ANL/IPNS/RP--89677-Vol.2

RECEIVED
MAY 06 1996
OSTI

EXPERIMENTAL REPORTS FOR EXPERIMENTS PERFORMED AT IPNS

MASTER

JANUARY 1991 – FEBRUARY 1996

MASTER



DISTRIBUTION OF THIS DOCUMENT IS UNLIMITED

15TH ANNIVERSARY 1981 – 1996

IPNS

Principal Author(s)	*Experiment Number*	*Title*
Glass, Liquid, and Amorphous Materials Diffractometer (GLAD)		**page 1**
A.G. Clare	1849	Measurement of Structure and Orientation in Bulk and Fiber Arsenic Selenide Glass
H.D. Cochran	1750	Structure of Dilute Supercritical Solutions IIb. Argon in Supercritical Krypton
H.D. Cochran	1859	Structure of Dilute Supercritical Solutions IIc. Argon in Supercritical Krypton
C. Cramer	1969	Structural Transitions in Fast Ion-Conducting Silver Iodide/Silver Selenate Glasses
A.J.G. Ellison	Disc.	Neutron Scattering Studies of Yb-Bearing Silicate Glasses
H.S. Schnyders/J.B. VanZytveld	2025	Structural Study of the Liquid Alloy $CeCu_6$
G.C. Straty	1628	Neutron Diffraction Investigation of Non-Ideal Binary Liquid Mixtures
K. Suzuya	Disc.	The Structure of Lead-Indium Phosphate Glass
P.Zhou/J.E. Fischer	2011	Local Structure of Lithium-Carbon Compounds
P.Zhou/J.E. Fischer	2155	Local Structure of Lithium-Carbon Compounds
J.W. Zwanziger	2154	Neutron Diffraction Study of the Structural Changes in Tellurite Glasses upon Modification with Sodium Oxide
General Purpose Powder Diffractometer (GPPD)		**page 12**
J. Allen	1385	Determination of the Structure of Lithium Dialuminate, $^7LiAl_2(OD)_7{\cdot}2D_2O$
M.T. Anderson/K.R. Poeppelmeier	NSF20	Determination of the Structure of the Perovskite-Related Compound La_2CuSnO_6
M.T. Anderson/K.R. Poeppelmeier	NSF27	Structure of Nd_2CuTiO_6 and Er_2CuTiO_6
R.C. Birtcher	1219	Irradiation-Induced Amorphization of U_3Si
R.C. Birtcher	1494	Irradiation-Induced Amorphization of U_3Si and U_3Si_2
R.C. Birtcher	1396	Irradiation-Induced Amorphization of U_3Si and U_3Si_2 (Also 1312, 1219, and 994)
R.C. Birtcher	2156	Crystallization of Amorphous U_3Si_2
S. Danyluk	1133	Non-Destructive Measurements of Residual Stresses in Thin, Short Plates of Yttrium-Barium-Copper Oxide Superconductors
H.A. Eick/G. Liu	1371	Determination of $BaMo(O,N)_3$ Structures at Various Temperatures
G.L. Hofman	D1994	Crystal and Microstructure of U_3Si_2 Fuel Plates after Reactor Irradiation
F. Izumi	1397	Crystal Structures of $YBa_2Cu_4O_8$ at Low Temperatures
J.A. Kaduk/S. Pei	2024	Hydrogen Bonding in Hydrated Sodium Aluminate, $NaAlO_2 \cdot 5/4H_2O$
J.A. Kaduk	1599	Crystal Structures of $KTiOPO_4$-type Nonlinear Optical Materials Above and Below the Curie Temperatures
N. Koura	2250	Crystal Structure of $(^7Li_{1-x}K_x)_2CO_3$ (x=0, 0.38, 0.50, 0.57) Determined by Neutron Powder Diffraction

Principal Author(s)	*Experiment Number*	*Title*
A.D. Krawitz	1644	Residual Stresses in WC-Co Measured by Neutron Diffraction
A.D. Krawitz/H.J. Prask	1226	Microstresses in Al_2O_3/SiC Ceramic Composites
D.S. Kupperman	D1992	Characterization of Residual Stresses in Metal-Ceramic Composite Compressor Rotors
D.S. Kupperman	P1994	Residual Strain in High Temperature Superconducting Tapes Measured by Neutron Diffraction
D.S. Kupperman/R.C. Birtcher	2152	Modification of Residual Stresses in Advanced Composites
G.A. Lager/R. Stoffregen	1571	Oxonium Ion Substitution in the Crystal Structure of Alunite
J. Lawrence	1934	Structure of the Heavy Fermion Compounds $CeCu_{2+x}Si_2$, $CePt_{2+x}$ and $YbInCu_4$
J. Lawrence	2031	Structure of the Heavy Fermion Compounds $CeCu_{2+x}Si_2$, $CePt_{2+x}$ and $YbInCu_4$
A.C. Lawson	1837	Crystal Structure of ζ-$Pu_{0.6}U_{0.4}$
A.C. Lawson	2013	Residual Strains in Ag-Cu In-situ Composites (Preliminary Results)
A.C. Lawson	1132	Crystal Structure of δ'-Plutonium
A.C. Lawson	1622	Debye-Waller Temperatures of $MoSi_2$
A.C. Lawson	1623	Debye-Waller Temperature and Thermal Expansion of Thorium Metal (10-300 K)
A.C. Lawson	1741	Thermal Expansion and Debye-Waller Factors of ZrC
M.A. Lewis	1490	Neutron Diffraction Study of Zeolite-A with Occluded Simulated IFR Waste Salt
K.H. Lii/S.L. Wang	1285	Neutron Powder Diffraction Study of $RbV_3P_4O_{17+x}$
C.-K. Loong	Disc.	Crystal Structure and Short-Range Oxygen Defects in La- and Nd-Modified ZrO_2
S.R. MacEwen	P1994	Microstructural Characterization of Al
K. Martin	1132	Residual Stress and Texture in Superconductor/Silver Composites
L.R. Morss	1143	Powder Diffraction Study of Li_5ReO_6 and Li_5NpO_6
G. Muralidharan	1795	Effect of Temperature and Composition on the Lattice Parameter Difference Between γ and γ' in Ni-Al-Si Alloys
J. Nipko	1967	f Electron-Phonon Coupling in $YbPO_4$ and $YbVO_4$
M. Ozawa	1971	Crystal Structure and Short-Range Defects in High-Temperature, High-Strength Nitride Ceramics
M. Ozawa	2068	Crystal Structure, Defects and Oxygen Storage in Ce Modified Zirconia
J.B. Parise	1434	Structure of Cristobalite, SiO_2, to 0.6 GPa
P.G. Radaelli/C.V. Segre	NSF12	Oxygen Deficiency in $ErBa_2Cu_3O_{7-x}$
L. Redey	2158	Neutron Diffraction Measurements of Metal-Hydride Electrodes (Phase 2)

Principal Author(s)	*Experiment Number*	*Title*
W.J. Reppart/S.C. Tang	1134	Structural Characterization of Basic Zeolites
W.J. Reppart/S.C. Tang	1262	Structural Characterization of Basic Zeolites
J.W. Richardson/E.T.C. Vogt	D1991	Structure Determination and Rietveld Refinement of the Aluminophosphate Molecular Sieve $AlPO_4$-8
J.W. Richardson/J.M. Carpenter	D1993	Characterization of Corrosion Products Generated from Failure of the IPNS Depleted Uranium Spallation Target
S. Roberts	1594	Temperature Dependence of Structure Parameters in UF_4
F.J. Rotella	Disc.	Palladium Deuteride Formation in the Cathode of an Electrochemical Cell: An In-situ Neutron Diffraction Study
K. Seff	1479	Location of Zn^{2+} and D^+ in Zeolite Y
C.V. Segre	NSF11	The Role of Pb-Substitution in the Bi-Sr-Cu-O System
T.R. Sendyka	1457	Local Structure of Superconducting Oxides
S. Skanthakumar	1761	Temperature Dependence of the Lattice Parameters in $HoP_{1-x}VxO_4$ ($0<x<1$)
T.E. Steyer/K.T. Faber	1261	Effect of Interfacial Films on the Residual Thermal Stresses in SiC-Al_2O_3 Composites
T.E. Steyer/K.T. Faber	1460	Effect of Interfacial Films on the Residual Stress in SiC-Al_2O_3 Composites
R.V. Strain	P1992	Neutron Diffraction Study of Irradiated $(U, Pu)O_{2-x}$ Fuel: Structure of Fuel-Sodium-Reaction-Product
T. Suzuki	1250	Neutron Diffraction Study of the Phase Transition in $Fe_{1/3}NbS_2$
J.T. Vaughey/K. Poeppelmeier	NSF18,NSF19	Structure of the New Copper Brownmillerite Phase $LaSrCuGaO_5$
J.T. Vaughey/K. Poeppelmeier	NSF21	The Structure of $LaSr_2Cu_2GaO_7$
J.T. Vaughey	NSF28	A Determination of the Structure of $HoSr_2Cu_2GaO_7$ and $HoSr_2Cu_2Ga_{0.85}Zn_{0.15}O_7$
J.T. Vaughey	NSF29	The Structural Determination of $LaSrCuGa_{0.85}Zn_{0.15}O_5$
J.W. White	1957	Approximant Structures in $Rb_3C_{60}(ND_3)_{2.5}$
J.T. Wood	2013	Residual Strains in Ag-Cu In-situ Composites

High Intensity Powder Diffractometer (HIPD) **page 75**

G.S. Girolami	Disc.	Nuclear and Magnetic Structure of $Cs_2Mn[V(CN)_6]$
K.W. Herwig/F. Trouw	1780	The Structure and Melting Temperatures of Alcohol Mixtures Adsorbed on Graphite
H. Nakotte	1925	Hybridization Effects in U_2T_2X Compounds: Magnetic Structures of U_2Rh_2Sn and U_2Ni_2In
H. Nakotte	1930	Magnetic and Crystallographic Structures of CeCuSn
A. Purwanto	1742	Magnetic and Structural Properties of URhIn
J.W. White	1778	In-Plane Ordering of Adsorbed Paraffin Molecules
J.W. White	1768	Tunnelling and Inelastic Scattering from Ternary Intercalates of C_{60}
J.W. White	1878	Inelastic Scattering from Ternary Intercalates of C_{60}

High-Resolution Medium-Energy Chopper Spectrometer (HRMECS) **page 83**

B. Chakoumakos/C.-K. Loong	2041	Hydrogen-Bonding Dynamics in Brucite
S.-K. Chan	1276	Determination of Phonon Density-of-States of the $YBa_2Cu_3O_{6.5}$ Superconductor
S.-K. Chan	1277	Determination of Phonon Density-of-States of the $YBa_2Cu_3O_{7-x}$ Superconducting Oxides
S.-K. Chan	NSF24	Determination of Phonon Density-of-States of the $YBa_2Cu_3O_{7-x}$ (x=0.71)
N. Choudhury	1851	Phonon Density of States of Forsterite and Enstatite
H. Conrad	1239	Molecular Spectroscopy of Insulin
H. Conrad	1612	Molecular Spectroscopy of Insulin
A.J.G. Ellison/C.-K. Loong	1697	Vibrational and Ligand-Field Spectroscopy in $3Na_2O{\cdot}R_2O_3{\cdot}6SiO_2$ (R=Yb) Glasses
M.A. Fradkin	1325	Kinetic Energies of the Individual Isotopes in Solid ^{3}He-^{4}He Solutions
M.A. Fradkin	1517	Single-Particle Response of Neon at High to Intermediate Momentum Transfers
M.A. Fradkin	1557	Density Dependence of the Single-Particle Response of Neon at High to Moderate Momentum Transfers
A.I. Goldman/C. Stassis	1388	Study of the Density-of-States and Localized Modes of the Icosahedral Al-Li-Cu Alloy
C.S. Johnson	1938	The Interaction of Water in MnO_2: Alpha-MnO_2
G.A. Lager	1904	Correlation Between Spectroscopic and Crystallographic Measurements in Alunite-Jarosite Minerals: Inelastic Neutron Scattering Studies
M. Loewenhaupt/C.-K. Loong	1841	Crystal-Field Spectroscopy of Hard Magnets RFe_4Al_8 (R=Tb and Dy)
C.-K. Loong	Disc.	Crystal-Field Excitations and Magnetic Properties of $TmPO_4$
C.-K. Loong	1588	f-Electron States in $ErPO_4$: A Joint Study of Neutron and Raman Spectroscopy
C.-K. Loong	1850	Local and Cooperative Jahn-Teller Effects in RMO_4 (R=Tb, Dy, Ho, Tm and M=P, V)
C.-K. Loong	1903	Hydrogen Vibrational Density-of-States of Water Physisorbed on Rare-Earth Modified ZrO_2 Fine Powders
S. Skanthakumar	1850	Crystal-Field Excitations and Magnetic Properties of Ho^{3+} on $HoVO_4$
L. Soderholm	1596	The Determination of Crystal Field Levels of Ho in $Pb_2Sr_2HoCu_3O_8$
M. Suzuki/S. Suzuki	1903	Hydrogen Vibrational Density-of-States of Water Physisorbed on Rare-Earth Modified ZrO_2 Fine Powders
S. Suzuki	2067	Atomic Dynamics of Si-Al-O-N Ceramic Alloys
K. Suzuya/C.-K. Loong	1981	Structural Properties of Amorphous Hydrogenated SiC Prepared by the Polymer Route
P. Vashishta	1984	Atomic Dynamics of Aluminum Nitride

Principal Author(s)	Experiment Number	Title
Low-Resolution Medium-Energy Chopper Spectrometer (LRMECS)		**page 108**
K. Bradley	1283	Coherent Scattering from Low Temperature, D_2O Hydrated Protein
B. Ewen	1842	Dynamics of Liquids Confined to Small Pores of Controlled Porous Glasses
M.A. Fradkin	1355	Para-Hydrogen Motion in Condensed Neon at Low Temperatures
J.A. Goldstone	1139	Crystal Field Levels in UCu_2Si_2
K.W. Herwig/F.R. Trouw	1393	A Study of the Inelastic Spectra of Ethanol Physisorbed on Graphite
S. Kern		Inelastic Magnetic Response in the System $(U_{0.45}Y_{0.55})Pd_3$
D.A. Peek	1034	Para-Hydrogen Motion in Condensed Neon Hosts
B.C. Sales	1974	The Structure of a Lead-Indium Phosphate Glass
U. Staub		Observations of CEF-Split Intermultiplet Transitions in Optically Opaque $EuBa_2Cu_3O_7$ Using Inelastic Neutron Scattering
H.L. Strauss	1774	The Diffusion of H_2 in Hexagonal Ice at Low Temperatures
S. Takahashi		Molecular Vibrations and Diffusion in $AlCl_3$-EMIC Molten Salts
Polarized Neutron Reflectometer (POSY)		**page 119**
S. Adenwalla	Disc.	90° Magnetic Structure in Fe/Cr Superlattices
S. Adenwalla	Disc.	2-D Character of the Magnetisation of Ultrathin Fe Films on MgO
S. Adenwalla	Disc.	Unidirectional Anisotropy in Co/CoO: A Neutron Reflection Study
S. Adenwalla	Disc.	Polarized Neutron Reflection Study of the Magnetic Field Distribution in Superconducting Nb Films
G.P. Felcher	Disc.	Observation of the Zeeman Splitting for Neutrons Reflected by Magnetic Layers
E.E. Fullerton	Disc.	Non-Oscillatory Antiferromagnetic Coupling in Sputtered Fe/Si Superlattices
G.H. Lander	1626	Examination of U-Based Multilayers
M. Loewenhaupt	Disc.	Microscopic Observation of the Magnetic Phase Transitions in Gd/Fe Multilayers
Y. Li	Disc.	Magnetic Depth Profile of Fe/Ni Bilayers
J.E. Mattson	Disc.	Oscillatory Interlayer Magnetic Coupling of Sputtered Fe/Nb Superlattices
Neutron Reflectometer (POSY II)		**page 129**
G. Agrawal	1353	Polymer Chain End vs. Chain Center Mobility
G. Agrawal	1714	Polymer Chain End vs. Chain Center Mobility: A Test of Reptation Theory
B.L. Carvalho	1417	Interlayer Diffusion in Langmuir-Blodgett Films
R.J. Composto/R. Oslanec	2027	Neutron Reflectivity Studies of Dry Polymer Brushes

Principal Author(s)	*Experiment Number*	*Title*
R.J. Composto	1412	Measurement of the Interdiffusion Profile at the Interface Between Linear and Cyclic Polystyrene Layers (I)
R.J. Composto	1662	Measurement of the Concentration Profiles at the Interface of a Homopolymer/Binary Polymer Mixture
K.H. Dai/E.J. Kramer	1633	Block Copolymers at Interfaces Between Homopolymers by Neutron Reflectometry
K.H. Dai/E.J. Kramer	1634	Ordering of a Triblock Copolymer Thin Film
K.H. Dai	1467	Neutron Reflectometry Study of Diblock Copolymer to the Interface Between Homopolymers
K.H. Dai	1569	Neutron Reflectometry Study of Diblock Copolymer to the Interface Between Homopolymers
W. Dozier	Disc.	Hydrogen Segregation at the Al/Si Interface, as Probed by Neutron Reflection
G.P. Felcher	Disc.	Topology of Forward Scattering of Neutrons from Imperfect Multilayers
J.S. Fodor	2102	Investigation of Density Variation and Pore Formation in Thin "Nanofoam"Films by Neutron Reflectivity
A. Hariharan	1464	Surface Segregation of Polymer Chains Due to Molecular Weight Effects
B.J. Heuser	2153	Neutron Reflectometry Study of Hydrogen Absorption by Metal Films
A. Karim	Disc.	Interdiffusion in Partially Deuterated Polymer Bilayers
A. Karim	1456	Study of Polyolefin Thin Films
M.S. Kent/D.W. Hua	1763	Interaction of Functionalized Elastomers with SiO_2 and the Correlation with Particle Dispersion Characteristics
M.S. Kent/W.-L. Wu	1950	The Influence of Silane Coupling Agents on Moisture Adsorption at the Epoxy/Glass Interface
M.S. Kent/A. Wong	1950	The Influence of Silane Coupling Agents on Moisture Adsorption at the Epoxy/Glass Interface
M.S. Kent	1949	Interaction of Functionalized Elastomers with SiO_2 and the Correlation with Particle Dispersion Characteristics
M.S. Kent	1951	Moisture Adsorption at the Copper/Epoxy Interface
J. Koberstein	1272	Surface Partitioning in Multicomponent Systems
S. Kumar/T. Russell	1299	Surface Segregation of Polymer Chains Due to Molecular Weight Effects
S. Kumar/T. Russell	1361	Surface Segregation of Polymer Chains Due to Molecular Weight Effects
S.K. Kumar	1753	Phase Separation and Surface Segregation in Binary Polymer Blends
M.R. Landry	1352	Determination of Interface Thickness Between Polymer Layers
T. Mansfield	1179	Surface Enrichment in Copolymers and Their Blends
L.J. Norton	1362	Surface Enrichment in Isotopic Polymer Alloys by Neutron Reflectometry
L.J. Norton	1363	Neutron Reflectometry Study of Segregation of End-Functionalized Polymers to Interfaces Between Polymers and Nonpolymers

Principal Author(s)	Experiment Number	Title
L.J. Norton	1465	Surface Enrichment in Isotopic Polymer Alloys by Neutron Reflectometry
L.J. Norton	1468	Neutron Reflectometry Study of Segregation of End-Functionalized Polymers to Interfaces Between Polymers and Nonpolymers
L.J. Norton	1567	Surface Enrichment in Isotopic Polymer Alloys by Neutron Reflectometry
L.J. Norton	1636	Surface Enrichment in Isotopic Polymer Alloys by Neutron Reflectometry
R.J. Roe	1233	Structure of Blends of Block Copolymer and Homopolymers
T.P. Russell/H.R. Brown	1350	Effect of Diblock Copolymers on Adhesion
T.P. Russell	1349	Interfacial Activity of Diblock Copolymers
T.P. Russell/A. Menelle	1477	Interfacial Activity of Diblock Copolymers
B. Sauer	1450	Diffusion of Polymers in Crosslinked Polymer Networks
N.C. Stoffel	1568	Polyimide Interfaces: Imidization and Interdiffusion by Neutron Reflectometry
J.G. Van Alsten		Interfacial Broadening Segmented Poly (Urethane Ureas) Studied by Neutron Reflection
D.J. Walsh/B.B. Sauer	1359	Neutron Reflection Studies of Polymer Interfaces
D.J. Walsh/B.B. Sauer	1359	Neutron Reflection Studies of Polymer Interfaces
D.J. Walsh/B.B.Sauer	1359	Neutron Reflection Studies of Polymer Interfaces
R.P. Wool		Structure of Polymer Interfaces
H. Zhang	1353	Evaluation of Minor Chain Reptation Model Using Triblock Interfaces

Quasielastic Neutron Spectrometer (QENS) **page 175**

M.C. Aronson/F.R. Trouw		Non-Fermi Liquid Scaling in UBe_{13}
V. Arrighi/J.S. Higgins	1581	Effect of Plasticizer on Polymer Dynamics
K. Edler	1958	Dynamics of Small Molecules in Large Pore Zeolites
K.W. Herwig/F.R. Trouw	1305	A Quasielastic and Low-Energy Inelastic Study of Ethanol on a Graphite Surface
K.W. Herwig/F.R. Trouw	1394	A Low-Energy Inelastic Study of Ethanol on a Graphite Surface
K.W. Herwig	1880	A Quasielastic Neutron Scattering Study of the Diffusive Motion of Water Molecules in a Water-Oil Microemulsion
K.W. Herwig	1881	Diffusion of Water in a Biological Gel Matrix
K.W. Herwig	1692	A Quasielastic Neutron Scattering Study of the Diffusive Motion of Water Molecules in a Water-Oil Microemulsion
S. Kern	1392	Thermal Behavior of the Inelastic Response of UF_4
E.W. Ong	1654	Molecular Motions in Ammonia-Ammonium Intercalated Titanium Disulfide
R.A. Robinson	1638	Quasielastic Scattering from YbBiPt
U. Staub/L. Soderholm	1954	Crystalline Electric-Field and Molecular-Field Behavior in $Y_{1-x}Tb_xBa_2Cu_3O_y$
H. Taub	1254	Quasielastic Neutron Scattering from Butane and Hexane Monolayers Adsorbed on Graphite

Principal Author(s)	*Experiment Number*	*Title*
A. Xenopoulos	1253	Lattice Dynamics of Polymer Chains II: Polyamides
J.W. White	1768	Tunnelling and Inelastic Scattering from Ternary Intercalates of C_{60}
J.W. White	1878	Inelastic Scattering from Ternary Intercalates of C_{60}

Small Angle Diffractometer (SAD) **page 191**

K.A. Carrado/P. Thiyagarajan	1402,1458	Magnesium Hydroxide Gels Monitored by SANS Contrast-Variation Techniques
R. Briber	1832	Small Angle Neutron Scattering in the Dilute Concentration Limit of PVME in PSD
J.M. Calo/P.J. Hall	1745	The Accessibility of Organic Liquids to the Pore Network of Activated Carbons
J.M. Calo/P.J. Hall	1968	Connectivity of Porosity in Coals
K.A. Carrado/P. Thiyagarajan	1889	SANS Studies of the Mechanism of Incorporation of Water-Soluble Polymers in Clays During Hydrothermal Crystallization
K.A. Carrado	1263	Characterization of Template-Mediated Layer Silicate Crystallization Processes by Small-Angle Neutron Scattering
H. Chen/G. Muralidharan	1185	Effect of Lattice Mismatch Strain on the Morphology Change in Ni-Al-Si Ternary Alloys
G.D. Cody	1825	The Solution Structure of the Coal Macromolecule
B. Crist/J.W. Rhee	1069,1146	Thermodynamics of Polyethylene-Copolymer Blends
B. Crist/J.W. Rhee	1282,1347	Thermodynamics of Model Polyethylene Blends
B. Crist/J.W. Rhee	1469	Thermodynamics of Model Polyethylene Blends
K. Edler	2017	Aging Process and Template Content in MCM-41
J.E. Epperson	1255	Time Resolved Neutron Small Angle Scattering
J.E. Epperson	1538	Determination of the Miscibility Gap in the Fe-Cr System
P.S. Goyal	1615	Clouding Phenomenon in Non-Ionic Micellar Solutions: Applicability of Baxter's Sticky Hard Sphere Model
X.H. Guo	1259	The Structure of Protein/SDS Complex in Low Ionic Strength Solution
B.J. Heuser/J.S. King	2009	SANS Investigation of Deuterium Precipitation in Nb: Effect of Deformation
B.J. Heuser/J.S. King	2009	SANS Investigation of Deuterium Trapping at Dislocations in Nb at Low Temperature
B.J. Heuser	1237	Dislocation-Deuterium Interaction in Pd
R.P. Hjelm	1820	Particle Morphology in Mixed Aqueous Colloids of Monoglycerides and Bile Salts
R.P. Hjelm	1227	SANS of Mixed Bile Salt-Lecithin Colloids
R.P. Hjelm	1291	SANS of Mixed Bile Salt-Lecithin Colloids
R.P. Hjelm	1507	Arrangement and Assembly of Lecithin and Bile Salts in Mixed Micelles
R.P. Hjelm	1710	SANS as a Probe of the Structure of Liquid Crystal Polymer-Reinforced Composites
R.P. Hjelm	Disc.	SANS as a Probe of Liquid Crystal Epoxy-Liquid Crystal Polymer Composites

Principal Author(s)	*Experiment Number*	*Title*
R.P. Hjelm	2072	Mixed Colloid-Drug Interactions in Drug Delivery Systems
H.W. Huang	1939	In-Plane Scattering of Peptides in Membranes
H.W. Huang	2079	In-Plane Scattering of Peptides in Membranes
H.W. Huang	2094	In-Plane Scattering of Peptides in Membranes
L.E. Iton/J.W. White	1370	ZSM-5 Crystallization by Liquid Phase Ion Transport
L.E. Iton/J.W. White	1575	ZSM-5 Crystallization by Liquid Phase Ion Transport
J. Kieffer	1499	Characterization of the Pore Structure in Activated Carbons
S. Kulkarni	1560	SANS from D_2O Swollen Reverse Osmosis and Ultrafiltration Membranes
C.W. Lantman/P.Thiyagarajan	Disc.	Block Copolymers
C.W. Lantman	1439	Effect of Sequence Distribution on Copolymer Adsorption
C.W. Lantman	1545	Copolymer Adsorption
A.C. Lawson	Disc.	Small Angle Neutron Scattering in $Ni_{1-x}Al_x$ Alloys
M.Y. Lin	1321	Critical Phase Transition of Binary Fluids in Random Media
A. Moini	1148	SANS Studies on the Formation of Sol-Clay Complexes and its Dependence on pH and Particle Size
G. Muralidharan	1246	Effect of Lattice Mismatch Strains on Phase Separation in Ni-Al-Si Alloys
G. Muralidharan	1562	Effect of Lattice Mismatch Strains on Phase Separation in Ni-Al-Si Alloys
G. Muralidharan	1649	Effect of Coherency Strains on the Kinetics of Coarsening in Ni-Al-Si Alloys
G. Muralidharan	1813	Effect of Coherency Strains on the Kinetics of Coarsening in Ni-Al-Si Alloys
G. Muralidharan	1875	Effect of the Interaction of Coherency Strains and Volume Fraction on the Coarsening of γ' in Ni-Al-Si Alloys
N.S. Murthy	1847	Distribution of Labeled Species in Polymers and Copolymers
N.S. Murthy	2044	Study of Amorphous Domains in Fibers, Blends and Networks
L.F. Nazar	1275	SANS Studies of the Microstructure of Alumina Sol-Gels
M. Ozawa	2057	Study of Porous Texture and Adsorption Process in Rare-Earth Modified Zirconia Gels
S. Schneider	2043	Small Angle Neutron Scattering Study of Phase Separation in Bulk Metallic Glasses
E.Y. Sheu/M. DeTar	1496	Reacted Asphaltenes in Polar Solvents
E.Y. Sheu	1238	Asphaltenes in Polar Solvents
E.Y. Sheu	1346	The Study of Asphaltene Formation Energy in Polar Solvents
E.Y. Sheu	1651	Structure of the Bioremediation Surfactants in Soil/Water/Surfactant Complexes
R.W. Siegel	1669	In-situ Sintering of Nanophase Pd

Principal Author(s)	Experiment Number	Title
P. Thiyagarajan/D.M. Tiede	1824	Physico-Chemical Properties of Detergents Used for Membrane Protein Crystallization in Presence of Salt, Small Amphiphiles and Polyethylene Glycol
P. Thiyagarajan	1948	The Solution Structure of Untreated and O-Methylated Coal Extracts in Pyridine: A Contrast Variation SANS Analysis
D.M. Tiede/P. Thiyagarajan	1823	Structure of Light Harvesting Complexes in Detergent Solutions
S.A. Visser	1341	Ionomer Chain Dimensions in the Vicinity of the Ionic Aggregates
J.W. White	1959	Surface Modification of Phase Separation in *n*-Paraffin Solutions
R. E. Winans	1896	SANS of Petroleum Resid and Their Interaction with Dispersed Catalysts
D.L. Worcester/A.E. Blaurock	1100	Hydrostatic Pressure Analysis of Teleost Myelin Stability
T.W. Zerda	2060	Density of Liquid Cyclohexane Inside Small Pores in Porous Glass

Single Crystal Diffractometer (SCD) **page 257**

L.R. Falvello/I. Pascual	1884	Single-Crystal Structure of Saccharinatotetraamminecopper(II) Saccharinate Hydrate
L.R. Falvello	1249	Hydrogen Bonding and Strain in Molecular Solid Solutions Exhibiting the Cooperative Jahn-Teller Effect
L.R. Falvello	1648	Hydrogen Bonding in the Crystal Structure of Vanadium Sulfate Hydrate
L.R. Falvello	1731	Hydrogen Bonding and Strain in Molecular Solid Solutions Exhibiting the Cooperative Jahn-Teller Effect
G.M. Frankenbach	1209	Analyzing Carboxylic Acid and Amino-Nitro Hydrogen-Bond Geometry in the Cocrystal of 4-Aminobenzoic Acid and 3,5-Dinitrobenzoic Acid by Use of 298 K X-Ray and 15 K Neutron Diffraction
M.A. Hitchman	1430	Neutron Diffraction Study of the Effect of Pressure on the Structure of $(NH_4)_2[CR(H_2O)_6](SO_4)_2$
W. Jauch/A.J. Schultz	1114	Accurate Determination of Changes in Structural Parameters in NiF_2 Due to Magnetic Ordering
J.S. Kallend	1483	Texture Analysis of $YBa_2Cu_3O_x$ Specimens
M. Kunz	1145	Crystal Chemistry and Crystal Physics of Neptunite
J.R. LaGraff	NSF15	Structure and Processing Relationships in Single Crystal $Y_{1-x}Pr_xBa_2Cu_3O_{7-d}$
C.-K. Loong	2056	Impurity-Induced Electronic Conductivity and Ferroelectricity in Ca-Doped $KTa_{1-x}Nb_xO_3$
J.S. Moore/D. Venkataraman	2073	Structural Studies on a Nanoporous Coordinational Network
H. Nakotte	1928	Magnetic Structure of UCu_3Al_2

Principal Author(s)	*Experiment Number*	*Title*
A. Palmer	1546	Structural Parameters in NiF_2 at 15 K from a Single Domain Crystal in a Magnetic Field
P.G. Radaelli	Disc.	Oxygen Defect Structure in Nd_2CuO_y
P.G. Radaelli	NSF	Structure of Superconducting $La_2CuO_{4+\delta}$ Phases ($\delta \approx 0.08, 0.12$) Prepared by Electrochemical Oxidation
J. Rakovan	1725	Differential Ordering in Minerals: The Role of Surface Structure During Growth
P. Reynolds	1835	The Crystal Structure of $Ru(ND_3)_6(SCN)_3$
A.J. Schultz	1210	Low Temperature Structure of $(NH_4)_2(TiOPO_4)_2$
A.J. Schultz	NSF	Structures of Reduced and Oxygenated $Nd_{2-x}\ Ce_xCuO_y$
A.J. Schultz	1625	The Low Temperature, High Pressure Crystal Structure of $K_2[FeCl_5(H_20)]$
C.J. Simmons	1430	Single Crystal Neutron Diffraction Study of $(NH_4)Cu(H_2O)_6(SO_4)_2$
C.J. Simmons	1529	Single Crystal Neutron Diffraction Study of $(NH_4)_2Cu(H_2O)_6(SO_4)_2$ at 15K Ambient and 1.5 kbar Pressure

Special Environment Powder Diffractometer (SEPD) **page 280**

R.H. Arendt	Pilot Center	Thermal Expansion Measurements Using Neutron Diffraction of $(Bi,Pb)_2Ca_2Sr_2Cu_3O_x$
R.H. Arendt	Pilot Center	Thermal Expansion Measurements Using Neutron Diffraction of $Bi_2CaSr_2Cu_2O_x$
S.J.L. Billinge/T. Egami	1457	Comparison of the Local Atomic Structure of Reduced and Unreduced Samples of $Nd_{1.83}Ce_{0.17}CuO_{4-y}$
W. Dmowski	1757	Local Structure of Superconducting $YBa_2Cu_4O_8$
T. Egami	1381	Local Structure of Superconducting Oxides
T. Egami	1381	Local Structure of Superconducting La-Nd-Sr-Cu-O and $YBa_2Cu_4O_8$
J. Fortner	1491	Structural Ordering in Liquid Potassium-Tellurium Alloys
M.A. Fradkin	1033	Structure Determination in BCC Solid ^3He-^4He
M.F. Garbauskas	Pilot Center	High-Temperature Neutron Diffraction Study of the Melting Behavior of $Bi_2CaSr_2Cu_2O_x$
J.T.S. Irvine/S.M. Fray	1858	Structural Study of $Na_2Bi_2O_5$ and $Pb_2Bi_6O_{11}$
F. Izumi	1398	Crystal Structures of $Tl_2Ba_2CuO_{6+z}$ Under High Pressure
G.H. Kwei/S.J.L. Billinge	1886	Determination of the Differential Pair Distribution Functions for $YBa_2Cu_3O_{6+x}$ Near T_c Using ^{63}Cu and ^{65}Cu Labeled Samples
F. Li/J.S. Lannin	1211,1289	Structure of Amorphous Carbon
C.-K. Loong	1971	Crystal Structure and Lattice Dynamics of Slip Cast β-Sialons
M.F. Mansuetto	1931	Structural Investigation of Lithiated Oxides for Rechargeable Lithium Batteries
H.D. Rosenfeld	1268	Local Structure of Superconducting La-Sr-Cu-O

Principal Author(s)	*Experiment Number*	*Title*
K.B. Schwartz	1323	Crystal Chemistry of Si/Al in Bi-Processed Aluminosilicates
T. Sendyka/T. Egami	1457	Local Structure of Superconducting Oxides
S. Teslic/T. Egami	1755	Local Structure of Relaxor Ferroelectric PLZT
B.H. Toby	1268	Local Structure of Superconducting $(Ba,K)BiO_3$
P.C. Trulove	1329	Structure of an Ambient-Temperature Molten Salt $ImHCl_2$
J.B. VanZytveld	1240	Structural Study of the Liquid Alloy $Mg_{0.50}Ba_{0.50}$

INSTRUMENT USED: GLAD	DATE OF REPORT: 5/11/95	EXPERIMENT NO.: 1849

TITLE: Measurement of Structure and Orientation in Bulk and Fiber Arsenic Selenide Glass

AUTHORS AND AFFILIATIONS: Alexis G. Clare, Wesley King, William LaCourse, NYSCC Alfred University and Adrian C. Wright, University of Reading UK

DATES OF EXPERIMENT: 19-23 Sept 1994

CHECK ALL APPLICABLE BOXES:

- [x] APPROVED BY PROGRAM COMMITTEE
- [ ] INSTRUMENT SCIENTIST ALLOCATION
- [ ] DO NOT PUBLISH
- [ ] PROPRIETARY RESEARCH
- [ ] PRT ALLOCATION

EXPERIMENTAL REPORT (or Abstract of Publication)

Figure 1 shows the total correlation functions for the bulk stoichiometric arsenic selenide sample.

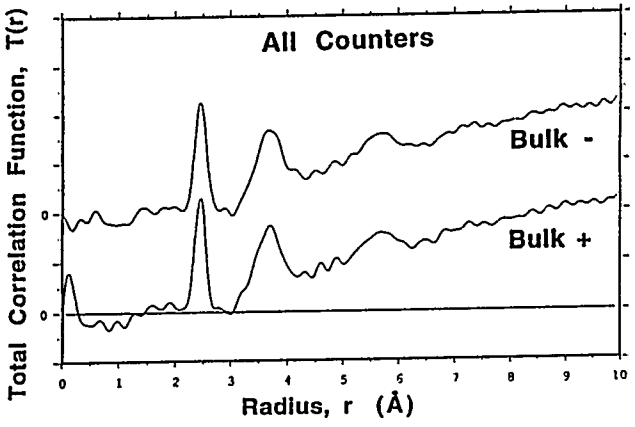


Figure 1 Total Correlation Functions of Bulk Oriented +45° (Q along axis) and -45° (Q along radius). All counters.

The 90° counter data indicated that the structure did not vary as a function of orientation for the bulk sample therefore analysis proceeded with the T(r) calculated from the sum of all counters. The three large peaks in the T(r) correspond to; As-Se first neighbors (2.4Å) As-As and Se-Se second neighbor distances at (3.7Å) and a peak at 5.7Å. The 2.4Å peak is very narrow and extremely symmetrical this is indicative of chemical ordering. The 5.7Å peak has most often been assigned to interlayer

correlations similar to those observed in the crystal. However, calculations of relative atomic positions in such a layer show that correlations corresponding to the large 12 membered rings that make up the layers in the crystal are absent from the T(r) observed in this experiment. This is consistent with T(r) data from previous experiments on this glass and yet remains unexplained. We proposed however that this correlation may be explained in terms of the spiral chains of As-Se bonds that make up the crystal. 5.7Å is a distance that appears repeatedly within those spirals, in addition the spirals will be separated by the same Van Der Waals interactions that appear in the layers which could add to that peak.

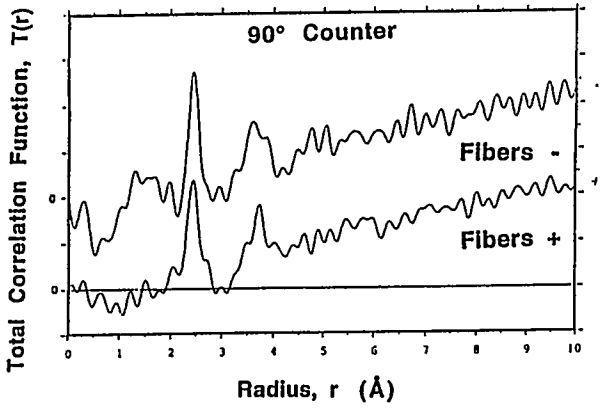


Figure 2 Total Correlation Functions of Fibers Oriented +45° (Q along axis) and -45° (Q along radius) 90° counter only

As can be seen while there is no change in the first peak indicating that the basic $AsSe_3$ tetrahedron is in tact, however, the second peak, as far as can be ascertained through the noise appears to have shifted such that the second neighbor distances axially are longer while radially shorter. This is extremely interesting and needs to be followed up. We are therefore applying for more time to look at just the fibers.

INSTRUMENT USED:	DATE OF REPORT:	EXPERIMENT NO.:
GLAD	May 25, 1994	1750

TITLE:
Structure of Dilute Supercritical Solutions IIb. Argon in Supercritical Krypton

AUTHORS AND AFFILIATIONS: H. D. Cochran, Oak Ridge National Laboratory
P. R. Bienkowski, V. M. Shah, S. B. Nogaja, E. L. Daggett, University of Tennessee

DATES OF EXPERIMENT:
February 22, 1994 to February 26, 1994

CHECK ALL APPLICABLE BOXES:

- [X] APPROVED BY PROGRAM COMMITTEE
- [ ] INSTRUMENT SCIENTIST ALLOCATION
- [ ] DO NOT PUBLISH
- [ ] PROPRIETARY RESEARCH
- [ ] PRT ALLOCATION

EXPERIMENTAL REPORT (or Abstract of Publication)

The aim of this experiment was to test our apparatus and to measure the partial structure factors of argon and krypton in a binary mixture at GLAD. The mixture consisted of 5 mole % argon in supercritical krypton at 220K and 980 psia. Isotope substitution with ^{36}Ar was to be used to extract the partial structure factors. Our apparatus (Londono *et al.* , 1993) consists of a high pressure vanadium sample cell 5 cm length by 1 cm internal diameter. The cell has a wall thickness of 0.036 cm where the neutron beam traverses it. The cell is enclosed in an aluminum vacuum shroud with vanadium windows. The sample cell holds about 5 grams of the gas mixture at 220K and 980 psia. A neutron beam size of 1 cm x 1.27 cm (using soller collimaters) was used with the sample in the downstream position at GLAD. The neutron beam traverses a total thickness of 0.142 cm of vanadium.

The following experiments were performed for the period February 23 to February 26, 1994 on the GLAD instrument.

1. 12 hrs. (total) instrument background.
2. 9 hrs. (total) vanadium rod.
3. 24 hrs. (total) empty cell.
4. 12 hrs. 5% natural argon in natural krypton at 220 K and 980 psia.
5. 6 hrs. pure krypton at 220 K and 980 psia.

The experiment with 5% natural argon in krypton and pure krypton were scheduled for 24 hrs each. The mixture run could not be completed successfully as the cell developed a leak resulting in the gradual loss of the gas mixture. The leak was repaired before carrying out the pure krypton experiment. However, this run had to be stopped as the cell started leaking again. Due to the vanadium in the sample cell and the windows, there was considerable scattering from the empty cell. As a result, the scattering from the krypton-argon mixture was only marginal compared to the empty cell. The small scattering from the sample and the short scattering times resulted in poor statistics, leading to unsatisfactory results.

Several modifications are being made to our apparatus to overcome the problems encountered during this trip. In order to reduce the empty cell scattering, an aluminum sample cell will be used instead of vanadium. The windows on the vacuum shroud will be replaced with aluminum windows. This should lead to a significant reduction in the scattering from the empty cell. The Bragg scattering from the aluminum cell will be corrected for during the data analysis. The problem of the leak in the cell has already been corrected. Since the normalized spectra from our empty instrument showed Bragg peaks, even though we had only vanadium in the path of the neutrons. we have decided to use boron carbide to shield our apparatus. We are in the process of making boron carbide "crispy" mix in order to make the shields. With these changes. we expect to have a successful experiment the next time we are up at GLAD.

References

Londono, J. D., V. M. Shah, G. D. Wignall, H. D. Cochran, and P. R. Bienkowski, "Small angle neutron scattering studies of dilute supercritical solutions. I. Pure supercritical neon," *J. Chem. Phys.*, 99(1), 466, (1993).

INSTRUMENT USED:	DATE OF REPORT:	EXPERIMENT NO.:
GLAD	January 12, 1995	1859

TITLE:
Structure of Dilute Supercritical Solutions IIc. Argon in Supercritical Krypton

AUTHORS AND AFFILIATIONS: H. D. Cochran, Oak Ridge National Laboratory, P. R. Bienkowski, V. M. Shah, E. L. Daggett, R. S. Dharmapurikar, University of Tennessee

DATES OF EXPERIMENT:
October 11, 1994 to October 15, 1994

CHECK ALL APPLICABLE BOXES:

- [X] APPROVED BY PROGRAM COMMITTEE
- [ ] INSTRUMENT SCIENTIST ALLOCATION
- [ ] DO NOT PUBLISH
- [ ] PROPRIETARY RESEARCH
- [ ] PRT ALLOCATION

EXPERIMENTAL REPORT (or Abstract of Publication)

The aim of this experiment was to measure the partial structure factors of argon and krypton in a binary mixture. The mixture consisted of 5 mole % argon in supercritical krypton at 220K and 1041 psia. Isotope substitution with ^{36}Ar was used to extract the partial structure factors. Since the mixture has only 5% argon in it, the argon-argon contribution to total scattering is neglected. Integral equation calculations have been done to validate this assumption. Hence, our goal was determine the krypton-krypton and the krypton-argon structure factors only.

Our apparatus (Londono *et al.*, 1993) consists of a high pressure aluminum sample cell 5 cm length by 1 cm internal diameter. The cell has a wall thickness of 0.036 cm where the neutron beam traverses it. The cell is enclosed in an aluminum vacuum shroud with aluminum windows. The sample cell holds about 5 grams of the gas mixture at 220K and 1041 psia. A neutron beam size of 1 cm x 1.27 cm (using soller collimaters) was used with the sample in the downstream position on GLAD. The neutron beam traverses a total thickness of 0.146 cm of aluminum. Boron carbide "crispy" mix was used to shield the vacuum shroud. A hot pressed boron carbide mask was used downstream to the sample to capture stray neutrons.

The following experiments were performed for the period October 11 to October 15, 1994 on the GLAD instrument.

1. Instrument background.
2. Vanadium rod.
3. Empty cell at 220 K.
4. 5% natural Ar in natural Kr at 220 K and 1041.4 psia.
5. 5% ^{36}Ar in natural Kr at 220 K and 1041.1 psia.

For both mixtures, the temperature of the cell was 219.93 ± 0.01 K and the temperature gradient between the top and the bottom of the cell was < 5 mK. The pressure in the cell was 1041.4 ± 0.1 psia over 21 hours for the natural argon mixture and 1041.1 ± 0.1 psia over 26 hours for the ^{36}Ar mixture.

Data analysis is going on at the present. Some preliminary results are given here. Figures 1 and 2 show the total distinct scattering for the natural Ar-Kr mixture and the ^{36}Ar-Kr mixture, respectively. Smoothing techniques were used to eliminate the aluminum Bragg peaks. The smoothed curves are shown by solid lines. The smoothed data was used to calculate the Faber-Ziman krypton-krypton (Figure 3) and krypton-argon (Figure 4) structure factors. Refinement of the GLAD data is under progress. Complimentary small angle neutron scattering experiments with the same mixtures and conditions have been completed at the SANS instrument at Oak Ridge National Laboratory. Preliminary results show good agreement between the GLAD and SANS results.

References

Londono, J. D., V. M. Shah, G. D. Wignall, H. D. Cochran, and P. R. Bienkowski, "Small angle neutron scattering studies of dilute supercritical solutions. I. Pure supercritical neon," *J. Chem. Phys.*, 99(1), 466, (1993).

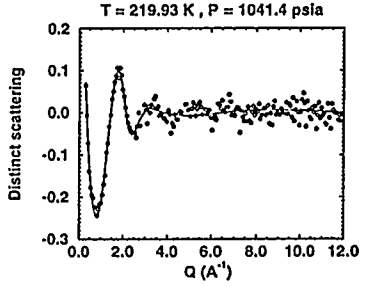


Figure 1: Total distinct scattering for natural Ar-Kr mixture

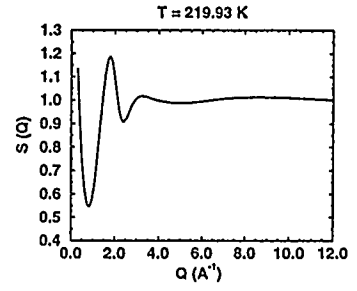


Figure 3: Krypton-krypton structure factor

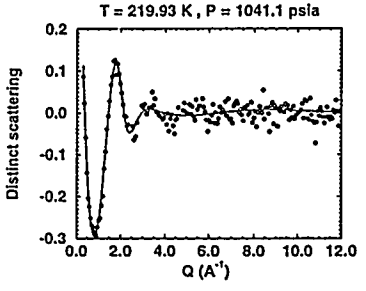


Figure 2: Total distinct scattering for ^{36}Ar-Kr mixture

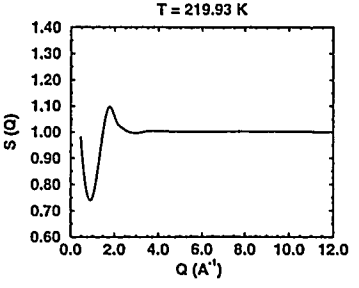


Figure 4: Krypton-argon structure factor

INSTRUMENT USED: GLAD	DATE OF REPORT: 02.13.1996	EXPERIMENT NO.: 1969

TITLE: Structural transitions in fast ion–conducting silver iodide/silver selenate glasses·

AUTHORS AND AFFILIATIONS: C. Cramer, D.L. Price, M.–L. Saboungi, and K.J. Volin, ANL, MSD 223

DATES OF EXPERIMENT: 12.09. – 12.12.1994

CHECK ALL APPLICABLE BOXES:

- ☐ APPROVED BY PROGRAM COMMITTEE
- ☐ INSTRUMENT SCIENTIST ALLOCATION
- ☐ DO NOT PUBLISH
- ☐ PROPRIETARY RESEARCH
- ☐ PRT ALLOCATION

EXPERIMENTAL REPORT (or Abstract of Publication)

AgI containing glasses are fast ion–conductors showing tremendous dc conductivities reaching values of about $10^{-2}\,\Omega^{-1}cm^{-1}$ at room temperature. So far, a lot of work has been done to link the high ionic conductivity to structural features of these glasses. A crucial question is how the AgI enters the glass network and whether this sort of glasses contain a biphasic structure with AgI rich regions .

To shed light on this question, we performed neutron diffraction experiments on GLAD diffractometer looking at the fast ion–conducting glass–forming system $x(AgI)_2 \cdot (1-x)Ag_2SeO_4$ at various temperatures. On the one hand, the static structure factor, S(Q), was determined at ambient temperature for glass compositions with x=0.40, 0.48, 0.54. On the other hand, glassy $0.48\,(AgI)_2 \cdot 0.52\,Ag_2SeO_4$ was studied at various temperatures between ambient temperature and 573 K. The variation of temperature allowed for determination of the structure in the glassy, partly crystallized and molten state of the same material. In addition, we looked at powder samples of the crystalline starting materials AgI and Ag_2SeO_4.

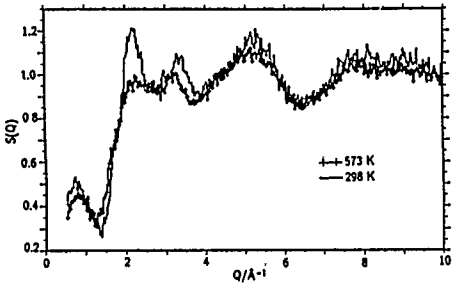


Fig. 1: S(Q) of $0.48\,(AgI)_2 \cdot 0.52\,Ag_2SeO_4$

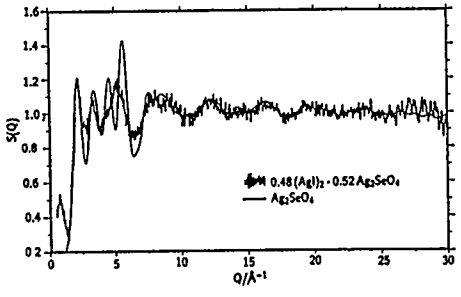


Fig. 2: S(Q) of $0.48\,(AgI)_2 \cdot 0.52\,Ag_2SeO_4$ and Ag_2SeO_4

At temperatures above 333 K (roughly 30 K above the glass temperature) the glass partially crystallizes. At 465 K, however, the complete sample is liquid. Fig. 1 shows the static structure factor of $0.48\,(AgI)_2 \cdot 0.52\,Ag_2SeO_4$ at 298 K and 573 K. Within experimental error, the S(Q) data taken at these temperatures are identical for Q–values higher than 10 $Å^{-1}$.

The structure factors of the solid and the melt are very similar to each other, larger deviations appearing just at Q=2.0 $Å^{-1}$ and Q≈ 3 $Å^{-1}$. Especially, at both temperatures diplayed in fig. 1, there is a peak at very low momentum transfer values, $\hbar Q$ (Q=0.75 $Å^{-1}$ at 298 K and Q=0.79 $Å^{-1}$ at 573 K).

EXPERIMENTAL REPORT (CONTD.)

These peaks reflect medium range order, the correlation length, $d = 2\pi/Q$ being approximately 8 Å. This medium range order survives the melting process. The partially crystallized glasses show Bragg peaks around Q≈ 0.8 $Å^{-1}$, whereas there is no intensity in this range in the structure factors of the crystalline starting materials AgI and Ag_2SeO_4. With increasing AgI content in the glasses, the intensity of the peak at very low Q slightly increases and its position is shifted to lower Q values.

From fig. 2 it can easily be seen that the structure factor of the glassy sample shows a strong similarity to the S(Q) of c–Ag_2SeO_4. (For better comparison with the amorphous samples, the structure factor of c–Ag_2SeO_4 has slightly been smoothed, yielding an envelope of Bragg peaks). This is remarkable because Ag_2SeO_4 does not form a network, instead the glasses consist of isolated ions (Ag^+, I^- and SeO_4^{2-}). The strong similarity between the glass structure and the structure of Ag_2SeO_4 can also be seen in the real space representations. Figs. 3 and 4 show the total structure factors T(r) (via $T(r) = 4\pi\rho_0 + \frac{2}{\pi}\int_0^{Q_{max}} Q\,[S(Q)-1]\sin(Qr)dQ$) of silver selenate and glassy $0.54\,(AgI)_2 \cdot 0.46\,Ag_2SeO_4$, respectively. The fits have been obtained by superposition of several Gaussians whose positions and weights are based on structural information about crystalline Ag_2SeO_4.

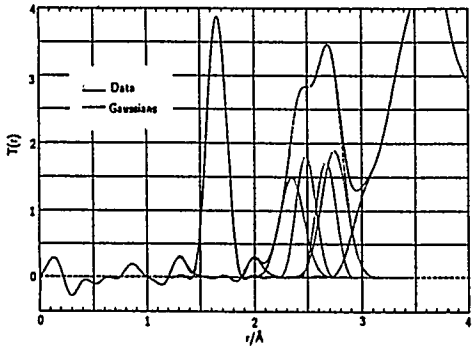


Fig. 3:T(r) of Ag_2SeO_4

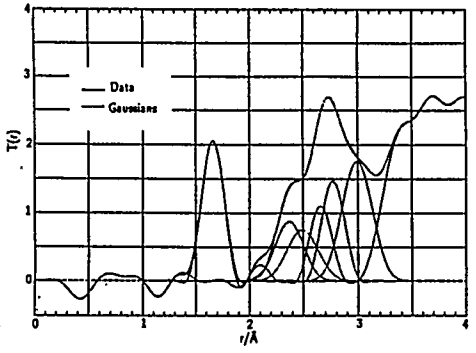


Fig. 4:T(r) of $0.54\,(AgI)_2 \cdot 0.46\,Ag_2SeO_4$

The atomic distances and coordination numbers that can be deduced from these fits are: i) in Ag_2SeO_4 Se–O: 1.65 Å (1 Se by 4 O), Ag–O: 2.35 Å (1 Ag by 2 O), 2.48 Å (1 Ag by 2 O), 2.67 Å (1 Ag by 2 O), O–O: 2.74 Å (1 O by 3 O); ii) in the glass forming system $x(AgI)_2 \cdot (1-x)Ag_2SeO_4$: Se–O: 1.66 Å in all glasses, 1.65 Å in the partly crystallized state, 1.67 Å in the melt. All coordination numbers of the SeO_4^{2-} units are the same as in Ag_2SeO_4 (tetrahedrons). All Ag–O distances are approximately the same as in silver selenate (±0.03 Å). An additional Gaussian which is assigned to Ag–I distances: 3.2 Å (1 I by 5 to 6 Ag) is needed to fit the glass data.

The following conclusions can be drawn: the glass structure can formally be constructed from the Ag_2SeO_4 structure by replacing x SeO_4^{2-} ions by 2x iodide ions. One half of the introduced iodide ions takes the vacant SeO_4^{2-} sites (the ionic radius of I^- (2.2 Å) is very similar to the "radius" of SeO_4^{2-} (2.4 Å)), the other half of the iodide ions enters vacant sites of the face–centered orthorhombic lattice. (That are those sites corresponding to tetrahedral vacancies in a face–centered cubic lattice. In c–Ag_2SeO_4 one half of these sites is occupied by selenate ions, the other half is vacant). By including the iodide ions into the lattice, it gets distorted, the long range order is lost, but the short range order is kept. Although iodide ions might be involved in the formation of medium range order that causes the peak in the structure factor at very low Q, there is no hint of formation of a biphasic structure with AgI clusters.

INSTRUMENT USED: HRMECS and GLAD	DATE OF REPORT: June 20, 1993	EXPERIMENT NO:

TITLE: **Neutron-scattering studies of Yb-bearing silicate glasses**

AUTHORS AND AFFILIATIONS:
A. J. G. Ellison, C.-K. Loong and J. Wagner, Argonne National Lab.

DATES OF EXPERIMENT: Feb 1993

CHECK ALL APPLICABLE BOXES:

- [ ] APPROVED BY PROGRAM COMMITTEE
- [X] INSTRUMENT SCIENTIST ALLOCATION
- [ ] DO NOT PUBLISH
- [ ] PROPRIETARY RESEARCH
- [ ] PRT ALLOCATION

EXPERIMENTAL REPORT (or Abstract of Publication)

Abstract

The static and dynamic magnetic response of the Yb^{3+} ions in $2Na_2O{\cdot}Yb_2O_3{\cdot}6SiO_2$ glass and the isochemical crystalline silicate $Na_3YbSi_3O_9$ has been studied by neutron diffraction, inelastic magnetic-scattering, and magnetic susceptibility measurements. The rare earth sites in the glass have an average coordination number of 5.6 ± 0.5 and give a mean rare earth-oxygen bond length of 2.23 Å; average Si-O and O-O coordination numbers and bond distances are comparable to those in vitreous SiO_2. The magnetic excitation spectrum of the $Na_3YbSi_3O_9$ material was analyzed by a crystal-field model using a method of descending symmetry. The magnetic susceptibility and the excitation spectrum of the Yb glasses can be described by a distribution of ligand-field effects on the Yb^{3+} ions that are similar to the nominal crystal field in crystalline $Na_3YbSi_3O_9$.

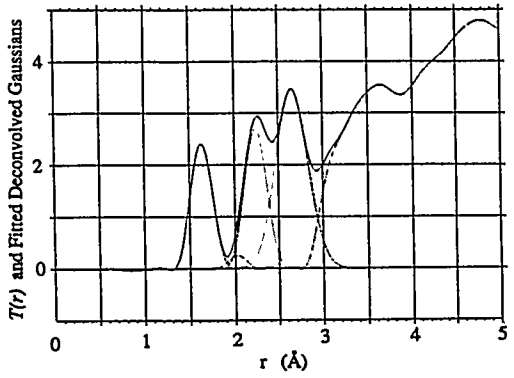


Figure 1. The total distribution function $T(r)$ of $2Na_2O{\cdot}Yb_2O_3{\cdot}6SiO_2$ glass. The peaks at 1.63, 2.24, and 2.65 Å correspond to the Si-O, Yb-O, and O-O nearest-neighbor distances, respectively. From the areas of the Si-O and Yb-O peaks we obtain average coordination numbers of 3.85 and 6.1 for Si and Yb, respectively.

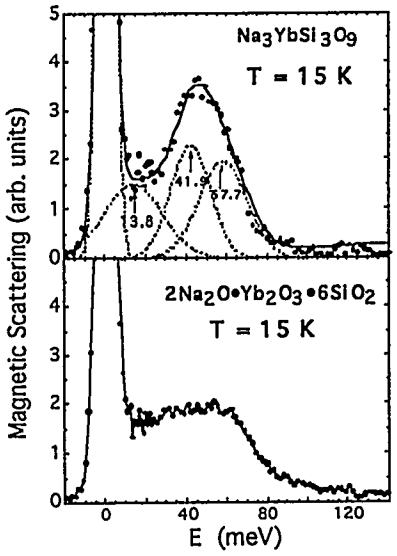


Figure Upper panel: The magnetic excitation spectrum of $Na_3YbSi_3O_9$ (circles) and a fit to the data (solid line) by a sum of four Gaussian functions centered at 0, 13.8, 41.9, and 57.5 meV denoted by the dotted lines. Lower panel: The magnetic excitation spectrum of the $2Na_2O{\cdot}Yb_2O_3{\cdot}6SiO_2$ glass (circles). The line is a guide to the eye.

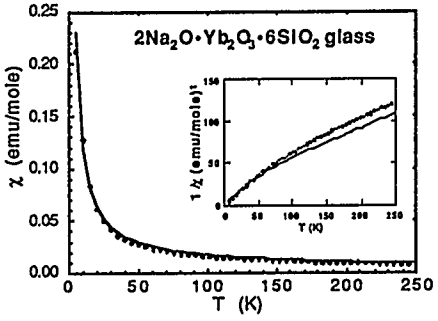


Figure 3. The measured paramagnetic susceptibility and the inverse susceptibility (inset) of the $2Na_2O{\cdot}Yb_2O_3{\cdot}6SiO_2$ glass (circles). The solid lines represent the calculated susceptibilities obtained from the crystal-field model using the nominal crystal-field parameters for crystalline $Na_3YbSi_3O_9$.

INSTRUMENT USED:	DATE OF REPORT:	EXPERIMENT NO.:
GLAD	December 20, 1995	2025

TITLE: Structural Study of the Liquid Alloy $CeCu_6$

AUTHORS AND AFFILIATIONS:
H.S. Schnyders and J.B. VanZytveld, Physics Dept., Calvin College, Grand Rapids, MI 49546

DATES OF EXPERIMENT:
September 20-22, 1995

CHECK ALL APPLICABLE BOXES:

- [x] APPROVED BY PROGRAM COMMITTEE
- [ ] INSTRUMENT SCIENTIST ALLOCATION
- [ ] DO NOT PUBLISH
- [ ] PROPRIETARY RESEARCH
- [ ] PRT ALLOCATION

EXPERIMENTAL REPORT (or Abstract of Publication)

We have studied the structure of liquid $CeCu_6$ on the GLAD apparatus at the IPNS at Argonne National Laboratory. A modification of the existing vacuum system enabled us to run the Howe vanadium furnace at 975 C, 37 degrees above the melting temperature of the alloy. The sample was contained in a cylindrical vanadium tube. A straight-forward analysis produced S(Q), and subsequently the radial distribution function N(r). S(Q) showed what we believe to be a significant pre-peak, which appears to be indicative of intermediate range order in the liquid. N(r) was decomposed via gaussian fitting to yield two peaks at r=2.5A and r=3.1A, of coordination numbers 3.58 and 5.56 respectively. The peak positions are very close to the Cu-Cu and Cu-Ce distances in the crystalline solid, and we also identify our peaks with these respective atom pairs. No Ce-Ce coordination was detected in the liquid; interestingly, the Ce first nearest neighbor shell of the crystal also contains no Ce atoms.

Our consideration of these similarities continues, as we believe it to hold the key to the negative temperature coefficient of the resistivity in liquid $CeCu_6$. We expect to publish our completed work in the Journal of Physics: Condensed Matter.

Many thanks are due David Price and Ken Volin, whose help was essential to the completion of the experiment and the analysis.

EXPERIMENTAL REPORT (CONTD.)

INSTRUMENT USED: GLAD

DATE OF REPORT: 12/21/94

EXPERIMENT NO: #1628

TITLE:
Neutron Diffraction Investigation of Non-Ideal Binary Liquid Mixtures

AUTHORS AND AFFILIATIONS:
G.C. Straty, B.D. Butler, H.J.M. Hanley
National Institute of Standards and Technology, Boulder Co. 80303

DATES OF EXPERIMENT:
9/23/94 - 9/27/94

APPROVED BY PROGRAM COMMITTEE

We have performed a series of neutron diffraction measurements on mixtures of cyclohexane and dodecane. The goal is to extract partial intermolecular structure factors which will yield insight into the origins of mixture excess properties. Contrast variation, where deuterium is substituted for hydrogen in some samples, was employed to make it possible to separate the total measured structure amplitude, $S(q)$, into its component parts $h_{CC}(q)$, $h_{DD}(q)$, and $h_{DC}(q)$, where the $h(q)$ represent structure functions due to intermolecular hydrogen-hydrogen pair correlations between the cyclohexane (C) and dodecane (D) molecules. It is hoped that these partial structure factors, and the radial distribution functions derived from them, will lead to a better understanding of the origins of the non-ideal mixing behavior of hydrocarbon liquids. While similar measurements have been performed on pure liquids [1-3] this is the first report of a neutron diffraction isotopic substitution (NDIS) measurement of a fluid mixture.

A mixture of cyclohexane and dodecane was chosen because these two molecules differ substantially in both size and conformation. The components were also readily available and their excess properties, such as excess volume, enthalpy, etc., are known. A series of experiments on both the pure liquids and mixtures were made using the GLAD instrument at IPNS. Measurements were made on the following samples:

(1) 100% C_6H_{12} (2) 100% C_6D_{12} (3) 50% C_6H_{12} 50% C_6D_{12}

(4) 100% $C_{12}H_{26}$ (5) 100% $C_{12}D_{26}$

(6) 50% C_6D_{12} 50% $C_{12}D_{26}$ (7) 50% C_6D_{12} 50% $C_{12}H_{26}$ (8) 50% C_6H_{12} 50% $C_{12}D_{26}$

Measurements were also made of the background scattering, scattering from an empty sample holder, and a vanadium standard. Samples were contained in cylindrical vanadium cells and data were collected for approximately 8 hrs per sample. The total neutron path length through the liquid was 1 mm.

Data analysis is currently in progress. Attempts are being made to first verify that the affect of isotopic substitution on ideal mixing of the deuterated and protonated variants of the same species (cyclohexane) are small by comparing derived structure functions of the samples (1) - (3). Second, we will attempt to extract the partial structure factors of each mixture component. In principle, this is possible from the data at the three different contrast ratios (6) - (8). If successful the structure factors will be inverted to obtain intermolecular pair correlation functions yielding clues to the origin of the mixture excess properties.

This work was partially funded by a grant from the Division of Chemical Sciences, Office of Basic Energy Research, U.S. Department of Energy.

[1] Narten, A.H., Habenschuss, A., Honnell, K.G., McCoy, J.D., Curro, J.G., and Schweizer, K.S. *J. Chem. Soc. Faraday Trans.* **88**, 1 (1992).

[2] Tromp, R.H., Postorino, P., Neilson, G.W., Ricci, M.A., and Soper, A.K. *J. Chem. Phys.* **101**, 6210 (1994)

[3] Londono, J.D., Annis, B.K., Turner, J.Z., and Soper, A.K. *J. Chem. Phys.* **101**, 7868 (1994)

INSTRUMENT USED:	DATE OF REPORT:	EXPERIMENT NO:
GLAD	June 16, 1995	discretionary

TITLE: **THE STRUCTURE OF A LEAD-INDIUM PHOSPHATE GLASS**

AUTHORS AND AFFILIATIONS:
K. SUZUYA*, D. L. PRICE*, C.-K. LOONG*, B. C. SALES**, AND L. A. BOATNER**
*Argonne National Laboratory, Argonne, IL 60439
**Oak Ridge National Laboratory, Oak Ridge, TN 37831

DATES OF EXPERIMENT: Sept. 1994

CHECK ALL APPLICABLE BOXES:

- [ ] APPROVED BY PROGRAM COMMITTEE
- [X] INSTRUMENT SCIENTIST ALLOCATION
- [ ] DO NOT PUBLISH
- [ ] PROPRIETARY RESEARCH
- [ ] PRT ALLOCATION

EXPERIMENTAL REPORT (or Abstract of Publication)

Lead-indium phosphate glasses exhibit a number of useful properties such as a high index-of-refraction, low preparation temperature and melt viscosity, and good chemical durability. The structure of such a glass (composition in wt. %: 65 PbO, 29 P_2O_5, 6 In_2O_3) has been investigated by total neutron scattering using the GLAD diffractometer at Argonne's spallation neutron source IPNS. Peaks corresponding to the P-O, Pb-O/In-O, and O-O pairs were observed in the radial distribution function. The short-range structure in the glass, in terms of average coordination numbers and bond distances, is compared with those of a pure P_2O_5 glass and with the crystal structure of lead pyrophosphate, $Pb_2P_2O_7$. Unlike silicate glasses in which the SiO_4 tetrahedra form a 3-dimensional network, the PO_4 tetrahedra in phosphate glasses form a chain-like structure. The structural modification by the lead cations in phosphate glasses appears to occur mainly in the medium range affecting the lengths and connectivity of the chain-like structure.

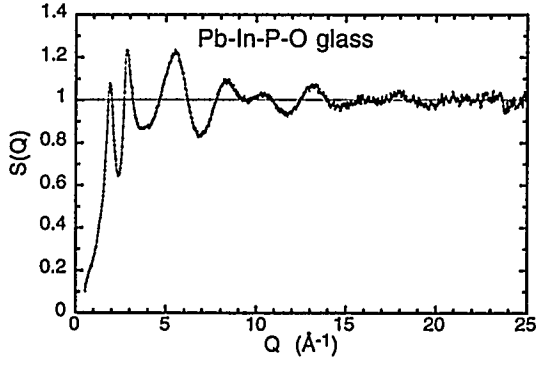


Figure 1. The structure factor of Pb-In-P-O glass.

EXPERIMENTAL REPORT (CONTD.)

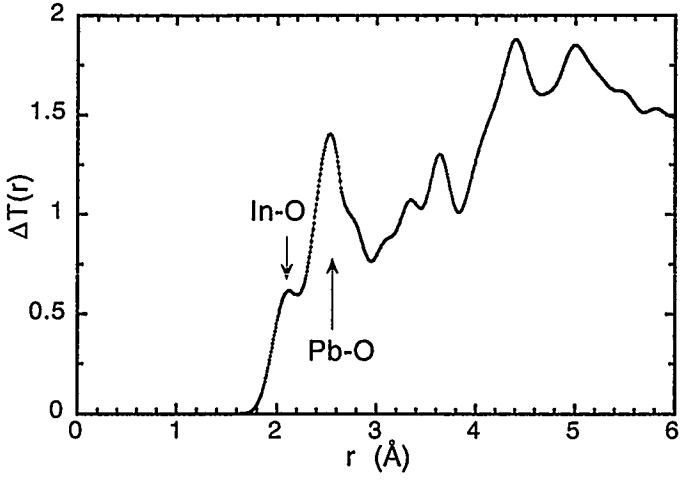


Figure 2. The residual $T(r)$ obtained by subtracting the fitted Gaussian functions for $T(r)$of the P-O glass from the $T(r)$ of the Pb-In-P-O glass. Small oscillations at $r < 2$ Å due to truncation errors in the Fourier transformations were ignored.

The results from the above analysis are consistent with the expected structure estimated from the diffraction data of a $(PbO)_{59}(P_2O_5)_{41}$ glass and the $Pb_2P_2O_7$ crystal. In the lead-phosphate glass, a "two-peak" structure, which was attributed to P-O and Pb-O + O-O spatial correlation at ~1.54 and 2.52 Å, respectively, was observed in the $T(r)$ curve. According to the crystal structure of $Pb_2P_2O_7$ the shortest bond distances for the P-O, Pb-O and O-O atomic pairs vary between 1.49 to 1.65, 2.43 to 3.35, and 2.46 to 2.60 Å, respectively. The qualitative agreement of the bond distances among these materials supports the notion that, within a short range comparable to nearest-neighbor distances, the spatial correlations between atoms in the glassy and crystalline phases of lead-phosphate are similar. The combined neutron-diffraction data of pure v-P_2O_5, $(PbO)_{59}(P_2O_5)_{41}$, and Pb-In-P-O glasses, in conjunction with the liquid chromatographic results of lead phosphate glasses confirm that the major structural modification on the introduction of metal cations in phosphate glasses occurs in the medium range involving the PO_4 chains.

We thank K. J. Volin (Argonne National Laboratory) for his assistance in the diffraction experiment as well as Ken Takeuchi and Koichi Ui (Tokyo University of Science) for their help in preparing the lead-phosphate glass. Work performed at Argonne and Oak Ridge National Laboratory is supported by the U. S. DOE-BES under contract Nos. W-31-109-ENG-38 and DE-AC05-84OR21400, respectively.

INSTRUMENT USED: GLAD	DATE OF REPORT: Aug 29, 95	EXPERIMENT NO.: 2011

TITLE: LOCAL STRUCTURE OF LITHIUM – CARBON COMPOUNDS

AUTHORS AND AFFILIATIONS: PING ZHOU AND J. E. FISCHER, DEPT. OF MAT. SCIENCE, U. PENNSYLVANIA

DATES OF EXPERIMENT: 6/17 to 6/21/95

CHECK ALL APPLICABLE BOXES:

- ☑ APPROVED BY PROGRAM COMMITTEE
- ☐ INSTRUMENT SCIENTIST ALLOCATION
- ☐ DO NOT PUBLISH
- ☐ PROPRIETARY RESEARCH
- ☐ PRT ALLOCATION

EXPERIMENTAL REPORT (or Abstract of Publication)

The goal of experiment (2011) on GLAD is to solve the local structure of disordered carbons produced from different organic precursors before and after Li doping. As planned, the pristine materials were measured between June 17 to 21, 95.

Graphite powder (Fisher) was measured first to calibrate the instrument and test the data analysis procedures. Its Radial Distribution Function (RDF) is plotted in Fig.1 (dotted curve). The data in Fig.1 are entirely consistent with the known graphite structure.

High hydrogen concentration (1-5 a.t.percent) in most of our carbon samples posed a severe problem due to the incoherent scattering (quasi-free and/or bonded). One observation is that the background is not only extremely large but also exhibits a large "droop" vs. Q in the higher angle detectors (Fig.2). The degree of the droop seems to correlate to the H concentration in the sample. A special trip to IPNS will be made in Sept. 95 to work with David Price on software to correct for this problem. This will hopefully consist of modifying an ISIS package to be compatible with GLAD format and instrument parameters.

Of the six carbons measured, one produced a satisfactory result due to its relatively low H level (0.1 a.t. percent). Its RDF is displayed as the solid curve in Fig.1 . Data sets from the other samples with greater H content will hopefully be salvaged by the aforementioned correction procedure. The pristine sample shown in Fig.1 (solid curve) is currently undergoing electrochemical doping and will be measured in its fully doped state during the upcoming run cycle.

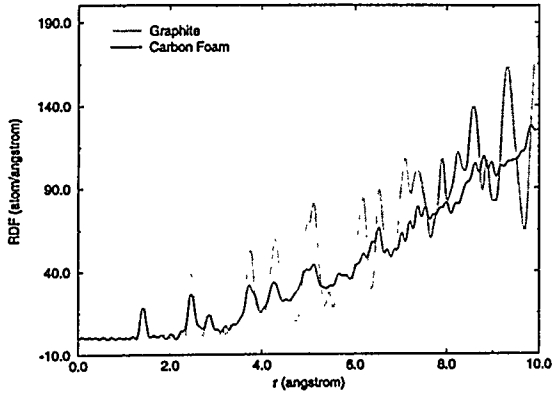


Fig.1 RDF of graphite powder(dotted curve) and a carbon foam (solid curve).

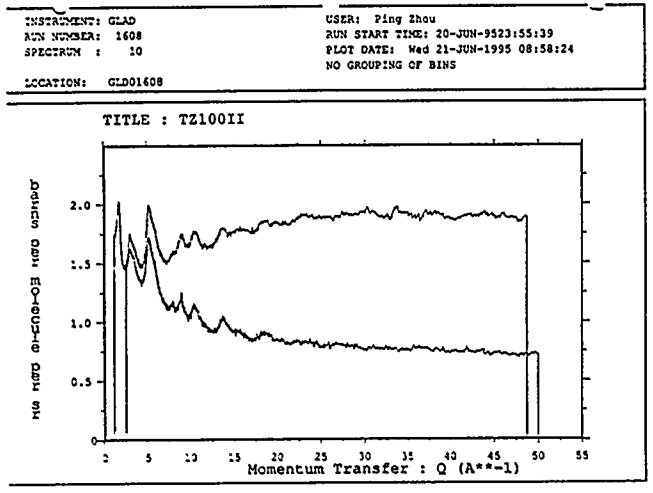


Fig.2. Diffraction data from detectors at 44 (top curve) and 90 degrees (bottom curve). The carbon sample contains 15 percent H.

INSTRUMENT USED: GLAD	DATE OF REPORT: FEB. 7, 96	EXPERIMENT NO.: 2155

TITLE: LOCAL STRUCTURE of LITHIUM-CARBON COMPOUNDS

AUTHORS AND AFFILIATIONS: PING ZHOU AND J.E. FISCHER MSE DEPT. U. PENNSYLVANIA

DATES OF EXPERIMENT: Nov. 8 - 13, 95

CHECK ALL APPLICABLE BOXES:

- [x] APPROVED BY PROGRAM COMMITTEE
- [ ] INSTRUMENT SCIENTIST ALLOCATION
- [ ] DO NOT PUBLISH
- [ ] PROPRIETARY RESEARCH
- [ ] PRT ALLOCATION

EXPERIMENTAL REPORT (or Abstract of Publication)

More on Experiment #2011

As mentioned in the previous report, a subroutine (SUBSELFGLD) was installed to solve the background problem in samples with high hydrogen content. The procedure involves estimating the self scattering by a Chebychev polynomial fit to the structure factor, made consistent with Krogh-Moe normalization (essentially, the requirement that RDF be zero below certain r) through a maximum-entropy method. In Figure 1 we plot the RDF of such a sample with H/C=0.15. A Lorch weighting factor was used to remove the spurious features due to truncation at 30Å^{-1}. The first peak is found at 1.44Å, very close to the C-C distance in graphite (1.42Å). The coordination number (area under the 1st peak) and bond angle (from the 2nd peak position at 2.47Å) are 3.1 and 120 degrees respectively, consistent with sp^2 bonding. The so-called intra-hexagonal peak is found at 2.85Å, double the bond length, a signature of planar hexagons. These results indicate that this particular material is remarkably similar to graphite on the length scale < 1 nanometer, and that reliable information can be extracted from samples containing a lot of H. The decrease in peak intensities relative to graphite is due to small particle sizes.

Experiment #2155

Experiment #2155 on GLAD was the continuation of #2011. A standard LiC_6 powder was measured. The averaged RDF is plotted in Figure 2 (solid curve) and compared with that of graphite (dotted curve). Two effects are observed due to lithium insertion between graphite layers: (1) elongation of C-C distance by 0.012Å, an effect well-established from traditional diffraction, and (2) a change in carbon layer stacking from alternating ABAB... to AA... The first effect is due to the charge transfer from the cations. By comparison with traditional diffraction results on LiC_6, we find that the C-C bond elongation observed here corresponds to Li_xC_6 with $x \sim 0.9$. This is consistent with the (independent) observation of a small amount of stage-II LiC_{12} in this sample. The second effect is manifested in the large differences in RDF at higher r. A negative peak is observed at 2.36Åand identified with the Li-C correlation, a characteristic of Li-C pair due to the negative neutron scattering length of Lithium. These results give us confidence that valuable information will be obtained from our Li-intercalated amorphous carbons.

We measured two lithiated samples prepared from carbon starting material containing 4 at.% hydrogen. These were doped electrochemically in 1M $LiClO_4$ and $LiPF_6$ solutions. The apparent hydrogen content increased dramatically after doping, no doubt resulting from formation of the ubiquitous "solid-electrolyte interphase" (reaction products of decomposed electrolyte solvent, Li metal etc..). This was quite evident from the huge increase in incoherent background (see report on #2011). Detailed analysis will require knowledge of the exact chemical composition, a task currently underway using a combination of elemental analysis, prompt gamma analysis and the newly developed subroutine SUBSELFGLD.

EXPERIMENTAL REPORT (CONTD.)

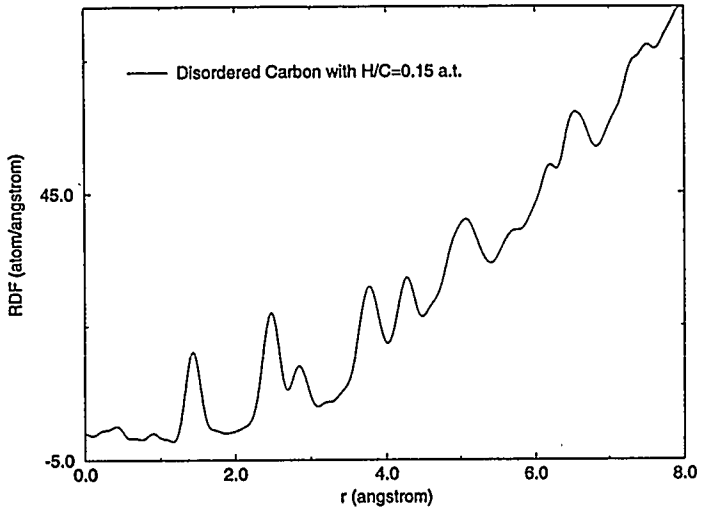


Figure 1. RDF of a carbon with H/C=0.15 a.t.

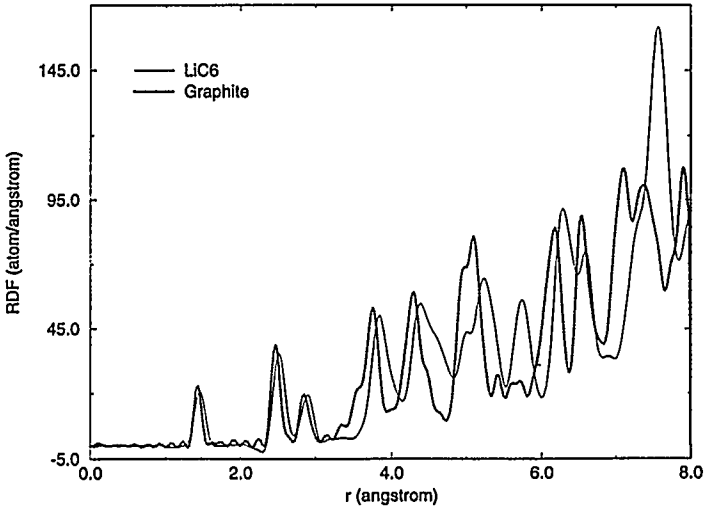


Figure 2. RDF's of LiC_6 (solid curve) and graphite (dotted curve).

INSTRUMENT USED: GLAD	DATE OF REPORT: 11/10/95	EXPERIMENT NO.: 2154

TITLE: *Neutron Diffraction Study of the Structural Changes in Tellurite Glasses upon Modification with Sodium Oxide*

AUTHORS AND AFFILIATIONS: J. W. Zwanziger and S. L. Tagg, Dept. of Chemistry, Indiana University; D. L. Price and M.-L. Saboungi, ANL

DATES OF EXPERIMENT: 10/26/95--10/31/95

CHECK ALL APPLICABLE BOXES:

- [X] APPROVED BY PROGRAM COMMITTEE
- [ ] PROPRIETARY RESEARCH
- [ ] INSTRUMENT SCIENTIST ALLOCATION
- [ ] PRT LOCATION
- [ ] DO NOT PUBLISH

EXPERIMENTAL REPORT (or Abstract of Publication)

Glasses based on tellurium dioxide are of interest due to their anomalous glass forming behavior (1) and their technological applications (2,3). We are studying the sodium tellurite system, $(Na_2O)_x(TeO_2)_{1-x}$, where glasses can be readily made between 10 and 30 mol-% sodium oxide. The stability of sodium tellurite glasses has been suggested to be dependent on modifier (Na_2O) concentration, with glasses most resistant to devitrification formed near the 20 mol-% crystalline composition, $Na_2Te_4O_9$. One possible explanation for this glass stability requires singly coordinated sodium cations (4). Our nuclear magnetic resonance data, however, indicate that the sodium cations in the glasses are between five and six coordinate (5,6). Since we have been able to learn a great deal about the modifier environment through NMR studies, we are now using neutron diffraction experiments to provide insight into how the tellurite matrix accommodates the addition of the modifier.

The glass samples, with compositions x = 0.12, 0.18, 0.20, 0.22, 0.28, were prepared by melting the stochiometric amount of tellurium dioxide and sodium carbonate at 750°C for approximately eight minutes. The liquid was then poured on to a stainless steel plate forming a brittle solid easily ground for analysis. Representative samples were confirmed to be amorphous by x-ray diffraction. The sodium tetratellurite crystalline sample $Na_2Te_4O_9$ was grown following the methods published previously (7), whereas crystalline samples of α-TeO_2 and Na_2TeO_3 were purchased commercially.

We utilized the Glass, Liquid, and Amorphous Materials Diffractometer (GLAD) at the Intense Pulsed Neutron Source. The glass and crystalline samples were run in 1.1 cm and 0.65 cm vanadium containers, respectively, for between 10 and 15 hours. The data was corrected for scattering from both the vanadium container and the instrument background and was normalized to the scattering from a pure vanadium rod. The corrections, including those for multiple-scattering, absorption and self-scattering, were all done using the Genie/ATLAS codes modified for the GLAD instrument.

The raw data was grouped into 19 clusters, each corrected to ensure that the self scattering and total scattering were equivalent at high momentum transfer. Due to the tellurium absorption, we did not include data in the Faber-Ziman structure factor S(Q) with energy greater than 1 eV, i.e., only neutrons with wavelengths between 0.286 and 3.0 Å were included (Figure 1(a)). The structure factor was transformed into real space using the fast Fourier transform method.

We are currently analyzing the total radial distribution functions of the crystalline and glassy samples. We have performed a least-squares fit of the total distribution function T(R) using gaussian functions for glassy $Na_2Te_4O_9$. Our preliminary interpretation of T(R) indicates a correlation at 1.9 Å which we ascribe to an interaction between tellurium and oxygen (Figure 1(b)). This assignment agrees well with Te-O bond distances known from crystallographic studies. We believe that our data contains important structural information and we are fitting the total distribution functions of the remaining samples.

EXPERIMENTAL REPORT (CONTD.)

References:

(1) J. Heo, D. Lam, G. H. Sigel, Jr., E. A. Mendoza, and D. A. Hensley, *J. Am. Ceram. Soc.* 75, 277 (1992).
(2) E. M. Vogel, M. J. Weber and D. M. Krol, *Phys. Chem. Glasses* 32, 231 (1991).
(3) R. El-Mallawany, *J. Appl. Phys.* 72, 1774 (1992).
(4) M. Zhang, S. Mancini, W. Bresser, and P. Boolchand, *J. Non-Cryst. Solids* 151, 149 (1992).
(5) S. L. Tagg, R. E. Youngman, J. W. Zwanziger, *J. Phys. Chem.* 99, 5111 (1995).
(6) J. W. Zwanziger, S. L. Tagg, J. C. Huffman, *Science* 268, 1510 (1995).
(7) S. L. Tagg, J. C. Huffman, J. W. Zwanziger, *Chem. Mater.* 6, 1884 (1994).

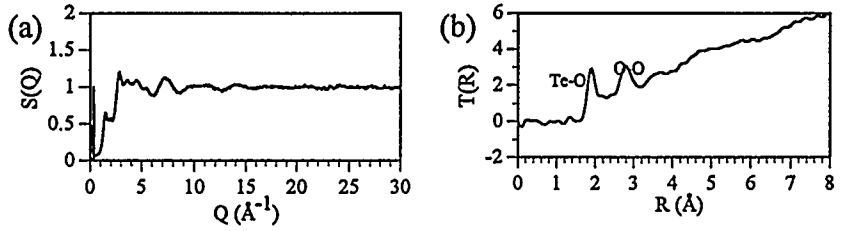


Figure 1: (a) Faber-Ziman structure factor S(Q) of glassy Na2Te4O9, obtained on the GLAD instrument at IPNS. (b) Total distribution function T(R), obtained from Fourier-transformation of S(Q). Preliminary assignments of the main peaks are indicated.

INSTRUMENT USED:	DATE OF REPORT:	EXPERIMENT NO.:
GPPD	February 8, 1990	1385

TITLE:
Determination of the Structure of Lithium Dialuminate, $^{7}LiAl_2(OD)_7 \cdot 2D_2O$

AUTHORS AND AFFILIATIONS:
J. Allen, J. Thiel and K. Poeppelmeier, Chemistry Dept. Northwestern Univ.

DATES OF EXPERIMENT: 11/08/90

☒ APPROVED BY PROGRAM COMMITTEE, OR

☐ PART OF INSTRUMENT SCIENTIST ALLOCATION

REPORT RECEIVED:

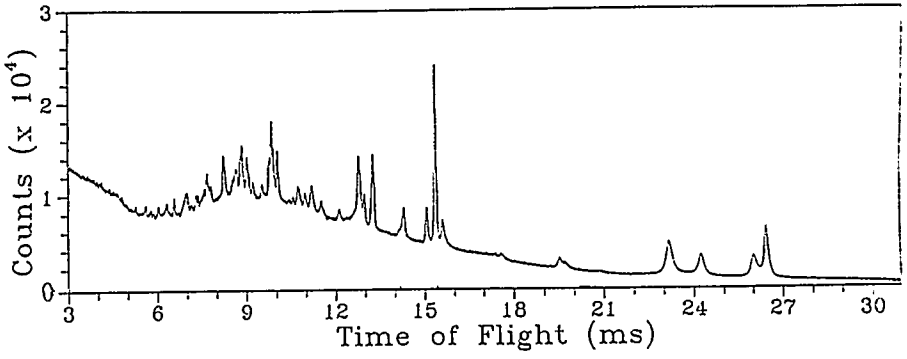
EXPERIMENTAL REPORT (or Abstract of Publication)

Lithium dialuminate was prepared in deuterated form and enriched in the lithium-7 isotope by reacting bayerite, $[Al(OD)_3]$, $^{7}Li(OD) \cdot D_2O$, and D_2O vapor.

X-ray Rietveld analysis of $LiAl_2(OH)_7 \cdot 2H_2O$ has led to a model which is similar to hydrotalcite, $[Mg_6Al_2(OH)_{16}]^{2+}(CO_3)^{2-} \cdot 4H_2O$, with dioctahedral sheets of bayerite converted to trioctahedral layers, $[LiAl_2(OH)_6]^{+}$, by the incorporation of lithium ion. A hydroxyl ion and two water molecules reside between the layers and are stabilized by hydrogen bonding. The analysis of the structure is complicated by a stacking disorder.

$^{7}LiAl_2(OD)_7 \cdot 2H_2O$ has been studied by neutron powder diffraction in order to refine the x-ray structural model by determining the distribution and chemical bonding of the lithium ion, hydroxide ion and water molecules. At this time, we are working toward the solution of this structure by using Rietveld refinement. The 148 degree data is attached.

EXPERIMENTAL REPORT (CONTD.)



INSTRUMENT USED:	DATE OF REPORT:	EXPERIMENT NO.:
GPPD	10/22/90	NSF - 20

TITLE: Determination of the Structure of the Perovskite-Related Compound La_2CuSnO_6

AUTHORS AND AFFILIATIONS: Mark T. Anderson and Kenneth R. Poeppelmeier
Department of Chemistry, Northwestern University

DATES OF EXPERIMENT: 7/26/90

☒ APPROVED BY PROGRAM COMMITTEE, OR

☐ PART OF INSTRUMENT SCIENTIST ALLOCATION

REPORT RECEIVED:

EXPERIMENTAL REPORT (or Abstract of Publication)

The structure of La_2CuSnO_6 was determined by Rietveld refinement of neutron powder diffraction data collected at room temperature. The structure was solved in space group $P2_1/m$ with a = 8.5102(1), b = 7.8147(1), c = 7.8171(1) Å, and β = 91.1521(7)° (Z = 4). The structure is best described as a 2 x 2 x 2 distorted perovskite with tilted oxygen polyhedra (nearly octahedral) around the Cu and Sn atoms with a layered arrangement of B cations, which is rare for perovskites that are stoichiometric in oxygen (we have yet to find other examples). The B cations have ordered to form $CuO_{4/2}$ and $SnO_{4/2}$ layers. The lanthanum atoms are displaced toward the copper-oxygen layers. The structural aspects of the compound are similar to high temperature superconductors. The magnetic susceptibility versus temperature profile for the compound indicates it is not a superconductor above 5 K. The compound appears to be a spin glass with a glass transition temperature $T_g \approx 130$ K.

As can be seen from the atomic coordinates in Table I, the oxygen atoms are significantly displaced from the ideal perovskite sites. The small contibution to the overall scattering of the oxygen atoms along with the absence of a single crystal made neutron diffraction a necessity to accurately determine the structure of La_2CuSnO_6. The excellent resolution of Bragg peaks and sensitivity of neutron diffraction to oxygen atom positions (b_O = 5.80, b_{La} = 8.24, b_{Cu} = 7.72, and b_{Sn} = 6.23 fm) compared to X-ray diffraction allowed unambiguous assignment of the indicies of about 40 diffraction peaks and the determination of the correct space group. The refinement of the structure proceeded smoothly to R_{wp} = 2.77% with R_{exp} = 1.84%.

Table I. Crystallographic Data for La_2CuSnO_6[a]

Atom	Site	x/a (σx)	y/b (σy)	z/c (σz)	B(Å²)(σB)	Occupancy
La1	2e	0.2118(3)	1/4	0.2792(4)	0.56(5)	1
La2	2e	0.1978(3)	1/4	0.7711(3)	0.50(4)	1
La3	2e	0.7574(2)	1/4	0.7855(3)	0.42(5)	1
La4	2e	0.7715(3)	1/4	0.2761(4)	0.81(5)	1
Cu1	2a	0	0	0	0.45(5)	1
Cu2	2c	0	0	1/2	0.43(5)	1
Sn1	2b	1/2	0	0	0.31(5)	1
Sn2	2d	1/2	0	1/2	0.24(6)	1
O1	4f	0.0363(2)	-0.0329(3)	0.2498(3)	0.44(4)	1
O2	4f	0.2699(2)	-0.0505(3)	-0.0476(3)	0.53(4)	1
O3	4f	0.2737(2)	0.0509(3)	0.5560(3)	0.65(4)	1
O4	4f	0.4298(2)	0.0450(3)	0.2495(3)	0.68(4)	1
O5	2e	0.0274(4)	1/4	0.0337(5)	0.64(6)	1
O6	2e	0.4599(4)	1/4	-0.0757(4)	0.73(6)	1
O7	2e	0.5826(4)	1/4	0.5237(4)	0.32(5)	1
O8	2e	-0.0157(4)	1/4	0.4706(4)	0.21(5)	1

[a]Space group $P2_1/m$ with a = 8.5102(1) Å, b = 7.8147(1) Å, c = 7.8171(1) Å, and β = 91.1521(7)°, Z = 4.

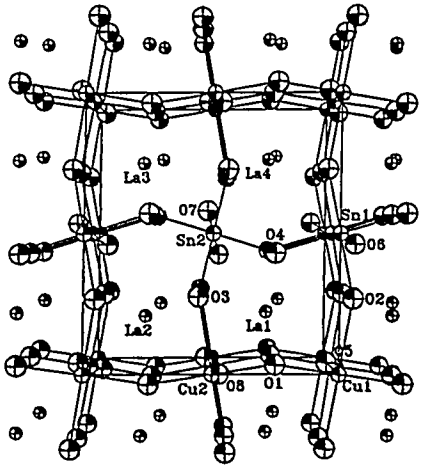


Figure 1. ORTEP of La_2CuSnO_6. The atom sizes are arbitrary. The view is down the [010] axis.

INSTRUMENT USED:	DATE OF REPORT:	EXPERIMENT NO.:
GPPD	9-9-91	NSF-27

TITLE: Structure of Nd_2CuTiO_6 and Er_2CuTiO_6

AUTHORS AND AFFILIATIONS: M. T. Anderson and K. R. Poeppelmeier
Department of Chemistry and the Science and Technology Center for Superconductivity
Northwestern University, Evanston, IL 60208-3113

DATES OF EXPERIMENT: May 17-18, 1991

☒ APPROVED BY PROGRAM COMMITTEE, OR

☐ PART OF INSTRUMENT SCIENTIST ALLOCATION

REPORT RECEIVED:

EXPERIMENTAL REPORT (or Abstract of Publication)

All superconductors with critical transition temperatures above 35 kelvins are layered cuprates. The synthesis of new cuprates and the investigation of their crystal chemistry is one of our main research thrusts. We have synthesized the series Ln_2CuTiO_6 (Ln = La, Nd, Sm, Eu, Gd, Tb, Dy, Ho, Er, Tm, Yb, Lu). As the series progresses from terbium to dysprosium, there is a structural change. We solved the structure of the neodymium and erbium compounds. To narrow the possible space groups, the peak positions in the neutron diffraction pattern were fit and the unit cell and systematic absences were determined. In both compounds the copper and titanium are randomly distributed. The materials thus lack copper-oxygen planes, which seem essential for superconductivity.

Nd_2CuTiO_6 is isostructural with $GdFeO_3$ (Table I). The copper and titanium form a corner-shared network of $(Cu,Ti)O_6$ octahedra. The octahedra tilt to reduce the neodymium atom coordination number form 12, found in an ideal perovskite, to 8 (3 + 2 + 3 configuration). The material is a semiconductor.

Er_2CuTiO_6 is isostructural with $YMnO_3$ (Table I). The copper and titanium are in trigonal bipyramidal coordination and form hexagonal $(Cu,Ti)O_{3/3}$ layers. The erbium cations are 7-coordinate and are in a capped trigonal antiprisms. The cation coordination numbers decrease with respect to the neodymium compound to provide favorable A—O bond distances for the smaller erbium cation. The material is green and is assumed to be an insulator.

EXPERIMENTAL REPORT (CONTD.)

Table I. Crystallographic Data for Nd_2CuTiO_6[a]

Atom	Site	x/a (σx)	y/b (σy)	z/c (σz)	B(Å²)(σB)	Occupancy
Nd	4c	-0.0110(3)	0.0609(3)	1/4	0.44(5)	1
Cu/Ti	4b	0	1/2	0	0.86(9)	1
O1	4c	0.0890(4)	0.4758(4)	1/4	0.38(6)	1
O2	8d	0.6983(3)	0.3031(3)	0.0462(2)	1.16(5)	1

[a]Space group *Pbnm* with a = 5.478 (2), b = 5.728 (2), c = 7.649 (2) Å, and Z = 2.

Table II. Crystallographic Data for Er_2CuTiO_6[a]

Atom	Site	x/a (σx)	y/b	z/c (σz)	B(Å²)(σB)	Occupancy
Er1	2a	0	0	0.2653(8)	0.69(7)	1
Er2	4b	1/3	2/3	0.2358(7)	0.55(4)	1
Cu/Ti	6c	0.3713(9)	0	0	0.24(8)	1
O1	6c	0.3167(6)	0	0.1677(8)	0.38(6)	1
O2	6c	0.6513(8)	0	0.3396(9)	1.09(7)	1
O3	2a	0	0	0.4822(15)	2.8(2)	1
O4	4b	1/3	2/3	0.0081(11)	3.5(1)	1

[a]Space group $P6_3cm$ with a = 6.1445 (5), c = 11.4980 (6) Å, and Z = 2.

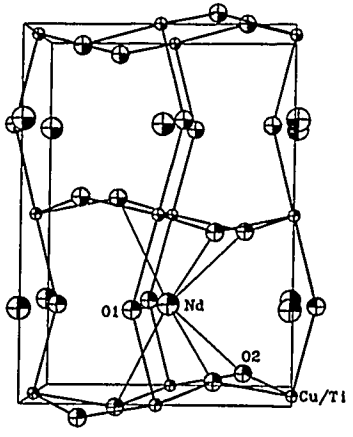


Figure 1. Structure of Nd_2CuTiO_6 viewed down the b axis.

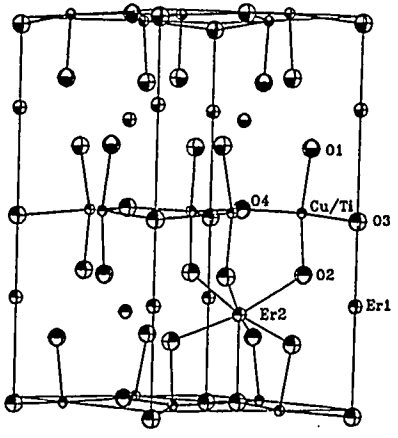


Figure 2. Structure of Er_2CuTiO_6.

INSTRUMENT USED:	DATE OF REPORT:	EXPERIMENT NO.:
GPPD	8/8/90	1219

TITLE:

Irradiation-Induced Amorphization of U_3Si

AUTHORS AND AFFILIATIONS:

R.C.Birtcher, G.L. Hofman, M.H. Mueller, J.W. Richardson, Jr., ANL

DATES OF EXPERIMENT: April, 1990 - October, 1990

☒ APPROVED BY PROGRAM COMMITTEE, OR

☐ PART OF INSTRUMENT SCIENTIST ALLOCATION

REPORT RECEIVED:

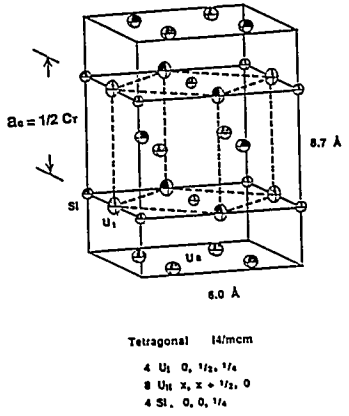
EXPERIMENTAL REPORT (or Abstract of Publication)

Uranium silicides have been considered for use as reactor fuels in high power as well as low enrichment applications. However, U_3Si was found to become amorphous under irradiation [1] and to become mechanically unstable to rapid growth by plastic flow [2,3]. U_3Si_2 appears to be stable against amorphization at low displacement rates, but the extent of this stability is uncertain. The present experiment follows in detail the changes in the crystal structures of U_3Si and U_3Si_2 introduced by neutron bombardment and subsequent uranium fission at room temperature. Neutron irradiations were performed at IPNS in the room temperature facility located adjacent to the neutron source [4]. In these specimens, damage was produced primarily by uranium fission in a manner identical to damage production in operating nuclear reactor fuel. The irradiations were performed in small steps (^{235}U burn-up < 3×10^{-8}) in order to closely follow the structural changes. After each irradiation and appropriate cool-down, diffraction data collected on GPPD were analyzed using Rietveld profile refinement.

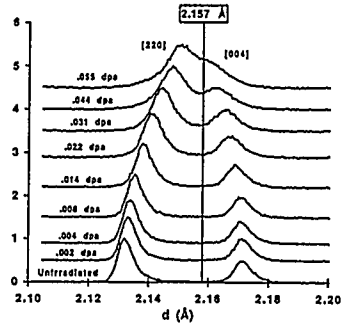
Results for U_3Si will be given in this report, while those for U_3Si_2 can be found in the accompanying report.

The U_3Si specimen used in this experiment contained precipitates of U_3Si_2 (< 15 volume %) and the uranium oxides UO_2 and UO (< 5 volume %) introduced during vacuum annealing.

Un-irradiated U_3Si is tetragonal, I4/mcm, $a_t = 6.0358(1)$, $c_t = 8.6925(1)$ Å, with atoms at locations shown in Figure 1. The base layer (z=0) contains U_{II} atoms only, the next layer (z=1/4) is 1/2 U_I and 1/2 Si, and the sequence repeats. The layer at z=1/2 (again U_{II} only) is rotated slightly relative to the base layer. If the U_{II} atoms are shifted to x=1/4, thus bringing the z=0 and z=1/2 layers into alignment and the axial ratio (c/a) is simultaneously reduced to √2, U_3Si then possesses the cubic Cu_3Au type structure ($a_c = a_t/\sqrt{2} = c_t/2$) shown by the dashed lines in Figure 1. This transformation is known to occur upon heating to 1038K [5], and is expected to occur under the above irradiation conditions. Continued irradiation should then drive the material amorphous.



The progress of the tetragonal-to-cubic (t→c) transformation was followed in two ways: (1) t→c lattice symmetry transformation (using refined lattice parameters, i.e., peak positions) and (2) t→c atomic structure transformation (using refined x-parameter for U_{II}; obtained from Rietveld analysis of the peak intensities). After 8 irradiation cycles (153×10^{18} protons or 0.05 displacements per U atom), the a- and c-axis changes were +0.8% and -0.4%, respectively. Extrapolation to cubic lattice symmetry ($a_t/\sqrt{2} = c_t/2$) results in an estimated transformation dose of 164×10^{18} or 0.070 dpa. Meanwhile, extrapolation of the calculated distance between the refined U_{II} position at each dose, and the idealized Cu_3Au position (1/4,3/4,0) (cubic atomic symmetry) results in an estimated dose of 0.065. The estimated amorphization dose (from ion irradiations) is 0.07 dpa, in close agreement with these transformation doses, suggesting that the high temperature cubic phase is unstable and will transform to the amorphous phase. In fact, Figure 2 shows the development of diffuse scattering between the $(220)_t$ and $(004)_t$ reflections long before the two peaks merge to become the $(002)_c$.



As the amorphization progresses, the crystallographic and amorphous forms can be studied simultaneously by combining conventional. Rietveld refinement of the crystallographic phases with Fourier-filtering analysis [6] of the non-crystalline scattering. This analysis will be described in future reports.

REFERENCES

1 D. G. Walker, J. Nucl. Mat. 37, 48 1970).
2 G. L. Hofman, J. Nucl. Mat. 140, 256 (1986).
3 R. C. Birtcher, C. W. Allen, L. E. Rehn and G. L. Hofman, J. Nucl. Mater. 152, 73 (1988).
4 R. C. Birtcher, T. H. Blewitt, M. A. Kirk, T. L. Scott, B. S. Brown and L. R. Greenwood, J. Nucl. Mater. 108 & 109, 3 (1982).
5 P. L. Blum, G.Silvestro and H. Vangoyan, C. R. Acad. Sci. 260, 5538 (1964).
6 J. W. Richardson, Jr. and J. Faber, Jr., Adv. X-ray anal. 29, 143 (1985).

INSTRUMENT USED:	DATE OF REPORT:	EXPERIMENT NO.:
GPPD	5 AUG 92	1494

TITLE:

Irradiation - Induced Amorphization of U_3Si and U_3Si_2

AUTHORS AND AFFILIATIONS:

R. C. Birtcher, M. H. Mueller and J. W. Richardson Jr. - ANL

DATES OF EXPERIMENT: Nov 91 - July 92

☒ APPROVED BY PROGRAM COMMITTEE, OR

☐ PART OF INSTRUMENT SCIENTIST ALLOCATION

REPORT RECEIVED:

EXPERIMENTAL REPORT (or Abstract of Publication)

NEUTRON IRRADIATED URANIUM SILICIDES STUDIED BY NEUTRON DIFFRACTION AND RIETVELD ANALYSIS

R. C. Birtcher, M. H. Mueller* and J. W. Richardson, Jr.
*Argonne National Laboratory, Argonne, IL 60439

The irradiation behavior of high-density uranium silicides has been a matter of interest to the nuclear industry for use in high power or low enrichment applications. Transmission electron microscopy studies have found that heavy ion bombardment renders U_3Si and U_3Si_2 amorphous at temperatures below about 250 C [1], and that U_3Si becomes mechanically unstable suffering rapid growth by plastic flow [2]. In this present work, crystallographic changes preceding amorphization by fission fragment damage have been studied by high-resolution neutron diffraction as a function of damage produced by uranium fission at room temperature. Initially, both silicides had tetragonal crystal structures. Crystallographic and amorphous phases were studied simultaneously by combining conventional Rietveld refinement of the crystallographic phases with Fourier-filtering analysis of the non-crystalline scattering component [3].

For U_3Si, damage introduced by irradiation results in a monotonic expansion of the a-axis and contraction of the c-axis with increasing irradiation dose. The net effect is an expansion of the tetragonal unit cell. The expansion, coupled with a concomitant shift of midplane/midcell uranium atoms to symmetric positions, would result in a new cubic unit cell of the Cu_3Au type. The phase transformation appears to be homogeneous and continuous without indication of coexistence of the initial and final phases. For U_3Si_2, both the a- and c-axes contract with increasing irradiation dose. Positional shifts of both uranium and silicon atoms continuously transform the U_3Si_2 toward a yet undetermined crystal structure. For both silicides, increases in background scattering reflect damage accumulation and/or amorphization. Damage in U_3Si saturates after a dose of 0.02 displacements per atom (dpa) and amorphization begins after an expansion of 1 at.% at 0.05 dpa.

The crystal structure refinements of unirradiated U_3Si and U_3Si_2, including the U_3Si_2 precipitates in U_3Si, agree with those previously obtained from X-ray diffraction [5,6]. Repeated irradiation produced structural changes in both alloys which resulted in a broadening and shifting of the Bragg peaks.

EXPERIMENTAL REPORT (CONTD.)

After 0.09 displacements per atom, the a-axis of U_3Si increased by 1% and the c-axis decreased by 0.5% , resulting in a net unit cell volume increase of 1.4%. The $(220)_T$ and $(004)_T$ reflections are gradually converging to the cubic $(200)_C$, Fig. 1, diffraction peaks broaden, and the diffuse background is significantly increased. Extrapolation of these peaks positions to total convergence yields the high temperature, cubic-phase lattice parameter. The initial increase in the diffuse background is thought to be due to defect accumulation while the large increase after 0.05 dpa is thought to be due to amorphization. The saturation of the initial increase occurs at a dose similar to that found for defect saturation in fission fragment irradiated metals [4]. The large increase in background scattering occurs in the dose regime required for amorphization of U_3Si by heavy ions [3].

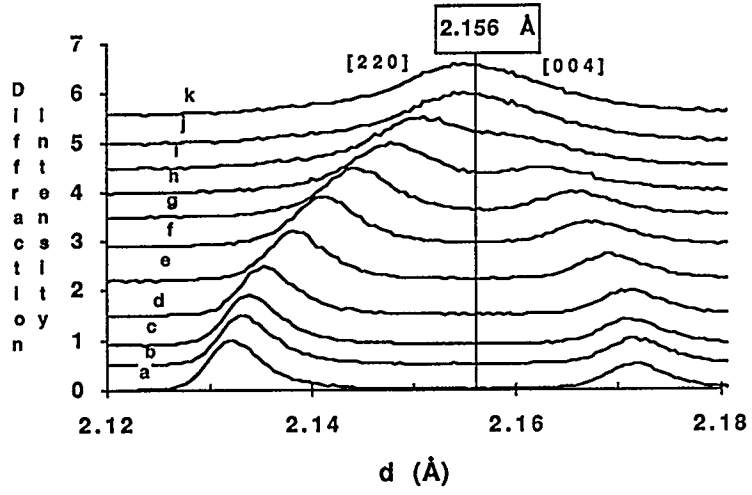


Fig 2. Changes in the $(220)_T$ and $(004)_T$ reflections of U_3Si produced by neutron irradiation. Background intensities have been subtracted, and peak intensities have been normalized to unity. The different curves correspond to damage levels of: a 0; b .002; c .004; d .006; e .014; f .022; g .031; h .044; i .055; j .071 and k .086 dpa. The vertical line at 2.157Å is half the lattice parameter of the high temperature cubic phase.

The U3Si2 unit cell volume decreases during irradiation, in contrast to the increase observed for U_3Si. There is little change in the c -axis while there is a strong contraction of the a-axis. With irradiation, the U_{II} site moves toward $(0,1/2,1/2)$ and pairs of Si atoms move away from each other and toward (1/4, 1/4,0) sites. Completion of this process would result in two uranium atoms occupying the same site or in formation of a phase with incorrect stoichiometry. Other U_3Si_2 phases have not been observed in thermodynamic studies.

1] D. G. Walker, J. Nucl. Mat. 37, 48 1970).
2] R. C. Birtcher, C. W. Allen, L. E. Rehn and G. L. Hofman, J. Nucl. Mater. 152, 73 (1988).
3] J. W. Richardson, Jr. and J. Faber, Jr., Adv. X-ray anal. 29, 143 (1985).
4] R. C. Birtcher, R. S. Averback and T. H. Blewitt, J. Nucl. Mat. 75,167 (1978).

INSTRUMENT USED:	DATE OF REPORT:	EXPERIMENT NO.:
GPPD	12 Feb 91	1396, 1312, 1219, 994

TITLE:
Irradiation-Induced Amorphization of U_3Si and U_3Si_2

AUTHORS AND AFFILIATIONS:
R.C. Birtcher, M.H. Mueller and J.W. Richardson Jr.

DATES OF EXPERIMENT:

☒ APPROVED BY PROGRAM COMMITTEE, OR

☐ PART OF INSTRUMENT SCIENTIST ALLOCATION

REPORT RECEIVED:

The irradiation behavior of high-density uranium silicides has been a matter of interest to the nuclear industry for use in high power or low enrichment applications. Transmission electron microscopy studies have found that heavy ion bombardme renders U_3Si and U_3Si_2 amorphous at temperatures below about 250 C [1], and that U_3Si becomes mechanically unstable suffering rapid growth by plastic flow [2,3]. In this present work, crystallographic changes preceding amorphization by fission fragment damage have been studied by high-resolution neutron diffraction as a function of damage produced by uranium fission at room temperature. Initially, both silicides had tetragonal crystal structures. Crystallographic and amorphous phases were studied simultaneously by combining conventional Rietveld refinement of the crystallographic phases with Fourier-filtering analysis of the non-crystalline scattering component [4].

Unirradiated U_3Si is tetragonal, space group I4/mcm, with a = 6.0358(1), c = 8.6925(1) Å, c/a = 1.440 and 16 atoms per unit cell. There are: 4 U_I at $\pm(0,1/2,1/4)$; 8 U_{II} at $\pm(x, x+1/2,0)$ with x=0.2251(1) and 4 Si at $(0,0,1/4)$. The base layer (z=0) contains only uranium atoms, the next layer ($z=1/4$) contains an equal number of uranium and silicon atoms, and the sequence repeats. The layer at $z = 1/2$ (U only) is rotated slightly relative to the base layer. This structure can be viewed as pseudo-cubic, in that if the U_{II} are shifted such that $x = 1/4$ and simultaneously the axial ratio (c/a) is reduced to $\sqrt{2}$, U_3Si would have the cubic Cu_3Au type structure ($a_C = a_T/\sqrt{2} = c_T/2$). This transformation also occurs upon heating to 1038K [12].

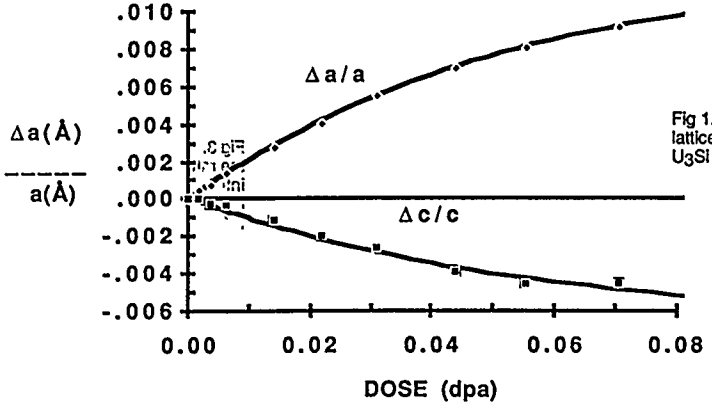


Fig 1. Variation of the lattice parameters of U_3Si with damage.

Lattice parameter changes produced by neutron irradiation of U_3Si are shown in Fig 1. After 0.07 displacements per atom, the a-axis increased by 1% and the c-axis decreased by 0.5% , resulting in a net unit cell volume increase of 1.4%. In addition, U_{II} is approaching the idealized Cu_3Au position ($1/4,3/4,0$), the $(220)_T$ and $(004)_T$ reflections are gradually converging to the cubic $(200)_C$, diffraction peaks broaden, and the diffuse background is significantly increased. The cubic transformation is illustrated in Fig. 2 by the convergence of the $(220)_T$ and $(004)_T$ reflections with increasing damage. Extrapolation of these peaks positions to total convergence yields the high temperature, cubic-phase lattice parameter.

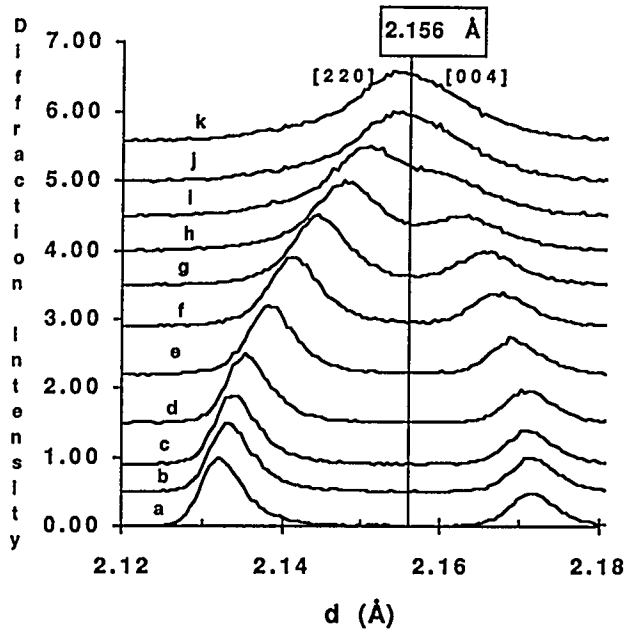


Fig 2. Changes in the $(220)_T$ and $(004)_T$ reflections of U_3Si produced by neutron irradiation. Background intensities have been subtracted, and peak intensities have been normalized to unity. The different curves correspond to damage levels of: a 0; b .002; c .004; d .006; e .014; f .022; g .031; h .044; i .055; j .071 and k .086 dpa. The vertical line at 2.157Å is half the lattice parameter of the high temperature cubic phase.

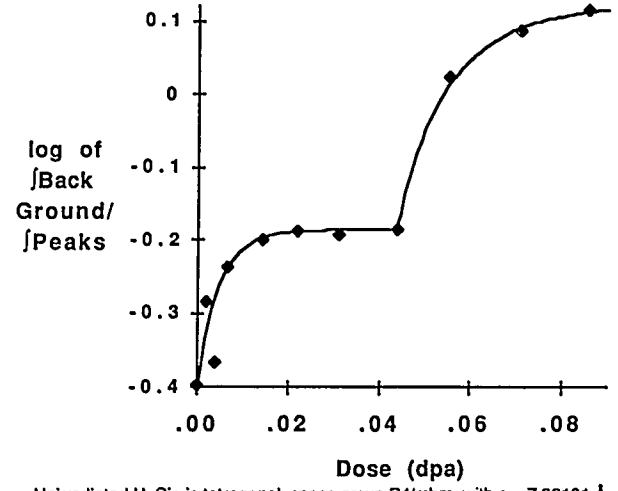


Fig 3. Variation of the ratio of integrated background to $(220)_T$ and $(004)_T$ peak intensities for U_3Si.

Unirradiated U_3Si_2 is tetragonal, space group P4/mbm, with a = 7.33101 Å, c = 3.90092 Å, c/a = 0.532 and 10 atoms per unit cell. There are U_I atoms at (0,0,0) and $(1/2,1/2,0)$; 4 U_{II} atoms at $\pm(x,x+1/2,1/2)$ with x=0.18186 and 4 Si at $\pm(x',$

These peak shifts indicate the accumulation of a homogeneous lattice strain and no direct formation of the cubic phase within the small volumes damaged by the fission fragments. Such direct formation of cubic material would be indicated by the growth of a [002] diffraction peak at 2.156Å rather than the merging of the tetragonal peaks. In addition at the highest dose of 0.086 dpa, the scattering contains less than 4% of the $[220]_C$ diffraction peak found for unirradiated material. The homogeneous nature of the transformations may be enhanced by the powder specimen which consists of single-crystal particles between 50 and 150 μm in diameter. Fig. 3 shows the variation with damage of the ratio of background scattering intensity to peak intensity over the range shown in Fig. 2. The initial increase is thought to be due to defect accumulation while the large increase after 0.05 dpa is thought to be due to amorphization. The saturation of the initial increase occurs at a dose similar to that found for defect saturation in fission fragment irradiated metals [13]. The large increase in background scattering occurs in the dose regime required for amorphization of U_3Si by heavy ions [3]. The Debye-Waller factors for all atomic sites increases with irradiation although the RMS values for Si atoms are somewhat less than for the U atoms. This may be indicative of deviations, static or dynamic, of U atoms from their ideal locations. In summary, neutron irradiation transforms the tetragonal crystal structure to either the high temperature cubic form and/or to an amorphous form.

Unirradiated U_3Si_2 is tetragonal, space group P4/mbm, with a = 7.33101 Å, c = 3.90092 Å, c/a = 0.532 and 10 atoms per unit cell. There are U_I atoms at (0,0,0) and ($^1/_2,^1/_2$,0); 4 U_{II} atoms at ±(x,x+$^1/_2,^1/_2$) with x=0.18186 and 4 Si at ±(x', x'+$^1/_2$,0) with x'=0.38383. Variations of the lattice parameters as a function of dose are shown in Fig. 4. There is little change in the c-axis while there is a strong contraction of the a-axis. The U3Si2 unit cell volume decreases during irradiation, in contrast to the increase observed for U_3Si. There are large out-of-plane displacements of U_I atoms along the [001] direction in all forms of the U_3Si_2, both unirradiated and irradiated; pure phase and second phase in U_3Si. These displacements increase from an initial value of 0.26Å at a rate of 2.7Å/dpa during irradiation. It is conceivable that the huge displacement parameter represents an average of random static displacements. With irradiation, the U_{II} site moves toward (0,$^1/_2,^1/_2$) and pairs of Si atoms move away from each other and toward (1/4, 1/4,0) sites. Completion of this process would result in two uranium atoms occupying the same site or in formation of a phase with incorrect stoichiometry. Other U_3Si_2 phases have not been observed in thermodynamic studies.

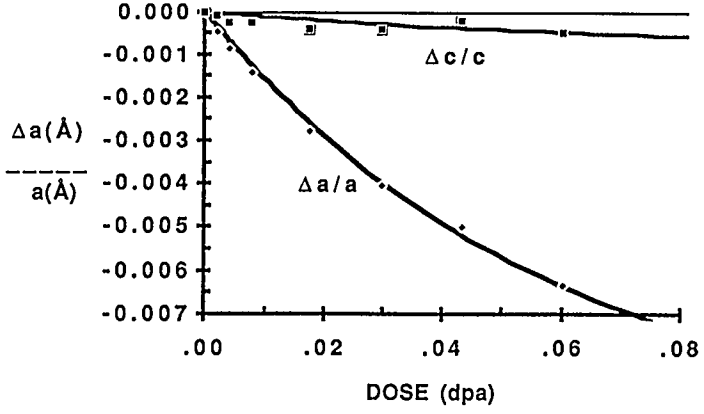


Fig 4. Variation of the lattice parameters of U_3Si_2 with damage.

REFERENCES

1 D. G. Walker, J. Nucl. Mat. 37, 48 1970).
2 G. L. Hofman, J. Nucl. Mat. 140, 256 (1986).
3 R. C. Birtcher, C. W. Allen, L. E. Rehn and G. L. Hofman, J. Nucl. Mater. 152, 73 (1988).
4 J. W. Richardson, Jr. and J. Faber, Jr., Adv. X-ray anal. 29, 143 (1985).
5 R. C. Birtcher, T. H. Blewitt, M. A. Kirk, T. L. Scott, B. S. Brown and L. R. Greenwood, J. Nucl. Mater. 108 & 109, 3 (1982
6 L. R. Greenwood, private communication.
7 D. M. Parkin and R. O. Elliott, Nucl. Inst. Meth. B16, 193 (1986).
8 H. M. Rietveld, J. Appl. Cryst. 2, 65 (1969).
9 J. D. Jorgensen, J. Faber, Jr., J. M. Carpenter, R. K. Crawford, J. R. Hauman, R. L. Hitterman, R. Kleb, G. E. Ostrowski, F. J. Rotella and T. G. Worlton, J. Appl. Cryst. 21, 321 (1989).
10 W. H. Zachariasen, Acta Cryst. 2, 94 (1949).
11 G. Kimmel and S. Nadiv, Acta Cryst. B31, 1351 (1975).
12 P. L. Blum, G.Silvestro and H. Vangoyan, C. R. Acad. Sci. 260, 5538 (1964).
13 R. C. Birtcher, R. S. Averback and T. H. Blewitt, J. Nucl. Mat. 75,167 (1978).

INSTRUMENT USED:	DATE OF REPORT:	EXPERIMENT NO:
GPPD	January 1996	2156

TITLE: Crystallization of Amorphous U_3Si_2

AUTHORS AND AFFILIATIONS: R. C. Birtcher (MSD Div., ANL), M. H. Mueller (FE Div., ANL) and J. W. Richardson (IPNS Div., ANL)

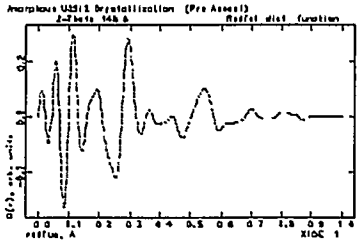
DATES OF EXPERIMENT: Sept. 22-23, 27-28; Oct. 25-26; Nov. 16-17; Dec. 11-12, 1995

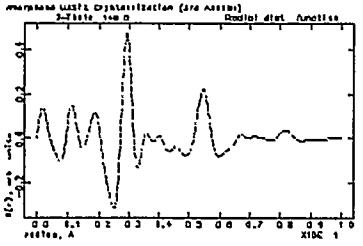
CHECK ALL APPLICABLE BOXES:

- [x] APPROVED BY PROGRAM COMMITTEE
- [ ] INSTRUMENT SCIENTIST ALLOCATION
- [ ] DO NOT PUBLISH
- [ ] PROPRIETARY RESEARCH
- [ ] PRT ALLOCATION

EXPERIMENTAL REPORT (or Abstract of Publication)

A specimen of U_3Si_2, made amorphous by room temperature neutron irradiation at IPNS, is being step annealed for one hour at increasingly higher temperatures. Anneals are made in a tube furnace, and after each anneal, neutron diffraction from the specimen is measured at room temperature on the GPPD. The annealing temperatures have been 161°C, 209°C, 242°C, the upper temperature limit for irradiation to amorphize U_3Si_2, and 305°C. Changes in the diffraction patterns (figure below shows d(r), extracted from Rietveld analysis of V containers, for unannealed and 3 times annealed samples; note changes in the 2.8-6 Å range) indicate that structural relaxation and atomic ordering occurred during the first two anneals. Crystallization of the amorphous material has not been detected. Additional anneals at higher temperatures will be made until crystallization occurs. Detailed analysis of the scattering patterns should yield measures of changes in atomic density and local order.





EXPERIMENTAL REPORT (CONTD.)

INSTRUMENT USED:	DATE OF REPORT:	EXPERIMENT NO.:
GPPD	August, 1990	1133

TITLE: Non-Destructive Measurements of Residual Stresses in Thin, Short Plates of Yttrium-Barium-Copper Oxide Superconductors

AUTHORS AND AFFILIATIONS:

Steven Danyluk, University of Illinois at Chicago

DATES OF EXPERIMENT: 10/23/89 and 12/18/89

☐ APPROVED BY PROGRAM COMMITTEE, OR

☐ PART OF INSTRUMENT SCIENTIST ALLOCATION

REPORT RECEIVED:

EXPERIMENTAL REPORT (or Abstract of Publication)

Summary

Short, cylindrical specimens (3.6cm dia., 0.8cm thick and 4.6cm dia., 0.5cm thick) of orthorhombic Yttrium-Barium-Copper oxide high temperature superconductor (T_c=91.5K) have been fabricated using a processing sequence developed at Argonne National Laboratory. Thin wafers (15, 3.5, and 0.8mm thick) were cut from these cylinders and the residual strains of these wafers were determined from neutron diffraction and shadow Moiré interferometry. Neutron diffraction, which probes through-thickness stresses over approximately the beam irradiation area (16mm^2), showed that the strains in the uncut cylinder were in the range of 0.05% and these strains varied with position in the cylinder. The strains could not be used to extract reliable values of residual stress. The shadow Moiré results were obtained on the thinnest wafer (0.8mm thick), and the in-plane residual stresses were determined to be compressive; approximately 1.5MPa at the center and 1.1 to 0.7MPa at the outer edge. These values of residual stress are significantly below those required to cause buckling or fracture.

EXPERIMENTAL REPORT (CONTD.)

INSTRUMENT USED:	DATE OF REPORT:	EXPERIMENT NO.:
GPPD	July 11, 1991	1371

TITLE:

Determination of $BaMo(O,N)_3$ Structures at Various Temperatures (1371)

AUTHORS AND AFFILIATIONS:
Harry A. Eick, Chemistry Dept. Michigan State University
G. Liu, Institute for Materials Research, McMaster University

DATES OF EXPERIMENT: April 20-22, 1991

☐ APPROVED BY PROGRAM COMMITTEE, OR

☐ PART OF INSTRUMENT SCIENTIST ALLOCATION

REPORT RECEIVED:

EXPERIMENTAL REPORT (or Abstract of Publication)

The specimen by X-ray powder diffraction was diphasic with a cubic $BaMoO_3$ perovskite-type phase and a rhombohedral Ba-Mo-O-N phase of unknown structure which exhibits interesting low-temperature magnetic behavior. Refinement was initiated on the cubic phase with the 295 K data set. Nitrogen substitution was considered; with the anion B_{iso} parameter fixed the composition refined to $BaMoO_{2.92}N_{0.06}$ with an R-factor of ~8%. B_{iso} parameters were: Ba (0.47), Mo (0.58), and O (0.57).

X-Ray powder diffraction data for the second (unknown) structure were consistent with space groups $R\bar{3}$, R32, or $R\bar{3}m$ with $a = 5.97$ and $c = 21.51$ Å. Two model structures were identified, $R\bar{3}m$ $BaRuO_3$ [P. C. Donohue, L. Katz, and R. Ward, *Inorg. Chem.* 4, 306 (1965)] ($a = 5.75$, $c = 21.6$ Å) and $R\bar{3}m$ $Ba_3Re_{2-x}O_9$ [C. Calvo, H.N. Ng, and B. L. Chamberland, *Inorg. Chem.* 17, 699 (1978)] ($a = 5.77$, $c = 20.80$ Å). X-Ray powder diffraction intensities calculated with the $Ba_3Re_{2-x}O_9$ parameters fit the data better. In this model the occupancy factor of Mo(2) at (0,0,1/2) is 0.079; it was omitted. The model did not refine; the thermal parameter of Ba1 (0,0,0) became non-positive while those for Mo1 and the anions became unreasonably large. Only atom Ba2 (0,0,0.2021) refined properly. The fit of the data at this point is illustrated in Figure 1. Starting with only Ba2 numerous Fourier analyses were computed and atoms added as indicated by the computational results. However, convergence could not be achieved.

Similar problems prevailed in diffraction data collected at a lower temperature.

The data in Figure 1 illustrate an additional problem. Some weak reflections (*e.g.*, $d = 2.045$, 2.135, 2.415, and 2.504 Å) are not accounted for positionally. These weak reflections were not apparent in the X-ray diffractograms and might result from a minor (unknown) third component. To attack this problem the synthesis reaction was analyzed as a function of temperature. Selected reaction data presented in Table I suggest that the desired phase will always be contaminated by $BaMoO_3$ or $MaMoO_4$ or both. They also suggest that the weak reflections belong to the Ba-Mo-O-N phase. A different synthesis procedures is being developed; refinement will be attempted again with data collected from a more phase-pure specimen.

Table I. Data illustrating synthesis kinetics of $BaMo(O,N)_3$.

Mole ratio (NH_3:$BaMoO_4$)	Temp. (°C)	Time (hr.)	Weight Loss (%)	Phases observed
3.59	610	6	0.47	$BaMoO_4$, $[BaMo(O,N)_3]$
3.89	610	6	1.25	$BaMoO_4$, $[BaMo(O,N)_3]$
4.38	610	12	1.53	$BaMoO_4$, $[BaMo(O,N)_3]$
4.72	610	12	1.92	$BaMoO_4$, $[BaMo(O,N)_3]$
5.39	650	12	2.47	$BaMoO_4$, $[BaMo(O,N)_3]$
6.02	650	3@12	4.16	$BaMoO_4$, $[BaMo(O,N)_3]$, $BaMoO_3$
11.73	650	2@12	5.25	$BaMoO_4$, $[BaMo(O,N)_3]$, $BaMoO_3$
28.06	650	2@12	5.96	$BaMoO_4$, $[BaMo(O,N)_3]$, $BaMoO_3$
125	650	2@12	6.43	$[BaMo(O,N)_3]$, $BaMoO_3$

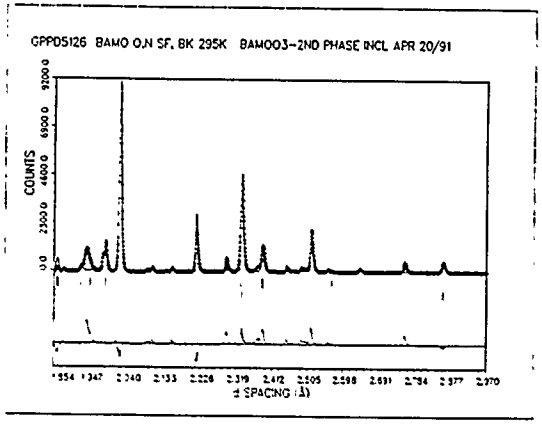


Figure 1. Rietveld difference plot (*d*-value range, 2.97-1.85 Å) which illustrates problems encountered in refinement of the Ba-Mo-O-N phase.

INSTRUMENT USED:	DATE OF REPORT:	EXPERIMENT NO:
GPPD	January 1996	D1994

TITLE: Crystal and Microstructure of U_3Si_2 Fuel Plates after Reactor Irradiation

AUTHORS AND AFFILIATIONS: G. L. Hofman (FE Div., ANL), R. C. Birtcher (MSD Div., ANL), J. W. Richardson (IPNS Div, ANL)

DATES OF EXPERIMENT: Mar. 16-17, 1994; June 20-21, 1995; Oct. 17-18, 1995

CHECK ALL APPLICABLE BOXES:

- [ ] APPROVED BY PROGRAM COMMITTEE
- [x] INSTRUMENT SCIENTIST ALLOCATION
- [ ] DO NOT PUBLISH
- [ ] PROPRIETARY RESEARCH
- [ ] PRT ALLOCATION

EXPERIMENTAL REPORT (or Abstract of Publication)

Neutron diffraction and SEM were been used to determine irradiation induced changes in reactor fuel plates containing U_3Si_2. The fuel plates were fabricated by hot rolling low enriched U_3Si_2 (45 volume %) and Al powders. Plates were irradiated at 150°C in the ORR reactor to 7% and 16% burnup of the uranium. Amorphization of U_3Si_2 after $4x10^{-6}$ burnup results in a 3.3% volume contraction. SEM examination shows the development of a several μm thick shell around each fuel particle due to Al diffusion into the particles. The shell thickness varies as the square root of the irradiation dose. Neutron diffraction shows that after the lower dose the fuel is amorphous (Figure 1), but that after higher dose it also contains a crystalline aluminide phase (Figure 2). The stability of U_3Si_2 fuel plates is believed to be associated with the volume contraction upon amorphization.

Neutron diffraction samples were prepared by slicing the fuel plates into small sections and sealing them into 3/8" dia. vanadium cans. Those vanadium cans were, in turn, sealed in 7/16" dia. vanadium cans and transported to IPNS for analysis. The samples were highly radioactive (150-200 R/hr @ 6 cm), so a specially designed remote handling apparatus was employed to eliminate personnel exposure to the radiation.

The results of Rietveld profile refinement (using GSAS: the Generalized Structure Analysis System) are shown in Figures 1 and 2. The strongly textured Al was modelled with the LeBail technique (whereby atomic structure factor constraints on calculated diffraction intensities are removed), while scattering from the vanadium canisters and crystalline UAl_3 were modelled in the traditional Rietveld manner. Modelling of UAl_3 peak broadening in the high dose (annealed sample) led to a prediction of ~800 Å UAl_3 particles. UAl_3 scattering intensities are roughly consistent with a total mass of 0.056 gms UAl_3 in the sample, implying a shell thickness of ~12 μm.

Superimposed on the crystalline scattering from Al, V and UAl_3 in the figures is the calculated pattern from the amorphous U_3Si_2 fuel. This calculated pattern is produced by GSAS under the assumption that the oscillatory amophous scattering is the Fourier transform of a correlation function corresponding to the local structure of amorphous U_3Si_2. The correlation function model includes a

EXPERIMENTAL REPORT (CONTD.)

series of variable parameters, positions and amplitudes characteristic of interatomic distances in the material. Refined values from this model for U_3Si_2 are very similar to interatomic distances found in crystalline U_3Si_2.

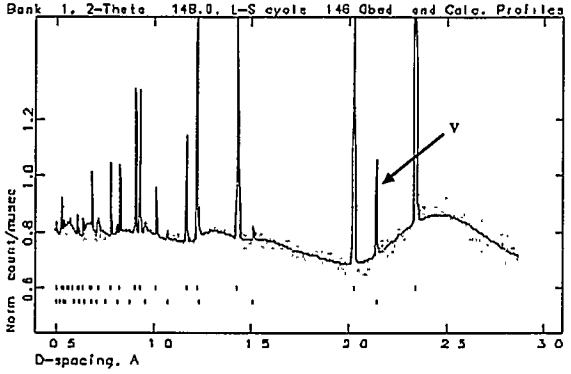


Figure 1. Rietveld profile refinement of a highly irradiated U_3Si_2-Al fuel plate showing scattering from crystalline Al and V, and amorphous U_3Si_2.

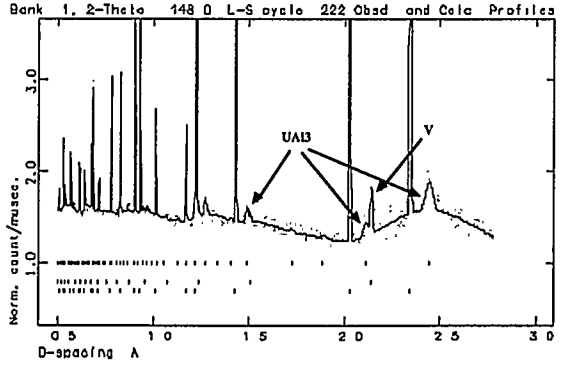


Figure 2. Rietveld profile refinement of a highly irradiated - and annealed - U_3Si_2-Al fuel plate showing scattering from crystalline Al and V, small (~800 Å) crystalline particles of UAl_3, and amorphous U_3Si_2.

INSTRUMENT USED:	DATE OF REPORT:	EXPERIMENT NO.:
GPPD	June 17, 1991	1397

TITLE:

Crystal Structures of $YBa_2Cu_4O_8$ at Low Temperatures

AUTHORS AND AFFILIATIONS: Natl. Inst. Res. Inorg. Mater.

F. Izumi, T. Matsumoto*, Y. Yamada*, *Natl. Res. Inst. Metals

DATES OF EXPERIMENT: March 14-16, 1991

☑ APPROVED BY PROGRAM COMMITTEE, OR

☐ PART OF INSTRUMENT SCIENTIST ALLOCATION

REPORT RECEIVED:

EXPERIMENTAL REPORT (or Abstract of Publication)

$YBa_2Cu_4O_8$ is a superconductor with a T_c of *ca.* 80 K. Kaldis *et al.*[1] reported that the *a* and *c* axes of superconducting $YBa_2Cu_4O_8$ shrank smoothly with lowering temperature, but that the *b* axis parallel to the direction of double CuO chains had a minimum length near T_c. They insisted that this anisotropic cell contraction results in a slight inflection in the orthorhombic distortion near T_c. However, relatively high *R* factors obtained in their Rietveld refinements indicate their sample of $YBa_2Cu_4O_8$ to be of poor quality. Samples containing lesser intergrowths should be used to draw unambiguous conclusions regarding the low-temperature anomalies in this superconductor. The low-temperature structure of $YBa_2Cu_4O_8$ is also very interesting in connection with redistribution of holes between two Cu sites: Cu(1) on the double CuO chains and Cu(2) on two-dimensional CuO_2 sheets.[2]

We prepared a sample of $YBa_2Cu_4O_8$ with high quality by the O_2-HIP method. High-resolution electron microscopy showed that this sample includes a very small portion of $YBa_2Cu_3O_{7-z}$-like intergrowths.[3]

TOF neutron-powder-diffraction data (15 points) were measured on the GPPD diffractometer over the temperature range from 10 K to 270 K. Preliminary Rietveld refinements indicated that our sample contained a very small amount of CuO. Then, the coexistence of this impurity was taken into account in subsequent refinements with the multi-phase capability of TOFLS.

The *b* values proved to be almost constant within the range of estimated standard deviations (Fig. 1). Thus, the above conclusion drawn by Kaldis *et al.*[1] evidently does not apply to high-quality samples of $YBa_2Cu_4O_8$. Samples with a considerable amount of oxygen deficiencies may exhibit such extraordinary cell contraction.

The most striking structural change in $YBa_2Cu_4O_8$ at low temperature is the contraction of a bond between Cu(2) and an apical oxygen atom, O(1) (Fig. 2). Such movements of Cu(2) and O(1) under low temperature may cause charge (hole) transfer from Cu(1) to Cu(2). Then,

we calculated the Madelung energies, E_M, of $YBa_2Cu_4O_8$ on the assumptions that the valences of Y, Ba, and O are respectively +3, +2, and –2 and that a positive charge of +4.5 is distributed between the Cu(1) and Cu(2) atoms. The minimum of the relative change in E_M, ΔE_M, proved to be nearly constant regardless of the number of holes per Cu(2), n_s. We have already reported that n_s increases with increasing pressure in $YBa_2Cu_4O_8$.[2] This difference in hole redistribution between two extreme conditions, *i.e.*, low temperature and high pressure, is very interesting; it should be investigated further in other superconductors.

References

1) E. Kaldis, P. Fischer, A.W. Hewat, E.A. Hewat, J. Karpinski, and S. Rusiecki, *Physica C*, **159**, 668 (1989).

2) Y. Yamada, J.D. Jorgensen, Shiyou Pei, P. Lightfoot, Y. Kodama, T. Matsumoto, and F. Izumi, *Physica C*, **173**, 185 (1991).

3) Y. Matui *et al.*, unpublished work.

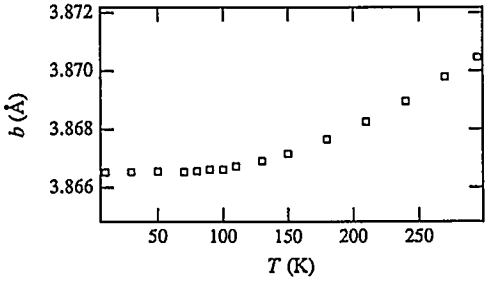


Fig. 1 *b vs.* temperature

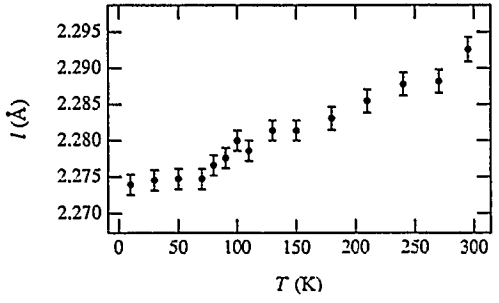


Fig. 2 Cu(2)–O(1) bond length *vs.* temperature

INSTRUMENT USED:	DATE OF REPORT:	EXPERIMENT NO..
GPPD	21 Nov 1995	2024

TITLE:
Hydrogen Bonding in Hydrated Sodium Aluminate, $NaAlO_2 \cdot 5/4H_2O$

AUTHORS AND AFFILIATIONS:
James A. Kaduk and Shiyou Pei, Amoco Corporation

DATES OF EXPERIMENT:
18-19 May 1995

CHECK ALL APPLICABLE BOXES:

- ☒ APPROVED BY PROGRAM COMMITTEE
- ☐ INSTRUMENT SCIENTIST ALLOCATION
- ☐ DO NOT PUBLISH
- ☐ PROPRIETARY RESEARCH
- ☐ PRT ALLOCATION

EXPERIMENTAL REPORT (or Abstract of Publication)

The crystal structure of hydrated sodium aluminate, $NaAlO_2 \cdot 5/4H_2O$, has been solved *ab initio* using synchrotron X-ray powder diffraction data [1]. The structure of the deuterated form, $NaAlO_2 \cdot 5/4D_2O$, was refined using time-of-flight neutron powder diffraction data collected at 20, 150 and 295K. The room temperature structure ($P\bar{7}2_1m$, a = 10.53044(9), c = 5.33672(6) Å, Z = 8) is maintained at low temperatures, and the lattice contracts isotropically. The structure consists of single layers of corner-sharing AlO_4 tetrahedra, joined into 4- and 8-rings. Three of the vertices are shared, and the fourth is a hydroxyl group, which points into the interlayer regions. The nearest O-O distances involving this hydroxyl groups are 3.2 Å.

All hydrogens were located, and refined anisotropically (Figure 1). The geometries of the two independent water molecules (at 20K) are typical:

Water Molecule	O-D, Å	D-O-D, °	H-bond O-O, Å	O-D···O, °
$O4(D4)_2$	1.030(3)	96.9(4)	2.68	171.2
$O5(D5)_2$	1.008(4)	100.3(6)	2.80	158.0

Both serve as proton donors in strong hydrogen bonds to framework oxygen atoms.

The hydroxyl hydrogen is ordered, and is directed toward only one of the two nearby hydroxyls from the adjacent layer (Figure 2):

Hydroxyl	O-D, Å	Al-O-D, °	H-bond O-O, Å	O-D···O, °
O1-D1	0.993(3)	115.1(2)	3.21	159.5

The orientation of the hydroxyl group seems determined more by its coordination to two Na cations than by the long hydrogen bonding interactions. The quantum mechanical calculations necessary to understand the details of the energetics turn out to be *very* large, and are still in progress.

1. J.A. Kaduk and S. Pei, *J. Solid State Chem.*, 115, 126-139 (1995).

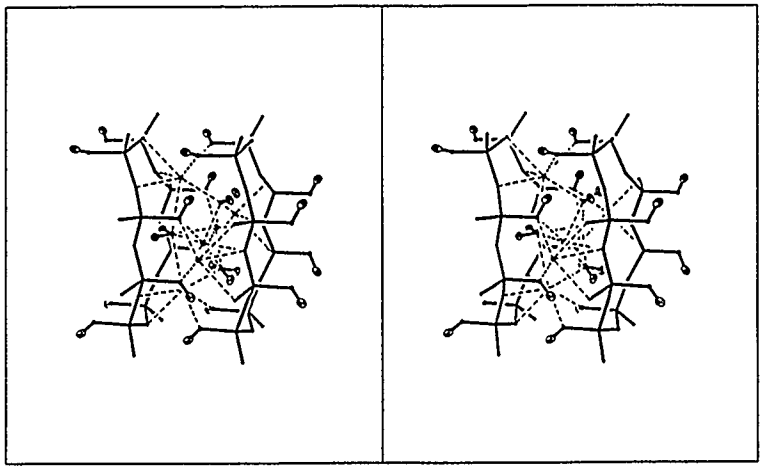


Figure 1. The crystal structure of $NaAlO_2 \cdot 5/4D_2O$ at 20K. The view is approximately down [110]. The dashed lines indicate the Na-O coordination. 50% probability ellipsoids.

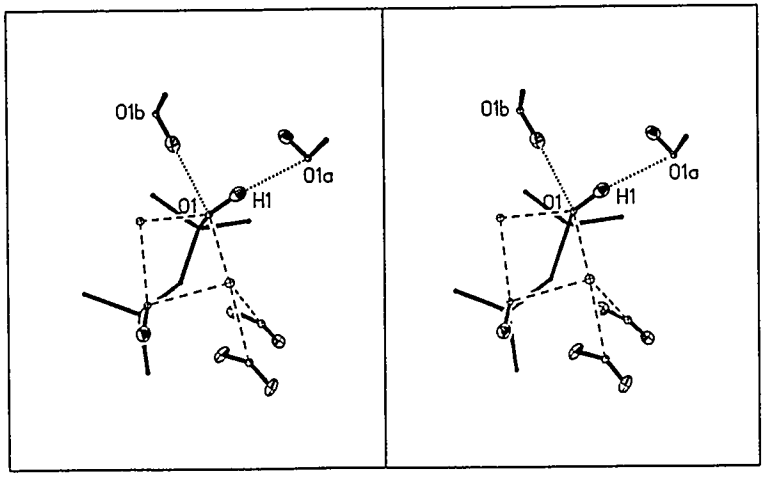


Figure 2. The environment of the hydroxyl group in $NaAlO_2 \cdot 5/4D_2O$ at 20K. The view is approximately down [001]. 50% probability ellipsoids.

INSTRUMENT USED:	DATE OF REPORT:	EXPERIMENT NO.:
GPPD	15 June 1993	1599

TITLE: Crystal Structures of $KTiOPO_4$-type Nonlinear Optical Materials above and below the Curie Temperatures

AUTHORS AND AFFILIATIONS: J.A. Kaduk, J. Faber, S. Pei, Amoco Corporation
R.H. Jarman, Amoco Technology Company

DATES OF EXPERIMENT: 23-28 April 1992

Approved by the Program Committee

REPORT RECEIVED:

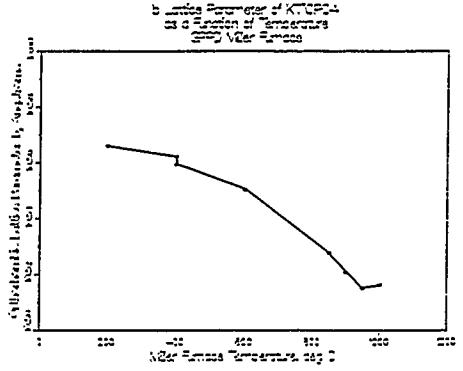
EXPERIMENTAL REPORT (or Abstract of Publication)

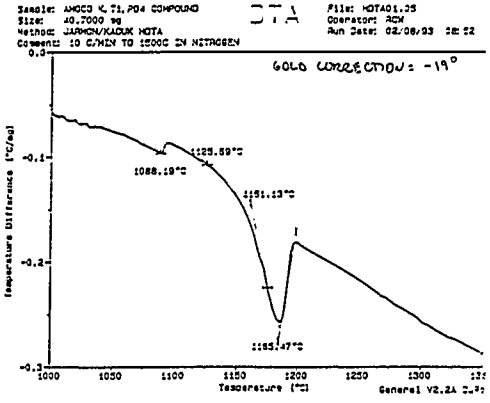
Powder patterns of $KTiOPO_4$ were collected at 200°, 400°, 850°, and 1000°C (on heating), and 950°, 900°, 600°, and 400°C (on cooling) on GPPD using the Miller furnace. The orthorhombic a- and c-axes (space group $Pn2_1a$) exhibit a monotonic increase with increasing temperature, but the b-axis decreases with increasing temperature until 950°C, at which temperature the b lattice parameter begins to increase.

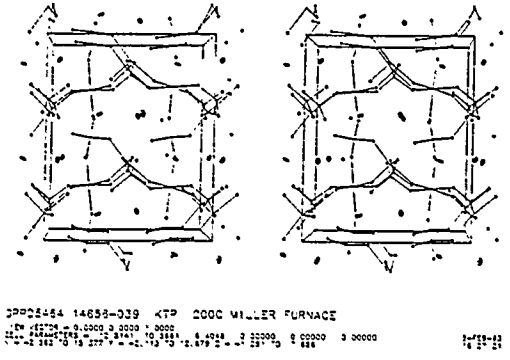
The Curie temperature of KTP is reported to be approximately 935°C, but the DTA curve is relatively featureless in this region. A small endothermic feature is observed, however at 1070°C, and the onset of incongruent melting occurs at approximately 1107°C.

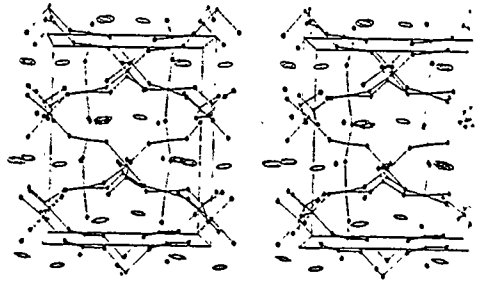
Refinement of the crystal structure at the various temperatures reveals no substantial framework changes. The anisotropic displacement coefficients of the K ions, which lie in channels, increase along the polar b-axis with increasing temperature. This increase is consistent with the documented greater ion mobility along this direction.

It appears that more than one subtle structural transition occurs in the temperature range 900-1100°C. Several patterns will need to be measured in this region to gain a greater understanding of the structural changes.









INSTRUMENT USED:	DATE OF REPORT:	EXPERIMENT NO:
GPPD	Feb 27, 1996	2250

TITLE: Crystal structure of $(^7Li_{1-x}K_x)_2CO_3$ (x=0, 0.38, 0.50, 0.57) determined by neutron powder diffraction

AUTHORS AND AFFILIATIONS:
N. Koura, Y. Idemoto, S. Kohara (Science University of Tokyo)
J. W. Richardson, Jr., and C.-K. Loong (ANL)

DATES OF EXPERIMENT:
Jan 1996

CHECK ALL APPLICABLE BOXES:

- [X] APPROVED BY PROGRAM COMMITTEE
- [ ] INSTRUMENT SCIENTIST ALLOCATION
- [ ] DO NOT PUBLISH
- [ ] PROPRIETARY RESEARCH
- [ ] PRT ALLOCATION

EXPERIMENTAL REPORT (or Abstract of Publication)

Molten carbonate is a very important electrolyte for the next generation fuel cells which show promising efficiency and attractive environmental features. The structural analysis of the melt should be done, because atomic structure and organization to a large extent decide the properties of melts, the cell performance, and the corrosion behavior of the cell components. Structural analyses of the Li/K carbonate system by the *ab-initio* calculations and molecular dynamics computer simulations were carried out at Science University of Tokyo. The crystal structure of the $(^7Li_{1-x}K_x)_2CO_3$ system was determined by powder diffraction using isotopic ^7Li samples at IPNS. Information regarding to the accurate location of alkali cation relative to the surrounding $(CO_3)^{2-}$ is very important.

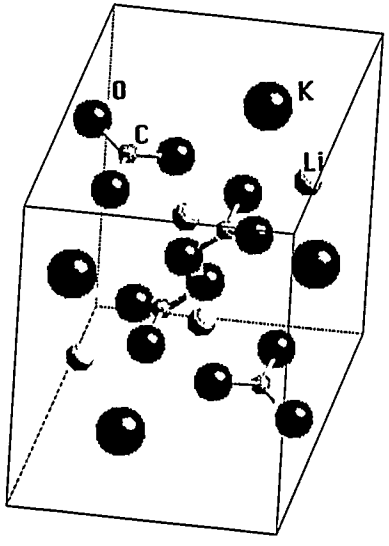


Fig. 1. The crystal structure of $(^7Li_{0.5}K_{0.5})_2CO_3$: monoclinic unit cell, space group $P2_1/c$.

EXPERIMENTAL REPORT (CONTD.)

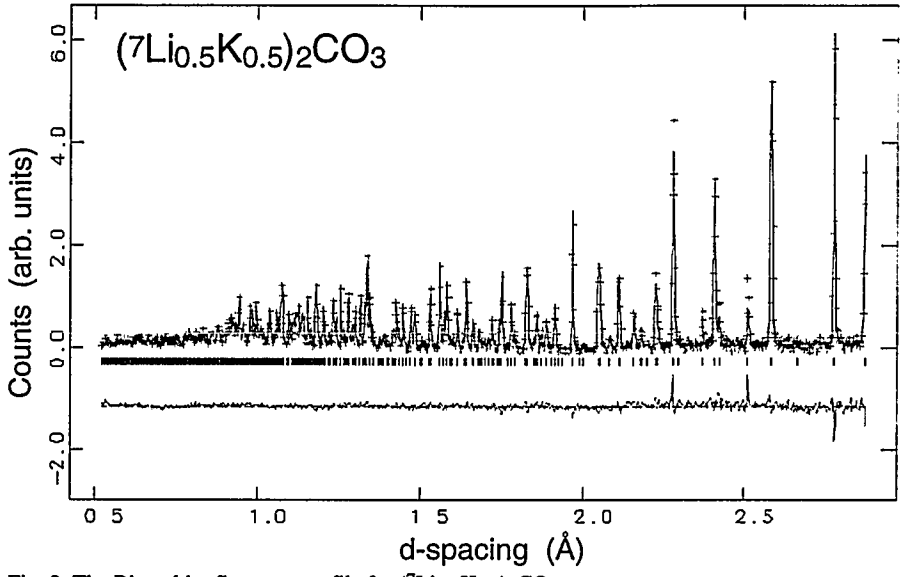


Fig. 2 The Rietveld refinement profile for $(^7Li_{0.5}K_{0.5})_2CO_3$.

INSTRUMENT USED:	DATE OF REPORT:	EXPERIMENT NO:
GPPD	February 1995	1644

TITLE: Residual Stresses in WC-Co Measured by Neutron Diffraction

AUTHORS AND AFFILIATIONS: A. D. Krawitz (Univ. of Missouri),
D. Mari (Mass. Inst. of Tech., Cambridge, Mass),
J. W. Richardson, Jr. (IPNS Div., ANL)

DATES OF EXPERIMENT: February 11-16, 1993

CHECK ALL APPLICABLE BOXES:

- [x] APPROVED BY PROGRAM COMMITTEE
- [ ] INSTRUMENT SCIENTIST ALLOCATION
- [ ] DO NOT PUBLISH
- [ ] PROPRIETARY RESEARCH
- [ ] PRT ALLOCATION

EXPERIMENTAL REPORT (or Abstract of Publication)

WC-Co composites are widely used as base materials for cutting tools. Their working temperature often exceeds 1300 K and it is essential to understand the physics of the materials at high temperature to improve the quality and performance of the tools. Recent studies have provided new understanding of the high temperature mechanical properties. The mechanical properties of WC-11wt% Co exhibit three different domains depending on temperature: elastic and brittle from room temperature to 900 K; tough with limited plasticity between 900 and 1100 K; and, easy deformation above 1100 K. Differences in coefficients of thermal expansion (CTE) of WC and Co, are likely to generate significant thermal residual microstresses during fabrication. In accordance with the CTE mismatch, WC and Co were found to be under compressive and tensile thermal stress, respectively, at room temperature. Upon heating, the magnitude of stress decreases up to 900 K. The WC stress unexpectedly attains a maximum (-100 MPa) at 1000 K, after which compression again increases. Stress measurements made during cooling follow a curve similar to that observed upon heating but the stress maximum in WC is tensile, with corresponding compression in Co, and it is shifted to lower temperature, i.e., hysteresis is observed (Figure 1). Measurements during a second heating and cooling cycle show reproducibility. The unusual increase in compressive stress magnitude in WC upon heating above 1000 K is attributed to W dissolution into the Co, forming WCo_3. The hysteresis is thought to be due to a difference between the heating and cooling kinetics of solution-precipitation of W from WC and WCo_3.

EXPERIMENTAL REPORT (CONTD.)

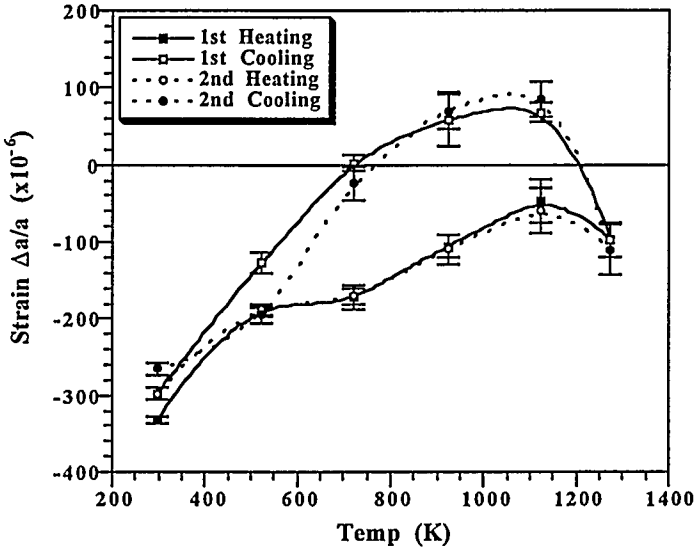


Figure 1. Residual strain in WC (a-lattice parameter) component of WC-Co composite as a function of temperature.

INSTRUMENT USED:	DATE OF REPORT:	EXPERIMENT NO.
GPPD	January 3, 1991	1226

TITLE: Microstresses in Al_2O_3/SiC Ceramic Composites

AUTHORS AND AFFILIATIONS:
Aaron. D. Krawitz, University of Missouri-Columbia, Columbia, MO 65211
Henry J. Prask, Reactor Radiation Division, NIST, Gaithersburg, MD 20899

DATES OF EXPERIMENT: February 22-24, 1990

√ Approved by Program Committee

REPORT RECEIVED:

EXPERIMENTAL REPORT

Residual microstresses in Al_2O_3 reinforced with SiC whiskers were studied. Two different types of whiskers at two different volume percentages were used: TWS 100 (≈ 0.4 μm diameter, ≈ 10 μm long) and TWS 400 (≈ 1.1 μm diameter, ≈ 50 μm long), each at 20 and 30 vol.%. Processing was the same for each whisker type: hot pressing into a disk 5 cm in diameter and ≈ 0.25 cm thick, at 6000 psi at 1700°C for 30 min. The samples for neutron study were cut from the center of the pressed disks, stacked and glued, and ground to cubes ≈ 0.9 cm on a side, with z parallel and x and y normal to the hot-pressing direction. Data were collected, on the GPPD, for all reflections in the range $0.767Å < d_{hkl} < 2.972Å$ for four different directions in the sample coordinate system: Q parallel and at 32° to the z and x directions. This was done by analyzing data from each bank of 148° detectors separately in an effort to see textural effects. In fact, no such effects were observed within experimental accuracy. The 113, 024, 116, and 300 Al_2O_3 reflections and the 111, 220, and 311 SiC reflections were used for analysis. Unstressed d-spacings were obtained from the starting materials, supplied as premixed, unsintered powders of the 30 vol.% material in both small and large whisker forms. Stresses were calculated using isotropic diffraction elastic constants.

Residual Stress. Results for the 20 vol.% sample with TWS 100 whiskers are shown in Table I. As expected from the difference in thermal expansion coefficients, and reported elsewhere, the whiskers are in a state of compression and the matrix is in tension. For each reflection of each phase the pressing direction is unique, with less average stress than in the orthogonal directions, which are essentially equivalent. The marked variation in stress magnitude for the same stress component for different reflections indicates that the use of bulk average elastic constants is not justified. The stress values averaged for all reflections of each constituent are shown in Table II. In the Al_2O_3, the stress is highest in the 30 vol.% material, as expected. For the 20 vol.% material, the stresses are higher for the big whiskers. In the SiC, the stress magnitude is highest in the 20 vol.% sample with small whiskers and lowest in the 30 vol.% sample with big whiskers. The stresses between the phases approximately balance in both the x and z directions, i.e. the expression $V_w\sigma_w + V_m\sigma_m = 0$, where w and m are whisker and matrix and V and σ are volume fraction and stress, respectively, does not exceed about 150 MPa.

Peak Breadth. The Al_2O_3 peak breadths are greater in the z than the x direction for both whisker contents and sizes in spite of the fact that the z-direction stresses are lower. Figure 1 shows the results for the small whisker samples. For the SiC, the breadths are generally greater for the small whiskers for both compositions and in both directions. Also, the 111 peak breadths are greater in the x-direction for both compositions and whisker sizes.

Table I. Average Microstresses in the 20 vol.% TWS 100 Sample

Phase	hkl	σ_{xx} (MPa)	σ_{yy} (MPa)	σ_{zz}* (MPa)
Al_2O_3	113	296(5)	299(18)	221(6)
	024	314(9)	325(34)	239(12)
	116	412(4)	416(14)	345(4)
	300	214(2)	228(8)	141(3)
SiC	111	-1126(14)	-1148(60)	-933(17)
	220	-1066(4)	-1030(19)	-894(6)
	311	-1180(4)	-1120(15)	-1094(5)

* Pressing direction.
** Standard deviations due to counting statistics in parentheses.

Table II. Averaged Stress Values for All Samples

Phase	Volume %	Whiskers	σ_{xx} (MPa)	σ_{yy} (MPa)	σ_{zz} (MPa)
Al_2O_3	20	TWS 100	200	197	103
	30	TWS 100	461	460	324
	20	TWS 400	309	317	237
	30	TWS 400	403	464	319
SiC	20	TWS 100	-1330	-1334	-1244
	30	TWS 100	-1148	-1117	-1127
	20	TWS 400	-1124	-1099	-974
	30	TWS 400	-1056	-1037	-937

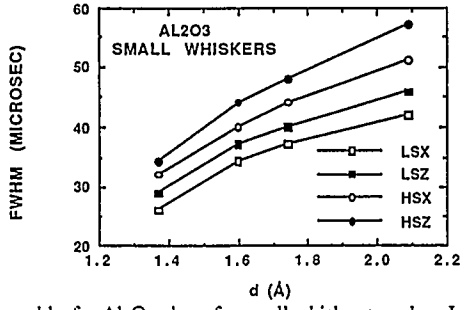


Fig. 1 Peak breadths for Al_2O_3 phase for small whisker samples. L,H is 20 and 30 vol.%, S is small whiskers, and X,Z are x- and z-directions, respectively.

INSTRUMENT USED:	DATE OF REPORT:	EXPERIMENT NO:
GPPD	September 1993	D1992

TITLE: Characterization of Residual Stresses in Metal-Ceramic Composite Compressor Rotors

AUTHORS AND AFFILIATIONS: D. S. Kupperman (ET Div., ANL), J. S. McPhee (Allison Gas Turbines), J. W. Richardson, Jr. (IPNS)

DATES OF EXPERIMENT: December 17-18, 1992

CHECK ALL APPLICABLE BOXES:

- [ ] APPROVED BY PROGRAM COMMITTEE
- [x] INSTRUMENT SCIENTIST ALLOCATION
- [ ] DO NOT PUBLISH
- [ ] PROPRIETARY RESEARCH
- [ ] PRT ALLOCATION

EXPERIMENTAL REPORT (or Abstract of Publication)

Allison Gas Tubines (AGT) has developed a highly advanced experimental aircraft engine which utilizes integrally bladed, reduced weight compressor rotors. This engine design offers a longer powerplant hot-section life and up to 30% weight reduction. The low weight, high-strength rotors are fabricated from silicon carbide-reinforced titanium metal matrix composite materials (see Figure 1 for a schematic representation of the composite components). Conventional jet engine rotors are manufactured from nickel-based metallic alloys. State-of-the-art developments in jet engine design, however, have revealed that enhancements in strength and heat-resistance can be realized with the use of metal-ceramic composites. The most critical impact of the use of composite materials is the corresponding increase in engine thrust to weight ratio. AGT's design makes extensive use of innovative materials in compressor rotors as well as in combustors and fuel nozzles.

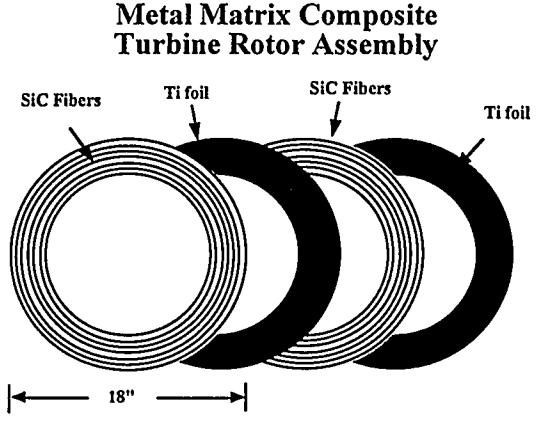


Figure 1. Schematic drawing of Ti - SiC composite rotor.

Integral to the development of this new technology is increased understanding of the physical properties of the composite material itself. Of particular concern are measures of the magnitude and

EXPERIMENTAL REPORT (CONTD.)

orientation of residual stresses developed during fabrication of the composite rings. Neutron diffraction is the only non-destructive analytical technique capable of providing the necessary data required to optimize design and fabrication criteria.

The composite materials of interest are composed of a two-phase titanium metal - silicon carbide ceramic mixture. For the neutron diffraction measurements, the rotor was mounted on a device used for positioning the sample in the neutron beam and rotated at 1 rpm, in order to sample over the entire assembly. With the SiC fibers oriented 45° to the incident beam, a single diffraction experiment (Figure 2) simultaneously measured residual strains in all phases present, in a number of orientations between axial and transverse. Because the Ti phase is non-cubic, this experiment was able to probe another degree of anisotropy, namely the difference in response of basal and axial reflections to residual stress.

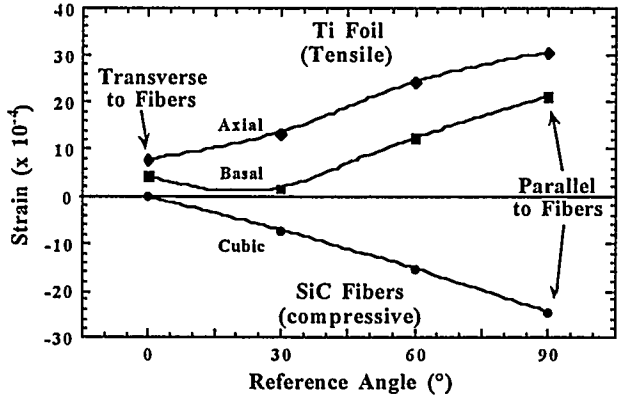


Figure 2. Measured residual strain in Ti - SiC composite rotor as a funtion of orientation relative to the SiC fiber axis.

INSTRUMENT USED:	DATE OF REPORT:	EXPERIMENT NO:
GPPD	June 1995	P1994

TITLE: Residual Strain in High Temperature Superconducting Tapes Measured by Neutron Diffraction

AUTHORS AND AFFILIATIONS: D. S. Kupperman (ET Division, ANL)
J. W. Richardson, Jr. (IPNS Div., ANL)
R. L. Hitterman (MSD Div., ANL)

DATES OF EXPERIMENT: Oct. 14-15, 1994 and Nov. 8-10, 1994

CHECK ALL APPLICABLE BOXES:

- [ ] APPROVED BY PROGRAM COMMITTEE
- [ ] INSTRUMENT SCIENTIST ALLOCATION
- [ ] DO NOT PUBLISH
- [x] PROPRIETARY RESEARCH
- [ ] PRT ALLOCATION

EXPERIMENTAL REPORT (or Abstract of Publication)

Differences in coefficients of thermal expansion of the constituents of a composite lead to residual stresses. The situation for the high temperature ceramic composite superconductor Bi–2223/Ag, in the form of a tape, is particularly complex because of the geometry and anisotropy of the superconductor. The thermal expansion of Ag ranges from 19 to 23 x 10–6 $°C^{-1}$. The thermal expansion coefficient for Bi–2223 is 14–24 x 10–6 $°C^{-1}$, with the greater expansion associated with the c axis (the expansion in the c–axis direction is ≈1.7 times that of the a–axis direction). It is difficult to predict even the sign of the residual stresses in the Ag or Bi–2223. We have measured by neutron diffraction the average strains in the Ag and BSCCO in various crystallographic directions. These data provide an experimental answer to the questions regarding magnitude and sign of fabrication–induced residual strain and provide data for validating models that are used to predict residual stresses.

For this experiment, a bundle of tape sections provided by ASC (each section was 100 μm thick and 20 mm long) filled a volume of about 10 mm in diameter and 20 mm high. The diffraction peaks were very sharp. The strains for various directions for the Ag and Bi–2223 are shown in Fig. 1. Ag tapes and Bi–2223 powder were used as references. The Ag strain is clearly tensile (up to 0.1%), whereas strains in the Bi–2223 are predominantly compressive for the c–axis directions and slightly tensile for directions in the a–b plane. The error in strain is ±0.02%. Experiments could also be carried out at elevated temperatures to establish the strain–free temperature and to study the formation of liquid phase.

EXPERIMENTAL REPORT (CONTD.)

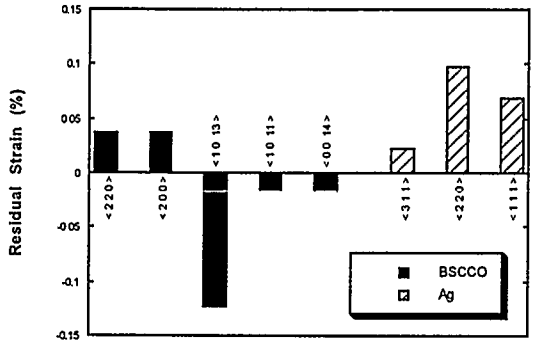


Fig. 1 Residual strains in Bi–2223/Ag monofilament supplied by ASC.

INSTRUMENT USED:	DATE OF REPORT:	EXPERIMENT NO:
GPPD	Nov. 21, 1995	2152

TITLE: Modification of Residual Stresses in Advanced Composites

AUTHORS AND AFFILIATIONS:
D. S. Kupperman, ET Div. ANL
R. C. Birtcher, MSD Div., ANL

DATES OF EXPERIMENT:
Jun. 19-21, 1995

CHECK ALL APPLICABLE BOXES:

- [x] APPROVED BY PROGRAM COMMITTEE
- [ ] INSTRUMENT SCIENTIST ALLOCATION
- [ ] DO NOT PUBLISH
- [ ] PROPRIETARY RESEARCH
- [ ] PRT ALLOCATION

EXPERIMENTAL REPORT (or Abstract of Publication)

Changes in the residual strain within ceramic/ceramic composites are being determined following room temperature neutron irradiation at IPNS. The residual strains are determined from neutron diffraction measurements on the GPPD. The systems under study are 10 and 20% SiC fibers in SiN and SiN fibers in Al_2O_3. A single irradiation has been completed and a second is underway. After the first irradiation, strain in the SiN matrix increased and the strain in the SiC fibers increased. These changes are believed to be driven by a large volume change in SiC produced when it is amorphized by irradiation. The strain in the SiN fibers in Al_2O_3 decreased after irradiation. The next irradiation step should generate greater changes in the lattice parameters and larger volume fractions of amorphous material that will be possible to resolve.

INSTRUMENT USED:	DATE OF REPORT:	EXPERIMENT NO.:
GPPD	June 14, 1993	1571

TITLE:
Oxonium ion substitution in the crystal structure of alunite

AUTHORS AND AFFILIATIONS:
George A. Lager, University of Louisville; Roger Stoffregen, AWK Consulting Engineers

DATES OF EXPERIMENT:
October 15-17, 1992

CHECK ALL APPLICABLE BOXES:

- [x] APPROVED BY PROGRAM COMMITTEE
- [ ] INSTRUMENT SCIENTIST ALLOCATION
- [ ] DO NOT PUBLISH
- [ ] PROPRIETARY RESEARCH
- [ ] PRT ALLOCATION

EXPERIMENTAL REPORT (or Abstract of Publication)

The following abstract was published in the Programs and Abstracts, American Crystallographic Association Meeting, Albuquerque, New Mexico, PA10, p. 80, 1993.

CRYSTAL STRUCTURE OF ALUNITE AS A FUNCTION OF TEMPERATURE. G. A. Lager, Department of Geography and Geosciences, University of Louisville, Louisville, KY 40292, R. E. Stoffregen, AWK Consulting Engineers, Turtle Creek, PA 15145, and J. W. Richardson, Jr., IPNS Division, Argonne National Laboratory, Argonne, IL 60439.

The crystal structure of synthetic alunite, $KAl_3(SO_4)_2(OD)_6$, has been refined from time-of-flight neutron-powder-diffraction data collected at 298 and 12 K, and at 298 K, after heating the sample in air at 673 K for 1 h. The objective of the study was to confirm the $D_3O^+ \Leftrightarrow K^+$ substitution, proposed on the basis of chemical and spectroscopic data, and to investigate the mechanism of dehydration. The sample was synthesized from a deuterated solution of K_2SO_4 and anhydrous $Al_2(SO_4)_3$ heated at a temperature of ~ 423 K for 4 d. Thermal gravimetric analyses of unheated alunite detected structurally-incorporated "water" in excess of the stoichiometric amount. This weakly-bound non-OH water (~ 6 wt% H_2O) is released rapidly between 473 and 673 K. A significant amount of OH water (~ 4 wt%) is also released in this temperature range, resulting in the breakdown of the alunite structure and the formation of $KAl(SO_4)_2$ as a second phase [30% mole fraction] in the heated sample. Rietveld refinements in space group R3m yielded the following agreement factors [R_{wp} (%)] and unit-cell parameters [a, c (Å)]: 298 K (unheated): 6.86, 7.0117 (1), 17.1631 (4); 12 K : 8.54, 7.0013 (1), 17.0736 (5); 298 K (heated): 4.74, 6.9755 (1), 17.3480 (3). The decrease in temperature to 12 K and loss of non-OH water at 673 K both have the effect of distorting the structure from the pseudocubic symmetry observed in unheated alunite at 298 K. One of the major structural changes in alunite after heating is a distortion of the sulfate tetrahedron, caused primarily by the translation of the S atom toward the apical O(1) atom. Initial attempts to locate the D_3O^+ ion by difference Fourier methods have been unsuccessful.

INSTRUMENT USED:	DATE OF REPORT:	EXPERIMENT NO.:
GPPD	1/29/95	1934

TITLE: Structure of the Heavy Fermion Compounds $CeCu_{2+x}Si_2$, $CePt_{2+x}$ and $YbInCu_4$

AUTHORS AND AFFILIATIONS: Jon Lawrence, UC Irvine; George Kwei, Livermore; Zachary Fisk, Florida State; Joe Thompson, Los Alamos

DATES OF EXPERIMENT: 12/8 - 12/10/94

CHECK ALL APPLICABLE BOXES:

- [x] APPROVED BY PROGRAM COMMITTEE
- [ ] INSTRUMENT SCIENTIST ALLOCATION
- [ ] DO NOT PUBLISH
- [ ] PROPRIETARY RESEARCH
- [ ] PRT ALLOCATION

EXPERIMENTAL REPORT (or Abstract of Publication)

$YbInCu_4$: Older low resolution x-ray studies suggest that this material has an isostructural phase transition, analogous to the α-γ transition in Ce metal. However, the transition temperature is not highly reproducible, and many samples have two transitions. Our goal was to verify that the transition is indeed isostructural, and to determine any differences between two samples: A, which had one transition, and B, which had two. We refined in the expected C15B structure; we constrained the Cu site occupancy to unity and allowed the Yb and In occupancies to vary (random distribution over the two sites corresponds to disordered C15, a plausible structure). The results are:

	a_0(Å)	f(In)	f(Yb)	σ	Wrp
	Sample A (T_c = 40K):				
20K	7.1359	1.060	0.973	89	0.0793
55K	7.1264	1.042	0.960	45	0.0767
	Sample B (T_c = 40 and 70K):				
20K	7.1293	1.083	0.928	164	0.0883
55K	7.1258	1.095	0.924	70	0.0802
100K	7.1246	1.093	0.933	136	0.0812

This confirms that the transition is isostructural. The site occupancies are closer to unity for sample A than for sample B; averaging these over temperature, accounting for scattering lengths and assuming complete occupancy of each site we arrive at stoichiometries $(Yb_{0.95}In_{0.05})(In_{0.97}Yb_{0.03})Cu_4$ for A and $(Yb_{0.89}In_{0.11})(In_{0.96}Yb_{0.04})Cu_4$ for B. This result suggests that the existence of multiple transitions is associated with greater site disorder. The larger R factors, and strain parameters σ for sample B reflect a substantially larger linewidth in this sample; indeed, it is probable that this reflects a spread of lattice constants, with both T_c and a_0 varying with varying site occupancy in the powder sample. The Los Alamos group has very recently been able to grow large quantities of small single crystals of $YbInCu_4$ which show a single transition at 40K; as a next step we would like to perform diffraction on a powder of these crystals to see whether they have more perfect order than sample A.

$CeCu_{2+x}Si_2$: Samples with excess Cu are heavy fermion superconductors; those with Cu deficiency are normal. The issue for our experiment was to determine any structural differences between two such samples. We took data at 20K, refining lattice constants, Si site positions (0,0,z), and relative site occupancies (with the Si site occupancy fixed at 1) in the tetragonal $ThCr_2Si_2$ crystal structure. The results are as follows:

A-$CeCu_{1.94}Si_2$: a_0 = 4.0860Å; c_0 = 9.9149Å; z(Si) = 0.3797;
f(Ce) = 0.999; f(Cu) = 0.997; f(Si) = 1; wRp = 0.0674
B-$CeCu_{2.10}Si_2$: a_0 = 4.0855Å; c_0 = 9.9147Å; z(Si) = 0.3795
f(Ce) = 1.005; f(Cu) = 1.003; f(Si) = 1; wRp = 0.0714

The scattering lengths (0.484, 0.772, 0.415 for Ce, Cu, Si respectively) are folded into the stated values of f, so that the site occupancies for A imply a stoichiometry $CeCu_{1.99}Si_2$; those for B could occur if 0.3% of the Ce sites were occupied by Cu, as per the formula $[Ce_{0.997}Cu_{0.003}]Cu_2Si_{1.994}$ which in terms of stoichiometry is $CeCu_{2.01}Si_2$. The Cu excess or deficiency measured in the experiment is clearly much smaller than expected on the basis of the stoichiometry of the melt. For B it is plausible that excess Cu forms in the grain boundaries; for our noise level, such a small Cu excess might not be detected, especially if the Cu occurs as very small crystallites. The new $LuNi_2B_2C$ superconductors form in the $ThCr_2Si_2$ structure, with the difference that the C atoms occupy the (1/2,1/2,0) site; so it is also plausible that excess Cu could go to this site, which we intend to test for by performing Fourier maps. Overall, the structural differences are very small; the lattice parameters and Si position differ only by a few parts in 10^{-4}, and the site occupancies are essentially unity; it remains unclear what such small differences have to do with superconductivity.

$CePt_{2+x}$: The recent discovery of evidence for 4f dispersion in photoemission studies of this compound has rekindled interest in the structure. Older low resolution x-ray experiments suggest that this compound grows for $0 \le x \le 1$ in the C15 Laves phase, with the Ce on a diamond lattice. We took data for $CePt_{2.5}$ at 20K. We refined in the C15B (F-43m) structure (the same as for $YbInCu_4$), assuming partial Pt occupancy of the Ce(1) site (the (000) sublattice) but only allowing Ce occupancy on the Ce(2) site (the (1/4,1/4,1/4) sublattice). We obtained good fits with the following parameters:

a_0 = 7.671Å; wRp = 0.0665;
f(Ce(1)): 0.683 Ce, 0.316 Pt; f(Ce(2)): 0.869 Ce; f(Pt(3)): 1 (constrained)

These occupancies correspond to a stoichiometry $CePt_{2.8}$ rather than that of the melt ($CePt_{2.5}$), suggesting absence of 10% of the Ce; there is no evidence for Ce segregation in the spectra, however. Given the scattering lengths (b = 0.484, 0.950 for Ce, Pt respectively) it is unlikely that there is any Pt on the Ce(2) site or any Ce on the Pt(3) site; this strengthens the case that the actual structure is C15B. Despite the reasonable R value for this structure, the small Ce(2) occupancy suggests problems with the refinement, which could perhaps be resolved by a more systematic study as a function of Pt excess x.

INSTRUMENT USED: GPPD	DATE OF REPORT: November 1, 1995	EXPERIMENT NO.: 2031

TITLE:
Structure of the Heavy Fermion Compounds $CeCu_{2+x}Si_2$ $CePt_{2+x}$ and $YbInCu_4$

AUTHORS AND AFFILIATIONS: Joe Thompson, Los Alamos Ntl. Lab
Jon Lawrence, UC Irvine; George Kwei, Livermore Ntl. Lab; Zachary Fisk, Florida State Univ.

DATES OF EXPERIMENT:
June 11-14, 1995

CHECK ALL APPLICABLE BOXES:

- [X] APPROVED BY PROGRAM COMMITTEE
- [ ] INSTRUMENT SCIENTIST ALLOCATION
- [ ] DO NOT PUBLISH
- [ ] PROPRIETARY RESEARCH
- [ ] PRT ALLOCATION

EXPERIMENTAL REPORT (or Abstract of Publication)

Experiment 2031 was a continuation of Experiment 1934; the objective was to characterize the structure of three heavy fermion compounds, $YbInCu_4$, $CePt_{2+x}$ and $CeCu_2Si_2$, via Reitveld refinement of the structure, based on diffraction data obtained on GPPD.

$YbInCu_4$: This has a valence transition at 40K analogous to the α-γ transition in cerium metal. In Expt 1934 we established3 that, while the lattice constant changes discontinuously by 0.15% at the transition, the C15B structure does not change. A second issue concerns the relationship between the degree of site disorder on the Yb and In sites and the temperature and sharpness of the transition. For Expt. 1934 we had studied two samples grown as polycrystals, establishing that a sample with a sharp transition at 40K had less site disorder than the sample with a higher temperature transition. For Expt. 2031 we studied a sample formed by powdering a set of flux-grown single crystal samples. We found that the single crystal samples had the least relative site disorder (f(In) - f(Yb) = 0.06, compared to 0.09 and 0.16 in the polycrystals). This shows that the process of flux growth does not lead to serious discrepancies in occupation, but indeed yields the most highly ordered samples, as well as the sharpest 40K transitions.

In performing these refinements, we also allowed the thermal factors to vary. Before publishing, we intend to perform a few more refinements, comparing the site occupancies obtained for the different samples when the thermal factors for each site are fixed at the same values for all three samples.

$CeCu_2Si_2$: This is a heavy fermion superconductor, where superconductivity at T_c = 0.6K occurs only for excess Cu in the starting composition, i.e. for $CeCu_{2+x}Si_2$. The idea was to determine what structural differences exist for superconducting and non-superconducting samples. Unfortunately, in Expt. 1934 we had inadvertantly studied two samples both of which contained copper deficiency (x = -0.08 and -0.05). For Expt. 2031, we studied a sample with x = 0.34, and we also established by a.c. susceptibility that only the latter sample had a sharp transition at T_c = 0.6K, while the two other samples had degraded transitions at lower temperatures. Allowing thermal factors to vary in the refinements, we find the following values for site occupancies (relative to a Si site occupancy of 1):

$CeCu_{2.3}Si_2$ f(Ce) = 0.984 f(Cu) = 1.000
$CeCu_{1.95}Si_2$ f(Ce) = 1.009 f(Cu) = 1.007

$CeCu_{1.92}Si_2$ f(Ce) = 1.004 f(Cu) = 1.001

In addition, for x = 0.3, fcc Cu exists as a second phase with approximately the correct phase fraction to correspond to $CeCu_2Si_2$ + 0.3Cu. Given the small observed differences, it appears that the structural differences may be too subtle to be determined in this manner.

As a final stage of analysis, we intend to 1) perform more refinements holding the thermal factors at the same values for all three samples, to get a better idea of the relative variations of the site occupancies; 2) include possible second phases (e.g. $CeSi_2$) for the copper deficient samples; and 3) use Fourier maps to study occupancy at other locations in the unit cell.

$CePt_{2+x}$: These C15 compounds appear to form for all x on the interval $0 \leq x \leq 1$. The compounds are of interest, due to recent photoemission experiments which give evidence for dispersion of the 4f levels. Our intent is to determine where the excess Pt goes: whether it goes randomly onto both the (0,0,0) and (1/4,1/4,1/4) Ce sublattices (disordered C15) or preferentially onto only one sublattice (disordered C15B). In Expt. 1934, we had studied only x = 0.5; for Expt 2031 we studied also x = 0, 0.25 and 3. We find that for all four samples the structure refines equally well, with R values approximately equal 2, under one of three assumptions: C15 with stoichiometry constrained to the nominal value; and either C15 or C15B with the stoichiometry unconstrained. For the latter cases the refinements give Pt occupancies which differ by as little as 5% to as much as 20% from the nominal value.

To choose between these alternatives we intend to perform electron microscopy on the samples to put better constraints on the actual stoichiometries.

INSTRUMENT USED: GPPD	DATE OF REPORT: 2 Dec 1993	EXPERIMENT NO.: 1837

TITLE: Crystal Structure of ζ-$Pu_{0.6}U_{0.4}$

AUTHORS AND AFFILIATIONS: A. C. Lawson, J. A. Goldstone, B. Cort, R. Martinez and T. Zocco, LANL, and J. W. Richardson, Jr., and M. H. Mueller, ANL

DATES OF EXPERIMENT: 14-21 July 1993

CHECK ALL APPLICABLE BOXES:

- ☐ APPROVED BY PROGRAM COMMITTEE
- ☒ INSTRUMENT SCIENTIST ALLOCATION
- ☐ DO NOT PUBLISH
- ☒ PROPRIETARY RESEARCH
- ☐ PRT ALLOCATION

EXPERIMENTAL REPORT (or Abstract of Publication)

We performed neutron diffraction experiments on GPPD at several temperatures on ζ-phase $Pu_{0.6}U_{0.4}$. (Fig. 1). In agreement with the x-ray results of Ellinger et al. [1], the structure is rhombohedral with a large unit cell. The density measurements of Ellinger et al. [1] show that there are 58 atoms in the rhombohedral unit cell.

A structure that meets these criteria is necessarily complex. We successfully fit our diffraction data with a centric structure (space group $R\bar{3}m$) that has 10 atoms in the assymetric unit. The atomic positions that we found are given in Table 1, and they are independent of temperature. The interatomic distances are quite reasonable. Because of the small difference of their scattering lengths, we were unable to detect any atomic ordering between Pu and U. The lattice constants have an intriguing temperature dependence, as shown in Fig. 2. The hexagonal unit cell of the structure is shown in Fig. 3; it is a stacking variant of the α-manganese structure. The complexity of this structure is consistent with the general behavior of the light actinides.

We also obtained data on the η-phase. It appears to be isomorphous with the η-phase in the Pu-Np system [2,3], but we have so far been unable to solve the structure.

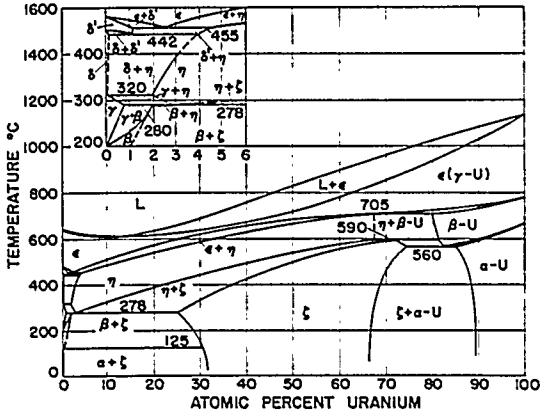


Fig. 1. Plutonium-uranium phase diagram.

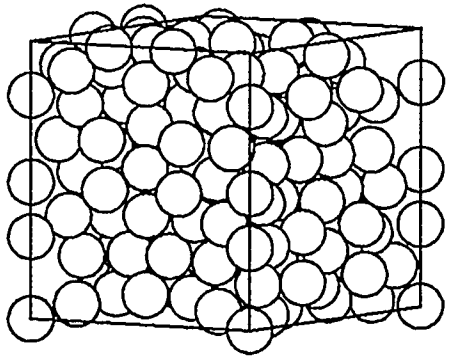


Fig. 3. Hexagonal unit cell of ζ-phase $Pu_{0.6}U_{0.4}$.

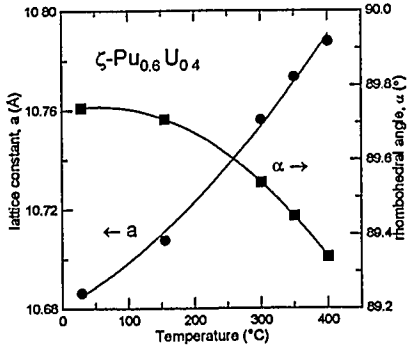


Fig. 2. Rhombohedral lattice constants of ζ-phase $Pu_{0.6}U_{0.4}$.

Table 1 - Atom Positions for ζ-$Pu_{0.6}U_{0.4}$ ($R\bar{3}m$)

atom	x	y	z	sym
Pu(1)	0.18301(30)	0.0000000(0)	0.0000000(0)	2(100)
Pu(2)	0.79609(15)	0.59219(29)	0.00741(20)	M(100)
Pu(3)	0.46215(15)	0.92431(29)	0.04064(20)	M(100)
Pu(4)	0.3333330(0)	0.6666670(0)	0.06830(35)	3M(100)
Pu(5)	0.80332(28)	0.40166(14)	0.08046(20)	M(010)
Pu(6)	0.65232(17)	0.64460(21)	0.09010(14)	1
Pu(7)	0.0000000(0)	0.0000000(0)	0.0974(4)	3M(100)
Pu(8)	0.23790(15)	0.47580(31)	0.13118(22)	M(100)
Pu(9)	0.12549(15)	0.25098(31)	0.13178(18)	M(100)
Pu(10)	0.88351(15)	0.76701(30)	0.15097(19)	M(100)

References

[1] F. H. Ellinger, R. O. Elliott and E. M. Cramer, "The Plutonium-Uranium System," J. Nucl. Matrer. 1 233-243 (1959).

[2] A. C. Lawson, J. A. Goldstone, J. Vaninetti, D. Eash, R. Martinez, J. Archuleta, B. Cort, R. O. Elliott, M. Stevens, R. Hitterman and J. Faber, "Neutron Diffraction Study of η-$Pu_{0.90}Np_{0.10}$," IPNS Progress Report 1988-1990, Argonne National Laboratory (1990) p 27.

[3] J. A. Goldstone, A. C. Lawson and B. Cort, "Thermal Expansion of η-$Pu_{0.90}Np_{0.10}$," LANSCE Experiment Reports, 1992 Run Cycle, Los Alamos National Laboratory, LA-12647-PR, p. 80.

INSTRUMENT USED: GPPD	DATE OF REPORT: 11 January 1995	EXPERIMENT NO 2013

TITLE: Residual Strains in Ag-Cu In-situ Composites (Preliminary Results)

AUTHORS AND AFFILIATIONS: A. C. Lawson and M. F. Stevens--LANL; J. Wood and J. D. Embury--McMaster University; J. W. Richardson, Jr.--ANL

DATES OF EXPERIMENT: 20 and 24 October 1994

CHECK ALL APPLICABLE BOXES:

- ☐ APPROVED BY PROGRAM COMMITTEE
- ☐ PROPRIETARY RESEARCH
- ☒ INSTRUMENT SCIENTIST ALLOCATION
- ☐ PRT ALLOCATION
- ☐ DO NOT PUBLISH

EXPERIMENTAL REPORT (or Abstract of Publication)

The deformation and strengthening of high-strength, two-phase wires and sheet is a highly complicated subject that is of great interest to both the metals-working industry and to the mechanical metallurgist. Perhaps most fascinating about these materials is the fact that strength levels greater than twice the expected "rule of mixtures" values can be realized. The debate concerning which strengthening mechanisms are operable at strains of *up to ten* has not resulted in a consistent picture of microstructural processes that can explain such effects. Although alignment of the second phase, substructural dislocation structures and dislocation obstacles (Orowan strengthening) have all been mentioned as possible strengthening mechanisms, it is clear that none by itself is sufficient to fully explain the levels achieved in many systems.

One important hypothesis that may help explain the synergistic strengthening achieved in two-phase materials is the storage of cold work and concomitant elastic energy at the interfacial regions of such alloys. The accumulation of dislocations in such regions may be responsible for increasing the effective surface energy of second phase obstacles to dislocation motion, thus increasing the angle to which dislocations would need to bow between obstacles before shearing them or generating loops. At the same time, second phase particles can contribute to the work hardening of the matrix by the transfer of elastic stresses to them. Both of these related processes can be probed through the use of neutron diffraction methods, where highly accurate measurements of strain can be made in embedded phases.

One system which has received much research attention regarding *in situ* composite strengthening is copper-silver. The special interest in this alloy class is for both high-strength and high-conductivity wire and sheet for pulsed magnetic field generation. Cu and Ag both have the fcc structure, but because of the large difference in lattice constants, the equilibrium structure of AgCu alloys is a two-phase lamellar mixture over a large portion of the composition range. The lattice constants from the literature are shown in Fig 1. We have used GPPD to make a preliminary study of residual strains in highly deformed two phase $Ag_{0.16}Cu_{0.84}$ alloys. The samples were cylinders of 3/16" diameter and 1.75" length that were machined from larger drawn specimens. The dimensions were carefully controlled to minimize systematic error, especially that arising form absorption. Measurements were made in sample directions parallel and perpendicular to the drawing stress, but no significant directional difference was found. The longitudinal strains are shown in Fig. 2. They are extremely large: about 2500 microstrain for Ag, and 4000 for Cu!

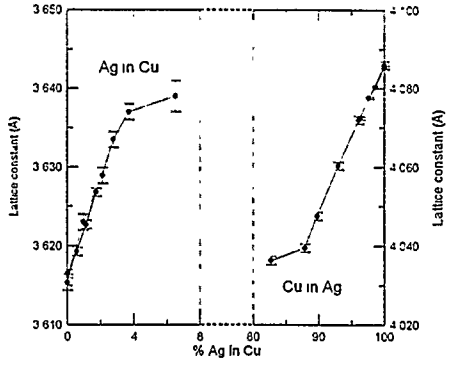


Fig. 1. Equilibrium lattice constants in the Ag-Cu system

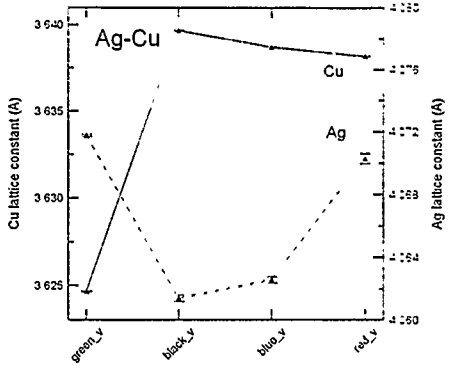


Fig. 2. Measured lattice constants of Ag-Cu *in situ* composites.

Knowledge of the bulk residual strains is very important for constraining models of the stress distribution. Accordingly, it would be of great interest to extend these measurements to samples with a greater range of imposed strains, so that the development of these distributions can be understood in greater detail. These measurements are essential to support the modeling effort that is underway on the mechanical properties of these materials.

J. Wood, PhD Thesis, MacMaster University, 1995.

INSTRUMENT USED:	DATE OF REPORT:	EXPERIMENT NO.:
GPPD	15 July 1992	1132

TITLE: Crystal Structure of δ' - Plutonium

AUTHORS AND AFFILIATIONS:
A.C. Lawson, J. Vaninetti, J. A. Goldstone, B. Cort, and J. W. Richardson (ANL)

DATES OF EXPERIMENT:
20-22 Feb 1990

CHECK ALL APPLICABLE BOXES:

- [X] APPROVED BY PROGRAM COMMITTEE
- [ ] INSTRUMENT SCIENTIST ALLOCATION
- [ ] DO NOT PUBLISH
- [ ] PROPRIETARY RESEARCH
- [ ] PRT ALLOCATION

EXPERIMENTAL REPORT (or Abstract of Publication)

During the course of powder diffraction study of the various phases of plutonium[1], we found some peculiarities in the pattern of δ'-Pu. The structure of this phase is known to be body-centered tetragonal[2], and it is an intermediate between the fcc d-phase and the bcc ε-phase. (See Fig. 1.) Our refinement of the δ'-phase was rather poor, even though the refinements of the neighboring δ- and ε-phases were of very good quality. Unfortunately the counting statistics were not good enough to reveal the source of difficulty, and the present experiment was designed to collect high-quality data on δ'-Pu. The experiment was carried out at 465°C and was a technical success.

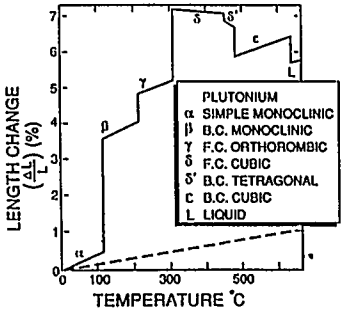


Fig. 1. Length Changes for the phases of Pu metal

The improved data did not show any distinctly new structural features, but we did find that some of the diffraction peaks were significantly shifted or broadened. The results of the peak analysis are shown in Figs. 2 and 3. Such broadening and shifting phenomenon are often symptomatic of stacking faults, and faulting would perhaps be expected in a transitional phase like δ'-Pu. We tried to develop a model along the lines of the usual model for stacking faults in fcc metals[3], but we have so far been unsuccessful in explaining our observations. Efforts to analyze these data are continuing.

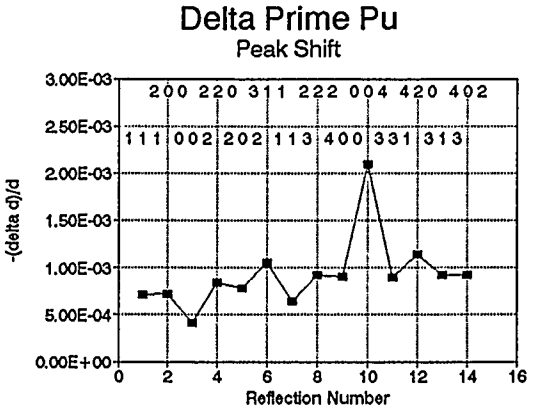


Fig. 2. Peak shifts for δ'-plutonium.

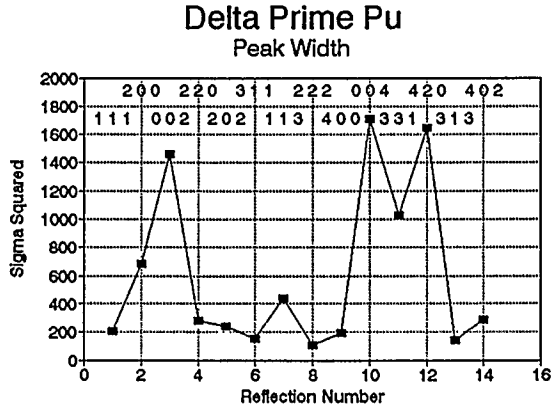


Fig. 3. Peak widths for δ'-plutonium.

[1] A. C. Lawson, B. Cort, J. A. Goldstone, D. Wozniak, R. L. Hitterman and J. W. Richardson, "Diffraction Studies of Plutonium Metal," IPNS Progress Report 1986-1988, Argonne National Laboratory (November 1988) p 50.

[2] J. Donohue, *The Structures of the Elements*, (New York, Wiley, 1974) p. 166.

[3] A. Guinier, *X-Ray Diffraction* (San Francisco, Freeman, 1963) pp 226-237.

INSTRUMENT USED:	DATE OF REPORT:	EXPERIMENT NO.:
GPPD	4 June 93	1622

TITLE:
Debye-Waller Temperatures of $MoSi_2$

AUTHORS AND AFFILIATIONS: A. C. Lawson, G. H. Kwei and J. J. Petrovic (LANL)
and J. W. Richardson, Jr., and R. L. Hitterman (ANL)

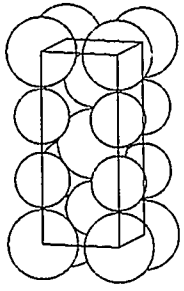
DATES OF EXPERIMENT:
19-21 February 1993

CHECK ALL APPLICABLE BOXES:

- [x] APPROVED BY PROGRAM COMMITTEE
- [ ] INSTRUMENT SCIENTIST ALLOCATION
- [ ] DO NOT PUBLISH
- [ ] PROPRIETARY RESEARCH
- [ ] PRT ALLOCATION

EXPERIMENTAL REPORT (or Abstract of Publication)

$MoSi_2$ is an intermetallic compound that is finding increasing application in high temperature ceramics [1]. As shown in Fig. 1, it crystallizes in the tetragonal $MoSi_2$ structure with two formula units per cell. We used GPPD to measure the Debye-Waller factors and lattice constants of $MoSi_2$ at 13 temperatures between 10 and 300K.

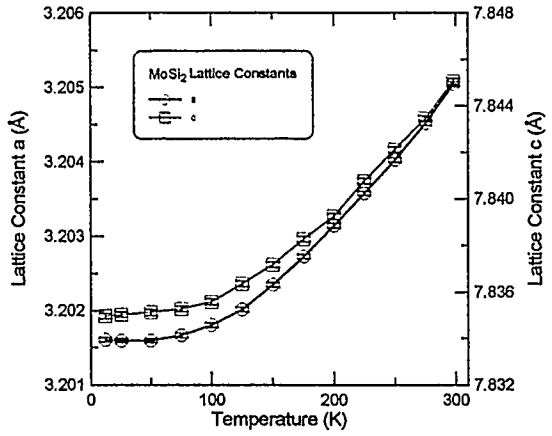


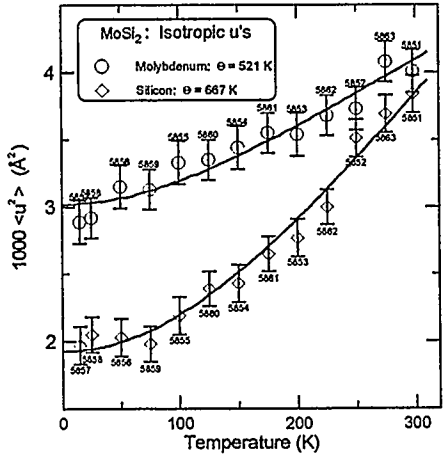
The lattice constants are shown in Fig. 2. The thermal expansion is somewhat anisotropic. Near room temperature the coefficient of thermal volume expansion is $2.0 \times 10^{-5} K^{-1}$.

The mean-square isotopic atomic displacements as determined from refinement of the Debye-Waller factors are plotted versus temperature in Fig. 3. The run numbers are shown as a check for thermal hysteresis. We used GSAS [2] to refine the data with the new Q^2 background function. We fitted the temperature dependence of the thermal factors in the usual way [2] to determine the atomic Debye-Waller temperatures (Θ_{DW}'s) for Mo and Si. The results are shown in the table. The Θ_{DW}'s do not scale with the square root of the atomic mass; this is indicative of strong bonding effects in $MoSi_2$. Attempts to determine the anisotrpies of the Debye-Waller temperatures were frustrated by strong correlations in the refinements.

element	Θ_{DW} (K)	atomic mass (g)
Molybdenum	521 (16)	95.9
Silicon	678 (10)	28.1

EXPERIMENTAL REPORT (CONTD.)





[1] A. K. Vasudevan and J. J. Petrovic, "A Comparative Overview of Molybdenum Disilicide Composites, in High Temperature Structural Silicides, Eds. A. C. Vasudevan and J. J. Petrovic (Elsevier Science Publishers, Amsterdam, 1992).

[2] A. C. Larson and R. B. Von Dreele, Generalized Crystal Structure Analysis System, LAUR 86-748 (1986) Los Alamos National Laboratory.

[3] A. C. Lawson, A. Williams, J. A. Goldstone, D. T. Eash, R. J. Martinez, J. I. Archuleta, D. J. Martinez, B. Cort, and M. F. Stevens, "Elastic Properties of Materials by Pulsed Neutron Diffraction," J. Less-Common Metals 167 353 (1991).

INSTRUMENT USED: GPPD	DATE OF REPORT: 15 Nov 1995	EXPERIMENT NO.: 1623

TITLE: Debye-Waller Temperature and Thermal Expansion of Thorium Metal (10-300K)

AUTHORS AND AFFILIATIONS: A. C. Lawson, B. Cort and F. A. Vigil, LANL, and J. W. Richardson, Jr., ANL

DATES OF EXPERIMENT: 20-21 Oct 1994

CHECK ALL APPLICABLE BOXES:

- ☒ APPROVED BY PROGRAM COMMITTEE
- ☐ INSTRUMENT SCIENTIST ALLOCATION
- ☐ DO NOT PUBLISH
- ☐ PROPRIETARY RESEARCH
- ☐ PRT ALLOCATION

EXPERIMENTAL REPORT (or Abstract of Publication)

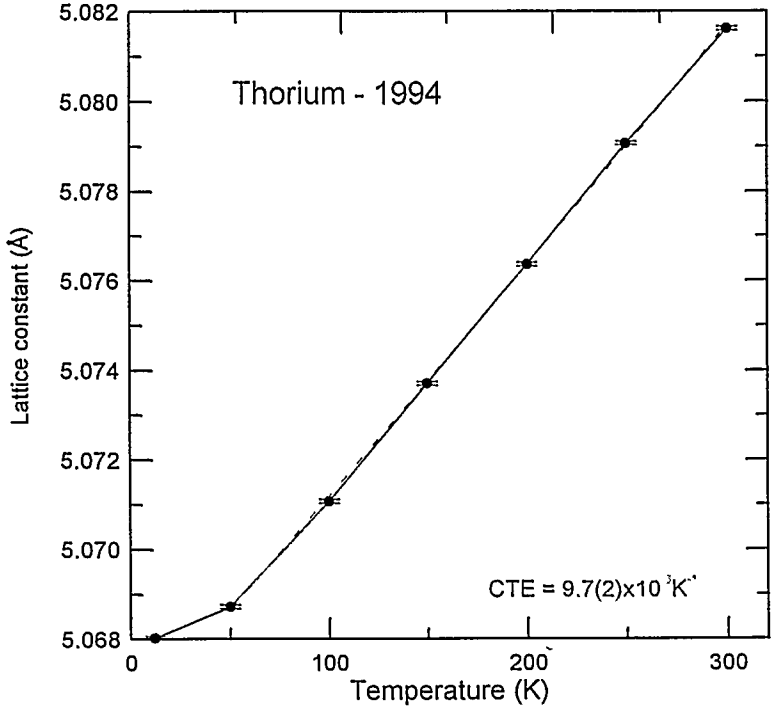


Fig. 1. Lattice constants of thorium metal.

Debye-Waller Temperature and Thermal Expansion of Thorium Metal (10-300K)

We used GPPD to make a neutron diffraction study of thorium metal between 10 and 300K. The specimen comprised several chunks of iodide crystal bar that had been prepared by the van Arkel process; it was doubly encapsulated in vanadium. We obtained diffraction patterns at 7 different temperatures below room temperature and used GSAS to analyze the data. Fig. 1 shows the lattice constants, and fig. 2 shows the thermal factors, each plotted versus temperature. From these data we obtain a linear thermal expansion coefficient of 9.7(2) x 10^{-6} K^{-1} (50 < T < 300 K) and a Debye-Waller temperature of 159(2)K. At low temperatures the Debye-Waller temperature shows no sign of the temperature dependence that is seen in U, Np and Pu; these measurements should be continued to higher temperatures.

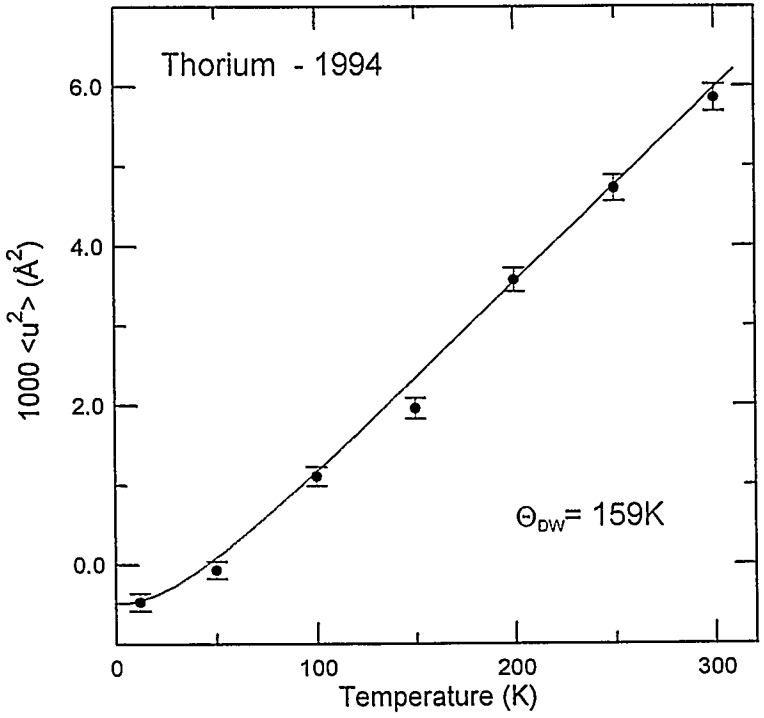


Fig. 2. Debye-Waller factors of thorium metal.

INSTRUMENT USED: GPPD	DATE OF REPORT: 1 Aug 1994	EXPERIMENT NO.: 1741

TITLE: Thermal Expansion and Debye-Waller Factors of ZrC.

AUTHORS AND AFFILIATIONS: A. C. Lawson and D. P. Butt (LANL)
and J. W. Richardson, Jr., and R. L. Hitterman (ANL)

DATES OF EXPERIMENT: 16-21 Nov 1993

CHECK ALL APPLICABLE BOXES:

- [X] APPROVED BY PROGRAM COMMITTEE
- [ ] INSTRUMENT SCIENTIST ALLOCATION
- [ ] DO NOT PUBLISH
- [ ] PROPRIETARY RESEARCH
- [ ] PRT ALLOCATION

EXPERIMENTAL REPORT (or Abstract of Publication)

ZrC_x is an important nuclear fuel material when combined in a solid solution with UC_x. Currently ZrC_x and $U_xZr_{1-x}C_y$ are primary candidates for missions requiring nuclear thermal propulsion, such as human missions to Mars. Understanding the mechanism(s) of diffusion is key to our ability to predict and control life limiting phenomena such as vaporization. Currently we believe that the diffusion of carbon is controlled by a vacancy mechanism, but we do not know the specific path [1]. We believe that there are three possible paths as follows:

- The carbon jumps in the <110> direction to a vacant carbon octahedral site..
- The carbon jumps in the <111> direction to a vacant octahedral site through an unoccupied tetrahedral site in the zirconium sublattice.
- The carbon jumps to a vacant carbon octahedral site through a zirconium vacancy that is associated with the carbon vacancy.

If we can determine the activation energy for vacancy formation, ΔH_v, it may then be possible to determine the rate controlling path by comparing ΔH_v to experimental activation energies for carbon diffusion. Theoretically we can measure ΔH_v using the relationship:

$$\frac{\Delta n}{n} = 3\left(\frac{\Delta l}{l} - \frac{\Delta a}{a}\right)$$

where $\Delta l/l$ and $\Delta a/a$ is the change in length of the crystal (l representing the bulk crystal, and a representing the lattice parameter), and $\Delta n/n$ is to the change in volume. If the change in volume is due to an increased population of vacancies then ΔH_v is equal to the activation energy of the difference $\Delta l/l - \Delta a/a$.

In order to get part of the information we need for the determination of ΔH_v, we measured $\Delta a/a$ of a hot-pressed bulk sample of polycrystalline ZrC_x by neutron powder diffraction on GPPD. The measurements at IPNS were carried out using the Miller furnace with an argon atmosphere. Data sets were collected in 100°C intervals from room temperature to 1300°C (ca. 1600 K). Subsequent additional measurements were made on part of the same sample below room temperature in a Displex refrigerator. The data were analyzed by Rietveld refinement using GSAS.

The lattice constants are shown in Fig. 1. There are two discontinuities in the lattice constant data. The first, at 1200 K, was occasioned by a thermocouple failure. In this case the sample was held overnight at 1200 K, and the experiment was continued with only one of the original two thermocouples. The discontinuity is believed to be a temperature error, estimated to be 23 K. The experiment was terminated by failure of the second thermocouple at 1600K. In this case the sample

was furnace quenched from 1600K to room temperature. The discontinuity with the low temperature experiments is believed to be caused by the difference in geometries between furnace and cryostat as is usually observed. The data above room temperature have been fitted to a quadratic function with allowance for the discontinuity at 1200 K. (The low temperature data are *not* fitted.) We find that the data are represented by $\Delta a/a = 5.85(2)^{-6} K^{-1} T + 7.75(2)x10^{-10} K^{-2} T^2$ (for T in Kelvin). $\Delta l/l$ will be measured on the same sample by conventional dilatometry in the near future, so that ΔH_v can be determined.

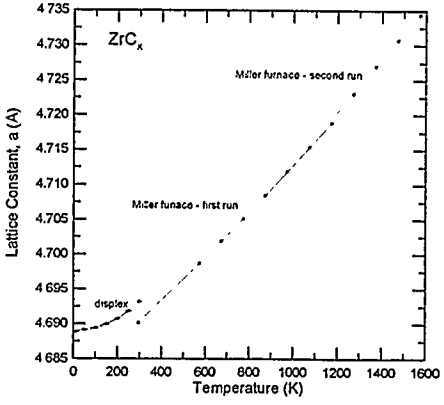


Fig. 1. Lattice constants versus temperature of ZrC.

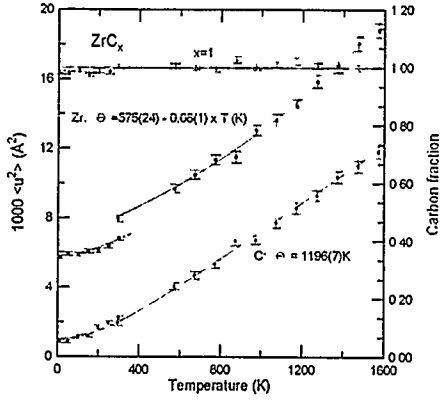


Fig. 2. Carbon fraction and Debye-Waller factors versus temperature of ZrC

We also determined the carbon fraction, x, and the Debye-Waller factors as a function of temperature, as shown in Fig. 2. The vacancy concentration is 1-x, and it is independent of temperature within the precision of the experiment — about 2%. The Debye-Waller temperature of carbon is temperature-independent at 1200K, while the Debye-Waller temperature of zirconium decreases at higher temperatures according to $\Theta_{DW} = 575(24)K - 0.08(1)T$. (In this case the low temperature data *are* fitted.) The mass-weighted average, $[\Sigma m_i\Theta_i^2/\Sigma m_i]^{1/2}$ is 721 K. The available literature values are those calculated from the Lindemann melting criterion: Θ(Zr) = 361 K and Θ(C) = 1370 K [2]; from the calculated phonon spectrum of HfC, checked against low temperature heat capacity: Θ_0(HfC) = 467 K [3]; and from resistivity measurements on ZrC: Θ_R = 647 K [4]. The different behaviors of carbon and zirconium with respect to the *temperature dependence of* Θ_{DW} show that the stability ZrC is determined to some extent by Zr-Zr bonding.

References

[1] R. W. Schmude, Jr., T. C. Wallace, Sr., and D. P. Butt, "Diffusion of Carbon in Zirconium Carbide," J. Nucl. Mat., in preparation.

[2] R. F. Voitovich and N. P. Shakhanova, Porosh. Met. #3(51) 75 (Russ.) 235 (Eng.) (1965).

[3] P. Roedhammer, E. Gmelin and W. Weber, Solid State Commun. *16* 1205 (1975).

[4] F. W. Clinard and P. Kempter, J. Less-Common Metals *15* 59 (1968).

INSTRUMENT USED:	DATE OF REPORT:	EXPERIMENT NO:
GPPD	January 1994	1490

TITLE: Neutron Diffraction Study of Zeolite-A with Occluded Simulated IFR Waste Salt

AUTHORS AND AFFILIATIONS: M. A. Lewis, B. Tani and S. Siegel (CMT Div., ANL), B. R. McCart (Augustana College), J. W. Richardson, Jr. (IPNS Div., ANL)

DATES OF EXPERIMENT: March 25-29, 1992

CHECK ALL APPLICABLE BOXES:

- [x] APPROVED BY PROGRAM COMMITTEE
- [ ] INSTRUMENT SCIENTIST ALLOCATION
- [ ] DO NOT PUBLISH
- [ ] PROPRIETARY RESEARCH
- [ ] PRT ALLOCATION

EXPERIMENTAL REPORT (or Abstract of Publication)

Segregation of cations based on size is observed in samples of zeolite-A loaded with simulated radioactive-waste (~5 wt.% Li, K, Cs and Ba, 1 wt.% Sr and Y, <1 wt.% Na) prepared from chloride salts. In contrast to traditional Na zeolite-A, for which all 8-ring access super (α) cages are identical and situated on a simple FCC lattice, these simulated rad-waste mixtures contain two types of α-cages situated on a NaCl-like lattice. The long range ordering of extra-framework ions is propagated by severe distortion of framework oxygens due to strong coordination with Li.

A sample was prepared by complexing zeolite-A with a ($LiCl$-KCl-$BaCl_2$-$CsCl$-$SrCl_2$) salt mixture resulting in the composition given above. This sample and a sample of synthetic Na zeolite-A were transferred in a dry box to sealed vanadium canisters. Refinement of the Na-A data produced the expected cubic (space group Fm3c) cell with Na^+ cations sited preferentially opposite 6-rings and secondarily off-center in 8-rings. Preliminary interpretation of the mixture data showed, in addition to a sizable 1.5% contraction of the unit cell, the existence of new diffraction lines indicative of lower crystallographic symmetry (see Figure 1). Careful study revealed that the new reflections are of the (hhl): h, l = 2n+1 type and that the correct space group is F432.

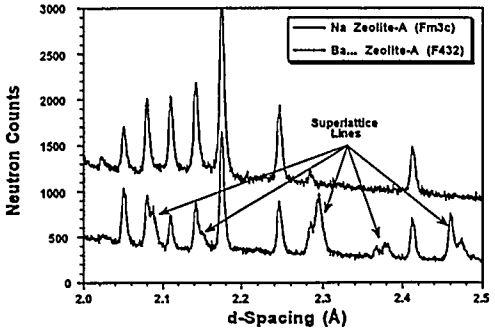


Figure 1. Comparison of section of diffraction patterns of Na-A and rad-waste zeolite-A

EXPERIMENTAL REPORT (CONTD.)

The two distinct α cages were labeled α_1 and α_2, and the single sodalite cage is labeled β. Predominant characteristics of the structural model are as follows: (1) Li^+ ions are strongly coordinated to all eight 6-rings of cage α_1, (2) a complex Li^+-K^+-Cl^- cluster "decorates" the α_1 cage surface, (3) 6-ring sites in the α_2 cage are alternately occupied by Ba^{2+}/Cs^+ and pairs of Li^+ ions, (4) Cl^- ions link the Ba^{2+}/Cs^+ and Li^+ ions, (5) Sr^{2+} is situated opposite a 6-ring, inside the β cage and (6) Li^+ ions are associated with 4-rings, in the β cage. Representative illustrations are given in Figure 2. In Figure 2a, from darkest to lightest, the extra-framework atoms are 6 Li^+ in six-rings, 6 K^+ near eight-rings, 6 Li^+ near four-rings and 6 Cl^- bridging Li^+'s and K^+'s. In Figure 2b, darkest to lightest ions are Li^+, Ba^{2+}/Cs^-, Sr^{2+} and Cl^-.

When modelling the precise bonding structure of encapsulated atoms and molecules in zeolites, we must necessarily grapple with the realization that the local symmetry of encapsulated moieties may not obey the long-range symmetry of the zeolite. From experience we know that these moieties tend to adjust their shape and orientation to conform with a sub-set of the zeolite's full symmetry. For example, the center of the α_1 and α_2 cages in the rad-waste zeolite complex have 43 point symmetry. In trying to fully detail the structure of the extra-framework atoms in the rad-waste mixture, we made extensive use of Fourier difference scattering density maps which provided starting coordinates for refineable atomic positions. Because the encapsulated materials need not obey the crystallographic symmetry, partial occupation is expected, so refinements for the extra-framework atoms included occupation factors as well as positional parameters.

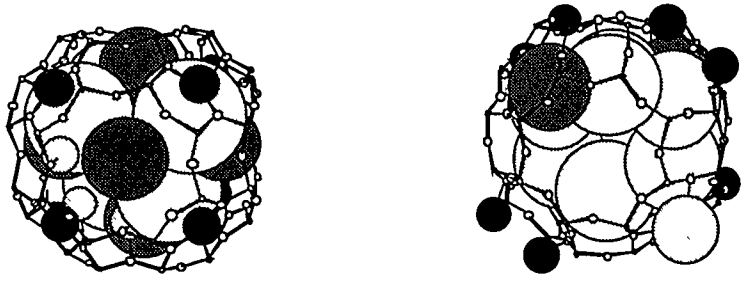


Figure 2. Illustrations of cation siting in (a) α_1 and (b) α_2 cages. Note the severe distortion of the 6-rings in α_1.

INSTRUMENT USED:	DATE OF REPORT:	EXPERIMENT NO.
GPPD	Feb. 19, 1991	1285

TITLE:

Neutron Powder Diffraction Study of $RbV_3P_4O_{17+x}$

AUTHORS AND AFFILIATIONS:

K. H. LII (Academia Sinica, Taipei), S. L. Wang (NTHU)

DATES OF EXPERIMENTS: May 20 to 21 1990

Δ APPROVED BY PROGRAM COMMITTEE, OR

Δ PART OF INSTRUMENT SCIENTIST ALLOCATION

REPORT RECEIVED:

EXPERIMENTAL REPORT (or Abstract of Publication)

Abstract submitted to Z. Kristallogr.

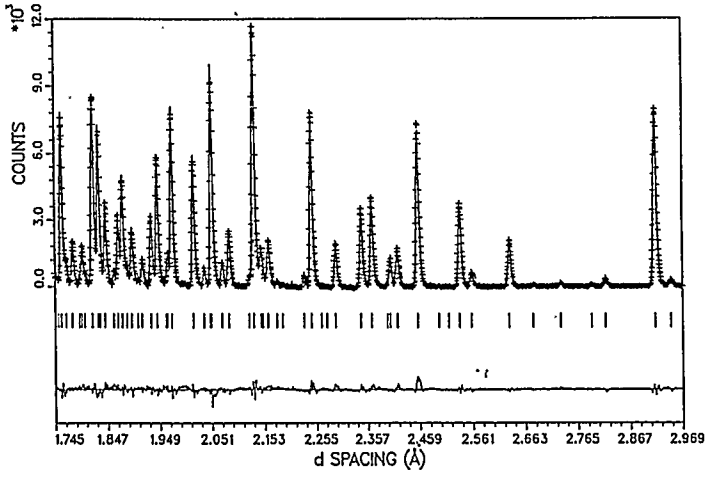
Rietveld refinement using high-resolution time-of-flight neutron powder diffraction data is reported for a mixed-valence vanadium pyrophosphate of $RbV_3P_4O_{16.97}$. This compound crystallizes in the tetragonal space group $P4_2/mnm$ (No. 136) with a = 13.65173(4), c = 7.31514(3) Å, V = 1363.320(8) $Å^3$, Z = 4, R_p = 0.0144, R_{wp} = 0.0213, and R_I = 0.0271 for 81 parameters and a total of 5059 data. The structure was previously determined using single-crystal X-ray diffraction with some remaining uncertainty in the oxygen content. Our neutron study shows that three oxygen sites are partially occupied, resulting somewhat different stoichiometry from the X-ray results. A good agreement between neutron and X-ray results in both atomic coordinates and thermal parameters was obtained for this complex structure. A comparison between the results from neutron powder and single-crystal X-ray data is given in detail.

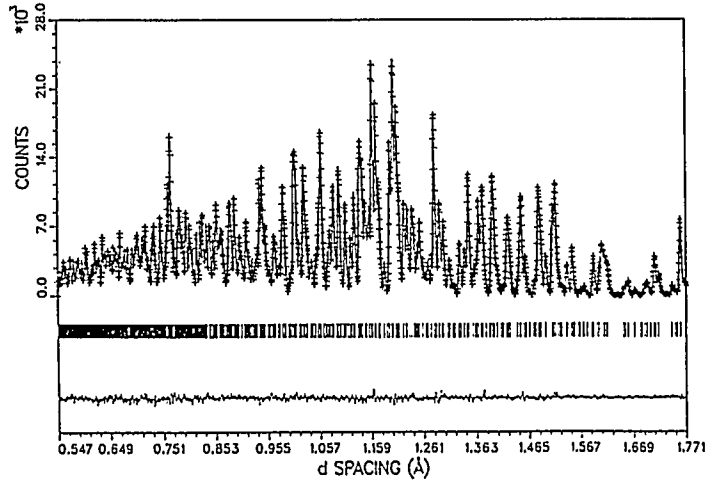
The figure shows the final Rietveld observed, calculated and difference plots of $RbV_3P_4O_{16.97}$.

EXPERIMENTAL REPORT (CONTD.)

Reference:

S. L. Wang and J. W. Richardson, Jr. (1991). Neutron Powder Diffraction Study of the Mixed-valance Vanadium Pyrophosphate $RbV_3P_4O_{16.97}$. Z. Kristallogr., submitted.





INSTRUMENT USED:	DATE OF REPORT:	EXPERIMENT NO:
GPPD	June 21, 1993	

TITLE:
Crystal Structure and Short-Range Oxygen Defects in La- and Nd-Modified ZrO_2

AUTHORS AND AFFILIATIONS:
C.-K. Loong[a], J. W. Richardson, Jr.[a], M. Ozawa[b], and M. Kimura[c]
[a]ANL, [b]Nagoya Inst. Tech. Japan, [c]Toyota Central Res. and Develop. Lab. Japan

DATES OF EXPERIMENT:
Nov. 1992

CHECK ALL APPLICABLE BOXES:

- [ ] APPROVED BY PROGRAM COMMITTEE
- [X] INSTRUMENT SCIENTIST ALLOCATION
- [ ] DO NOT PUBLISH
- [ ] PROPRIETARY RESEARCH
- [ ] PRT ALLOCATION

EXPERIMENTAL REPORT (or Abstract of Publication)

Abstract (submitted to J. Alloys and Compounds)

The crystal structure of rare-earth modified zirconia and the associated oxygen defects were studied by neutron diffraction. A Rietveld analysis of the neutron powder patterns of heat treated samples of La- and Nd-10mol%-ZrO_2 revealed the composition of a major tetragonal phase (space group $P4_2/nmc$) and a minor cubic phase (space group Fm3m). The short-range oxygen defects structure was examined by a Fourier-filtering technique. A real-space correlation function, obtained from a Fourier transform of the filtered residual diffuse scattering, showed evidence of static, oxygen-vacancy induced atomic displacements along the <111> and other directions of the pseudocubic cell.

Table I. The crystal structure derived from Rietveld refinement.

	$La_{0.1}Zr_{0.9}O_{1.95}$ heated at 600°C	$Nd_{0.1}Zr_{0.9}O_{1.95}$ heated at 600°C	$Nd_{0.1}Zr_{0.9}O_{1.95}$ heated at 800°C
Tetragonal $P4_2/nmc$ [a]			
a (Å)	3.6447 (5)	3.6346 (5)	3.6293 (3)
c (Å)	5.2034 (10)	5.2020 (11)	5.1895 (8)
z	0.0324 (6)	0.0392 (8)	0.0412 (6)
Composition (%)	94.8	74.5	74.7
Cubic Fm3m [b]			
a (Å)	5.1149 (20)	5.1403 (11)	5.1540 (7)
Composition (%)	5.2	25.5	25.3
Weighted R (%)	4.7	6.8	6.0

[a] 2 Zr (a) 3/4, 1/4, 3/4; 1/4, 3/4, 1/4;
4 O (d) 1/4, 1/4, z; 1/4, 1/4, z+1/2; 3/4, 3/4, -z; 3/4, 3/4, -z+1/2.
[b] 4 Zr (a) 0, 0, 0; F.C.
8 O (c) ±(1/4, 1/4, 1/4); F.C.

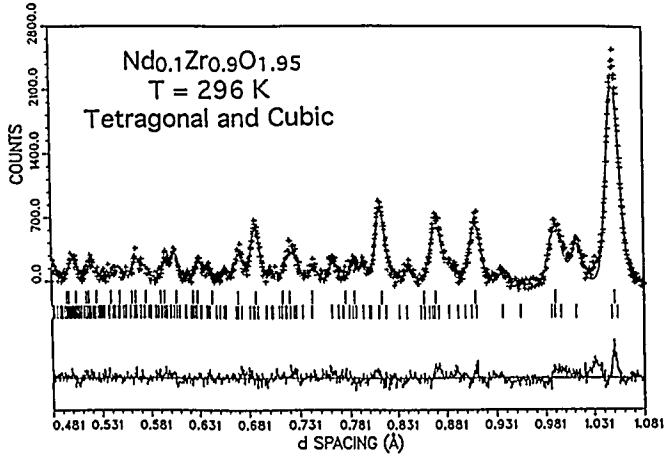


Figure. 1 Correlation function, D(r), calculated from the filtered residual intensities from the Rietveld refinement of the $Nd_{0.1}Zr_{0.9}O_{1.95}$ data (see Fig. 1). The features below 2 Å are noise due the truncation of data.

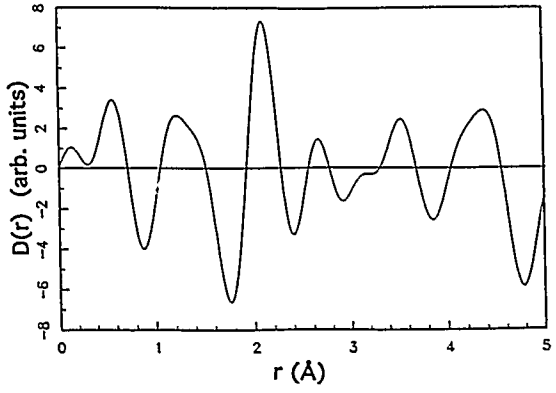


Figure. 2 Final Rietveld profile fit for the $Nd_{0.1}Zr_{0.9}O_{1.95}$ sample after Fourier-filtering. Only the 0.48-1.08 Å region of d-spacing is shown.

INSTRUMENT USED:	DATE OF REPORT:	EXPERIMENT NO:
GPPD	January 1996	P1994

TITLE: Microstructural Characterization of Al

AUTHORS AND AFFILIATIONS: S. R. MacEwen (Alcan International), E. Daniels (ES Div., ANL), J. W. Richardson, Jr. and G. L. Burr (IPNS Div., ANL)

DATES OF EXPERIMENT: March 1995, May 1995, September 1995

CHECK ALL APPLICABLE BOXES:

- [ ] APPROVED BY PROGRAM COMMITTEE
- [ ] INSTRUMENT SCIENTIST ALLOCATION
- [ ] DO NOT PUBLISH
- [x] PROPRIETARY RESEARCH
- [ ] PRT ALLOCATION

EXPERIMENTAL REPORT (or Abstract of Publication)

Grain size, crystallographic texture, the presence and amount of minority phases, and dislocation density define the essential ingredients of the metallurgical microstructure of Al products. Traditionally, microstructure has been characterized by a combination of direct techniques, including optical microscopy, TEM, SEM, and microprobe analysis, used to quantify grain size and shape, and X-ray diffraction used to determine crystallographic texture and the identity of minority phase particles extracted from the matrix; along with a variety of indirect mechanical test procedures, such as tensile and fracture toughness tests, which can be related to microstructure. No single one of these tests, however, is sufficient to completely characterize microstructure.

The primary objective of this project is to develop neutron diffraction techniques which provide a "signature" of Al microstructure that captures the salient features in a single, cost-effective experiment.

Microstructural data accessible to neutron diffraction include: (i) precise measurement of Al lattice parameter, (ii) crystallographic texture of Al, (iii) microstrain, a measure of dislocation density, produced by cold work, and (iv) presence and quantities of minority phases.

Data are analysed using GSAS (Generalized Structure Analysis System), a suite of programs designed for crystal structure refinement from powder diffraction data. By positioning Al sheet samples oriented 45° to the incident neutron beam in the GPPD, neutrons scattered into the $2\theta = -90°$ and +90°banks are scattered from planes whose diffraction vectors are perpendicular and parallel to the plane of the sheet, respectively. A single GSAS analysis, separately refining data from $2\theta = \pm148°$, ±90° and ±60° detector banks, generates parameters defining the microstructure of crystalline constituents in each of the 6 orientations, thereby quantifying anisotropy in grain orientation (in Al and minority phases) and microstrain directly.

Lattice constants (Al sheet) - Pure Al has lattice constant a_0 ~4.05 Å. The Al lattice can be expanded or contracted, depending upon the respective atomic radii of retained additive elements in the Al. Each alloy composition will have a corresponding baseline lattice constant, which may vary with processing. Mathematical corrections for subtle (as small as 0.25 mm) sample positioning errors, coupled with the inherently high resolution of the GPPD, result in an estimated lattice constant accuracy of ~0.00005 Å.

Inverse Pole Figures - As illustrated in Figure 1, dramatic differences in diffraction intensities normal to and in the plane of Al sheet are common. Precise knowledge of texture is exceedingly valuable for assessment of mechanical behavior. An Inverse Pole Figure (IPF) is a measure of crystallographic texture (Figure 2) which relates the intensities of individual reflections (crystallographic orientations) in textured samples to those expected for a randomly oriented sample. An IPF is generated from the integrated intensities of discrete diffraction peaks calculated by GSAS.

With a complete set (including all sample orientations) of IPF's, an Orientation Distribution Function (ODF) can be generated, relating all crystallographic orientations with all sheet orientations. From this the mechanical properties of Al sheet could be predicted very precisely. For expediency we limit ourselves to a total of 11 IPF's from two sets of sheets for each sample.

EXPERIMENTAL REPORT (CONTD.)

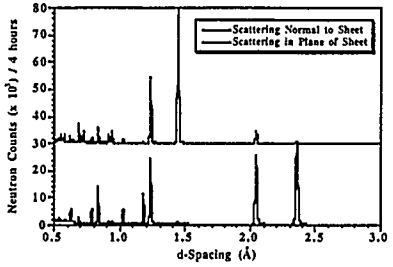


Figure 1. Raw data from the $2\theta = \pm90°$ detector banks showing strong texture typical of Al sheet

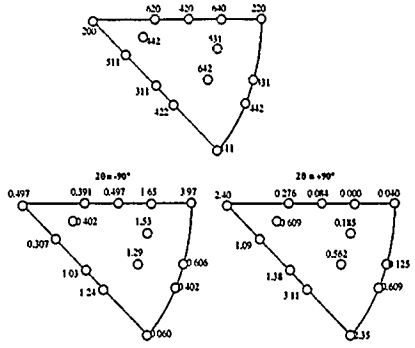


Figure 2. Inverse Pole Figure derived from data shown in Figure 1.

Microstrain and Particle Size broadening - Unstrained samples generate diffraction data with peak breadths equivalent to the resolution limit of the diffractometer. Microstrain from cold work or other disruptive forces will cause broadening of peaks. Alternatively, if the crystalline particles have a diameter of ~1000 Å or less, the resulting diffraction peaks will be broadened. These two mechanisms for broadening are distinguishable by GSAS. Most samples studied here suffer exclusively from microstrain broadening. Figure 3 illustrates the ability to resolve microstrain due to rolling reduction of Al sheet.

Minority Phases - Many Al alloy compositions contain minority intermetallic precipitate phases. These phases are often important to the mechanical behavior of the final product. GSAS is capable of generating microstructural data for up to 6-8 phases in addition to Al. Accuracy and precision will be limited according to the relative contributions of each to the diffraction patterns. As an example, refinement of a typical Al alloy composition (Figure 4), using $2\theta = \pm148°$, ±90° and ±60° detector banks, identified Mg_2Si precipitates present at an estimated 0.46(1) wt% level.

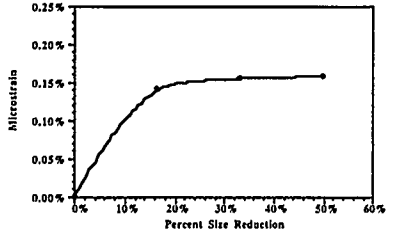


Figure 3. Calculated microstrain as a function of percent size reduction in Al sheet.

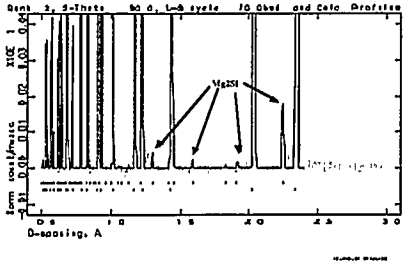


Figure 4. Rietveld profile fit showing modelling of Mg_2Si minority phase (0.5 wt%) in Al sheet.

INSTRUMENT USED:	DATE OF REPORT:	EXPERIMENT NO.:
GPPD	15 July 1992	1132

TITLE: Residual Stress and Texture in Superconductor/Silver Composites

AUTHORS AND AFFILIATIONS: K. Martin, J. Bingert, A.C. Lawson, M. Bourke, J.A. Goldstone, G.H.Kwei, D. Korzekwa, R. Trujillo, S. Atencio, D. Zaremba (LANL), and J.W. Richardson, (ANL)

DATES OF EXPERIMENT: 16-19 May 1992

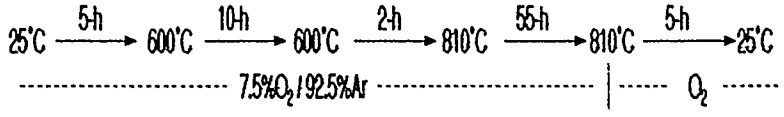
CHECK ALL APPLICABLE BOXES:

- [X] APPROVED BY PROGRAM COMMITTEE
- [ ] INSTRUMENT SCIENTIST ALLOCATION
- [ ] DO NOT PUBLISH
- [ ] PROPRIETARY RESEARCH
- [ ] PRT ALLOCATION

EXPERIMENTAL REPORT (or Abstract of Publication)

This experiment was done in support of a program to fabricate composite tape of silver metal and superconducting ceramic. Residual strains are known to have drastic effects on superconducting properties of materials. It is therefore desirable to know what strains are induced through differential thermal expansion during temperature cycling of the composite. This can conveniently be studied by means of neutron powder diffraction using the sample itself as a strain gauge. If the orientation of the tape is preserved, different components of the strain can be measured. In our experiments, a copper container served as a reference standard. We used GPPD at IPNS to obtain very high d-spacing resolution.

$SrCO_3$, $CaCO_3$ and CuO (Sr:Ca:Cu = 1.91:2.03:3.06) were milled and then calcined at 950°C for 48-h. This pre-reacted mixture of calcium and strontium cuprates was then milled with the appropriate amounts of Bi_2O_3 and PbO to form the composition $Bi_{1.84}Pb_{0.34}Sr_{1.92}Ca_{2.01}Cu_{3.07}O_x$. This powder was packed into an alumina firing boat and was sintered at 845°C in air for 96-h and then quenched. The sample was then mortar and pestle ground, sieved to 400 mesh and then fired again in air at 845°C for 96-h. The x-ray pattern of the sample after this firing showed mostly Bi-2223 with some Bi-2212, $(Ca_{1-x}Sr_x)_2PbO_4$, and $(Ca_{1-x}Sr_x)_2CuO_3$. This powder was packed into a silver tube. The silver-superconductor composite was swaged and drawn and then rolled into a tape 0.106" x 0.008" x ~130 feet long. Thirty two pieces of lengths of 6.5" were cut from this 130' roll of tape. Great care was taken both in the cutting and in the post processing of these pieces to preserve the rolling direction and side (top to bottom) orientation. The tape pieces were loaded flat into a large bore furnace and processed according to the following schedule:



After post processing the 6.5" wires were clipped into small pieces ~0.32" long. Again, the rolling direction of the tape and the top to bottom orientation of each of these small pieces was carefully preserved. Four hundred and sixty five pieces of tape were packed into a copper box of dimensions 0.32" x 0.32" x 1.5". The tape was stacked three rows across and 155 rows high. (See Fig. 1.)

We used three days of beam-time on GPPD to obtain diffraction patterns at three tempreatures: 298K, 100K and 298K again. Long counting times were necessary because of the high absorption of the silver. The sample was oriented in the cryostat so that the +90° bank counted neutrons scattered from crystal planes normal to the tape transverse direction, and the -90° detector bank counted neutrons scattered from planes normal to the

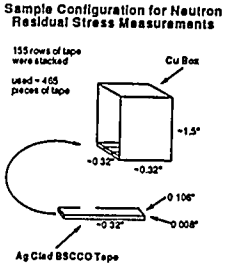


Fig. 1. Sample configuration.

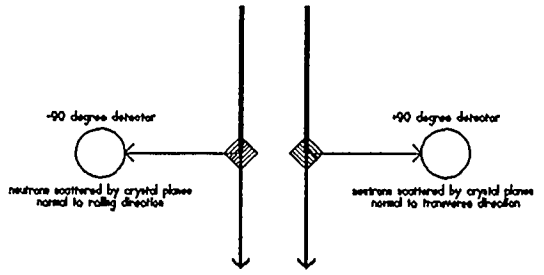


Fig. 2. Diffractometer configuration.

tape rolling direction. (See Fig. 2) Observations in the normal direction were not made. Rietveld refinements were carried out with GSAS: each combination of sample phase and detector bank was treated as an individual phase except for the copper calibrant. We found that the 2212-phase was the dominant superconductor phase after processing; but other phases were present, and the overall quality of the patterns was not very high. The precision of the experiment was limited by the large (~1%) microstrain that was observed in the 2212-superconductor.

The experiment verified that the thermal expansions of the silver substrate and the 2212-superconductor are significantly different. (See Fig. 3) However, we did not detect any significant differences in lattice constant between the rolling and transverse directions induced by nearly 200K of temperature change. (The apparent difference in the silver lattice constant is believed to be due to uncertainties in temperature.) This means that the composite can accommodate the thermal stresses that are necessarily present in the cycling of the material. We did not observe a significant difference in preferred orientation between the rolling and transverse directions.

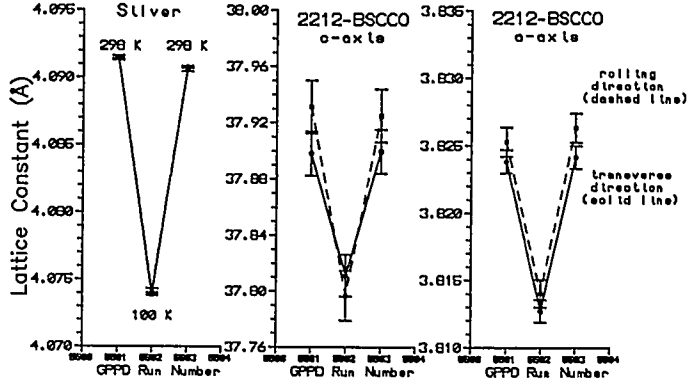


Fig. 3. Lattice constants for the Ag/BSCCO composite.

INSTRUMENT USED:	DATE OF REPORT:	EXPERIMENT NO.:
GPPD	August 16, 1990	1143

TITLE: Powder Diffraction Study of Li_5ReO_6 and Li_5NpO_6

AUTHORS AND AFFILIATIONS: L. R. Morss and E. H. Appelman, Chemistry Division, Argonne National Laboratory; D. Martin-Rovet, CNRS, 295 rue Saint-Jacques, 75005 Paris, France

DATES OF EXPERIMENT: Feb. 26; March 23; May 20; July 26, 1990

☒ APPROVED BY PROGRAM COMMITTEE, OR

☐ PART OF INSTRUMENT SCIENTIST ALLOCATION

REPORT RECEIVED:

EXPERIMENTAL REPORT (or Abstract of Publication)

The objectives of this study were to confirm the crystal structure recently reported (1) for Li_5ReO_6 by single-crystal X-ray diffraction and to establish whether the corresponding and interesting Np(VII) compound Li_5NpO_6 is isostructural or whether its structure is the one originally proposed (2) from X-ray powder patterns. In carrying out this project we actually studied five samples at GPPD.

The initial series of experiments were performed on Li_5ReO_6 (stoichiometric) and on Li_5ReO_6 prepared with an excess of lithium (Li:Re ratio 6:1). The goals were to confirm the Li_5ReO_6 structure and to ascertain whether the excess lithium in the second preparation produced Li_6ReO_6. The first experiment confirmed the monoclinic C2/m structure for Li_5ReO_6 and the second experiment showed that a two-phase mixture of Li_5ReO_6 and Li_2CO_3 was produced from a carefully mixed and heated sample of 12 Re + Li_2CO_3.

The next experiment was carried out with a Li:Np ratio of 4:1 under nearly the same conditions. The product was Li_4NpO_5, which we have now confirmed to be isostructural with Li_4UO_5, which was studied by both X-ray and neutron powder diffraction (3). We successfully refined our IPNS data in space group I4/m, a = 6.6993 Å, c = 4.4200 Å, with atomic parameters and bond lengths very similar to those of Hoekstra and Siegel (3) for Li_4UO_5. A report on X-ray powder diffraction of Li_4NpO_5 is consistent with our results (4).

Since all of our experiments were done with ^7Li, and since we needed $^7Li_2O_2$ for our synthesis of Li_5NpO_6, we confirmed the structure of Li_2O_2 in a subsequent run at GPPD (5). Our final experiment was carried out with 3 grams of Li_5NpO_6, which showed an X-ray powder pattern identical to that found earlier by Keller (2) and by us, and which was confirmed as a Np(VII) compound by spectrophotometry. Our GPPD data show peaks reasonably consistent with the C2/m Li_5ReO_6 model but there are some unindexable peaks that do not correspond to any plausible impurity. Therefore the refinement of Li_5NpO_6 is still in progress.

EXPERIMENTAL REPORT (CONTD.)

References

(1) T. Betz and R. Hoppe, Z. Anorg. Allg. Chem. 512, 19 (1984).

(2) C. Keller and H. Sieffert, Inorg. Nucl. Chem. Lett. 5, 51 (1969).

(3) H. Hoekstra and S. Siegel, J. Inorg. Nucl. Chem. 26, 693 (1964).

(4) C. Keller, L. Koch, and K. H. Walter, J. Inorg. Nucl. Chem. 27, 1205 (1965).

(5) H. Föppl, Z. Anorg. Allg. Chem. 291, 12 (1957).

INSTRUMENT USED:	DATE OF REPORT:	EXPERIMENT NO:
GPPD	12/20/93	1795

TITLE:
Effect of Temperature and Composition on the Lattice Parameter difference between γ and γ' in Ni-Al-Si Alloys

AUTHORS AND AFFILIATIONS:
G. Muralidharan (ANL/Univ of Illinois), J. R. Richardson(IPNS/ANL), F. J. Rotella(IPNS/ANL), J. E. Epperson(MSD/ANL), Haydn Chen(Univ of Ill.)

DATES OF EXPERIMENT:
Oct 21, 24 and Dec. 17

CHECK ALL APPLICABLE BOXES:

- [x] APPROVED BY PROGRAM COMMITTEE
- [ ] INSTRUMENT SCIENTIST ALLOCATION
- [ ] DO NOT PUBLISH
- [ ] PROPRIETARY RESEARCH
- [ ] PRT ALLOCATION

EXPERIMENTAL REPORT (or Abstract of Publication)

Objective: To obtain the lattice parameter difference between γ and γ' in Ni-Al-Si alloys.

Experimental Work: The overall aim of this work is to measure the difference between the lattice parameters of two phases (γ and γ') that are in coherent equilibrium in several Ni-Al-Si alloys. The various samples have already been used in a Small Angle Neutron Scattering (SANS) study designed to measure the coarsening rates in these alloys. A sample with the composition of Ni-6 at. % Si - 6.0 at. % Al was used first. The alloy had been cast, homogenized, rolled and punched to a disk of size 12.5 mm. diameter and 1.5 mm. thick. Powder data was collected from the sample using the GPPD and fitting was attempted using Rietveld codes.
Significant difficulties were encountered during the fitting:
1) It was found that the peak intensities for the matrx did not reflect a true powder average. The matrix was assumed to be F.C.C. with Ni, Al and Si being substitutional in the sites.
2) The second phase peaks were very broad and very weak.

Texture was suspected for (1) and a set of experiments designed to reduce the effect of texture, was carried out. Two runs were done, one with the sample rotated about its cylindrical axis and the another with the sample rotating about an axis perpendicular to the cylindrical axis. It was found that this did not entirely rid the pattern of the difficulties with the peak intensities. Two possible causes are being examined
1. The rotation did not completely eliminate the texture.
2. The structure of the matrix is different from the assumed structure: maybe one or more of the interstitial sites are occupied.

EXPERIMENTAL REPORT (CONTD.)

Experiments are currently being carried out to study this in further detail. Future experiments will thus need two or more runs for a complete analysis on one sample, since it is planned to rotate the sample about atleast two difference axes.
To reduce the effect of (2), the samples will be aged *ex-situ* to have large precipitates so that the peaks are sharper.

INSTRUMENT USED:	DATE OF REPORT:	EXPERIMENT NO:
GPPD	Jan 15. 1996	1967

TITLE:
f electron-phonon coupling in $YbPO_4$ and $YbVO_4$

AUTHORS AND AFFILIATIONS:
J. Nipko and S. Kern (Colorado State Univeristy), M. M. Abraham and L. A. Boatner (Oak Ridge National Lab), J. W. Richardson, Jr. and C.-K. Loong (ANL)

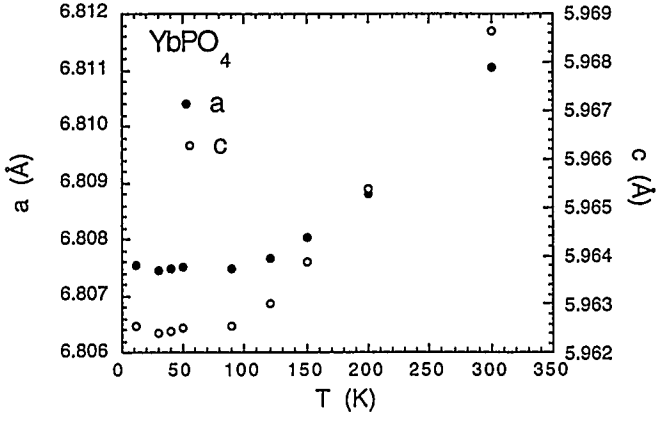
DATES OF EXPERIMENT:
Dec. 18, 1994 and Feb. 14, 1995

CHECK ALL APPLICABLE BOXES:

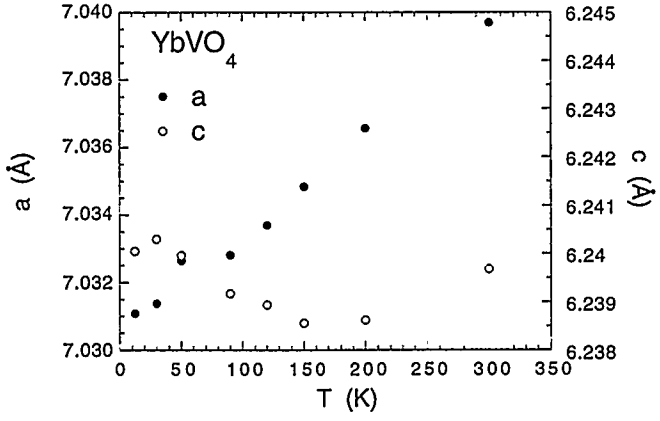
- [X] APPROVED BY PROGRAM COMMITTEE
- [ ] INSTRUMENT SCIENTIST ALLOCATION
- [ ] DO NOT PUBLISH
- [ ] PROPRIETARY RESEARCH
- [ ] PRT ALLOCATION

EXPERIMENTAL REPORT (or Abstract of Publication)

Interactions between the crystal-field-split states and the host lattice in rare-earth (RE) orthovanadates, RVO_4 (R = rare earth elements) have previously been investigated by a number of experimental techniques. These interactions may affect a variety of physical properties of the system, including the thermal expansion, magnetoelasticity, and Jahn-Teller-type transitions. Although many studies have been performed on the RVO_4 with R= Tb, Dy, Ho, and Tm, very little experimental work has been done on $YbVO_4$. We have investigated the Yb^{3+} crystal-field (CF) level structure in $YbVO_4$ using inelastic magnetic neutron-scattering measurements and CF model calculations. We also determined the temperature dependence of the a and c lattice parameters of the tetragonal unit cell by neutron diffraction and observed a minimum at ~125 K in the c parameter. This anomaly in the thermal expansion is interpreted as a coupling of the anisotropic low-lying CF states of the Yb^{3+} ions and the crystal lattice at low temperatures.



EXPERIMENTAL REPORT (CONTD.)



INSTRUMENT USED:	DATE OF REPORT:	EXPERIMENT NO:
GPPD	Jan 15. 1996	1971

TITLE:
Crystal structure and short-range defects in high-temperature. high-strength nitride ceramics

AUTHORS AND AFFILIATIONS:
M. Ozawa and S. Suzuki (Nagoya Institute of Technology)
J. W. Richardson, Jr. and C.-K. Loong (ANL)

DATES OF EXPERIMENT:
Sept 18-19, 1994

CHECK ALL APPLICABLE BOXES:

- [X] APPROVED BY PROGRAM COMMITTEE
- [ ] INSTRUMENT SCIENTIST ALLOCATION
- [ ] DO NOT PUBLISH
- [ ] PROPRIETARY RESEARCH
- [ ] PRT ALLOCATION

EXPERIMENTAL REPORT (or Abstract of Publication)

The crystal structures of β′-Sialon ceramics, $Si_{6-z}Al_zO_zN_{8-z}$ ($0 \le z \le 6$), prepared by a novel slip-cast method were studied by neutron scattering techniques. A Rietveld analysis of the diffraction patterns shows that samples of $z < 4$ form a single-phase solid solution of Si-Al-O-N isostructural to β-Si_3N_4 (space group $P6_3/m$). Within this structure there is a consistent preferred occupation of O on the 2c sites and N on the 6h sites. For $z > 4$ the materials exhibit multiple-phase structure.

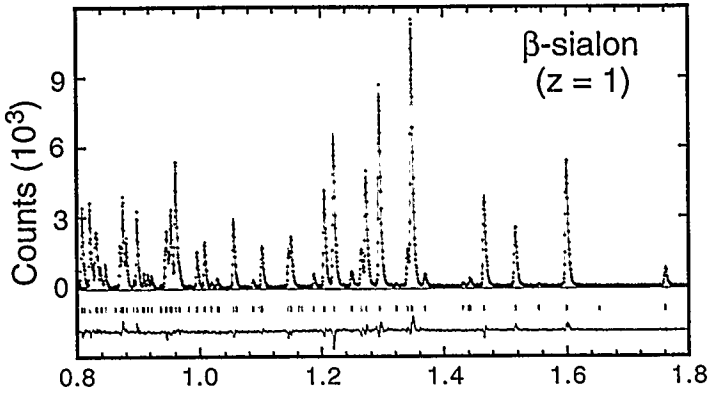


Figure 1. Rietveld profile fit in the 0.8-1.8 Å region of d-spacing for the z = 1 sialon sample. The symbols are the observed, background subtracted intensities. The solid line represents the calculated crystalline intensities. The tick marks indicate the positions of the Bragg reflections. The difference between the observed and calculated intensities is shown at the bottom of the figure.

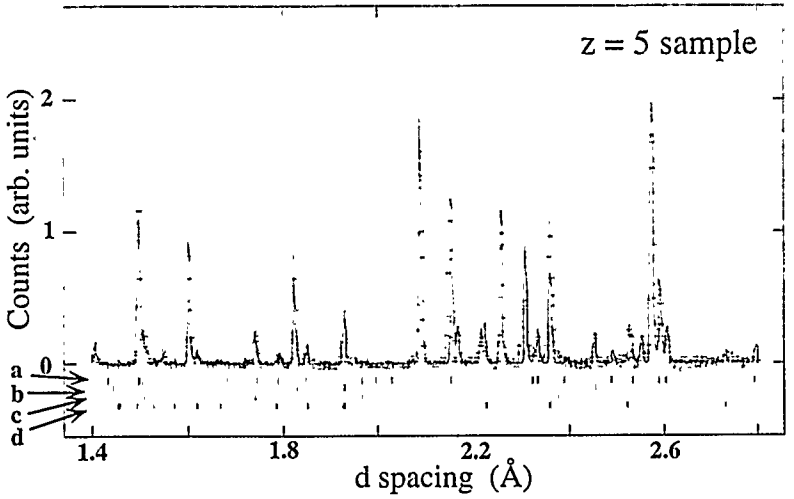


Figure 2. Rietveld profile fit in the 1.4-2.8 Å region of d-spacing for the z = 5 sample. The crystalline phases labeled a, b, c, and d correspond to $SiAl_5O_5N_3$, q-$Si_3Al_{12}O_9N_{10}$, a-Al_2O_3, and bȼ-$SiAl_4O_2N_4$, respectively. The LeBail technique was applied to the fit whereby structure factor calculations for the q-$Si_3Al_{12}O_9N_{10}$ and bȼ-$SiAl_4O_2N_4$ phases were ignored.

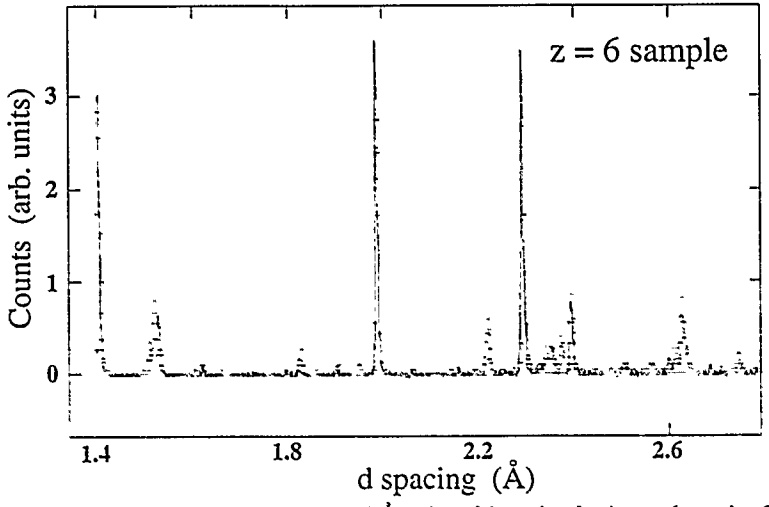


Figure 3. Rietveld profile fit in the 1.4-2.8 Å region of d-spacing for the z = 6 sample. Only the Al_3O_3N phase was used in the fit.

INSTRUMENT USED:	DATE OF REPORT:	EXPERIMENT NO:
GPPD	Jan 15, 1996	2068

TITLE:
Crystal structure, defects and oxygen storage in Ce Modified zirconia

AUTHORS AND AFFILIATIONS:
M. Ozawa and S. Suzuki (Nagoya Institute of Technology),
J. W. Richardson, Jr. and C.-K. Loong (ANL)

DATES OF EXPERIMENT:
June 18, 1995

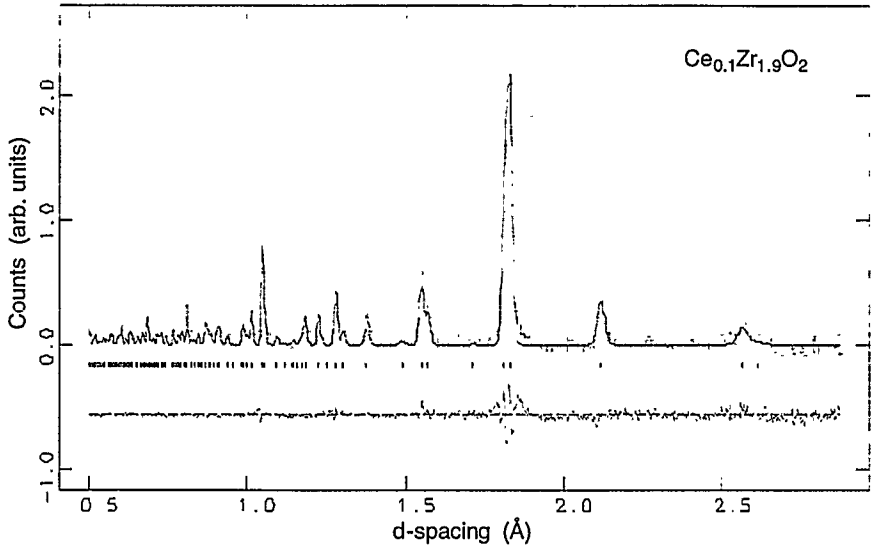
CHECK ALL APPLICABLE BOXES:

- [X] APPROVED BY PROGRAM COMMITTEE
- [ ] INSTRUMENT SCIENTIST ALLOCATION
- [ ] DO NOT PUBLISH
- [ ] PROPRIETARY RESEARCH
- [ ] PRT ALLOCATION

EXPERIMENTAL REPORT (or Abstract of Publication)

Zirconia is an active isosynthesis catalyst which is capable of selective conversion of synthesis gas into branched hydrocarbons. It can also be used as a catalytic support of metallic active components in automobile exhaust emission control. A key requirement for these catalytic functions is the ability in retaining the large surface area, structural stability, and surface acidity/basicity over a wide range of temperatures. This is often achieved by preparing fine, promoter-modified zirconia powders using low-temperature processing methods which start from mixing multi-component molecular precursor solutions. Adding promoters such as a few mol. % of certain rare-earth oxides (including yttria) to zirconia may stabilize the cubic and tetragonal phases and prevent sintering of the material at high temperatures. Ce-doped ZrO_2 has an additional benefit of oxygen storage capability owing to the Ce^{3+} and Ce^{4+} fluctuations. An understanding of the relationship between catalytic performance and sample variables such as crystalline morphology, defects, and porous texture is of fundamental importance to the development of zirconia-based catalytic systems.

EXPERIMENTAL REPORT (CONTD.)



The powder-diffraction pattern and Rietveld refinement of10 mol% Ce-doped zirconia powder, heat-treated at 600°C, measured on GPPD at room temperature. Unlike the case of La- and Nd-doped ZrO_2, only the monoclinic structure was observed in Ce-ZrO_2. In addition, no evidence was found for oxygen defects in the material.

INSTRUMENT USED:	DATE OF REPORT:	EXPERIMENT NO.:
G SPPD	8/18/92	1434

TITLE:
Structure of Cristobalite, SiO_2, to.6 GPa

AUTHORS AND AFFILIATIONS: J. B. Parise, SUNY, Stony Brook; J.D. Jorgensen, Materials, Argonne; M.A. Saltzberg, E.I. Dupont

DATES OF EXPERIMENT:
16-20 June 1992

CHECK ALL APPLICABLE BOXES:

- [X] APPROVED BY PROGRAM COMMITTEE
- [ ] INSTRUMENT SCIENTIST ALLOCATION
- [ ] DO NOT PUBLISH
- [ ] PROPRIETARY RESEARCH
- [ ] PRT ALLOCATION

EXPERIMENTAL REPORT (or Abstract of Publication)

The compression mechanism for both SiO_2, cristobalite, and Ca-partially stabilized cristobalite ($Ca_{x/2}Si_{2-x}Al_xO_4$), has been investigated using structural data derived from neutron powder diffraction. The data, collected from samples contained in a gas pressure apparatus up to 6 GPa, suggest collapse of the corner-connected framework from rotations of the rigid SiO_4-tetrahedra. The Ca-stabilized material has a higher bulk modulus, suggesting the alkaline earth ion occupies positions within the cavities formed by the (Si, Al)-O framework.

The structure and response to temperature and pressure of the SiO_2 polymorph, cristobalite, is of considerable interest recently. Yeganeh-Haeri *et al.* have reported a relatively low pressure phase transition[1] in this material as well as a negative Poisson's ratio[2]. This later observation is particularly interesting since it implies the low pressure form, α-cristobalite, unlike other silica and silicates, contracts laterally when compressed and expands laterally when stretched. Given these unusual observations we thought it worthwhile to investigate the low pressure structure, below 1 GPa, using neutron diffraction. The experiments were carried out in a gas pressure apparatus[3] attached to the SPPD instrument. This equipment ensures hydrostatic conditions; it delivers data devoid of Bragg peaks from the high pressure cell, and with sufficient peak-to-background to obtain reliable structure refinements using the Rietveld technique.

The pure SiO_2 cristobalite was obtained as an x-ray diffraction standard[4]. By way of comparison a chemically stabilized cristobalite (CSC) was also prepared[5]. Data were collected with increasing pressure at room temperature and with decreasing pressure at 60 K.(Fig. 1). The structures of the two materials were refined using an automated procedure introduced at the IPNS[6].

The structural response of cristobalite has been analyzed in terms of the rotation of rigid tetrahedra[7,8]. Using this approach we find the polyhedral tilt of these units[7,8] is larger for the pure SiO_2 framework (Fig 2); this, along with the evidence summarized in Fig. 1, suggests the Ca is

indeed incorporated into the cavities of the structure and serves as a brace against collapse at higher pressures.

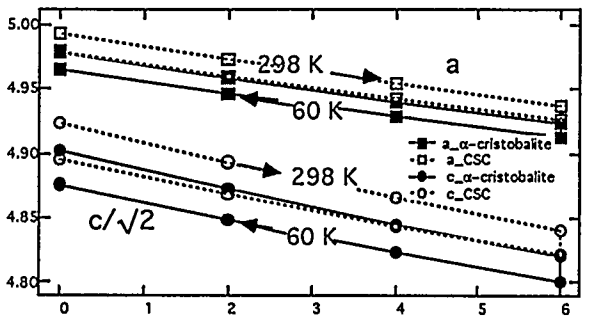


Figure 1. Variation of the a and c/√2 cell parameters for the tetragonal (pseudo cubic) α-cristobalite and chemically stabilized cristobalite (CSC) structure, emphasizing the greater compressibility of the c relative to the a unit cell parameter. The arrows indicate the direction in which pressure was increased at 298 K and decreased at 60 K. As expected the cell for the Ca-containing framework is larger.

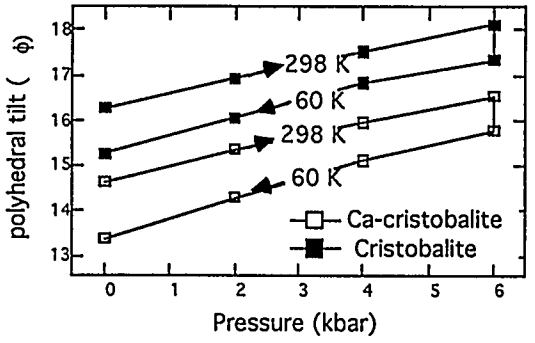


Figure 2. Variation in SiO_4 polyhedra tilt[7,8] as a function of pressure at 298 and 60 K. Note that pressure is increasing at 298 and decreasing at 60 K. The lower polyhedral tilt, and the lower rate of increase of this tilt as a function of pressure, for the Ca-stabilized material, is indicative of the presence of Ca in the open parts of the structure, bracing it against collapse.

1. Yeganeh-Haeri A. *et al.* (1991) Eos 71 (No. 43), *Fall Meeting, American Geophysical Union, Supplement*, 1671.
2. Yeganeh-Haeri A.; Weidner, D. W.; Parise, J. B. (1992) *Science*, 257, 650
3. Jorgensen, J. D.; Shiyou, P.; Lightfoot, P.; Hinks, D. G.; Veal, D. W.; Dabrowski, B.; Paulikas, A. P.; Kleb, R. (1990) *Physica* C 171, 93
4. in a10 gm. batch from X-Ray Diffraction Accessories, 1652 Princeton Drive, State College, PA 16803.
5. A clear sol was prepared from Ludox AS-40® , aluminum nitrate nonahydrate, and calcium nitrate hexahydrate in proportions to form a final composition of 93 mole% SiO_2: 4.7% Al_2O_3: 2.3% CaO. This clear sol was spray dried in a Niro spray-dryer, yielding amorphous powder with a d_{50} of about 8 μm. This precursor was calcined at 1100°C for 24 hours to form CSC.
6. Rotella, F. J.; Hitterman; R. L. (1992) abstract PC72, *American Crystall. Assoc.* Collected Abs., Pittsburgh.
7. Taylor, D. (1972) *Min. Mag.* 38, 593
8. O'Keefe, M.; Hyde, B. G. (1976) *Acta. Crystallog.* B32, 2923

INSTRUMENT USED:	DATE OF REPORT:	EXPERIMENT NO.:
GPPD	6-1-90	NSF-12

TITLE: Oxygen deficiency in $ErBa_2Cu_3O_{7-x}$

AUTHORS AND AFFILIATIONS: Paolo G. RADAELLI and Carlo U. SEGRE (IIT)

DATES OF EXPERIMENT: 2-5 Mar 1990

☐ APPROVED BY PROGRAM COMMITTEE, OR

☐ PART OF INSTRUMENT SCIENTIST ALLOCATION

REPORT RECEIVED:

EXPERIMENTAL REPORT (or Abstract of Publication)

Neutron diffraction studies on the $ErBa_2Cu_3O_{6+\delta}$ system

A series of $ErBa_2Cu_3O_{6+\delta}$ samples with variable oxygen content has been prepared by mixing oxygen-rich $ErBa_2Cu_3O_7$ and oxygen deficient $ErBa_2Cu_3O_6$ powders in different proportions. The samples have been sealed in quartz ampules under vacuum and slowly cooled from 400°C to 50°C over a period of two months, in order to achieve near-thermal-equilibrium. Neutron diffraction data were collected at room temperature using the General Purpose Powder Diffractometer, and analyzed by the Rietveld structural refinement technique.

An initial series of structural Rietveld refinements were made assuming that each sample was either single phase orthorombic (O) or single phase tetragonal (T). Isotropic strain and isotropic particle size broadening parameters were used to refine the peak shapes. Using this simple model we observed significant anomalies in some of the refined structural parameters of these samples, especially if compared with samples prepared at higher temperature: in particular the behavior of the a and b lattice parameters near the tetragonal-to-orthorombic transition is not the one expected for a second order transition. In addition no discontinuity in the c-axis parameter has been observed near the composition where superconductivity first appears ($\delta \approx 0.35$): the observation of a c-axis discontinuity in $YBa_2Cu_3O_{6+\delta}$ samples has been recently related to a charge-transfer mechanism between Cu-O chains and $Cu\text{-}O_2$ planes, which is thought to enhance the carrier concentration on the planes and ultimately lead to superconductivity. Another peculiarity is the behavior

EXPERIMENTAL REPORT (CONTD.)

of the occupation of the O1 (chain) and O5 (antichain) positions as functions of the total oxygen content: over the entire orthorombic region n(O5) converges to a small value (≈ 0.05), while n(O1) decreases almost linearly. At the transition the use of a different structural model forces the two occupations to be equal. No sign of the characteristic chain disorder near the transition can be detected in these samples.

A detailed analysis of the differences between the observed and the calculated diffraction patterns shows that the simple model applied to refine these data was not completely satisfactory: in all the samples an hkl-dependance of the peak width and a pronounced asymmetry in the peak shapes can be observed. In addition, the isotropic strain broadening parameter σ_1 displays a large positive anomaly in the region $0.25<\delta<0.5$. Several refinement models were applied in order to improve the fit, including a microtwin-related anisotropic particle size broadening model. A two-phase model applied to the samples in the region of σ_1-anomaly has been proved to be very successful: samples with oxygen content $0.35<\delta<0.5$ were refined using two orthorombic phases (O+O'), while for the samples with $0.25<\delta<0.35$ one orthorombic and one tetragonal phase (O'+T) were used. The phase fraction of the O' phase never exceeds 65%, and peaks at $\delta \approx 0.35$. The success of this model suggests that large inhomogeneities in the oxygen distribution may have developed in this compositional region. Although a true thermodynamic phase separation is certainly a possible explanation for these inhomogeneities, other mechanisms cannot be completely ruled out a this point.

Superconducting transition temperature and phase fraction were measured using a Lake Shore Cryotronics model 7000 AC susceptometer: both these quantities and the refined phase fraction of the O phase go to zero at the same value of the oxygen content $\delta \approx 0.35$, well inside the orthorombic region: in the contest of a true thermodynamic phase separation this would indicate that only the O phase is superconducting.

INSTRUMENT USED:	DATE OF REPORT:	EXPERIMENT NO:
GPPD	22Feb96	2158

TITLE: Neutron Diffraction Measurements of Metal-Hydride Electrodes(Phase 2)

AUTHORS AND AFFILIATIONS:
Laszlo Redey, CMT, ANL. Gary Burr, Jim Richardson, IPNS, ANL.

DATES OF EXPERIMENT:
Oct. 25-27, 1995, Nov 20-21 1995

CHECK ALL APPLICABLE BOXES:

- [x] APPROVED BY PROGRAM COMMITTEE
- [ ] INSTRUMENT SCIENTIST ALLOCATION
- [ ] DO NOT PUBLISH
- [ ] PROPRIETARY RESEARCH
- [ ] PRT ALLOCATION

EXPERIMENTAL REPORT (or Abstract of Publication)

Lanthanum-nickel hydride($LaNi_5D_x$) has been of interest as a battery material because of the ability of the intermetallic alloy to absorb large amounts of hydrogen(deuterium). It has been shown that substitution of some of the nickel with aluminum will increase the capacity of the electrode ten-fold. Rietveld profile refinements NPD data on operating electrochemical cells have been performed to gain insight into the relationship between structural and electrochemical phenomena.

Our neutron powder diffraction studies on the aluminum substituted alloys($LaNi_{5-y}Al_y$) indicate that the addition of small amounts of aluminum(y = 0.12, 0.16) into the alloy leads to significant strain in the alloy. The strain was noticed when compared to the peak width in the $LaNi_5$ alloy. To determine the nature of the strain, the unit cell symmetry was lowered from hexagonal(P6/mmm) to orthorhombic(Cmmm). The refinement and peak fitting improved greatly. In the orthorhombic cell, the aluminum preferentially substitutes into one of the three available nickel sites(2c). When the aluminum concentration is increased to y = 0.60, the peak widths are comparible to those of $LaNi_5D_x$.

The working electrochemical cell consists of a rolled $LaNi_{5-y}Al_y$ electrode in the neutron beam with a NiO(OD) counterelectrode, positioned outside of the beam, in a KOD/D_2O electrolyte solution, all sealed in a quartz tube. Contributions from the electrolyte and quartz tube are modeled by the GSAS program.

Refinement of deuterium occupancy in a $LaNi_{5-y}Al_y$ electrode indicates that the alpha phase(where x is small) in $LaNi_{4.88}Al_{0.12}D_x$ can accept much more deuterium than the alpha phase for $LaNi_5D_x$(x = 1.2 versus 0.5 for $LaNi_5D_x$). No additional detuerium sites were identified. This is indicative of the aluminum contibuting additional stability to deuterium in present sites. A representative data set is shown in Fig. 1. with the calculated pattern and difference plot. The difference plot illustrates that no additional phases are present in the material. The Rietveld refinement was able to show that the deuteriums were preferentially loaded in sites near the aluminum.

A slow and steady decrease in the deuterium concentration(x) during a discharging cycle of a $LaNi_{4.88}Al_{0.12}D_x$ cell was observed and illustrated in Fig. 2. Each consecutive data set was 30 minutes in duration. The change in x is similar to that measured by the elcetrochemical cell. Also cell volume in the same cycle also illustrated a similar decrease. There is also peak widening observed in all materials containing deuterium. This includes $LaNi_5D_x$ and $LaNi_{5-y}Al_yD_x$(where y=0.12 and 0.60), which is due to the mobile nature of the deuteriums.

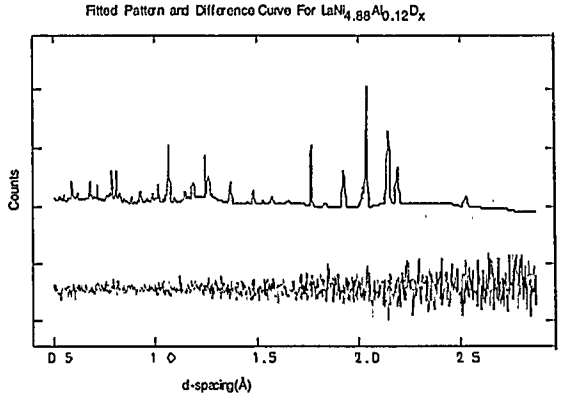


Fig. 1. Fitted pattern and difference curve for $LaNi_{4.88}Al_{0.12}D_x$

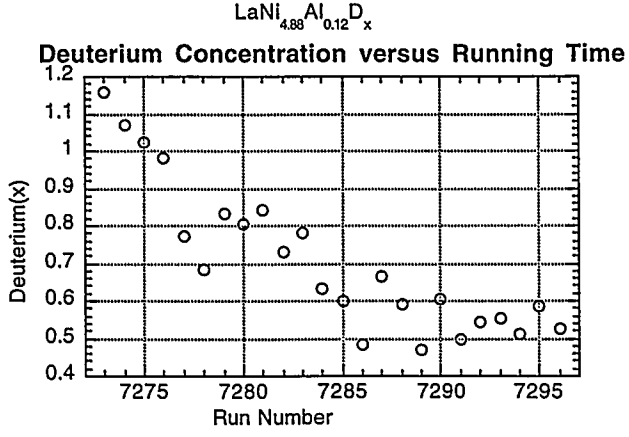


Fig. 2. Plot of deuterium concentration versus time in $LaNi_{4.88}Al_{0.12}D_x$

INSTRUMENT USED:	DATE OF REPORT:	EXPERIMENT NO:
GPPD	21Nov95	2158

TITLE: Neutron Diffraction Measurements of Metal-Hydride Electrodes(Phase 2)

AUTHORS AND AFFILIATIONS:
Laszlo Redey, CMT, ANL. Gary Burr, Jim Richardson, IPNS, ANL.

DATES OF EXPERIMENT:
Oct. 25-27, 1995, Nov 20-21 1995

CHECK ALL APPLICABLE BOXES:

- [x] APPROVED BY PROGRAM COMMITTEE
- [ ] INSTRUMENT SCIENTIST ALLOCATION
- [ ] DO NOT PUBLISH
- [ ] PROPRIETARY RESEARCH
- [ ] PRT ALLOCATION

EXPERIMENTAL REPORT (or Abstract of Publication)

In the second stage of this proposal, it was planned to use in situ NPD to investigate the beta phase of $LaNi_5D_x$. The beta phase is present where $0.5<x<3.0$. It is necessary to force the x value this high using up to 5 atmospheres of deuterium gas above the sample. It was learned that a sample in which aluminum has been doped for nickel in $LaNi_5D_x$ would lead to large x values in the electrochemical cell and form the beta phase without the need for a pressurized cell. For this reason, we report on the NPD results gathered on samples in electrochemical cells with the following nomenclatures: $LaNi_{5-y}Al_yD_x$ and $LaNi_5D_x$.

First, we report on the structural analysis of the aluminum doped starting material($LaNi_{5-y}Al_y$). Our studies confirm that the aluminum preferentially substitutes on one of the nickel sites, whereas the second site is fully occupied with nickel. Also, we confirmed the presence of anisotropic peak broadening for this material, which is not present in $LaNi_5$. We believe that there is a lowering of the symmetry for the hexagonal unit cell to an orthorhombic cell, with analysis continuing on this.

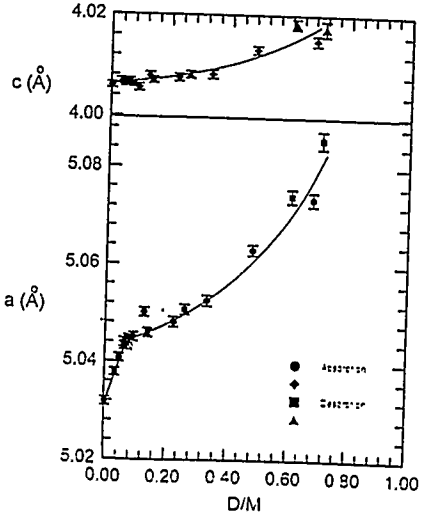
As a part of the previous proposal, an attempt was made to improve the resolution in the determination of the x value in $LaNi_5D_x$. In this regard, the amount of sample was increased while the amount of electrolyte was reduced, thus improving the signal to noise ratio and reducing the error in x.

Our first attempt to observe the conversion between alpha and beta phases, in order to reproduce literature work, was on $LaNi_{4.8}Al_{0.2}D_x$. The sample was electrochemically cycled(charged and then followed with a discharge to insert and remove deuterium) several times before placing in the diffractometer. A data set of the "fully charged" material was collected for several hours before the discharging, in situ, was begun. Unfortunately, cycling of a cell degrades the cell(decreases the maximum amount of deuterium inserted) and this "fully charged" material was significantly degraded that there was not enough deuterium to form a significant amount of the beta phase material.

EXPERIMENTAL REPORT (CONTD.)

The GSAS analysis of the lattice parameters in the alpha phase of $LaNi_{4.8}Al_{0.2}D_x$ was compared to the lattice parameters in the literature for $LaNi_5D_x$, it could be determined that this analysis was of equal quality of the previous literature studies. Fig. 1 is a literature plot of lattice parameter for the alpha phase versus deuterium concentration(D/M on the abscissa is deuterium x value divided by the total metal present{La+Ni+Al}). Based on the change the lattice parameters between deuterated and pristine alloy indicates that we had not reached the point where beta phase would form(D/M of 0.16). This electrochemical cell studied was cycling between D/M of 0.04-0.12. Based on Fig. 1., this would lead to a change in the lattice parameter of approximately 0.006 Å, whereas our refinements showed a change of 0.005 Å. Also, our error bars associated with lattice parameters are similar to those reported in Fig.1.

A plot of x value for the alpha phase determined from the current of the electrochemical cell versus time is similar to that observed when data sets are refined for deuterium concentration. For example, in $LaNi_5D_x$, the change in x when discharged from the "fully charged" material to the discharged material, as determined from the cell current, was 0.40 moles. When the two endmembers were refined using GSAS, the refined values for x were 0.50(10) and 0.20(10) moles. This puts the two measurements within good agreement, and we believe that this study could be used analyze a range of electrodes of this type for in situ measurements.



INSTRUMENT USED: GPPD	DATE OF REPORT: July 10, 1990	EXPERIMENT NO.: 1134

TITLE:
Structural Characterization of Basic Zeolites

AUTHORS AND AFFILIATIONS:
W. J. Reppart and S. C. Tang, Shell Development Company

DATES OF EXPERIMENT: March 24-25, 1990

X APPROVED BY PROGRAM COMMITTEE, OR

PART OF INSTRUMENT SCIENTIST ALLOCATION

REPORT RECEIVED:

EXPERIMENTAL REPORT (or Abstract of Publication)

Base catalysis over alkali-modified molecular sieves is an area of growing interest.[1,2] The goal is that of producing strongly basic zeolites to extend the well-known chemistry of acidic catalysts. Acidic zeolites are commercially used for cracking, rearrangements, and alkylation of aromatic rings, while basic zeolites can be used for double bond isomerization (with no concomitant skeletal isomerization), dehydrogenation, and selective oxidation. In spite of their industrial potential, basic zeolites have received very little attention as far as their characterization is concerned. To partially remedy this situation, we at Shell have been engaging in a synthesis as well as a multi-techniques characterization effort in order to understand the workings of this new class of solid bases.

Basic zeolites are generally prepared by either ion-exchange or impregnation (or both) of acidic zeolites with alkali metal salts. For example, Hathaway and Davis[1] prepared a basic zeolite capable of selectively dehydrogenating isopropanol to acetone by reacting NaY-zeolite with both CsOH and Cs acetate. Since there are many distinct crystallographic sites available for occupancy in any given zeolitic framework, as well as possible locations on the exterior surfaces of the zeolite, it is difficult to ascertain the siting of the catalytically active species in these basic zeolites. In order to determine the location of the impregnated metal, we, in March of this year, obtained time-of-flight neutron powder diffraction (NPD) data on two samples of Y-zeolite: a conventional NaY, and a Zn impregnated NaY-zeolite.

Surprisingly, in spite of the fact that there are over 60 crystal structure determinations of X or Y-zeolites, on either single crystals or powder samples, none have involved zinc. Nearly every element in the Periodic Table has been ion-exchanged into zeolite Y, and the literature on the behavior of these zeolites are voluminous. In general, due to the large size of the supercage, metal species within the supercages cannot be exactly located crystallographically. The charge balancing cations, however, are readily locatable at the Y-zeolite sites I, I', II', and II (Figure 1).

In order to carry out the Rietveld analysis on the NPD data, we have previously obtained GSAS from Dr. Robert Von Dreele at Los Alamos National Laboratory. Both datasets were refined in the space group Fd3m. Using GSAS, the framework for both structures refined smoothly, and then using difference Fourier technique, the cations or water molecules were located and refined.

For the NaY sample, we found the various Na^+ cations and water molecules were quite similar to the dehydrated NaY reported by Marti et al..[4] Chemical analysis determined the unit cell formula for the NaY sample to be $Na_{48}Ca_2Al_{52}Si_{140}O_{384}(H_2O)_{125}$. For the ZnNaY, chemical analysis determined the unit cell formula to be $Na_{44}Ca_2Zn_2Al_{52}Si_{140}O_{384}(H_2O)_{66}\cdot 10ZnO$. From the elemental composition, it is clear that there is an excess of possible cationic species (Na^+, Ca^{+2}, and Zn^{+2}) to balance out the 52 negative charges from the Al. From the preparation step, the zinc can reside in three possible places: 1) the surface of the crystallites, 2) the supercages, and 3) a specific cation site. The Rietveld analysis is not capable of detecting the zinc on the crystallite surfaces, and unless the zinc has somehow been localized (immobilized) within the supercages, it too cannot be detected. The Rietveld analysis can, however, detect the presence of zinc at the specific cationic sites. The neutron powder diffraction showed two significant differences between the NaY and ZnNaY samples, namely that ZnNaY has greater neutron density at site I, and that ZnNaY's site I' is further into the sodalite cage than usual. We interpreted these differences as being that there are Zn^{+2} ions at site I, along with Na^+, and that there is a water molecule at site I' instead of Na^+. It can be speculated that with the addition of the divalent Zn substituting for the monovalent Na, there would be fewer atoms needed for charge balancing, and thereby providing more room in the sodalite cage for the water molecule. Future work will involve comparing these current results with those from a completely zinc ion-exchanged Y-zeolite.

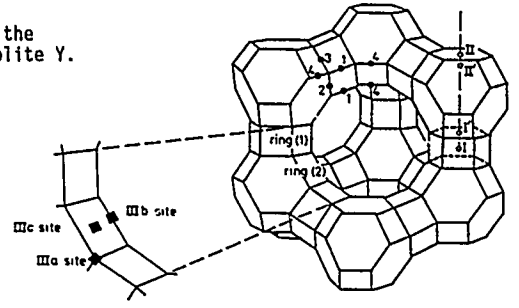


Figure 1. Illustration of the structure of zeolite Y.

REFERENCES:

1. P. E. Hathaway and M. E. Davis, J. Catal., 116, 263 (1989).
2. A. Corma, V. Fornes, R. M. Martin-Aranda, H. Garcia, and J. Primo, Appl. Catal., 59, 237 (1990).
3. J. Marti, J. Soria, and F. H. Cano, J. Colloid and Interface Sci., 60, 82 (1977).
4. O. B. Yang, S. I. Woo, and R. Ryoo, J. Catal., 123, 375 (1990).

INSTRUMENT USED: GPPD	DATE OF REPORT: February 13, 1991	EXPERIMENT NO.: 1262

TITLE:
Structural Characterization of Basic Zeolites

AUTHORS AND AFFILIATIONS:
W. J. Reppart and S. C. Tang, Shell Development Company

DATES OF EXPERIMENT: September 11-12, 1990

X APPROVED BY PROGRAM COMMITTEE, OR

PART OF INSTRUMENT SCIENTIST ALLOCATION

REPORT RECEIVED:

EXPERIMENTAL REPORT (or Abstract of Publication)

Base catalysis over alkali-modified molecular sieves is an area of growing interest. The goal is that of producing strongly basic zeolites to extend the well-known chemistry of acidic catalysts. Acidic zeolites are commercially used for cracking, rearrangements, and alkylation of aromatic rings, while basic zeolites can be used for double bond isomerization (with no concomitant skeletal isomerization), dehydrogenation, and selective oxidation. In spite of their industrial potential, basic zeolites have received very little attention as far as their characterization is concerned. Basic zeolites are generally prepared by either ion-exchange or impregnation (or both) of acidic zeolites with alkali metal salts. In order to determine the location of the metal species, we, in March of 1990, obtained time-of-flight neutron powder diffraction (NPD) data on two samples of Y-zeolite: a conventional NaY, and a Zn impregnated NaY-zeolite (designated as im-ZnNaY). In September of 1990, we returned to Argonne and obtained NPD data on another ZnNaY-zeolite, but one in which the Zn has been ion-exchanged into the zeolite rather than impregnated. First a dataset was taken on a hydrated Zn-ion-exchanged-NaY zeolite (designated as ie-ZnNaY), then the sample was transferred to a 450°C furnace and kept there for 2 hours, it was then cooled to room temperature, and another NPD dataset taken on it (designated as hie-ZnNaY) with the GPPD.

Using GSAS, both datasets were refined in the space group Fd-3m. The framework for both structures refined smoothly, and then using difference Fourier technique, the cations or water molecules were located and refined. In general, due to the large size of the supercage, metal species within the supercages cannot be exactly located crystallographically. The charge balancing cations, however, are readily locatable at the Y-zeolite sites I, I′, II′, and II. The hydration level of metal-exchanged zeolites greatly influences the locations of the cations. For hydrated Y-zeolites, most of the metal cations are generally located at site I′ and in the supercage, with site I (the center of the hexagonal prism) being empty. Upon dehydration, some of the metal cations migrate from the supercage into the smaller cells, thus occupying site I. Chemical analysis determined the unit cell formula for the ie-ZnNaY sample to be $Na_{12.3}Zn_{19.8}Al_{52}Si_{140}O_{384}\cdot x(H_2O)$. The presence of a substantial quantity of Na was expected since it is extremely difficult to completely exchanged out a NaY zeolite. It was not possible, on the basis of the Rietveld analysis, to distinquish unambiguously between Zn and Na cations for the ie-ZnNaY and hie-ZnNaY samples. On Table I, the results of the Rietveld analysis on the cation distribution for the 4 samples (NaY, im-ZnNaY, ie-ZnNaY, hie-ZnNaY) are compared. Based on the results obtained thus far, several observations can be made. First of all, it is clear that neither ie-ZnNaY nor hie-ZnNaY has cations located at site I; this indicates that the heat treatment at 450°C alone was not sufficient to engender the migration of cations from site I′ to site I. Secondly, the site II′ is not always occupied, and the assignment of an O atom from a water molecule to that position is by analogy to an earlier report for NaY. Thirdly, for all the ZnNaY samples examined, neutron density can be found at both x=y=z=0.25 (the usual site II location) and at x=y=z=0.27, which are 1 Å apart. We attribute this to disorder in the position of the metal cation, and denote these sites as II and IIb. Fourthly, based on the occupancy level at site I and the position of the O at site I′ for the Zn-impregnated NaY sample, a combined occupancy of Zn and Na for site I can be assigned. Lastly, there seems to be an apparent high degree of disorder for several of the cation positions for the ie-ZnNaY and hie-ZnNaY samples, as evidence by the large thermal parameters for those positions. Future work will involve attempting to discern the location of Zn versus Na in these samples by anomalous dispersion measurements at a synchrotron X-ray facility.

Table 1. Cation Locations for Zeolite Samples

Site		NaY	im-ZnNaY	ie-ZnNaY	hie-ZnNaY
I	x=y=z=	0.0	0.0	0.0	0.0
	atom	Na	Zn,Na[1]	-	-
	SOP	0.574	1.123[2]	-	-
	U_{iso}, Å^2	0.027	0.031	-	-
I′	x=y=z=	0.0729	0.1164	0.0634	0.0554
	atom	Na	O	Zn,Na[1]	Zn,Na[1]
	SOP	0.223	0.287	0.762[2]	0.787[2]
	U_{iso}, Å^2	0.027	0.031	0.123	0.020
II′	x=y=z=	0.1712	-	-	0.2037
	atom	O	-	-	O
	SOP	0.432	-	-	0.220
	U_{iso}, Å^2	0.027	-	-	0.077
II	x=y=z=	0.2485	0.2475	0.2334	0.2378
	atom	Na	Zn,Na[1]	Zn,Na[1]	Zn,Na[1]
	SOP	0.428	0.469[2]	0.454[2]	0.338[2]
	U_{iso}, Å^2	0.027	0.031	0.018	0.020
IIb	x=y=z=	-	0.2733	0.2663	0.2701
	atom	-	Zn,Na[1]	Zn,Na[1]	Zn,Na[1]
	SOP	-	0.353[2]	0.655[2]	0.343[2]
	U_{iso}, Å^2	-	0.031	0.144	0.075

[1] Either Zn, or Na, or both. [2] SOF refined assuming only Na present.

INSTRUMENT USED:	DATE OF REPORT:	EXPERIMENT NO:
GPPD	Dec. 1991	D1991

TITLE: Stucture Determination and Rietveld Refinement of the Aluminophosphate Molecular Sieve $AlPO_4$-8

AUTHORS AND AFFILIATIONS: J. W. Richardson, Jr. (IPNS), E. T. C. Vogt (AKZO Chemicals Nederland bv, Amsterdam)

DATES OF EXPERIMENT: Oct. 12-14, 1989 and Dec. 11, 1989

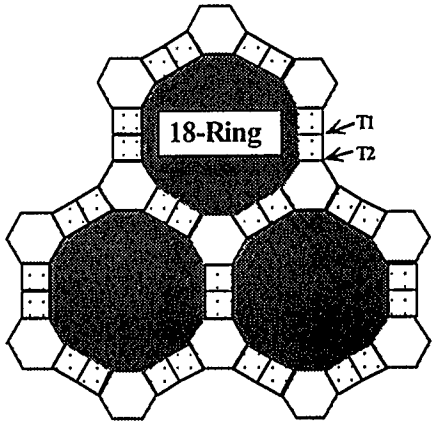
CHECK ALL APPLICABLE BOXES:

- [ ] APPROVED BY PROGRAM COMMITTEE
- [x] INSTRUMENT SCIENTIST ALLOCATION
- [ ] DO NOT PUBLISH
- [ ] PROPRIETARY RESEARCH
- [ ] PRT ALLOCATION

EXPERIMENTAL REPORT (or Abstract of Publication)

The 18-ring pore molecular sieve $AlPO_4$-54 (otherwise known as VPI-5) recrystallizes to the 14-ring sieve $AlPO_4$-8. This recrystallization appears to be reversible under proper conditions, as could be explained on the basis of the structural relationship between the two materials. $AlPO_4$-54 has an 18-ring channel bounded by six 6-rings and six pairs of adjoining 4-rings. In the conversion to $AlPO_4$-8, two-thirds of the adjoining 4-rings are converted to 6-rings and reconnected to form a smaller, 14-ring channel bounded by eight 6-rings, two pairs of adjoining 4-rings and two single 4-rings. The space group for $AlPO_4$-8 ($Cmc2_1$: a=33.0894(25), b=14.6832(13), c=8.3630(6) Å at room temperature) is a direct sub-group of that for $AlPO_4$-54 ($P6_3cm$: a=18.549(1), c=8.404(1) Å for de-hydrated form; orthohexagonal setting: a=32.128, b=18.549, c=8.404 Å). Interconversion of the two structures may be facilitated by extra-coordination of framework aluminum atoms with water molecules. The observed small adsorption capacity of $AlPO_4$-8 can be explained by stacking faults where, within a single channel, different pairs of adjoining 4-rings are left unbroken.

AlPO-54 to AlPO-8 Transformation



AlPO-54

12 Å channels

J. W. Richardson, Jr. (Argonne National Lab.)

J.V. Smith, J.J. Pluth (Univ. Chicago)

Hexagonal topology
2 types of Al,P

Issues
- Stability of AlPO-54
- Role of water
- Structures

Irreversible??

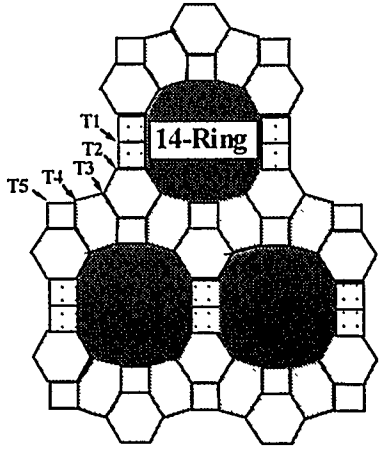
AlPO-8

8-9 Å channels

J. W. Richardson, Jr. (ANL)

E.T.C. Vogt (AKZO Chem., Amsterdam)

Orthorhombic topology
5 types of Al,P



INSTRUMENT USED:	DATE OF REPORT:	EXPERIMENT NO:
GPPD	January 1994	D1993

TITLE: Characterization of Corrosion Products generated from Failure of the IPNS Depleted Uranium Spallation Target

AUTHORS AND AFFILIATIONS: J. W. Richardson, Jr. (IPNS) and J. M. Carpenter (IPNS)

DATES OF EXPERIMENT: Dec. 15-17, 1993

CHECK ALL APPLICABLE BOXES:

- [ ] APPROVED BY PROGRAM COMMITTEE
- [x] INSTRUMENT SCIENTIST ALLOCATION
- [ ] DO NOT PUBLISH
- [ ] PROPRIETARY RESEARCH
- [ ] PRT ALLOCATION

EXPERIMENTAL REPORT (or Abstract of Publication)

Near the end of 1992 the IPNS depleted uranium target failed. Metallurgical examination of the target assembly after failure indicated that failure was most probably caued by leakage in the zircaloy cladding, resulting in corrosion of the uranium.

Rietveld profile analysis revealed the composition of the extracted material. Put very succinctly, we see three interaction products: UO_2, β-UH_3 and UO_3, along with α-U (unreacted "fuel"), V (sample was contained in two thin walled cans) and a trace of Fe (see Figure 1 for Rietveld profile plot). These results are based on distinct - but not necessarily unambiguous - features observed in the data, and should be considered tentative pending critical review by experts.

According to the relative scattering of the various phases and the known amount of vanadium, from the ~200 mg sample there were (roughly) 80 mg of UO_2, 55 mg β-UH_3, 40 mg α-U, 6 mg UO_3 and 3 mg Fe. Based on these data, of all reacting uranium atoms 63% formed UO_2, 32% β-UH_3 and 5% UO_3. As background for a critical review of the analysis, what follows is a description of the evidence for each of the phases, from most important to least.

β-UH_3 - This is the non-metastable (stable?) form of UH_3. The peaks are rather broad, indicating small particles; the Rietveld refinement suggests ~1500 Å (0.15 mm). This is the only phase which on the face of it has an expanded lattice relative to literature values.

UO_2 - The peaks of this phase are likewise very broad, consistent with ~500 Å particles. The lattice parameter corresponds to very nearly stoichiometric amounts of uranium and oxygen.

UO_3 - This phase was not necessarily expected. It was, however, the only logical phase we could find with a major reflection at d = 2.08 Å. The lattice parameter is in excellant agreement with the literature value and the fit looks good.

EXPERIMENTAL REPORT (CONTD.)

Rietveld Profile Plot (Depleted Uranium - Corrosion Products)

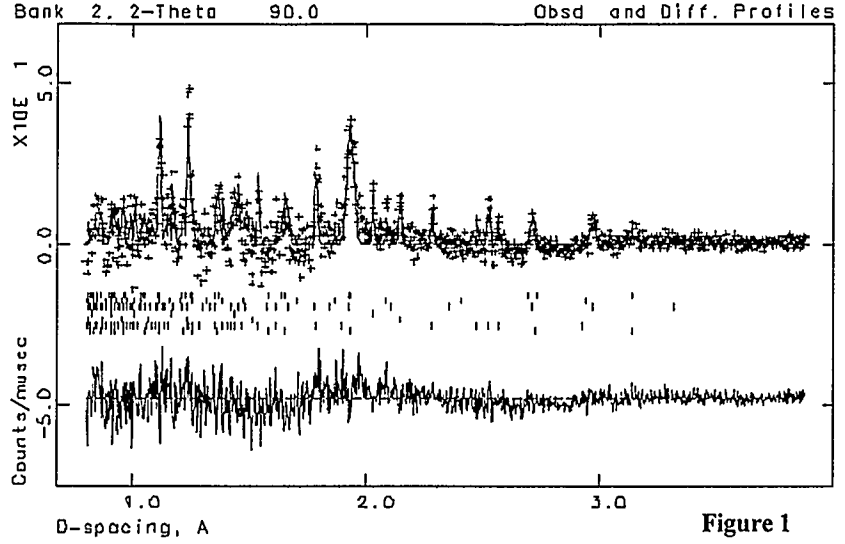


Figure 1

α-Uranium - The most obvious evidence for this phase is the famous triple (002), (021), (111) reflections at d~2.5-2.6 Å. Refined lattice parameters suggest possible dissolution of something in the uranium lattice. In earlier work with U/Zr and U/Pu/Zr alloys, we observed similar lattice distortions due to solubility. In those cases where larger (than U) atoms of Zr and Pu were substituted into the lattice the a- and c-axes expanded and the b-axis contracted. We observe the opposite effect here, which might be expected with hydrogen or oxygen solubility.

Vanadium - The characteristic (110) reflection at d = 2.14 Å is always the most apparent contribution from our V cans, and is isolated from reflections from all other phases.

Iron - The (110) reflection for iron is at lower d-spacing (2.03 Å) than that for vanadium. Although this phase was not expected, it is the only reasonable phase with a major reflection at this d-spacing. The Fe scattering is most likely due small filings from the probe used to remove the corrosion material (the predicted 3 mg of Fe has a volume of 0.0004 cm^3).

INSTRUMENT USED:	DATE OF REPORT:	EXPERIMENT NO.:
GPPD	29-JUL-92	1594

TITLE:
Temperature Dependence of Structure Parameters in UF4

AUTHORS AND AFFILIATIONS: S. Roberts, B. Cort, G. H. Lander
S. Kern (Colorado State U.), J. W. Richardson, Jr., F. J. Rotella, J. Hayward

DATES OF EXPERIMENT:
June 5 - June 8, 1992

CHECK ALL APPLICABLE BOXES:

- [X] APPROVED BY PROGRAM COMMITTEE
- [ ] INSTRUMENT SCIENTIST ALLOCATION
- [ ] DO NOT PUBLISH
- [ ] PROPRIETARY RESEARCH
- [ ] PRT ALLOCATION

EXPERIMENTAL REPORT (or Abstract of Publication)

Correlation of Motional Effects in UF_4

UF_4 has been run on the GPPD at 15,50,100,200 and 300K. UF_4 exists in a monoclinic structure, space group C2/c, with two Uranium sites of differing symmetry and seven different fluorine positions. We found that the cell volume decreases as the temperature is raised from 15K to room temperature.

We have extended the Rietveld analysis program capabilities to handle as many as 10,000 reflections; this has permitted us to obtain stable values of the anisotropic temperature factors for all atoms in the unit cell. In all, 84 parameters have been refined. The lattice parameters are listed in the Table below:

T(K)	a(Å)	b(Å)	c(Å)	beta(°)
15	12.8051	10.7864	8.3758	126.191
50	12.8038	10.7849	8.3747	126.192
100	12.8001	10.7842	8.3716	126.189
200	12.7959	10.7860	8.3690	126.213
300	12.7944	10.7901	8.3687	126.247

The Figure shows the temperature variation of these parameters, as well as that of the cell volume. It is seen that the decrease in cell volume has flattened out by room temperature. There is a 0.2% change in volume in going from 15K to 300K.

The room temperature parameters are in good agreement with those obtained previously by X-ray (1) and neutron (2) diffraction, but our temperature factors, when converted from anisoptropic betas to isotropic B's, are different. There are small changes in the lattice parameters that occur when the refinement is changed from one using isotropic temperature factors to one using a complete set of anisotropic ones.

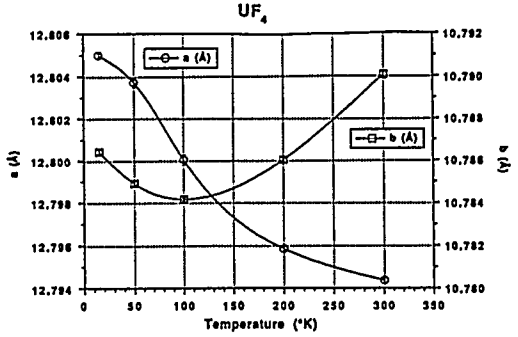
Without a determination of the temperature variation of the isomorphic, but electronically inert, ThF_4, we cannot say whether this unusual behavior is structural, or related to electronic effects produced by the $5f^2$,U^{4+} ion. An analysis of the variation of the anisotropic temperature parameters is now underway.

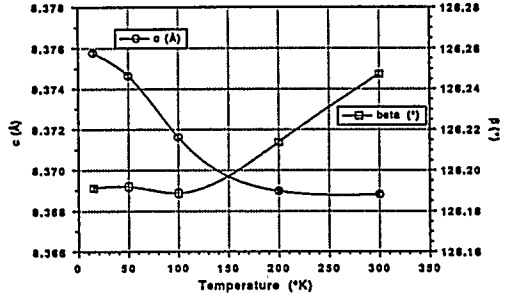
References

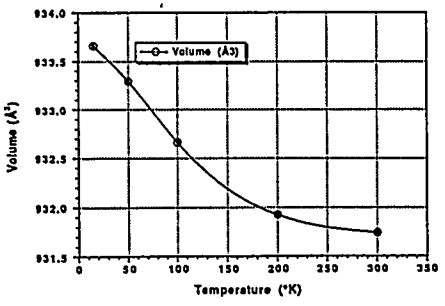
1. W.H.Zachariasen Acta Cryst. 2 388 (1949)

2. A.C.Larson,R.B.Roof,and D.T.Cromer Acta Cryst. 17 555(1964)

EXPERIMENTAL REPORT (CONTD.)







INSTRUMENT USED:	DATE OF REPORT:	EXPERIMENT NO.:
GPPD	2/5/91	----

TITLE: Palladium Deuteride Formation in the Cathode of an Electrochemical Cell: An In situ Neutron Diffraction Study

AUTHORS AND AFFILIATIONS: F. J. Rotella and J. W. Richardson, Jr., IPNS Division; L. Redey, Chemical Technology Division; and G. P. Felcher, R. L. Hitterman, and R. Kleb, Materials Science Division; Argonne National Laboratory

DATES OF EXPERIMENT: 7/24-27/89 and 8/2/89

☐ APPROVED BY PROGRAM COMMITTEE, OR

☒ PART OF INSTRUMENT SCIENTIST ALLOCATION

REPORT RECEIVED:

EXPERIMENTAL REPORT (or Abstract of Publication)

Abstracts of contributed papers of this work have been published:

G. P. Felcher, R. L. Hitterman, L. Redey, J. W. Richardson, Jr. and F. J. Rotella, Bull. Am. Phys. Soc. 35(3), 370 (1990)

F. J. Rotella, J. W. Richardson, Jr., L. Redey, G. P. Felcher and R. L. Hitterman, Program and Abstracts, Am. Cryst. Assoc. Mtg., Series 2, ISSN 0569-4221. 18, 64 (1990)

A "research highlight" describing this experiment was written for the IPNS Progress Report 1988-1990 - "*In situ* Neutron Diffraction Study of Palladium Deuteride Formation in the Cathode of an Electrochemical Cell: A Status Report", F. J. Rotella, J. W. Richardson, Jr., L. Redey, G. P. Felcher, R. L. Hitterman, and R. Kleb, pp. 35-37. The following is a summary of the research highlight.

Neutron diffraction measurements as a function of charging time of the palladium cathode in a working electrochemical cell were performed using the GPPD. The cell, with a wrought Pd rod as cathode, Pt anode and circulating LiOD-saturated D_2O electrolyte, all contained in a quartz tube, was designed to minimize the contribution of amorphous scattering from the liquid electrolyte and quartz tube and to eliminate crystalline scattering from elements of the cell other than the Pd cathode. Diffraction data as a function of charging time (to approximately 62.6 h) were collected while the cell was being galvanostatically charged and cell voltage was monitored.

What has been learned from this experiment to date:

(1) the orientation of crystallites in the Pd rod is not random nor is it amenable to a simple texture model, limiting the ability to extract quantitative structural information from the data.

(2) the observed Bragg intensities from Pd and the two observed hydride phases, α-PdD_x and β-PdD_x, are all consistent with fcc (Fm3m) unit cells.

(3) the observed Bragg intensities from β-PdD_x are fully consistent with deuterium occupation of octahedral lattice sites.

(4) the β-deuteride phase begins to form after about 2.5 h of charging (Figure 1), while the formation of α-deuteride appears to begin upon charging.

(5) the resolution of the data is sample-limited, making it impossible to distinguish between the Pd and α-PdD_x phases - the FWHM of the (2 2 0) reflection shows virtually no variation with charging time.

(6) the FWHM of the β-deuteride diffraction peaks is broadened by a factor of at least 2½ relative to the GPPD resolution at 2θ = -90° after 62.6 h of charging, and its variation with d is best fit with a straight line (Figure 2), indicating that deuterium absorption introduces a significant strain in the Pd cathode.

(7) assuming that deuterium absorption does not change the texture in the Pd rod substantially, the ratio of I(2 2 0) of the β-deuteride to that of the Pd/α-deuteride, normalized by F^2(2 2 0) of $PdD_{1.0}$ and Pd respectively, should provide an approximate measure of the deuterium absorbed by the Pd cathode (Figure 3); after 62.6 h of charging, x in PdD_x is approximately 0.2.

We are incorporating a model for sample texture based on spherical harmonics [M. Järvinen, M. Merisalo, A. Pesonen and O. Inkinen, J. Appl. Cryst. 3 (1970), 313] into the IPNS Rietveld analysis software in the hope that it will allow the present experiment to yield quantitative structural information. Additionally, we are exploring the possibility of producing texture-free Pd cathode material for future experiments. In any case, measurements are planned to much longer charging times. In an initial attempt, after approximately 128 h of charging, macroscopic strain in the Pd cathode caused the quartz tube to break and the cell to fail.

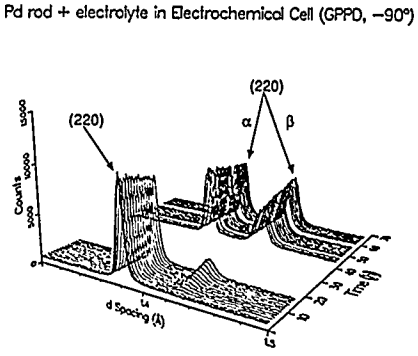


Figure 1

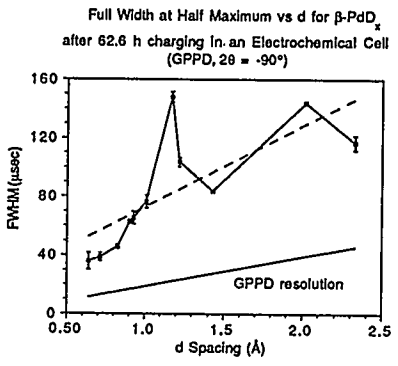


Figure 2

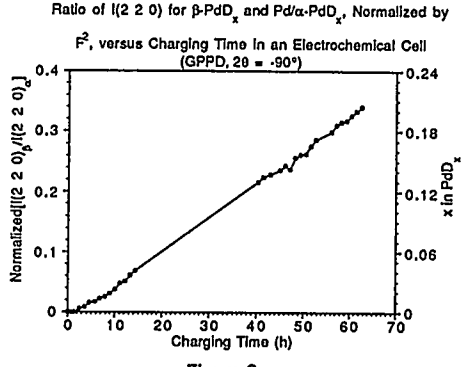


Figure 3

INSTRUMENT USED:	DATE OF REPORT:	EXPERIMENT NO.:
GPPD	9/16/91	1479

TITLE:

LOCATION OF Zn^{2+} AND D^+ IN ZEOLITE Y

AUTHORS AND AFFILIATIONS:
Karl Seff, Petrie Peapples-Montgomery and Tao Sun
Chemistry Department, University of Hawaii, Honolulu, HI 96822

DATES OF EXPERIMENT: June 13-15, 1991

☒ APPROVED BY PROGRAM COMMITTEE, OR

☐ PART OF INSTRUMENT SCIENTIST ALLOCATION

REPORT RECEIVED:

EXPERIMENTAL REPORT (or Abstract of Publication)

Abstract 1

Fully dehydrated, fully Zn^{2+}-exchanged zeolite Y has been synthesized by the reduction of all H^+ ions in H-Y by zinc vapor. The solvent-free redox reaction goes to completion at 420 °C with about 0.2 torr of Zn^0 to give $Zn_{27.5}Si_{137}Al_{55}O_{384}$($a_o$ = 24.4688(3) Å). The crystal structure was determined in the cubic space group $Fd\bar{3}m$ by pulsed-neutron powder-diffraction methods at 10 K and was refined to R_p = 0.0268 and R_{wp} = 0.0368. Two different Zn^{2+} positions were found in the structure. The Zn(1) position is located on a threefold axis in the sodalite unit adjacent to a single six-ring, 2.183(12) Å from three nearest framework oxygens. The Zn(2) position is also on a threefold axis in the sodalite unit, adjacent to a double six-ring, 2.228(15) Å from three nearest framework oxygens. It must be true, on the basis of refined fractional occupancy parameters and to avoid 3.1 Å Zn(1) - Zn(2) distances, that half of the sodalite cavities contain four Zn(1) ions arranged tetrahedrally, and that the other half contain about three Zn(2) ions similarly arranged.

Abstract 2

Zeolite Y largely ion-exchanged with Pb^{2+} was dehydrated and treated with excess D_2S. The sample was maintained at 10^{-6} torr and 25 °C for 24 h to remove excess D_2S. The product crystal structure was determined at 10 K by pulsed-neutron powder diffraction techniques in the cubic space group $Fd\bar{3}m$ with a_o = 24.7027(3) Å. Least-squares refinement converged to the final residuals R_p = 0.0320 and R_{wp} = 0.0430. The crystallographic results indicate that the formula of this material is approximately $(Pb^{2+})_6(PbSD^+)_6Na_3D_{34}Si_{137}Al_{55}O_{384}$. The 34 deuterium ions occupy two crystallographic sites: one is close to a framework oxygen at the side of a hexagonal prism, and the other is close to a framework oxygen of a single 6-ring. Both deuterium positions are in the supercages where they can hydrogen bond to SD^- ions. The O-D distances are both 1.26(3) Å, a little longer than an O-H bond, perhaps because of hydrogen-bonding. Lead cations occupy three different positions, all on threefold axes. Pb(1) occupies site II in the supercage, 2.85 Å from three framework oxygens. This long Pb(1)-oxygen distance suggests that SD^- ions, needed to balance charge and stoichiometry but not located in this work, interact strongly with Pb(1) ions in the supercages. Two other Pb^{2+} positions each approach three framework oxygens: Pb(2)-O = 2.504(23) Å and Pb(3)-O = 2.553(22) Å, normal strong Pb-O interactions. Pb(2) and Pb(3) lie within sodalite cavities, Pb(2) at Site I' and Pb(3) at site II'. Sodium ions are found at the centers of hexagonal prisms. These results indicate that PbS is molecularly dispersed as $PbSD^+$ in this structure.

INSTRUMENT USED:	DATE OF REPORT:	EXPERIMENT NO.:
GPPD	6-1-90	NSF 11

TITLE:
The role of Pb- substitution in the Bi-Sr-Ca-O System

AUTHORS AND AFFILIATIONS:
Carlo U Segre, Justin Akujeze and P. Radaelli

DATES OF EXPERIMENT: 2-5 Mar 1990

☐ APPROVED BY PROGRAM COMMITTEE, OR

☐ PART OF INSTRUMENT SCIENTIST ALLOCATION

REPORT RECEIVED:

EXPERIMENTAL REPORT (or Abstract of Publication)

The role of Pb substitution in the $Bi_{2+x}Sr_{2-x}CuO_6$ system

Several Pb-doped $Bi_{2+x}Sr_{2-x}CuO_6$ samples have been prepared by solid state reaction and splat-cooling method. Lead has been formally substituted both for bismuth and strontium in a range of composition varying from 0.1 to 0.6 formula units. Neutron diffraction data have been collected at room temperature on GPPD, and analyzed by the Rietveld refinement technique. The space group A2aa has been used, and partial occupancy has been allowed for both the Bi and the Sr sites in order to clarify which of these atoms Pb substitutes for; due to the relative closeness of the scattering factors of Pb and Bi, this information can be accessed only on high quality data; a complete understanding of the structural model is also required. The general features of the diffraction pattern of this series of samples are well reproduced by the refinement: it is clear that the orthorombicity of the cell, which is pseudotetragonal in the undoped compound, increases with lead concentration. Besides, the modulation peaks of the undoped material disappear with the lead doping. In some cases quite low values of the R-factors can be obtained ($R_w \approx 2.1$). It is clear, however, that the details of the structural model are still to be understood, especially in the samples with high lead concentration. In addition the presence of an amorphous background in some of the samples raises serious doubts about the quality of the entire series. Further work is presently in progress in order to improve the quality of the samples and find a model which gives a more accurate description of the structure of this class of compounds.

EXPERIMENTAL REPORT (CONTD.)

INSTRUMENT USED: SEPD	DATE OF REPORT: 6/15/93	EXPERIMENT NO.: 1457

TITLE: LOCAL STRUCTURE OF SUPERCONDUCTING OXIDES

AUTHORS AND AFFILIATIONS: T. R. SENDYKA, W. DMOWSKI, T. EGAMI
UNIVERSITY OF PENNSYLVANIA

DATES OF EXPERIMENT: 8-12 DEC, 1992

CHECK ALL APPLICABLE BOXES:

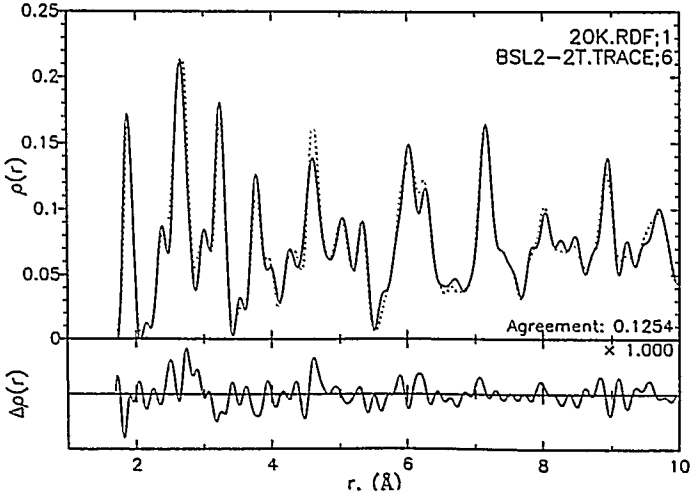
- [x] APPROVED BY PROGRAM COMMITTEE
- [ ] INSTRUMENT SCIENTIST ALLOCATION
- [ ] DO NOT PUBLISH
- [ ] PROPRIETARY RESEARCH
- [ ] PRT ALLOCATION

EXPERIMENTAL REPORT (or Abstract of Publication)

The changes with temperature of the local atomic structure of $La_{2-x}Sr_xCuO_4$ was studied using the pair distribution function (PDF) analysis. The 2-1-4 systems were looked at the variety of temperatures for lanthanum compositions x=0.125 and x=0.15. In this material the x=0.15 is the maximum T_c composition, while x=0.125 is the composition where the critical temperature is slightly suppressed. The exact nature of this suppression is not well understood for the compound doped with strontium, while in the analogous compound doped with barium the deep suppression of T_c is associated with the appearance of new low temperature tetragonal phase (LTT).

The atomic structure of the strontium doped compound has been examined in detail. The local structure of all the 2-1-4 compound is different from the average structure as determined by usual crystallographic techniques. Detailed modeling has been performed for the case of $La_{1.85}Sr_{0.15}CuO_4$. The oxygens atoms are shifted in the c-axis direction from their average positions. A fraction of apical oxygens is shifted towards the CuO_2 planes, and in-plane oxygens are shifted collectively in 5x5 Å domains. The result of the PDF fit is presented below. The agreement factor for this model is A=0.125, comparing with the A=0.155 for the average structure. Solid line represents the experimental PDF.

Model with oxygens moving along c-axis in domains



INSTRUMENT USED:	DATE OF REPORT:	EXPERIMENT NO:
GPPD	Dec15, 1993	1761

TITLE: **Temperature Dependence of the Lattice Parameters in $HoP_{1-x}V_xO_4$ ($0 < x < 1$)**

AUTHORS AND AFFILIATIONS: **S. Skanthakumar, C.-K. Loong, L. Soderholm, and J. W. Richardson, Jr., (ANL), M. M. Abraham and L. A. Boatner (Oak Ridge National Lab.)**

DATES OF EXPERIMENT: **7/21-7/22, 7/26-7/27, 10/21-10/22, 11/12-11/13 and 12/8-12/9/1993**

CHECK ALL APPLICABLE BOXES:

- [X] APPROVED BY PROGRAM COMMITTEE
- [ ] INSTRUMENT SCIENTIST ALLOCATION
- [ ] DO NOT PUBLISH
- [ ] PROPRIETARY RESEARCH
- [ ] PRT ALLOCATION

EXPERIMENTAL REPORT (or Abstract of Publication)
Abstract submitted for the March 1994 Meeting of the American Physical Society.

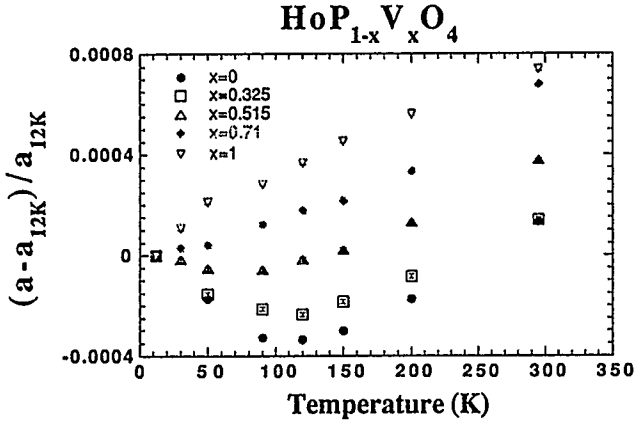
Anomalies in the Temperature Dependence of the Lattice Parameters in $HoP_{1-x}V_xO_4$ ($0 < x < 1$)

S. Skanthakumar, C.-K. Loong, L. Soderholm (ANL), J. W. Richardson, Jr., M. M. Abraham and L. A. Boatner (Oak Ridge National Lab.)

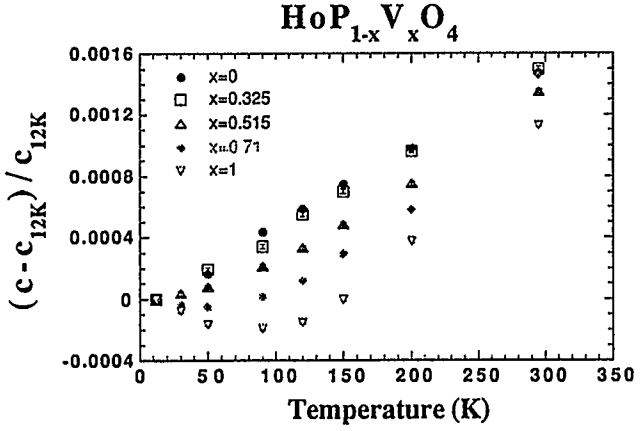
Abstract

$HoP_{1-x}V_xO_4$ crystallizes in the tetragonal zircon structure ($I4_1/amd$) in which Ho occupies a single site of D_{2d} symmetry, while P and V are surrounded by tetrahedra of oxygen atoms. Neutron powder-diffraction techniques have been used to study the temperature dependence of the lattice parameters in these materials. Below T ≈ 100K, the lattice parameter *a* of $HoPO_4$ increases with decreasing temperature while *c* decreases, which is in agreement with a previous x-ray study[1]. In $HoVO_4$, the above behavior is reversed, that is, *a* decreases with decreasing temperature while *c* increases. In the mixed compounds, such anomalous temperature dependence of the lattice parameter is reduced. This anomaly in the thermal expansion is related to the difference of the Ho^{3+} ionic ground state in $HoPO_4$ and $HoVO_4$. Inelastic magnetic neutron-scattering results revealed that $HoPO_4$ has a highly anisotropic Γ_5 doublet ground state, while $HoVO_4$ has a nonmagnetic singlet ground state. Possible coupling of the crystalline lattice with the Ho^{3+} ground-state moments in this system is discussed. [1]. V. I. Sokolov, Z. A. Kazei and N. P. Kolmakova, Physica B 176, 101 (1992).

A. Temperature dependence of the lattice parameter a for different V concentrations x ($0 < x < 1$).



B. Temperature dependence of the lattice parameter c for different V concentrations x ($0 < x < 1$).



INSTRUMENT USED:	DATE OF REPORT:	EXPERIMENT NO.:
GPPD	12/7/90	1261

TITLE:
Effect of Interfacial Films on the Residual Thermal Stresses in SiC-Al_2O_3 Composites

AUTHORS AND AFFILIATIONS: T. E. Steyer and K. T. Faber
Department of Materials Science & Engineering, Northwestern University, Evanston, IL 60208

DATES OF EXPERIMENT: September 8 - 11, 1990

☑ APPROVED BY PROGRAM COMMITTEE, OR

☐ PART OF INSTRUMENT SCIENTIST ALLOCATION

REPORT RECEIVED:

EXPERIMENTAL REPORT (or Abstract of Publication)

The purpose of this study was to examine the effects of tailored interfaces on the residual thermal stress in hot-pressed β-SiC whisker-reinforced α-Al_2O_3 composites. Theory [1] predicts that incorporating a compliant coating such as carbon at the whisker–matrix interface will reduce the residual thermal stresses in this system.

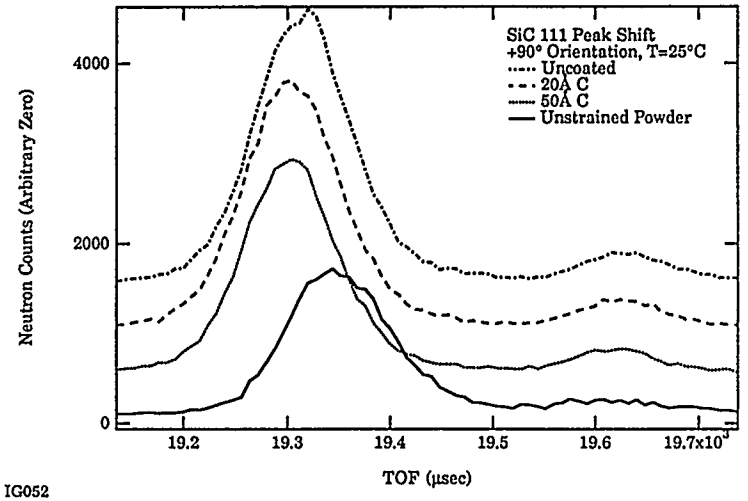
Four composites with distinctly different interfaces were fabricated for this study: no interfacial carbon coating, 20Å C coating, 50Å C coating, and a composite with a 50Å C coating processed 100°C higher than the previous three samples. Due to the anisotropic character of hot-pressed whisker composites, the samples were positioned in the diffractometer such that data from the hot-pressing axis and normal to the hot-pressing axis could be easily deconvoluted. Individual peaks were fit using TOFMANY analysis. Strains were determined from differences between hkl-spacings in the composites and a powder standard as a function of temperature (25, 300, 400, 600, 800, and 1000°C). An example of the peak shift to shorter time-of-flight from powder to composites is shown in Figure 1 for the SiC <111> peak corresponding to the axial direction in the whisker.

Experimental determination of the coefficients of thermal expansion for the strain-free powder were calculated in a straight-forward manner similar to that discussed by Krawitz et al.[2] An overview of the thermal expansion data for the powder standard, Δl/l vs T, is shown in Figure 2.

Figure 3 shows the compressive strain in the SiC <111> versus test temperature. During the thermal cycling from room temperature to 1000°C and returning to room temperature, neutron runs were performed at 25, 400, 800, 1000, 600, and 300°C in order to observe any hysteresis effect due to the presence of glassy interphases. A marked effect is observed in the uncoated composite which may be attributed to segregation of sintering aids to the whisker–matrix interface resulting in a glass interphase.

1. Hsueh, C.-H., P.F. Becher, and P. Angelini, *Effects of Interfacial Films on Thermal Stresses in Whisker-Reinforced Ceramics.* J. Am. Ceram. Soc., 1988. 71(11): p. 929-933.

2. Krawitz, A.D., D.G. Reichel, and R. Hitterman, *Thermal Expansion of Tungsten Carbide at Low Temperature.* J. Am. Ceram. Soc., 1989. 72(3): p. 515-517.



IG052

Figure 1

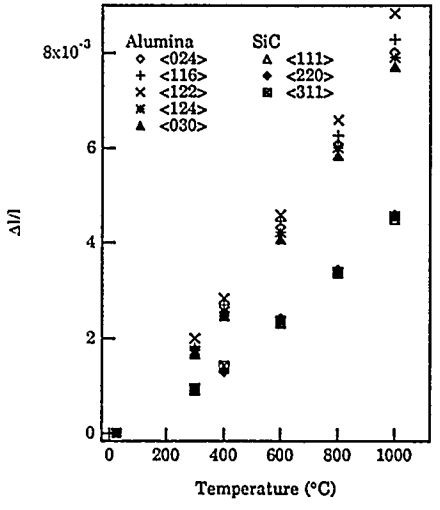


Figure 2

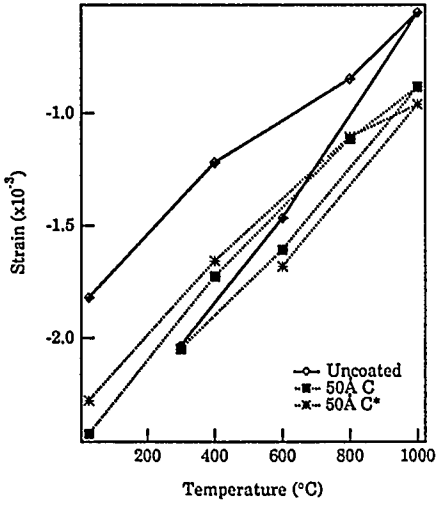


Figure 3

INSTRUMENT USED:	DATE OF REPORT:	EXPERIMENT NO.:
GPPD	7-Jan-94	1460

TITLE:
Effect of Interfacial Films on the Residual Stress in SiC-Al2O3 Composites

AUTHORS AND AFFILIATIONS:
T.E. Steyer and K.T. Faber; Northwestern University, Dept. of Materials Science and Eng., 2225 N. Campus Drive, Evanston, IL 60208-3108

DATES OF EXPERIMENT:
June 4-8, 1991

CHECK ALL APPLICABLE BOXES:

- [x] APPROVED BY PROGRAM COMMITTEE
- [ ] INSTRUMENT SCIENTIST ALLOCATION
- [ ] DO NOT PUBLISH
- [ ] PROPRIETARY RESEARCH
- [ ] PRT ALLOCATION

EXPERIMENTAL REPORT (or Abstract of Publication)

An experiment was performed to examine the effects of compliant interfacial coatings on the residual thermal stress of hot-pressed α–Al_2O_3 reinforced with β–SiC whiskers. For this study, uncoated SiC whiskers and SiC whiskers with 50 Å graphite coatings were used to make composites with a 30 v/o whisker loading. Neutron diffraction was performed to determine average strains for various crystallographic reflections in the whisker and matrix as a function of temperature to assess the strain-free temperature and explore the effects of thermal cycling to 1000°C. Strain was calculated by measuring interplanar spacings from the composites relative to measured interplanar spacings of a strain-free powder of a similarly processed material which was annealed following powder processing.

Crystallographically, the SiC <111> peak is important since the {111} family contains the axial [111] direction. Unfortunately, a radial [2$\bar{2}$0] peak contained in the <220> reflection is unresolved due to overlap with the Al_2O_3 <211> peak. The other resolvable SiC whisker peak, the <311> reflection, does not contain an axial or radial direction, but is useful because it has no analogue in the hexagonal SiC polytypes.

Various Al_2O_3 reflections are resolvable as a function of temperature including, in order of decreasing interplanar spacing, the <104>, <111>, <024>, <116>, <124>, and <300> peaks. The magnitude of strain measured in the Al_2O_3 matrix is much smaller than in the SiC whiskers because the neutron technique measures the strain averaged over the entire volume, and the strain in the matrix decreases as $1/x^2$ where x is the distance from the whisker.

The reduction in the absolute value of residual strain with temperature shown in figure 1 is consistent with residual strains due to thermal expansion mismatch, ε_T, where $\varepsilon_T \propto (\alpha_w - \alpha_m)(T_{SF} - T)$, α is the thermal expansion coefficient for the whisker and matrix, and T is the temperature of interest. The strain-free temperature, T_{SF}, represents the temperature above which creep, grain boundary sliding, or other thermal mechanisms are active to dissipate the strains in the system. Extrapolating the whisker strains as a function of temperature from the ambient to 1000°C data collected yields a strain-free temperature of 1270°C for composites with uncoated SiC whiskers and 1330°C for composites with 50 Å carbon-coated SiC whiskers.

EXPERIMENTAL REPORT (CONTD.)

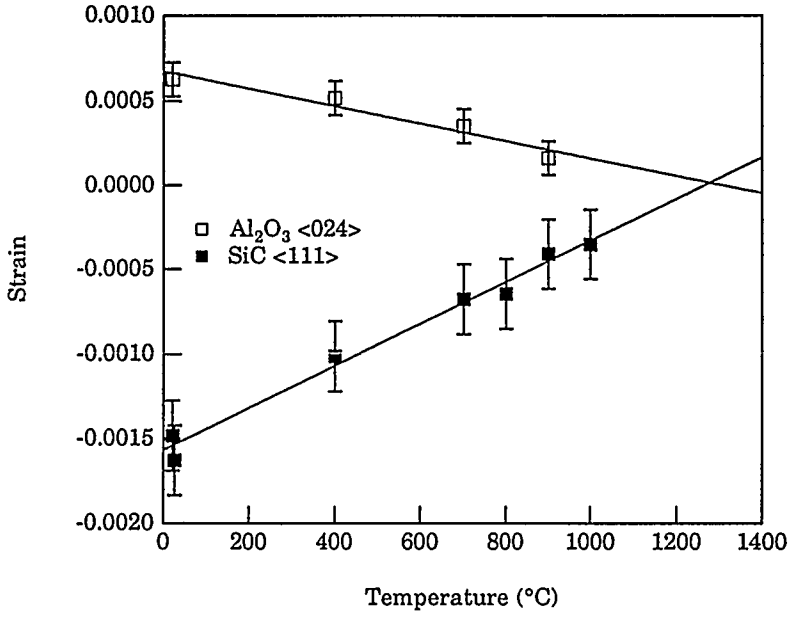


Figure 1: Residual thermal strains measured *in situ* to 1000°C for a Al_2O_3–30% SiC whisker sample.

INSTRUMENT USED:	DATE OF REPORT:	EXPERIMENT NO:
GPPD	August 1992	P1992

TITLE: Neutron Diffraction Study of Irradiated $(U,Pu)O_{2-x}$ Fuel: Structure of Fuel-Sodium-Reaction-Product

AUTHORS AND AFFILIATIONS: R. V. Strain and M. H. Mueller (Fe Div., ANL)
J. W. Richardson, Jr. (IPNS Div., ANL)

DATES OF EXPERIMENT: April 16-18, 1992

CHECK ALL APPLICABLE BOXES:

- [ ] APPROVED BY PROGRAM COMMITTEE
- [ ] INSTRUMENT SCIENTIST ALLOCATION
- [ ] DO NOT PUBLISH
- [x] PROPRIETARY RESEARCH
- [ ] PRT ALLOCATION

EXPERIMENTAL REPORT (or Abstract of Publication)

As part of DOE-PNC RBCB (Run Beyond Cladding Breach) program we studied the fuel-sodium-reaction product (FSRP) and other changes in the fuel that occur as a result of RBCB operation. The GPPD was used to obtain crystallographic data on samples that were operated in the RBCB mode. The overall goal of the neutron diffraction studies for the RBCB program is to determine the structure of the FSRP and the fuel itself over a range of temperatures encompassing the operating temperatures of the outer regions of the oxide fuel in a LMR (500 to 1000°C). It is assumed that the FSRP is similar to sodium-uranate (Na_3UO_4), but little reliable data is available for the compound formed between sodium and mixed-oxide fuel, particularly for the conditions that may exist in an actual reactor (temperature, pressure, and fission-products). Reaction between sodium and the fuel reduces the oxygen content of the fuel; these changes in the fuel O/M could be monitored by measurement of the lattice constants of the fuel. Comparison of differences between intact and breached pins would provide data to elucidate the effect of RBCB operation. A previous study has indicated that both sodium uranate (Na_3UO_4) and the FSRP (Na_3MO_4 where M is U and Pu in the same ration as in the fuel) is a simple cubic material at low temperature and a FCC material at higher temperature with a lattice constant of 9.56 Å. A smaller unit cell with a lattice constant of between 4.77 and 4.88 Å has also been reported for the reaction product. Our measurement of 4.7974 Å for the lattice constant of the FSRP appears to be in good agreement with the bulk of the data. However, there is too little FSRP in this sample to determine the exact structure of Na_3MO_4. Estimated errors on the stoichiometry values for Na and O would be roughly 0.7, i.e., $Na_{3\pm0.7}(U,PU)O_{4\pm0.7}$.

The lattice parameter of mixed-oxide fuel can be used to measure the deviation of the oxide from stoichiometry. Stoichiometric $(25\%Pu\text{-}75\%U)O_{2.00}$ is reported to have a lattice constant of 5.4519 Å and the lattice constant of fuel (25%Pu) in equilibrium with FSRP at 800°C was reported as 5.469 Å. Our value for the lattice parameter of the fuel corresponds to an O/M of 1.973, while the fuel in equilibrium with FSRP corresponds to an O/M of 1.950. It is likely that the FSRP present

EXPERIMENTAL REPORT (CONTD.)

in our sample was in equilibrium with the fuel so it is unlikely that the fuel was at its equilibrium O/M. The measured lattice constant for the fuel in our sample agrees well with the data quoted above as it indicates a reduction from its original O/M of 1.98, but a value above the expected equilibrium value.

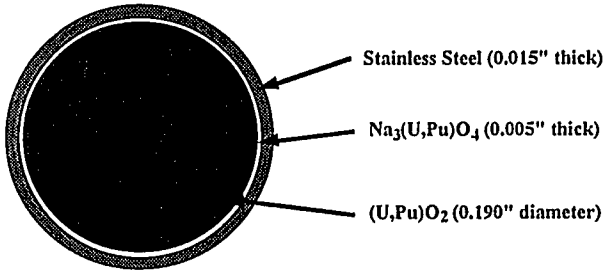


Figure 1. Schematic showing the sub-surface reaction zone.

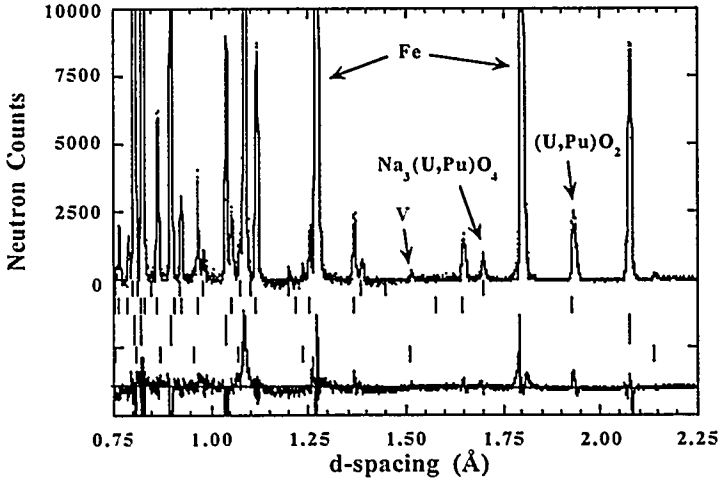


Figure 2. Rietveld profile refinement fit.

INSTRUMENT USED:	DATE OF REPORT:	EXPERIMENT NO.:
GPPD	Oct. 19, 1990	1250

TITLE:

Neutron diffraction study of the phase transition in $Fe_{1/3}NbS_2$

AUTHORS AND AFFILIATIONS:

T. Suzuki, S. Ikeda and J. W. Richardson

DATES OF EXPERIMENT: Jul., 1990

☑ APPROVED BY PROGRAM COMMITTEE, OR

☐ PART OF INSTRUMENT SCIENTIST ALLOCATION

REPORT RECEIVED:

EXPERIMENTAL REPORT (or Abstract of Publication)

$Fe_{1/3}$ NbS_2 has been investigated and reported as an antiferro magnetism with Néel temperature 50K [1),2),3)]. Recently, we investigated the isomorphous compound $Fe_{1/3}$ $NbSe_2$ and found the low temperature phase below 180K [4)]. In this study, we confirm the vacancies at Fe atom sites have a very important role in the phase transition of these layered dicharcogenide intercalations. We have found the structural phase transition with very large and complicated thermal hysteresis below 30K in $Fe_{1/3}$ NbS_2 . We also measured the magnetic susceptibility of this compound and observed Néel temperature as 47K. We have done the neutron diffraction to reveal the structure of these phases. We could not find the phase above mentioned but found a new magnetic phase below 47K.

We show the spectrum obtained at 50K in Fig.1. We can fit the calculated spectrum to the observed one by the Rietvelt method program. From obtained parameters we can see our sample has vacancies of 13% at Fe atom site. Other parameters are almost same as obtained by B. Van Laar et al. [1)]. Then it is possible that our sample occurs a structural phase transition like as $Fe_{1/3}$ $NbSe_2$. Nevertheless, we obtained the different spectrum from both that expected by the structural phase transition found by X-ray diffraction experiments and that of B. Van Laar et al. below 40K. They observed the magnetic order with a orthohexagonal unit cell. Nevertheless, we observed the super lattice peaks with a hexagonal unit cell whose lattice constant is $2a_o$.

The temperature dependence of the super lattice peaks observed in present experiment is shown in Fig. 2. We suppose these peaks come from magnetic ordering because they disappears at Néel temperature as shown in Fig. 2 and can not be observed by a X-ray diffraction experiment. Observed peaks are shown in Table 1. Then we found the new magnetic phase different from that of previous authors. We are calculating the magnetic structure by the spectrum at low temperature. However, we can not

EXPERIMENTAL REPORT (CONTD.)

understand why we can not observe the expected structural phase transition and the magnetic phase found by us is different from that of the previous authors. Further investigation for the detailed thermal hyseterisis in the phase transition of $Fe_{1/3}$ NbS_2 is needed.

1) B. Van Laar, H. M. Rietvelt and D. J. W. IJDO, J. Solid St. Chem. 3, 154 1971.
2) F. W. Boswell, A. Prodan, W. R. Vaughan, and J. M. Corbett, Phys. Stat. Sol. (a)45, 469 1978.
3) O. Gorochov, a. Le Blanc-Soreau and J. Rouxel, P. Imbert and G. Jehanno, Phil. Mag. B, 43, 1981.
4) T. Suzuki, S. Tomiyoshi, and H. Asano, KENS Repotr 7, KEK Internal (1988) p.41.

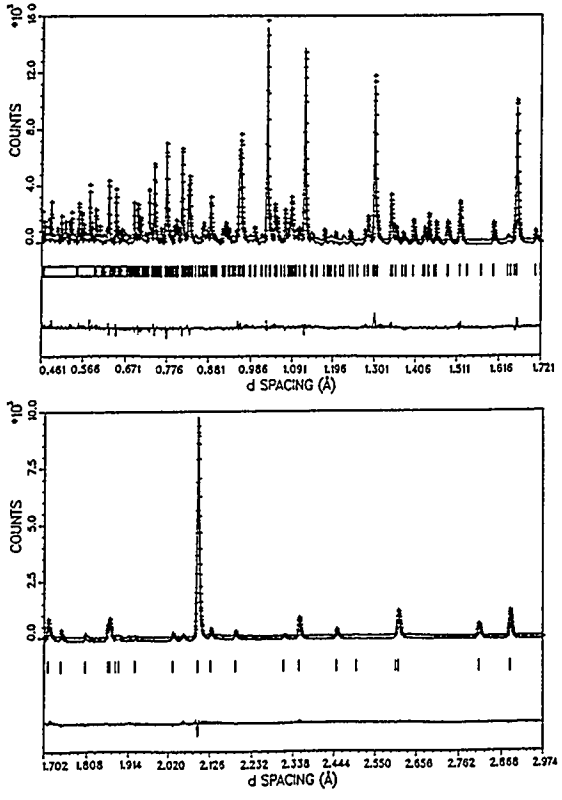


Fig. 1 Diffraction spectrum and Rietvelt fit at 50K.

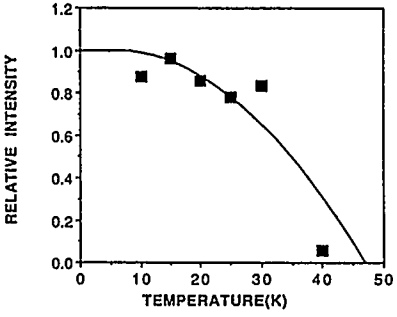


Fig. 2 The temperature dependence of super lattice peaks observed below 40K.

d	H	K	L
7.65	1/2	0	1
5.67	1/2	1/2	0
4.19	1/2	1/2	2
3.61	1/2	1	1
3.33	1/2	1/2	3
	3/2	0	0
2.70	3/2	1/2	1

Table 1. Observed peaks are shown. They can be able to index by a hexagonal unit cell with lattice constant $2a_o$.

INSTRUMENT USED:	DATE OF REPORT:	EXPERIMENT NO.:
GPPD	Oct. 23, 1990	NSF #18, 19

TITLE: Structure of the New Copper Brownmillerite Phase $LaSrCuGaO_5$

AUTHORS AND AFFILIATIONS: J. T. Vaughey and Kenneth Poeppelmeier, Dept of Chemistry and the Science and Technology Center for Superconductivity, Northwestern University

DATES OF EXPERIMENT: July 24 - 25, 1990

☒ APPROVED BY PROGRAM COMMITTEE, OR

☐ PART OF INSTRUMENT SCIENTIST ALLOCATION

REPORT RECEIVED:

EXPERIMENTAL REPORT (or Abstract of Publication)

X-ray work in our lab has concentrated on the synthesis and characterization of new perovskite-related copper oxides with fixed oxygen deficiencies. We recently completed the single crystal structure of the new brownmillerite-related phase $LaSrCuGaO_5$ and found it to be made up of copper-oxygen planes separated by gallium-oxygen tetrahedra. The A-cations (La,Sr) in the structure were randomly distributed over one crystallographic site.

It was subsequently found that the polycrystalline samples of this material could be made p-type with different lanthanum/strontium ratios up to approximately $La_{0.85}Sr_{1.15}CuGaO_5$. Magnetic susceptibility experiments indicated the samples remain paramagnetic down to 4K. A neutron structure determination of $La_{0.87}Sr_{1.13}CuGaO_5$ was undertaken to find out what structural modifications were created by the substitution of strontium for lanthanum.

It was found that the cell was elongated along the a-axis (the long axis of the unit cell and perpendicular to the copper-oxygen planes) by approximately 0.17Å, while the in-plane dimensions b and c were only slightly changed. The cell elongation was found to occur in the gallium-oxygen bonds. The long axial copper oxygen bonds (2.49Å) did not change. Within the copper planes the copper-oxygen bond lengths were found to go from 1.96Å (X2) and 1.89Å (X2) to 1.92 (X2) and 1.93 (X2).

The cell found for $LaSrCuGaO_5$ from the single crystal study was a = 16.383Å; b = 5.533Å; c = 5.330Å. The unit cell of the polycrystalline sample was found to be a = 16.551Å; b = 5.522Å; c = 5.345Å. Both solutions are in the non-centrosymmetric space group Ima2 (#46). The final R_{wp} was 5.16% (R_{exp} = 1.68%). No superstructure due to lanthanum/strontium ordering was detected, and no oxygen non-stoichiometry could be found. Work on the compound $LaSr_2Cu_2AlO_7$ continues but has been slowed by the presence of additional phases in the ceramic samples.

The refined atomic positions for $La_{0.87}Sr_{1.13}CuGaO_5$ are :

Atom	Wyckoff Sym.	x	y	z	B
La	8c	.60705	.01295	.04065	0.59616
Sr	8c	.60705	.01295	.04065	0.59616
Cu	4a	.50000	.00000	.54390	0.49284
Ga	4b	.75000	.56888	.00000	0.47592
O1	8c	.49508	.24956	.79340	0.63493
O2	8c	.64955	.04937	.56557	1.16646
O3	4b	.75000	.61949	.64455	0.65963

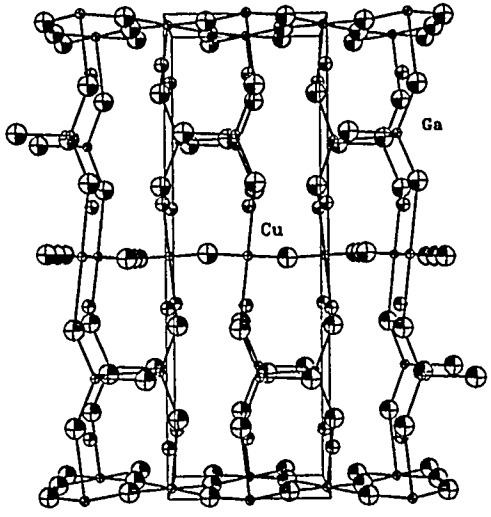


Figure 1. The structure of $La_{0.87}Sr_{1.13}CuGaO_5$ viewed down the b-axis. Atom sizes are arbitrary.

INSTRUMENT USED:	DATE OF REPORT:	EXPERIMENT NO.:
GPPD	February 8, 1991	NSF-21

TITLE: The Structure of $LaSr_2Cu_2GaO_7$

AUTHORS AND AFFILIATIONS: J. T. Vaughey and K. Poeppelmeier
Department of Chemistry, Northwestern University
The Science and Technology Center for Superconductivity, Evanston IL 60208

DATES OF EXPERIMENT: Nov. 8 & 9, 1990

☒ APPROVED BY PROGRAM COMMITTEE, OR

☐ PART OF INSTRUMENT SCIENTIST ALLOCATION

REPORT RECEIVED:

EXPERIMENTAL REPORT (or Abstract of Publication)

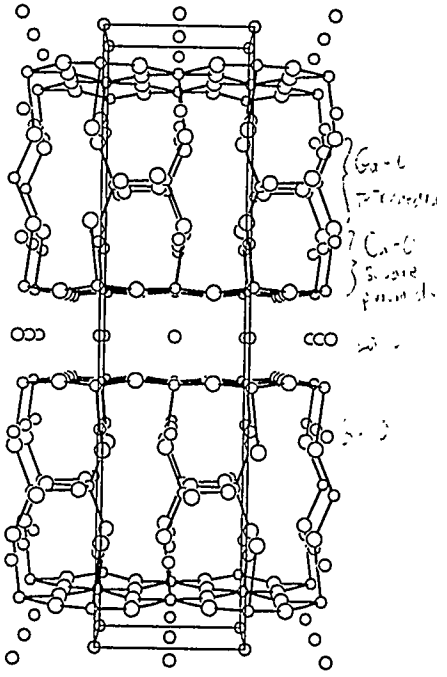
Work in our lab has concentrated on the detailed study of oxygen-deficient perovskite-related compounds. A recent example of this work was the structural determination of the new brownmillerite related copper oxide $La_{0.87}Sr_{1.13}CuGaO_5$ by neutron diffraction techniques (NSF-18). An investigation of the lanthanum/strontium solid solution in that compound led to the discovery of the compound $LaSr_2Cu_2GaO_7$. This compound was the subject of IPNS experiment NSF-21.

The structure was solved in space group Ima2 (#46) with lattice parameters of a = 23.1425(9)Å, b = 5.5662(2)Å, c = 5.4648(2)Å. The structure of the compound is closely related to that of the 93K superconductor $YBa_2Cu_3O_7$ except that the square planar copper atom has been replaced by a tetrahedral gallium atom. This replacement creates a large supercell that is related to a perovskite cube by $6a_p \times \sqrt{2}a_p \times \sqrt{2}a_p$. In comparison to the brownmillerite related compound $LaSrCuGaO_5$, the average copper bond length in the plane has increased 0.02Å, while the apical oxygen distance has decreased from 2.49Å to 2.34Å. However, it must be noted that the coordination of the copper also has changed from six to five. In $LaSr_2Cu_2GaO_7$, the lanthanum and strontium are unequally mixed over two eight coordinate sites. The lanthanum prefers (70%-30%) a position in between the copper oxygen square pyramids, comparable to that of yttrium in $YBa_2Cu_3O_7$, while the strontium is in a position nearer the gallium tetrahedra. The final R_p was 3.29% (R_{wp} = 4.62%).

EXPERIMENTAL REPORT (CONTD.)

Table of Atomic Positions

Atom	x	y	z	B	occ.
La(1)	0.0	0.0	0.0	0.448	0.70
La(2)	0.15101	0.98586	0.99851	0.361	0.30
Sr(1)	0.15101	0.98586	0.99851	0.361	0.70
Sr(2)	0.0	0.0	0.0	0.448	0.30
Cu	0.07788	0.49920	0.99646	0.319	1.00
Ga	0.25	0.42852	0.03702	0.497	1.00
O(1)	0.07350	0.24778	0.24629	0.525	1.00
O(2)	0.06998	0.75131	0.74918	0.512	1.00
O(3)	0.17817	0.54898	0.96907	0.846	1.00
O(4)	0.25	0.37524	0.38202	0.891	1.00



INSTRUMENT USED:	DATE OF REPORT:	EXPERIMENT NO.:
GPPD	Sept. 23, 1991	NSF 28

TITLE: A Determination of the Structure of $HoSr_2Cu_2GaO_7$ and $HoSr_2Cu_2Ga_{.85}Zn_{.15}O_7$

AUTHORS AND AFFILIATIONS: J. T. Vaughey, E. F. Hasty, D. A. Groenke, and K. R. Poeppelmeier, The Science and Technology Center for Superconductivity, and the Department of Chemistry, Northwestern University, Evanston, IL 60208-3113

DATES OF EXPERIMENT: May 19, 1991

☒ APPROVED BY PROGRAM COMMITTEE, OR

☐ PART OF INSTRUMENT SCIENTIST ALLOCATION

REPORT RECEIVED:

EXPERIMENTAL REPORT (or Abstract of Publication)

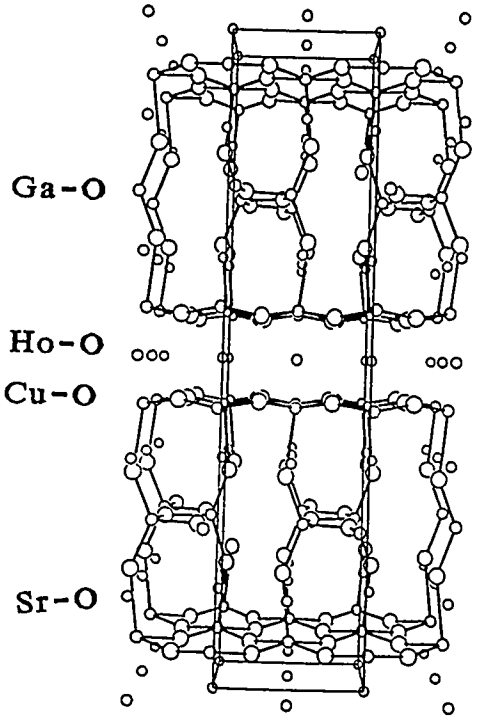
Previously we determined the structure of a new perovskite related copper oxide by powder neutron diffraction, $LaSr_2Cu_2GaO_7$ (IPNS-NSF- 18). It was found that this compound possessed a non-centrosymmetric (Sp. Grp Ima2(No. 46)) structure related to $YBa_2Cu_3O_7$. Doubling of the unit cell was observed in comparison to '123' is the result of oxygen ordering in the gallium oxygen plane. It was also found that the lanthanum and strontium were unequally mixed over two crystallographic sites. Both sites are eight coordinate but with different coordinations. The lanthanum was found to prefer a site between the copper-oxygen planes, while the strontium was found to prefer a position near the gallium chains. The lanthanum was found to have a 70/30 preference for the site between the planes. In this study, we determined the structure of $HoSr_2Cu_2GaO_7$. Holmium being smaller than lanthanum (1.01Å compared to 1.16Å) may have a more distinct site preference for one position over the other. The holmium compound was found to be isostructural with the lanthanum analog. The unit cell was found to be a = 22.823(1)Å, b = 5.4806(2)Å, c = 5.3950(2)Å. In this study, it was found that the holmium only occupied the between plane position in the structure. The final R-factors were $R_{profile}$ = 3.39%, $R_{wtd\ profile}$ = 4.52%, R_{riet} = 8.71%. This result was in agreement with a X-ray single crystal study completed at about the same time, however, the crystal contained a substantial amount of aluminum contamination from the crucible materials.

Solution of the data set of $HoSr_2Cu_2Ga_{0.85}Zn_{0.15}O_7$ has yet to be completed, however a result similar to that seen for $LaSrCuGa_{0.85}Zn_{0.15}O_5$ (IPNS - NSF- 29), that the zinc mixes over the both the gallium and copper sites is expected.

EXPERIMENTAL REPORT (CONTD.)

Refined Positional Parameters for $HoSr_2Cu_2GaO_7$

Atom	x	y	z	B
Ho	0	0	0	0.13(2)
Sr	0.15097(5)	-0.0140(1)	-0.0031(9)	0.45(2)
Cu	0.07285(5)	0.4994(3)	-0.0029(8)	0.22(1)
Ga	0.25	0.42912(4)	0.0373(8)	0.92(5)
O1	0.06586(9)	0.2460(8)	0.2454(11)	0.39(4)
O2	0.06191(10)	0.7485(9)	0.7471(11)	0.47(4)
O3	0.17592(8)	0.5422(3)	-0.1983(11)	0.85(4)
O4	0.25	0.3793(6)	0.3889(10)	1.04(6)



The Structure of $HoSr_2Cu_2GaO_7$

INSTRUMENT USED:	DATE OF REPORT:	EXPERIMENT NO.:
GPPD	Sept. 23, 1991	NSF 29

TITLE: The Structural Determination of $LaSrCuGa_{0.85}Zn_{0.15}O_5$

AUTHORS AND AFFILIATIONS: J. T. Vaughey, E. F. Hasty, D. A. Groenke, and K. R. Poeppelmeier, The Science and Technology Center for Superconductivity and Department of Chemistry, Northwestern University, Evanston, IL 60208-3113

DATES OF EXPERIMENT: May 19, 1991

☒ APPROVED BY PROGRAM COMMITTEE, OR

☐ PART OF INSTRUMENT SCIENTIST ALLOCATION

REPORT RECEIVED:

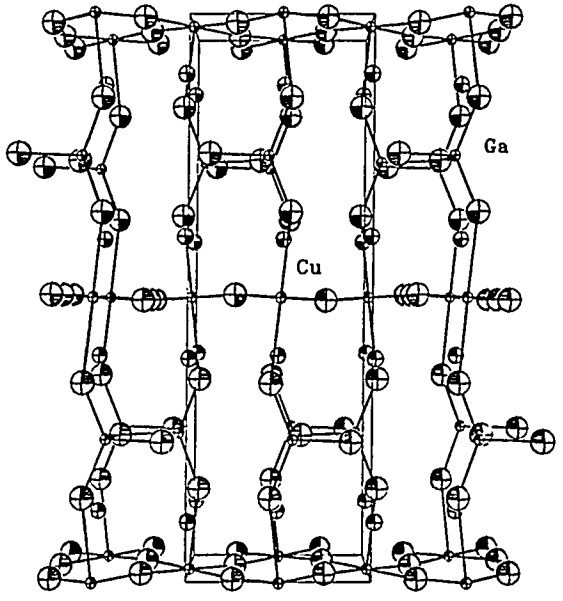
EXPERIMENTAL REPORT (or Abstract of Publication)

Previous studies in our labs has focused on the structure and properties of copper perovskite related structures that contained fixed oxygen deficiencies. In previous neutron studies conducted at the IPNS facility at Argonne National Laboratory, we determined the structure and effect of doping on a new brownmillerite related copper oxide, $La_{0.87}Sr_{1.13}CuGaO_5$. In comparison to the undoped parent compound, $LaSrCuGaO_5$, this compound possessed much higher conductivity and lower paramagnetism. Subsequently we discovered an alternative approach at achieving the same carrier concentration level, namely zinc substitution for gallium. In this study, we determined the structure of the endmember of the series, $LaSrCuGa_{0.85}Zn_{0.15}O_5$. Our study concluded that, contrary to our initial beliefs, that zinc was equally distributed over both the tetrahedral chain and copper plain sites. This result is in agreement with other studies on layered copper oxides where zinc has been previously found to substitute easily for copper. It would have been exceedingly difficult to determine the such site mixing occurrences but for the significant difference in neutron scattering lengths exhibited by the cations under study.

EXPERIMENTAL REPORT (CONTD.)

Refined Positional Parameters for $LaSrCuGa_{0.85}Zn_{0.15}O_5$

Atom	x	y	z	B	occup.
La/Sr	0.60742(7)	0.0123(3)	0.0378(6)	0.51(2)	1.0
Cu	0.5	0	0.5402(8)	0.28(4)	0.922(1)
Ga	0.75	0.5665(4)	0	0.71(6)	0.928(1)
Zn1	0.75	0.5665(4)	0	0.71(6)	0.072(1)
Zn2	0.5	0	0.5402(8)	0.28(4)	0.078(1)
O1	0.4946(1)	0.2492(9)	0.7919(9)	0.54(3)	1.0
O2	0.6484(1)	0.0491(3)	0.5617(7)	1.19(5)	1.0
O3	0.75	0.6172(6)	0.6397(7)	0.93(6)	1.0



The Structure of $LaSrCuGa_{.85}Zn_{.15}O_5$

INSTRUMENT USED: GPPD	DATE OF REPORT: 2/23/95	EXPERIMENT NO.: 1957

TITLE: Approximant structures in $Rb_3C_{60}(ND_3)_{2.5}$

AUTHORS AND AFFILIATIONS: J.W. White, P.A.Reynolds, W.K.Fullagar
Research School of Chemistry, Australian National University

DATES OF EXPERIMENT: 12/14/94 TO 12/16/94

CHECK ALL APPLICABLE BOXES:

- X APPROVED BY PROGRAM COMMITTEE
- ☐ INSTRUMENT SCIENTIST ALLOCATION
- ☐ DO NOT PUBLISH
- ☐ PROPRIETARY RESEARCH
- ☐ PRT ALLOCATION

EXPERIMENTAL REPORT (or Abstract of Publication)

During a study of the superconducting alkali-metal doped compound Rb_3C_{60}, it was discovered that large amounts of ammonia could be absorbed by this material, with a concomitant loss in superconductivity. Subsequent investigations revealed that the conventional X-ray powder diffraction signature had also been drastically altered, and that the material was multiphase and disordered, best described as like an icosahedral glass. We have completed a powder X-ray diffraction pattern from a sample of nominal $Rb_3C_{60}(ND_3)_{2.5}$ after it has been throughly annealed and aged at the Photon Factory's Australian National Beamline Facility. To allow a complete structural characterisation this material has also been examined by neutron diffraction on GPPD. Both patterns can be completely indexed with three phases - 2 known, viz. orthorhombic RbC_{60} and a poorly crystalline Rb_3C_{60}. The third unknown phase is I-centred orthorhombic with a = 12.626 b= 11.687 c= 10.972Å, and is the majority phase.

The neutron and X-ray diffraction patterns have been simultaneously refined using a common structural model with the Rietveld refinement package GSAS. The known structures of RbC_{60} and Rb_3C_{60} were used. The structured diffuse background in the neutron pattern is characteristic of orientationally disordered C_{60}. It was modelled by the Fourier filter technique. The observed and fitted patterns, after allowing positional and some thermal parameters to refine are shown below. Some constraints were used e.g. C_{60} was constrained to be cubic, and N-D bonds 1.01Å in length. The Rb_3C_{60} peak profiles were extremely broad and did not fit well. This material is evidently reprecipitated since the starting Rb_3C_{60} was of much better crystal quality. To improve refinement of the unknown phase approximately 10% of the total patterns were excluded in regions where the two known phases scattered strongly from a re-refinement. We currently obtain the values shown in the Table (C values excluded) with agreement factors R_W= 0.047 χ^2=6.1.

Table

Atom	x	y	z	population
Rb(1)	0.2227(5)	0.5	0.0	1
Rb(2)	0.5	0.1896(5)	0.0	1
N(1)	0.0	0.5	0.255(2)	0.91(1)
D(1)	0.056(1)	0.561(1)	0.249(3)	0.46(1)
D(2)	0.0	0.5	0.346(2)	0.91(1)

Perhaps the most interesting feature of this result is that we have obtained $Rb_4C_{60}(ND_3)_2$ by disproportionation of C_{60}^{3-} to C_{60}^{4-} and C_{60}^{1-}. Rb_3C_{60} consists of an FCC arrangement of C_{60}s, with Rb ions disordered over both tetrahedral and octahedral sites. Addition of ammonia causes disproportionation into RbC_{60} and $Rb_4C_{60}(ND_3)_2$, in both of which the Rb sites are ordered. The $Rb_4C_{60}(ND_3)_2$ is related to the Rb_4C_{60} structure in that both are basically BCC arrangements of C_{60}s, however Rb_4C_{60} is tetragonal with some tetrahedral holes empty and others partially occupied. Addition of ammonia causes complete Rb ordering and a lowering of symmetry to orthorhombic.

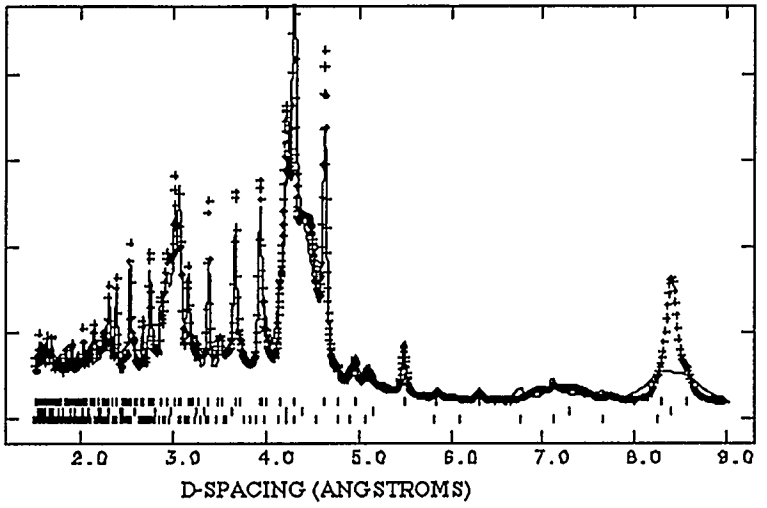


Figure 1. X-ray diffraction pattern from annealed Rb3C60(ND3)2.5 with fitted profile. The tick marks correspond to peak positions for the 3 phases.

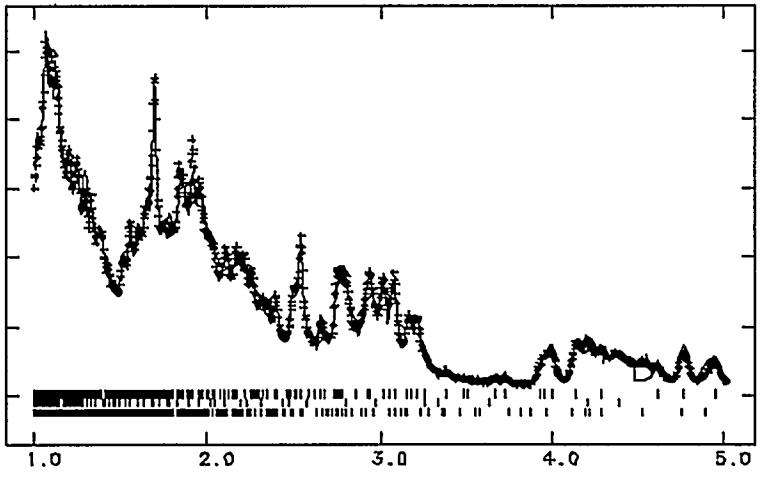


Figure 2. Neutron diffraction pattern from annealed Rb3C60(ND3)2.5 with profile

INSTRUMENT USED: GPPD	DATE OF REPORT: Aug. 2, 1995	EXPERIMENT NO.: 2013

TITLE: Residual Strains in Ag-Cu In-situ Composites

AUTHORS AND AFFILIATIONS: Y.T. Wood[1], A.C. Lawson[2], J.D. Embury[1], M.F. Stevens[2]
[1]McMaster University, Canada, [2]LANL

DATES OF EXPERIMENT: May 19-20, 1995

CHECK ALL APPLICABLE BOXES:

- [x] APPROVED BY PROGRAM COMMITTEE
- [ ] INSTRUMENT SCIENTIST ALLOCATION
- [ ] DO NOT PUBLISH
- [ ] PROPRIETARY RESEARCH
- [ ] PRT ALLOCATION

EXPERIMENTAL REPORT (or Abstract of Publication)

It is well known that heavily deformed, two-phase metals like copper-niobium and copper-silver alloys are able to attain strength values well in excess of either of the individual constituents (Figure 1). The mechanisms responsible for this strengthening, however, are not well understood.

Residual stress in a material can be an indication of strengthening by the transfer of load to a stronger second phase. Microstructural characterization by scanning and transmission electron microscopy has shown qualitatively that residual stresses develop in the wires as the level of deformation increases. Strengthening in single-phase materials is generally limited to roughly 1% of the calculated theoretical strength. For a material like copper, this equates to a strength of the order of 400 MPa. Estimates derived from the qualitative studies suggest that the residual stresses reach values of the order of 50 – 100% of the theoretical strength.

Verifying i) the existence and ii) the magnitude of the residual stresses as well as understanding how they develop during the deformation process is valuable for a number of reasons: i) it will provide insight into the strengthening mechanisms that are operative in these materials, and ii) it may lead to an alternative fabrication method for high-strength whiskers.

Samples were prepared from rods of Cu-24wt%Ag and Cu-12.5wt%Nb in conditions ranging from fully annealed to a true (logarithmic) strain of 1.86. All samples were machined to a similar diameter of 4.75mm (3/16") to maintain a constant scattering volume. Strain measurements were made in the radial direction. The average residual stress in the longitudinal direction can then be calculated as:

$$\sigma_l = -\frac{E\,\varepsilon_r}{\nu}$$

where E is Young's modulus, ν is Poisson's ratio, and the subscripts l and r indicate the longitudinal and radial directions. The experimental results are shown below along with the calculated residual stresses.

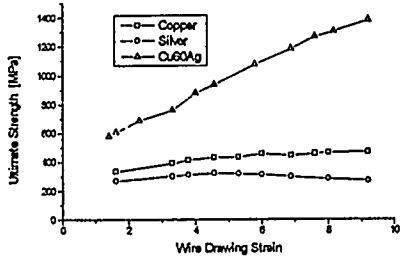


Figure 1. The evolution of strength with wire drawing strain for a two-phase material and it's single-phase constituents.

In both the Cu-Ag and Cu-Nb wires, the second phase is subject to a longitudinal tensile stress while the copper matrix is in compression. In the case of Cu-Ag, the calculated stresses are similar to the strength levels reached in the monolithic materials (Figure 1). The niobium filaments, however, are subject to very large residual stresses – in agreement with the qualitative observations made previously. It is important to note that similar experiments employing x-rays on the same samples measured strains (and therefore stresses) of the order of half of the values obtained by neutrons. This is likely due to the relaxation of residual stresses at the free surface of the sample combined with the shallow penetration of the x-rays.

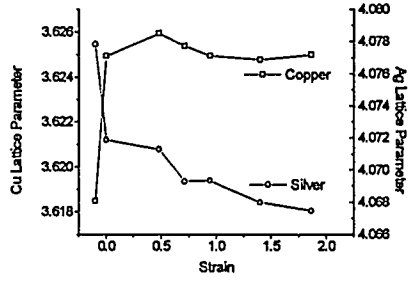


Figure 2.Copper and silver lattice parameters as a function of imposed strain.

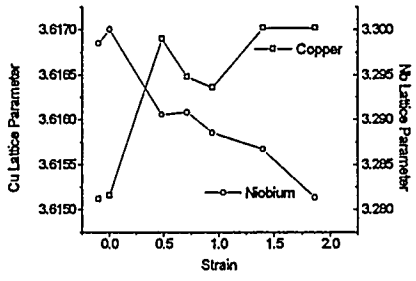


Figure 3.Copper and niobium lattice parameters as a function of imposed strain.

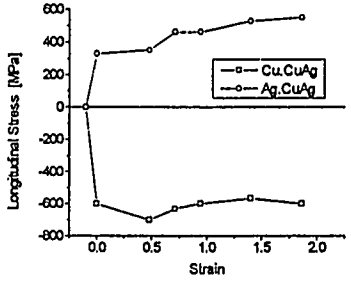


Figure 4.Calculated longitudinal stress as a function of strain in copper-silver rod.

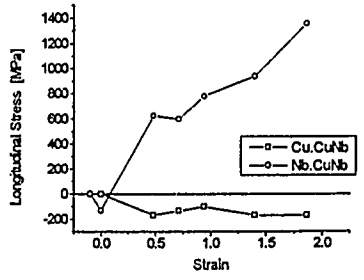


Figure 5.Calculated longitudinal stress as a function of strain in copper-niobium rod.

INSTRUMENT USED:	DATE OF REPORT:	EXPERIMENT NO.:
HIPD	November 16, 1995	DISC.

TITLE: Nuclear and magnetic structure of $Cs_2Mn[V(CN)_6]$

AUTHORS AND AFFILIATIONS: Prof. G. S. Girolami, S. M. Holmes (Univ. of Illinois, Urbana-Champaign), A. J. Schultz (IPNS)

DATES OF EXPERIMENT: June, 1995

CHECK ALL APPLICABLE BOXES:

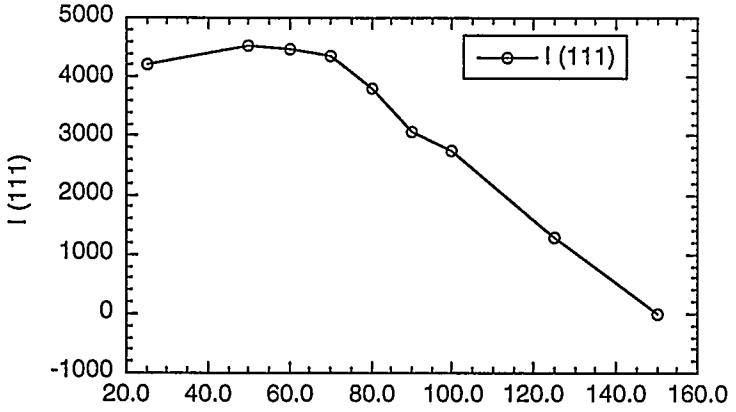
- [ ] APPROVED BY PROGRAM COMMITTEE
- [ ] PROPRIETARY RESEARCH
- [X] INSTRUMENT SCIENTIST ALLOCATION
- [ ] PRT LOCATION
- [ ] DO NOT PUBLISH

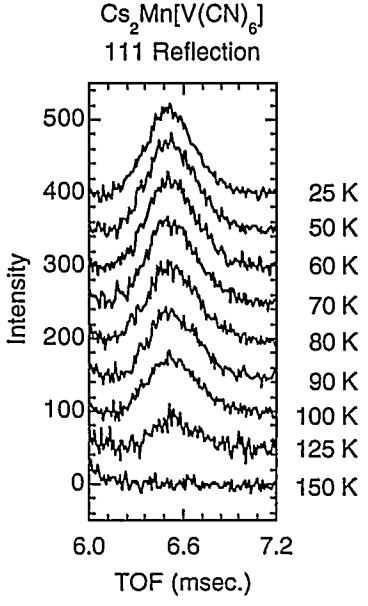
EXPERIMENTAL REPORT (or Abstract of Publication)

Molecular magnets offer the potential of magnetic materials in combination with other properties associated with molecules and polymers. In addition, these materials are prepared by relatively low-temperature organic or organometallic synthetic procedures. Although a wide variety of such materials are known, the long-range magnetic ordering usually occurs at temperatures well below 30 K.

We have prepared several vanadium containing analogs of Prussian blue derived from salts of the hexacyanovanadate(II) ion.[4] One of these, $Cs_2Mn^{II}[V^{II}(CN)_6]$, has features characteristic of a three-dimensional ferrimagnet with a Néel transition at 125 K. We have measured neutron diffraction data on HIPD on this material in the temperature range of 25–150 K and observe magnetic Bragg scattering due to longe-range ordering. Since the nuclear structure is face-centered cubic, the appearance of intensity for the 111 peak is attribute to magnetic Bragg scattering and the shape of the curve vs. T is similar to that found in other magnetization experiments.

EXPERIMENTAL REPORT (CONTD.)





INSTRUMENT USED:	DATE OF REPORT:	EXPERIMENT NO.:
HIPD	12/17/93	1780

TITLE:
The Structure and Melting Temperatures of Alcohol Mixtures Adsorbed on Graphite

AUTHORS AND AFFILIATIONS:
K. W. Herwig (Research Reactor, University of Missouri), F. R. Trouw (IPNS, ANL)

DATES OF EXPERIMENT:
10/12/93 to 10/25/93

CHECK ALL APPLICABLE BOXES:

- [XX] APPROVED BY PROGRAM COMMITTEE
- [ ] INSTRUMENT SCIENTIST ALLOCATION
- [ ] DO NOT PUBLISH
- [ ] PROPRIETARY RESEARCH
- [ ] PRT ALLOCATION

EXPERIMENTAL REPORT (or Abstract of Publication)

Although vapor pressure isotherms and heat of adsorption measurements demonstrated over 20 years ago that n-alcohols would adsorb onto the basal planes of graphite,[1] it is only recently that microscopic probes have been used to study these systems. With the application of neutron and x-ray scattering to these systems has come the identification of a variety of unique and intriguing phenomena.[2-6] Common to all of these studies is the observation that hydrogen bonding plays a dominant role in stabilizing the two-dimensional structure, as it does in determining the corresponding bulk structures of the alcohols. One of the striking features seen in several of these systems is the unusually high melting temperature exhibited by the adsorbed monolayer. Indeed, monolayers of both ethanol and n-propanol have melting temperatures far in excess of their corresponding bulk melting temperatures. A combination of neutron diffraction, quasielastic scattering, and a molecular dynamics simulation enabled us to propose a melting mechanism for ethanol physisorbed on graphite. Melting in this system occurs via a two-step process. In the first step, ethanol molecules orientationally disorder normal to the graphite surface. This step provides the excess area required for the molecules to translationally disorder, but melting cannot occur until the molecules have sufficient energy to break the hydrogen bonds which stabilize the structure.

These observations prompted our investigation into the structures and melting temperatures of mixtures of alcohols having different lengths adsorbed on graphite. Some preliminary measurements on a nearly equal mixture of ethanol and methanol indicated that a mixed, crystalline phase formed which melted at a temperature intermediate to that of the respective monolayer melting points. Only a single Bragg peak was observed at a d-spacing the same as the strongest reflection from pure adsorbed ethanol.

In this experiment, we began with a monolayer of n-butanol adsorbed on graphite. It's diffraction pattern is shown in Fig. 1. The strongest peaks can be indexed on a rectangular unit cell with lattice constants 13.04 Å and 5.02 Å, with an area of 32.7 Å^2/molecule. Recent vapor pressure isotherm measurements yield a specific area of 32.9 Å^2/molecule,[3] in very good agreement with this proposed unit cell. A profile analysis is in progress for a more detailed comparison to the diffraction profile. The melting temperature of the n-butanol monolayer was determined to be approximately 250 K, nearly 70 K above the bulk melting temperature of 183 K.

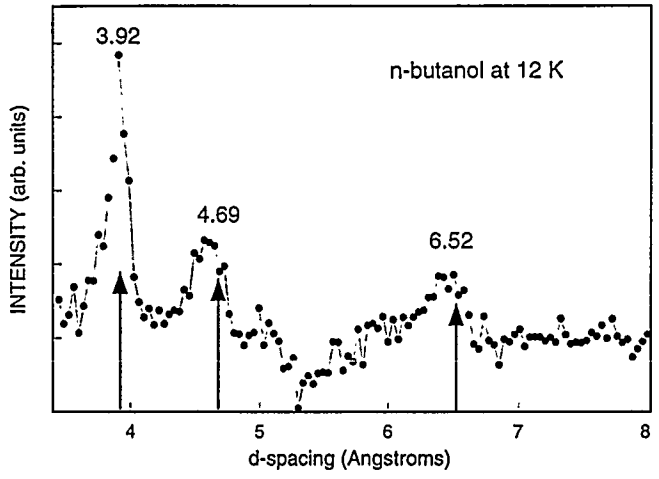


Figure 1. Diffraction profile of n-butanol on graphite. The scattering due to the graphite substrate has been subtracted.

The monolayer of n-butanol was subsequently warmed to a temperature where the film was liquid, and approximately one monolayer of ethanol added. The sample was cooled slowly to 12 K and a diffraction pattern collected, which closely resembled that of the pure n-butanol sample. The specimen was then warmed to 300 K, and again slowly cooled to 12 K. The resulting diffraction profile was again very similar to that seen for the pure n-butanol sample. We can conclude that the higher affinity for the graphite surface of n-butanol(afforded by its longer hydrocarbon backbone), as compared with ethanol, results in preferential segregation of the butanol at the graphite surface. As the temperature is lowered this film crystallizes into the same structure as observed for the pure n-butanol sample. No additional peaks or changes in the profile were observed upon the addition of the ethanol, and we can conclude that the ethanol in the sample is in a disordered state.

REFERENCES

[1] N. N. Avgul and A. V. Kiselev, in *Chemistry and Physics of Carbon*, edited by P. L. Walker, Jr. (Marcel Dekker, New York, 1970), Vol. 6, p. 1.
[2] K. Morishige, K. Kawamura, and A. Kose, J. Chem. Phys. **93**, 5267 (1990).
[3] K. Morishige, K. Hayashi, K. Izawa, I. Ohfuzi, and Y. Okuda, Phys. Rev. Lett. **68**, 89 (1992).
[4] K. W. Herwig and F. R. Trouw, Phys. Rev. Lett. **69**, 89 (1992).
[5] K. Morishige, J. Chem. Phys. **97**, 2084 (1992).
[6] K. Morishige, N. Kawai, and M. Shimizu, Phys. Rev. Lett. **70**, 3904 (1993).

INSTRUMENT USED:	DATE OF REPORT:	EXPERIMENT NO:
HIPD	Nov. 20, 95	1925

TITLE:

Hybridization effects in U_2T_2X compounds: Magnetic Structures of U_2Rh_2Sn and U_2Ni_2In

AUTHORS AND AFFILIATIONS:

H. Nakotte, A. Purwanto and R.A. Robinson

LANSCE, Los Alamos National Laboratory, Los Alamos NM 87545, USA

K. Prokeš, J.C.P. Klaasse, P.F. de Châtel and F.R. de Boer

University of Amsterdam, 1018 XE Amsterdam, The Netherlands

L. Havela and V. Sechovský,

Department of Metal Physics, Charles University, 12 116 Prague 2, The Czech Republic

L.C.J. Pereira, A. Seret, J. Rebizant and J.C. Spirlet

European Commission, Joint Research Center,

Institute for Transuranium Elements (ITU), 76125 Karlsruhe, Germany

F. Trouw

IPNS, Argonne National Laboratory, Argonne IL 60439-4814, USA

DATES OF EXPERIMENT:

Dec. 9-20, 1994

CHECK ALL APPLICABLE BOXES:

- [x] APPROVED BY PROGRAM COMMITTEE
- [ ] INSTRUMENT SCIENTIST ALLOCATION
- [ ] DO NOT PUBLISH
- [ ] PROPRIETARY RESEARCH
- [ ] PRT ALLOCATION

EXPERIMENTAL REPORT (or Abstract of Publication)

submitted to Phys. Rev B (in press)

The tetragonal intermetallic compounds U_2Ni_2In and U_2Rh_2Sn have been studied by means of specific-heat, electrical-resistivity and neutron-diffraction techniques. At low temperatures, both compounds order antiferromagnetically in a magnetic unit cell doubled along the c axis, and we find 5*f* moments of 0.60 and 0.38 μ_B/U-atom for U_2Ni_2In and U_2Rh_2Sn, respectively. For U_2Ni_2In, our refinement also indicates a possible Ni moment of 0.37 μ_B perpendicular to the U moments. We discuss the development of the 5*f* moments together with findings on other isostructural U_2T_2X (T = transition metal, X = In, Sn) compounds and confirm that the trends expected due to 5*f*-ligand hybridization also hold for this family of uranium compounds. Our analysis indicates different arrangements of the 5f moments in the two compounds (non-collinear arrangement within the basal plane for U_2Ni_2In and collinear arrangement along the *c* axis for U_2Rh_2Sn), although both compounds have nearest-neighbor U-U distances along the *c* axis. This would mean that the magnetocrystalline anisotropy in U_2T_2X compounds is not determined by nearest-neighbor U-U links alone.

EXPERIMENTAL REPORT (CONTD.)

INSTRUMENT USED:	DATE OF REPORT:	EXPERIMENT NO:
HIPD	Nov. 20, 95	1930

TITLE:

MAGNETIC AND CRYSTALLOGRAPHIC STRUCTURES OF CeCuSn

AUTHORS AND AFFILIATIONS:

H. Nakotte, A. Purwanto and R.A. Robinson
LANSCE, Los Alamos National Laboratory, Los Alamos NM 87545, USA
E. Brück, K. Prokeš and F.R. de Boer
University of Amsterdam, 1018 XE Amsterdam, The Netherlands
Yang Fu-ming
Academica Sinica, Beijing, China
F. Trouw
IPNS, Argonne National Laboratory, Argonne IL 60439-4814, USA

DATES OF EXPERIMENT:

Dec. 14-17, 1994

CHECK ALL APPLICABLE BOXES:

- [x] APPROVED BY PROGRAM COMMITTEE
- [ ] INSTRUMENT SCIENTIST ALLOCATION
- [ ] DO NOT PUBLISH
- [ ] PROPRIETARY RESEARCH
- [ ] PRT ALLOCATION

EXPERIMENTAL REPORT (or Abstract of Publication)

In order to determine the crystallographic and magnetic structures of CeCuSn, we performed neutron-diffraction studies on CeCuSn at 4.2, 7.5 and 15 K using the HIPD spectrometer at ANL.

At 15 K, we find only nuclear intensities, which are best fitted using the hexagonal $CaIn_2$ structure with the following structural parameters:

space group: $P6_3mmc$

		x	y	z	
Ce	2b	0	0	1/4	
Cu/Sn	4f	1/3	2/3	x	x = 0.0259

a = 459.49 ± 0.01 pm c = 782.68 ± 0.02 pm

reduced χ^2 = 10.5%

EXPERIMENTAL REPORT (CONTD.)

However, some peaks remain unindexed in this structure. Although we believe that these peaks should be attributed to an unidentified secondary phase, at present, we cannot completely exclude that these reflections belong to the parent phase indicating some modified version of the above structure. Further analysis is underway to clarify this.

Below T_N = 8.5 K, additional magnetic peaks evolve as can be seen in the difference plot shown in Fig. 1. This observation should enable us to solve the low-temperature magnetic structure when having unambiguously solved the nuclear structure.

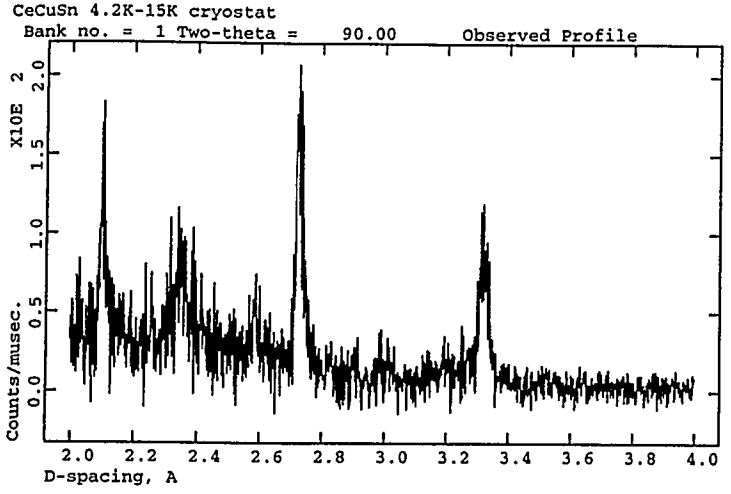


Fig. 1: Difference plot (4.2-15K) of a part of the neutron-diffraction data taken in the 90° bank of HIPD.

INSTRUMENT USED:	DATE OF REPORT:	EXPERIMENT NO:
HIPD	July 12, 1994	1742

TITLE: **Magnetic and Structural Properties of URhIn**

AUTHORS AND AFFILIATIONS:
A. Purwanto [1,2]
R. A. Robinson [1]
F. Trouw [3]
F. J. Rottella [3]
V. Sechovsky [4]
H. Nakotte [1]

[1] LANSCE, Los Alamos National Lab., USA
[2] New Mexico State University, USA
[3] IPNS, Argonne National Lab., USA
[4] Charles University, Prague, The Czech Republic

DATES OF EXPERIMENT:
18 - 20 November 1993

CHECK ALL APPLICABLE BOXES:

- [x] APPROVED BY PROGRAM COMMITTEE
- [ ] INSTRUMENT SCIENTIST ALLOCATION
- [ ] DO NOT PUBLISH
- [ ] PROPRIETARY RESEARCH
- [ ] PRT ALLOCATION

EXPERIMENTAL REPORT (or Abstract of Publication)

This work is part of a larger program to understand the magnetic properties of ternary (1:1:1) U intermetallics. As one varies the degree of *5f-d* hybridization by moving down or across the periodic table, a rich variety of magnetic behavior is observed: progressing from itinerant magnetism, through the heavy-fermion state to localised magnetism with complicated *5-f* magnetic ordering. We have investigated such compounds crystallizing in a variety of structures: the cubic MgAgAs, the hexagonal $CaIn_2$ and Fe_2P, and the orthorhombic $CeCu_2$ structure type or their ordered variants. Most of them have U-moments systematically aligned perpendicular to the nearest U-U distance. In this work, we concentrated on URhIn which crystallizes in the ordered variant of Fe_2P structure type, namely; ZrNiAl.

Our high-field magnetization measurement indicates that URhIn has U-moment of approximately $1\mu_B$. By comparing results for free powder with those for powder frozen in random orientation, we concluded that URhIn exhibits easy-plane anisotropy. This contradicts most of U intermetallics crystallizes in Fe_2P or in ordered variant ZrNiAl type structure which have U moment oriented along the *c*-axis.

We did the neutron experiment using HIPD at IPNS for four different temperatures: 1.5K, 4.2K, 12K and 300K. A preliminary crystallographic

EXPERIMENTAL REPORT (CONTD.)

structure refinement, done with GSAS, confirmed that URhIn crystallizes in hexagonal symmetry. We have not checked whether the structure crystallizes in the ordered ZrNiAl or the disordered Fe_2P structure type. The diffraction pattern shows at least two significant unindexed peaks indicating the presence of an impurity phase.

The nuclear refinement of the low temperature data indicated that the nearest U-U distance is marginally along the *c*-axis which is consistent with the high temperature data. Based on the result from other ternary (1:1:1) U-intermetallics, we expected the U moment to be in the basal plane. The possible magnetic structures based on the Shubnikov magnetic space group are shown in fig. 1, indicating that there are only two structures (a) and (b) with U moments in the basal plane. However, there was no detectable extra magnetic intensity at low temperatures. Statistical analysis of our 1.5 K data indicate that any long-range order U moment must be less than 0.6 μ_B for model (b)(0.3 μ_B for model (a) and 0.2 μ_B for model (c)).

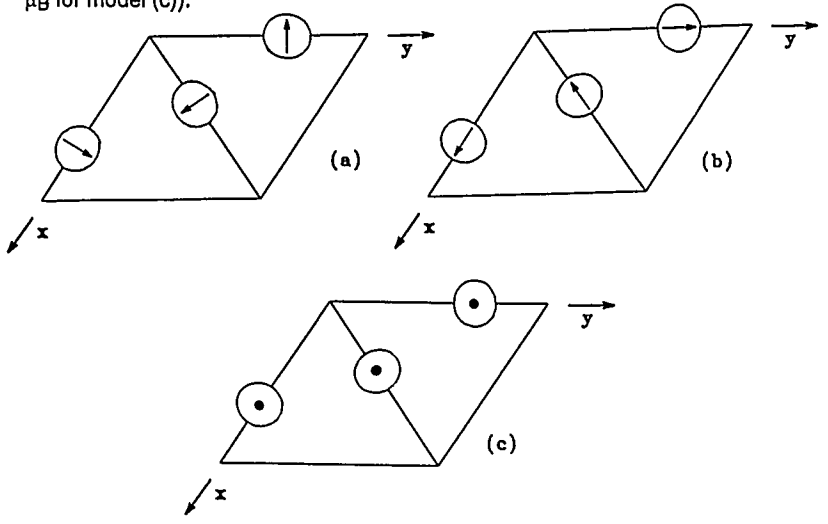


Fig. 1. The Shubnikov magnetic space group of $P\bar{6}2m$. In (a), the U moments are perpendicular to the mirror plane, while in (b) and (c), the moments are parallel to the mirror planes. Note that in the model (a) and (b), the moments lie within the hexagonal basal plane, while in (c) they are ferromagnetically coupled along the *c*-axis. For clarity, only the U atoms are drawn.

INSTRUMENT USED: HIPD	DATE OF REPORT: 10TH DECEMBER, 1993.	EXPERIMENT NO: 1778
TITLE: In-Plane Ordering of Adsorbed Paraffin Molecules		
AUTHORS AND AFFILIATIONS:	J.W. White, E.P. Gilbert and P. Reynolds Research School of Chemistry, Australian National University	
DATES OF EXPERIMENT: 12TH-14TH NOVEMBER, 1993.		

CHECK ALL APPLICABLE BOXES:

- ☐ APPROVED BY PROGRAM COMMITTEE
- ☐ INSTRUMENT SCIENTIST ALLOCATION
- ☐ DO NOT PUBLISH
- ☐ PROPRIETARY RESEARCH
- ☐ PRT ALLOCATION

EXPERIMENTAL REPORT (or Abstract of Publication)

Introduction

Recently, there has been considerable interest in the structures formed by paraffin molecules at the liquid/graphite interface. These molecules have been shown to undergo physisorption onto the basal plane of graphite with the alkane molecule taking up an all-trans conformation parallel to the surface and producing a highly ordered lamellar structure. Very little is currently known, however, about multilayer structures of this kind and in particular confinement in structures whose dimensions are close to those of the molecules. The gallery structure in high surface area and partially oriented graphites, such as grafoil, allow this problem to be studied. The aim of this experiment was to begin to characterise the structures and determine the packing parameters which result from the adsorption of a deuterated alkane in a graphitic adsorbent.

Results

A 95%:5% by mole fraction mixture of $C_{30}D_{62}$ and $C_{36}H_{74}$ was prepared; the ratio chosen to minimise small angle scattering by the Grafoil substrate. Grafoil disks were outgassed at 350°C to a pressure of 10^{-6} torr and, under dry Helium gas, six of these disks were put into contact with a melt of the hydrocarbon mixture. After evacuation to 10^{-5} torr at room temperature, the disks and melt were sealed in a glass vessel and the system allowed to equilibrate at 250°C overnight followed by slow cooling. The amount of mixture used was calculated to be sufficient for pore filling to occur and no solid was observed on the walls of the vessel after cooling. The 'filled' disks were subsequently studied on the HIPD instrument. Three of these filled disks and three outgassed disks were also sealed in a glass vessel and treated as above to produce 'half-filled' disks. The half-filled disks and a sample of the bulk crystalline deuterated hydrocarbon were, in addition, studied on the HIPD instrument. In all experiments, the grafoil was oriented such that the neutron momentum transfer was parallel to the graphite basal plane.

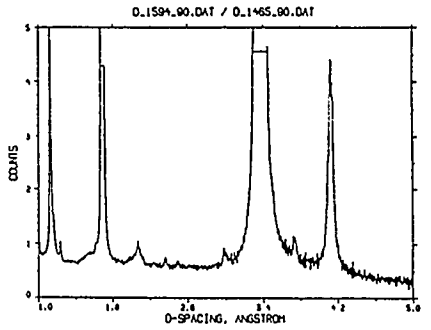


Figure 1. Diffraction pattern from 'filled' grafoil disks.

Diffraction from the 'filled' grafoil disks showed five non-graphite peaks attributable to the adsorbed $C_{30}D_{62}$ (figure 1). The spectrum was observed to be quite different from that of the bulk crystalline sample (figure 2). We have found that the five peaks may be indexed on a 7.42 x 4.96Å rectangular cell which agrees with the a and b dimensions of the $C_{30}H_{62}$ orthorhombic unit cell. It appears, therefore, that the molecules adsorb with their chains perpendicular to the graphite basal plane in a lattice identical to that of the bulk orthorhombic phase and not, as expected, in a parallel orientation. The only features common to the 'filled' and 'half-filled' samples were a weak peak corresponding to d~4.2Å and several strong graphite peaks. We have also observed a series of peaks for the 'half-filled' sample around d=2.6Å which appear to be consistent with a rectangular lattice of dimensions 5.15 x 5.44Å.

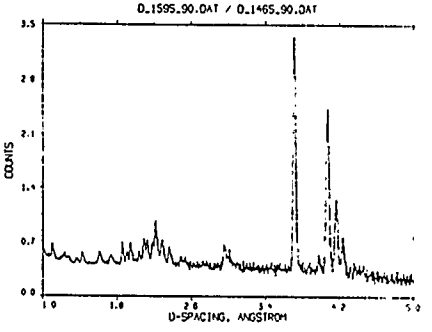


Figure 2. Diffraction pattern from bulk crystalline $C_{30}D_{62}$.

INSTRUMENT USED: QENS, HIPD	DATE OF REPORT: 12/12/93	EXPERIMENT NO.: 1768
TITLE: Tunnelling and Inelastic Scattering from Ternary Intercalates of C_{60}		
AUTHORS AND AFFILIATIONS:	J. W. White*, P. Reynolds*, R. Durand*, F. Trouw‡ * Research School of Chemistry, Australian National University ‡ IPNS, Argonne National Laboratory	
DATES OF EXPERIMENT: 10/11/93 to 17/11/93		

CHECK ALL APPLICABLE BOXES:

- ☐ APPROVED BY PROGRAM COMMITTEE
- ☐ INSTRUMENT SCIENTIST ALLOCATION
- ☐ DO NOT PUBLISH
- ☐ PROPRIETARY RESEARCH
- ☐ PRT ALLOCATION

EXPERIMENTAL REPORT (or Abstract of Publication)

We have found that alkali metal C_{60} intercalates, such as Rb_3C_{60} may be ternarily doped with ammonia at room temperature to produce phases which resemble those which we have previously studied in the graphite alkali metal intercalation compounds.[1,2] This doping also changes the superconducting behaviour of the C_{60} intercalate.

The mechanism of superconductivity in these compounds has been suggested to be explainable by the BCS theory of superconductivity [3] which is based on electron-phonon coupling. In particular the intramolecular modes of C_{60} having symmetry Hg have been implicated in this interaction [4]. Changes in the superconducting behaviour should therefore be apparent as changes in the strengths and widths of these modes.

To examine the NH_3 tunnelling and the effect of doping on the C_{60} Hg vibrational modes we examined two samples on QENS. The first was Rb_3C_{60} doped with ca. 4 moles of NH_3 per C_{60}. The second was Rb_3C_{60} doped with ca. 1 mole of ND_3 per C_{60}. The results indicate that doping with ammonia does strongly affect the vibrational modes of C_{60} and that doping at a stoichiometry of ca. 1:1 of ammonia:Rb_3C_{60} results in a mixture of two phases, pure Rb_3C_{60} and $Rb_3C_{60}(ND_3)_4$. The inelastic spectrum from QENS shows prominent NH_3 librational peaks for the NH_3 material.

HIPD Diffraction results (see Fig. 1)

The pattern of the ND_3 doped material exhibits a mixture of strong sharp, and weak broad peaks. The latter correspond with similar peaks in the NH_3 doped material. The ND_3 material is a mixture of ca. 80% pure Rb_3C_{60} and 20% $Rb_3C_{60}(ND_3)_{4\pm1}$. This is confirmed by Rietveld fitting of the profiles (see Fig. 2), from which we obtain the first Rb_3C_{60} structure. Examination of this structure shows voids around the Rb site at $^1/_2,^1/_2,^1/_2$ of a size capable of accommodating ammonia molecules. The NH_3 doped material has a similar cell size, indicating filling of voids by ammonia, but the cell indexes as primitive cubic, not Fm3m, as in Rb_3C_{60}. In addition peaks are broad, and somewhat shifted indicating poorer crystal quality.

QENS Inelastic results :

The inelastic spectra from QENS for the NH_3 and ND_3 materials (see Fig. 3) clearly show the prominent NH_3 librational peaks for the NH_3 material, at 3.7 and 8.4 meV. We also observe distinct differences at higher energies in which the relatively sharp Rb_3C_{60} peaks at 43.9, 49.6 and 60.4 meV are broadened in the $Rb_3C_{60}(NH_3)_4$. Thus ammonia doping markedly affects the "C_{60}" vibrational modes although we cannot yet definitively say if this broadening is due to electron phonon interaction or due to structural disorder.

1 ..... Two Dimensional Caesium-ammonia Solid Solutions in $C_{28}Cs(NH_3)_x$
Carlile C.J., Jamie I. McL., Lockhart G., and White J.W., *Mol. Phys.*, 76, 173, (1992)

2 ..... Temperature Dependence of the Lattice Dynamics of Rb_3C_{60}
White J.W., Lindsell G., Pang, L., Palmisano A., Sivia D.S., and Tompkinson J.,
Chem. Phys. Lett., 191, 92-96, (1992)

3 ..... Theory of Superconductivity
Bardeen J., Cooper L.N., Schrieffer J.R., *Phys. Rev.*, 108(5), 1175, (1957)

4 ..... Schluter M.A., *preprint*

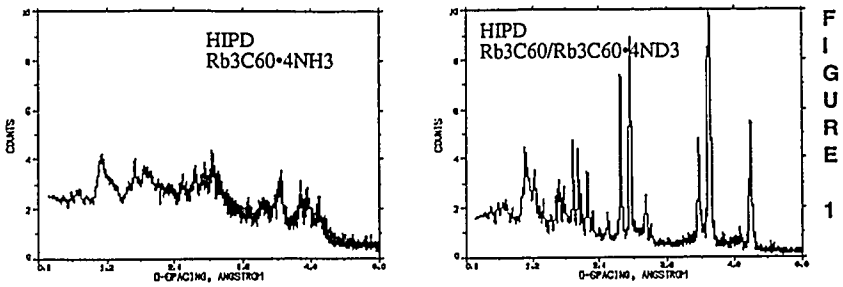


FIGURE 1

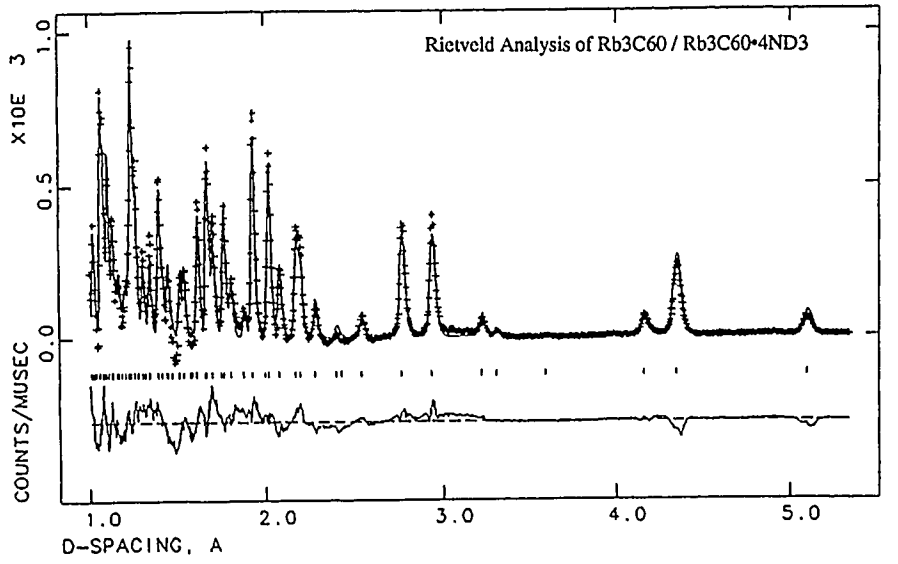


FIGURE 2

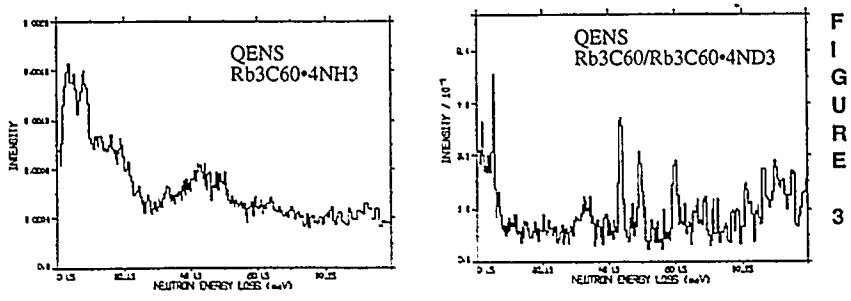


FIGURE 3

INSTRUMENT USED: QENS, HIPD	DATE OF REPORT: 8/2/94	EXPERIMENT NO.: 1878

TITLE: Inelastic Scattering from Ternary Intercalates of C_{60}

AUTHORS AND AFFILIATIONS: J. W. White, P. Reynolds, R. Durand
Research School of Chemistry, Australian National University

DATES OF EXPERIMENTS: 4/12/94 to 4/25/94

CHECK ALL APPLICABLE BOXES:

- X APPROVED BY PROGRAM COMMITTEE
- ☐ INSTRUMENT SCIENTIST ALLOCATION
- ☐ DO NOT PUBLISH
- ☐ PROPRIETARY RESEARCH
- ☐ PRT ALLOCATION

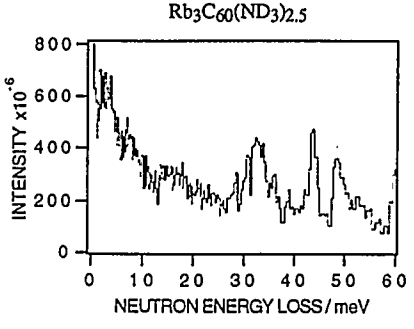
EXPERIMENTAL REPORT (or Abstract of Publication)

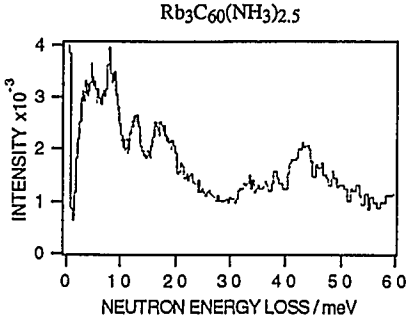
This is a continuation of Experiment No. 1768 in which two ammonia doped Rb_3C_{60} samples were examined by elastic (HIPD) and inelastic (QENS) neutron scattering. As outlined in the report on #1768, this is an experiment to elucidate the mechanism of high temperature superconductivity in these materials.

Two further samples, of improved crystallinity and different doping were examined on QENS and HIPD. We now have results from Rb_3C_{60}; $Rb_3C_{60}(NH_3)_{0.96}$; $Rb_3C_{60}(NH_3)_{2.5}$ and $Rb_3C_{60}(ND_3)_{2.5}$.

These new results confirm that the internal vibrational modes of C_{60} in Rb_3C_{60} are strongly affected by ammonia doping, the density of states reverting to something much closer to that in pure C_{60}. In addition there are now, by comparison of spectra, sufficient data to assign all the observed inelastic peaks both in the tunnelling (μeV) and vibrational (meV) regions. The NH_3 and ND_3 torsional and tunnelling peaks may be fitted by a model in which the -NH_3 rotor exists within a threefold potential with a mean barrier height of 12 meV.

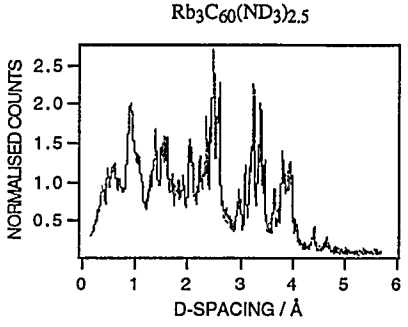
QENS Inelastic Results The new QENS inelastic spectrum for $Rb_3C_{60}(NH_3)_{2.5}$ shows more structure than the $Rb_3C_{60}(NH_3)_{0.96}$ spectrum of #1768. In addition to the lattice peak at 4 meV and the NH_3 torsional mode at 8.5, we can now resolve two further torsional peaks at 13.0 and 17.5 meV. In addition for ND_3 we observe torsions at 7.9 and 16.3 meV. All these energies may be fitted by a threefold rotational potential with barrier height 12 meV. δ bending modes of N-Rb-N may be assigned at 35 and 45 meV (NH_3) and 27 meV (ND_3) at their expected values. A comparison of Rb_3C_{60} and $Rb_3C_{60}(NH_3)_{2.5}$ shows similar C_{60} internal vibrational modes, many very narrow. But in $Rb_3C_{60}(NH_3)_{2.5}$, as in C_{60} itself, the $H_g(2)$ (54 meV) and T_{1u}(70-74 meV) modes are apparent which they are not in Rb_3C_{60}. This appears to be due to strong electron-phonon coupling.

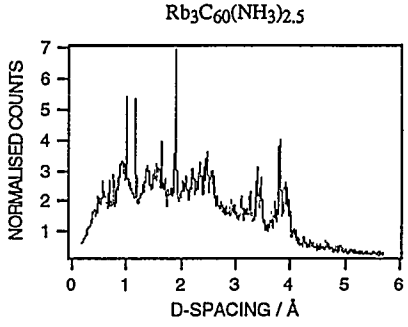




EXPERIMENTAL REPORT (CONTD.)

HIPD Diffraction Results The diffraction patterns here show many more resolved peaks than the previous samples, reflecting the improved crystallinity. The peaks indexed as primitive cubic are now much split. The material is not single phase, but is composed of a number of superlattices all derived from a basic cubic $Im\bar{3}m$ (a=12.10Å) cell, by modulation along the three principal axes. This is supported by both X-ray diffraction measurements, and measurements on the corresponding lithium compounds. The C_{60} - C_{60} distances remain constant while the modulation doubles and in aged samples the cell dimensions triple with substantial rearrangement of unit cell contents. These superlattices may be interpreted as low order approximants to an icosahedral quasicrystal. The peaks observed correspond to those strongest in such a quasicrystal. We can infer that the commensurate modulation is such as to produce, for much of the unit cell content, a more icosahedral local coordination around the C_{60} fragments.





INSTRUMENT USED:	DATE OF REPORT:	EXPERIMENT NO:
HRMECS	Oct 1. 1995	2041

TITLE:
Hydrogen-bonding dynamics in Brucite

AUTHORS AND AFFILIATIONS:
Bryan Chakoumakos (Oak Ridge National Lab)
C.-K. Loong (ANL)

DATES OF EXPERIMENT:
May 17-21, 1995

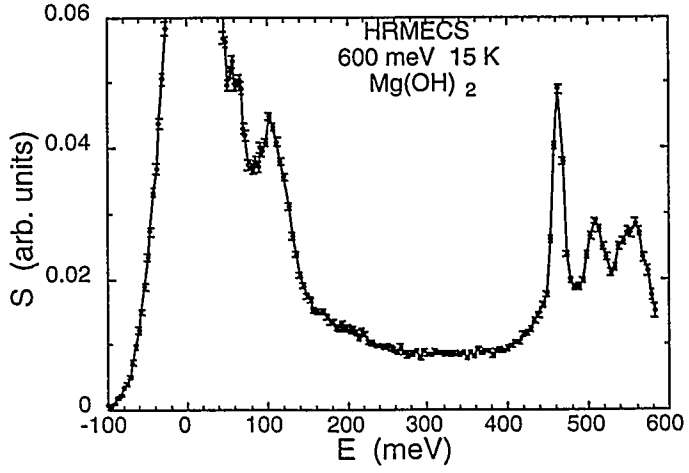
CHECK ALL APPLICABLE BOXES:

- [X] APPROVED BY PROGRAM COMMITTEE
- [ ] INSTRUMENT SCIENTIST ALLOCATION
- [ ] DO NOT PUBLISH
- [ ] PROPRIETARY RESEARCH
- [ ] PRT ALLOCATION

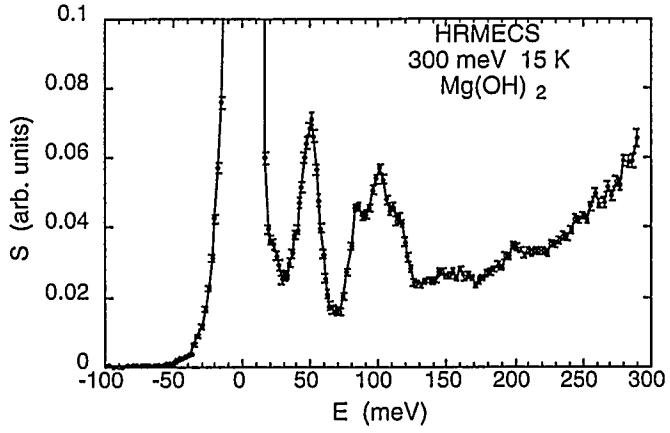
EXPERIMENTAL REPORT (or Abstract of Publication)

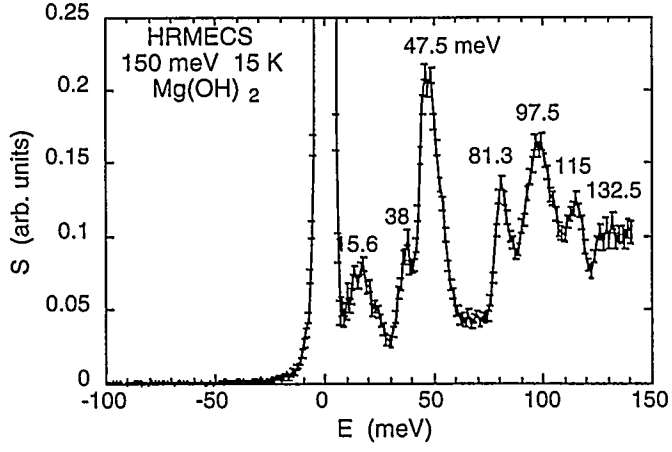
The pressure and temperature dependence of hydrogen bonding in crystals is critically important to understanding their stability. Brucite, $Mg(OH)_2$, is of particular interest because its simple structure can be viewed as a model system. Moreover, brucite is of geophysical interest because it is an end-member for a variety of hydrous minerals that are hosts for water in the crust and mantle of the Earth. Information regarding the structure or dynamics of this water-containing model system under high pressure is valuable to an eventual understanding of the thermodynamic properties of minerals under various pressure-temperature conditions in the earth.

We used inelastic neutron scattering to examine the hydrogen bonding dynamics of $Mg(OH)_2$ as a function of temperature (15-300 K), and correlate this information with high precision structural refinements of $Mg(OD)_2$. The inelastic spectra provided a measure of hydrogen motion in lattice modes, librations, bending, stretch vibrations as well as combination modes over an energy region of 0-600 meV from which unique information concerning H-bonding dynamics can be obtained.



EXPERIMENTAL REPORT (CONTD.)





INSTRUMENT USED:	DATE OF REPORT:	EXPERIMENT NO.:
HRMECS	October 30, 1990	1276

TITLE: Determination of Phonon Density-of-States of the $YBa_2Cu_3O_{6.5}$ Superconductor

AUTHORS AND AFFILIATIONS:

S.-K. Chan, B. W. Veal, and C.-K. Loong, Argonne National Laboratory

DATES OF EXPERIMENT: July 17-31, 1990

☒ APPROVED BY PROGRAM COMMITTEE, OR

☐ PART OF INSTRUMENT SCIENTIST ALLOCATION

REPORT RECEIVED:

EXPERIMENTAL REPORT (or Abstract of Publication)

Introduction

The lattice dynamics of $YBa_2Cu_3O_{6.5}$ are important to the understanding of the transition of the system from a superconductor to a semimetal and of the nature of the ordering of oxygen atoms in the chains. A theoretical calculation [1] has recently been completed for this composition, leading to phonon dispersions and density of phonon states. Since there exists no experimental information for this composition, phonon density of states were measured for the first time and compared with the calculation and also with data for other compositions.

Experiment and Results

The polycrystalline sample of $YBa_2Cu_3O_{7-x}$ with nominal composition $x \approx 0.1$ used in a previous experiment (Experiment 1277) was reoxygenated to nominal composition $x \approx 0.5$. Phonon density of states (DOS) were investigated at 15 K using the high-resolution median energy chopper spectrometer for the energy range 0-80 meV. The results are presented in Fig. 1 (squares) together with those for nominal composition $x \approx 0.1$ (circles) for the purpose of comparison. The anomalous peaks above 80 meV are due to contamination. It is seen that in the low energy range, there is hardening of the phonon modes for $x \approx 0.5$ in relation to those for $x \approx 0.1$ and, in the higher energy range, there is some relative shifting of the peaks for the two compositions. The phonon DOS calculated for x = 0, 0.5, and 1 are shown in Fig. 2 for comparison. The structure for x = 0.5 on which the calculation was carried out was based on the model of Alario-Franco et al. [2]. The theoretical results indicate a close resemblance of the DOS for the x = 0 and x = 0.5 compositions and a rather large departure of the DOS for the x = 1 composition from those for x = 0 or x = 0.5 in the mid and high energy range. The similarity of the results for x = 0 and x = 0.5 predicted in the calculation is borne out by experiment.

References

[1] C. H. Chen and S.-K. Chan, to be published.
[2] M. A. Alario-Franco et al., Mat. Res. Bull. 22, 1685 (1987).

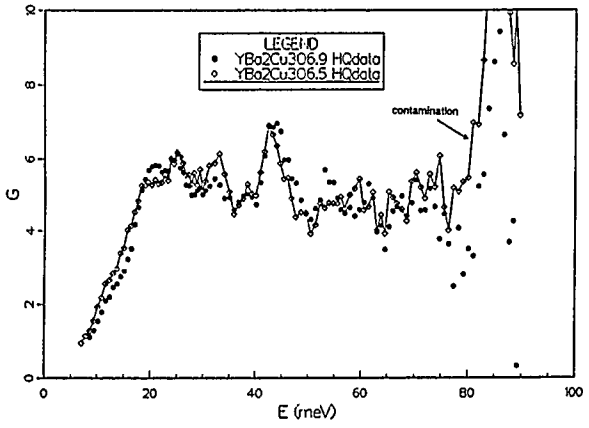


Fig. 1. Weighted DOS measured at 15 K for $YBa_2Cu_3O_{7-x}$, x = 0.1, 0.5

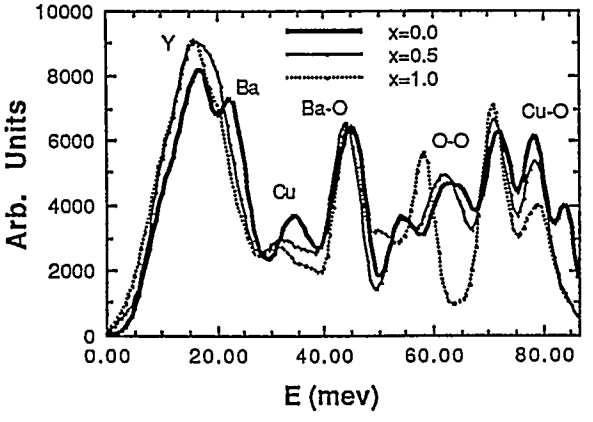


Fig. 2. Calculated DOS for $YBa_2Cu_3O_{7-x}$, x = 0, 0.5, 1.

INSTRUMENT USED:	DATE OF REPORT:	EXPERIMENT NO.:
HRMECS	October 30, 1990	1277

TITLE: Determination of Phonon Density-of-States of the $YBa_2Cu_3O_{7-x}$ Superconducting Oxides

AUTHORS AND AFFILIATIONS:

S.-K. Chan, B. W. Veal, and C.-K. Loong, Argonne National Laboratory

DATES OF EXPERIMENT: July 17-31, 1990

☒ APPROVED BY PROGRAM COMMITTEE, OR

☐ PART OF INSTRUMENT SCIENTIST ALLOCATION

REPORT RECEIVED:

EXPERIMENTAL REPORT (or Abstract of Publication)

Introduction

The lattice dynamics of $YBa_2Cu_3O_{7-x}$ ($x \approx 0.1$) are important to the understanding of the phonon and lattice properties of the superconducting ceramic oxides and of the possible role of phonons in superconductivity. A calculation of the lattice dynamics has recently been carried out based on the Born-von Karman model [1]. The phonon dispersion, density of phonon states and elastic stiffness constants have been obtained. The last information has been used to compare calculated surface wave velocity with experimental measurements on de-twinned single crystals. To test the validity of the calculation and to resolve the discrepancies between previous data from neutron experiments of Renker et al. [2] and Rhyne et al [3], the density of phonon states were measured at 15 K over the energy range 0-80 meV.

Experiment and Results

A polycrystalline sample (~100 g) of nominal composition $x \simeq 0.1$ was prepared and characterized with SQUID magnetization. Phonon density of states (DOS) were investigated at 15 K using the high-resolution medium energy chopper spectrometer. Results of the weighted phonon DOS are shown in Fig. 1 by the circles. In the same figure, results for $x \approx 0.5$ (Experiment 1276) are also shown by the squares for comparison. The regime above 80 meV exhibits anomalous peaks due to contamination. Our data are closer to those obtained previously by Renker et al. (Fig. 2) than to those obtained by Rhyne et al. (Fig. 3). The positions of the peaks of the weighted phonon DOS measured for $x \approx 0.1$ can be compared with those of the phonon DOS calculated for $x = 0$ (Fig. 4) although the absolute heights of the peaks are not relevant. It is seen that the correspondence of the positions of the peaks between the calculation (for $x = 0$) and the experimental measurements (for $x \approx 0.1$) is very good. Most of the features up to 80 meV obtained in the calculation are borne out by experiment.

References

[1] C. H. Chen and S.-K. Chan, to be published.
[2] B. Renker et al., Z. Phys. B71, 437 (1988).
[3] J. J. Rhyne et al., Phys. Rev. B36, 2294 (1987).

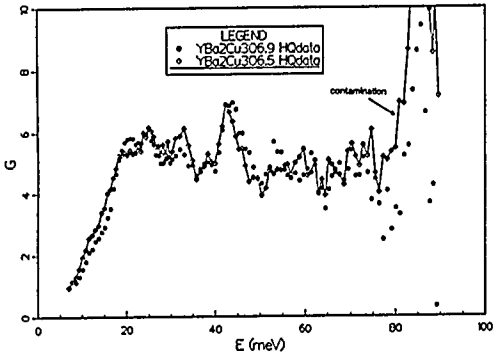


Fig. 1. Weighted DOS measured at 15 K

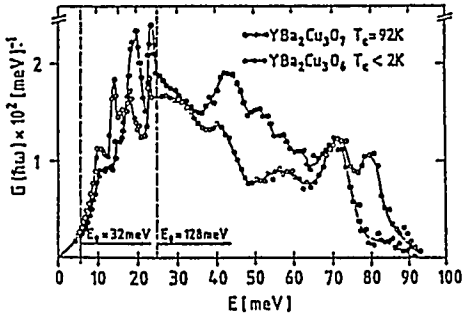


Fig. 2. DOS of $YBa_2Cu_3O_7$ and $YBa_2Cu_3O_6$ [2]

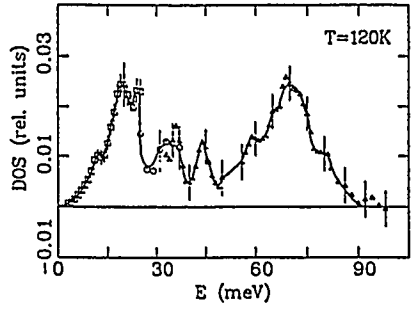


Fig. 3. DOS of $YBa_2Cu_3O_7$ [3]

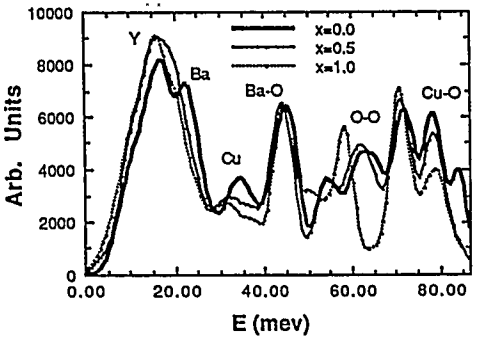


Fig. 4. Calculated DOS for $YBa_2Cu_3O_{7-x}$, $x = 0, 0.5, 1$ [1]

INSTRUMENT USED:	DATE OF REPORT:	EXPERIMENT NO.:
HRMECS	July 12, 1991	NSF-24

TITLE:
Determination of Phonon Density-of-States of the $YBa_2Cu_3O_{7-x}$ (x = 0.71)

AUTHORS AND AFFILIATIONS:
S.-K. Chan, B. W. Veal, and C.-K. Loong, Argonne National Laboratory

DATES OF EXPERIMENT: April 8-17, 1991

☒ APPROVED BY PROGRAM COMMITTEE, OR

☐ PART OF INSTRUMENT SCIENTIST ALLOCATION

REPORT RECEIVED:

EXPERIMENTAL REPORT (or Abstract of Publication)

Introduction

The lattice dynamics of $YBa_2Cu_3O_{7-x}$ as a function of x are important to the understanding of the origin of the instabilities of the tetragonal and the orthorhombic phases and may also provide guidance to the possible role of phonons in the superconducting transformation of these ceramic oxides. The generalized phonon density-of-states (DOS) for nominal x = 0.1 and 0.5 have already been measured (July 16-30, 1990) using the HRMEC at IPNS [1]. The results indicate a softening of the phonon modes for the x = 0.1 composition in relation to those for the x = 0.5 in the low energy range and a systematic shifting of peaks between the two compositions in the higher energy range. These experimental results compare favorably with a theoretical calculation of the lattice dynamics [2]. Measurements of the DOS for one more composition x on the nonsuperconducting side of the phase boundary would provide an adequate description of the dependence on x of the phonon profile. In the original proposal, the composition x = 1 was chosen. However, towards the x = 1 end of the composition range, decomposition of the oxides into separate phases becomes quite probable. To avoid the occurrence of such an eventuality, the nominal composition x = 0.71 was used instead. This composition places the sample in the nonsuperconducting regime without getting near to the range where decomposition becomes probable.

Experiment and Results

A sample (~80 g) of $YBa_2Cu_3O_{7-x}$ (x = 0.71) was prepared under well-controlled conditions that yielded minimally stressed grains. Generalized phonon DOS were measured in the range 0-80 meV at 15 K using the HRMECS with neutron energy E_0 = 100 meV. To obtain better resolution for the lower energy range 0-30 meV, the measurements were also repeated with neutron energy E_0 = 40 meV. Results for the DOS are shown, respectively, in Figs. 1 and 2. In relation to the generalized phonon DOS of the fully oxygenated $YBa_2Cu_3O_{6.9}$ shown in Fig. 3, one notices that there is (1) a hardening of the phonon modes in the energy range 8-17 meV, (2) a loss of the hump at 20-22 meV, (3) the appearance of a new peak at 27 meV, (4) the appearance of a stronger peak at 33 meV, (5) a shift to lower energy of the major structure 42-47 meV, and (6) a loss of the peak structure at 53 meV. These experimental findings will be interpreted in terms of a lattice dynamics calculation [2].

References

[1] S.-K. Chan, B. W. Veal, and C.-K. Loong, IPNS Progress Report and to be published.
[2] C. H. Chen and S.-K. Chan, to be published.

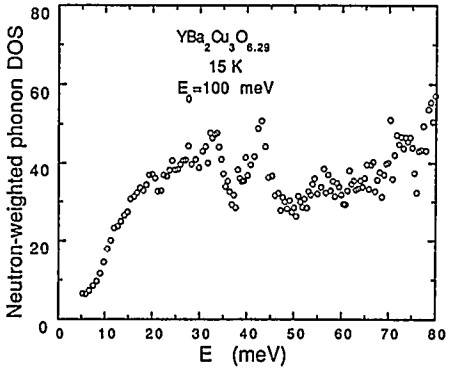


Fig. 1. DOS for $YBa_2Cu_3O_{6.29}$ measured with neutron energy E_0 = 100 meV

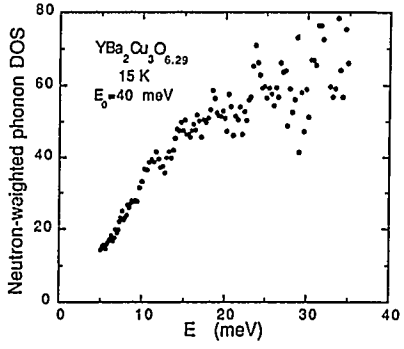


Fig. 2. DOS for $YBa_2Cu_3O_{6.29}$ measured with neutron energy E_0 = 40 meV

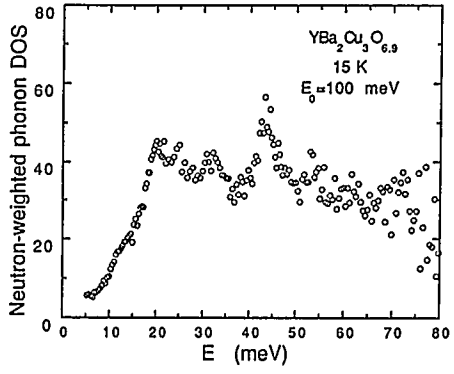


Fig. 3. DOS for $YBa_2Cu_3O_{6.9}$ measured with neutron energy E_0 = 100 meV

INSTRUMENT USED:	DATE OF REPORT:	EXPERIMENT NO:
HRMECS	April. 20, 1995	1851

TITLE:
Phonon density of states of forsterite and enstatite

AUTHORS AND AFFILIATIONS:
N. Choudhury and S. Ghose (University of Washington, Seattle)
C.-K. Loong (IPNS-ANL)

DATES OF EXPERIMENT:
Nov, 1993

CHECK ALL APPLICABLE BOXES:

- [ ] APPROVED BY PROGRAM COMMITTEE
- [X] INSTRUMENT SCIENTIST ALLOCATION
- [ ] DO NOT PUBLISH
- [ ] PROPRIETARY RESEARCH
- [ ] PRT ALLOCATION

EXPERIMENTAL REPORT (or Abstract of Publication)

Enstatite and forsterite are important rock-forming silicates occurring in terrestrial and lunar rocks and meteorites, and are considered to be the major constituent of the earth's upper mantle. The goal of our phonon measurements is an eventual understanding of the physical and thermodynamic properties of these minerals under high pressure-temperature conditions prevalent in the earth. Structurally enstatite $Mg_2Si_2O_6$ is distinct from forsterite Mg_2SiO_4. While both contain octahedral bands, enstatite contains single tetrahedral silicate chains, whereas forsterite contains isolated silicate tetrahedra. Salient differences in their densities of states (DOS) have been clarified on the basis of lattice dynamical calculations which are in excellent agreement with the experimental data. The DOS in both have mainly a three-peak structure. The broad peak in the 20-80 meV range in both minerals is due to the Mg-translations and the librations of the SiO4 groups. Above 80 meV, the contributions in both cases are mainly from the internal vibrations of the silicate groups. In enstatite, the bridging oxygens in the silicate chain are vibrationally distinct from the bon-bridging oxygens. Consequently, the Si-O stretching vibrations in enstatite can be resolved into a bridging (80-120 meV) and non-bridging (110-140 meV) set. There is no contribution to the vibrational spectra in the 80-100 meV range in forsterite, with the internal vibrations contributing in the 100-140 meV range.

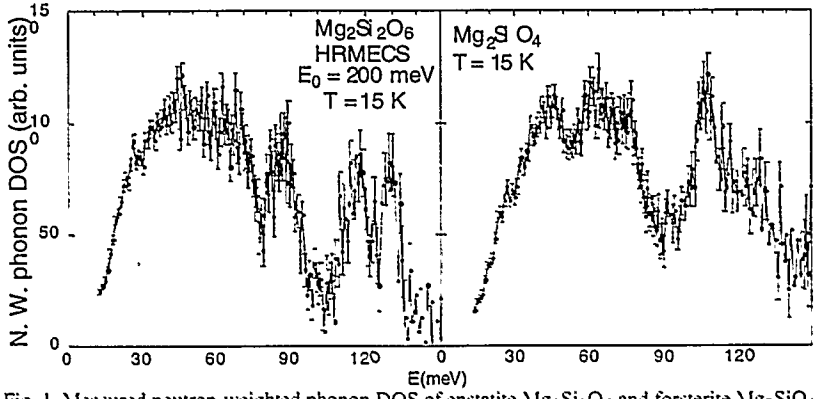


Fig. 1 Measured neutron-weighted phonon DOS of enstatite $Mg_2Si_2O_6$ and forsterite Mg_2SiO_4.

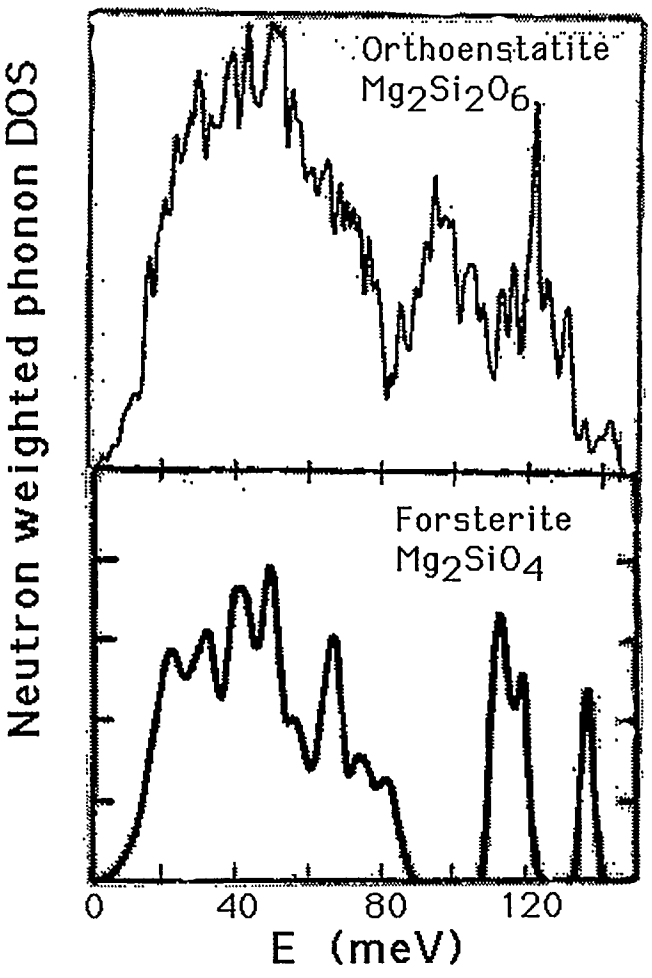


Fig. 2. Calculated phonon DOS of enstatite $Mg_2Si_2O_6$ and forsterite Mg_2SiO_4 using a rigid-ion model.

INSTRUMENT USED:	DATE OF REPORT:	EXPERIMENT NO.:
HRMECS	06-11-1990	1239

TITLE:
MOLECULAR SPECTROSCOY OF INSULIN

AUTHORS AND AFFILIATIONS:
H.Conrad, KFA Julich; A.Wollmer, RWTH Aachen; D.L.Price, MSD; D.J.LePoire, IPNS

DATES OF EXPERIMENT: 05-10 through 05-20-90

☒ APPROVED BY PROGRAM COMMITTEE, OR

☐ PART OF INSTRUMENT SCIENTIST ALLOCATION

REPORT RECEIVED:

EXPERIMENTAL REPORT (or Abstract of Publication)

The present experiment is a continuation of an earlier HRMECS measurement on the dynamics of insulin in its polycrystalline and dissolved forms, respectively [1]. This former experiment has been the very first one ever done on a protein applying neutron down scattering. Accordingly, compared to upscattering trials with cold neutrons [2], a rich but still not very well resolved spectrum has been measured. Most likely this had two reasons: Firstly, inadequate instrumental resolution due to relatively high incoming energy. Secondly, the insulin sample has been measured only at room temperature. Crystalline proteins contain up to 50% mother liquor in the unit cell, which might result in motional broadening of spectral lines because of weak steric hindrance by the surrounding liquor.

Therefore we performed the present measurements with 300meV neutrons and did comparative low temperature (12 K) and room temperature runs. It turned out that indeed the low temperature data showed more pronounced structure than the room temperature data, as can be seen from figures 1 and 2. Also included in fig. 1 is the RAMAN spectrum of polycrystalline insulin [3]. Although a complete assignment of neutron and RAMAN data is still not possible, several clearly separated peaks are present in the low temperature neutron data, which correspond unambiguously to the respective RAMAN lines. A more thorough interpretation of the neutron results has still to be done and will be published elsewhere. A brief qualitative interpretation of the relative neutron intensities has already been given in [1].

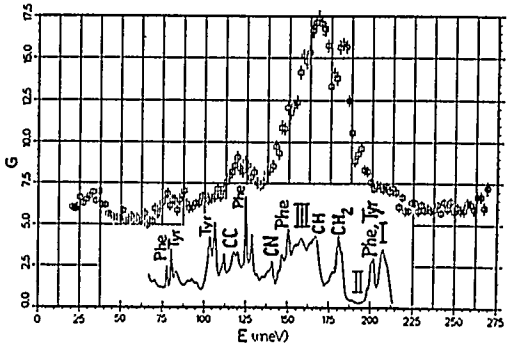


Figure 1:

Generalized frequency distribution of polycrystalline insulin measured at 12 K. The line spectrum at the bottom represents the RAMAN data [3]. The roman numbers label the amide I,II,III bands. CH and CH resp. denote deformation vibrations of these groups. Tyr, Phe, C-C, C-N label the fingerprint lines for two examples of amino acids and two other typical molecular groups.

EXPERIMENTAL REPORT (CONTD.)

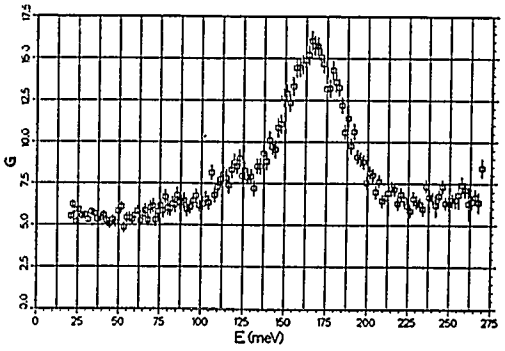


Figure 2:

Generalized frequency distribution of polycrystalline insulin measured at room temperature.

The low frequency peaks now clearly visible might correspond to the peaks predicted by MD simulations [4], but at least the 30 meV peak could also correspond to a van Hove singularity of the crystal modes. The insulin solution measurements of the previous experiment [1] could not be repeated and improved because of lack of beam time. The solution data would be free of collective excitations of that kind.

An important question is the biochemical stability of insulin on cooling to very low temperatures. Although the only reliable answer can come from biochemical investigations still to be performed, we checked this by comparing two 12 K runs intermitted by a room temperature one. Figure 3 shows the difference data of the respective frequency distributions.

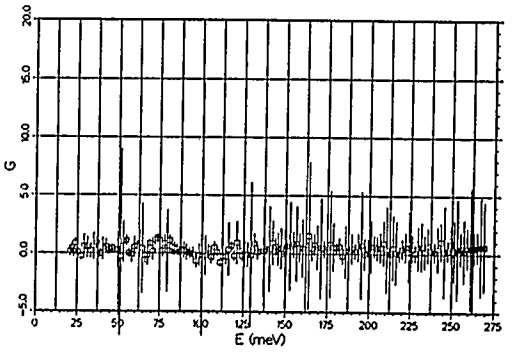


Figure 3:

Difference data of the frequency spectra of two low temperature runs intermitted by a 40 h room temperatur run.

References:

[1] Report on HRMECS-experiment No. 1108
[2] S. Cusack, J. Smith, J. Finney, M. Karplus and J. Trewhella (1986) Physica 136B, 256-259.
[3] N.-T. Yu, B.H. Jo, R.C.C. Chang and J.D. Huber (1974) Arch.Biochem.Biophys. 160, 614-622.
[4] IPNS proposal to HRMECS experiment No. 1108

INSTRUMENT USED:	DATE OF REPORT:	EXPERIMENT NO.:
HRMECS	09–06–93	1612

TITLE:

Molecular Spectroscopy of Insulin

AUTHORS AND AFFILIATIONS:
H. Conrad, KFA Jülich; A. Wollmer, RWTH Aachen; G. Kneller, CEN Saclay; C. Loong, IPNS;

DATES OF EXPERIMENT: 07–14 through 07–20–93

☒ APPROVED BY PROGRAM COMMITTEE, OR

☐ PART OF INSTRUMENT SCIENTIST ALLOCATION

REPORT RECEIVED:

EXPERIMENTAL REPORT (or Abstract of Publication)

The present experiment is a continuation of an earlier run on the dynamics of insulin (see report on HRMECS expt. # 1239). It was planned, when molecular dynamics calculations of insulin by one of us (G.K.) covering the whole experimental frequency range of the previous run (# 1239) became available after finishing that experiment. The calculated frequency distribution $G(\omega)$ obtained by Fourier transforming the velocity autocorrelation function is shown in Figure 1.

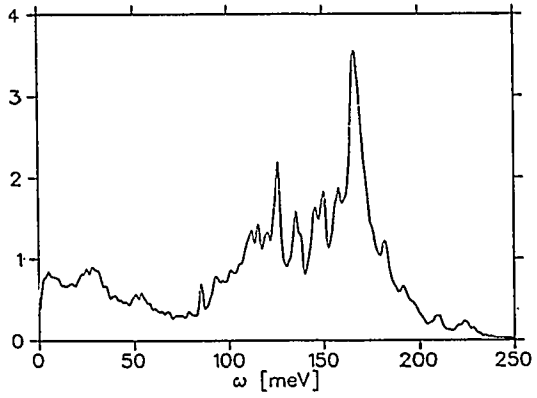


Figure 1

Calculated frequency spectrum of insulin based on the velocity autocorrelation function deduced from molecular dynamics trajectories (G.Kneller, unpublished)

The experimental data of run # 1239 essentially resembled the calculated spectrum, although the absolute intensities of some spectral lines appeared to be different. Furthermore and very importantly both the statistical accuracy and the energy resolution of the experimental data were not sufficient everywhere over the frequency range measured. As we had covered only about 30 % of the available beam cross section of HRMECS due to lack of a sufficient amount of the very expensive insulin (we actually used 2 grams for the previous run, an amount, which made the biochemists wonder about the usefulness of neutron scattering!), we hoped to improve the results by investing in sample material.

When starting the present measurements it turned out that the booster target installed at IPNS during our previous experiment was no longer available. As a consequence the expected gain due to the extended sample is compensated by the loss in primary neutron intensity due the depleted uranium target. In fact, the precision of the data look strikingly similar to that already obtained before. Even the improvements with the spectrometer (T_0 chopper, Soller collimator) did not significantly change the background conditions for this experiment, except from slightly lower contributions beyond about 225 meV. Therefore we only show one example of a measured frequency spectrum for the scattering angle with the best counting statistics in Figure 2. The data were taken with E_0 = 300 meV and a temperature of 12 K.

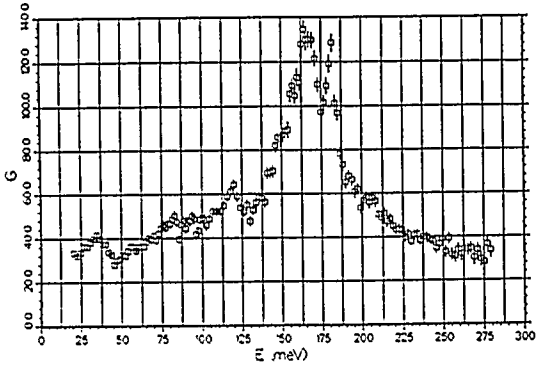


Figure 2

Frequency spectrum of bovine insulin for a scattering angle of 18.3 degrees

The average over all scattering angles shown in Figure 3 demonstrates a not yet eliminated momentum transfer dependence in the data, which means we are still dealing with a generalized frequency distribution $G(Q,\omega)$.

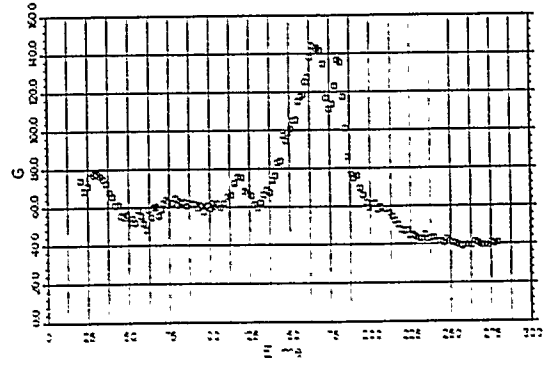


Figure 3

Frequency spectrum averaged over all scattering angles

INSTRUMENT USED:	DATE OF REPORT:	EXPERIMENT NO:
HRMECS	June 1, 1994	1697

TITLE:
Vibrational and ligand-field spectroscopy in $3Na_2O{\cdot}R_2O_3{\cdot}6SiO_2$ (R=Yb) Glasses

AUTHORS AND AFFILIATIONS:
A. J. G. Ellison and C.-K. Loong (ANL)

DATES OF EXPERIMENT:
Dec 18-19, 1992, March 16-18, 1993

CHECK ALL APPLICABLE BOXES:

- [X] APPROVED BY PROGRAM COMMITTEE
- [ ] INSTRUMENT SCIENTIST ALLOCATION
- [ ] DO NOT PUBLISH
- [ ] PROPRIETARY RESEARCH
- [ ] PRT ALLOCATION

EXPERIMENTAL REPORT (or Abstract of Publication)

The static and dynamic magnetic response of the Yb^{3+} ions in $3Na_2O{\cdot}Yb_2O_3{\cdot}6SiO_2$ glass and the isochemical crystalline silicate $Na_3YbSi_3O_9$ has been studied by neutron diffraction, inelastic magnetic-scattering, and magnetic susceptibility measurements. The rare earth sites in the glass have an average coordination number of 5.6 ± 0.5 and give a mean rare earth-oxygen bond length of 2.23 Å; average Si-O and O-O coordination numbers and bond distances are comparable to those in vitreous SiO_2. The magnetic excitation spectrum of the $Na_3YbSi_3O_9$ material was analyzed by a crystal-field model using a method of descending symmetry. The magnetic susceptibility and the excitation spectrum of the Yb glasses can be described by a distribution of ligand-field effects on the Yb^{3+} ions that are similar to the nominal crystal field in crystalline $Na_3YbSi_3O_9$.

(J. Alloys Compounds, **207/208** (1994) 170-173)

EXPERIMENTAL REPORT (CONTD.)

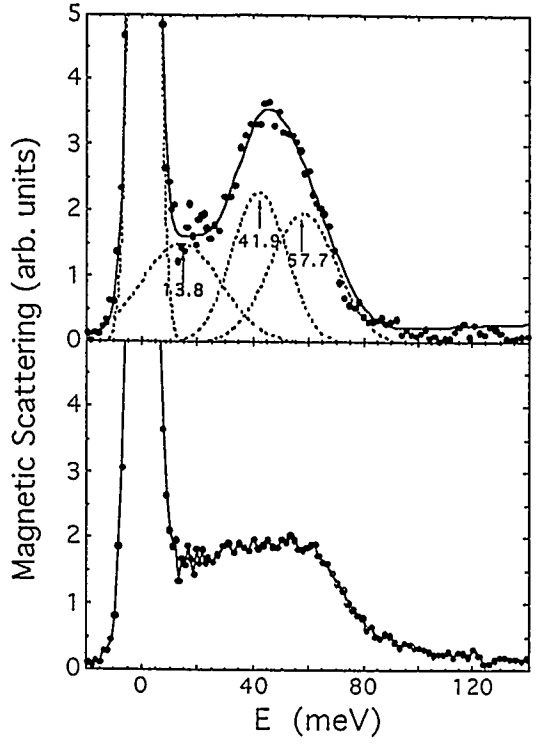


Fig. 2. Upper panel: The magnetic excitation spectrum of $Na_3YbSi_3O_9$ (circles) and a fit to the data (solid line) by a sum of four Gaussian functions centered at 0, 13.8, 41.9, and 57.5 meV denoted by the dotted lines. Lower panel: The magnetic excitation spectrum of the $3Na_2O \cdot Yb_2O_3 \cdot 6SiO_2$ glass (circles). The line is a guide to the eye. $T = 15$ K.

INSTRUMENT USED:	DATE OF REPORT:	EXPERIMENT NO.:
HRMECS	January 3rd, 1991	#1325

TITLE:

Kinetic Energies of the Individual Isotopes in Solid ^{3}He - ^{4}He Solutions

AUTHORS AND AFFILIATIONS:

M. A. Fradkin (UIUC), S. X. Zeng (UIUC), R. O. Simmons (UIUC)

DATES OF EXPERIMENT: 9/5/90 - 9/14/90

☒ APPROVED BY PROGRAM COMMITTEE, OR

☐ PART OF INSTRUMENT SCIENTIST ALLOCATION

REPORT RECEIVED:

EXPERIMENTAL REPORT (or Abstract of Publication)

In this experiment we intended to measure the single-particle kinetic energies of the individual isotopes in a homogeneous bcc solution of ^{3}He and ^{4}He. Solid solutions of ^{3}He and ^{4}He exhibit complicated phase diagrams at low temperature; understanding of these unusual solids is still incomplete. In particular, there is no information whatsoever about kinetic energies of the isotopic constituents, which are expected to differ considerably. Unfortunately due to a thermal short between the sample cell and the inner radiation shield of the cryostat we were unable to cool the sample into the solid phase to the desired temperature of 2.4 K. This limitation prevented us from investigating the bcc phase. Instead we took data on a dense fluid mixture, $^3He_{0.05}$ - $^4He_{0.95}$. These data, which we are currently analyzing, should provide us with the single-particle kinetic energies of the individual isotopes in the fluid phase as well as knowledge (best ^{3}He concentration, accumulation of necessary statistics, etc.) which will be useful when the bcc solid solution experiment is again attempted.

INSTRUMENT USED:	DATE OF REPORT:	EXPERIMENT NO.:
HRMECS	7/31/1991	#1517

TITLE: **Single-Particle Response of Neon at High to Intermediate Momentum Transfers**

AUTHORS AND AFFILIATIONS: M. A. Fradkin, S. X. Zeng, R. O. Simmons
University of Illinois at Urbana-Champaign

DATES OF EXPERIMENT: June 4-12, 1991

☒ APPROVED BY PROGRAM COMMITTEE, OR

☐ PART OF INSTRUMENT SCIENTIST ALLOCATION

REPORT RECEIVED:

EXPERIMENTAL REPORT (or Abstract of Publication)

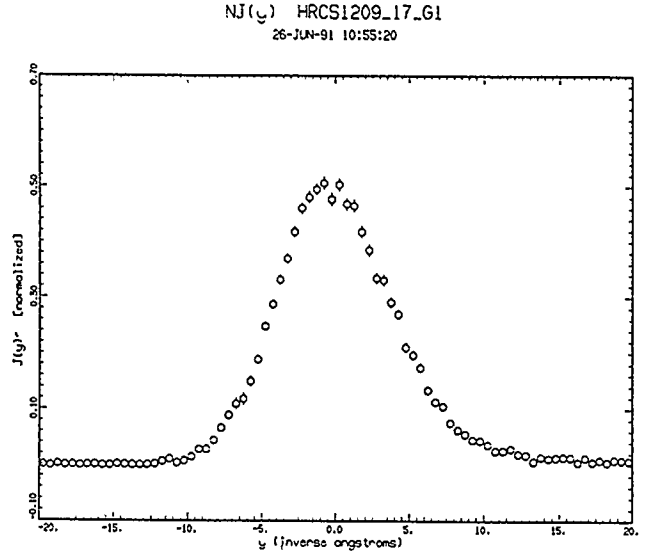
In this experiment we measured the response S(Q,E) of a liquid neon sample over the range of momentum transfers: 10.4 Å^{-1} - 27.6 Å^{-1}. The sample, natural liquid neon, was produced in situ by condensing research grade neon gas in a multi-tubed aluminum cell. For all data sets the sample was held at approx. 27 K at a pressure slightly above its saturated vapor pressure. Data were taken at four different incident energies in order to study the momentum transfer dependance of the liquid neon's response. The incident energies were chosen such that the range of momentum transfer in each data set overlaps those in another data set. (see table). This provides a valuable consistency check for instrument resolution corrections. A typical J(y) (Compton profile) is shown in the figure.

Analysis is currently in progress using a newly developed sophisticated Monte Carlo simulation of the instrument, created by R. C. Blasdell at IPNS. This simulation will permit the effects of instrument resolution and multiple scattering to be deconvoluted from the measured response.

Momentum Transfer as a Function of Scattering Angle and Incident Energy

	Scattering Angle			
Incident Energy	87°	106°	121°	136°
125 meV	10.4 Å^{-1}	12.0 Å^{-1}	13.0 Å^{-1}	13.8 Å^{-1}
195 meV	13.1	15.0	16.3	17.2
300 meV	16.2	18.6	20.2	21.4
500 meV	20.9	24.0	26.0	27.6

EXPERIMENTAL REPORT (CONTD.)



This research supported by US DOE contracts DOE-DE-FGO2-91ER45439 and W-31-1090-ENG-38

INSTRUMENT USED:	DATE OF REPORT:	EXPERIMENT NO.:
HRMECS	10/20/92	1557

TITLE: Density Dependence of the Single-Particle Response of Neon at High to Moderate Momentum Transfers

AUTHORS AND AFFILIATIONS: M. A. Fradkin, S.-X. Zeng, and R. O. Simmons
University of Illinois at Urbana-Champaign (UIUC)

DATES OF EXPERIMENT: 7/7/92 - 7/21/92

☐ APPROVED BY PROGRAM COMMITTEE, OR

☐ PART OF INSTRUMENT SCIENTIST ALLOCATION

REPORT RECEIVED:

EXPERIMENTAL REPORT (or Abstract of Publication)

This experiment is a continuation of experiment #1517 and represents an extension of our previous measurements of Final State Effects (FSE) in liquid Ne. With the data taken in the present experiment we now have scattering data over a range of momentum transfers at two different sample densities. These data permit the density dependence of FSE in this system to be investigated.

In order to identify FSE contributions to the liquid response we are employing in our analysis the formalism of Sears[1]. In this formalism J(y), the longitudinal momentum distribution function, is written as an asymptotic expansion whose terms are symmetric and antisymmetric in the West scaling variable y,

$$[1] \quad J(y) = J_{IA}(y) - A_3\left(\frac{J_{IA}^3(y)}{dy^3}\right) + A_4\left(\frac{J_{IA}^4(y)}{dy^4}\right) - \ldots$$

with

$$[2] \quad A_3 = \frac{M\langle\nabla^2 V\rangle}{36\hbar^2 Q}$$

J(y) is the observed longitudinal momentum distribution function, $J_{IA}(y)$ is the longitudinal momentum distribution function in the Impulse Approximation, V is the interatomic potential, M is the mass of the scatterer, and <...> represents a thermal average. The sample conditions (T = 35 K, P = 7.6 MPa, V_{molar} = 18.0 cc/mole) for the present experiment were chosen to be near existing neutron diffraction measurements of g(r), the radial distribution function[2]. Knowledge of g(r) is necessary to compute the average value of Laplacian which appears in the expression for the coefficient of the first antisymmetric term in Eq. 2. The density dependence of the A_3 coefficient is explicitly contained in g(r).

Utilizing the accurate pair-potentials which exist for Ne the first term in the Sears' expansion may be determined and compared with our experimental results.

In experiment #1517 scattering data were obtained at four different incident neutron energies (125, 195, 300, and 500 meV) on a liquid Ne sample (T = 26.9 K, P = 0.7 MPa, V_{molar} = 16.7 cc/mole). Analysis of experiment #1517 is still in progress. The reduction in neutron flux due to the re-installation of the depleted Uranium target necessitated longer data collection times in experiment #1557 than those used in experiment #1517, hence in #1557 we obtained data at only two incident energies, 125 and 195 meV. These incident energies allow the scattering in the range of momentum transfers from 104 to 172 nm^{-1} to be explored with the HRMECS high angle detector banks. The incident energies were chosen such that the range of momentum transfers in the 125 meV data set overlaps those in the 195 meV data set. This overlap provides a valuable consistency check of instrument resolution and multiple scattering corrections which must be thoroughly accounted for in order to unambiguously identify FSE contributions to the liquid response. The sample cell used in the present experiment differs from the cell used in #1517 by the addition of 0.063 cm thick Cadmium disks placed at 1.0 cm intervals in the cell tubes to reduce sample multiple scattering.

References

[1] V. F. Sears, Phys. Rev. B, 30, 44 (1984)
[2] L. A. De Graaf and B. Mozer, J. Chem. Phys. 55, 4967 (1971)

INSTRUMENT USED:	DATE OF REPORT:	EXPERIMENT NO.:
HRMECS	Jan 31, 1991	1388

TITLE: Study of the Density-of-States and Localized Modes of the Icosahedral Al-Li-Cu Alloy

AUTHORS AND AFFILIATIONS:
A.I. Goldman & C. Stassis, Physics Dept., Iowa State University

DATES OF EXPERIMENT: 11-10-1991 to 11-19-1991

☒ APPROVED BY PROGRAM COMMITTEE, OR

☐ PART OF INSTRUMENT SCIENTIST ALLOCATION

REPORT RECEIVED:

EXPERIMENTAL REPORT (or Abstract of Publication)

This experiment aims at the determination of the phonon densities-of-states (DOS) of quasicrystalline materials and their reference crystalline compounds. These single-phase alloy systems are very difficult to prepare in large quantities (> 20 g). In the period of Nov. 10 - 19, 1990 we have focused our investigations on quasicrystalline and polycrystalline $Al_{65}Cu_{23}Fe_{12}$. We chose this system instead of the $Al_{5.1}Li_3Cu$ originally proposed for the reasons of availability of samples and its interesting dynamic properties as revealed in recent x-ray and neutron studies.

The quasicrystalline and the polycrystalline materials, each about 25 grams, were studied on HRMECS at room temperature using an incident neutron energy of 70 meV. Figures 1 and 2 show the measured scattering function S(E) for crystalline (Xtal) and quasicrystalline (QXtal) $Al_{65}Cu_{23}Fe_{12}$, respectively. A total of 50 hrs of data for the Xtal and 72 hrs for the QXtal samples were collected. We find that the features around 8, 14, and 25 meV in the DOS show some interesting differences between the Xtal and QXtal phases in both their intensities and widths. It is tempting to attribute these differences to the phonon dynamics due to changes in global and local symmetries from the Xtal to the QXtal materials. Unfortunately, the relatively poor statistics of the data prevents a definite identification of these features to the interesting physical properties, such as the existence of a set of energy gaps and/or localized states in the QXtal phase. The main reason for the poor data is insufficient samples given the current flux level of HRMECS. In addition, during this running period technical problems in the T_0-rotor controller have reduced the efficiency of the chopper system from 95+% to ~80%.

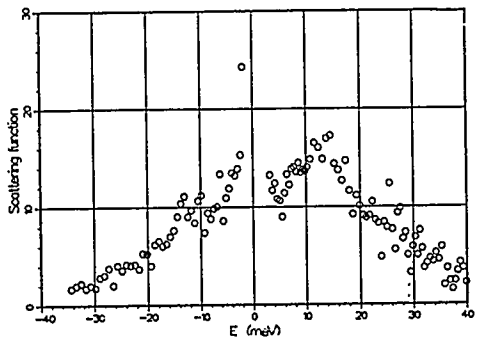


Figure 1. Measured scattering function S(E) of polycrystalline $Al_{65}Cu_{23}Fe_{12}$.

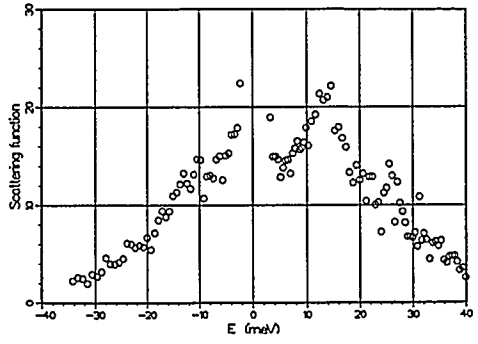


Figure 2. Measured scattering function S(E) of quasicrystalline $Al_{65}Cu_{23}Fe_{12}$.

To establish the ability of phonon DOS measurements by HRMECS under identical experimental conditions, we show in Figure 3 the measured neutron-weighted phonon DOS of vanadium obtained in a 7 hr calibration run using a 50 g vanadium plate. The data agree[1] very well with other neutron measurements and lattice dynamics calculations.

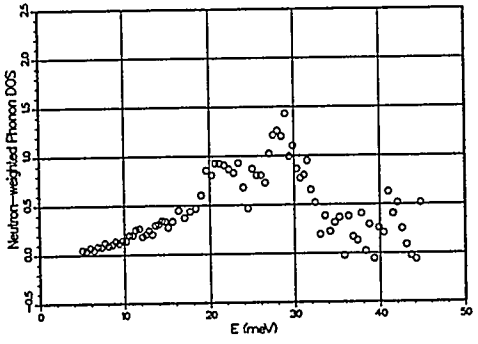


Figure 3. Measured neutron-weighted phonon density-of-states (under the incoherent approximation) of vanadium. The data have not been corrected for multiphonon scattering.

We conclude that although the present measurements indicate interesting difference in the phonon spectra between the QXtal and Xtal phases of $Al_{65}Cu_{23}Fe_{12}$, the experiment should be repeated using larger samples to improve the statistics of data.

[1] G. Dolling and A. D. B. Woods, in *Thermal Neutron Scattering*, Ed. P. A. Egelstaff, Academic (New York, 1965), Chapter 5, p. 211.

INSTRUMENT USED:	DATE OF REPORT:	EXPERIMENT NO.:
HRMES	May 23, 1995	1938

TITLE: The Interaction of Water in MnO_2: Alpha-MnO_2

AUTHORS AND AFFILIATIONS:
C. S. Johnson (CMT), M.M. Thackeray (CMT), and C.-K. Loong (IPNS)

DATES OF EXPERIMENT:
2/28/95 to 3/8/95 (6 runs); Run #1731-1736

CHECK ALL APPLICABLE BOXES:

- [X] APPROVED BY PROGRAM COMMITTEE
- [ ] INSTRUMENT SCIENTIST ALLOCATION
- [X] DO NOT PUBLISH
- [X] PROPRIETARY RESEARCH
- [ ] PRT ALLOCATION

EXPERIMENTAL REPORT (or Abstract of Publication)

INTRODUCTION: MnO_2 materials are of interest as electrodes for aqueous Zn/MnO_2 and Li/MnO_2 batteries. We are investigating α-MnO_2 as a potential cathode material for these batteries. Alpha-MnO_2 has a framework structure containing MnO_6 octahedra. It has been commonly believed that α-MnO_2 structure is stabilized by a foreign cation such as K^+ or Ba^{2+} within the interstitial space of the framework. We have recently synthesized an α-MnO_2 structure, without "stabilizing" cations. In our product, it was found by powder X-ray diffraction and neutron diffraction analysis (SEPD) that water molecules exist within the framework. Additional thermogravimetric data collected on this material showed that about 5% weight water was also present as surface water. The superficial and tunnel-bound water may be removed by heat-treating. Dehydrated α-MnO_2 is stable to approximately 400°C. The water molecules are important for the discharge of Zn/MnO_2 cells, whereas the MnO_2 must be anhydrous for Li/MnO_2 battery applications.

EXPERIMENTAL: The HRMECS spectrometer was used to assess the molecular vibrational interaction of water with a hydrated and a dehydrated α-MnO_2 samples. Samples were cooled to 25 or 15 K prior to exposing them to the chopped neutron beam. Data were collected at high and low angle neutron scattering angles and first at an incident spectrometer energy of 600 meV as defined by the chopper's rotation. Upon initial data inspection, it was deemed necessary to also perform the experiment at 250 meV to gain additional information. Data from empty aluminum foil envelopes were collected to correct for background.

RESULTS: (a) MnO_2·0.25H_2O. The baseline corrected spectra obtained at 600 meV and 250 meV are shown in Figures 1 and 2. Table 1 summarizes the information derived from these spectra in terms of peak number, energy, relative intensity and preliminary vibrational assignment.

(b) Anhydrous MnO_2. The baseline corrected spectra collected at 600 meV and 250 meV are shown in Figures 3 and 4. The spectra are essentially featureless in terms of hydrogen interactions, which confirmed that the water had been entirely removed from the α-MnO_2 structure on heat treatment.

(c) MnO_6-MnO_6 lattice vibrations. Figure 5 is a spectrum calculated from the scattering data. A peak due to the phonon is observed at about 68 meV (548 cm^{-1}) (see Table 1).

A full interpretation of the spectra will be reported together with the structural data that is being obtained from the neutron diffraction experiments (SEPD).

Table 1. Inelastic Neutron Scattering Data from Hydrated α-MnO_2.

Peak Number	Energy		Relative Intensity	Assignment
	meV	cm^{-1}		
1	68	548	NA	lattice vibration
2	75.00	605	medium, broad	Mn-O stretch
3	117	944	weak	?
4.00	140	1129	medium, narrow	HOH bend (op)
5.00	200.00	1613	strong, narrow	HOH bend (ip)
6	420.00	3387	strong, broad	-OH group stretch
7	490	3952	medium, broad	combination mode

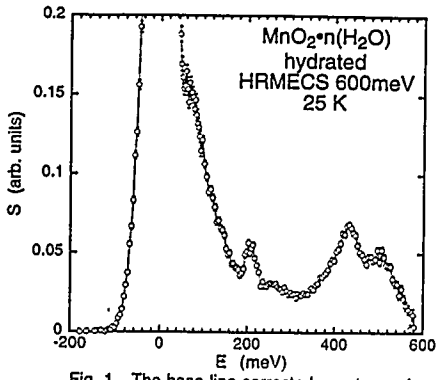


Fig. 1. The base-line corrected spectrum of α-MnO2·0.25H_2O at 600 meV.

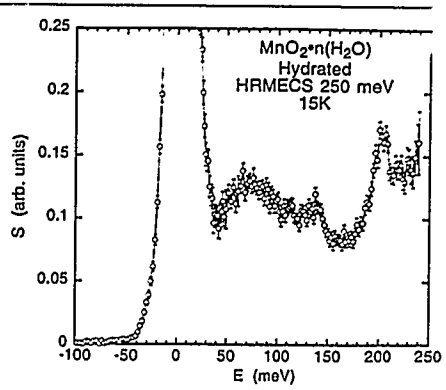


Fig. 2. The base-line corrected spectrum of α-MnO_2·0.25H_2O at 250 meV.

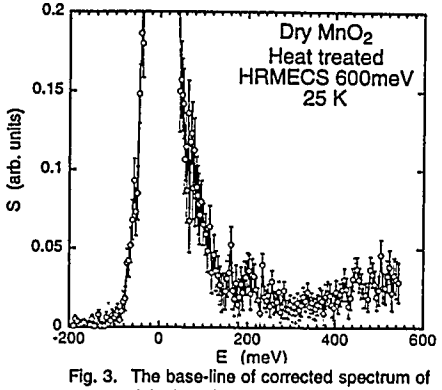


Fig. 3. The base-line of corrected spectrum of dehydrated α-MnO_2 at 600 meV.

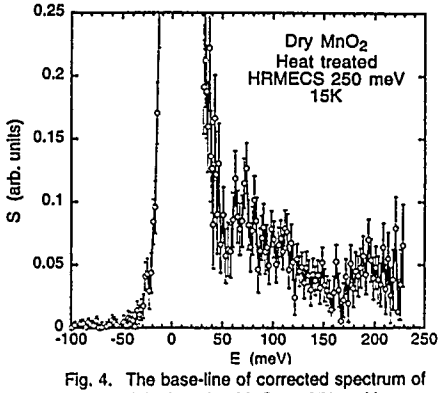


Fig. 4. The base-line of corrected spectrum of dehydrated α-MnO_2 at 250 meV.

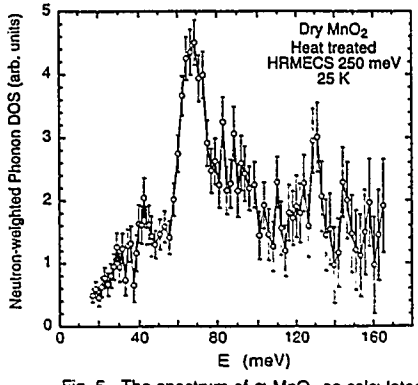


Fig. 5. The spectrum of α-MnO_2 as calculated from neutron scattering data.

INSTRUMENT USED:	DATE OF REPORT:	EXPERIMENT NO:
HRMECS	August 10, 1994	1904

TITLE: Correlation between spectroscopic and crystallographic measurements in alunite-jarosite minerals: inelastic neutron scattering studies

AUTHORS AND AFFILIATIONS:
G.A. Lager, University of Louisville; G.A. Swayze, U.S. Geological Survey; F J. Rotella, ANL/IPNS; C.-K. Loong, ANL/IPNS

DATES OF EXPERIMENT:
May 20-23, 1994

CHECK ALL APPLICABLE BOXES:

- [ ] APPROVED BY PROGRAM COMMITTEE
- [X] INSTRUMENT SCIENTIST ALLOCATION
- [ ] DO NOT PUBLISH
- [ ] PROPRIETARY RESEARCH
- [ ] PRT ALLOCATION

EXPERIMENTAL REPORT (or Abstract of Publication)

Paper to be presented at the Annual Meeting of the Geological Society of America, Seattle, Washington, October 1994.

NEUTRON-SCATTERING STUDIES OF SYNTHETIC OXONIUM ALUNITE.

LAGER, G.A., Department of Geography and Geosciences, University of Louisville, Louisville, KY 40292; SWAYZE, G.A., U.S. Geological Survey, P.O. Box 25046, Denver, CO 80225; RICHARDSON, J.W., Jr., ROTELLA, F.J., LOONG, C.-K., IPNS Division, Argonne National Laboratory, Argonne, IL 60439.

A synthetic, polycrystalline sample of end-member oxonium alunite [$H_3OAl_3(SO_4)_2(OH)_6$] has been investigated using elastic and incoherent, inelastic neutron-scattering (IINS) methods. The objectives of these experiments were to confirm the presence of the oxonium ion, and to correlate crystallographic and spectroscopic measurements for remote-sensing applications in the near-infrared region. Elastic scattering data were collected at 295 and 15 K for a deuterated analogue on the GPPD diffractometer, and analyzed using the Rietveld method. At both temperatures, neutron density equivalent to one oxygen atom per formula unit was observed at the 12-coordinated, monovalent cation site [0,0,0]. A trigonal arrangement of associated D atoms, consistent with the geometry of the D_3O^+ ion, could not be located near the [0,0,0] position in difference-Fourier projections, suggesting orientational disorder of the D_3O^+ ion. IINS measurements were made on a non-deuterated oxonium alunite at 15 K using the HRMECS chopper spectrometer with 50 and 600 meV incident energies. Because of the large incoherent scattering cross-section of hydrogen, the spectra are dominated by molecular vibrations and rotations involving hydrogen atoms. However, the fundamental vibrations of H_3O^+ could not be identified with certainty because of overlap with H_2O and Al-O-H bands. A detailed spectral analysis will be made upon completion of IINS measurements on low-temperature (423 K) K-alunite, and partially dehydrated oxonium alunite (1 h @ 523 K). Work performed at Argonne National Laboratory is supported by the U.S. DOE-BES under contract No. W-31-109-ENG-38.

EXPERIMENTAL REPORT (CONTD.)

INSTRUMENT USED:	DATE OF REPORT:	EXPERIMENT NO:
HRMECS	Aug. 15 1994	1841

TITLE: Crystal-field Spectroscopy of Hard Magnets RFe_4Al_8 (R=Tb and Dy)

AUTHORS AND AFFILIATIONS: M. Loewenhaupt (IFF/KFA-Jülich) and C.-K. Loong (ANL)

DATES OF EXPERIMENT: 5/10-5/18/94

CHECK ALL APPLICABLE BOXES:

- [X] APPROVED BY PROGRAM COMMITTEE
- [ ] INSTRUMENT SCIENTIST ALLOCATION
- [ ] DO NOT PUBLISH
- [ ] PROPRIETARY RESEARCH
- [ ] PRT ALLOCATION

EXPERIMENTAL REPORT (or Abstract of Publication)

CRYSTAL FIELD AND EXCHANGE INTERACTIONS IN DyT4Al8

(T = Fe, Mn)§, M. Loewenhaupt*, C.-K. Loong**, P. Tils*, and W. Hahn*, * Institut für Festkörperforschung, D-52425 Jülich, Germany; **Argonne National Laboratory, Argonne, Illinois 60439, U. S. A.

We investigated the magnetic excitations in polycrystalline samples of a hard magnet $DyFe_4Al_8$ and a related compound $DyMn_4Al_8$ by neutron spectroscopy using the HRMECS chopper spectrometer of Argonne's spallation neutron source IPNS. For both compounds the magnetic spectra are dominated by the response of the Dy^{3+} ions. For $DyMn_4Al_8$ we observed pure crystal-field transitions within the Dy^{3+} J=15/2 ground multiplet which is split into 8 doublets under low point-group symmetry. For $DyFe_4Al_8$ we have to include an additional exchange interaction to account for the ferromagnetically[1] ordered Fe sublattice. We will discuss our results in the light of other measurements on RT_4Al_8 compounds, with special emphasis on the neutron data by Moze et al.[2] Work performed at Argonne National Laboratory is supported by the U. S. DOE-BES under the contract No. W-31-109-ENG-38.

1 The actual ordering is a long (60Å) spiral, see W. Schäfer *et al. Mat. Sci. Forum* **27-28** (1988) 243.

2 O. Moze *et al. Sol. State Comm.* **76** (1990) 331; and *ibid*, **72** (1989) 249.

§ to be presented in the Materials Research Society Fall Meeting, Boston 1994

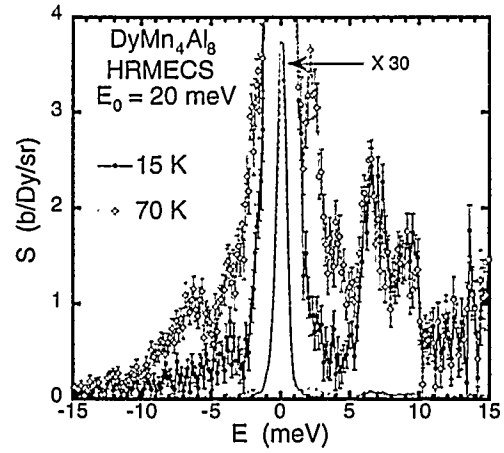


Figure 1. The magnetic spectrum of $DyMn_4Al_8$ showing well-defined crystal-field transitions within the Dy^{3+} J=15/2 ground multiplet.

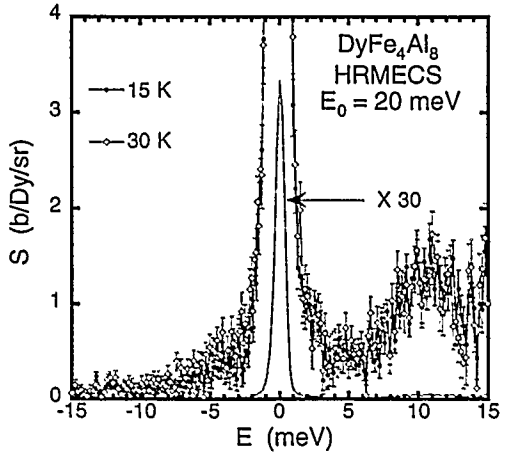


Figure 2. The magnetic spectrum of $DyFe_4Al_8$ showing the effects of the Fe molecular fields on the crystal-field transitions of the Dy^{3+} ions. In these hard magnets the large ferromagnetic moments originate from the d-electrons of the Fe ions but interplay of f- and d-magnetism is important for achieving the desirable properties.

INSTRUMENT USED: HRMECS	DATE OF REPORT: July 30, 1992	EXPERIMENT NO:

TITLE: Crystal-field excitations and magnetic properties of $TmPO_4$

AUTHORS AND AFFILIATIONS: C.-K. Loong, and L. Soderholm (ANL), M. M. Abraham and L. A. Boatner (Oak Ridge National Lab.), and N. Edelstein (Lawrence Berkeley Lab.)

DATES OF EXPERIMENT: 4/14-4/22/1992

CHECK ALL APPLICABLE BOXES:

- [ ] APPROVED BY PROGRAM COMMITTEE
- [X] INSTRUMENT SCIENTIST ALLOCATION
- [ ] DO NOT PUBLISH
- [ ] PROPRIETARY RESEARCH
- [ ] PRT ALLOCATION

EXPERIMENTAL REPORT (or Abstract of Publication)
The manuscript has been prepared, to be submitted to J. Chem. Phys.

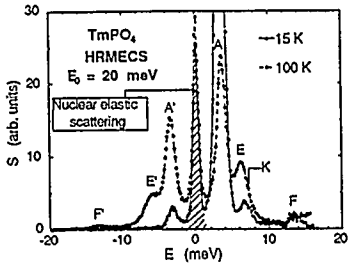
Crystal field excitations and magnetic properties of $TmPO_4$

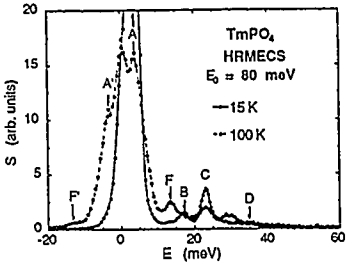
C.-K. Loong and L. Soderholm (ANL), M. M. Abraham and L. A. Boatner (Oak Ridge National Lab.), and N. M. Edelstein (Lawrence Berkeley Lab.)

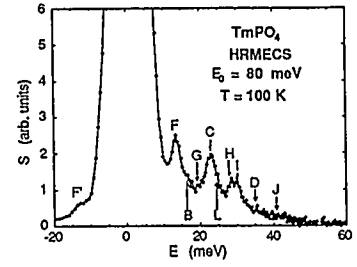
Abstract

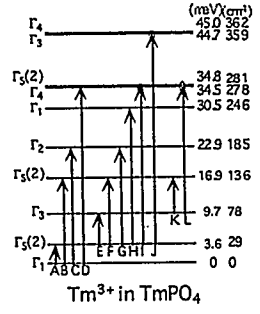
The magnetic-excitation spectrum of $TmPO_4$ has been studied using neutron scattering techniques. Sharp crystal-field transitions were observed at 15 and 100 K, yielding new information regarding the energy-level structure of the Tm^{3+} ground-multiplet splitting. The data were analyzed using a Hamiltonian that included the atomic free-ion and crystal-field interactions for an f^{12} configuration. By using the Tm free-ion parameters derived from optical spectroscopy of Tm^{3+} diluted in a $LuPO_4$ host, a set of crystal-field parameters were obtained for Tm^{3+} in pure $TmPO_4$. The calculated magnetic spectra of $TmPO_4$ agree very well with results of neutron and Raman measurements. The calculated bulk magnetic susceptibility of $TmPO_4$ exhibits a large anisotropy in the directions both parallel and perpendicular to the crystallographic c axis at low temperatures. A significant contribution to the specific heat from the Tm^{3+} crystal field states was found at temperatures below 100 K.

A. Observed crystal-field excitations within the Tm^{3+}: $^3H_6$ ground multiplet:

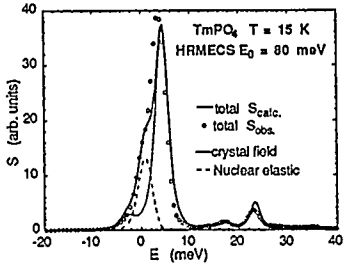


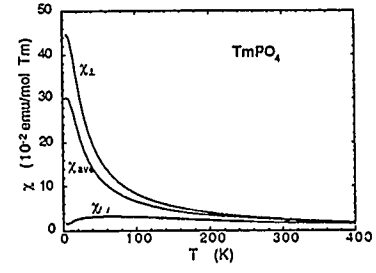






B. Left panel: calculated total scattering (CF & nuclear elastic) compared with data; Right panel: calculated magnetic susceptibility.





INSTRUMENT USED:	DATE OF REPORT:	EXPERIMENT NO:
HRMECS	July 30, 1992	1588

TITLE: f-electron states in $ErPO_4$: a joint study of neutron and Raman spectroscopy

AUTHORS AND AFFILIATIONS: C.-K. Loong, L. Soderholm and J. P. Hammonds (ANL), M. M. Abraham and L. A. Boatner (Oak Ridge National Lab.), and N. Edelstein (Lawrence Berkeley Lab.)

DATES OF EXPERIMENT: 3/5-3/14/1992

CHECK ALL APPLICABLE BOXES:

- [X] APPROVED BY PROGRAM COMMITTEE
- [ ] INSTRUMENT SCIENTIST ALLOCATION
- [ ] DO NOT PUBLISH
- [ ] PROPRIETARY RESEARCH
- [ ] PRT ALLOCATION

EXPERIMENTAL REPORT (or Abstract of Publication)

Manuscript submitted to the 37th MMM Conference, to be published in J. Appl. Phys. (April 1993)

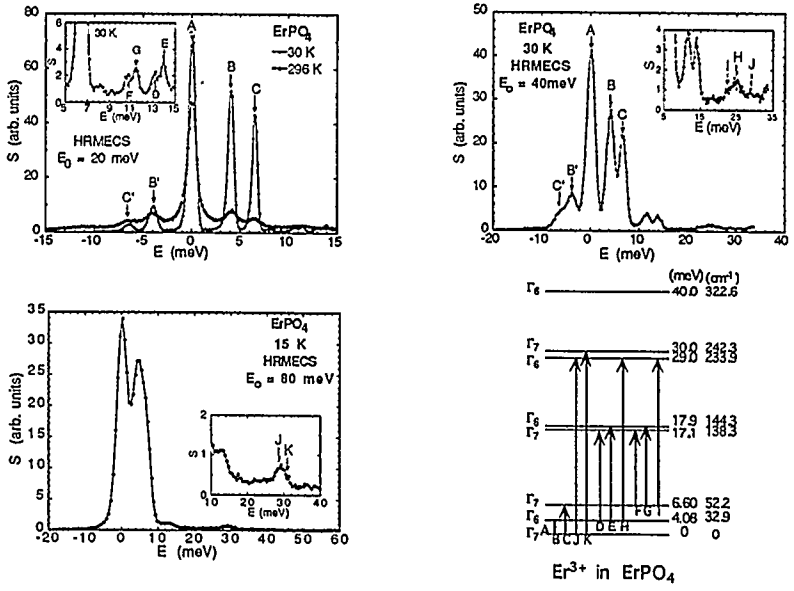
NEUTRON SCATTERING STUDY OF CRYSTAL-FIELD TRANSITIONS IN $ErPO_4$

C.-K. Loong, L. Soderholm, and J. P. Hammonds, Argonne National Laboratory, Argonne, IL 60439, M. M. Abraham and L. A. Boatner, Oak Ridge National Laboratory, Oak Ridge, TN 37831, N. M. Edelstein, Lawrence Berkeley Laboratory, Berkeley, CA 94720.

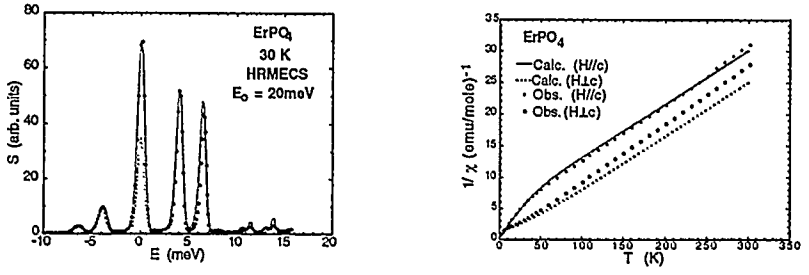
The crystal-field splitting of the Er^{3+} ground multiplet, $^4I_{15/2}$, in $ErPO_4$ is investigated by inelastic neutron scattering. Six excitations from the Γ_7 ground state to the excited states, and several transitions between the excited states have been identified. The observed transition energies and intensities are used to refine the parameters of the crystal-field potential under the scheme of intermediate coupling. The calculated magnetic susceptibility, $\chi(T)$, agrees well with experimental values from single-crystal measurements. A comparison of neutron data with optical absorption, nonresonance and resonance Raman scattering measurements has been made.

Work performed at Argonne, Oak Ridge and Lawrence Berkeley Laboratories is supported by the U. S. DOE, Basic Energy Sciences, Chemical Sciences and Materials Sciences Divisions under Contract Nos. W-31-109-ENG-38 (ANL), DE-AC05-84OR21400 (ORNL), and DE-AC03-76SF00098 (LBL), respectively.

A. Observed crystal-field excitations within the Er^{3+}: $^4I_{15/2}$ ground multiplet:



B. Left panel: calculated total (CF & nuclear elastic scattering, solid curve) and nuclear elastic (dotted curve) scattering compared with data (circles); Right panel: magnetic susceptibility.



INSTRUMENT USED:	DATE OF REPORT:	EXPERIMENT NO:
HRMECS	Feb 21, 1996	1850

TITLE:
Local and cooperative Jahn-Teller effects in RMO_4 (R=Tb, Dy, Ho, Tm and M=P,V)

AUTHORS AND AFFILIATIONS:
C.-K. Loong and L. Soderholm (ANL)
M. M. Abraham and L. A. Boatner (Oak Ridge National Lab)

DATES OF EXPERIMENT:
Sept 19-25, 1993

CHECK ALL APPLICABLE BOXES:

- [X] APPROVED BY PROGRAM COMMITTEE
- [ ] INSTRUMENT SCIENTIST ALLOCATION
- [ ] DO NOT PUBLISH
- [ ] PROPRIETARY RESEARCH
- [ ] PRT ALLOCATION

EXPERIMENTAL REPORT (or Abstract of Publication)

Rare Earth Crystal Field Spectroscopy by Neutron Magnetic Scattering: from Xenotime to High-T_c Superconductors

C.-K. Loong and L. Soderholm

Argonne National Laboratory, Argonne, IL 60439-4814

Abstract

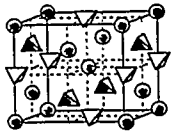
Optical spectroscopy is one of the traditional methods used to determine the overall splitting of the rare-earth ion energy states within an f^N configuration in either solution or solid state of transparent materials. This technique can provide data over a wide energy range with good resolution, and the obtained parameters for the empirical Hamiltonian reflect the "best fit" of the observed energies. Absolute-intensity measurements of optical transitions and their comparison with theory, however, are difficult. Magnetic scattering of thermal neutrons arises from an interaction of the neutron magnetic moment with the convection and spin current of the scatterer. Such a weak interaction does not involve any excited intermediate states of the system and requires only a first-order perturbation treatment to calculate the scattering cross section. However, neutron spectroscopy probes only states at energies less than ~1 eV.

(J. Alloys Compounds, **207/208** (1994) 153-160)

EXPERIMENTAL REPORT (CONTD.)

Xenotime
RPO_4 (R=Tb-Lu, Y & Sc)

Crystal Structure:
tetragonal zircon
($I4_1/amd$)



R-ion site point-group symmetry:
D_{2d}



R P O

RPO_4: R	Tb	Dy	Ho	Er	Tm	Yb
T_N (K)	2.2	3.4	1.35	<0.4		
Ground state (major J,J_M)	$6,\pm5$	$\frac{15}{2},\pm\frac{15}{2}$	$8,\pm7$	$\frac{15}{2},\pm\frac{7}{2}$	$6,0$	$\frac{7}{2},\pm\frac{3}{2}$
$g_{//}$	12.7	19.4	17 2	6.6	0	1.6
$g_\perp$	0	~0	0	4.3	0	3.2
Estimated exchange field (kG)	5.2	3	2.4			

Fig. 1. Upper diagram: the unit cell of xenotime, which contains four formula units of RPO_4. Lower portion: the Néel temperatures, J_M of the major components $|J,J_M\rangle$ in the ground state wavefunctions, spectroscopic splitting g-factors of the ground states ($\|$ and $\perp$ denote the magnetic field directions parallel and perpendicular to the c-axis, respectively), and the exchange field strength estimated from a molecular-field approximation.

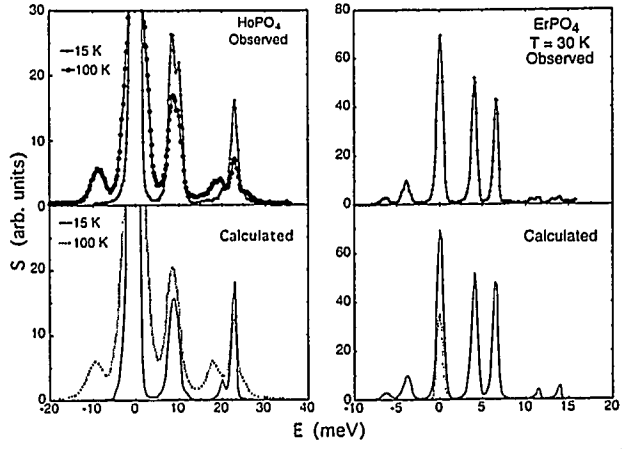


Fig. 3. The observed (upper panels) and calculated (lower panels) neutron scattering functions for $HoPO_4$ and $ErPO_4$. The lines in the observed spectra are guides to the eye. The solid line in the calculated spectrum of $ErPO_4$ represents the sum of magnetic- and nuclear elastic (dashed line) scattering.

INSTRUMENT USED:	DATE OF REPORT:	EXPERIMENT NO:
HRMECS	Aug. 11 1994	1903

TITLE: Hydrogen vibrational DOS of water physisorbed on rare-earth modified ZrO_2 fine powders

AUTHORS AND AFFILIATIONS: C.-K. Loong, and L. E. Iton (ANL), Masakuni Ozawa (Nagoya Institute of Technology, Japan)

DATES OF EXPERIMENT: 5/17-5/24/1994

CHECK ALL APPLICABLE BOXES:

- [X] APPROVED BY PROGRAM COMMITTEE
- [ ] INSTRUMENT SCIENTIST ALLOCATION
- [ ] DO NOT PUBLISH
- [ ] PROPRIETARY RESEARCH
- [ ] PRT ALLOCATION

EXPERIMENTAL REPORT (or Abstract of Publication)

The manuscript has been prepared, to be submitted to J. Chem. Phys.

Hydrogen Vibrational Density of States of Adsorbed Water on Rare-earth Modified Zirconia*

C.-K. Loong[a], L. E. Iton[a], and Masakuni Ozawa[b]

[a]Argonne National Laboratory, Argonne, Illinois 60439, U. S. A.

[b]Nagoya Institute of Technology, Tajimi, Gifu, 507, Japan.

Rare-earth (RE) doped ZrO_2 prepared by a method of coprecipitation from aqueous solution shows many properties such as good thermal stability and large surface area (~80 m^2/g) that are suitable for use as catalyst supports and sorbents for a variety of molecules. We have measured the vibrational densities of states of surface hydroxyl groups as well as physisorbed water molecules in $La_{0.1}Zr_{0.9}O_{1.95}$ and $Nd_{0.1}Zr_{0.9}O_{1.95}$ by inelastic neutron scattering. The spectrum of dry RE-ZrO_2 exhibits a peak at about 455 meV characteristic of the O-H stretch vibrations of surface hydroxyl groups. At a submonolayer coverage of H_2O this peak broadens and shifts to a slightly lower energy. At higher coverage three bands, corresponding to the O-H stretch (~430 meV), H-O-H bend (~200 meV) and librational motion (~80 meV), were observed. The decreasing energy and larger width of the O-H stretch band with increasing H_2O coverage indicate the influence of hydrogen bonding on the motion of water molecules.

*To be presented at The International Conference on Neutron Scattering, Sendai, Japan 11-14 October 1994. Proceedings to be published in Physica B.

P2 B-50, C.-K. Loong et al. Hydrogen vibrational .... Figure 1.

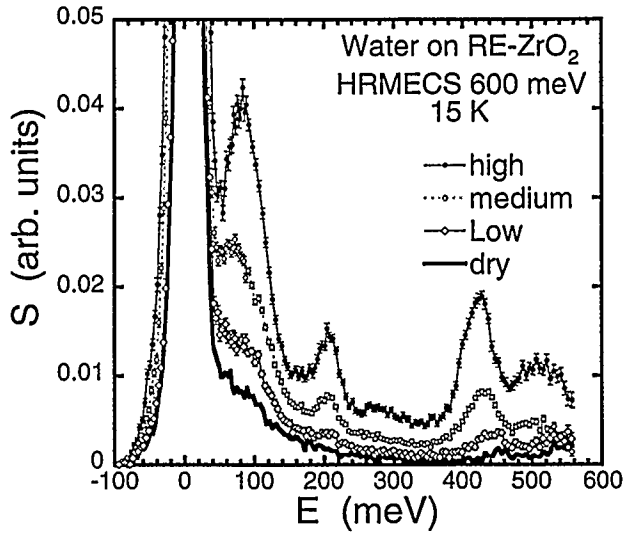


Figure 1. The observed scattering functions of water adsorbed on RE-ZrO_2 for the dry, low-, medium-, and high-water content powders.

INSTRUMENT USED: HRCS	DATE OF REPORT: AUG15, 1994	EXPERIMENT NO: 1850

TITLE: **Crystal-Field excitations and Magnetic properties of Ho3+ on $HoVO_4$**

AUTHORS AND AFFILIATIONS:
S. Skanthakumar, C.-K. Loong, and L. Soderholm, (ANL),
M. M. Abraham and L. A. Boatner (Oak Ridge National Lab.)

DATES OF EXPERIMENT: **9/17/93 - 9/26/93**

CHECK ALL APPLICABLE BOXES:

- [X] APPROVED BY PROGRAM COMMITTEE
- [ ] INSTRUMENT SCIENTIST ALLOCATION
- [ ] DO NOT PUBLISH
- [ ] PROPRIETARY RESEARCH
- [ ] PRT ALLOCATION

EXPERIMENTAL REPORT (or Abstract of Publication)
Abstract of the paper submitted to the Physical Review B for publication

Crystal-Field Excitations and Magnetic Properties of Ho^{3+} in $HoVO_4$

Abstract

The magnetic excitations in $HoVO_4$ were studied by neutron scattering and susceptibility techniques. Well-defined transitions between the crystal-field-split states of the Ho^{3+} ions were observed at 15, 40, and 100 K. The magnetic spectra were analyzed using a single-ion crystal-field model which includes intermediate coupling of the LS states of Ho. A quantitative comparison of the observed energies and intensities with the model was made and used to refine the five crystal-field parameters needed to calculate the Ho ionic wavefunctions and other magnetic properties. The nonmagnetic, Γ_1-singlet ground state (containing about 90% pure $|8,0\rangle$ component) of the Ho ions, in conjunction with the next higher doublet state situated at 2.5 meV, strongly influence the low-temperature magnetic behavior. The calculated magnetic susceptibility, which exhibits an "easy plane" coinciding with the crystallographic a-b plane at low temperatures, agrees very well with the experimental data obtained from single-crystal measurements. The magnetic properties of $HoVO_4$ are contrasted with those of an isostructural compound $HoPO_4$ which has a 98% pure $|8,7\rangle$-doublet ground state. The difference in the crystal-field-level structure between these two compounds is reflected in a sign change of the B_0^2 crystal-field parameter. In spite of the overall tetragonal crystal structure of $HoVO_4$, which predicts double degeneracy for each Γ_5 state, a small splitting in the first-excited doublet was clearly observed at low temperatures.

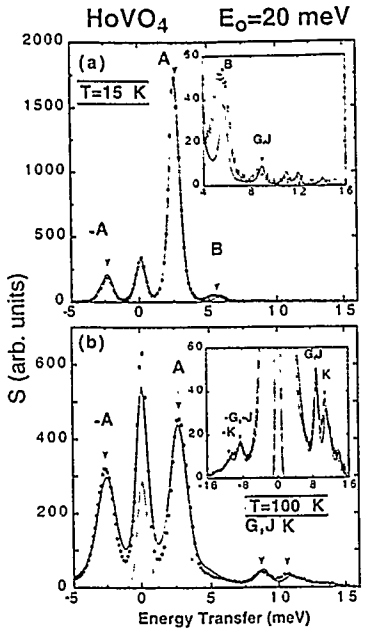


Fig. 1. The observed (solid circles) and calculated (solid curve) scattering functions for an incident energy of 20 meV at (a) 15 K and at (b) 100 K. The labels of the peaks correspond to the crystal-field transitions as shown in Fig. 2. The broken line indicates the nuclear contribution to the elastic peak.

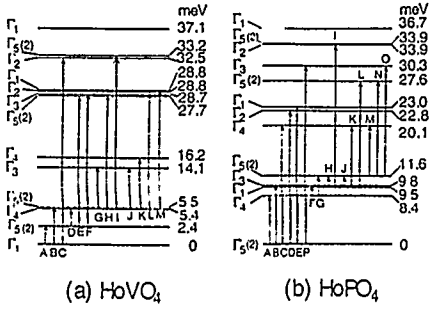


Fig. 2. The schematic diagram of the crystal-field splitting of the Ho^{3+} ground multiplet ($^5I_8$) in (a) $HoVO_4$ and (b) $HoPO_4$. The experimentally observed transitions are labeled by the letters.

S. Skanthakumar
Aug 18, 94

INSTRUMENT USED:	DATE OF REPORT:	EXPERIMENT NO.:
HRMECS	31 July 92	1596

TITLE:

The Determination of Crystal Field Levels of Ho in $Pb_2Sr_2HoCu_3O_8$

AUTHORS AND AFFILIATIONS:

L. Soderholm, C.-K. Loong (ANL), Simon Xue, John Greedan and Milan Maric (McMaster Univ.)

DATES OF EXPERIMENT: 30 July 91 - 9 Aug 91

☒ APPROVED BY PROGRAM COMMITTEE, OR

☐ PART OF INSTRUMENT SCIENTIST ALLOCATION

REPORT RECEIVED:

EXPERIMENTAL REPORT (or Abstract of Publication)

EXPERIMENTAL REPORT (CONTD.)

The experiments on $Pb_2Sr_2HoCu_3C_3$ were performed as part of an ongoing program devoted to the electronic properties of f-elements in superconductor-related materials. In particular, we are interested in the lighter-lanthanide and actinide substituted members of superconducting series which do not superconduct. We believe that magnetic interactions between the f-electrons and the CuO conduction electrons are sufficient to inhibit superconductivity [1]. Since this interaction is magnetic, there must be unpaired spin density on the rare earth site. The magnitude of the magnetic moment of the ground state can be very sensitive to the crystal field environment [2], and therefore a quantitative knowledge is necessary of the crystal field splittings for the Russell Saunders ground multiplets. For the most part, these materials are good conductors, and therefore opaque to UV-visible radiation, making inelastic neutron scattering the technique of choice when determining the energy level splittings. The experiments described here on $Pb_2Sr_2HoCu_3O_8$ represent our first attempts to characterize the crystal field environment at the rare earth site within the series $Pb_2Sr_2RCu_3O_8$.

The experiments were run during the time that IPNS operated at a reduced current of 5μA. Despite the reduced current, we were easily able to obtain good data at 15 K with incident neutron energies of 80, 20, and 8 meV. There were peaks observed at 0, 0.4, 1.37, 1.7, 4.8, 8, 12, 12.5, 58, and 60 meV, and from their Q-dependence we assign them all to crystal field transitions.

The site symmetry of the rare earth is mmm, therefore 9 B^n_m crystal field parameters are necessary to model the environment. The small data/parameter ratio can be partially overcome by using superposition modeling to determine a set of starting parameters [3]. From this modeling, we determined that, like the previously investigated $RBa_2Cu_3O_7$ series, the site symmetry at Ho is very nearly cubic. Unfortunately, because or the ratio of 4th to 6th order crystal field parameters, there are 5 nearly degenerate states expected at low energy (3 originating from the Γ_4 and 2 from the Γ_3 in cubic notation). Since these data were collected at 15 K, we expect that all 5 energy states will have appreciable occupation, and therefore the observed transitions could occur between either the ground and excited states higher states or between excited states. Slight changes in any of the crystal field parameters cause large changes in the transition intensities calculated for various transitions, therefore we are not able, at this time, to assign an energy level scheme that we can confidently use as a basis to refine our crystal field. More work is necessary before this project can be completed.

This work is supported by DOE-BES under contract W-31-109-ENG-38.

REFERENCES

[1] C.-K. Loong and L. Soderholm in High Temperature Superconductors, Eds: S.K. Malik and S.S. Shah, Nova Science Publishers, N.Y. (in press).
[2] L. Soderholm, C.-K. Loong, G.L. Goodman, and B.D. Dabrowski, Phys. Rev. B41 (1991) 7923.
[3] see for example L. Soderholm, C.-K. Loong and S. Kern, Phys. Rev. B45 (1992) 10062.

INSTRUMENT USED:	DATE OF REPORT:	EXPERIMENT NO:
HRMECS	Dec. 2, 1995	1903

TITLE:
Hydrogen vibrational density-of-states of water physisorbed on rare-earth modified ZrO_2 fine powders

AUTHORS AND AFFILIATIONS:
M. and S. Suzuki (Nagoya Institute of Technology)
C.-K. Loong and L. E. Iton (ANL)

DATES OF EXPERIMENT:
April 15-24, 1994

CHECK ALL APPLICABLE BOXES:

- [X] APPROVED BY PROGRAM COMMITTEE
- [ ] INSTRUMENT SCIENTIST ALLOCATION
- [ ] DO NOT PUBLISH
- [ ] PROPRIETARY RESEARCH
- [ ] PRT ALLOCATION

EXPERIMENTAL REPORT (or Abstract of Publication)

Rare-earth (RE) doped ZrO_2 prepared by a method of coprecipitation from aqueous solution shows many properties such as good thermal stability and large surface area (~80 m^2/g) that are suitable for use as catalyst supports and sorbents for a variety of molecules. We have measured the vibrational densities of states of surface hydroxyl groups as well as physisorbed water molecules in $La_{0.1}Zr_{0.9}O_{1.95}$ and $Nd_{0.1}Zr_{0.9}O_{1.95}$ by inelastic neutron scattering. The spectrum of dry RE-ZrO_2 exhibits a peak at about 455 meV characteristic of the O-H stretch vibrations of surface hydroxyl groups. At a submonolayer coverage of H_2O this peak broadens and shifts to a slightly lower energy. At higher coverage three bands, corresponding to the O-H stretch (~430 meV), H-O-H bend (~200 meV) and librational motion (~80 meV), were observed. The decreasing energy and larger width of the O-H stretch band with increasing H_2O coverage indicate the influence of hydrogen bonding on the motion of water molecules.

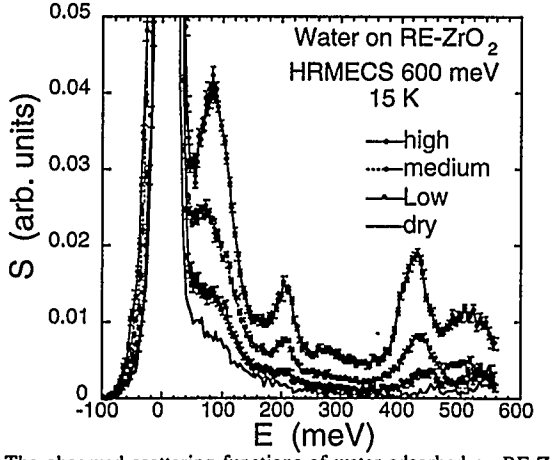


Figure 1. The observed scattering functions of water adsorbed on RE-ZrO_2 for the dry, low-, medium-, and high-water content powders.

EXPERIMENTAL REPORT (CONTD.)

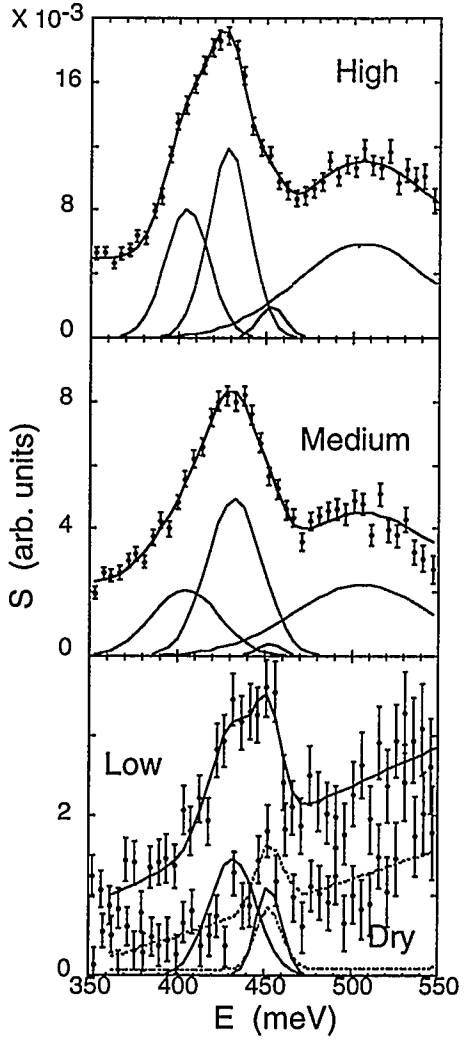


Figure 2. The O-H stretch vibration band and the combination band fitted to a sum of multiple Gaussian functions and a background for the dry (dashed curves) and low-water content (solid curves) samples, medium-water content sample, and high-water content sample.

INSTRUMENT USED:	DATE OF REPORT:	EXPERIMENT NO:
HRMECS	Jan 15. 1996	2067

TITLE:
Atomic Dynamics of Si-Al-O-N ceramic alloys

AUTHORS AND AFFILIATIONS:
S. Suzuki and M. Ozawa (Nagoya Institute of Technology)
J. W. Richardson, Jr. and C.-K. Loong (ANL)

DATES OF EXPERIMENT:
April 4-9, 1995

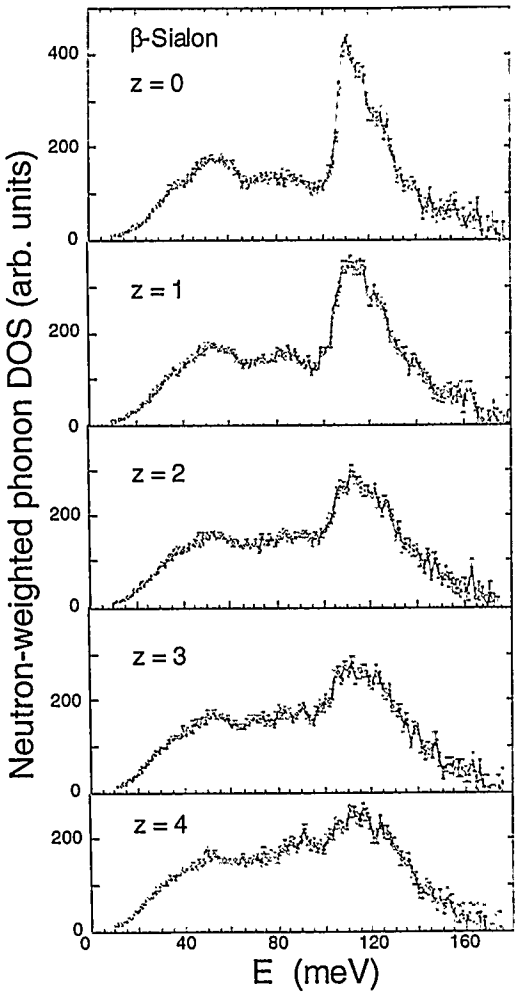
CHECK ALL APPLICABLE BOXES:

- [X] APPROVED BY PROGRAM COMMITTEE
- [ ] INSTRUMENT SCIENTIST ALLOCATION
- [ ] DO NOT PUBLISH
- [ ] PROPRIETARY RESEARCH
- [ ] PRT ALLOCATION

EXPERIMENTAL REPORT (or Abstract of Publication)

The crystal structure and phonon densities of states (DOS) of β′-sialon ceramics, $Si_{6-z}Al_zO_zN_{8-z}$ ($0 \le z \le 4$), prepared by a novel slip-cast method were studied by neutron-scattering techniques. The samples of $z < 4$ form a single-phase solid solution of Si-Al-O-N isostructural to β-Si_3N_4 (space group $P6_3/m$). Within this structure there is a consistent preferential occupation of the 2c sites by O and the 6h sites by N. The phonon DOS of β′-sialon displays phonon bands at about 50 and 115 meV. These features are considerably broader than the corresponding ones in β -Si_3N_4 powder.

EXPERIMENTAL REPORT (CONTD.)



INSTRUMENT USED:	DATE OF REPORT:	EXPERIMENT NO:
HRMECS	Jan 15. 1996	1981

TITLE:
Structural properties of amorphous hydrogenated SiC prepared by the polymer route

AUTHORS AND AFFILIATIONS:
K. Suzuya (MSD-IPNS)
C.-K. Loong (IPNS-ANL)

DATES OF EXPERIMENT:
Feb 1-7, 1995

CHECK ALL APPLICABLE BOXES:

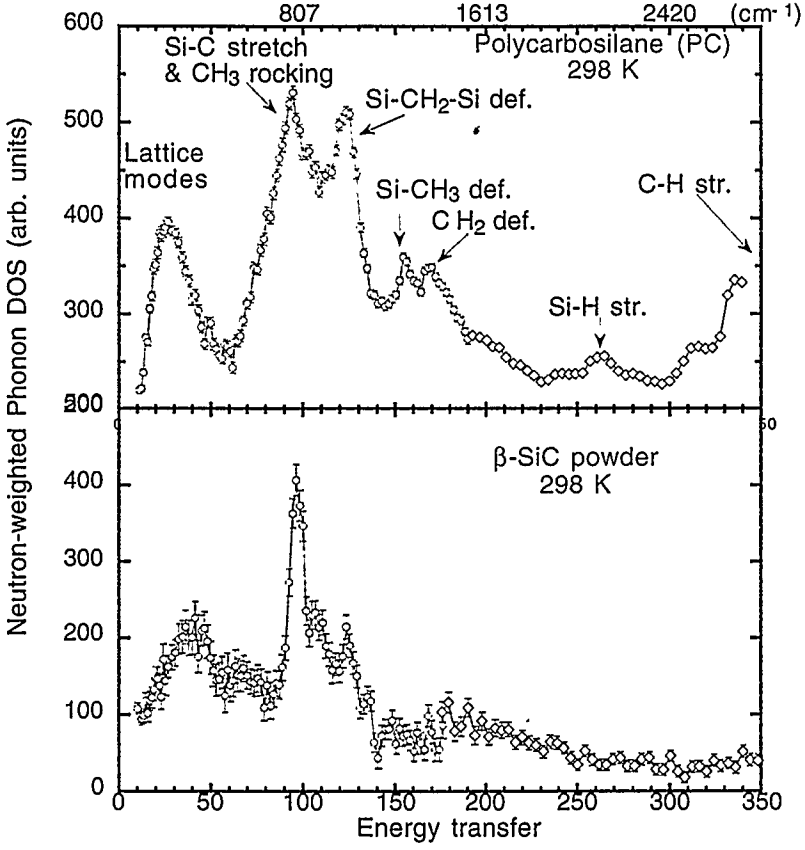
- [X] APPROVED BY PROGRAM COMMITTEE
- [ ] INSTRUMENT SCIENTIST ALLOCATION
- [ ] DO NOT PUBLISH
- [ ] PROPRIETARY RESEARCH
- [ ] PRT ALLOCATION

EXPERIMENTAL REPORT (or Abstract of Publication)

The preparation of flexible SiC fibers with a tensile strength of 62 X 108 Nm-2 through the conversion of polycarbosilane (PC) to b-SiC by novel heat treatments was developed by a research group at Tohoku University (Yajima et al. 1976). It is thought that dehydrogenation first occurs during the pyrolysis process (T < 1110 K), forming a carbon-rich, amorphous silicon carbide phase which consists of strong Si-C-Si bonds. Formation of b-SiC like microcrystals follows in subsequent heating. At higher temperatures (T > 1570 K), losing the excess carbon leads to rapid increase of SiC crystallite size and reduction of tensile strength. Therefore, an understanding of the structural evolution from polymeric precursor to ceramic is of fundamental importance to the development of useful ceramic products.

EXPERIMENTAL REPORT (CONTD.)

Dynamic Response of Polycarbosilane and SiC



The neutron spectra of polycarbosilane. the polymeric precursor of pyrolytic SiC fiber (top) and \fb\n-SiC powder (bottom).

INSTRUMENT USED:	DATE OF REPORT:	EXPERIMENT NO:
HRMECS	Jan 31, 1996	1984

TITLE:
Atomic dynamics of alumimum nitride

AUTHORS AND AFFILIATIONS:
P. Vashishta, R. Kalia (Louisiana State University)
C.-K. Loong (IPNS-ANL)

DATES OF EXPERIMENT:
Dec 15-20, 1994

CHECK ALL APPLICABLE BOXES:

- [X] APPROVED BY PROGRAM COMMITTEE
- [ ] INSTRUMENT SCIENTIST ALLOCATION
- [ ] DO NOT PUBLISH
- [ ] PROPRIETARY RESEARCH
- [ ] PRT ALLOCATION

EXPERIMENTAL REPORT (or Abstract of Publication)

Phonons are thought to play a crucial role in the high thermal conductivity of AlN and ZrN. Using time-of-flight neutron spectroscopy, we have measured the phonon spectra of AlN and ZrN up to 300 meV (2400 cm^{-1}). The one-phonon density of states (DOS) of AlN exhibits relatively sharp bands at about 33, 63, 83 and 91 meV. In addition, distinct multiple-phonon excitations were observed at ~173 and 255 meV. The phonon DOS of ZrN displays similar features with the corresponding phonon energies shifted toward lower energies. The measured DOS of AlN is compared with results of molecular-dynamics simulations.

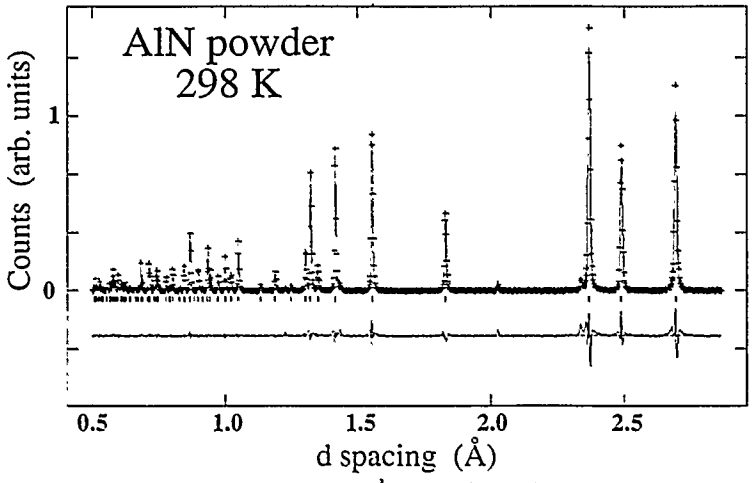


Figure 1. Rietveld profile fit in the 0.8-1.8 Å region of d-spacing for the AlN powder at room temperature. The symbols are the observed, background subtracted intensities. The solid line represents the calculated crystalline intensities. The tick marks indicate the positions of the Bragg reflections. The difference between the observed and calculated intensities is shown at the bottom of the figure.

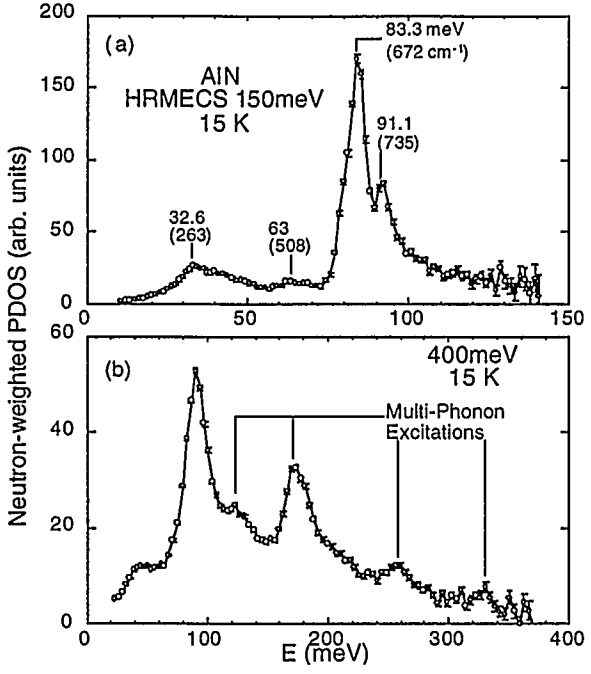


Figure 2. The observed neutron-weighted phonon DOS of AlN at 15 K, obtained from HRMECS runs with an incident energies of 150 meV (a), and 400 meV (b).

INSTRUMENT USED:	DATE OF REPORT:	EXPERIMENT NO.:
LRMECS	March 6th, 1991	1283

TITLE:

Coherent Scattering from Low Temperature, D_2O Hydrated Protein.

AUTHORS AND AFFILIATIONS:

K. Bradley (Brown University), S.-H. Chen (MIT), H. Crespi (ANL)

DATES OF EXPERIMENT: 1990

☒ APPROVED BY PROGRAM COMMITTEE, OR

☐ PART OF INSTRUMENT SCIENTIST ALLOCATION

REPORT RECEIVED:

This experiment, in conjunction with experiment number 1192, consisted of a series of measurements of the fully *in vivo* deuterated protein C-phycocyanin. Fully deuterated protein in large enough quantities to probe with neutron scattering is only available by growing the parent organism, in this case the microorganism cyanobacteria, in a completely deuterated growth medium. Typically about one-half of a protein's atoms are hydrogen, and so it is only through using a deuterated sample that coherent scattering can be measured without an intense incoherent background.

In this work, inelastic coherent scattering from C-phycocyanin has been measured in the energy range of -25 to 60 meV. Dry phycocyanin was measured at room temperature and hydrated (with D_2O) phycocyanin was measured at room temperature and 20 K. It has been known by biologists that completely dried protein becomes biologically inactive while the later addition of adsorbed water will reactivate the protein. They postulate that the lack of surface water destroys the protein's flexibility because internal shifting of different protein substructures is required in many biological processes. Support for this idea has been most recently expressed by Cusack, Doster and Petry [1], [2], who point to changes in the quasielastic scattering from myoglobin as evidence of a glass transition where internal motion in normal (hydrogenated) proteins with surface D_2O is frozen out at around 200 K. They also report that quasielastic scattering is vastly reduced by dehydration of the sample and speculate on the connection between temperature and hydration effects.

Analysis to date of our work on LRMECS shows two important points. The first of which, illustrated in figure 1, is that the average protein structure takes on different configurations based on both temperature and degree of adsorbed water. The low-q peak appears to correspond to residue–residue correlations in the protein while the peaks above 2 $Å^{-1}$ correspond to atomic bonds in the D_2O–protein system. The region of $S(q)$ associated with residue–residue correlations changes its character in distinctly different ways with both temperature and hydration levels while the local atomic correlations remain relatively unchanged. This point is being explored further through a series of experiments on a high resolution diffractometer at SACLAY. The second point is that the *change* in quasielastic scattering with both temperature and hydration depends on momentum transfer. That is, the change in diffusion associated with the 1.5 Å peak is quite different than the change in diffusion associated with the 6 Å peak as a function of both hydration and temperature. This is shown in figure 2. We believe that this difference is due to the fact that quasielastic scattering at 1.5 Å is associated with residue–residue motion, while quasielastic scattering at 3 and 6 Å is associated with local atom–atom motions. We are continuing to analyze the LRMECS data to understand how the full $S(q,\omega)$ scattering signal depends on the protein dynamics and are designing concurrent experiments to pursue these above points further.

[1] S. Cusack and W. Doster, *Biophys. J.* **58**, 243 (1990).

[2] W. Doster, S. Cusack and W. Petry, *Phys. Rev. Lett.* **65**, 1080 (1990).

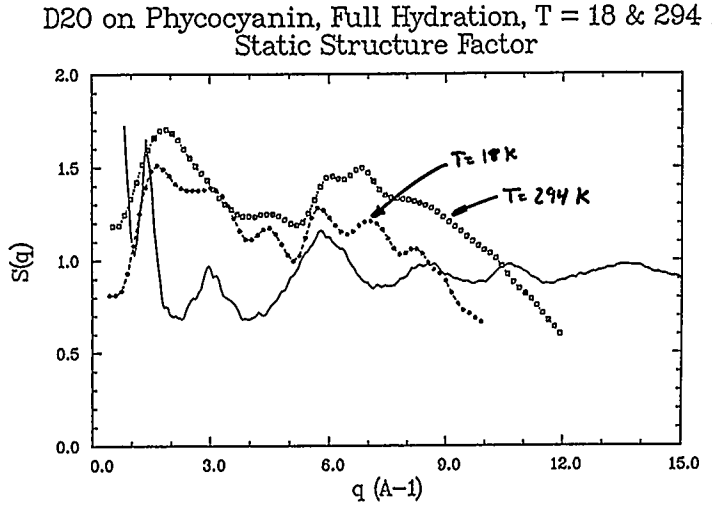


Figure 1: Comparison of the total structure factor of fully hydrated (with D_2O) C-phycocyanin at T = 18 K and T = 294 K. Solid line is an estimate of the protein's static structure factor using information from x-ray scattering.

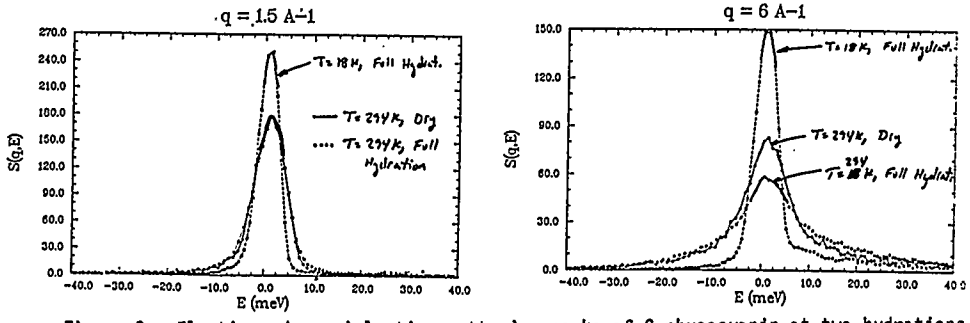


Figure 2: Elastic and quasielastic scattering peaks of C-phycocyanin at two hydrations and two temperatures indicating how the quasielastic component changes in different fashions with these parameters depending on the q-region probed.

INSTRUMENT USED:	DATE OF REPORT:	EXPERIMENT NO:
LRMECS	Dec 1, 1995	1842

TITLE:
Dynamics of liquids confined to small pores of controlled porous glasses

AUTHORS AND AFFILIATIONS:
B. Ewen, Yu. B. Mel'nichenko and J. Schuller (MPI für Polymerforschung)
C.-K. Loong (ANL)

DATES OF EXPERIMENT:
April 22-May 15, 1994

CHECK ALL APPLICABLE BOXES:

- [X] APPROVED BY PROGRAM COMMITTEE
- [ ] INSTRUMENT SCIENTIST ALLOCATION
- [ ] DO NOT PUBLISH
- [ ] PROPRIETARY RESEARCH
- [ ] PRT ALLOCATION

EXPERIMENTAL REPORT (or Abstract of Publication)

Dynamics of hydrogen-bonded liquids confined to mesopores: A dielectric and neutron spectroscopy study

Yu. B. Mel'nichenko,[a] J. Schüller, R. Richert, and B. Ewen
Max-Planck-Institut für Polymerforschung, Ackermannweg 10, 55128 Mainz, Germany

C.-K. Loong
Argonne National Laboratory, Argonne, Illinois 60439-4814

(Received 20 March 1995; accepted 4 May 1995)

In this paper we present and discuss experimental results on molecular mobility in propylene glycol and its three oligomers confined to the ~100 Å pores of a controlled porous glass. The objective is to elucidate the finite size effects on the dynamics of hydrogen-bonded liquids of different molecular weights but identical chemical composition. The methods of dielectric and neutron spectroscopy have been employed to investigate both the low- and high-frequency features as a function of temperature. We find that all fluids in pores separate into two distinct liquid phases. (i) molecules physisorbed at the surface which exhibit a dramatic frustration of their mobility related to a substantial *positive* shift of the glass transition temperature T_g by up to $\Delta T_g \sim +47$ K; and (ii) relatively "free" molecules in the inner pore space subject to only moderate retardation of the α and normal mode relaxation and substantial broadening of the distribution of relaxation times. The shift in T_g for the α process with $\Delta T_g \sim +5$ K is maximal for the monomer liquid and gradually diminishes with increasing molecular weight or decreasing intermolecular hydrogen bonding. The inelastic neutron spectrum of confined propylene glycol shows the boson peak as expected in bulk strong and intermediate glass formers in the vicinity of T_g. This effect can be attributed to the finite-size induced crossover from long wave vibrations characteristic of a continuous medium to localized vibrations in a confined geometry. © *1995 American Institute of Physics.*

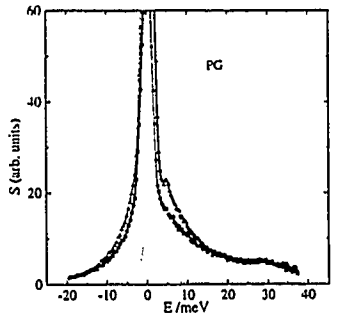


FIG. 10. Energy dependence of the dynamic structure factor $S(E)$ for bulk (■) and confined (Δ) PG at $T = T_g = 167$ K. The dashed line represents the spectrum for the pure CPG.

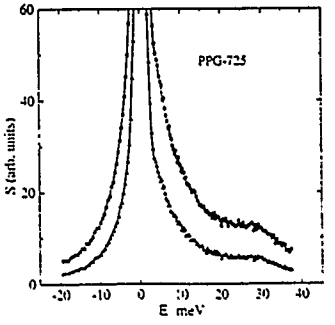


FIG. 11. Energy dependence of the dynamic structure factor $S(E)$ for bulk (■) and confined (▲) PPG-725 at $T = T_g = 197$ K. To avoid crowding, the spectrum for the bulk liquid is arbitrary shifted upward.

INSTRUMENT USED:	DATE OF REPORT:	EXPERIMENT NO.:
LRMECS	7/12/1991	#1355

TITLE:
Para-Hydrogen Motion in Condensed Neon at Low Temperatures

AUTHORS AND AFFILIATIONS: M. A. Fradkin, S. X. Zeng, R. O. Simmons
(University of Illinois at Urbana-Champaign)

DATES OF EXPERIMENT: 3/5-19/1991

☒ APPROVED BY PROGRAM COMMITTEE, OR

☐ PART OF INSTRUMENT SCIENTIST ALLOCATION

REPORT RECEIVED:

EXPERIMENTAL REPORT (or Abstract of Publication)

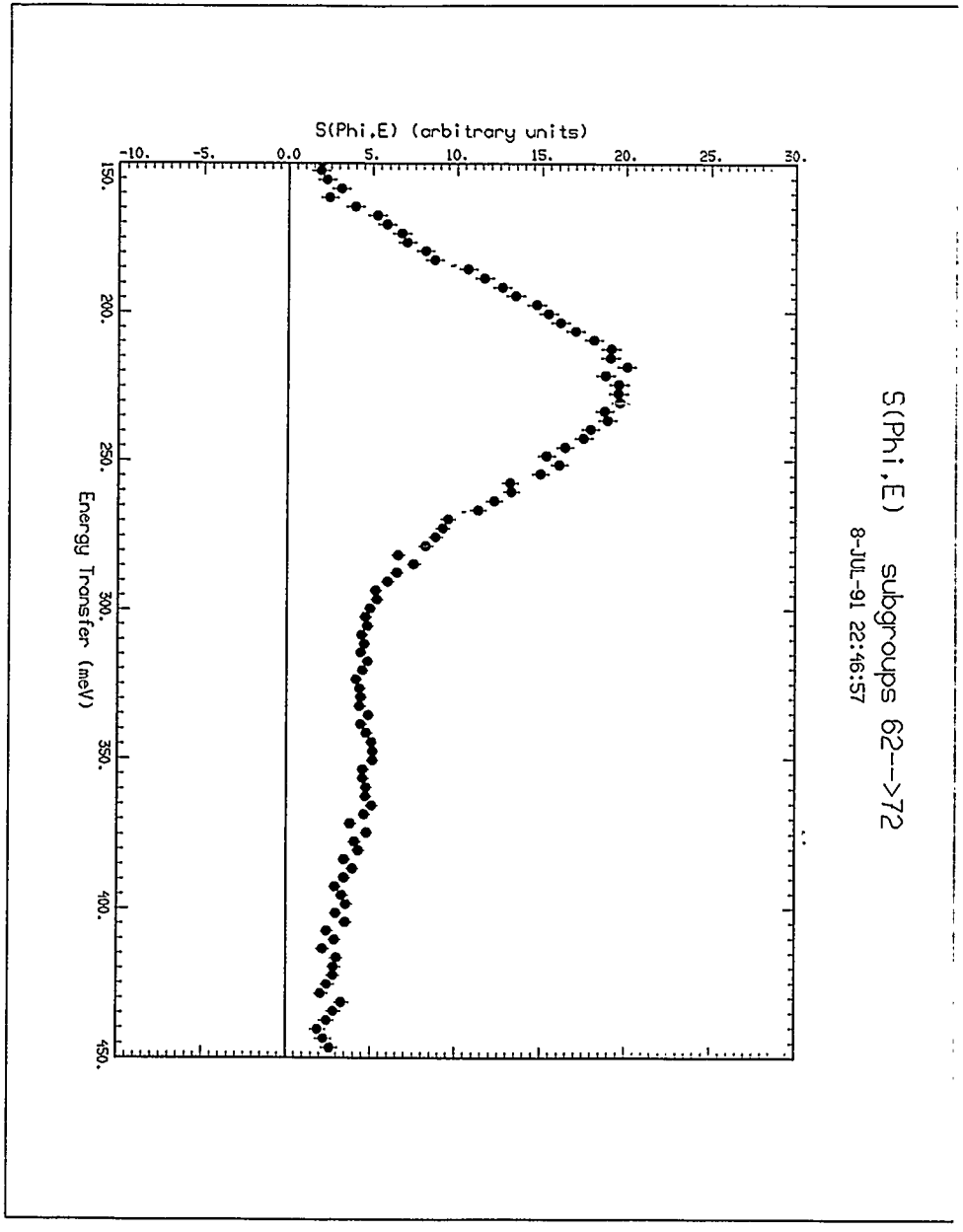
In this experiment we have extended previous deep inelastic neutron scattering work on the para-hydrogen - neon system. The previous experiment (see IPNS report #1034) was performed on a sample consisting of approximately 1% para-hydrogen embedded in solid neon at a temperature of 23.5 K. Analysis of this previous experiment indicated that the para-hydrogen had not dissolved in the solid neon as intended, rather pockets of para-hydrogen gas were formed. In the present experiment we sought to disperse the para-hydrogen by using a more dilute concentration, 0.5%. This smaller concentration afforded an additional advantage: multiple scattering was reduced although longer data collection times were required.

Data were taken on three samples: The first was with the sample cell filled with the solid para-hydrogen - neon mixture, the second was a background sample in which the sample cell was filled with solid neon, and the third was with the sample cell completely empty. For all three cases the temperature was approximately 4.7 K and the incident neutron energy 500 meV.

We are currently analyzing the scattering data. Preliminary analysis indicates that the center-of-mass single-particle kinetic energy of the para-hydrogen is approximately 50 K. This is appreciably less than the previously obtained pure para-hydrogen 4.7 K vapor pressure solid value of 92.6 K[1]. A typical para-hydrogen recoil spectrum is shown in figure 1. The observed peak corresponds to a rotational transition from the J = 0 state to the J = 3 state.

This research was supported by US DOE contracts DOE-DE-FG02-91ER45439 and W-31-1090-ENG-38

1. K. W. Herwig, Thesis (unpublished), University of Illinois (1988)



INSTRUMENT USED:	DATE OF REPORT:	EXPERIMENT NO.:
LRMECS	May 1, 1990	1139

TITLE: Crystal Field Levels in UCu_2Si_2

AUTHORS AND AFFILIATIONS: Joyce A. Goldstone, A. C. Lawson, A. Giorgi, LANL; P. Vorderwisch, Hahn-Meitner-Institut; C. K. Loong, IPNS; B. R. Cooper, West Virginia Univ.; Joe Vanimetti, LANL

DATES OF EXPERIMENT: January 23-30, 1990

☒ APPROVED BY PROGRAM COMMITTEE, OR

☐ PART OF INSTRUMENT SCIENTIST ALLOCATION

REPORT RECEIVED:

EXPERIMENTAL REPORT (or Abstract of Publication)

UCu_2Si_2 is the prototype of a series of recently discovered high-field ferromagnetic materials.[1] The origin of the magnetic properties of UCu_2Si_2 is interesting especially because of its difference in properties with respect to $CeCu_2Si_2$ and URu_2Si_2. $CeCu_2Si_2$ is a superconductor and shows well defined crystal field levels.[2] In contrast, URu_2Si_2 is a heavy fermion antiferromagnet and a superconductor, but no crystal field transitions could be observed.[3] As a first step toward the microscopic understanding of this new class of materials, we conducted an experiment at IPNS on LRMECS to search for crystal field levels.

We began our search using an incident energy of 200 meV, as there was a possibility that the crystal field levels might occur at higher energies than in the cerium analogue. Figure 1 shows the data taken at this energy. No interesting features exist in this data above an energy of approximately ~80 meV. We then changed the incident energy energy to 90 meV. With this incident energy, data were taken on the UCu_2Si_2 sample at 15K and 150K, on the nonmagnetic analogue sample $ThCu_2Si_2$ at 75K, and background and calibration runs were completed. The $ThCu_2Si_2$ sample was used to determined the phonon contribution to the scattering from UCu_2Si_2. Figure 2 shows a comparison of the data taken at 15K and 150K for UCu_2Si_2, no obvious change is visible. Figure 3 shows the UCu_2Si_2 data taken at 15K plot with the $ThCu_2Si_2$ data. Data have been corrected for the background, the number of monitor counts, the difference in sample amounts, and the difference in scattering cross section (29.3 barns for the U compound and 32.6 barns for the Th compound). The high angle data in figure 3a agree quite well. The low angle data in figure 3b shows increased scattering intensity for the UCu_2Si_2 over the $ThCu_2Si_2$ data, however no additional peaks are evident.

We conclude from these data that there are no high energy crystal fields in UCu_2Si_2. We now suspect that this compound behaves similarly to the Ce analogue and that if distinct crystal field levels can be observed that the energy region of interest in few meV range. To investigate this regime, higher resolution will be needed.

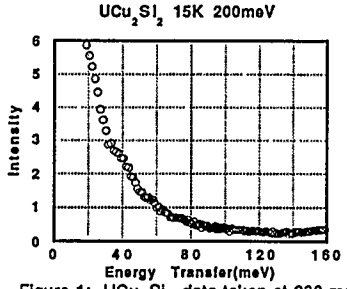


Figure 1: UCu_2Si_2 data taken at 200 meV incident energy.

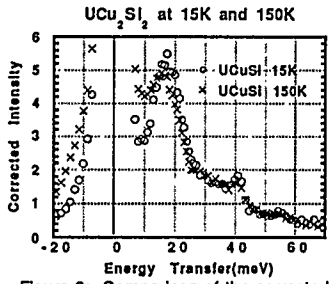


Figure 2: Comparison of the corrected UCu_2Si_2 data at 15K and 150K.

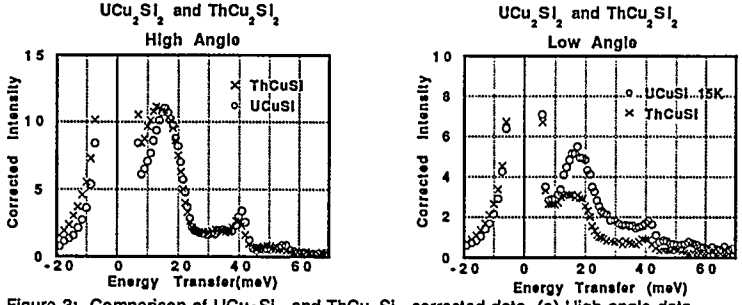


Figure 3: Comparison of UCu_2Si_2 and $ThCu_2Si_2$ corrected data. (a) High angle data shows the good agreement between the U-compound and the Th-compound. (b) The low angle data show some increased scattering in the U-data over the Th-data, but no new peals are resolved.

[1] A. L Giorgi, A. C. Lawson, J. A Goldstone, K. G. Volin, and J. D. Jorgenson, "Magnetic Structure of UCu_2Si_2 and $U(Cu_{0.75}Mn_{0.25})_2Si_2$", J. Appl. Phys. 63 (1989) 3604.
[2] E. Holland-Moritz, W. Weber, A. Severing, E. Zirngiebl, H. Spille, W. Baus, S. Horn, A. P . Murani, AND J. L. Ragazzoni, "Crystal-Field and Magnetic Excitations in $CeCu_{2\pm0.2}Si_2$", Phys. Rev. B39 (1989) 6409.
[3] U. Walter, C. K. Loong, M. Lowenhaupt and W. Schlabitz, "Evidence of a Gaplike Excitation in URu_2Si_2", Phys. Rev/. B33 (1986) 7875.

INSTRUMENT USED: LRMECS	DATE OF REPORT: 7/25/91	EXPERIMENT NO.: 1393

TITLE:

A STUDY OF THE INELASTIC SPECTRA OF ETHANOL PHYSISORBED ON GRAPHITE

AUTHORS AND AFFILIATIONS:

K. W. Herwig and F. R. Trouw IPNS/ANL

DATES OF EXPERIMENT: 9/12/90 -9/19/90 and 2/15/91 - 2/29/91

☒ APPROVED BY PROGRAM COMMITTEE, OR

☒ PART OF INSTRUMENT SCIENTIST ALLOCATION

REPORT RECEIVED:

EXPERIMENTAL REPORT (or Abstract of Publication)

The structure and dynamics of hydrocarbons physisorbed onto a graphite surface have been the subject of numerous investigations.[1] These efforts have concentrated on systems where the adsorbate-adsorbate interactions are relatively simple. Interactions between molecules of alcohols, such as ethanol, are more complicated because of the possibility of hydrogen bonding. Our goal in this experiment was to probe the inelastic spectra of such a physisorbed species, ethanol on graphite, over a wide range of energy and momentum transfers.

For purposes of comparison, we also measured the spectra from a bulk specimen of ethanol, C_2H_5OH. Figure 1 shows the spectra obtained using 160 meV incident neutrons on LRMECS. Although the experiment could have benefited from better resolution, many features are readily observable in the spectra. A fit to the spectra (using Gaussian line shapes) gave peak positions: 34, 54, 92, 101, 110, and 138 meV. Infrared and Raman measurements[2,3] assigned these peaks to various internal modes of the molecule, a CH_3 torsion, CCO in-plane bend, COH torsion, combination, symmetric CCO stretch, and asymmetric CCO stretch, respectively. There are some indications in the neutron spectra of additional peaks at 69 and 117 meV which were not observed in the Raman and infrared experiments.

Figure 2 shows the spectra obtained from C_2H_5OH physisorbed onto GRAFOIL. (GRAFOIL is a partially oriented, recompressed exfoliated graphite with a surface area of approximately 22 m^2/gm.) Significant differences can be observed between the spectra obtained from the bulk and physisorbed species. Fits to the spectra in Fig. 2 gave peak positions of 34, 60, 82, 91, 102, 105, and 138 meV. The two lowest energy peaks probably correspond to the CH_3 torsion and CCO in-plane bend modes respectively. The most significant difference is the presence of a strong peak in the physisorbed spectra at 82 meV which was not present in the bulk spectra. The origin of this peak is still an open question and a further experiment is planned to aid in its interpretation.

We were also interested in probing the inelastic spectra at high energy transfers. Figure 3 shows the spectra obtained from C_2H_5OH physisorbed on graphite taken with an incident energy of 650 meV on LRMECS. Two peaks are observed in the inelastic spectra at energy transfers of 192 and 382 meV. The lower energy peak can be associated with rocking modes of the CH_3 group. The higher energy peak is likely composed of several modes due to stretching vibrations of the protons. Because the sample was fully protonated, it is impossible to separate out these motions. A further experiment is planned on a partially deuterated specimen. This measurement will focus solely on the behavior of the hydroxyl proton and should yield unique information about the strength of the hydrogen bond in the physisorbed species.

EXPERIMENTAL REPORT (CONTD.)

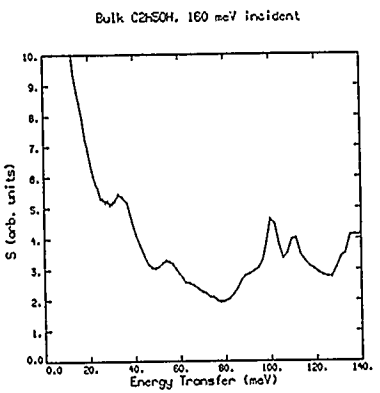


Fig. 1 The inelastic spectra of bulk ethanol.

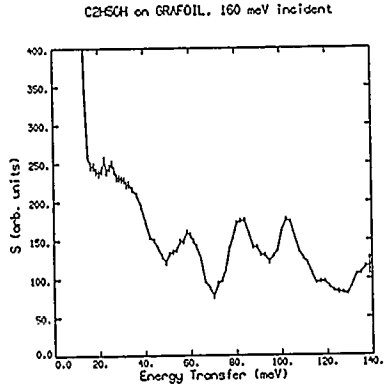


Fig. 2 The inelastic spectra of C_2H_5OH physisorbed on graphite using 160 meV incident neutrons.

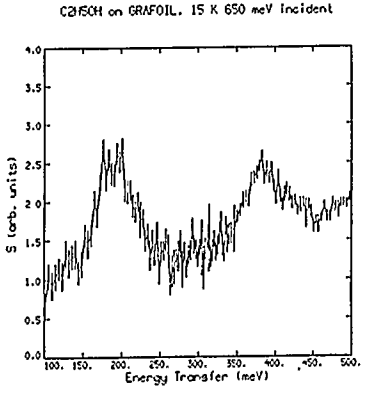


Fig. 3 The inelastic spectra of C_2H_5OH physisorbed on graphite using 650 meV incident neutrons.

REFERENCES

[1] See for example, Neutron Scattering Studies of the Structure, Phase Transitions, and Dynamics of Commensurate Herringbone Monolayers Physisorbed on Graphite, H. Taub in The Time Domain in surface and Structural Dynamics, NATO ASI series, ed. G.J. Long and F. Gradjean, p. 467-498, 1988.

[2] J. P. Perchard and M. L. Josien, J. Chim. Phys. 65, 1834 (1968).

[3] J. P. Perchard and M. L. Josien, J. Chim. Phys. 65, 1856 (1968).

INSTRUMENT USED:	DATE OF REPORT:	EXPERIMENT NO.:
LRMECS	20-Jan-1993	

TITLE: Inelastic magnetic response in the system $(U_{0.45}Y_{0.55})Pd_3$

AUTHORS AND AFFILIATIONS: G.H. Lander, EITU, Karlsruhe
S. Kern, CSU, Fort Collins, Co. C.K. Loong & D. Hinks, ANL

DATES OF EXPERIMENT: 13-17 July 1992

☒ APPROVED BY PROGRAM COMMITTEE, OR

☐ PART OF INSTRUMENT SCIENTIST ALLOCATION

REPORT RECEIVED:

EXPERIMENTAL REPORT (or Abstract of Publication)

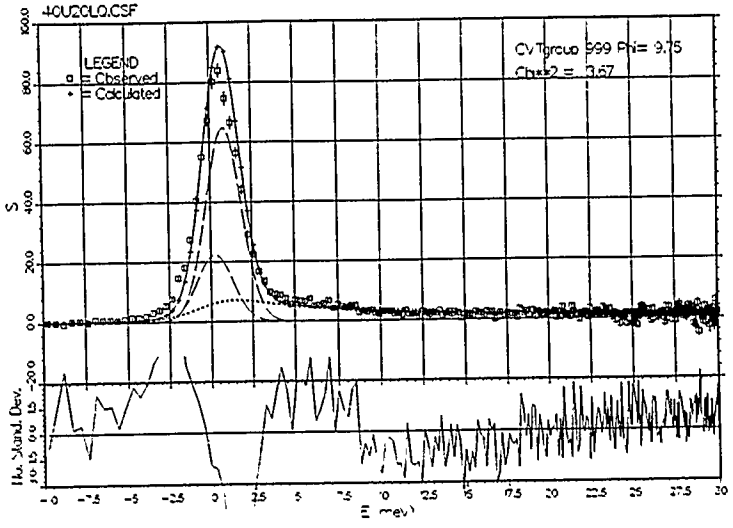


Figure: Experimental spectrum (E_I=40 meV, T=20 K) from LRMECS at low Q values. The data have been fit with the resolution function and a relaxation function (dotted line) of half-width 3 meV. Notice the absence of excitations in the region -4 < E < 25 meV.

A considerable number of experiments have been conducted over the last few years on the system $(U_XY_{1-X})Pd_3$. It is well known that UPd_3 is a localized ($5f^2$) system, and recent work on this has shown that some interesting quadrupolar effects occur at low temperature. The disadvantage of the pure UPd_3 material is that the crystal structure is hexagonal with *two* inequivalent U sites, one of hexagonal and one of quasi-cubic symmetry, in the unit cell. Doping with Y has the advantage that the cubic $AuCu_3$ structure is stabilised for $x < 0.5$, and all sites are equivalent. The coordination of the U atom is then similar to that of the quasi-cubic site in the pure compound. The transport and photoemission work on $(U_XY_{1-X})Pd_3$ have been interpreted as strong evidence for a Kondo resonance behavior in the region of low U concentration, i.e. $x < 0.3$. Moreover, the theory of Cox[1] has been used to interpret much of the bulk data in the low x concentration region and this theory explicitly requires that the ground state of the uranium be a non-magnetic doublet of the $5f^2$ configuration, the most likely candidate being the doublet of symmetry Γ_3. No direct low-energy spectroscopic evidence has been reported to confirm this ground state.

The initial aim of our neutron investigations are to investigate the crystal-field states of these materials. A secondary aim, equally important, is to examine the relaxation spectrum as a function of temperature. This can give information on any possible Kondo behaviour of the system. We started with a sample of x=0.45. This contains enough U atoms to be able to see a magnetic signal at IPNS, but it still within the $AuCu_3$ phase. The material was found to be single phase with a= 4.0818 Å at RT. The experiments were performed on LRMECS.

At 20 K with E_0=120 meV a weak peak at ~ 35 meV was observed. This is presumably the higher-lying states of the CF multiplet that were observed previously in pure UPd_3 {also at IPNS during our investigation of the $U(Pd,Pt)_3$ system[2]}. However, in pure UPd_3 the quasi-cubic states have a singlet ground state with their excited doublet at ~ 1.5 meV. To investigate this possibility we reduced the incident energy to 40 meV. The results are shown in the figure. This shows definitively that there are no excitations up to ~ 25 meV. A small quasielastic component, with a FWHM of ~ 3 meV is fitted to the data, but given that the resolution of LRMECS is also about 2-3 meV at this E_I this fitting should be taken as suggestive only. Further experiments on this sample will be proposed for QENS, and other x values are also being prepared.

Refs:
[1] D L Cox, Phys. Rev. Letters, 59, 1240 (1987)

[2] K A McEwen, W G Stirling, C K Loong, G H Lander, and D Fort, J. Magn. and Magn. Matls. 76-77, 426 (1988)

INSTRUMENT USED:	DATE OF REPORT:	EXPERIMENT NO.:
LRMECS	July30,1989	1034

TITLE: Para-hydrogen Motion in Condensed Neon Hosts

AUTHORS AND AFFILIATIONS:
D. A. Peek, Jon T. Nelson, R. O. Simmons (University of Illinois, Urbana-Champaign)

DATES OF EXPERIMENT: Jan. 24 - Feb. 3 1989

☐ APPROVED BY PROGRAM COMMITTEE, OR

☐ PART OF INSTRUMENT SCIENTIST ALLOCATION

REPORT RECEIVED:

EXPERIMENTAL REPORT (or Abstract of Publication)

A one percent solution of hydrogen gas was introduced into a sample cell containing natural neon that had been cooled with a displex to 23.5K (solid) and 25.5K (liquid). Conversion to para-hydrogen was quickened by forcing it through a chamber containing a paramagnetic salt.

The kinetic energy was measured by fitting the data to three gaussians. The three peaks, corresponding to rotational transitions in the hydrogen of J=0 to 1,3,5, fit the Young and Koppel model nicely with chi-squared fits of around one.

Preliminary analysis of the data indicates that the hydrogen gas didn't absorb into the solid neon as intended, instead pockets of gas were formed where the gas had a classical kinetic energy (34.4 ± 2K where 3/2 kT is 35K). For the liquid however, the kinetic energy was not classical (46.7 ± 1 5K where 3/2 kT is 38.3K), indicating that it was absorbed into the neon (figure 1) On a previous run the kinetic energy of neon was measured to be 52 8 ± 3 7K at a sample temperature of 25.8K [1].

This research was supported in part by the U.S. Department of Energy, Division of Material Sciences, under contract DOE-DE-AC02-76ER01198.

REFERENCES

1) M. C. Schmidt, D. A. Peek, I. Fujita, and R. O. Simmons, Jap. Jou. of Appl. Phys. 26, Suppl. 26-3, 451 (1987)

EXPERIMENTAL REPORT (CONTD.)

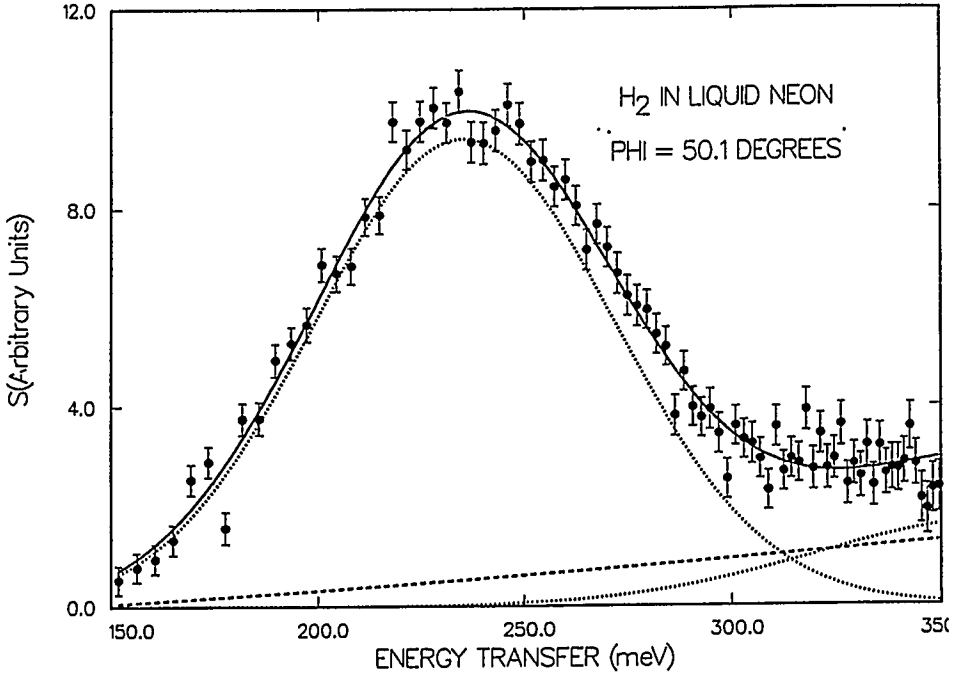


Figure 1. J=0-3 transition peak for para-hydrogen

INSTRUMENT USED:	DATE OF REPORT:	EXPERIMENT NO:
LRMECS	June 16, 1995	1974

TITLE: **THE STRUCTURE OF A LEAD-INDIUM PHOSPHATE GLASS**

AUTHORS AND AFFILIATIONS:
B. C. SALES**, AND L. A. BOATNER**, K. SUZUYA*, D. L. PRICE*, C.-K. LOONG*,
*Argonne National Laboratory, Argonne, IL 60439
**Oak Ridge National Laboratory, Oak Ridge, TN 37831

DATES OF EXPERIMENT: Sept. 1994

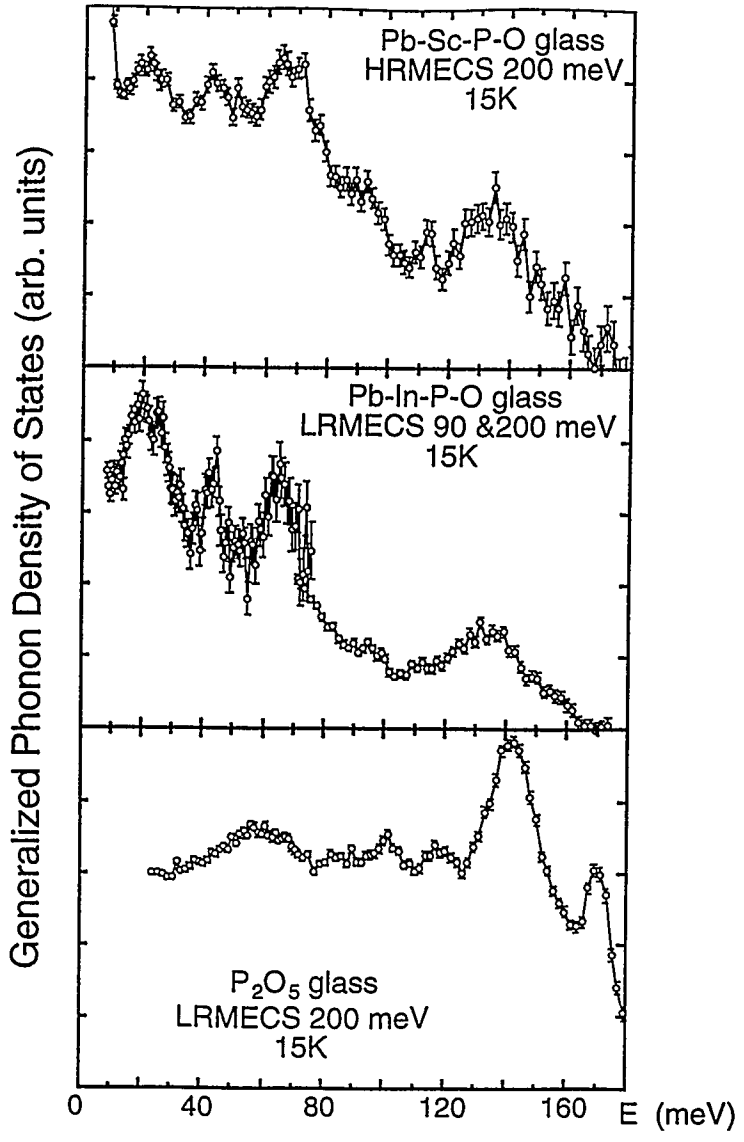
CHECK ALL APPLICABLE BOXES:

- [X] APPROVED BY PROGRAM COMMITTEE
- [ ] INSTRUMENT SCIENTIST ALLOCATION
- [ ] DO NOT PUBLISH
- [ ] PROPRIETARY RESEARCH
- [ ] PRT ALLOCATION

EXPERIMENTAL REPORT (or Abstract of Publication)

Two new glass systems based on a range of lead-scandium phosphate and lead-indium phosphate compositions have recently been developed at Oak Ridge National Laboratory. These glasses exhibit many useful properties such as a high index-of-refraction, low preparation temperature and melt viscosity, and good chemical durability. The evolution of the corner-linked PO_4 tetrahedra chains structure in the amorphous-to-crystalline transformation of these glasses have been studied by liquid chromatography. This technique requires the materials to be dissolved in aqueous high-pH solution and examines only the phosphate chain structures. Neutron scattering provides a more complete analysis of the structure and dynamics of the glasses nondestructively.

We have studied the dynamic response to structural modification by the Pb cations in a $PbO(65\ wt\%)P_2O_5(29\%)R_2O_3(6\%)$ (R = Sc and In) glasses by inelastic neutron scattering. The figure below displays the observed neutron-weighted phonon densities of states (PDOS) of the Pb-R-P-O glass as compared with the pure P_2O_5 glass. These spectra reveal a different dynamic response to medium-range ordering: 1) the stretch vibrations of the P=O (doubly bonded P and terminal O) at 170 meV (1360 cm^{-1}) disappear in the lead phosphate glass; 2) the highly disordered P-O-P bending/torsion band below 80 meV in pure P-O glass is replaced by "more organized" Pb-O/P-O vibrational bands. These features suggest a substantial reduction of the Q^3 (branching) and Q^2 (middle) configurations in the 3-D network of corning sharing PO_4 tetrahedra and a development of short chains of PO_4's admixed with the modifying Pb ions. This result is in qualitative agreement with those obtained from a liquid-chromatography study.



01 25 95 10:25 ☎708 252 4163 ANL IPNS 300 003

INSTRUMENT USED: LRMECS	DATE OF REPORT: 26.1.95	EXPERIMENT NO.:

TITLE: See below

AUTHORS AND AFFILIATIONS: See below

DATES OF EXPERIMENT:

CHECK ALL APPLICABLE BOXES:

- ☒ APPROVED BY PROGRAM COMMITTEE
- ☐ INSTRUMENT SCIENTIST ALLOCATION
- ☐ DO NOT PUBLISH
- ☐ PROPRIETARY RESEARCH
- ☐ PRT ALLOCATION

EXPERIMENTAL REPORT (or Abstract of Publication)

OBSERVATIONS OF CEF-SPLIT INTERMULTIPLET TRANSITIONS IN OPTICALLY OPAQUE $EuBa_2Cu_3O_7$ USING INELASTIC NEUTRON SCATTERING

U. Staub[1], L. Soderholm[1], R. Osborn[2], E. Balcar[3], and V. Trunov[4]
[1] Chemistry Division, Argonne National Laboratory, Argonne, Il-60439, USA
[2] Material Sciences Division, Argonne National Laboratory, Argonne, Il-60439, USA
[3] Atominstitut der Oesterriechischen Universitäten, A-1020 Vienna, Austria
[4]St. Petersburg Nuclear Physics Institute, Gatchina, St. Petersburg, 188350 Russia.

ABSTRACT

Inelastic neutron scattering (INS) results on the intermultiplet transitions J=0 → 1 and J=1 → 2 in optically opaque $EuBa_2Cu_3O_7$ are reported whereas these multiplets are split by the crystalline electric field (CEF). The low J values of these multiplets are influenced to first order only by the second order CEF parameters. B_0^2, B_2^2 and the spin-orbit coupling parameter were obtained by fitting the splitting of the J=1 multiplet and the energy separation between the J=0 and 1 multiplets. The J=0 → 1 splitting observed here is smaller than previously seen by optical spectroscopic studies on a variety of transparent, ionic compounds, necessitating the inclusion of a free-ion parameter in the fitting procedure. Additional spectroscopic information on the J=2 multiplet indicate that additional free ion parameters must be included to adequatly model the observed low energy separation between the two lowest J-multiplets. Priliminary calculation on the Q-dependence of the CEF split J=0 → 1 transitions and the comparison with the observations are presented.

to be puplished in the Proceedings of the MRS Fall Meeting 28. Nov.-2.Dec. 1994 Boston.

INSTRUMENT USED: LRMECS	DATE OF REPORT: Aug. 15 1994	EXPERIMENT NO: 1774

TITLE: The diffusion of H_2 in hexagonal ice at low temperatures

AUTHORS AND AFFILIATIONS: H. L. Strauss, and Z. Chen (Dept. Chemistry, U. C. California, Bekerley, CA 94720), and C.-K. Loong (ANL)

DATES OF EXPERIMENT: 7/22-7/29/93

CHECK ALL APPLICABLE BOXES:

- [X] APPROVED BY PROGRAM COMMITTEE
- [ ] INSTRUMENT SCIENTIST ALLOCATION
- [ ] DO NOT PUBLISH
- [ ] PROPRIETARY RESEARCH
- [ ] PRT ALLOCATION

EXPERIMENTAL REPORT (or Abstract of Publication)
The manuscript has been prepared, to be submitted to J. Chem. Phys.

THE DIFFUSION OF H_2 IN HEXAGONAL ICE AT LOW TEMPERATURES*

Herbert L. Strauss and Zhang Chen
Department of Chemistry, University of California, Berkeley CA 94720
and

C.-K. Loong
IPNS, Argonne National Laboratory, Argonne IL 60439

The diffusion of hydrogen molecules in hexagonal D_2O ice (Ih) in a temperature range of 25 - 60 K was investigated by quasielastic neutron scattering. The observed spectra consist of a narrow elastic peak and a broad quasielastic component. A single-particle diffusion coefficient for H_2 in D_2O ice was obtained using a simple model of diffusion.

*submitted to J. Chem. Phys.

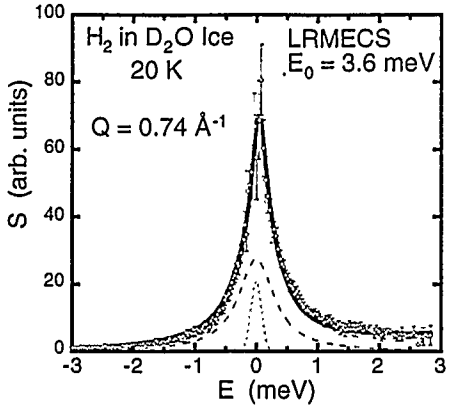


Figure 1. The spectrum of H_2 in D_2O ice at 25 K with a mean wave vector Q = 0.74 Å-1. The spectrum was taken with an incident energy of 3.6 meV. The solid line corresponds to a fit of the data by the sum of resolution-limited Gaussian (dotted line), a Lorentzian (dashed line), and a linear background.

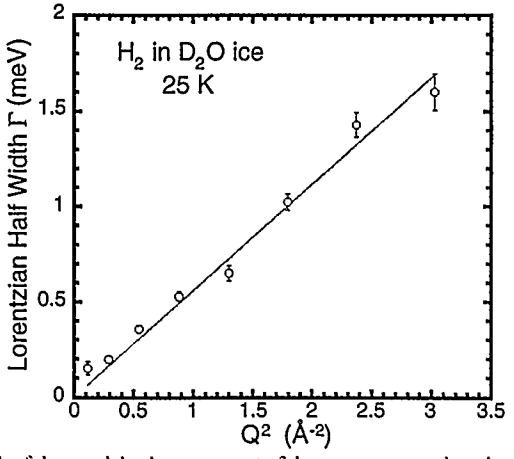


Figure 2. The width of the quasielastic component of the neutron scattering plotted against the wave vector, Q, squared. The limiting slope at small Q gives the diffusion constant.

INSTRUMENT USED: LRMECS	DATE OF REPORT: Aug. 6, 1992	EXPERIMENT NO:

TITLE:
Molecular vibrations and diffusion in $AlCl_3$-EMIC molten salts

AUTHORS AND AFFILIATIONS:
S. Takahashi, Nisshin Steel, Japan
M.-L. Sabungi and D. L. Price, ANL

DATES OF EXPERIMENT:
March 1992

CHECK ALL APPLICABLE BOXES:

- [ ] APPROVED BY PROGRAM COMMITTEE
- [X] INSTRUMENT SCIENTIST ALLOCATION
- [ ] DO NOT PUBLISH
- [ ] PROPRIETARY RESEARCH
- [ ] PRT ALLOCATION

EXPERIMENTAL REPORT (or Abstract of Publication)

Inelastic scattering spectroscopy has been applied to probe the structure and dynamics of ionic species in $AlCl_3$ - 1-ethyl-3-methyl imidazolium chloride (EMIC) molten salts. Two compositions, 46 and 67 mol% of $AlCl_3$, were chosen for study at 25, 243, and 297 K with incident energies of 60 and 90 meV. Ample evidence have indicated the important roles in the distinct electrochemical properties of the dominant anions, $AlCl_4^-$ and $Al_2Cl_7^-$ in the 46 and 67 mol% composition, respectively.

Fig. 1 shows the neutron-weighted vibrational spectra of 46 mol% $AlCl_3$ -54 mol% EMIC and 67 mol% $AlCl_3$ -33 mol% EMIC at 25 K. Although the observed scattering is dominated by vibrations of H atoms in the EMIC cations, some differences can be seen in the regions near 100, 160, 215, and 390 cm^{-1}. Similar different features were also observed at higher temperatures. It is believed that the $AlCl_4^-$ anion displays a T_d structure as compared to a C_2 structure of the $Al_2Cl_7^-$ anions in these molten salts. The observed frequency shifts and intensity changes in the neutron spectra of the two compositions may arise from the different internal vibrational frequencies involving the Al and Cl atoms in the $AlCl_4^-$ and $Al_2Cl_7^-$ ionic species. Inelastic experiments using deuterated EMIC salts would help clarify this interpretation of the data.

We also studied the quasielastic scattering of 67 mol% $AlCl_3$ - 33 mol% EMIC at room temperature using LRMECS with an incident energy of 4 meV. An energy resolution of 0.24 meV in the elastic region can be achieved in this configuration. A quasielastic component in the scattering function is clearly evident, as shown in Fig. 2. Analysis of the data in terms of molecular diffusion of the EMIC cations is currently in progress.

EXPERIMENTAL REPORT (CONTD.)

In parallel with the inelastic neutron studies, we have also performed neutron diffraction, electrochemical analyses, Raman scattering, IR and NMR measurements on these molten salts. The results of these experiments as well as from *ab initio* molecular-orbital calculations seem to corroborate the preliminary analysis of the neutron data.

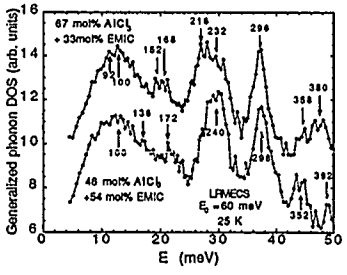


Figure 1. The observed neutron-weighted vibrational spectra of 46 mol% $AlCl_3$ - 54 mol% EMIC and 67 mol% $AlCl_3$ - 33 mol% EMIC at 25 K. The upper spectrum is displaced by 5 units in the vertical direction. The labeled frequencies (in cm^{-1}) matches well to the frequencies from *ab initio* calculations.

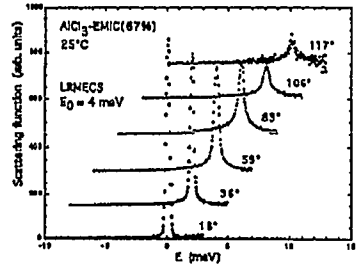


Figure 2. Quasielastic scattering of 67 mol% $AlCl_3$ - 33 mol% EMIC at 25°C using LRMCS with an incident energy of 4 meV.

References:

1. S. Takahashi, I.Saeki and K.Akimoto, J. Surf. Fin. Soc. Japan, 40, 42 (1989).
2. S. Takahashi, M.-L. Saboungi, R. J. Klingler, M. J. Chen, and J. W. Rathke, submitted to J. Electrochem. Soc.

INSTRUMENT USED: POSY	DATE OF REPORT: February 1996	EXPERIMENT NO.: Discretionary

TITLE: 90^{o} Magnetic Structure in Fe/Cr Superlattices

AUTHORS AND AFFILIATIONS: S. Adenwalla, G.P. Felcher, E. Fullerton and S.D. Bader
Argonne National Lab.

DATES OF EXPERIMENT:

CHECK ALL APPLICABLE BOXES:

- ☐ APPROVED BY PROGRAM COMMITTEE
- ☒ INSTRUMENT SCIENTIST ALLOCATION
- ☐ DO NOT PUBLISH
- ☐ PROPRIETARY RESEARCH
- ☐ PRT ALLOCATION

EXPERIMENTAL REPORT (or Abstract of Publication)

90^{o} Magnetic Structure in Fe/Cr Superlattices

S. Adenwalla, G.P. Felcher, E. Fullerton and S.D. Bader

Argonne National Laboratory, Argonne IL 60439

We present Polarized Neutron Reflectivity (PNR) and magnetization measurements on a [Fe(14A)/Cr(74A)] superlattice. At this thickness of Cr, the bilinear coupling constant is expected to be small. Our measurements indicate the presence of biquadratic coupling in the superlattice. Both the magnetization and PNR data are consistent with his scenario. The data shows that the sample is single domain. and that the magnetic structure is coherent through the depth of the sample. Below the magnetic ordering temperature of the Cr spacer layer, our measurement s indicate a dramatic change in the nature of the coupling.

INSTRUMENT USED:	DATE OF REPORT:	EXPERIMENT NO.:
POSY	February 1996	Discretionary

TITLE:
2-D Character of the Magnetisation of Ultrathin Fe Films on MgO

AUTHORS AND AFFILIATIONS: S. Adenwalla, Y. Park, and G. P. Felcher (Argonne National Lab.) and M. Teitelman (Institute for Applied Physics, Russian Academy of Science)

DATES OF EXPERIMENT:

CHECK ALL APPLICABLE BOXES:

- ☐ APPROVED BY PROGRAM COMMITTEE
- ☒ INSTRUMENT SCIENTIST ALLOCATION
- ☐ DO NOT PUBLISH
- ☐ PROPRIETARY RESEARCH
- ☐ PRT ALLOCATION

EXPERIMENTAL REPORT (or Abstract of Publication)

2-D Character of the Magnetisation of Ultrathin Fe films on MgO*

S. ADENWALLA, Y. PARK, G.P. FELCHER, Argonne National Laboratory, Argonne IL 60439 and M. TEITELMAN, Institute for Applied Physics, Russian Academy of Science, Nizhny Novgorod, 603600, Russia. Recent Polarized Neutron Reflectometry (PNR) measurements[1] have shown that 4 Å thick films of bcc Fe on (100) MgO are ferromagnetic at low temperature but in order to be saturated a magnetic field in excess of 1000 Oe needs to be applied in the film's plane. Such behavior may stem from uniaxial anisotropy. However, the initial measurements could be fitted as well with the logarithmic approach to saturation predicted for a 2-dimensional film in absence of anisotropy. New measurements of M(H,T) have been taken both by PNR and and Kerr effect on thin films of bcc Fe grown under various conditions. PNR is capable of measuring the absolute magnetisation, but only in the plane of the film, while the Kerr effect is used to detect the presence of axial and planar components of the magnetization. The preliminary results indicate the complete absence of hysteresis in the magnetization loop, with zero magnetization in zero applied field for the thinnest samples. The magnetization decreases with increasing temperatures very gradually, with a behavior to be compared with the linear decay expected for a 2-d ferromagnet.

[1] Y.Y. Huang, C. Liu and G.P. Felcher, Phys. Rev.47, 183 (1993)

*Supported by US-DOE, BES-MS contract #W-31-109-ENG-38.

EXPERIMENTAL REPORT (CONTD.)

INSTRUMENT USED:	DATE OF REPORT:	EXPERIMENT NO.:
POSY	February 1996	Discretionary

TITLE: Unidirectional Anisotropy in Co/CoO: A Neutron Reflection Study

AUTHORS AND AFFILIATIONS: S. Adenwalla, R. Siebrechht and G.P. Felcher (Argonne National Lab.) and K. Takano and A. Berkowitz (University of California-San Diego)

DATES OF EXPERIMENT:

CHECK ALL APPLICABLE BOXES:

- ☐ APPROVED BY PROGRAM COMMITTEE
- ☒ INSTRUMENT SCIENTIST ALLOCATION
- ☐ DO NOT PUBLISH
- ☐ PROPRIETARY RESEARCH
- ☐ PRT ALLOCATION

EXPERIMENTAL REPORT (or Abstract of Publication)

UNIDIRECTIONAL ANISOTROPY IN Co/CoO: A NEUTRON REFLECTION STUDY, S. Adenwalla, R. Siebrecht and G.P. Felcher, Argonne National Laboratory, Argonne IL 60439*; K. Takano and A. Berkowitz, Center for Magnetic Recording Research, University of California-San Diego, La Jolla CA92093-2720.

It is well known that many ferromagnetic/antiferromagnetic couples, cooled in a magnetic field, display a hysteresis loop biased by an exchange field, H_e, of the order of a few tens of Oersteds. The effect is thought to have its origin on a configuration of the antiferromagnetic spins at the interface that does not switch entirely when the magnetization is reversed. Our samples consist of pairs Co/CoO, each 100 Å thick, epitaxially deposited on (111) sapphire. In these films Co is magnetized in the plane and the antiferromagnetic propagation axis is perpendicular to the surface. Polarized Neutron Reflectometry is used to determine and compare the various Fourier components of the spin depth profiles in the two magnetic states. The preliminary results rule out the extreme model, where the antiferromagnetic configuration remain rigidly the same for the two magnetic states. Further experiments will verify if the magnetization reversal gives rise to an extended antiferromagnetic domain wall, as proposed by Malozemoff.

INSTRUMENT USED:	DATE OF REPORT:	EXPERIMENT NO.:
POSY	February 1996	Discretionary

TITLE: Polarized Neutron Reflection Study of the Magnetic Field Distribution in Superconducting Nb Films

AUTHORS AND AFFILIATIONS:
S. Adenwalla, E.E. Fullerton and G.P. Felcher (Argonne National Lab.)

DATES OF EXPERIMENT:

CHECK ALL APPLICABLE BOXES:

- ☐ APPROVED BY PROGRAM COMMITTEE
- ☒ INSTRUMENT SCIENTIST ALLOCATION
- ☐ DO NOT PUBLISH
- ☐ PROPRIETARY RESEARCH
- ☐ PRT ALLOCATION

EXPERIMENTAL REPORT (or Abstract of Publication)

Polarized Neutron Reflection Study of the Magnetic Field Distribution in Superconducting Nb films S. ADENWALLA, ERIC E. FULLERTON, G.P. FELCHER,Argonne National Laboratory, Argonne IL 60439. Polarized Neutron Reflectometry has been quite successful[1,2] in measuring the penetration depth in both Type I and Type II superconductors below the critical field H_{c1}. For this kind of experiment the typical sample is a film of thickness much larger than the penetration depth and the measurements are taken with the magnetic field applied parallel to the surface. The present experiment was aimed at discerning the distribution of magnetic fields at $H_{c1}<H<H_{c2}$. The presence of a fluxoid lattice was expected to perturb the spin-dependence of the specular reflectivity (which measures the laterally averaged magnetic depth profile) as well as to give rise to off-specular diffraction spots. We carried out measurements on Nb films of thickness ranging from 5000A to 2um, the thinnest film having a Tc (9.1K) already very close to the bulk value. The spin-dependent reflectivities were found to evolve, when taken at increasing fields (above H_{c1}), in a manner consistent with that expected for superconductors containing a fairly well ordered flux lattice.

1. G.P. Felcher, R.T. Kampwirth, K.E. Gray and Roberto Felici, PRL **52**, 1539 (1984).
2. Huai Zhang, J. W. Lynn, C.F. Majkrzak, S.K. Satija, J.H. Kang and X.D. Wu, Phys. Rev. **B52**, 10395 (1995).

EXPERIMENTAL REPORT (CONTD.)

INSTRUMENT USED:	DATE OF REPORT:	EXPERIMENT NO.:
POSY	February 1996	Discretionary

TITLE: Observation of the Zeeman Splitting for Neutrons Reflected by Magnetic Layers

AUTHORS AND AFFILIATIONS: G.P. Felcher and S. Adenwalla (Argonne National Lab.)
V.O. DeHaan, A.A. Van Well (I.R.I. Delft University of Technology)

DATES OF EXPERIMENT:

CHECK ALL APPLICABLE BOXES:

- ☐ APPROVED BY PROGRAM COMMITTEE
- ☒ INSTRUMENT SCIENTIST ALLOCATION
- ☐ DO NOT PUBLISH
- ☐ PROPRIETARY RESEARCH
- ☐ PRT ALLOCATION

EXPERIMENTAL REPORT (or Abstract of Publication)

Observation of the Zeeman Splitting for Neutrons Reflected by Magnetic Layers

G.P. FELCHER, S. ADENWALLA
Argonne National Laboratory, Argonne IL 60439
and V.O. DE HAAN, A.A. VAN WELL
I.R.I., Delft University of Technology, 2629 JB Delft, The Netherlands

The Zeeman splitting was measured for neutrons specularly reflected from a magnetic layer in a particular geometry. The neutron spins were quantized along an external magnetic field H, and the reflecting layer was magnetized in a different direction, causing some of the reflected neutrons to flip spin. The laws of conservation of energy and momentum for the spin-flipped neutrons impose the condition $\theta_f^2 = \theta_i^2 \pm 1.47 \times 10^{-7} H \cdot \lambda^2$, where θ_i, θ_f are respectively the incident and reflected angles in radians, H is expressed in kOe and λ (the neutron wavelength) in Å. Neutrons reflected and spin-flipped are reflected at an angle significantly different from the angle of incidence even in fields of a few kOe, although the Zeeman splitting energy amounts to less than 10^{-7} eV.

INSTRUMENT USED:	DATE OF REPORT:	EXPERIMENT NO.:
POSY	February 1996	Discretionary

TITLE: Non-oscillatory Antiferromagnetic Coupling in Sputtered Fe/Si Superlattices

AUTHORS AND AFFILIATIONS: E.E. Fullerton, J.E. Mattson, S.R. Lee, C.H. Sowers, Y.Y. Huang, G.Felcher and S.D. Bader (Argonne National Lab.) and F.T. Parker (University of California-San Diego).

DATES OF EXPERIMENT:

CHECK ALL APPLICABLE BOXES:

- ☐ APPROVED BY PROGRAM COMMITTEE
- ☒ INSTRUMENT SCIENTIST ALLOCATION
- ☐ DO NOT PUBLISH
- ☐ PROPRIETARY RESEARCH
- ☐ PRT ALLOCATION

EXPERIMENTAL REPORT (or Abstract of Publication)

Non-oscillatory antiferromagnetic coupling in sputtered Fe/Si superlattices.

Eric E. Fullerton, J.E. Mattson, S.R. Lee†, C.H. Sowers, Y.Y. Huang, G. Felcher and S.D. Bader
Materials Science Division, Argonne National Laboratory, Argonne, IL 60439
F. T. Parker
Center for Magnetic Recording Research 0401, University of California at San Diego, La Jolla, CA 92093-0401

A series of sputtered Fe(30Å)/Si(x) superlattices were grown for x=10-40Å. Magnetization and Kerr hysteresis loops, and neutron-reflectivity measurements identify antiferromagnetic (AF) coupling of the Fe layers at room temperature for x=15Å nominal thickness, with switching fields of 6kOe. X-ray structural analyses indicates that the spacer medium is *crystalline* for x<20Å, while sputtered Si layer is *amorphous* (*a*). Failure to detect oscillations in the AF coupling for thicker Si layers is due to the formation of *a*-Si, as opposed to the crystalline silicide responsible for the coupling.

EXPERIMENTAL REPORT (CONTD.)

INSTRUMENT USED:	DATE OF REPORT:	EXPERIMENT NO.:
POSY	16 Jan 93	1626

TITLE: Examination of U-based multilayers

AUTHORS AND AFFILIATIONS:
G.H. Lander, EITU, T.S. Plaskett, IBM C. Chang G. Felcher, ANL

DATES OF EXPERIMENT: 5-12 Nov. 1992

☒ APPROVED BY PROGRAM COMMITTEE, OR

☐ PART OF INSTRUMENT SCIENTIST ALLOCATION

REPORT RECEIVED:

EXPERIMENTAL REPORT (or Abstract of Publication)

A particularly interesting series of materials have been prepared over the last few years by the group at IBM, Yorktown Heights, using uranium based alloys in thin-film form. The motivation for these studies [1-4] has been to exploit the high anisotropy, and hence the large Kerr effect, known to exist in U-based alloys [5] with the high Curie temperatures available from 3d-transition elements to produce room-temperature materials with a large magneto-optical Kerr effect. These could have potentially interesting technological applications. A great many materials were fabricated over the last 4 years and their optical and bulk magnetic properties examined. Some success has been reported, especially in obtaining large Kerr rotations, but the most successful materials have been the multilayers made recently [3-4] that have, indeed, shown T_C near RT.

Our first experiments on POSY (Nov. 92) were with a thin film consisting of glass /Co (200 Å)/$[U\text{-}As/Co]_n$ with the amorphous U-As layer of thickness 80Å, the Co thickness 20Å, and n=12 repeat layers. Fig. 1 shows the reflectivity for the two spin states for this material. The peak at q ~ 0.029 $Å^{-1}$ corresponds to a multilayer spacing of 108(3) Å, which is close to the intended thickness of 100 Å. The oscillations at small q are the important aspect for the analysis of the polarization, which is shown in Fig. 2. Perhaps the most striking aspect of this figure is the low avergae polarization up to q ~ 0.015 $Å^{-1}$. [At higher values of q the signal is dominated by the Co underlayer] This low value indicates that the net moment in the multilayers is small, suggesting that the U and Co moments are aligned antiparallel. It is known from the optical work that significant moments of ~ 1 μ_B are on both types of atoms.

References:

[1] P. P. Freitas and T. S. Plaskett, Phys. Rev. Letters 64, 2184 (1990)
[2] R. J. Gambino et al., J. Appl. Phys. 69, 4750 (1991)
[3] T. S. Plaskett et al., J. Appl. Phys. 70, 5855 (1991)
[4] T. S. Plaskett et al., (preprint 1992)
[5] W. Reim and J. Schoenes, in "Handbook of Ferromagnetic Materials", North-Holland, Amsterdam, Vol. 5, p. 133

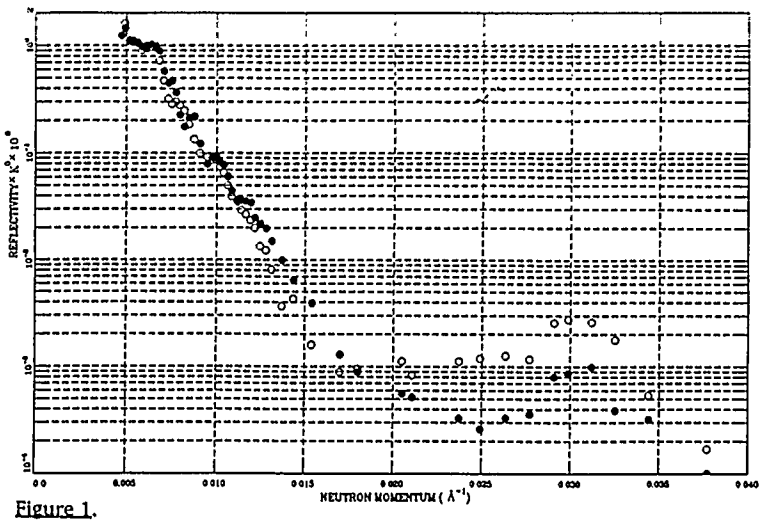


Figure 1.

Reflectivity as a function of momentum transfer for the sample with U-As thickness of 80Å, and n=12 repeats. The different symbols correspond to the different spin states of the neutrons.

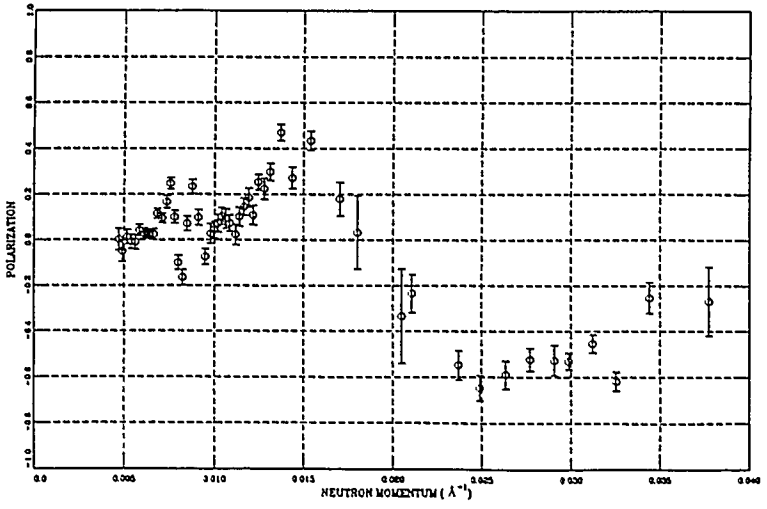


Figure 2.

Polarization of the signal from the multilayer as deduced from Fig. 1

INSTRUMENT USED:	DATE OF REPORT:	EXPERIMENT NO.:
POSY	February 1996	Discretionary

TITLE: Microscopic Observation of the Magnetic Phase Transitions in Gd/Fe Multilayers

AUTHORS AND AFFILIATIONS: M. Loewenhaupt, W. Hahn (IFF), Y.Y. Huang, G.P. Felcher (Argonne National Lab.) and S.S.P. Parkin (IBM Almaden)

DATES OF EXPERIMENT:

CHECK ALL APPLICABLE BOXES:

- ☐ APPROVED BY PROGRAM COMMITTEE
- ☒ INSTRUMENT SCIENTIST ALLOCATION
- ☐ DO NOT PUBLISH
- ☐ PROPRIETARY RESEARCH
- ☐ PRT ALLOCATION

EXPERIMENTAL REPORT (or Abstract of Publication)

Microscopic Observation of the Magnetic Phase Transitions in Gd/Fe Multilayers.* M. LOEWENHAUPT, W. HAHN, IFF, Forschungzentrum Julich, Y.Y. HUANG, G.P. FELCHER, Argonne National Laboratory, S.S.P. PARKIN, IBM Almaden --- At low temperature Gd/Fe multilayers are magnetically ordered. The individual layers of Gd and Fe are ferromagnetic, but the Gd magnetization is opposite to that of Fe. As a result, a sample like [Fe 35 Å/ Gd 50 Å] multilayer is ferrimagnetic with the Gd moments aligned toward a weak magnetic field. Raising of the field is predicted to cause a phase transition from the ferrimagnetic to a twisted configuration which depends on the nature of the atoms in the outermost layer[1]. The spin-dependent reflectivity of a sputtered [Fe 35 Å/ Gd 50 Å]x15 film has been measured with polarized neutrons at 15 K and in magnetic fields up to 0.7 T. The low field measurements were entirely consistent with the ferrimagnetic configuration. As the field is increased, the reflectivity of the front face (Fe-terminated) starts evolving at 0.1T, whilst the reflectivity of the back face (Gd-terminated) remains practically unchanged until 0.5T. More extensive testing is now being made of the validity of the model, by least-square fitting the reflectivity to twisted structure, and by probing the polarization of the reflected neutrons. This should be altered by a twisted configuration of atomic moments.

*Supported by US-DOE, BES-MS contract #W-31-109-ENG-38.

[1]J.G. LePage and R.E. Camley, Phys. Rev. Lett. 65, 1152 (1990)

EXPERIMENTAL REPORT (CONTD.)

INSTRUMENT USED:	DATE OF REPORT:	EXPERIMENT NO.:
POSY	February 1996	Discretionary

TITLE: Magnetic Depth Profile of Fe/Ni Bilayers

AUTHORS AND AFFILIATIONS: Yi Li, C. Polaczyk, F. Klose, Ch. Rehm, H. Maletta and D. Riegel (Hahn-Meitner-Institut) and G.P. Felcher and S. Adenwalla (Argonne National Lab.)

DATES OF EXPERIMENT:

CHECK ALL APPLICABLE BOXES:

- ☐ APPROVED BY PROGRAM COMMITTEE
- ☒ INSTRUMENT SCIENTIST ALLOCATION
- ☐ DO NOT PUBLISH
- ☐ PROPRIETARY RESEARCH
- ☐ PRT ALLOCATION

EXPERIMENTAL REPORT (or Abstract of Publication)

Magnetic Depth Profile of Fe/Ni bilayers

Yi Li, C. Polaczyk, F. Klose, Ch. Rehm, H. Maletta, and D. Riegel
Hahn-Meitner-Institut, Glienicker Straße 100, 14109 Berlin, Germany
andG.P. Felcher and S. Adenwalla
Material Science Division, Argonne Nat. Lab., USA

Abstract. Magnetization measurements of a series of Fe/Ni bilayers were carried out by spin-polarized neutron reflectometry and SQUID magnetometry. The bottom layer of Ni had the same thickness for all samples (140 Å) while the top layer of Fe varied from sample to sample (16-80 Å). The magnetic moment of iron was found to be dependent on the layer's thickness. For Fe layers of 32 Å or less the Fe magnetization was an order of magnitude smaller than that of bulk bcc Fe, indicating that Fe is either in a non magnetic state or that its ordering is antiferromagnetic. For Fe layers of 60 Å or more, the Fe moment was found to be in the plane of the film, constant throughout its entire layer, and with a value (2.0 μ_B/atom) approaching that of bulk iron. This result might be attributed to a structural phase transition from the fcc to the bcc structure.

EXPERIMENTAL REPORT (CONTD.)

INSTRUMENT USED: POSY	DATE OF REPORT: February 1996	EXPERIMENT NO.: Discretionary

TITLE: Oscillatory Interlayer Magnetic Coupling of Sputtered Fe/Nb Superlattices

AUTHORS AND AFFILIATIONS: J.E. Mattson, E.E. Fullerton, C.H. Sowers, Y.Y. Huang, G.P. Felcher and S.D. Bader (Argonne National Lab.)

DATES OF EXPERIMENT:

CHECK ALL APPLICABLE BOXES:

- ☐ APPROVED BY PROGRAM COMMITTEE
- ☒ INSTRUMENT SCIENTIST ALLOCATION
- ☐ DO NOT PUBLISH
- ☐ PROPRIETARY RESEARCH
- ☐ PRT ALLOCATION

EXPERIMENTAL REPORT (or Abstract of Publication)

OSCILLATORY INTERLAYER MAGNETIC COUPLING OF SPUTTERED Fe/Nb SUPERLATTICES*

J.E. Mattson+, Eric.E. Fullerton, C.H. Sowers, Y.Y. Huang, G.P. Felcher

and S.D. Bader

Material Science Division, Argonne National Laboratory, Argonne, IL 60439

The saturation field of sputtered Fe/Nb superlattices oscillates as a function of the Nb thickness, with a periodicity of ~9 Å. In contrast to the case of Fe/Cr superlattices, the concurrent magnetoresistance oscillations were found to be very weak. Yet polarized neutron reflection measurements confirmed that even for the Fe/Nb superlattices with high saturating field the magnetic ground state is of the + - + - type. Neutron and X-rays measurements indicated that, while the crystalline and antiferromagnetic order is well developped along the thickness of the film, the average lateral size of the crystallites (as well as of the magnetic domains) is quite small. This effect (thought to be related to the gross mismatch of the iron and the niobium crystal lattices) may be the cause of the high overall resistance of the material , and its weak dependence from the magnetization.

EXPERIMENTAL REPORT (CONTD.)

INSTRUMENT USED: POSY II	DATE OF REPORT: AUG 1 1992	EXPERIMENT NO.: 1353.

TITLE: POLYMER CHAIN END VS. CHAIN CENTER MOBILITY

AUTHORS AND AFFILIATIONS: G.AGRAWAL, R.P.WOOL (UNIV. OF ILLINOIS)
W.D. DOZIER, G.FELCHER (ANL) T.P. RUSSELL (IBM)

DATES OF EXPERIMENT: 6/5 - 6/8/92, 6/11 - 6/14 192

CHECK ALL APPLICABLE BOXES:

- [X] APPROVED BY PROGRAM COMMITTEE
- [X] INSTRUMENT SCIENTIST ALLOCATION
- [ ] DO NOT PUBLISH
- [ ] PROPRIETARY RESEARCH
- [ ] PRT ALLOCATION

EXPERIMENTAL REPORT (or Abstract of Publication)

From this set of experiments we wanted to find if the centers of a polymer chain followed the chain ends as predicted by the Reptation theory.

Experiments were conducted on HDH/DHD bilayer samples, where HDH represents polystyrene chains deuterated at the centers and DHD represents chains deuterated at the ends. Both the triblock layers were half deuterated. Therefore initially, if the chain ends moved faster than the chain centers, the D concentration would increase in the top layer followed by an equal decrease in the bottom layer. The width of concentration ripple, thus formed at the interface could be observed by Neutron Reflectometry. If the entire chain moved in a Fickian manner, then the initial concentration profile would have been retained. This experiment was different than the other polymer interdiffusion experiments reported in literature. Both Karim [1] and Reiter [2] had followed the interdiffusion distance of the entire chain with time. Their results support the Reptation theory but we hoped that the current experiments would provide a definitive answer.

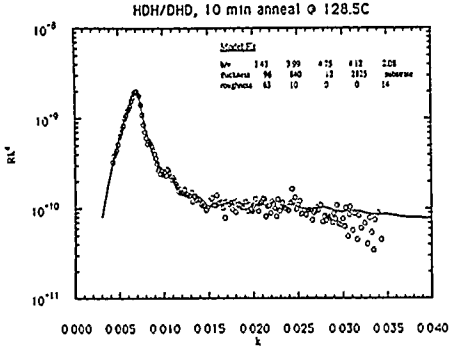
Both the layers had an equal molecular weight of 630K and 50% deuteration. Various annealing times based on an earlier computer simulation study [3] were chosen. The annealing temperature was chosen to be 128.5 °C such that the reptation time was around 24 hrs. Annealing was done under vacuum of 30 in. Hg. Scattering lengths of each layer was determined separately with monolayer samples of individual layers. Sample curves along with the fits are given below in Figures 1-3. It was found that due to end segregation in the top layer, the concentration of ends in the top layer at the polymer interface was less than the ends concentration in the bottom layer. This lead to an asymmetric interface initially (Figures 1-2) which also favors the hypothesis of the chain ends leading the chain centers. Concentration ripple as described earlier forms at higher annealing times (Figure 3).

Our earlier results support the Reptation theory. To completely verify our aim, we would need to do additional experiments. In future it would be of help to (a) use samples with no end segregation, (b) to conduct experiments at annealing times exceeding the Reptation time such that the fickian diffusion could be observed and (c) to use different molecular weight to generalize the results.

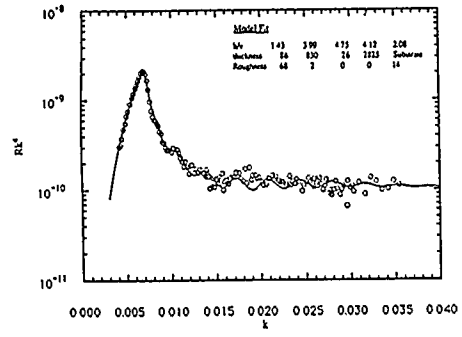
References:
1. A. Karim, Ph.D. Thesis, Northwestern University, 1990.
2. G. Reiter and U. Steiner, J. Phys. II, 1, pp. 659-671, 1991.
3. G. Agrawal, R.P. Wool, W.D. Dozier, T.P. Russell, Bull. of Am. Phys. Soc., 37(1), Q'33 4, 1992.

EXPERIMENTAL REPORT (CONTD.)

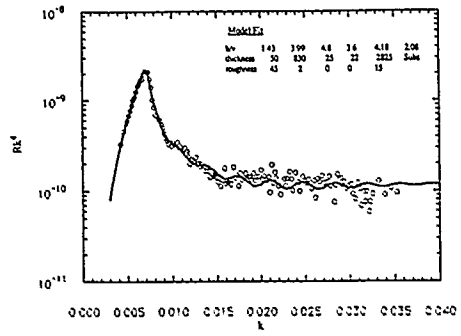
HDH/DHD, 10 min anneal @ 128.5C



HDH/DHD, 90 min anneal @ 128.5C



HDH/DHD, 8 hrs anneal @ 128.5 C



INSTRUMENT USED: POSY - II	DATE OF REPORT: 6/15/93	EXPERIMENT NO: 1714

TITLE: Polymer Chain End Versus Chain Center Mobility: A test of Reptation theory

AUTHORS AND AFFILIATIONS: G. Agrawal & R.P. Wool (UIUC), W.D. Dozier & G.P. Felcher (ANL), T. Russell (IBM)

DATES OF EXPERIMENT: 11/14-17/93 & 12/8-11/93

CHECK ALL APPLICABLE BOXES:

- [x] APPROVED BY PROGRAM COMMITTEE
- [ ] INSTRUMENT SCIENTIST ALLOCATION
- [ ] DO NOT PUBLISH
- [ ] PROPRIETARY RESEARCH
- [ ] PRT ALLOCATION

EXPERIMENTAL REPORT (or Abstract of Publication)

From this set of experiments we wanted to find if the centers of a polymer chain followed the chain ends as predicted by the Reptation theory.

Experiments were conducted on HDH/DHD bilayer samples, where HDH represents polystyrene chains deuterated at the centers and DHD represents chains deuterated at the ends. Both the triblock layers were half deuterated. Therefore initially, if the chain ends moved faster than the chain centers, the D concentration would increase in the top layer followed by an equal decrease in the bottom layer. The concentration ripple, thus formed at the interface could be observed by Neutron Reflectometry. If the entire chain moved in a Fickian manner, then the initial concentration profile would have been retained. This experiment was different than the other polymer interdiffusion experiments reported in the literature. Richter et. al. (neutron spin echo) [1] reported a marked decrease in diffusion at tube length scales but all the observations reported were for times less than the Rouse time, where reptation does not govern the polymer dynamics. Monte-Carlo simulation studies of Skolnick et. al. [2] did not show existence of any tube, while Kremer and Grest [3] reported contrary results, i.e. polymer chains experienced constraints due to a tube.

In our experiments both the layers had an equal molecular weight of about 230K. However the deuteration in HDH and DHD was 50% and 38% respectively. Various annealing times based on an earlier computer simulation study [4] were chosen. The annealing temperature was chosen to be 118 °C such that the reptation time was around 30 hrs. Annealing was done under vacuum of 30 in. Hg. Scattering lengths of each layer was determined separately with monolayer samples of individual layers. Sample curves along with the fits are given below in Figure 1. It was found that at annealing times greater than 7:30 hrs, a component similar to the fickian diffusion between the HDH and DHD had to be added to the rippled concentration profile. The components due to the rippled concentration profiles are shown in Figures 2 and 3..

These results support the existence of the tube and hence the reptation. To completely verify our aim, we would need to extend these measurements to the strongly entangled (M/M_e~35) and to the unentangled regimes (M/M_e~1). The molecular weight (233,000) used in this study is considered weakly entangled (M/M_e~11).

References:
1. D. Richter, R. Butera, L.J. Fetters, J.S. Huang and B. Ewen, *Macromolecules*, 25, 6156 (1992).
2. J. Skolnick, R. Yaris and A. Kolinski, *J. Chem. Phys.*, 88, 1407 (1988); J. Skolnick and R. Yaris, *ibid*, 88, 1418 (1988).
3. K. Kremer and G. Grest, *J. Chem. Phys.*, 92, 5057 (1990).
4. G. Agrawal, R.P. Wool, W.D. Dozier, T.P. Russell, Bull. of Am. Phys. Soc., 37(1), Q'33 4, 1992.

EXPERIMENTAL REPORT (CONTD.)

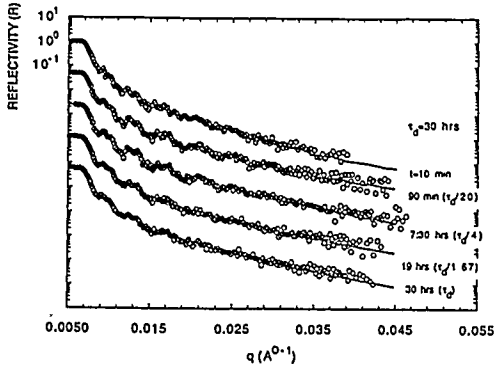


FIGURE 1.

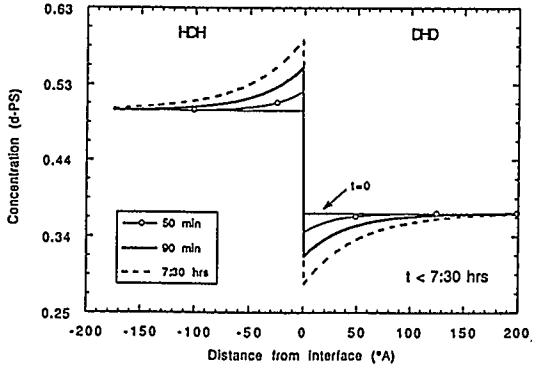


FIGURE 2.

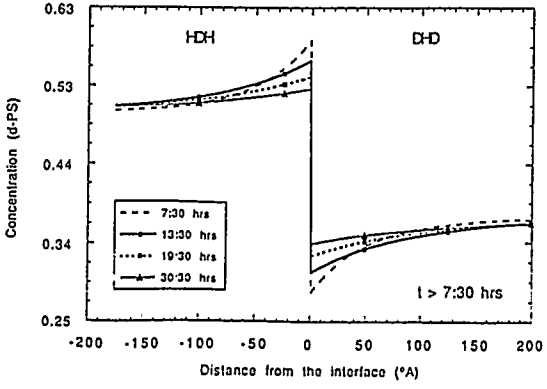


FIGURE 3.

INSTRUMENT USED:	DATE OF REPORT:	EXPERIMENT NO.:
POSY II	1/31/91	1417

TITLE:
Interlayer Diffusion in Langmuir-Blodgett Films

AUTHORS AND AFFILIATIONS:
B. L. Carvalho & S. H. Chen, M.I.T.; W. Dozier and G. Felcher, Argonne Nat. Lab.

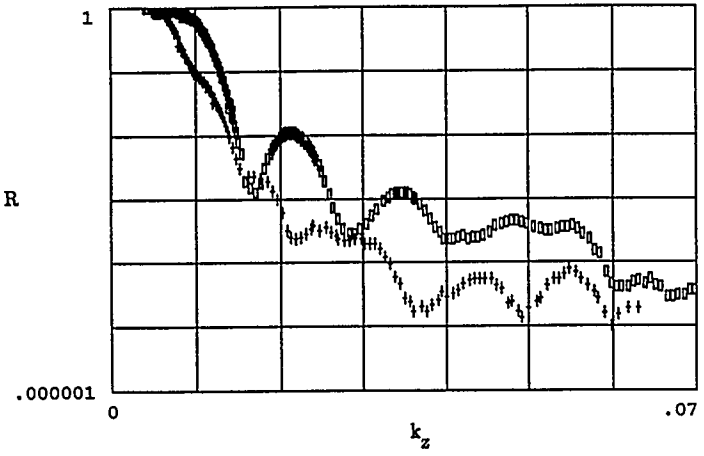
DATES OF EXPERIMENT: 12/1/90 - 12/2/90

☒ APPROVED BY PROGRAM COMMITTEE, OR

☐ PART OF INSTRUMENT SCIENTIST ALLOCATION

REPORT RECEIVED:

EXPERIMENTAL REPORT (or Abstract of Publication)



Neutron reflectivity,R, is plotted as a function k_z for the as–made sample (square) and after a heat treatment of 98° C for 7.5 hours (cross).

The neutron reflection technique was used to study interlayer diffusion in a Langmuir–Blodgett film composed of deuterated and protonated cadmium arachidate. The film was made by depositing 8 layers of protonated cadmium arachidate onto a hydrophyllic silicon substrate; 9 layers of deuterated cadmium arachidate was then deposited onto this protonated layer. When this multilayer film was made the pH of the subphase was held at 6.6; such a pH leads to a cadmium:amphiphile stoichiometry of 1:2. This film and others prepared under the same conditions were uniformly light brown in color. The obtained neutron reflectivity spectra were dominated by specular reflection with little, if any, off–specular scattering. This lack of diffuse scattering in the neutron reflectivity spectra coupled with the even coloring of our films leads us to believe that we can consistently produce films suitable for the neutron reflection technique.

The main result of our November run is shown in the figure below. In this figure, neutron reflectivity, R, is plotted as a function of the z component of the neutron, k, for the as–made sample and for the sample after it was subjected to 98 C for 7.5 hours. The interference fringes for $k < 0.05$ Å^{-1} are primarily the result of the top 9 deuterated layers while the Bragg peak at $k = 0.055$ Å^{-1} is the product of the regular repeat of head groups through the film's thickness. In a first approach to fitting these reflectivity curves we have neglected the effect of the head groups on the refractive index profile and used an error function to model the broadening of the deuterated/protonated interface. This preliminary analysis indicates that the deuterated/protonated interface for the as–made sample has a roughness less than 15 Å and that this interface broadens to over 100 Å after the heat treatment. A crude calculation based on these breadths indicates that the diffusion coefficient is of the order 10^{-17}cm^2/sec. The significant finding that these two experimental reflectivity curves show is that despite the large scale diffusion of amphiphiles the Bragg peak is preserved. This is the first time that interlayer diffusion is shown to exist in a crystalline amphiphilic multilayer system.

This run was cut short by the unexpected shut down of the pulse source. The remaining experiments will be performed in February 1991 and this report will be updated soon after that.

INSTRUMENT USED: POSY II	DATE OF REPORT: 10 November 1995	EXPERIMENT NO.: 2027

TITLE: Neutron Reflectivity Studies of Dry Polymer Brushes

AUTHORS AND AFFILIATIONS: R.J. Composto, R. Oslanec, University of Pennsylvania

DATES OF EXPERIMENT: Sept. 18-22, 1995

☒ APPROVED BY PROGRAM COMMITTEE, OR

☐ PART OF INSTRUMENT SCIENTIST ALLOCATION

REPORT RECEIVED:

EXPERIMENTAL REPORT (or Abstract of Publication)

The adsorption of block copolymers from a homopolymer melt was studied as a function of matrix species and the molecular weight of the non-adsorbing block of a block copolymer using neutron reflectivity (NR). The block copolymer is poly(deuterated styrene - *block* - methylmethacrylate) (dPS-*b*-PMMA) which contains short MMA and long dS blocks. In this report we present neutron reflectivity experiments which provide us with a better understanding of the fundamental behavior of block copolymer adsorption in a melt. Our experiments consist of the following parts:

1) Effect of matrix molecular weight. In this part, the effect of matrix molecular weight on the volume fraction and coverage of adsorbed dPS-*b*-PMMA layer was investigated. The molecular weights of dPS and PMMA blocks were 104,700 and 4,400 g/mol, respectively. For brevity, we refer to this material as the 104K copolymer. The matrix was polystyrene (PS) which represents a nearly neutral environment for the dPS. Molecular weights of PS (Mw) were chosen such that they range from above to below the molecular weight of the dPS block, namely 30,000, 50,000, 90,000, 200,000 and 650,000 g/mol. The copolymer was blended with the matrix polymer in solution such that the volume fraction of the copolymer was 0.05. This value was maintained for all samples in this report. The blend was deposited by spin coating onto Si wafers covered with a thin layer of silicon oxide. Ellipsometry measurements revealed that the film thicknesses ranged from 2200 to 2400Å. The samples were annealed in vacuum oven at 173°C for 5.5 days. Neutron reflectivity experiments were performed at incident angles of 0.25° and 0.65°. Figure 1 shows the reflectivity profiles from the 104K copolymer in a PS matrix having Mw = 30,000 and 90,000 g/mol. This figure shows that an increase in matrix molecular weight results in an increase in reflectivity and a change in reflectivity curve. Similar changes were observed as the matrix molecular weights were varied. These experiments suggest that the matrix molecular weight has a measurable effect on the adsorbed amount and profile shape of the copolymer. Evaluation of the reflectivity profiles is in progress.

2) Effect of the interaction parameter, χ, between matrix and dPS block. In this experiment, the 104K copolymer was blended with poly(styrene-*co*-4-bromostyrene) (PBrS) [1] with 12 molar% of bromostyrene units. The molecular weight of PBrS was 223,700 g/mol [2]) and the χ parameter between dPS and PBrS at T=173°C was 2.1×10^{-3} [3]. The sample was prepared and annealed in the same way as mentioned the in previous section. The thickness of the film was 2200Å as determined from ellipsometry. Figure 2 shows the reflectivity profiles obtained from this 104K copolymer in matrices of PS and PBrS. Clearly, the reflectivity increases upon changing the matrix from neutral to weakly repulsive. This experiment serves as a preliminary test for a more systematic study of the effect of χ on copolymer adsorption. This study is currently underway.

3) Effect of non-adsorbing dPS block length. The dPS-*b*-PMMA with molecular weights of dPS and PMMA of 22,000 and 1,600 g/mol, respectively (22K copolymer), was blended with PS matrix of molecular weight 90,000 g/mol. The sample preparation including annealing was identical to that in section 1. The thickness of the film determined from the ellipsometry was 2380Å. Figure 3 shows a comparison of reflectivity curves obtained from the 104K and 22K copolymers in a PS matrix. Here, the shape of the reflectivity curve changes as one decreases the copolymer Mw. Moreover, the amplitude of interference oscillations is much stronger for low Mw copolymer. These reflectivity experiments are being evaluated. The results will then serve as a starting point for a more systematic study of the effect of the non-adsorbing dPS molecular weight on adsorption.

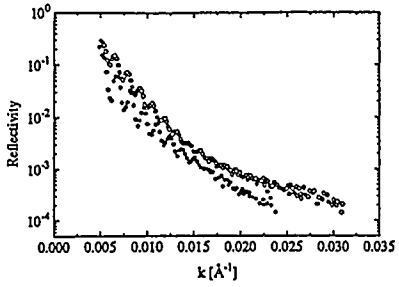


Fig.1 Reflectivity from the 104K copolymer blended with PS of molecular weight 30,000 g/mol (solid circles) and 90,000 g/mol (open circles). Samples were annealed at 173°C for 5.5 days.

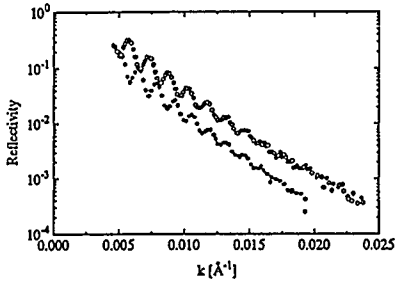


Fig.2 Reflectivity from the 104K copolymer blended with PS of molecular weight 200,000 g/mol (solid circles) and PBrS of molecular weight 223,700 g/mol (open circles). Samples were annealed at 173°C for 5.5 days.

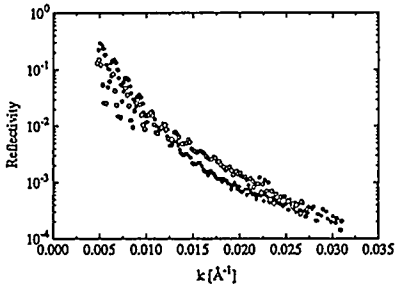


Fig.3 Reflectivity from the 104K (solid circles) and 22K (open circles) copolymers blended with PS of molecular weight 90,000 g/mol. Samples were annealed at 173°C for 5.5 days.

References

[1] PBrS was prepared using a procedure by R.P. Kambour, J.T. Bendler and R.C. Bopp, *Macromolecules*, 16, 753 (1983).
[2] The molecular weight of the PS before bromination was 200,000g/mol which is identical with one of the matrix polymers in sec. 1.
[3] G.R. Strobl and G. Urban, *Coll. Pol. Sci.*, 266, 398 (1988); F. Bruder and R. Brenn, *Macromolecules*, 24, 5552 (1991).

This work was supported by NSF-DMR-PYI Program, Grant 91-58462, NSF MRL Program, Grant 92-20668. NSF/International Grant 94-17523, ACS/PRF Grant 27593AC7 and DOE, Grant W-31-109-ENG-38.

INSTRUMENT USED:	DATE OF REPORT:	EXPERIMENT NO.:
POSY II	14 August 1991	1412

TITLE: Measurement of the Interdiffusion Profile at the Interface between Linear and Cyclic Polystyrene Layers (I)

AUTHORS AND AFFILIATIONS: Russell J. Composto (Univ. of Pennsylvania), Richard S. Stein (Univ. of Massachusetts), G. Hadziiannov (Univ. of Groningen) ~~W. Dozier (ANL)~~

DATES OF EXPERIMENT: April 16-18, 1991

☐ APPROVED BY PROGRAM COMMITTEE, OR

☐ PART OF INSTRUMENT SCIENTIST ALLOCATION

REPORT RECEIVED:

EXPERIMENTAL REPORT (or Abstract of Publication)

Because the adhering and joining of polymers is a diffusion controlled process, the molecular welding of polymer surfaces is of great practical interest. In this report, we limit our study to the early stage of healing where the initial disposition of chain ends at the interface will play an important role. Namely, if reptation is the dominate diffusion mechanism, only those chain ends near the interface can protrude across the boundary and entangle with molecules on the opposite side. To understand the importance of chain ends, we report short-time interdiffusion experiments using the neutron reflectivity technique to study systems of linear and cyclic molecules.

Because chain-end displacements on length scales much less than the molecular size can provide a significant increase in the mechanical resistance to interface separation, techniques with a spatial resolution of 10Å or less are necessary. Karim and co-workers have shown that neutron reflectivity is ideally suited for measuring the narrow concentration gradients which occur during the early stage of healing [1]. Figure 1 shows the reflectivity profile from a linear deuterated polystyrene (DPS) and cyclic polystyrene (CPS) diffusion couple before and after annealing for 7 minutes at 110°C. The molecular weights are 60 000 and 45 000 for the DPS and CPS, respectively. The reptation and Rouse times for the CPS polymer are 114 and 6.5 minutes, respectively. Upon annealing, the amplitudes of the oscillations decrease as a result of the broadening of the initially sharp interface. To test whether the cyclic molecules provide an additional interfacial resistance , a complimentary experiment was performed with a diffusion couple consisting of the same DPS and a linear polystyrene (PS) layer of molecular weight 46 000. As shown in Fig. 2, the amplitudes of the interference oscillations have again decreased after 7 minutes of annealing. However, upon a qualitative comparison, the oscillations appear to be more heavily damped for DPS/PS suggesting a broader interface and hence more interdiffusion in the linear molecule system. Because the linear/linear system has more chain ends available for interdiffusion, these results seem plausible Simulations of the experimental data are in progress. In addition, a comparison of our work with previous studies of the short time interdiffusion of linear systems is desirable [1,2].

[1] A. Karim, Dissertation (Northwestern University, 1990)
[2] T.P. Russell, A. Karim, A . Mansour and G.P. Felcher Macromolecules 21: 1890-93,1988.

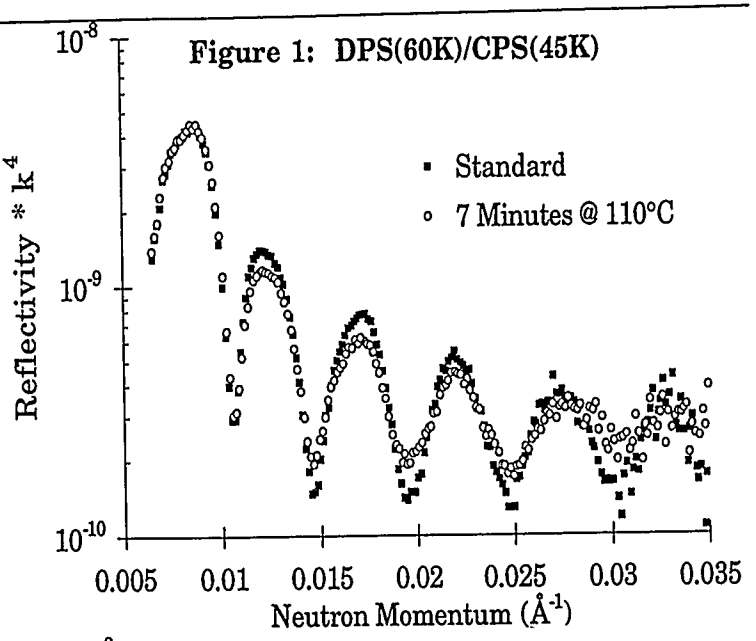


Figure 1: DPS(60K)/CPS(45K)

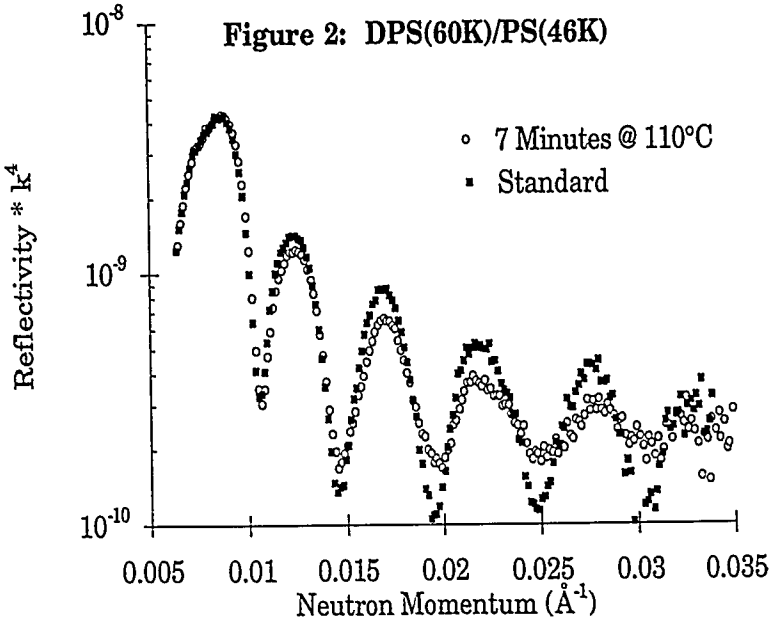


Figure 2: DPS(60K)/PS(46K)

INSTRUMENT USED:	DATE OF REPORT:	EXPERIMENT NO.:
POSY II	22 June 1993	1662

TITLE: Measurement of the Concentration Profiles at the Interface of a Homopolymer/Binary Polymer Mixture

AUTHORS AND AFFILIATIONS: R. J. Composto, A. Faldi, and J. Genzer, University of Pennsylvania; P.Garrett, Monsanto Chemical Co.

DATES OF EXPERIMENT: Feb. 19-22, 1993

☒ APPROVED BY PROGRAM COMMITTEE, OR

☐ PART OF INSTRUMENT SCIENTIST ALLOCATION

REPORT RECEIVED:

EXPERIMENTAL REPORT (or Abstract of Publication)

Using neutron reflectivity (NR) and dynamic secondary-ion mass spectrometry, we found that the interfaces of thin films of poly(styrene-co-acrylonitrile) (SAN) blends are enriched with the lower acrylonitrile component [1]. Following this demonstration of NR's sensitivity to segregation near air/polymer and buried interfaces, a systematic study of DSAN23, containing 23 weight percent AN, and SAN27 blends showed that the surface excess of DSAN23 increases from 15Å to 60Å as the DSAN volume fraction, ϕ, increases from 0.05 to 0.020. Correspondingly, the DSAN23 segregation to the silicon oxide interface increases from 5 Å to 31 Å as ϕ increases from 0.05 to 0.020 [2]. In this report we present neutron reflectivity experiments aimed at understanding and controlling the concentration profiles at polymer surfaces and interfaces in two systems: (i) a copolymer blend of DSAN23:SAN27 containing DSAN23 as the majority component and, (ii) an immiscible system of an SAN blend interfaced with polycarbonate.

Figure 1 shows the reflectivity profile of a DSAN 23:SAN27 blend at ϕ=0.80. The blend was annealed for 3.5 days at 200 °C and had a thickness of 550Å. In agreement with previous experiments [1], the simulated volume fraction profile exhibits DSAN23 enrichment at both the air and substrate interfaces. This simulation also shows that DSAN23, although the majority component, does not the "saturated" the surface. This observation suggests that the chemical potential difference driving DSAN23 to the surface decreases as ϕ increases. Figure 2 shows the derivative of the bare surface energy $df_s/d\phi_1$ as a function of volume fraction of DSAN23. Multiplication of this factor by kT/b^3, where b is the unit cell dimension of the Flory-Huggins lattice, gives the surface energy difference. Note that the surface energy difference for this copolymer system depends more strongly on ϕ_1 than in the DPS:PS system (solid line). Further modelling is in progress.

Figure 3 shows the reflectivity from a tri-layer sample of PC/ DSAN23:SAN27 /PC before and after annealing for 12 hours at 140°C. A DSAN23 volume fraction of 0.18 was chosen so that PC and the SAN blend have the same scattering length densities. This contrast matching dramatically increases the sensitivity of NR to small amounts of interfacial segregation. Moreover, a tri-layer geometry will ensure identical segregation to both polymer interfaces, thus simplifying data analysis.

Before annealing (closed circles) the reflectivity profile is featureless because the PC and SAN have the same neutron refractive index. However, upon annealing, interference maxima and minima appear because of composition changes in the PC and/or SAN layers. PC and DSAN23 have limited solubility (less than 3wt%) and the interfacial width between them is 50Å [4]. Upon adding SAN27 to the DSAN23, the interfacial width should narrow as predicted by fracture toughness measurements which show a maximum adhesion at an AN content of 24% [5]. Moreover, the DSAN23 should enrich the interface just as in the "hard wall" experiments discussed in Fig. 1. Precise analysis of the tri-layer geometry requires revision of existing software and is currently underway. Further experiments on the PC/SAN system are planned.

In conclusion, we have found that the interfacial segregation in copolymer blends depends strongly on the bulk composition. However, even when the lower surface energy polymer is the majority component, the surface is not completely covered by this polymer. A theoretical model is being developed to explain this limitation. Upon replacing the silicon oxide "hard wall" with a polycarbonate "soft wall", reflectivity experiments suggest that segregation to this internal interface occurs. These experiments are of great practical importance because the adhesive strength between multiphase materials is determined by intermolecular penetration.

This work was supported by The Chemical Group of Monsanto Co., NSF (DMR, MRL, and IMR programs) and the Petroleum Research Fund.

EXPERIMENTAL REPORT (CONTD.)

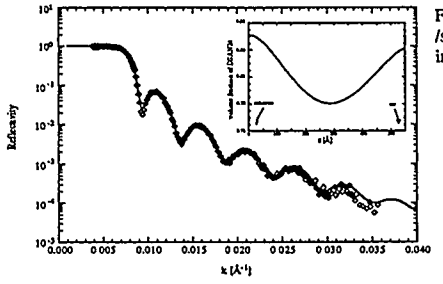


Fig.1 Reflectivity from a DSAN23(0.8): SAN27 /silicon sample after annealing @ 200°C. The inset shows the volume fraction of DSAN23.

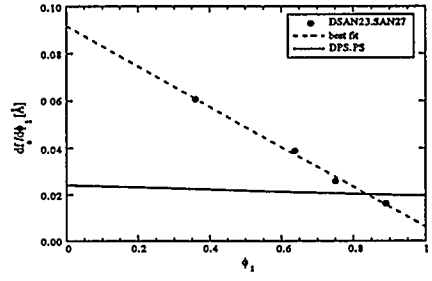


Fig.2 Derivative of bare surface energy with respect to volume fraction DSAN23. The dashed line is best fit where $df_s/d\phi_1$=-0.0855ϕ_1+0.0917. For comparison, data for deuterated polystyrene, DPS, and polystyrene, PS, mixtures is given [3].

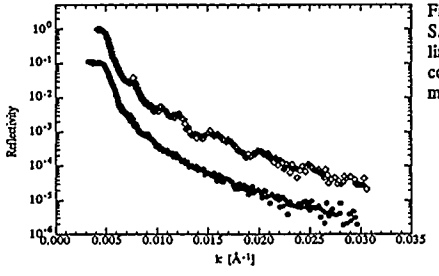


Fig.3 Reflectivity from a PC/DSAN23(0.18): SAN27/PC before (solid circles) and after annealing @ 140 °C (open diamonds). The reflectivity corresponding to the standard sample has been multiplied by 10^{-1}.

[1] Mansfield, T., Stein, R.S., Composto, R.J., Rafailovich, M.H., Sokolov, J., and Schawarz, S.A., *Physica B* 173, 207 (1992).
[2] Mansfield *et al*, in preparation.
[3] Jones, R.A.L., Kramer, E.J., Rafailovich, M.H., Sokolov, J., and Schwarz, S.A., *Phys.Rev.Lett.* 62, 280 (1989).
[4] Mansfield, T., PhD Thesis, University of Massachusetts.
[5] Janarthanan, V., Stein, R.S., and Garrett, P.D., submitted for publication.

INSTRUMENT USED: POSYII	DATE OF REPORT: 6/1/1993	EXPERIMENT NO.: 1633
TITLE: Block Copolymers at Interfaces between Homopolymers by Neutron Reflectometry		
AUTHORS AND AFFILIATIONS: Kevin H. Dai and E. J. Kramer, Dept of Materials Sci. & Eng., Cornell University		
DATES OF EXPERIMENT: 3/12-3/16, 1993		

CHECK ALL APPLICABLE BOXES:

- [x] APPROVED BY PROGRAM COMMITTEE
- [ ] INSTRUMENT SCIENTIST ALLOCATION
- [ ] DO NOT PUBLISH
- [ ] PROPRIETARY RESEARCH
- [ ] PRT ALLOCATION

EXPERIMENTAL REPORT (or Abstract of Publication)

By neutron reflectometry, we have measured the segment density profile of the deuterated polystyrene block of poly(deutero-styrene-b-2-vinylpyridine) (dPS-PVP) diblock copolymers segregating to the interface between the immiscible homopolymer PS and poly(4-vinyl benzoic acid) (PVBA) from the PS homopolymer phase. A layer of PVBA homopolymer was spun onto a silicon substrate, and subsequently coated by a layer of PS homopolymer doped with the dPS-PVP copolymer. The degree of polymerization for the dPS-PVP copolymers used in this experiment are 597–59 and 520–22, respectively. The bilayer specimens with 597–59 and 520–22 diblock copolymers were annealed at 178°C and 156°C, respectively. It should be noted that the annealing temperatures are above the glass transition temperature of PS and dPS-PVP whereas it is well below that of PVBA which is 265°C. By forward recoil spectrometry, we have recently shown that the adsorption of dPS-PVP diblock copolymer to the PS/PVBA interface is greatly enhanced over the segregation to the PS/PVP interface. This enhanced segregation of diblock copolymer is caused by an additional attractive interaction between the PVP block and the PVBA homopolymer resulting from the formation of hydrogen bonds. Figure 1 shows the neutron reflectivity (R) data plotted as Rkz^4 versus kz, where kz is the perpendicular component of the neutron wave vector. The insert shows the scattering length density (b/V) profiles required to generate the fits (solid line in Figure 1). Figure 2 shows the dPS volume fraction versus depth profiles converted from the (b/V) profiles. The width of the dPS block "brush" of the 597-59 and 520-22 copolymers at the PS-PVBA interface are estimated to be $3.4R_g$ and $2.5R_g$, respectively, where R_g is the radius of gyration of the polymer coil representing its size in the un-stretched state. Therefore, the copolymer chains at the PS/PVBA interface are significantly stretched. In addition, the volume fraction of dPS block is nearly equal to one at the interface which indicates the interface is almost totally occupied by the copolymer chains, i.e. very few homopolymer PS chains penetrate to the interface.

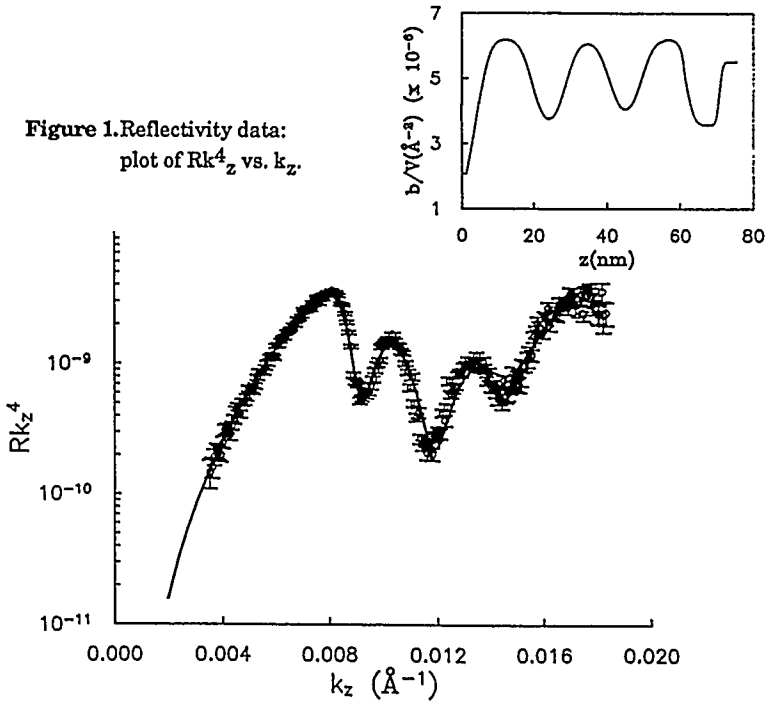
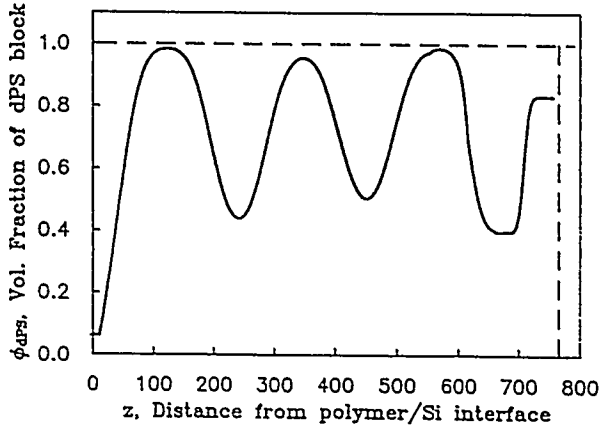


Figure 1. Reflectivity data: plot of Rk^4_z vs. k_z.

Figure 2. Volume fraction vs. depth profile of the dPS block.



INSTRUMENT USED: POSYII	DATE OF REPORT: 6/1/1993	EXPERIMENT NO.: 1634
TITLE: Ordering of a Triblock Copolymer Thin Film		
AUTHORS AND AFFILIATIONS: Kevin H. Dai and E. J. Kramer, Dept of Materials Sci. & Eng., Cornell University		
DATES OF EXPERIMENT: 11/8-11/12, 1993		

CHECK ALL APPLICABLE BOXES:

- [X] APPROVED BY PROGRAM COMMITTEE
- [ ] INSTRUMENT SCIENTIST ALLOCATION
- [ ] DO NOT PUBLISH
- [ ] PROPRIETARY RESEARCH
- [ ] PRT ALLOCATION

EXPERIMENTAL REPORT (or Abstract of Publication)

We have measured the neutron reflectivity of a triblock copolymer thin film to study its ordering phenomena due to microphase separation. The triblock polymer, poly(2–vinylpyridine–b–deutero–styrene–b–2–vinylpyridine)[PVP-dPS-PVP] was synthesized anionically and the degree of polymerization was determined to be 101-577-101. A layer of the triblock copolymer was spun onto a silicon substrate and then annealed at 178°C under vacuum for 5 days. Figure 1 shows the neutron reflectivity (R) data plotted as Rk_z^4 versus k_z, where k_z is the perpendicular component of the neutron wave vector while the insert shows the scattering length density (b/V) profile required to generate the fit (solid line in Figure 1). As seen, the oscillating feature of the neutron scattering length density (b/V) profile indicates the formation of an ordered structure of the triblock copolymer film. We have measured the thickness of this film, i.e. 765Å, using X-ray reflectometry, in collaboration with Rafailovich and Sokolov at SUNY Stony Brook. X-ray reflectometry unambiguously demonstrates that no islands are formed on the air surface of the film; such islands would be formede if the thickness of the film was not "matched" with the microdomain spacing. Figure 2 shows the volume fraction of dPS block versus depth profile converted from the (b/V) profile. This result leads us to conclude that a layer of adsorbed PVP is formed adjacent to the silicon surface and followed by two periods of microphase ordered structure and then a layer of dPS preferentially adsorbed adjacent to the air surface. The microphase structure has been determined to be cylinderical microdomains of PVP in a matrix of dPS by TEM[1]. The morphology revealed by TEM also indicates that the cylinders are not straight, but form a meander structure within the plane of the film. This observation provides an explanation for the observed dPS volume fraction in the PVP-rich layer, i.e. ~0.4-0.5, which would be too high for a perfect microphase structure consistenting of straight cylinders. The spacing between the cylinderical microdomains along the direction normal to the surface is estimated to be approximately 210Å, again consistent with our observations of island formation as a function of film thickness[2] by atomic force microscopy.

Reference:

1. Y. Liu, W. Zhao, X. Zheng, A. King; A. Singh, M. H. Rafailovich, J. Sokolov, X. Zhao, K. H. Dai, E. J. Kramer, S. A. Schwarz, *Bull. Amer. Phys. Soc.*, 38, 409 (1993).
2. W. Zhao, Y. Liu, X. Zheng, M. H. Rafailovich, J. Sokolov, X. Zhao, K. H. Dai, E. J. Kramer, S. K. Singh, R. Plano, S. A. Schwarz, *Bull. Amer. Phys. Soc.*, 38, 295 (1993).

Figure 1. Reflectivity data: plot of Rk^4_z vs. k_z.

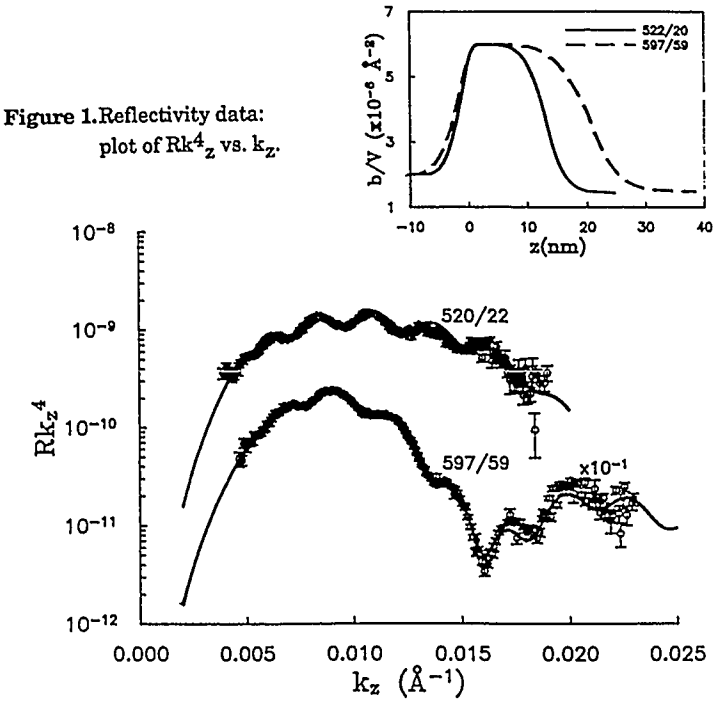
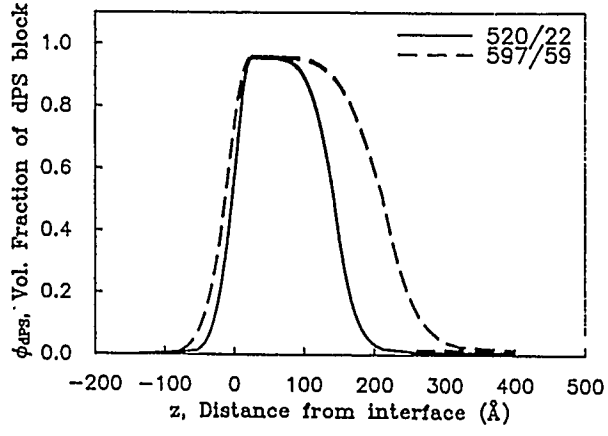


Figure 2. Volume fraction vs. depth profile of the dPS block.



INSTRUMENT USED: POSY II

DATE OF REPORT: 8/2/91

EXPERIMENT NO: 1467

TITLE: Neutron Reflectometry Study of Diblock Copolymer to the Interface between Homopolymers

AUTHORS AND AFFILIATIONS: K.H. Dai, L.J. Norton, E.J. Kramer (Cornell U)

DATES OF EXPERIMENT: 5/14-5/18

_APPROVED BY PROGRAM COMMITTEE, OR

_PART OF INSTRUMENT SCIENTIST ALLOCATION

REPORT RECEIVED:

EXPERIMENTAL REPORT (or Abstract of Publication)

Utilizing neutron reflectometry, we have measured the segment density profile of the deuterated polystyrene (dPS) block in a dPS-poly(2-vinylpyridine) (PVP) diblock copolymer at the interface between immiscible homopolymer PS and PVP. The samples were made by spin-casting a layer of PVP homopolymer on a silicon substrate, and subsequently spin-casting a second layer of PS homopolymer doped with various concentrations of the dPS-PVP copolymer. The bilayer specimens were then annealed at 178°C to allow equilibrium segregation of the diblock copolymer to the interface to occur. The initial concentration of diblock copolymer was varied so that six samples spanning a ϕ_∞, volume fraction of diblock copolymer remaining in the PS homopolymer phase after segregation, range from 0.004 to 0.1 were produced. Because of its superior depth resolution (~5Å), neutron reflectometry provides the capability to reveal the density profile near the buried interface [1]. The neutron reflection results for the sample with ϕ_∞=0.025 are shown in Figure 1 as a plot of Rk^4 versus k, where k is the perpendicular component of the neutron wave vector . The insert shows the scattering length density profile required to generate a best fit (solid line) to the reflectivity data at these angles. The dPS volume fraction profile (solid line) corresponding to the scattering length density profile is shown in Figure 2 with the profile (dashed line) predicted from a self-consistent mean field theory (SCMF) [2]. The interaction parameter χ for the theory was established by fitting to the segregation isotherm measured by forward recoil spectrometry [3,4]. As seen in Figure 2, the shape of the measured dPS profile is similar to the profile predicted by the SCMF except that the measured profile is broadened at the interface relative to the SCMF prediction. This excess broadening is observed for all ϕ_∞'s. We believe that most of this interface broadening is due to the apparent roughness of the equilibrium interface encouraged by the decrease in interfacial tension accompanying the copolymer segregation.

Reference:

1. Russell, T.P.; Anastasiadis, S.H.; Menelle, A.; Felcher, G.P.; Satija, S.K., Macromolecules, 1991, 24, 1575.
2. Shull, K.R.; Kramer, E.J., Macromolecules, 1990, 23, 4769.
3. Shull, K.R.; Kramer, E.J.; Hadziioannou, G.; Tang, W., Macromolecules, 1990, 23, 4780.
4. Dai, K.H.; Kramer, E.J.; Shull, K.R., Macromolecules in press.

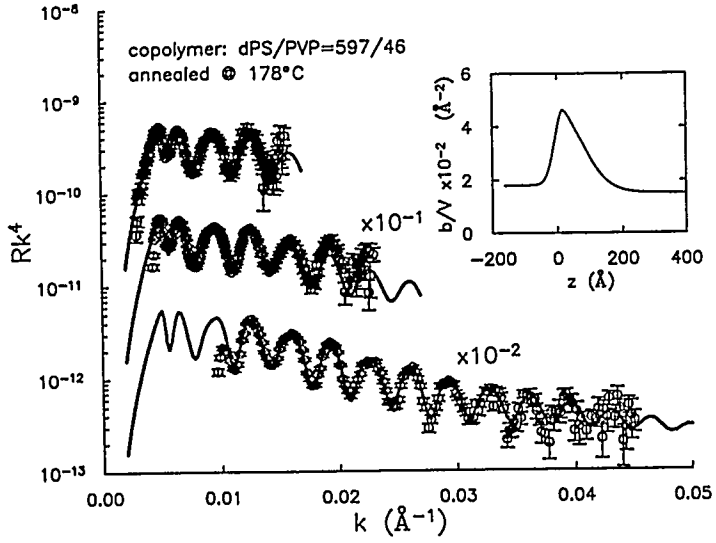


Fig.1 Reflection spectrum: Rk^4 vs. k

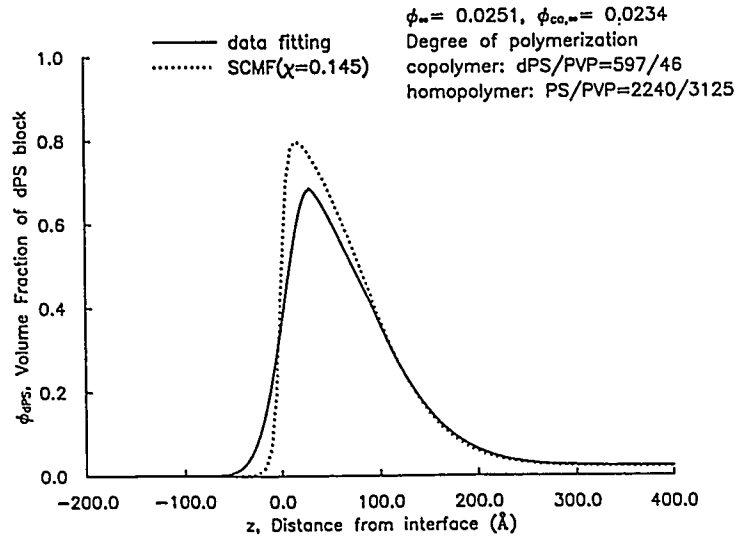


Fig.2 Concentration profile of deuterated PS block

INSTRUMENT USED: POSY II | DATE OF REPORT: 8/3/92 | EXPERIMENT NO: 1569

TITLE: Neutron Reflectometry Study of Diblock Copolymer to the Interface between Homopolymers

AUTHORS AND AFFILIATIONS: K.H. Dai, L.J. Norton, E.J. Kramer, J.M.J.Frechet (Cornell U)

DATES OF EXPERIMENT: 5/7-5/12

_APPROVED BY PROGRAM COMMITTEE, OR

_PART OF INSTRUMENT SCIENTIST ALLOCATION

REPORT RECEIVED:

EXPERIMENTAL REPORT (or Abstract of Publication)

Utilizing neutron reflectometry (NR) [1], we have measured the segment density profile of the deuterated polystyrene (dPS) block in a dPS-poly(2-vinylpyridine) (PVP) diblock copolymer at the interface between immiscible homopolymer PS and poly(4-vinyl benzoic acid) (PVBA). A layer of PVBA homopolymer was spun onto a silicon substrate, and subsequently coated by a layer of PS homopolymer doped with the dPS-PVP copolymer. The bilayer specimens were then annealed at 178°C to allow the segregation of the diblock copolymer to the interface to achieve equilibrium. We have recently measured the adsorbed amount of the copolymer at the PS-PVBA interface by forward recoil spectrometry (FRES). Results show a remarkable increase in the areal density Σ of diblock copolymer as compared to that at the corresponding PS-PVP interface. This enhanced adsorption is caused by an attractive interaction between the PVP block and the PVBA homopolymer due to hydrogen bond formation. In general, increasing Σ increases the fracture toughness G_c of the interface because more chains need to be broken during fracture. However, increasing Σ to large value may cause the copolymer blocks to stretch significantly. This stretching in turn may decrease the entanglement between the blocks and the homopolymer, leading to a saturation or even a decrease in G_c.[2] Figure 1 shows the neutron reflectivity (R) data plotted as Rk^4 versus k, where k is the perpendicular component of the neutron wave vector while Figure 2 shows the scattering length density profile required to generate this fit (solid line in Figure 1) with the corresponding profile for the same block copolymer at PS-PVP interface shown as a dashed line. Three conclusions can be drawn: (1) The width of the dPS block "brush" at the PS-PVBA interface is nearly 3 times larger than that at the PS-PVP interface. (2) The interface between the stretched chains in the dPS brush and the PS homopolymer is sharper in the PS-PVBA case and in fact almost as sharp as the dPS distribution at the interface between PS and PVBA. (3) The maximum scattering length density at the PS-PVBA interface is very close that of dPS which indicates the interface is almost totally occupied by the copolymer chains, i.e. very few homopolymer PS chains penetrate to the interface.

Reference:

1.Russell, T.P.; Anastasiadis, S.H.; Menelle, A.; Felcher, G.P.; Satija, S.K., Macromolecules, 1991, 24, 1575.

2.Wahiyama, J.; Creton, C.; Kramer, E. J., submitted for publication.

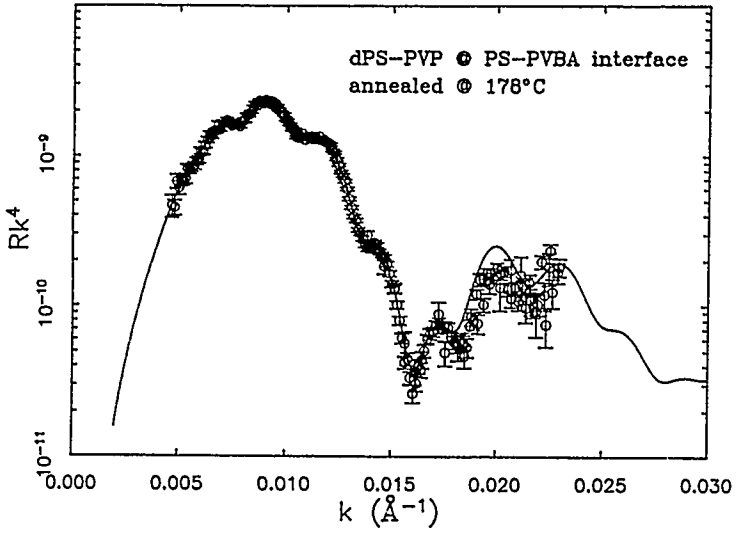


Figure. 1 Reflection spectrum: Rk^4 vs. k

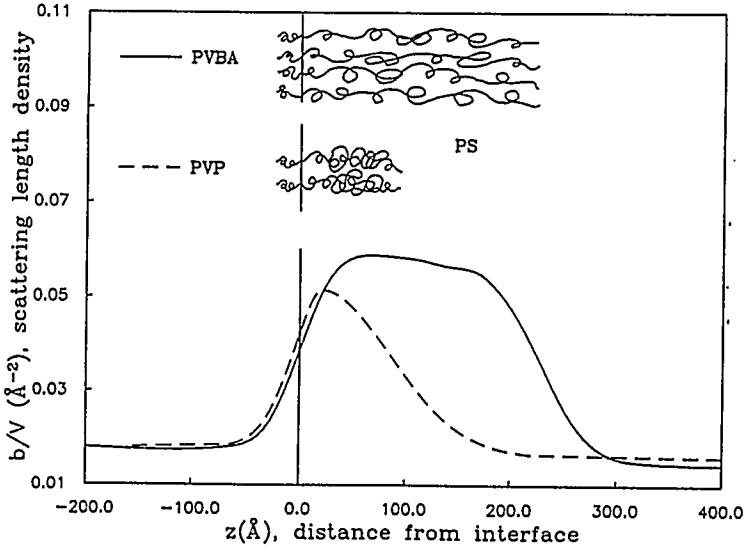


Figure.2 Scattering length density profile at the PS-PVP (dashed line) and PS-PVBA (solid line) interfaces.

INSTRUMENT USED:	DATE OF REPORT:	EXPERIMENT NO.:
POSY II	February 1996	Discretionary

TITLE: Hydrogen Segregation at the Al/Si Interface, as Probed by Neutron Relection

AUTHORS AND AFFILIATIONS: W. Dozier, Y.Y. Huang and G.P. Felcher (Argonne National Lab.)
A.D. Marwick, IBM, Yorktown Heights

DATES OF EXPERIMENT:

CHECK ALL APPLICABLE BOXES:

- ☐ APPROVED BY PROGRAM COMMITTEE
- ☐ PROPRIETARY RESEARCH
- ☒ INSTRUMENT SCIENTIST ALLOCATION
- ☐ PRT ALLOCATION
- ☐ DO NOT PUBLISH

EXPERIMENTAL REPORT (or Abstract of Publication)

Hydrogen Segregation at the Al/Si (111) Interface, as probed by Neutron Reflection* W. DOZIER, Y.Y. HUANG and G.P. FELCHER, Argonne National Laboratory, A.D. MARWICK, IBM Yorktown Heights Neutron reflection is an excellent probe to measure the profile of hydrogen segregated at a buried interface Al/Si. This is because the refractive index, n, of Al is undistinguishable from that of Si. n-1 is -5.32×10^{-6} and -5.30×10^{6} for Al and Si respectively for 4.0 Å neutrons, whereas for hydrogen $n-1=3.82 \times 10^{6}$ at liquid hydrogen density ($0.07 g/cm^3$). Even a small amount of hydrogen excess at the Al/Si interface creates an optical gap, which dramatically alters neutron reflectivity. Measurements were done on two aluminum films, 1670 Å thick, epitaxially deposited on the (111) surface of a polished Si single crystal. One of the samples was kept as standard; the other was charged with a dose of 10^{16} hydrogen atoms/cm^2. The reflectivity of the standard was a smooth function of the momentum transfer, agreeing well with that expected for an Al film on Si except for a thin (~20Å) oxidized layer. The reflectivity of the charged sample showed the characteristic interference pattern of neutrons reflected from the surface and the Al/Si interface. Best fitting was obtained by setting a concentration of 0.13 H/Al at the interface. Hydrogen is contained in a slab, 60 Å thick, at the interface; on the aluminum side, the H content is graded approximately like an error function with half-thickness of 30 Å. The uncertainty of these values is less than 20%.

EXPERIMENTAL REPORT (CONTD.)

INSTRUMENT USED:	DATE OF REPORT:	EXPERIMENT NO.:
POSY II	February 1996	Discretionary

TITLE: Topology of Forward Scattering of Neutrons from Imperfect Multilayers

AUTHORS AND AFFILIATIONS: G.P. Felcher and R.J. Goyette (Argonne National Lab.), S. Anastasiadis and T.P. Russell (IBM) and M. Foster and F. Bates (University of Minnesota)

DATES OF EXPERIMENT:

CHECK ALL APPLICABLE BOXES:

- ☐ APPROVED BY PROGRAM COMMITTEE
- ☒ INSTRUMENT SCIENTIST ALLOCATION
- ☐ DO NOT PUBLISH
- ☐ PROPRIETARY RESEARCH
- ☐ PRT ALLOCATION

EXPERIMENTAL REPORT (or Abstract of Publication)

EXPERIMENTAL REPORT (CONTD.)

Topology of forward scattering of neutrons from imperfect multilayers

G.P. Felcher and R.J. Goyette
Argonne National Laboratory, Argonne IL 60439
S.Anastasiadis* and T.P. Russell
IBM Almaden Research Center, San Jose CA 95120
M.Foster** and F. Bates,
Dept. of Chemical Engineering, University of Minnesota, Minneapolis MN 55455

Neutrons sent at grazing incidence on imperfect multilayers of polymers are scattered both out of and within the plane of reflection. In the latter geometry the scattered intensity is highly structured in two series of ridges, whose loci can be labelled in terms of the neutron momenta. Intersecting ridges show evidence of mode coupling. Similar topology is expected for X-rays scattering.

INSTRUMENT USED:	DATE OF REPORT:	EXPERIMENT NO.:
POSY II	11/8/95	2102

TITLE: Investigation of Density Variation and Pore Formation in Thin "Nanofoam" Films by Neutron Reflectivity

AUTHORS AND AFFILIATIONS: Jeffrey S. Fodor, University of Maryland College Park, Robert M. Briber, University of Maryland College Park, Thomas P. Russell, IBM Corporation

DATES OF EXPERIMENT: 10/27/95 - 10/39/95

CHECK ALL APPLICABLE BOXES:

- [X] APPROVED BY PROGRAM COMMITTEE
- [ ] PROPRIETARY RESEARCH
- [ ] INSTRUMENT SCIENTIST ALLOCATION
- [ ] PRT LOCATION
- [ ] DO NOT PUBLISH

EXPERIMENTAL REPORT (or Abstract of Publication)

Low dielectric constant nanofoam materials are produced by spin casting thin uniform films of tri-block copolymers, consisting of a poly-amic-acid center block and two polypropylene oxide (PPO) end blocks onto a substrate. Thermal treatment under an oxygen free atmosphere effectively converts the poly-amic-acid block into a stable polyimide. Subsequent thermal treatment in air results in decomposition of the polypropylene oxide end blocks into low molecular weight products that diffuse out of the polyimide matrix, resulting in voids typically on the order of 5-80 nm in size [1-4]. The morphology and pore structure of the foamed material is a very important consideration in relation to performance of the final product. Ideally, the average density of the film would be uniform thoughout its depth, however, substrate/polymer interactions and the processing steps described above have the potential of causing density variation across the sample thickness. Characterization of the unfoamed and foamed material as well as the effects of imidization and foaming on morphology and structure is a key issue in the development and improvement of these materials.

This report briefly summarizes very recent neutron reflectivity experiments on thin film fluorinated polyimide/polypropylene oxide triblock copolymer nanofoams as a function of thermal foaming, and film thickness. The experiments were conducted on the instrument, POSY II, at the Intense Pulsed Neutron Source. Two modes of data collection were attempted: 1) a batch type foaming process, where the samples were removed from the reflectometer between measurements and foamed at 300 °C in air for cumulative lengths of time, and 2) and in-situ process, where data acquisition occurred concomitantly with the foaming process at 220 °C (The lower temperature was used in an attempt to obtain reasonable time resolution between acquired reflectivity data sets.) Both modes proved to be reasonable, however, due to time constraints only a limited amount of data was collected using the latter mode of operation.

Two thicknesses were considered, thin (910 Å) and thick (9730 Å) films, in an attempt to discern the effects of thickness on the foaming process. The measured reflectivity as a function of foaming time (time spent at 300 °C in air) for the two thicknesses considered, are plotted in Figures 1 and 2. Clearly, there are dramatic changes taking place, the most evident occurring within the first hour of the foaming process. In the thinner film (Figure 1) the data seem to indicate a moderate thinning of the film accompanied by an overall change in the average scattering length density profile, and a shift of the critical angle to slightly larger k values. In the thicker film (not shown) equally dramatic changes take place. Again there is a shifting of the critical angle to larger k values, while at high k values there is clearly a decrease in the magnitude of the reflectivity. The data acquired by the in-situ mode of collection, show very similar behavior.

Presently, a very limited amount of data analysis has be undertaken, however, our initial modeling of the unfoamed thin (910Å) sample has indicated that the reflectivity cannot be described by a simple uniform average scattering length density profile across the film thickness, even if we assume the presence of an oxide layer on the substrate surface. (Prior to spinning the film the Si wafers were etched using a buffered hydrofluoric acid solution which should have removed any oxide layer that might have existed.) The data for the unfoamed 910Å film is plotted in Figure 2, along with a preliminary first model of the reflectivity as determined by the profile indicted in the inset of the Figure. Clearly, refinement to the model needs to be undertaken. However, assuming that this

model is reasonable and recalling that this is the unfoamed material, it appears that a non- uniform scattering length density profile exists prior to foaming. Such a non-uniformity may arise either from the imidization process or preferential interactions between the substrate and one of the copolymer blocks. Further analysis of the data and future experimentation is needed to clarify these issues.

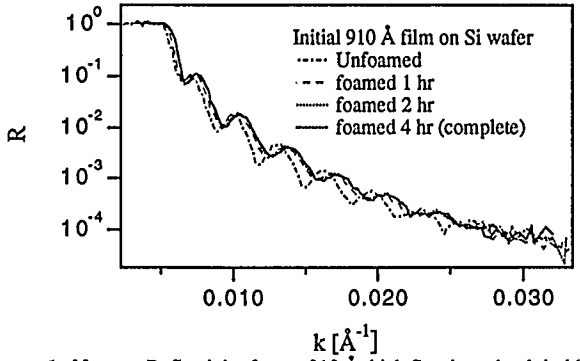


Figure 1. Neutron Reflectivity from a 910 Å thick fluorinated polyimide / PPO triblockco-polymer film after foaming for increasing lengths of time (indicated in the legend)

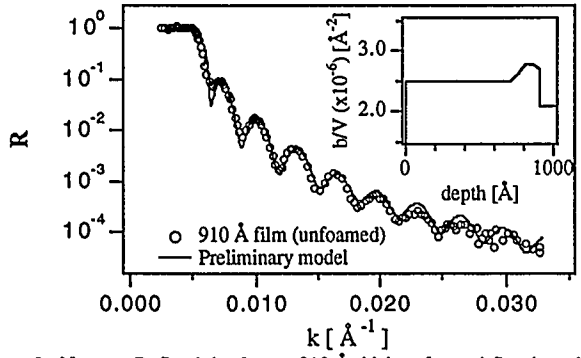


Figure 2. Neutron Reflectivity from a 910 Å thick unfoamed fluorinated polyimide / PPO triblock co-polymer film along with a very initial model of the reflectivity. The model is based on the scattering length profile given in the inset of the Figure.

References

1. Hedrick, J. L.; Labadie, J. W.; Russell, T. P.; Palmer, T. *Polymer*, **1991**, 32, 950.

2. Hedrick, J. L.; Labadie, J. W.; Russell, T. P.; Hofer, D. C.; Wakharkar, V. *Polymer*, **1993**, 34, 4717.

3. Charlier, Y.; Hedrick, J. L.; Russell, T. P.; DePietro, R. *Polymer Preprints (Am Chem. Soc., Div. Polym. Mater. Sci. Eng.)* **1995**, 72, 389.

4. Carter, K. R., et. al. *Polymer Preprints (Am. Chem. Soc., Div. Polym. Mater. Sci. Eng.)* **1995**, 72, 383.

INSTRUMENT USED:	DATE OF REPORT:	EXPERIMENT NO.:
POSY 2	2 Aug 1991	1464

TITLE:

Surface segregation of polymer chains due to molecular weight effects

AUTHORS AND AFFILIATIONS:
Arvind Hariharan, Sanat Kumar, Dept. of Polymer Science, Penn State University)
Thomas P. Russell (IBM, Almaden Research Center, San Jose)

DATES OF EXPERIMENT: May 14-16, May 18-21

☐ APPROVED BY PROGRAM COMMITTEE, OR

☐ PART OF INSTRUMENT SCIENTIST ALLOCATION

REPORT RECEIVED:

EXPERIMENTAL REPORT (or Abstract of Publication)

INTRODUCTION

In the past[1,2] we reported neutron reflectivity measurements on the surface behavior of blends of deuterated and protonated polystyrene of disparate molecular wights, at an overall composition of 50%. The results of the experiments showed that when the molecular weight of the deuterated component (PSD) was fixed, and the shorter chain was the protonated component (PSH) in the blend, the PSH partitioned preferentially to the air surface if its molecular weight was smaller than a certain critical value. On the other hand, a significant enhancement of the deuterated component to the air surface was observed when the PSH molecular weight in the blend exceeded this critical value, this result being consistent with the earlier findings of Jones *et al.*[3]

Frequently, the anionic synthesis of polystyrene standards is performed by using *sec*-butylithium as the initiator causing the first unit in the chain to be a *sec*-butyl group. Similarly, the termination of the living polymer chain in such a synthesis is accomplished by using any one of a variety of terminating agents which, in general, again cause the other end to be usually different from the middle segments. In addition, initiators and terminators that are protonated are normally used in the synthesis of the deuterated component. In the first set of experiments that were performed[1,2] (which we will refer to as set I) all the samples that were used were synthesized by using *sec*-butylithium as the initiator and methanol as the terminator. It is well known that energetic effects arising from differences in the chemical nature of the units making up the ends of a polymer chain versus the internal repeat units could cause significant perturbations to the macroscopic properties of a polymer. The set of experiments that we report here (which we will refer to as set II) were devoted to the study of the isotope effect in polymer blends whose ends were made to be chemically similar to those in the middle of the chain. *"Properly" endcapped samples were therefore used in these experiments to confirm that the observed crossover in the type of component that partitioned preferentially to the surface was not driven by chain end energetic effects.* These polystyrene samples were synthesized anionically by using benzyl potassium as the initiator and methanol as the terminator so that both ends of the chain were similiar to the repeat units in middle of the chain.[4] For the deuterated component, per-deuterated counter-parts of the initiator and the terminator were used. This ensured that both the components in the blend had completely symmetric structures.

RESULTS AND DISCUSSION

Thin films of blends of deuterated and protonated polystyrene were spin-coated from toluene onto silicon surfaces and annealed for 5 days at 433 °C. The PSD molecular weight was fixed at 551K (DP=5298) for all the samples and the PSH molecular weight was allowed to vary from 12K (DP=115) to 169K (DP=1625). The compositions of all the films were fixed at 50% by weight. The reflectivity from each of these samples was measured and analyzed by fitting to an exponential concentration profile from the air surface by minimizing χ^2 (which took values of the order of *ca.* 9 for good fits).

In Figure 1 the volume fraction of the deuterated component (ϕ) is plotted as a function of the degree of polymerization (DP) of the protonated chains in the blend. The circles in the Figure refer to experiment set I while

the squares refer to set II.[1,2] The line passing through the points describes the general trend that has been observed and is not quantitative. The dotted line in the Figure at a composition of 0.5 denotes the bulk volume fraction of all the samples and deviations of the data points from this line represent a segregation or depletion of the deuterated component at the air surface.

The main observations and conclusions that one can draw from this Figure are summarized below.

1. The deuterated component is depleted from the air surface due to the corresponding preferential paritioning of the protonated component when its DP is lower than 471 (MW=49K). This partitioning is highest for the lowest DP of the PSH (=115) that was considered.

2. As the PSH chain length is increased, a concomitant increase in the surface volume fraction (ϕ) of the deuterated component is observed leading to a situation where at the highest DP of 1625, there is a significant segregation of the segments of the deuterated polymer to the air surface.

3. The most important observation of this study is made by comparing the curve corresponding to set I to that corresponding to set II. One can immediately see that identical trends are observed in the variation of Φ as a function of the DP of the PSH. In addition, the DP of the PSH at which no preferential segregations occur is at a value of *ca.* 500 for both sets of experiments. This suggests that any energetic differences between the *sec*-butyl groups which formed the end of the polymer chains in the samples used in set I and the middle (styrene) repeat units were insignificant in modifying the surface properties of the blend. One can thus conclude that the observed crossover in the type of component that segregated to the air surface was driven purely by the effect of chain length differences between the components in the blend and the isotope effect, and not by any chain end energetic effects.

REFERENCES

1. Kumar, S.K.; Russell, T.P. *IPNS Report* # (1299).
2. Hariharan, A.; Kumar, S.K.; Russell, T.P *Bulletin of the American Physical Society*, March, 1991.
3. Jones, R.A.L.; Kramer, E.L.; Rafailovich, M.L.; Sokolov, J.; Schwarz, S.A. *Phys. Rev. Lett.*, 1989, 62, 2801.
4. Bucca, D.; Gordon, B. Submitted to *Macromolecules* 1991.

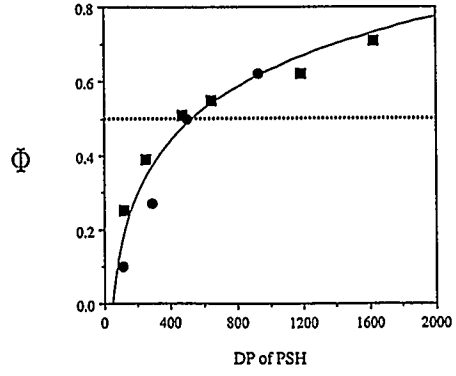


Figure 1. Variation of the volume fraction of the deuterated polystyrene (ϕ) (longer chains) at the air surface as a function of the degree of polymerization of the protonated polystyrene (shorter chains). The circles and the squares refer to set I and set II respectively. The line describes the general trend and is not quantitative.

INSTRUMENT USED: POSY 2	DATE OF REPORT: 12/3/95	EXPERIMENT NO.: 2153

TITLE: Neutron Reflectometry Study of Hydrogen absorption by Metal Films

AUTHORS AND AFFILIATIONS: Brent J. Heuser, Alan E. Munter, Neil R. Guillermo, Univ. IL, Dept N.E.

DATES OF EXPERIMENT: Nov. 15-19, 1995

CHECK ALL APPLICABLE BOXES:

- [x] APPROVED BY PROGRAM COMMITTEE
- [ ] INSTRUMENT SCIENTIST ALLOCATION
- [ ] DO NOT PUBLISH
- [ ] PROPRIETARY RESEARCH
- [ ] PRT ALLOCATION

EXPERIMENTAL REPORT (or Abstract of Publication)

Successful *in situ* neutron reflectivity measurements of hydrogen and deuterium absorption in Pd thin films from the gas phase were performed on POSY 2 in November of 1995. The Pd depositions were magnetron sputtered onto polished 3 mm thick Si single crystal substrates. The films were held at constant gas pressure during NR measurements in the POSY 2 environmental cell. These experiments were motivated by the believe that neutron reflectometry could provide accurate measurements of hydrogen profiles in metal thin films. This believe is confirmed by the observations presented below.

Figure 1 shows the reflectivity measurement of a 500 Å Pd film exposed to 1 atm. of D_2 gas at approximately 300 K. Also shown is a measurement of the same Pd film before deuterium absorption, with the data terminated beyond 0.022 1/Å for a more clear presentation. The most noticeable effect is the shift of the critical edge to higher k_z. The shifting of the critical edge is the result, we believe, of deuterium absorption into the Pd thin film. This absorption increases the overall scattering length density of the 500 Å film (both D and Pd have positive scattering lengths, while the scattering length of H is negative) and extends the range of total reflection out to higher k_z.

Another effect of deuterium absorption is a slight dampening of the thickness interference oscillations, most noticeable at high k_z. At first thought this dampening might seem counter-intuitive and in contradiction of the observed higher critical edge. The interference oscillations would have been strengthened only if the absorbed deuterium concentration profile did not vary significantly with depth. The fact that the oscillations were weakened implies a non-uniform deuterium depth profile.

The deuterium depth profile, obtained from a best fit of the data in Fig. 1 using a genetic algorithm, is shown in Fig. 2. (The fit corresponding to this profile is shown in Fig. 1.) Also shown in Fig. 2 is the hydrogen concentration depth profile determined from an *in situ* neutron reflectivity measurement with the same Pd deposition. The Pd film was exposed to 60 torr H_2 gas at 300 K in this case. The two profiles share a few similarities. First, they indicate that both deuterium and hydrogen are excluded from the Pd/Si interface (at a depth of zero in Fig. 2). This exclusion extends in each case out to approximately 200 Å from the interface or approximately a third of the film. We believe this is the result of the Pd film being constrained at the interface, thereby limiting the lattice expansion required for hydrogen and deuterium uptake. Secondly, both concentration profiles exhibit a peak in the mid- to upper-half of the film. Finally, the concentration at the peak of the profiles are found to be similar, 0.8 D/Pd and 0.6 H/Pd. For reference, the minimum concentration of the hydride phase in Pd is 0.6 H (or D)/Pd. We believe, therefore, that the film may have undergone the hydride phase transformation during each absorption, at least in the region near the peak of the concentration profile.

The fact that the two concentration profiles are very similar (similar in the sense that the two profiles are approximate mirror images about the bulk Pd Nb value) gives us confidence that the profiles in Fig. 2 are physically meaningful. Hydrogen and deuterium should follow the same profile once equilibrium is reached, assuming the chemical potentials of the gas phase in each case are equal and that the film is not damaged from one measurement to the other. Actually, we cannot accept either of these assumptions. Although the chemical potentials of H and D with respect to bulk Pd are known, the solubility law is certainly altered in thin-film geometry. At the high gas pressures involved here, 1 atm. D_2 and 60 torr H_2, we do believe, though, that the system is beyond the two-phase co-existence region of the phase diagram, even in thin-film geometry. This is confirmed by the peak concentration values quoted above. For reference, the two-phase region pressure for bulk Pd is approximately 14 torr D_2 and 4 torr H_2.

With regard to film damage during absorption, Fig. 3 shows the NR measurement of same Pd film before hydrogen absorption and after vacuum annealing (180 °C for 1 hour) to remove absorbed hydrogen The most obvious effect is the non-reversible increase in thickness (oscillation period decreases) after hydrogen absorption. This is not the result of annealing since the film was pre-anneal under identical conditions prior to exposure to H_2 and D_2 gas. Fits to both data sets (not shown) indicate that while the thickness was altered irreversibly, the scattering length density of the film returned the pre-hydrogen level. That level, by the way, was 98% of bulk Pd.

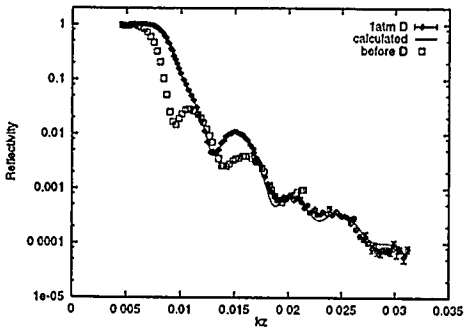


Fig. 1. NR measurement of 500 Å Pd film with and without D. Best fit to latter corresponds to Fig. 2 D profile.

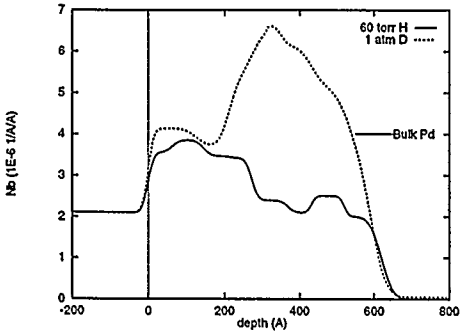


Fig. 2. Hydrogen and deuterium concentration profiles in 500 Å Pd film determined from the fit of *in situ* NR measurements.

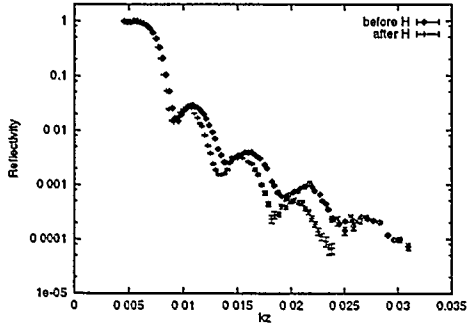


Fig. 3. NR measurement before H absorption and after H-outgassing anneal. Differences due to non-reversible lattice damage to thin Pd film.

INSTRUMENT USED:	DATE OF REPORT:	EXPERIMENT NO.:
POSY 2	10 AUGUST 90	

TITLE: INTERDIFFUSION IN PARTIALLY DEUTERATED POLYMER BILAYERS

AUTHORS AND AFFILIATIONS:

A. KARIM, G.P. FELCHER – ANL AND T.P. RUSSELL IBM, SAN JOSE, CA

DATES OF EXPERIMENT: MAY 1990

☒ APPROVED BY PROGRAM COMMITTEE, OR

☒ PART OF INSTRUMENT SCIENTIST ALLOCATION

REPORT RECEIVED:

EXPERIMENTAL REPORT (or Abstract of Publication)

EXPERIMENTAL REPORT (CONTD.)

Interdiffusion at the bilayer polymer interface: evidence for reptation, G.P. Felcher, A. Karim and T.P. Russell, International discussion meeting on relaxations in complex systems, Heraklion, Crete, Greece, June 18 1990 (Invited). To be published in Journal of non - crystalline solids (North Holland).

INTERDIFFUSION AT THE BILAYER POLYMER INTERFACE : EVIDENCE FOR REPTATION

G. P. Felcher and A. Karim
Materials Science Division
Argonne National Laboratory
and
T. P. Russell
IBM Research Division
Almaden Research Center
San Jose, CA 95120

Abstract

Neutron reflection is used to study the interdiffusion in equal molecular weight polystyrene bilayer melts with a spatial resolution of 1nm. Interfacial widths and concentration profiles at the bilayer interface are obtained for annealing times up to and beyond the time (reptation time, τ_d) in which the molecule has moved by its own length. For annealing times $t<\tau_d$, the reptation model predicts a mean square displacement of monomers whose time evolution is a power law. The detailed profile is expected to exhibit a discontinuity (sharp gradient) of density at the interface between the two polymers. For relatively light weight polymers of M~ 233000, the mean square displacements of monomers is in general agreement with reptation predictions; the discontinuity at the interface is only observed when the molecular weights are large, M~1,000,000. The discontinuity is present even for low concentrations of the deuterated polymer where isotopic slowing down effects are negligible, thus confirming the sharp gradient as being due to reptation.

INSTRUMENT USED:	DATE OF REPORT:	EXPERIMENT NO.:
POSY 2	07/28/91	1456

TITLE: STUDY OF POLYOLEFIN THIN FILMS

AUTHORS AND AFFILIATIONS: ALAMGIR KARIM, UNIVERSITY OF MINNESOTA
PROF. FRANK S. BATES, UNIVERSITY OF MINNESOTA AND DR. GIAN P. FELCHER, ARGONNE NATIONAL LAB.

DATES OF EXPERIMENT: JUNE 14 - 22

☒ APPROVED BY PROGRAM COMMITTEE, OR

☐ PART OF INSTRUMENT SCIENTIST ALLOCATION

REPORT RECEIVED:

EXPERIMENTAL REPORT (or Abstract of Publication)

POLYOLEFIN BLOCK COPOLYMER (PEP-PE)

Neutron reflection was used to investigate the thin film to bulk like behavior in a symmetric block copolymer. The copolymer was partially deuterated poly(ethylene propylene) - poly(ethylene) or PEP-PE, in which the PE block is crystallizable. The model profile fit to the reflectivity from as cast films of approximately 2000 and 900 Å thickness corresponded to a homogeneous layer of the block copolymer. The 2000Å film was subsequently annealed in situ in the neutron flight path at a small reflection angle of 0.4° under flowing N_2 gas. From bulk rheology measurements, it is known that the PE block of the copolymer has a crystal melting temperature, T_m = 108°C and an order-disorder transition temperature, T_{odt} = 159 °C. At an equilibrated temperature of 124°C ($T_m<T<T_{odt}$) in the in situ reflection measurements, a sharp first order Bragg peak in the reflectivity indicated a layering of the PEP and PE blocks parallel to the substrate surface. While the limited momenta range of the data ruled out the possibility of observation of higher order Bragg peaks and a hence a more detailed interpretation, the d-spacing of ~ 460 Å is close to that obtained from bulk SANS measurements which correspond to lamellar layering. Further annealing and equilibration at 143 °C leads to a total disappearance of the first Bragg peak; presumably the block copolymer is in its disordered state. The complete disappearance of the first Bragg peak is surprising and has never been observed in other block copolymer systems; even well above the T_{odt} in other systems, ordering is induced by preferential wetting of a block at the surface which is propagated into the bulk as an oscillatory pattern by virtue of connectivity of the individual blocks. The fact that the Bragg peak is regained upon cooling and remains quenched in below T_m shows that the sample has not degraded (which would lead to irreversible disordering). The thinner 900 Å film did not show any Bragg peak in the reflectivity upon annealing.

We plan to investigate in depth the above phenomena in a series of thin films of a recently synthesized PEP-PE, in which the PE is almost fully deuterated. The large contrast for neutrons between the two blocks will be advantageously used in answering key questions on ordering, crystallinity and chain folding in polyolefin block copolymers.

ASYMMETRIC BLOCK COPOLYMER (PEP-PEE)

We have used neutron reflection to study the surface and bulk like properties of the asymmetric block copolymer, poly(ethylene propylene) - poly (ethylethylene) or PEP-PEE in which the PEP(deuterated) composition is 75%. A wide range of film thicknesses (500 - 5000 Å) was studied. The films could be divided into 3 categories: thin, intermediate and thick. In films of intermediate thickness, such as 1290Å, the reflectivity showed a distinct first order Bragg peak and a very diffuse second peak. These could be fit by a model profile corresponding to rows of nearly hexagonally packed PEE rods surrounded by the PEP phase in the bulk. Both the air and silicon surface were determined to be covered with ~60Å layers of almost pure PEE. The dimensions of the PEE hexagons were only slightly different from that obtained from bulk SANS measurements. Static secondary ions mass spectroscopy (SIMS) confirmed the presence of a deuterated PEE layer at the air surface of the thin film.

A better understanding of the surface behavior is obtained by delineating the bulk properties from surface behavior, as in the ultra thin film of 500 Å. The reflectivity from it corresponds to a model profile which is essentially just the air and silicon surface profile of the 1290 Å thick film. The presence of highly reflecting PEE at both surfaces causes large total film thickness fringes to appear in the reflectivity. Annealing the sample above its bulk T_{odt} followed by slow cooling caused a mixing of the PEE phase near the silicon surface with the interior of the sample, and further enrichment of PEE at the air surface. Due to the decrement of PEE at the silicon surface the average scattering length density of the sample was almost the same as that of silicon itself. Its effect on the reflectivity is a dramatic absence of total film thickness fringes. The effect of annealing is remarkable given the fact that both blocks were well above their glass temperature even at ambient room temperature.

The thickest film of 5000Å showed very structured off - specular scattering after annealing. A unique feature is that the surface of the sample remains smooth as seen under the phase contrast microscope, which means that all the off-specular scattering arises from in plane structures or inhomogeneities within the bulk of the film. A rotation of the sample by 90° about is axis in the neutron beam produced the same off-specular scattering, indicating either a random distribution of rods or more likely, a radial distribution of rods arising from the spin casting process.

We plan to further investigate the surface wetting properties and the effect of annealing in more detail and also study the corresponding behavior in homopolymer blends of PEP and PEE. In addition the off-specular scattering from thick films will be related to block copolymer morphology by systematic investigation of samples that are spun off-center in order to orient the PEE rods in a given direction.

INSTRUMENT USED:	DATE OF REPORT:	EXPERIMENT NO.:
POSYII	8/11/94	1763

TITLE: Interaction of Funtionalized Elastomers with SiO_2 and the Correlation with Particle Dispersion Characteristics

AUTHORS AND AFFILIATIONS:

M.S. Kent -Sandia Nat. Labs., D.-W. Hua - U. of NM

DATES OF EXPERIMENT: Dec. 7-9, 1993

☐ APPROVED BY PROGRAM COMMITTEE, OR

☐ PART OF INSTRUMENT SCIENTIST ALLOCATION

REPORT RECEIVED:

EXPERIMENTAL REPORT (or Abstract of Publication)

Many materials of technological importance are composed of a polymer matrix containing filler particles. The interface between the polymer matrix and the filler particles can be an important contributor to the mechanical properties and the degree of dispersion of the filler particles. Good adhesion which can be carefully controlled is required to optimize these properties. The goal of this work is to determine the degree of adsorption and the interfacial concentration profile of functionalized elastomer chains in a nonfuntionalized elastomer matrix in contact with a silica surface as a function of the type of functional group, the number of such groups per chain, the relative lengths of the functionalized and matrix chains, and the relative concentrations.

We examined this problem with neutron reflection from the interface between an elastomer matrix and a thermally grown oxide layer on the surface of a silicon wafer. We mixed a small amount (1% by wt.) of functionalized, fully deuterated 50 kg/mol elastomer chains with non-functionalized protonated 50 kg/mol elastomer chains and spin-coated a roughly 4000 Å layer of the mixture onto a silicon wafer with a thermally grown oxide layer of 166 Å. The samples were then annealed in a vacuum oven at 40 °C for 10 hours. We examined the adsorption behavior for two types of functional groups: one terminated with a dimethylchlorosilyl group (d-PBD1), and another terminated with a trichlorosilyl group (d-PBD2). The reflectivity data are shown in Figure 1, along with the data for a bare silicon wafer with the same thermal oxide layer.

The curve through the data for the bare silicon wafer corresponds to a thermal oxide layer of 166 Å layer with $Nb = 3.4 \times 10^{-6}$ and 17 Å roughness. We observe that the data for the d-PBD1 sample are nearly identical to the data for the bare silicon wafer. This indicates that little or no adsorption of the d-PBD1 chains to the interface has occurred. The presence of the matrix PBD chains has little effect on the reflectivity since the scattering length density of PBD is close to that air. In contrast, the data for the sample containing d-PBD2 is shifted to lower q. This indicates a significant adsorption of the d-PBD2 chains to the interface. The curve through these data corresponds to a 22 Å layer at the interface with $Nb = 5.1 \times 10^{-6}$ and 32 Å roughness.

We are working to correlate this information with three types of measurements on the silica-filled elastomer material: SANS measurements, dynamic mechanical measurements, and with measurements of the degree of dispersion of the silica filler.

EXPERIMENTAL REPORT (CONTD.)

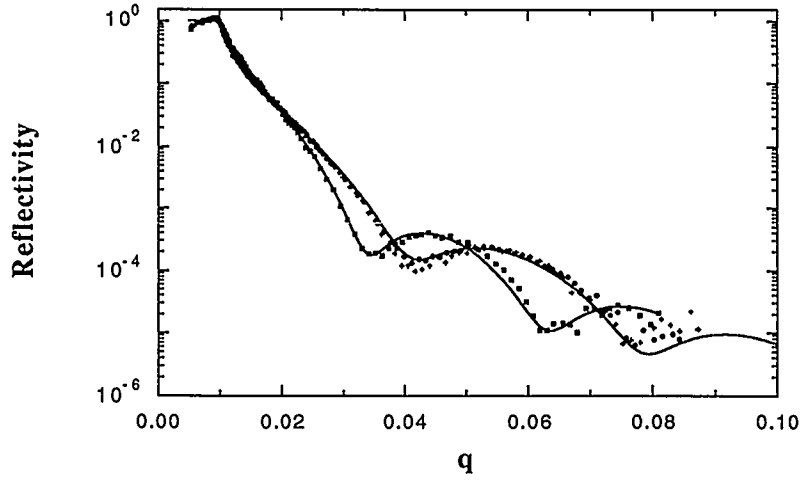


Fig. 1 Reflectivity from thin film samples of polybutadiene coated onto silicon wafers with 166 Å thermal oxide: (•) - bare silicon wafer, (+) - PBD with 1.0 wt % d-PBD1, (■) - PBD with 1.0 wt % d-PBD2. Preliminary fits are indicated by the curves through the data. The data for the sample with d-PBD1 is very similar to that for the bare silicon wafer, indicating that the d-PBD1 chains do not adsorb at the surface. The data for the sample with d-PBD2 is quite different and indicates strong adsorption. The curve through the data represents a 22 Å layer of d-PBD2 at the interface with $Nb = 5.1 \times 10^{-6}$ and 32 Å roughness.

INSTRUMENT USED:	DATE OF REPORT:	EXPERIMENT NO.:
POSYII	2/1/95	1950

TITLE: The Influence of Silane Coupling Agents on Moisture Adsorption at the Epoxy/Glass Interface

AUTHORS AND AFFILIATIONS:

M.S. Kent -Sandia Nat. Labs., Wen-Li Wu - NIST

DATES OF EXPERIMENT: Nov. 17-20, Dec. 10-13, 1994

☑ APPROVED BY PROGRAM COMMITTEE, OR

☐ PART OF INSTRUMENT SCIENTIST ALLOCATION

REPORT RECEIVED:

EXPERIMENTAL REPORT (or Abstract of Publication)

Many materials of technological importance involve the interface of a polymer matrix with glass. It is standard practice in industry to use silane coupling agents to promote adhesion at these interfaces. However, under high temperature conditions adhesive failures still occur, particularly after exposure to humidity. Standard references on the use of silanes[1] discuss the notion of mixing hydrophobic and hydrophilic silanes to achieve hydrophobic (or less hydrophilic) interfaces while still maintaining good adhesion promotion. We propose to test this concept for the first time by directly examining the moisture adsorption in situ with neutron reflectivity for a variety of coatings. We will examine the partitioning of moisture among the silane layer and the the surface layer of the substrate. We will relate this information to adhesive measurements to determine what role, if any, interface moisture plays in adhesive failures.

In our investigations, two types of samples were prepared. In the first group, the silane finishes were spin coated onto the oxide surfaces of silicon wafers. These samples were examined by impinging the neutron beam onto the sample from the air side and reflecting off the silicon substrate. The samples were examined dry and after 18 days exposure to saturated D_2O at 22 °C. For the second group of samples, a roughly 2 micron deuterated epoxy layer was roll-coated over the silane finish. The reflectivity was obtained with the beam impinging onto the interface from the silicon side. The epoxy layer is thick (and rough) enough so that the epoxy / air interface makes no contribution to the reflectivity, while being thin enough to allow moisture to diffuse to the interface on a practical time scale. Reflectivity data were obtained from these samples in the dessicated state, after 18 days exposure to a saturated D_2O atmosphere at 22 °C, and then again after 2 days exposure to saturated D_2O at 80 C.

A sample of the reflectivity data from the group 1 samples is shown in Figure 1. For this silane coating in the dry state (under vacuum), we observe that the reflectivity is decreased from that of the bare silicon wafer. The data can be modelled by including an increased roughness due to the silane coating. In the wet state, the reflectivity is increased above that of the bare silicon wafer. This can be accounted for by the presence of D_2O in the silane layer. The magnitude of these effects (roughness and D_2O adsorption) were found to vary with the three types of coatings examined.

For the group 2 samples, the reflectivity from all samples after 18 days in sat. D_2O at 22 C were identical to the data in the dry state. However, after 2 days exposure to sat. D_2O at 80 C, significant changes in the reflectivity were observed, an example of which is shown in Figure 2. Again, the results varied with the type of surface treatment.

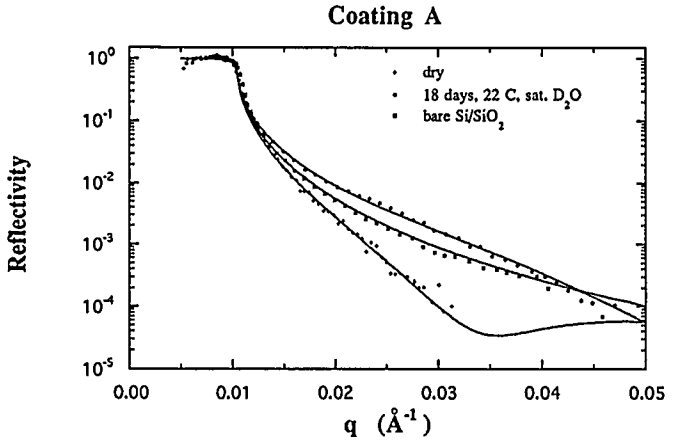


Fig. 1 Reflectivity from silicon wafers coated with a silane finish.

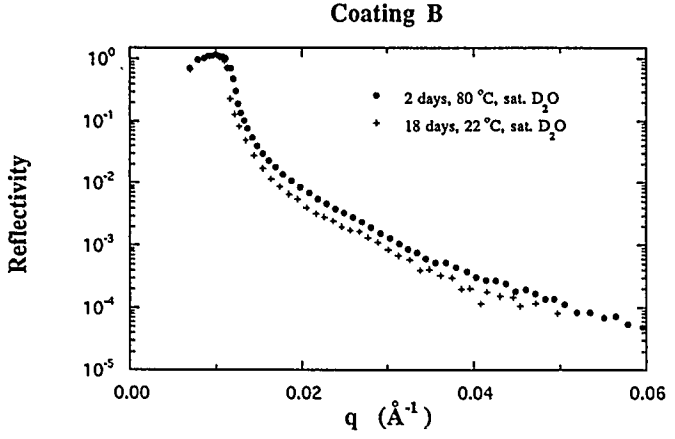


Fig. 2 Reflectivity from silicon wafers coated with a silane finish and a deuterated epoxy.

INSTRUMENT USED: POSYII	DATE OF REPORT: 11/16/95	EXPERIMENT NO.: 1950

TITLE: The Influence of Silane Coupling Agents on Moisture Adsorption at the Epoxy/Glass Interface

AUTHORS AND AFFILIATIONS: M.S. Kent -Sandia Nat. Labs., A. Wong, IPNS

DATES OF EXPERIMENT: Oct. 23-26, 1995

CHECK ALL APPLICABLE BOXES:

- ☐ APPROVED BY PROGRAM COMMITTEE
- ☐ INSTRUMENT SCIENTIST ALLOCATION
- ☐ DO NOT PUBLISH
- ☐ PROPRIETARY RESEARCH
- ☐ PRT ALLOCATION

EXPERIMENTAL REPORT (or Abstract of Publication)

Many materials of technological importance involve the interface of a polymer matrix with glass. It is standard practice in industry to use silane coupling agents to promote adhesion at these interfaces.[1] However, while silane coupling agents improve resistance to moisture substantially, adhesive failures still occur after exposure to high temperature and humidity. In one particular example from the printed circuit board industry, a technology involving direct chip attachment to circuit boards has tremendous market potential, but current board materials (glass cloth impregnated with epoxy) are unable to pass the required test conditions of 85 °C and 80 % relative humidity for 72 hours. This is due to failure of the glass/silane/epoxy interface. The goal of this work is to investigate the mechanisms that lead to failure of glass/silane/epoxy systems under these extreme conditions.

In this experiment, we examined the absorption of D_2O into a thin film (100Å) of a commercial silane coupling agent finish after conditioning for 21 hrs at 80 °C in at saturated D_2O atmosphere. A sample of the results are shown in Figure 1. After conditioning we observe a dramatic increase in the reflectivity, indicating significant uptake of D_2O in the silane layer. To understand the mechanism of adhesion loss after such conditioning treatments, it is important to determine if the uptake of deuterium is related to simple absorption of D_2O into the silane layer or to a chemical effect, such as the hydrolysis of siloxane bonds : -Si-O-Si- + D_2O → 2SiOD. To address this, we exposed the conditioned samples to vacuum for various periods of time. The data shown in Figure 1 indicate that roughly half of the deuterium uptake is lost fairly rapidly after exposure to vacuum. This is likely to be due to physically adsorbed D_2O. Reflectivity data after a much longer period in vacuum (not shown) indicates a further loss but at a much greatly reduced rate. The origin of this slower loss of deuterium will be the subject of future work.

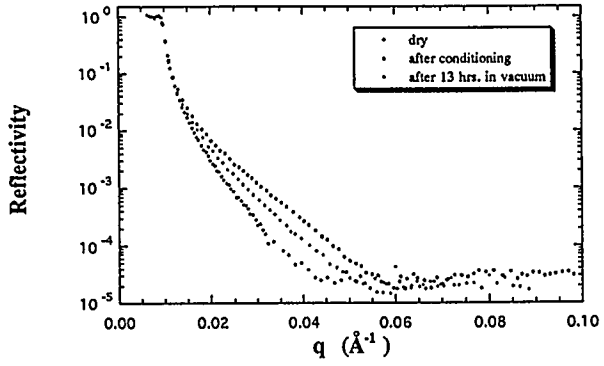


Fig. 1 Reflectivity from silicon wafers coated with a silane finish dry, after exposure to high temperature high humidity conditioning, and then after a period of 13 hrs in vacuum..

1. E. P. Plueddemann, *Silane Coupling Agent s*, 2nd ed., Plenum Press, New York, 1991. L. H. Lee, *Fundamentals of Adhesion*, Plenum Press, New York, 1991.

INSTRUMENT USED:	DATE OF REPORT:	EXPERIMENT NO.:
POSYII	2/1/95	1949

TITLE: Interaction of Funtionalized Elastomers with SiO_2 and the Correlation with Particle Dispersion Characteristics

AUTHORS AND AFFILIATIONS:

M.S. Kent -Sandia Nat. Labs.

DATES OF EXPERIMENT: Dec. 13-14, 1994

☒ APPROVED BY PROGRAM COMMITTEE, OR

☐ PART OF INSTRUMENT SCIENTIST ALLOCATION

REPORT RECEIVED:

EXPERIMENTAL REPORT (or Abstract of Publication)

Many materials of technological importance are composed of a polymer matrix containing filler particles. The interface between the polymer matrix and the filler particles can strongly affect the degree of dispersion of the filler particles and the mechanical properties. Good adhesion which can be carefully controlled is required to optimize properties. The goal of this work is to determine the degree of adsorption and the interfacial concentration profile of functionalized elastomer chains in a nonfuntionalized elastomer matrix in contact with a silica surface as a function of the type of functional group, the number of such groups per chain, the relative lengths of the functionalized and matrix chains, and the relative concentrations.

We previously examined this problem with neutron reflection from the interface between an elastomer matrix and a thermally grown oxide layer on the surface of a silicon wafer. We mixed a small amount (1% by wt.) of functionalized, fully deuterated 50 kg/mol elastomer chains with non-functionalized protonated 50 kg/mol elastomer chains and spin-coated a roughly 4000 Å layer of the mixture onto a silicon wafer with a thermally grown oxide layer of 166 Å. The samples were then annealed in a vacuum oven at 40 °C for 10 hours. We examined the adsorption behavior for two types of functional groups: one terminated with a dimethylchlorosilyl group (d-PBD1), and another terminated with a trichlorosilyl group (d-PBD2). The reflectivity data indicated that only the d-PBD2 chain adsorbed at the interface.

In the present experiment we further examined the adsorption behavior of d-PBD1 by treating a bare oxidized wafer with a solution of d-PBD1 in hexane. A range of concentrations were used. After 2 hours the wafers were removed from the solutions and rinsed exhaustively with methanol and hexane. The samples were then examined by neutron reflectivity. A sample is shown in Figure 1.

These results are representative of several samples examined. In all cases the reflectivity was identical to that of a bare Si/SiO_2 surface. Therefore we conclude that no reaction or strong adsorption occurs for d-PBD1, even from solution. This result is consistent with our previous observation.

We are working to correlate the adsorption information with three types of measurements on the silica-filled elastomer material: SANS measurements, dynamic mechanical measurements, and with measurements of the degree of dispersion of the silica filler.

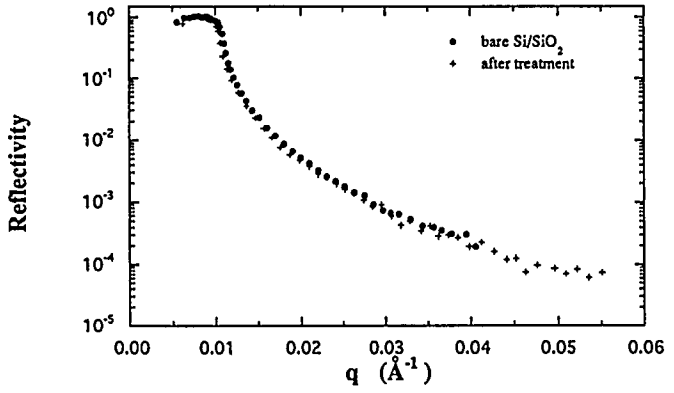


Fig. 1 Reflectivity from silicon wafers with a chemically grown oxide, bare and after exposure to a solution of d-PBD1 in hexane. These data indicate that no chemcial reaction or strong adsorption occurs between d-PBD1 and the surface of the silicon wafer.

INSTRUMENT USED:	DATE OF REPORT:	EXPERIMENT NO.:
POSYII	2/1/95	1951

TITLE: Moisture Adsorption at the Copper/Epoxy Interface

AUTHORS AND AFFILIATIONS:

M.S. Kent -Sandia Nat. Labs.

DATES OF EXPERIMENT: Nov. 21-22, 1994

☐ APPROVED BY PROGRAM COMMITTEE, OR

☐ PART OF INSTRUMENT SCIENTIST ALLOCATION

REPORT RECEIVED:

EXPERIMENTAL REPORT (or Abstract of Publication)

The goal of this experiment was to examine the adsorption of water to a copper epoxy interface. However, this experiment could not be performed because the epoxy unexpectedly dewet from the copper substrate. Therefore an alternative, but related experiment was performed. This involved measuring the conformation of a block copolymer adsorbed to the copper surface. This block copolymer was designed as a coupling agent for the copper/epoxy interface: one block was functionalized with an imidazole group to bond to the copper surface while the second block was functionalized with an amine group to bond to the epoxy. A key question in this project is whether the copolymer adsorbs in a layered fashion, such that the second block is on top and thus available to bond to the epoxy, or whether both blocks adsorb to the copper surface.

To answer this question, a 280 Å thin film of copper was sputtered onto the surface of a polished silicon wafer. The sample was then exposed to a solution of the block copolymer for 2 hours. Several concentrations and several solvents were used. Two block copolymers were examined which varied in the molecular weight of the second block. The molecular weights were 15-15 and 15-40 kg/mol. The first block (imidazole-functionalized) of each copolymer was partially deuterated. The results for all samples and concentrations were nearly identical. A sample is shown in Figure 1. These data indicate that the copolymer does indeed adsorb in a layered fashion, with the first block adsorbing preferentially at the Cu surface. The result observed in Figure 1 is quite distinct from the results expected if both blocks adsorbed or if the second block adsorbed preferentially at the Cu surface. Adhesion measurements involving this system are currently underway.

EXPERIMENTAL REPORT (CONTD.)

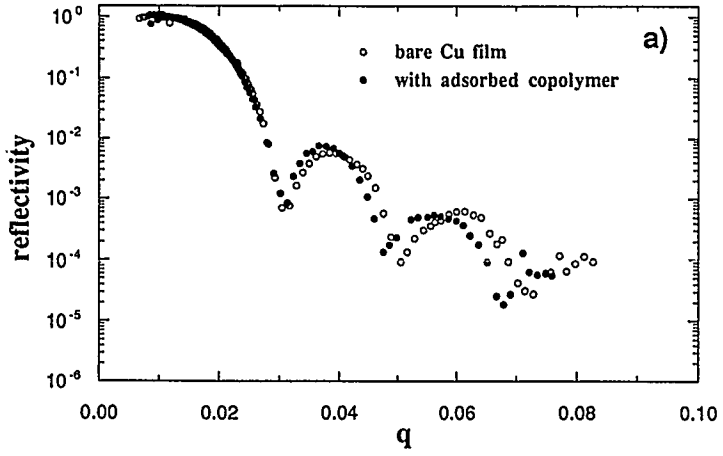


Figure 1. a) Neutron reflectivity for a bare Cu film and after adsorption of the block copolymer. Comparison with calculated curves strongly suggests that the imidazole functionalized block selectively adsorbs.

INSTRUMENT USED:	DATE OF REPORT:	EXPERIMENT NO.:
POSY II	5-29-91	1272

TITLE:
Surface Partitioning in Multicomponent Systems

AUTHORS AND AFFILIATIONS:
J. Koberstein, J. Elman (U of Connecticut), T. Long (E. Kodak), I. Yilgor (Goldschmidt)

DATES OF EXPERIMENT: July 23-27 1990

☐ APPROVED BY PROGRAM COMMITTEE, OR

☐ PART OF INSTRUMENT SCIENTIST ALLOCATION

REPORT RECEIVED:

EXPERIMENTAL REPORT (or Abstract of Publication)

Polymer end groups can profoundly effect many polymer properties (miscibility, adhesion, tribology and morphology) even though these moieties represent a very small fraction of the total chain. Monofunctionally terminated polymers were analyzed by Neutron Reflectivity (NR), ellipsometry, and X-ray Photoelectron Spectroscopy (XPS) to determine the spacial distribution of polymer termini within such films. Single layers of normal, proton tipped polystyrene (PS), and PS with either fluorocarbon* or lithium carboxy termini were spun cast on Si or fused silica substrates. These polymer chains were selectively deuterated (about 20%) at the functional tip by anionic synthesis for neutron contrast. Spin casting produced duplicate samples of two different thicknesses: approximately 1000 or 500 Å. Double layer samples that paired carboxy or proton tipped PS with amine or methyl di-terminated poly(dimethylsiloxane) (PSMS) were also prepared in the hopes of observing end group distribution at a buried interface.

XPS was performed on samples at Eastman Kodak before being brought to Argonne National Labs (ANL) to ascertain if the single layer films' annealing procedure (16 hours in air at 110C) introduced any unwanted oxidation. Table 1 shows trace amounts of oxygen in these films and no silicone contamination. In addition the XPS spectra showed strong pi -> pi* transitions as would be expected for an aromatic polymer like PS. The carboxy PS did show a bit more oxygen (1.1%) which could be attributed to a contaminant, minor oxidation or preferential orientation of carboxy groups. The NR results will eliminate at least one of these possibilities. The fluoro tipped PS showed an excess of fluorine as compared to the predicted stoichiometric amount. This is expected for such a low energy end group and is consistent with the NR profile. In addition the ratio of F to Si (24) was very interesting as it indicates the fluorocarbon portion of the terminus to be vertical thus shielding the single silane atom. A horizontal geometry would have given a normal stoichiometric ratio of 13. The proton tipped PS showed a slight (0.3%) fluorine contamination probably from the Teflon filter used to prepare spin coating solutions. Even if this 0.3% were subtracted to correct the fluoro tip data, then the F/Si would equal 22, still well above 13. Table 2 shows good agreement between total film thickness as measured by a single wavelength ellipsometer (a Rudolf Research instrument) and the corresponding NR fits to the data.

NR was obtained on the POSY II instrument at ANL. Presently the fits are close to optimal but should not be taken as the final profiles. A fully deuterated PS "standard" was run, and can be described as a homogeneous film (about 95% d) with a 9 Å layer of contaminating hydrocarbon at the surface. Two thicknesses of proton tipped PS showed similar behavior. This contaminating hydrocarbon layer could also contain an enhanced concentration of sec butyl end groups.

The fluoro tipped PS was also run at two thicknesses and both show striking preferentially adsorption of the deuterated ends to the surface followed immediately by a layer deficient in deuteration. If the first layer of this PS is oriented with fluoro tips at the surface then there must be a linked layer next that is low in deuteration (the hydrogenous portion of these oriented polymer chains). This description is consistent with the XPS data. The Li^+ carboxy NR data was the hardest to fit as it has gradients in % deuteration at the surface and at the Si wafer interface. The model consists of a depletion layer at the surface (high energy carboxy groups pulled away to minimize

*fluoro tip is $-SiCH_2CH_2(CF_2)_5CF_3$ (CH_3 / CH_3)

EXPERIMENTAL REPORT (CONTD.)

surface energy), followed by a homogeneous film, another depletion layer and finally a significant concentration of carboxy groups at the oxide layer of the Si wafer. Thus the 1% oxygen seen with XPS must be a contamination or the result of some oxidation. It is interesting to note that in both the fluoro and carboxy cases the depletion layer is perceptibly thicker than the associated highly deuterated (=functional tip) layer.

The spin casting of double layers to examine a buried interface presented experimental difficulties. A thick (1000 Å) film of PS was first cast from a toluene solution. This was followed by a thin (300 Å) layer of PDMS cast from an isopropanol solution. Exposure of PS to a wash of pure isopropanol showed no loss of PS as measured by ellipsometry. However although no intermixing occurred the bilayer films did optically scatter. This indicated that the PDMS layer was discontinuous or comprised of several areas of differing thickness. Surprisingly NR data was reasonable for two of the three samples. The fits to the two good films showed the PDMS layer to be far thinner than expected (20 A versus the original 300A). It is possible that much of the PDMS moved off the sample during annealing. XPS was preformed following NR to see if any PDMS was indeed still present. A PDMS layer should consist of 50% carbon, 25% silicon and 25% oxygen (XPS doesn't detect hydrogen). If the PDMS layer was compromised then one should see an enhancement of the carbon signal (contributed by PS) at the expense of the other two elements. Table 3 reveals an unexpected result: the % carbon is very close to the predicted value of 50, however silicon is enhanced slightly (28%) and oxygen diminished (21%). One can conclude that PDMS predominates at the surface, but is either unusually oriented or has been damaged by the neutron beam.

TABLE 1:
XPS of Single Layer Samples

PS (80h/20d) end group	%Carbon	%Oxygen	%Fluorine	%Silicon
Proton	99.8.	0.2	< 0.1	< 0.1
Fluoro	94.5	0.5	4.8*	0.2*
Li^+ Carboxy	98.6	1.1	0.3	< 0.1

*F/Si = 24

TABLE 2:
Total Film Thickness

PS (80h/20d) end group	Neutron Reflectivity (Å)	Ellipsometry (Å)
Proton	a) 450'+ 10 (SiO_2)	461
	b) 1077 + 10 (SiO_2)	1087
Fluoro	a) 436 + 10 (SiO_2)	460
	b) 1082 + 10 (SiO_2)	1092
Li^+ Carboxy	a) 1054 + 10 (SiO_2)	1056

TABLE 3:
XPS of Double Layer Samples

PS (80h/20d) end group	PDMS end group	%Carbon	%Oxygen	%Silicon
Li^+ Carboxy	Methyl	50.5	21.0	28.5
Proton	Amine	51.0	20.9	28.1
Li^+ Carboxy	Amine	50.4	21.9	27.7

INSTRUMENT USED:	DATE OF REPORT:	EXPERIMENT NO.:
POSY2	8/1/90	1299

TITLE:
Surface segregation of polymer chains due to molecular weight effects

AUTHORS AND AFFILIATIONS:
Sanat Kumar, Penn State University; Thomas Russell, IBM - San Jose

DATES OF EXPERIMENT: 5/19/90-5/23/90

☒ APPROVED BY PROGRAM COMMITTEE, OR

☐ PART OF INSTRUMENT SCIENTIST ALLOCATION

REPORT RECEIVED:

EXPERIMENTAL REPORT (or Abstract of Publication)

1. INTRODUCTION

The goal of the proposed experimental plan was to study the effects of polydispersity on the behavior of a thin polymer melt film near a surface. The experimental program was divided into two sections:

(i) Mixtures of different chain length isotopic polymers (polystyrene in our case) were prepared to study the effects of polydispersity on surface behavior. In this context it should be emphasized that Kramer and his coworkers (1) have studied mixtures of equal chain lengths of PSH and PSD and found that the segments of the PSD chains were preferentially partitioned to the air surface at equilibrium. The effects of chain lengths of the two isotopic polymers on the surface segregation observed will be the major focus of this report.

(ii) In the second stage of this work we examined mixtures where one component was a deuterated polystyrene (molecular weight 500K) mixed with a low molecular weight protonated PS (10K- 50K) that was end terminated with a -COOH molety at one or both chain ends. Theoretical predictions (2) on such systems suggest that the carboxylic acid terminated chains will be strongly segregated to the substrate (silicon in this case) and will thus cause a preferential partitioning of the short chains to the substrate interface. We have performed preliminary neutron reflectivity measurements which verify qualitatively that chains with -COOH end tags do segregate to the silicon surface. Complete quantitative analyses have not performed, and an exhaustive set of experiments are plannned.

2. EFFECTS OF DEUTERATION

As noted earlier Kramer and his coworkers (1) have studied the case where one has a mixture of PSH (molecular weight 1.80×10^6) and PSD (1.03×10^6) and found that the PSD was preferentially partitioned to the air surface. Further experiments by this group have indicated that the segregation decreased as the chain length of the PSH was reduced (up to a minimum of *ca.* 100K) for a constant length for the PSD.(2) In all cases, however, the PSD segregated to the air surface for the one composition examined (15% PSD in the bulk) suggesting that the effects of chain length did affect the magnitude but not the species that segregated to the surface.

To extend our understanding on the effects of tagging we performed a series of experiments where the PSD molecular weight was fixed at 500K. The molecular weight of the PSH (11.2K, 30K, 52K, and 96K) and the composition of the two species in the bulk (fixed at three different values of 10, 50 and 90% of PSD) were then varied in a systematic fashion to understand the effects of these variables on the segregation obtained. Films were formed by dissolving blends of the PSD and PSH with different compositions in toluene and then spinning onto a silicon substrate. This then is the as cast sample. In all cases the cast sample was then annealed at 433K for a period of 5 days to ensure the attainment of equilibrium. In one case we prepared an additional as cast sample (corresponding to 50% of 30K PSH with the 500K PSD) to study the effects of annealing on the segregation obtained.

In Figure 1 we plot neutron reflectivity data as Rk^4 vs. k for three different samples: the unannealed sample, an annealed sample of 50% 11.2K PSH/500K PSD and an annealed sample 50% 96K PSH/500K PSD. It is clear, if one assumes that the unannealed sample is uniform in concentration, that the 11.2K PSH sample behaves in a fashion that is very different from the 96K sample. Preliminary analysis would suggest that in the former case the PSH would go to the air surface, while the PSD would go to the air surface in the latter. While the latter result is in agreement with past experimental work on such systems, the results with the 11.2K PSH (where it is suggested that the PSH segregates to the air surface) is not, and suggests that the effects of tagging are indeed very complicated and the species from an isotopic blend that segregates to the air surface depends not only on its tagging but also on the chain lengths of the two species in consideration.We have analyzed the neutron reflectivity data by assuming that the concentration profile of the two species in the vicinity of the surface follow an exponential profile with a correlation length that is characteristic of each system. In all cases best fits were obtained by minimizing the χ^2, which is a measure of error between the reflectivity obtained from the suggested concentration profile and the experimental reflectivity. Figure 2 illustrates a typical example, and one may see that excellent fits can be obtained to the experimental data through such considerations.

EXPERIMENTAL REPORT (CONTD.)

Finally, in Table I we list the parameters that define the concentration profiles for all the 50% bulk samples that were examined in this work. Several facts need to be noted. First, the unannealed sample (50% 30K PSH/ 500K PSD) does not have a uniform concentration profile along the z axis. This can be seen by observing that ϕ_b (the bulk volume fraction of the deuterated species) is different from the surface volume fraction of the deuterated species (ϕ_1). This implies that the protonated short chains are segregated to the air surface in the casting process. On annealing this depletion of deuterated species from the air surface is magnified with a concomitant decrease in the correlation length. Thus, it is clear that changes on annealing are indeed small. Second, it can be seen in the case of the 50% 11.2K PSH that the surface is strongly enriched in the PSH, and that this enrichment of the protonated species does drop off to the case of no enrichment of either species in the case of the 52K PSH. This result is consistent with a recent theoretical model (4) which suggests that the no enrichment should occur for either species if one had a PSH of molecular weight 58K mixed with a PSD of 500K. Further, the PSD segregates to the air surface when one proceeds to the case where one has 96K PSH. These preliminary results suggest that, at this composition, the species partitioning to the air surface does indeed depend on the chain length of the two polymers in consideration and that one could even access samples wherein no segregation occurs due to tagging of one of the components of the binary blend. This is a particularly exciting result since it points to the fact that, in specific cases, tagging does not cause a significant perturbation to the results obtained in a surface sensitive experiment. We have also examined two different compositions for all the PSH/PSD molecular weight mixtures that were considered in Table I. These corresponded to 10% and 90% by volume of the PSD in the bulk. Preliminary analysis of the neutron reflectivity data suggests that, for all the different PSH molecular weights at these compositions, the deuterated polymer segregates to the air surface. These results, suggest that the effects of deuteration are not only strongly chain length dependent but also composition dependent, and that the deuterated species apparently partitions to the air surface when one has large quantities of either species in the bulk film.

REFERENCES

1. R.A.L. Jones, E.J. Kramer, M.L. Rafailovich, J. Sokolov, S. Schwarz, *Phys. Rev. Lett*,62,2801,1989.
2. A. Hariharan, S.K. Kumar, T.P. Russell To be submitted to *Macromolecules*.
3. E.J. Kramer *Personal Communication*, 1990.
4. S.K. Kumar, T.P. Russell Submitted to *Macromolecules*, 1990.

TABLE 1

SYSTEM	ϕ_b	ϕ_1	Correlation Length (nm)
50% 30K PSH/500K PSD Unannealed	0.47	0.40	5.7
50% 11.2K PSH/500K PSD	0.48	0.10	2.7
50% 30K PSH/500K PSD	0.46	0.27	3.1
50% 52K PSH/500K PSD	0.48	0.50	8.9
50% 96K PSH/500K PSD	0.52	0.62	12.8

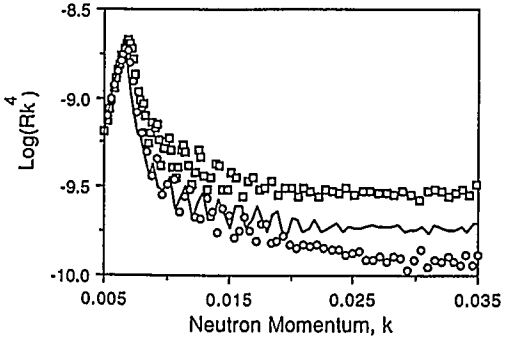


Figure 1: Neutron reflectivity data plotted as Rk^4 vs neutron momentum, k (A^{-1}) for three different sample. (——) is unannealed 30K PSH, (o) is annealed 50% PSH annealed, and (o) is 96K PSH annealed. All samples are 50% in the bulk, and the PSD is of molecular weight 500K.

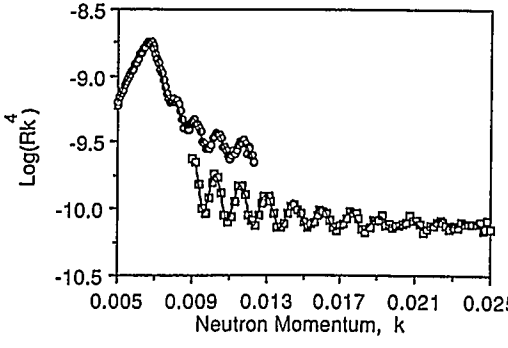


Figure 2: Neutron reflectivity data plotted as Rk^4 vs neutron momentum, k (A^{-1}) for a 50% 52K PSH/500K PSD. (o) is experimental data at low angle, while (o) are data are at high angle. Line is fit to the experimental data obtained using parameters in Table 1. The high angle results have been offset along the y-axis for clarity.

INSTRUMENT USED:	DATE OF REPORT:	EXPERIMENT NO.:
POSY2	1/29/91	1361

TITLE:

SURFACE SEGREGATION OF POLYMER CHAINS DUE TO MOLECULAR WEIGHT EFFECTS

AUTHORS AND AFFILIATIONS:
S.K. Kumar, Department of Materials Science and Engineering, Pennsylvania State University, University Park, PA. T.P. Russell, IBM Almaden Research Center, San Jose, CA.

DATES OF EXPERIMENT: 11/3/90-11/7/90

☐ APPROVED BY PROGRAM COMMITTEE, OR

☐ PART OF INSTRUMENT SCIENTIST ALLOCATION

REPORT RECEIVED:

EXPERIMENTAL REPORT (or Abstract of Publication)

The goal of the proposed experimental plan was to follow up on our earlier research (IPNS project # 1299) and study the effects of polydispersity on the behavior of a thin polymer melt film near a surface. Mixtures of different chain length isotopic polymers (polystyrene in our case) at different compositions were prepared to study the effects of polydispersity and composition on surface behavior. In this context it should be emphasized that Kramer and his coworkers (1) have studied mixtures of equal chain lengths of PSH and PSD and found that the segments of the PSD chains were preferentially partitioned to the air surface at equilibrium. The effects of chain lengths, and bulk compositions of the two isotopic polymers on the surface segregation observed will be the major focus of this report.

Earlier, we have reported neutron reflectivity measurements on polystyrene (PSH)/ deuterated-polystyrene (PSD) mixtures, at fixed bulk composition (*ca.* 50% by weight) and constant PSD molecular weight (5×10^5) for different values of the PSH chain length, near an air surface (2). It was illustrated that a reversal of the isotopic effect could be achieved for PSH molecular weights less than *ca.* 5×10^4 for this composition and PSD chain length, and that the protonated segments partitioned to an air surface in these cases. Specific combinations of the chain lengths of isotopic polymers could thus be used if one desired to study polymer interfaces without perturbations induced due to the effects of tagging. These experimental results were aparently in qualitative agreement with the predictions of an earlier theoretical model which suggested the reversal of the isotopic effect for PSH of a molecular weight less than *ca.* 6×10^4 (3).

To verify the general applicability of the results presented earlier, we have resorted to a set of experiments wherein the bulk compositions of the two polymers were maintained constant at *ca.* 50%, and the same range of PSH molecular weights were examined. However, in this case the PSD molecular weight was changed so that we now examined mixtures where the deuterated component was of molecular weight *ca.* 10^4. The theory presented in reference 2 predicts that the reversal of the isotope effect should now occur for a PSH molecular weight of *ca.* 3×10^4. We begin by examining the data at the two PSD molecular weights in Figure 4. Data are plotted in the form, A(surface) *vs.* PSH Chain Length, where A(surface) is defined as

$$A(\text{surface}) = (\phi_s-\phi_b)/\phi_b \qquad (1)$$

where ϕ_s and ϕ_b correspond to the experimentally determined PSD surface and bulk volume fractions, respectively. A(surface) is thus a non-dimensionalized quantity that expresses the relative enhancement of the PSD segments at the air surface. Two results are clear from this Figure,

(i) The absolute enhancement, A (surface), is always larger in the case of the lower PSD molecular weight. This suggests that PSD segments from chains of lower molecular weight are found preferentially at this surface compared to the case where one had a PSD molecular weight of 5×10^5. This can be argued to be an entropic effect, and is apparently in agreement with heuristic reasoning.

EXPERIMENTAL REPORT (CONTD.)

(ii) The PSH molecular weight where the reversal of the isotopic effect occurs is smaller in the case where the PSD molecular weight is lower. These trends are apparently in qualitative agreement with the theory presented earlier for the prediction of isotopic reversal (3). However, quantitative comparisons have not been made due to the fact that the error bars on the experimental data will allow for a shift in the cross over molecular weight of the order of *ca.* 10^3.

At this stage of the proposal we are therefore certain of the fact that a reversal of the isotope effect can effectively be obtained by tailoring the molecular weights of the isotopic polymers in the blend. Clearly, other polymers have to be examined to establish the general validity of these, results. We have also conducted two other studies, but their analyses have not been completed to date. The results of these experiments are summarized in a qualitative fashion.

(i) To delineate the effect of bulk compositions we have taken system comprising PSD of molecular weight 5×10^5 and allowed the PSH molecular weight, and overall bulk compositions vary. In contrast to our earlier report (2) we find that there is some composition dependence on A(surface); however there is no reversal of isotope effect as one traverses composition from pure PSH to pure PSD. These results are still in analysis and hence no quantitative statements can be made at this time.

(ii) In our experiments we normally spin a polystyrene film on a substrate (typically, Si with a native oxide overlayer) and conduct our neutron reflectivity measurements. We find that, in general, we are extremely sensitive to changes at the air surface, but not to any concentration profiles in the vicinity of the substrate. We found, however, that we could be sensitive to concentration profiles at both interfaces in the case where the scattering length density of the bulk film is close to that of Si (in this case corresponding to *ca.* 10vol% PSD in the bulk film). To generalize this contrast matching concept, and to check its validity, we have chosen to conduct experiments with a glass substrate. The glass substrate is particularly important in this context since its scattering length density corresponds to a different composition, *ca.* 42% PSD in the film. We have thus conducted two experiments where an identical 42% PSD film was cast on Si and glass substrates, and we find tentatively that the Si substrate experiments allow us to delineate the air profile, while the glass substrate allow for a probe of both interfaces. These experiments have not been analyzed in detail and hence we defer making any conclusions in this context at this stage.

REFERENCES

1. R.A.L. Jones, E.J. Kramer, M.L. Rafailovich, J. Sokolov, S. Schwarz, *Phys. Rev. Lett*,62,2801,1989.
2. S.K. Kumar, T.P. Russell *IPNS Progress Report for Project # 1299*, 1990.
3. S.K. Kumar, T.P. Russell Submitted to *Macromolecules* 1990.

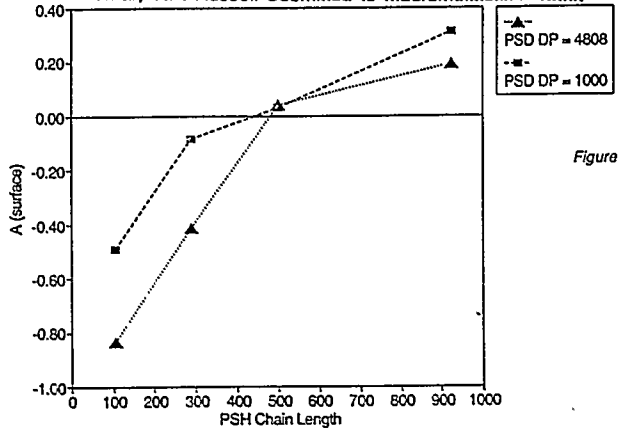


Figure 1: Experimentally determined relative enhancement of the segments of the PSD chains at the air surface, A(surface), as function of the chain length of the PSH chains for two different PSD chain lengths. The bulk films were prepared with *ca.* 50wt% of each species. PSD chain lengths are (▲) 4008, and (■) 1000.

INSTRUMENT USED:	DATE OF REPORT:	EXPERIMENT NO.:
POSY II	August 15, 1994	1753

TITLE:

Phase Separation and Surface Segregation in Binary Polymer Blends

AUTHORS AND AFFILIATIONS: Sanat K. Kumar, Tania M. Slawecki (Penn State University); Alamgir Karim (NIST); Thomas P. Russell (IBM Almaden Research Center)

DATES OF EXPERIMENT: 9/20-23/93, 11/20-24/93, 3/20-29/94

☐ APPROVED BY PROGRAM COMMITTEE, OR

☐ PART OF INSTRUMENT SCIENTIST ALLOCATION

REPORT RECEIVED:

EXPERIMENTAL REPORT (or Abstract of Publication)

Our goal in these experiments was to examine the role of surface segregation on the phase behavior of thin films of binary polymer blends. We have primarily focused upon the "classic" lower critical solution temperature system of PS/PVME, where the polystyrene component was deuterated to provide contrast in our neutron studies. From previous investigations, we anticipated the preferential segregation of PVME to both surfaces in our thin film samples, thereby leaving a dPS-enriched region in the middle of the film. This should effectively alter the "bulk" blend composition and thus shift its location relative to the bulk phase envelope. We also needed information from off-specular scattering data to give us further insight into the behavior of our thin polymeric films in the vicinity of the two-phase boundary.

Samples were prepared by spin-coating blends of different composition onto Si wafers which had been stripped of their native oxide layer. The resulting ~85 nm-thick films were then heated progressively under vacuum over a range of temperatures from the phase-mixed regime (403 K) until, at a temperature well inside the calculated bulk spinodal for the blend, we observed a large damping of the reflectivity thickness oscillations and the sudden onset of off-specular scattering. At each temperature, an "equilibrium" configuration was established by repeatedly measuring the reflectivity over a limited k-range until no differences were observed between successive scans.

Three blends of 20%, 30% and 40% dPS weight % content were run successfully on the POSY2 reflectometer. Table 1 lists the fit parameters for two of the blend samples studied and analyzed at present. We observe that with increasing temperature, while no dramatic changes take place in the variation of the layer roughness near the Si surface, large changes take place at the free surface of the film. This change begins to take place at 443 K for the 30% dPS blend and, possibly, at 438 K for the 20% dPS blend. Atomic force microscopy has revealed to us that the surface has undergone a gross roughening at this point, with features on the order of 100 nm. This result is consistent with the apparent decrease in overall dPS content of the film as the spaces between protruding surface features is averaged in with the scattering length density of the film, effectively lowering it.

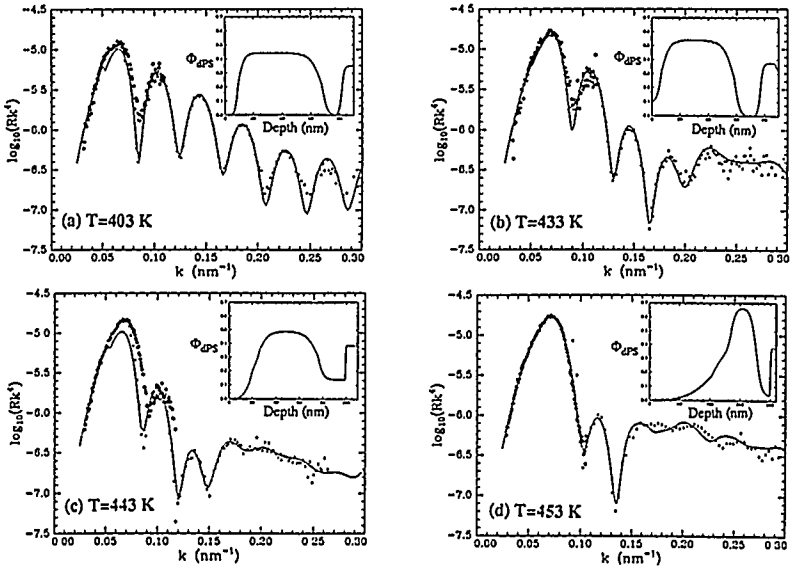
Graphs 1a-d show best fits to the 30% dPS blend sample at 403 K, 433 K, 443 K, and 453 K respectively. Insets to these graphs portray the corresponding concentration profiles used to

generate these reflectivities. Clearly, in the phase-mixed state (403 K) the preferential segregation of PVME to both the free and Si surfaces forms a trilayer-like structure with the dPS-enriched layer being the middle layer. We attribute the thin layer that appears before the Si surface to a residual oxide layer on the Si. At 433 K, the free surface of the profile is still essentially smooth but the dPS content in the middle of the film is shown to increase, consistent with the increase in surface segregation of the PVME. Large changes in the concentration profile begin to manifest themselves at 443 K as the free surface begins to roughen.

Table 1

T (K)	30%dPS/70%PVME					20%dPS/80%PVME				
	Film Thickness	R_{air}	R_{Si}	χ^2	%dPS	Film Thickness	R_{air}	R_{Si}	χ^2	%dPS
403	80.7 nm	.32 nm	.41 nm	.11	30.8	82.5 nm	.07 nm	2.2 nm	2.7	19.0
413	77.8 nm	.36 nm	.80 nm	2.1	30.7	82.7 nm	.05 nm	2.5 nm	2.8	19.1
423	77.4 nm	.1 nm	.67 nm	2.1	31.0	82.5 nm	.1 nm	2.9 nm	3.2	19.1
433	76.8 nm	.1 nm	1.2 nm	2.1	32.5	82.2 nm	.01 nm	3.4 nm	1.6	17.8
438	——	——	——	——	——	82.4 nm	2.7 nm	3.4 nm	5.7	16.8
443	81.6 nm	7.8 nm	1.6 nm	3.4	26.1					
453	97.2 nm	45.4 nm	.65 nm	3.7	17.5					

Graphs 1a-d



INSTRUMENT USED:	DATE OF REPORT:	EXPERIMENT NO.:
Posy-II	August 1, 1991	1352

TITLE:
Determination of Interface Thickness Between Polymer Layers

AUTHORS AND AFFILIATIONS:
M. R. Landry, Eastman Kodak Company, Rochester, NY 14650-2110

DATES OF EXPERIMENT: March 12-14, 1991

☐ APPROVED BY PROGRAM COMMITTEE, OR

☐ PART OF INSTRUMENT SCIENTIST ALLOCATION

REPORT RECEIVED:

EXPERIMENTAL REPORT (or Abstract of Publication)

Although the purpose of this particular NR experiment was a feasibility study, our ultimate intent is to expand upon the work of Russell and coworkers[1,2] in which the segment density distribution between two immiscible homopolymers with a diblock copolymer localized at their interface was probed. From a practical standpoint, it may be useful to determine the interfacial activity of not only block (-b-) copolymers, but also graft (-g-) and to a lesser extent, random (-r-) copolymer architectures in immiscible polymer blends. For this end, film specimens of dPS/P(dS-b-MMA)/PMMA, dPS/P(MMA-g-dS)/PMMA, dPS/P(S-r-MMA)/PMMA, and dPS/PMMA were prepared by spin coating a thick 3000 Å layer of dPS followed by floatation transfer of a 300 Å copolymer film and a 1000 Å PMMA upper layer, all onto 5-cm diameter polished Si wafers. A second set of four samples with the same copolymers as intermediate layers were prepared, except that the homopolymer pair was PSOH [poly(p-hydroxystyrene)] / dPS. With PSOH and PMMA being a miscible pair[3], the latter experiment is the complement of a similar one for PXE/PMMA with PS-b-PMMA at the interface, with PS and PXE being miscible, reported in reference 2. Presumably there is a much stronger interaction between PMMA and PSOH than PXE and PS due to H-bonding between the former pair. For each of the samples in this study, the primary objective was to determine the width of the interfacial region between the immiscible polymer pairs of dPS/PMMA or PSOH/dPS as a function of the copolymer architecture.

The ultimate lesson learned from this first trip to Argonne was the importance of careful sample preparation, which includes controlled annealing conditions. Several of the samples were rendered useless by apparent decomposition of the polymer layers on the Si substrates, both at 165°C (for dPS/PMMA) and 195°C (for PSOH/dPS), despite heating all samples under vacuum. Some surface abrasion or extensive roughness of a few other samples also affected reflectivity profiles (for example, see figure 1 for the dPS/PMMA homopolymer bilayer) by effectively damping the oscillations from the upper PMMA layer. Two of the PSOH/dPS films, one containing the diblock dPS-b-PMMA, the other with the graft PMMA-g-dPS copolymer, provided reasonable reflectivity profiles suitable for further analysis. Because of the caveats, the reflectivity profiles were quantitatively fit with less rigor than if the sample quality was improved; for example, the results below are reported for merged data sets with $\Delta k/k$ assumed to be constant, and no χ^2 minimization was performed.

Figure 2 shows the Rk^4 vs. k plot for the sample PSOH/dPS-b-PMMA/dPS, with dPS being the top layer. The fit shown for this data gives a lower PSOH layer thickness of 3000 Å (measured by ellipsometry) with $b/V = 1.06 \times 10^{-6}$ Å^{-2}, covered by a 1025 Å dPS layer, $b/V = 6.61 \times 10^{-6}$ Å^{-2}, and a top layer roughness of 30 Å.The interfacial width was fit as 10 Å using a Gaussian function to model the segment density profile. The data were not sensitive enough to distinguish between the scattering length density difference between PSOH and the PMMA half of the diblock copolymer. The results of fitting the reflectivity profile for PSOH/PMMA-g-dPS/dPS (NR profile not shown) were similar, with a narrower interface of 5 Å. The relative thickness of the interfaces with added copolymers for the dPS/PSOH pair is in marked contrast with our result of 25 Å for an interface width for the dPS/PMMA pair with no added copolymer from fig. 1. At this time we hesitate to conclude whether the difference in interfacial widths measured with the block and graft copolymers for the dPS/PSOH pair is significant given the uncertainty of adequate sample preparation. It is felt however, that the differences between the homopolymer pairs is noteworthy and that these investigations warrant repeating. Additional experiments are also being planned for these materials.

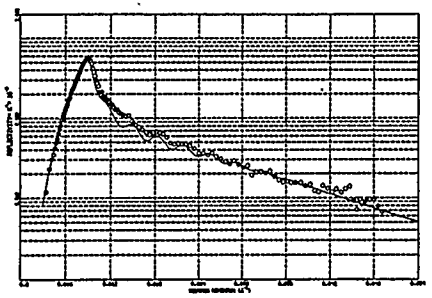


Fig. 1

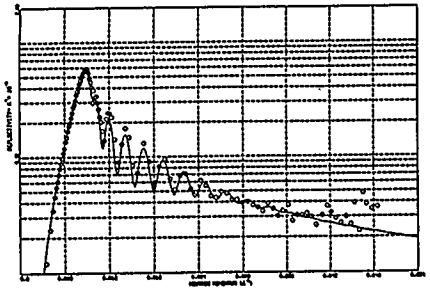


Fig. 2

[1] T.P.Russell, S.H.Anastasiadis, A. Menelle, G.P.Felcher, and S.K.Satija, *Macromolecules*, 24, 1575(1991).
[2] H.R.Brown, K.Char, T.P.Russell, IPNS Progress Report 1988-1990, Argonne National Laboratory, p. 123.
[3] C.J.Serman, Y.Xu, P.C.Painter, M.M.Coleman, *Macromolecules*, 22, 2015(1989).

INSTRUMENT USED:	DATE OF REPORT:	EXPERIMENT NO.:
Posy II	9 Aug. 1990	1179

TITLE:
Surface Enrichment in Copolymers and their Blends

AUTHORS AND AFFILIATIONS: T Mansfield, R.S. Stein, RJ Composto *
R Mendelsen & P Garrett ** * Univ of Massachusetts ** Monsanto Chemical Company

DATES OF EXPERIMENT: May 1990

☒ APPROVED BY PROGRAM COMMITTEE, OR

☐ PART OF INSTRUMENT SCIENTIST ALLOCATION

REPORT RECEIVED:

EXPERIMENTAL REPORT (or Abstract of Publication)

SAN copolymers are random copolymers of styrene and acrylonitrile. Blends of SAN with different AN contents can form miscible or partially miscible systems depending on the difference in AN content. We have chosen to investigate blends of DSAN24 (deuterated SAN with 24 w% AN content) with SAN27, a system that is miscible under the experimental conditions we chose, but not far from the coexistence curve.

The essence of the experiment is to spin cast a solution of the blend onto a polished silicon substrate to form a film and measure its neutron reflectivity, NR, before and after annealing at approximately T_g + 60°C. In all cases, appreciable changes in the NR of these samples was observed upon annealing, suggesting that significant changes in the concentration profiles occurred. We present in this report a preliminary summary of the features of the concentration profiles in these samples.

NR data and consideration of the sample preparation procedures both suggest that the unannealed films are nearly homogeneous in composition.

Concentration profiles deduced from NR simulations suggest that DSAN24 preferentially segregates to both the polymer/vacuum and polymer/substrate interfaces during annealing. These features are consistent with SIMS experiments done on annealed films. The concentration profile, $\Phi(z)$, used in the NR simulations is an exponential function with a decay length, ξ, on the order of the radius of gyration of these polymers. The simulated and experimental data for a film of volume fraction 0.3 are shown in Figure 1. The relation between the volume fraction of DSAN24 at the surface and in the bulk for films of different compositions is shown in Figure 2.

It is possible to estimate a value of χ for this blend using the theory of Binder and Schmidt[1]. Figure 3 shows a comparison of our experimental Z^* values with those obtained using Binder's theory[2]. We obtain a value of 8.9×10^{-4} for χ.

We plan to do small angle neutron scattering experiments with this system in the near future. We hope to compare the values of χ and ξ obtained from the SANS experiment with the values of χ and ξ obtained from the measurement of concentration profiles.

[1]Schmidt and Binder J Phys. (Paris) 46, 1631 (1985)
[2]D. E. Sullivan and M. M. Telo de Gama, in *Fluid Interfacial Phenomena*, edited by C. A. Croxton (Wiley, New York, 1986), pp. 45-134

EXPERIMENTAL REPORT (CONTD.)

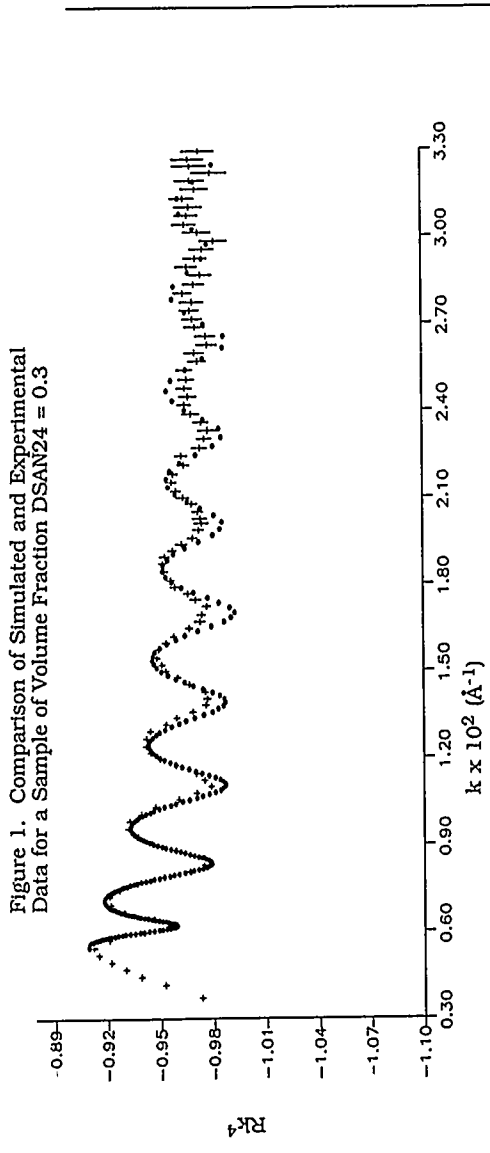


Figure 1. Comparison of Simulated and Experimental Data for a Sample of Volume Fraction DSAN24 = 0.3

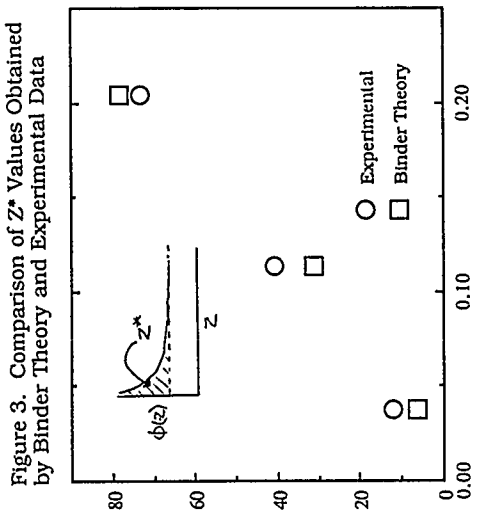


Figure 3. Comparison of Z* Values Obtained by Binder Theory and Experimental Data

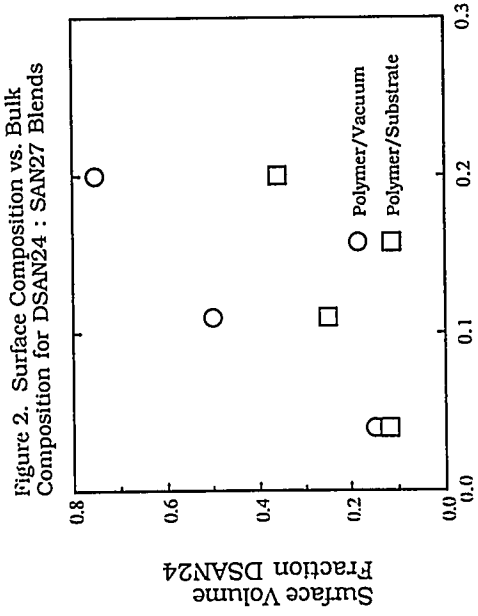


Figure 2. Surface Composition vs. Bulk Composition for DSAN24 : SAN27 Blends

INSTRUMENT USED: POSY II | DATE OF REPORT: 1/31/91 | EXPERIMENT NO: 1362

TITLE: Surface Enrichment in Isotopic Polymer Alloys by Neutron Reflectometry

AUTHORS AND AFFILIATIONS: L.J. Norton, E.J. Kramer (Cornell U); R.A.L. Jones (Cambridge U); F.S. Bates (U Minnesota).

DATES OF EXPERIMENT: 9/15-9/18/90

__ APPROVED BY PROGRAM COMMITTEE, OR

__ PART OF INSTRUMENT SCIENTIST ALLOCATION

REPORT RECEIVED:

EXPERIMENTAL REPORT (or Abstract of Publication)

We have measured neutron reflectivities from the surface of films of deuterated polyethylenepropylene (d-PEP) and protonated polyethylenepropylene (PEP) blends as a function of bulk volume fraction and annealing temperature. After annealing, the surface is enriched in dPEP with an enrichment much stronger than that in polystyrene/deuterated polystyrene blends [1,2] as expected from the higher D/C or H/C ratio in the dPEP/PEP blend. While pursuing a set of measurements intended to determine the true equilibration time scale of the composition profile we observed an interesting and potentially useful feature in the reflectivity.[5] Figure 1 shows the reflectivity R versus k, the perpendicular component of the neutron wave vector, for a sample with a bulk volume fraction dPEP ϕ_∞=0.08 annealed at 70°C for 40 hours. The fit is calculated from the scattering length density profile shown in Figure 2. The bulk of the film has a scattering length density less than both the enriched surface layer and the silicon substrate creating an effective potential well. At certain k values below k_c, the critical value for total reflection from silicon, interference between reflections from the silicon interface and from the air-polymer surface leads to an increase in the amplitude of the neutron (standing) wave function in the polymer film. At these k values there is considerable incoherent scattering from the highly protonated bulk and a corresponding decrease in R. Two resonances can be seen at k ~ 0.0029 and 0.0041 $Å^{-1}$. We expect that when present, resonances of this type will put new constraints on the scattering length density profile as well as probe its long wavelength features.

References

1.) R.A.L. Jones, E.J. Kramer, M.H. Rafailovich, J. Sokolov, S. A. Schwarz, Phys. Rev. Lett. 62 280 (1989)

2.) R.A.L. Jones,L.J. Norton, E.J. Kramer, R.J. Composto, R.S. Stein, T.P. Russell, A. Karim, A. Mansour, G.P. Felcher, M.H. Rafailovich, J. Sokolov, X. Zhou, and S. A. Schwarz, Europhys. Lett.,12 41-46 (1990).

3.) M. Born and E. Wolf, *Principles of Optics*, Pergamon Press, Oxford 1975.

4.) I.Schmidt and K. Binder, J. Physique (Paris) 46 1631 (1985).

5.) R.A.L. Jones et al. in preparation.

Figure 1

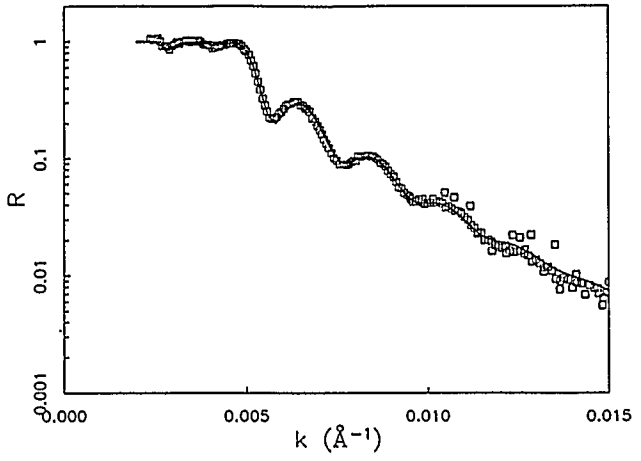
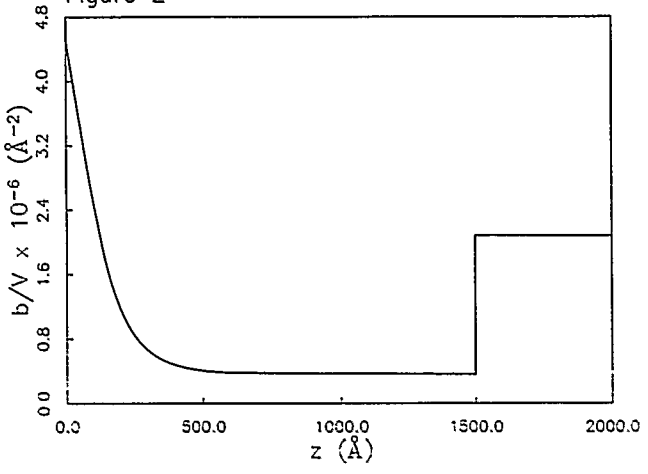


Figure 2



INSTRUMENT USED: POSY II | DATE OF REPORT: 1/31/91 | EXPERIMENT NO: 1363

TITLE: Neutron Reflectometry Study of Segregation of End-Functionalized Polymers to Interfaces between Polymers and Nonpolymers

AUTHORS AND AFFILIATIONS: L.J. Norton, E.J. Kramer (Cornell U); K. Shull (IBM-ARC); R.A.L. Jones (Cambridge U); Lewis Fetters (Exxon).

DATES OF EXPERIMENT: 11/13-11/18,12/2-12/5

__ APPROVED BY PROGRAM COMMITTEE, OR

__ PART OF INSTRUMENT SCIENTIST ALLOCATION

REPORT RECEIVED:

EXPERIMENTAL REPORT (or Abstract of Publication)

We have measured neutron reflectivity, R, from blends of polystyrene (PS) with deuterated polystyrene (dPS) terminated at one end by either -OH or -OLi. When a blend is spun onto a bare silicon substrate and annealed we have seen with forward recoil spectrometry (FRES) that the end-functionalized polymer segregates to the silicon interface and have measured the integrated interface excess. To investigate the degree of stretching of the end-functionalized chain away from the silicon interface we have measured NR from samples consisting of various bulk volume fractions ϕ_∞ (0.13, 0.064, 0.035, 0.022) of the end-functionalized dPS in molecular weight M=670,000 PS. The R from an annealed -OLi sample (ϕ_∞=0.064 in M=670,000) is displayed in Figure 1, a plot of k^4R versus k, the perpendicular component of the neutron wave vector. The fit is calculated from the concentration profile shown in the inset and contains a maximum in the volume fraction away from the interface as seen in previous work [1]. Profiles for end-anchored chains derived from simple theories (e.g. a step function brush [2,3] or a parabolic brush [4]) do not predict this maximum. Figure 2, a plot of the maximum volume fraction versus ϕ_∞ , shows that the -OLi end segregates slightly more strongly than the -OH group. Using self-consistent mean-field calculations[5] we plan to quantify the interaction energy of each end group with silicon and test the possibility that the maximum away from the interface is a consequence of the relative preference of the PS over the dPS monomers for the silicon.

References:

1) R.A.L. Jones et al., IPNS report January 1990.
2) S. Alexander, J. Phys. (Paris) 38, 983 (1977).
3) P.G. de Gennes, J. Phys. (Paris) 37, 1443 (1976).
4) S.T. Milner, T. A. Witten and M. E. Cates, Macromolecules 21, 2610 (1988).
5) K.S. Shull, J. Chem. Phys., in press.

Figure 1

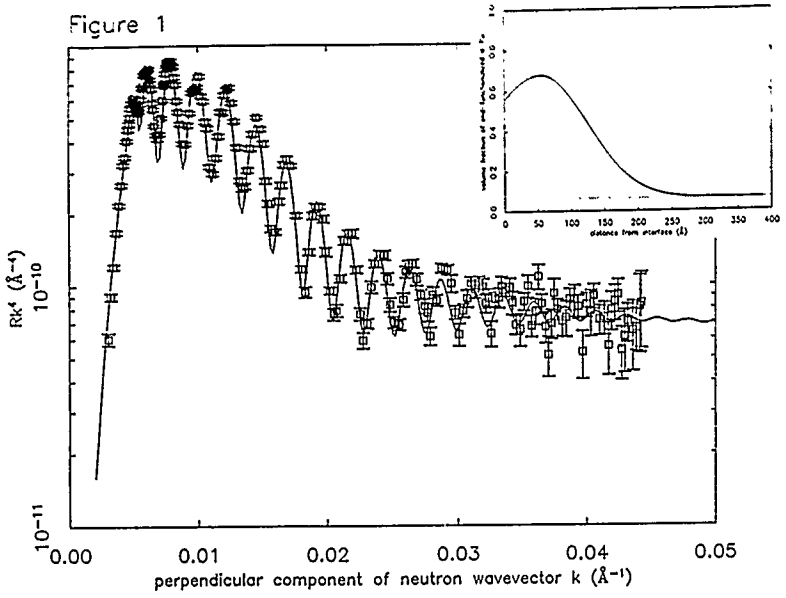
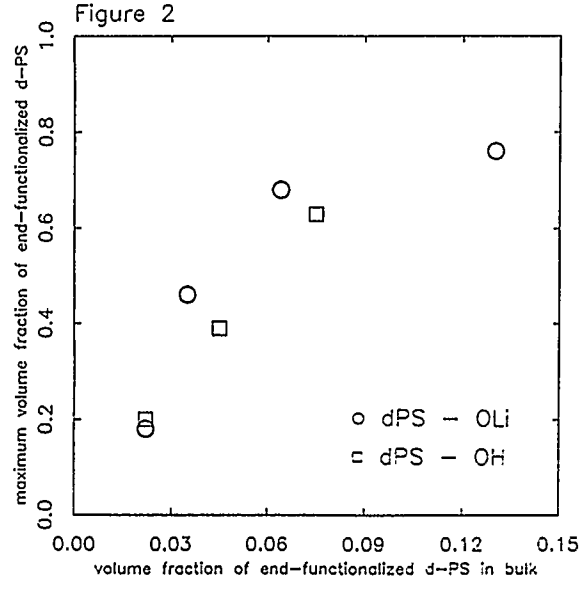


Figure 2



INSTRUMENT USED: POSY II

DATE OF REPORT: 8/2/91

EXPERIMENT NO: 1465

TITLE: Surface Enrichment in Isotopic Polymer Alloys by Neutron Reflectometry

AUTHORS AND AFFILIATIONS: L.J. Norton, E.J. Kramer (Cornell U); R.A.L. Jones (Cambridge U); F.S. Bates (U Minnesota).

DATES OF EXPERIMENT: 2/17-2/21/91, 2/24-2/26/91

_ APPROVED BY PROGRAM COMMITTEE, OR

_ PART OF INSTRUMENT SCIENTIST ALLOCATION

REPORT RECEIVED:

EXPERIMENTAL REPORT (or Abstract of Publication)

We have measured neutron reflectivities from the surface of films of deuterated and protonated polyethylenepropylene (dPEP and PEP) blends as a function of bulk volume fraction and annealing temperature. After annealing, the surface is enriched with dPEP and segregated much more strongly than that of comparable dPS/PS blends as expected from the higher D/C ratio in the dPEP/PEP blend. In our earlier work we saw signs of unexpectedly long equilibration time scales. In this work on blends with symmetric molecular weight of 160,000, we tested for equilibration by annealing samples for 3 and 12 days at 70°C. Both samples had initial bulk volume fractions ϕ_0=0.32 and identical reflectivities. The data for these samples are shown in Figure 1 as a plot of Rk^4 versus k, where k is the perpendicular component of the neutron wave vector. The composition profile required to generate a best fit (solid line) to the data is shown in Figure 2. The surface is substantially more enriched in dPEP than predicted by theory (dashed curve) [3], probably due to a break down of the mean-field theory for large surface concentrations. Analysis of the reflectivity data is continuing for samples of various ϕ_0(0.10, 0.12, 0.15, 0.20) annealed at both 35 and 70°C for a minimum of 9 days.

References

1.) R.A.L. Jones, E.J. Kramer, M.H. Rafailovich, J. Sokolov, S. A. Schwarz, Phys. Rev. Lett. 62 280 (1989)

2.) R.A.L. Jones,L.J. Norton, E.J. Kramer, R.J. Composto, R.S. Stein, T.P. Russell, A. Karim, A. Mansour, G.P. Felcher, M.H. Rafailovich, J. Sokolov, X. Zhou, and S. A. Schwarz, Europhys. Lett.,12 41-46 (1990).

3.) I.Schmidt and K. Binder, J. Physique (Paris) 46 1631 (1985).

Fig.1 Reflection spectrum: Rk^4 vs. k

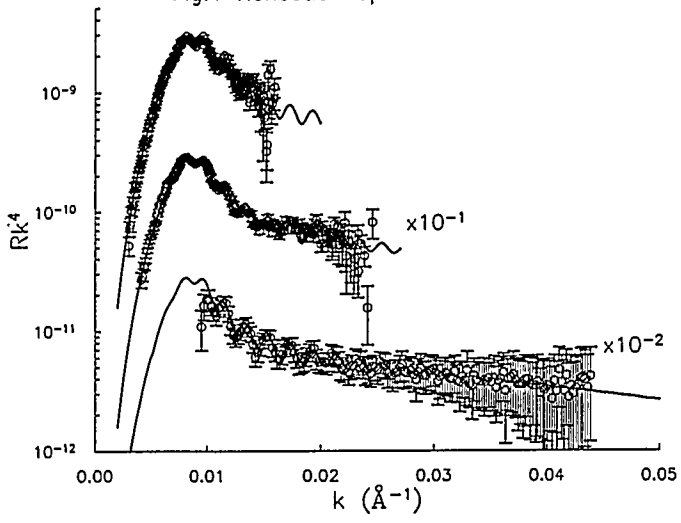
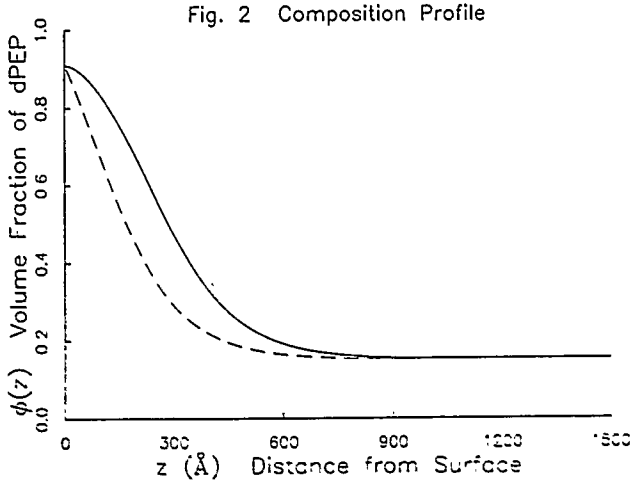


Fig. 2 Composition Profile



INSTRUMENT USED: POSY II | DATE OF REPORT: 8/2/91 | EXPERIMENT NO: 1468

TITLE: Neutron Reflectometry Study of Segregation of End-Functionalized Polymers to Interfaces between Polymers and Nonpolymers

AUTHORS AND AFFILIATIONS: L.J. Norton, E.J. Kramer (Cornell U); K. Shull (IBM-ARC); R.A.L. Jones (Cambridge U); Lewis Fetters (Exxon).

DATES OF EXPERIMENT: 3/9-3/11/91

__ APPROVED BY PROGRAM COMMITTEE, OR

__ PART OF INSTRUMENT SCIENTIST ALLOCATION

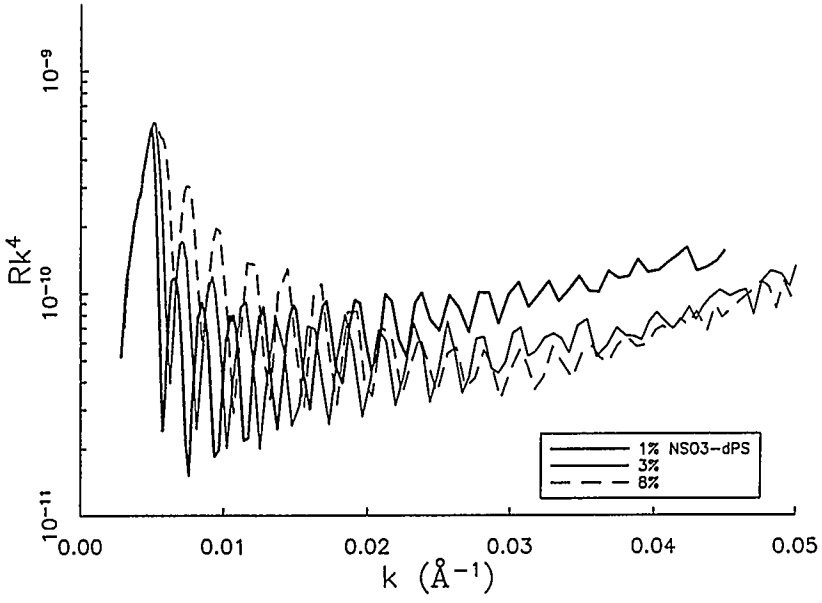
REPORT RECEIVED:

EXPERIMENTAL REPORT (or Abstract of Publication)

We have measured neutron reflectivity, R, from blends of polystyrene (PS) with deuterated polystyrene (dPS) terminated at one end by $-[N^+(CH_3)_2(CH_2)_3SO_3^-]$, a zwitter ion. The blend was spuncast onto a silicon wafer which had undergone rapid thermal annealing at 900°C for 60sec in an oxygen ambient to create a silicon dioxide, SiO_2, film approximately 45Å thick. When these films are annealed we have seen with forward recoil spectrometry (FRES) that the end-functionalized polymer segregates to the SiO_2 interface and have measured the integrated interface excess. To investigate the degree of stretching of the end-functionalized chain away from the oxide interface we have measured NR from samples consisting of a range of bulk volume fractions ϕ_∞ of the end-functionalized dPS in molecular weight M=670,000 PS. In Figure 1, plotted as Rk^4 versus k, where k is the perpendicular component of the neutron wave vector, the systematic changes in the data of the segregated samples as a function of ϕ_∞ is shown. Analysis of this data is underway to determine the segment density profile away from the interface. In addition, using self-consistent mean-field calculations [1] we plan to quantify the interaction energy of the end group with SiO_2 and compare the results with values for other end groups and other interfaces. [2,3]

References:
1) K.S. Shull, Journal of Chemical Physics, 94, 5723 (1991).
2) R.A.L. Jones et al., submitted to Macromolecules.
3) L.J. Norton et al, in preparation.

Figure 1: NSO3–dPS/670kPS/SiO2



INSTRUMENT USED: POSY II

DATE OF REPORT: 8/3/92

EXPERIMENT NO: 1567

TITLE: Surface Enrichment in Isotopic Polymer Alloys by Neutron Reflectometry

AUTHORS AND AFFILIATIONS: L.J. Norton, E.J. Kramer (Cornell U); A. Karim (NIST); M.D. Gehlsen, F.S. Bates (U Minnesota).

DATES OF EXPERIMENT: 7/17-23/92

__ APPROVED BY PROGRAM COMMITTEE, OR

__ PART OF INSTRUMENT SCIENTIST ALLOCATION

REPORT RECEIVED:

EXPERIMENTAL REPORT (or Abstract of Publication)

In our early studies of surface enrichment we measured the neutron reflectivities from an isotopic blend of protonated and deuterated polyethylenepropylene (PEP and dPEP) both with degree of polymerization N=2286 and a difference in the fraction of deuteration $\Delta x_D = 1$. We found that the deuterated component segregated to the surface [1,2] and that the detailed shape of the profile differed substantially from theoretical predictions [3]. We believe that this behavior is a result of the breakdown of the mean-field approximation at large concentrations of the deuterated chains and an improper accounting of the chain configuration near the surface.

In order to facilitate the development of a more complete theory of surface segregation we have measured the neutron reflectivites on a new blend with N=7910 and $\Delta x_D = 0.5$. Recently Gehlsen et al. [4] found for PEP/dPEP blends that the Flory parameter χ (which describes the strength of the interaction between segments of the two components) is independent of N and takes the form $\chi = (\Delta x_D)^2 [\ 0.571/T - 0.000656\ ]$. In this experiment N and Δx_D were chosen in order to keep the value of χN, and therefore the critical temperature and the coexistence curve, nearly the same as the original system. Films 1000Å thick with initial bulk concentrations $\phi_0 = 0.12, 0.20, 0.30$ were annealed at 25°C for a minimum of 7 days. Data for these samples, taken at $\Theta = 0.4°$, are shown in Figure 1 as a plot of Rk^4 versus k, where k is the perpendicular component of the neutron wave vector. The systematic increase in the amplitude of the oscillations indicates an increase in surface concentration of the dPEP as ϕ_0 increases and broadening of the composition profile near the surface away from the mean-field prediction. Analysis is continuing to determine the detailed shape of the profiles.

References

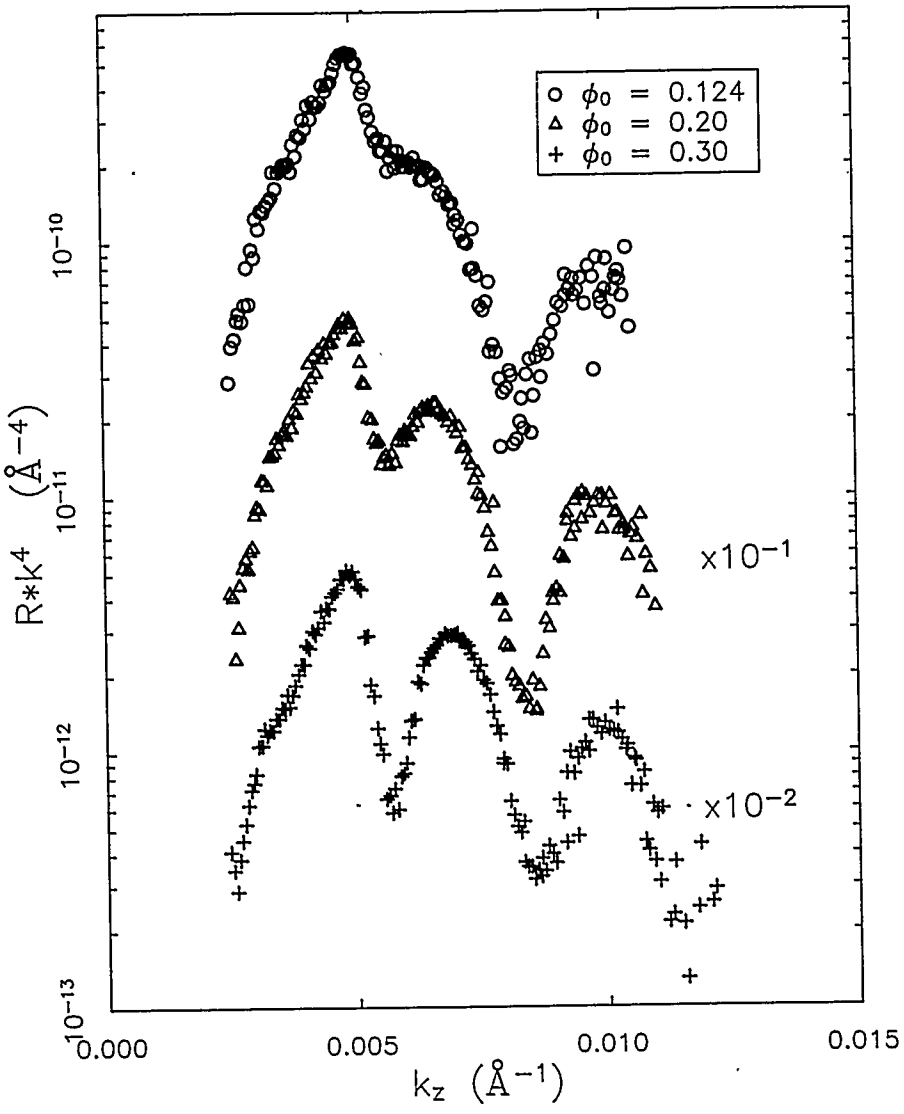
1) R.A.L. Jones, E.J. Kramer, M.H. Rafailovich, J. Sokolov, S. A. Schwarz, Phys. Rev. Lett. 62 280 (1989); R.A.L. Jones, L.J. Norton, E.J. Kramer, R.J. Composto, R.S. Stein, T.P. Russell, A. Karim, A. Mansour, G.P. Felcher, M.H. Rafailovich, J. Sokolov, X. Zhou, and S. A. Schwarz, Europhys. Lett.,12 41-46 (1990).

2) IPNS Reports 1/91, 8/91; L.J.Norton et al., in preparation.

3) I.Schmidt and K. Binder, J. Physique (Paris) 46 1631 (1985).

4) M.D. Gehlsen, J.H. Rosedale, F.S. Bates, G.D. Wignall, L. Hansen, K. Almdal, Phys. Rev. Lett. 68 2452 (1992).

Figure 1



INSTRUMENT USED: POSY II	DATE OF REPORT: 5-18-93	EXPERIMENT NO.: 1636
TITLE: Surface Enrichment in Isotopic Polymer Alloys by Neutron Reflectometry		
AUTHORS AND AFFILIATIONS: L. J. Norton, E. J. Kramer (Cornell U); A. Karim (NIST); F. S. Bates, M. D. Gehlsen, J. H. Rosedale (U Minnesota)		
DATES OF EXPERIMENT: 10/16-20/92 2/14-19/93		

CHECK ALL APPLICABLE BOXES:

- ☒ APPROVED BY PROGRAM COMMITTEE
- ☐ INSTRUMENT SCIENTIST ALLOCATION
- ☐ DO NOT PUBLISH
- ☐ PROPRIETARY RESEARCH
- ☐ PRT ALLOCATION

EXPERIMENTAL REPORT (or Abstract of Publication)

In earlier studies of surface enrichment we measured the neutron reflectivity from an isotopic blend of protonated and deuterated polyethylenepropylene (PEP and dPEP) having degree of polymerizations N_h=2360 and N_d=2140, respectively, and the dPEP having a deuteration fraction f_d = 0.99. Figure 1 shows a composition profile (solid line) for a sample annealed to equilibrium at 35°C. The depth from the surface is scaled by the average radius of gyration, $R_g^2=Na^2/6$, where a is the statistical segment length. The deuterated component has segregated to the surface[1,2] and the detailed shape of the profile differs substantially from the theoretical prediction[3] shown with a dashed line. Jones[4] recently calculated the effect of long range surface forces on the shape of the composition profile. No experimentally measurable deviation of the profile from the short range force case was observed. Therefore, we believe that our results indicate a breakdown of the approximations of mean-field theory at large concentrations of the deuterated chains which probably fails to account properly for the perturbed chain configuration near the surface.

In order to facilitate the development of a more complete theory of surface segregation we have measured the neutron reflectivity from a blend with N=7910 and f_d = 0.532. Recently Gehlsen et al.[5] found for PEP/dPEP blends that the Flory parameter χ (which describes the strength of the interaction between segments of the two components) is independent of N and takes the form $\chi = f_d^2\ [\ 0.571/T - 0.000656\ ]$. A systematic variation of both f_d and N maintains χN, and thus the bulk thermodynamics, while varying the surface energy difference and correlation length for concentration fluctuations. A series of films, with a thickness of ~3000Å (~10R_g), were annealed at 25°C for a minimum of 15 days. Figure 2 shows the composition profile from one of these samples with nearly the same bulk concentration ϕ_∞ as in figure 1. Qualitatively similar deviations from the mean-field prediction are observed. Analysis of the other samples is continuing to investigate these deviations as ϕ_∞ is varied.

EXPERIMENTAL REPORT (CONTD.)

Figure 1

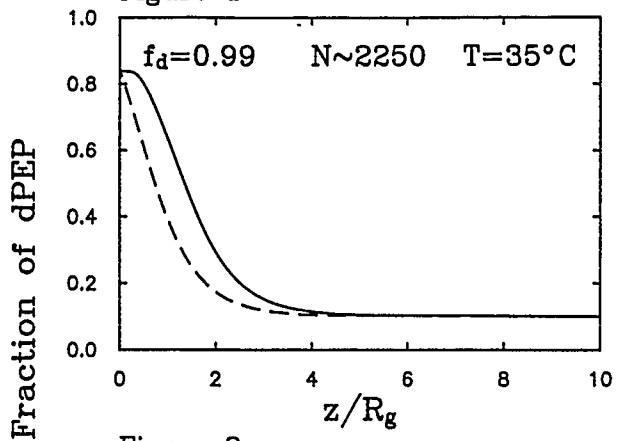
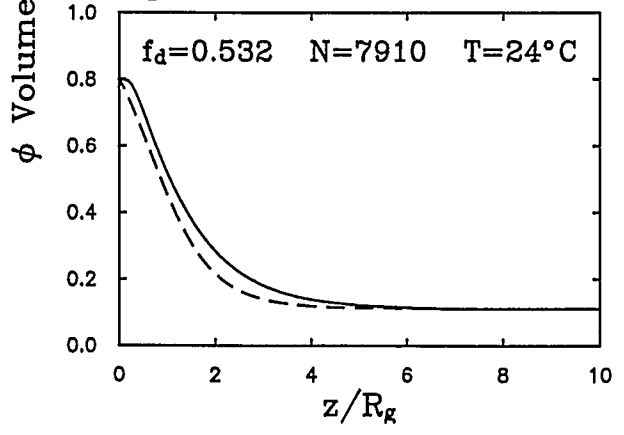


Figure 2



References

1) R.A.L. Jones, E.J. Kramer, M.H. Rafailovich, J. Sokolov, S. A. Schwarz, Phys. Rev. Lett. 62 280 (1989); R.A.L. Jones, L.J. Norton, E.J. Kramer, R.J. Composto, R.S. Stein, T.P. Russell, A. Karim, A. Mansour, G.P. Felcher, M.H. Rafailovich, J. Sokolov, X. Zhou, and S. A. Schwarz, *Europhys. Lett.*,12 41-46 (1990).

2) IPNS Reports 1/91, 8/91; L.J.Norton et al., *in preparation.*

3) I.Schmidt and K. Binder, *J. Physique* (Paris) 46 1631 (1985). N. Nakanishi and P. Pincus, *J. Chem. Phys.* 90,10 (1989).

4) R. A. L. Jones, *Phys. Rev. E*, 47 1437 (1993).

5) M.D. Gehlsen, J.H. Rosedale, F.S. Bates, G.D. Wignall, L. Hansen, K. Almdal, *Phys. Rev. Lett.* 68 2452 (1992).

INSTRUMENT USED:	DATE OF REPORT:	EXPERIMENT NO.:
POSY II	01/30/91	No. 1233

TITLE:
Structure of Blends of Block Copolymer and Homopolymers

AUTHORS AND AFFILIATIONS:
R.J. Roe and K.J. Jeon, University of Cincinnati and: T.P. Russell, Almaden Research Center, IBM

DATES OF EXPERIMENT: June 22-26, 1990

☐ APPROVED BY PROGRAM COMMITTEE, OR

☐ PART OF INSTRUMENT SCIENTIST ALLOCATION

REPORT RECEIVED:

EXPERIMENTAL REPORT (or Abstract of Publication)

The objective of the experiment was to measure the neutron reflectivity of thin polymer samples supported on a silica substrate, and then analyze the data to obtain the distribution of matter across the cross-section of the film. The samples consisted of blends of styrene-butadiene diblock copolymer with various amounts of added polystyrene. In the samples various permutations of the three components involved, i.e., the styrene block, the butadiene block, and the polystyrene, were deuterated to produce contrast. These blends, dissolved in toluene, were spin cast onto the silica substrate to produce thin film of thickness on the order of 0.1 μm. Previous investigations, by members of our group and by some other workers, have shown that in such thin films, after thermal annealing for an appropriate length of time, the block copolymer organizes itself into microdomain lamellae parallel to the film surface. The reflectivity measurement would therefore reveal the thickness of the lamellae and the concentration distribution of the added polystyrene, when either one of the styrene block and the polystyrene is deuterated.

EXPERIMENTAL REPORT (CONTD.)

The reflectivity measurements were done with only some of the samples prepared because of the limitation in the allocated beam time. The reflectivity profiles obtained were, however, somewhat different from what we expected from intuitive consideration on the basis of the model of the structure we had in mind. Quantitative interpretation of the measured reflectivity profile to deduce the distribution of deuterated species across the film thickness direction also turned out to be very difficult. Although the possibility of the structure of the films which is entirely different from our preconceived models could not be totally ruled out, we came rather to suspect that in the samples a sufficient degree of ordering of the block copolymer lamellae parallel to the film surface was in fact not attained. A scrutiny of the film preparation procedure revealed that the temperature of the film annealing may have been too high, in comparison to the chemical stability of the material, leading to cross-linking which prevented sufficient chain mobility to achieve the desired ordering.

Since then we have re-evaluated our sample preparation procedure, checking the structure of the obtained films by means of DSIMS. The latter technique gives a reasonably good indicator of the extent of ordering in the films, but of course does not have the sufficient spatial resolution required in this research project. The knowledge of the concentration profile of the added homopolymer in the block copolymer lamellae will have important bearing in testing the several theories proposed to explain the structure of block copolymers under a variety of conditions and the solubility of the homopolymers in the block copolymer. We plan to continue this project, and a new set of samples are new being prepared.

INSTRUMENT USED:	DATE OF REPORT:	EXPERIMENT NO.:
POSY II	1/30/91	1350

TITLE: EFFECT OF DIBLOCK COPOLYMERS ON ADHESION

AUTHORS AND AFFILIATIONS:
T.P.Russell, H.R.Brown IBM

DATES OF EXPERIMENT: 12/90

☑ APPROVED BY PROGRAM COMMITTEE, OR

☐ PART OF INSTRUMENT SCIENTIST ALLOCATION

REPORT RECEIVED:

REPORT

The adhesion between two immiscible polymers is generally weak due to the lack of interpenetration of the polymer molecules across the narrow interface between the two homopolymers. Typically this interface is on the order of 10-50Å. One means by which the adhesion can be improved is by use of a diblock copolymer where one of the blocks resides preferentially in one homopolymer and the other block in the other homopolymer. This has been shown in the case of PS and PMMA homopolymers where a symmetric diblock copolymer of PS and PMMA, denoted P(S-b-MMA) is placed at the interface between the two homopolymers.[1] The detailed segment density distributions of the different components in this system has been treated previously by neutron reflectivity[2] and is the current subject of an alternate proposal (IPNS#1349).

The subject of this work is the extension of these studies to the case where the homopolymers have different chemical structures from the diblock copolymer and where the segmental interaction parameter, χ, plays a role. In particular studies were performed on bilayers of perdeuterated PMMA and poly(2,6-dimethyl-phenylene oxide), denote PXE, where a symmetric diblock copolymer of P(S-b-MMA) was placed at the interface. Previous studies have shown that the interface formed between PMMA and PXE is quite sharp with an effective interfacial width of 33Å and the fracture energy of the bilayer formed is not measurable. However, the addition of P(S-b-MMA) where the molecular weight of each block of the copolymer is $\sim 5 \times 10^4$ results in a substantial increase in the fracture energy to ~ 200 J/m^2.

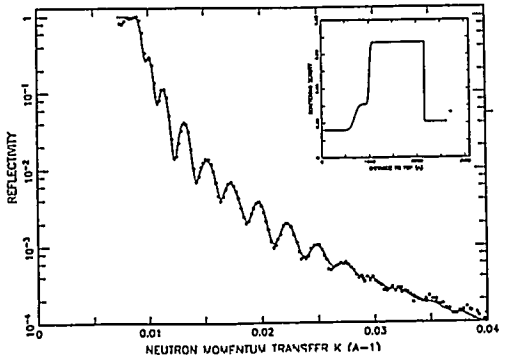
The specimens for the neutron reflectivity measurements were prepared by spin coating a layer of d-PMMA onto a Si substrate. On separate substrate a ~250Å film of P(d-S-b-d-MMA) was prepared, floated off onto a pool of water and retrieved with the d-PMMA coated substrate. In a similar manner a film of PXE was transferred on top of the bilayer forming a trilayered specimen. This trilayer was annealed at 160°C for 120 hrs and quenched to room temperature to perform the reflectivity measurements. The reflectivity profile obtained from this trilayer is shown in Figure 1. Use of a simple bilayer model with a hyperbolic tangent or error function to describe the interface did not yield satisfactory agreement with the observed reflectivity. Only by inclusion of a small step in the scattering length density profile, as shown in the inset of Figure 1, was reasonable agreement found. In these calculations the width of the step, representing the d-PS segments of the copolymer, was 315±30Å. This represents a substantial stretching of the PS segments of the copolymer at the interface which is quite different from the results obtained for the case where the homopolymer and diblock copolymer segments are the same[3]. This stretching results from the favorable interactions between the PS segments of the copolymer and the PXE homopolymer segments.

EXPERIMENTAL REPORT (CONTD.)

Limited experimental time precluded a systematic investigation of this problem which requires a consecutive variation of the labelling of the homopolymer and diblock copolymer segments. These are the subject of a current proposal. In addition, we have obtained the deuterated analog of PXE which dramatically enhances the capability and variability of determining the segment density profiles.

REFERENCES

1. H.R.Brown, 1989. *Macromolecules* 22, 2859.
2. T.P.Russell, A.Menelle, S.H.Anastasiadis, G.P.Felcher and S.K.Satija, 1991. *Macromolecules* in press.



INSTRUMENT USED:	DATE OF REPORT:	EXPERIMENT NO.:
POSY II	1/25/91	1349

TITLE:

INTERFACIAL ACTIVITY OF DIBLOCK COPOLYMERS

AUTHORS AND AFFILIATIONS:

T.P.Russell, IBM; A.Menelle, IBM; G.P.Felcher, IPNS; S.K.Satija, NIST

DATES OF EXPERIMENT: 12/90

☒ APPROVED BY PROGRAM COMMITTEE, OR

☐ PART OF INSTRUMENT SCIENTIST ALLOCATION

REPORT RECEIVED:

REPORT

Neutron reflectivity was used to investigate the behavior of diblock copolymers at the interface between homopolymers. In these experiments homopolymers of polystyrene, PS, and poly(methylmethacrylate), PMMA, with molecular weights of $\sim 10^4$ and $5x10^4$ were used. The diblock copolymer was a symmetric diblock copolymer of PS and PMMA, denoted P(S-b-MMA), where the molecular weights of each block was $5x10^4$. The specimens were prepared by casting films of PMMA onto an Si substrate. Films of the P(S-b-MMA) were prepared on separate substrate, floated off onto a pool of water and retrieved with the PMMA coated substrate. In a similar manner a layer of PS was prepared thereby making a trilayered specimen. The specimens were annealed at 160°C for 240 hrs under vacuum to allow the specimens to come to equilibrium and were then quenched to room temperature to perform the reflectivity measurements. Reflectivity measurements were performed at several different angles of incidence to cover a neutron momentum range up to $\sim 0.045 Å^{-1}$.

These studies represent an extension of the studies performed on the same diblock copolymers but where the molecular weights of the homopolymers were 10^5 and 10^6.[1] In all of these experiments, selective labelling of the blocks of the copolymer and/or the homopolymers permitted the isolation of each component. For simplicity in the interpretation of the reflectivity profiles the labelling of the components in three of the experiments were H/H:H/D, H/H:D/D and H/D:D/H where the letters indicate the labelling of the PS/P(S-b-MMA)/PMMA in the trilayer, respectively. Additional experiments were performed on H/D:D/H and H/H:D/H trilayers.

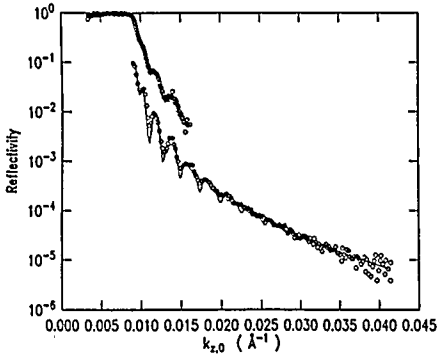
A typical reflectivity profile is shown in Figure 1 for a H/H:D/D specimen. The reflectivity profile is characterized by a sharp drop in the reflectivity past the critical angle with essentially a single frequency oscillation superposed. Since, in the first three cases mentioned above, the reflectivity measurements can not distinguish between the segments of the copolymer and homopolymer with the same labelling, these three cases reduce to a simple bilayer model. In fact, considering the reflectances, to a very good approximation the reflectivity results from a single layer of deuterated material. Independent optical ellipsometry measurements of all the film thicknesses reduced the number of parameters in the calculations to essentially the width of the interface between the H and D layers. A typical fit to the reflectivity profile is shown as the solid line in the figure. As can be seen, good agreement between the calculated and measured reflectivities was found.

EXPERIMENTAL REPORT (CONTD.)

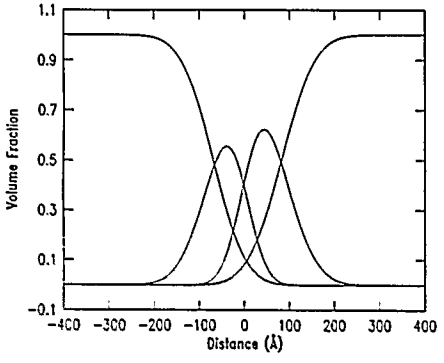
From the scattering length density profiles used to calculate the reflectivity profiles, a simultaneous set of equations can be used to determine the concentration profiles of the PS and PMMA homopolymers and block copolymers at the interface. These results can then be directly compared to the results determined from the H/H:D/H and H/D:D/H experiments. The segment density distributions determined in this manner are shown in Figure 2 for the case where the homopolymer molecular weights were $5x10^4$. Analysis is still in progress for the 10^4 case. In comparison to the results obtained previously, the measurements here show that the amount of copolymer segregated at the interface is lower which is in keeping with the reduced molecular weights. As in the previous cases,[1] there is substantial penetration of the homopolymers into the interfacial region.

REFERENCES

1. T.P.Russell, A.Menelle, S.H.Anastasiadis, G.P.Felcher and S.K.Satija, 1991. *Macromolecules* in press.



PSH(50K)/PSD:PMMAD(50:50)/PMMAD σ_i=80Å



PS(50K)/P(S-b-MMA)(50K-50K)/PMMA(50K)

INSTRUMENT USED:	DATE OF REPORT:	EXPERIMENT NO.:
POSY-II	7/18/91	1477

TITLE:

Interfacial Activity of Diblock Copolymers

AUTHORS AND AFFILIATIONS:
T.P.Russell, A.Menelle; IBM ARC, 650 Harry Road, San Jose, CA 95120

DATES OF EXPERIMENT: 4/91

☐ APPROVED BY PROGRAM COMMITTEE, OR

☐ PART OF INSTRUMENT SCIENTIST ALLOCATION

REPORT RECEIVED:

EXPERIMENTAL REPORT (or Abstract of Publication)

Experiments were performed on the interfacial behavior of polystyrene, PS, polymethylmethacrylate, PMMA, diblock copolymers, denoted P(S-b-MMA), at the interface between the immiscible homopolymer pairs of PS and PMMA and poly(2,6-dimethylphenylene oxide), PXE. In particular, the segment density profiles for four different systems were evaluated by combining a series of reflectivity measurements at three different angles of incidence. Specifically the systems investigated are tabulated below (molecular weights are indicated in the parentheses)

PS(11K)/PS:PMMA(50K:50K)/PMMA(146K)

PS(300K)/PS:PMMA(150K:150K)/PMMA(300K)

PXE(30K)/PS:PMMA(50K:50K)/PMMA(75K)

PXE(30K)/PS:PMMA(150K:150K)/PMMA(75K)

Experiments were performed on trilayer specimens where a layer of the copolymer was sandwiched between layers of the two homopolymers. All specimens were annealed for at least 120 hrs. at 170°C under vacuum and cooled to room temperature where the reflectivity measurements were performed. Four sets of experiments were performed for each of the first two systems where the labelling of the components was varied as: H/H:H/D; H/H:D/D; H/D:D/D and H/D:D/H. In the first three cases the analysis of the reflectivity profiles was quite straightforward since the specimens reduce to a simple bilayer separated by an interface which was well described by an error function. In the final case, a four layer model had to be used with interfaces between H/D:D and D:D/H. The segment density profiles evaluated from the fits of the reflectivity profiles were simultaneously solved to yield the scattering length density profiles of the PS and PMMA homopolymers and the blocks of the copolymers. The final results of these analyses are shown in Figures 1 and 2.

From these profiles there are several features worth noting. First, as the molecular weight of the copolymer increases the copolymer behaves more efficiently as a barrier between the two immiscible homopolymers. That is to say, the penetration of the homopolymers into the interfacial region is markedly decreased in the case of the 150K:150K copolymer. As can be seen there is virtually no overlap of the two homopolymers in the interfacial region. In the case of the 50K:50K copolymer, on the other hand, the PS and PMMA homopolymers overlap significantly in the interfacial region. Secondly, the amount of copolymer at the interface between the homopolymer increases with increasing molecular weight. For the 150K:150K case, the concentration of the copolymer is essentially unity whereas for the 50K:50K case, a total copolymer volume fraction of only 0.8 is seen. It is also interesting to note that the sum of the PMMA homopolymer segments and PMMA segments in the copolymer can be taken

EXPERIMENTAL REPORT (CONTD.)

These results are being combined with those from different molecular weights of the PS and PMMA homopolymers and are being compared to current theoretical predictions.

For the cases involving the PXE homopolymer, the unavailability of deuterated PXE forced the use of only three experiments where the labelling of the PS:PMMA and PMMA homopolymer were varied. The fourth experiment, useful for providing an internal check, is not mandatory. The concentration profiles required to fit the H/H:H/D and H/H:D/D data reduced to a simple two layer model with a single interface. However, the H/D:D/D scheme required the use of three a layer model where the PSD block of the copolymer formed a separate layer showing that the homopolymer was being stretched into the PXE layer due to the favorable interactions between the PS and PXE segments. At present the concentration profiles have been determined but further checks on the fitting procedure are in progress. The results on these analyses will be forthcoming shortly.
which yields the interfacial width between the PS and PMMA segments. In the case of the 150K:150K copolymer, the interfacial width is 90±5Å which compares well with previous results obtained on PS(100K)/PS:PMMA(50K:50K)/PMMA(100K) and PS(10^6)/PS:PMMA(50K:50K)/PMMA(10^6). This width is nearly 80% broader than the width found in the corresponding pure diblock copolymers and represents a reduction in the interfacial tension between the homopolymers. For the PS(11K)/PS:PMMA(50K:50K)/PMMA(146K), on the other hand, the interfacial width was found to be 118±5Å which is significantly broader. This results reflects directly the reduction in the interfacial tension due to the low molecular weight of the PS homopolymer.

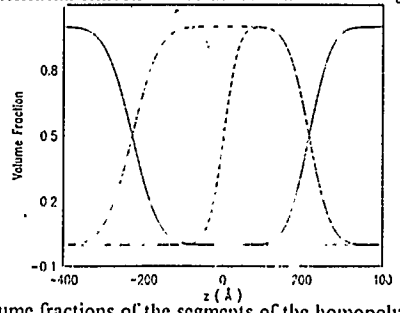


Figure 1. Volume fractions of the segments of the homopolymers and diblock copolymers at the interface where the system is: PS(300K)/PS:PMMA(150K:150K)/PMMA(300K).

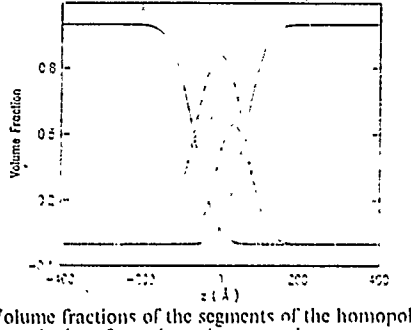


Figure 2. Volume fractions of the segments of the homopolymers and diblock copolymers at the interface where the system is: PS(11K)/PS:PMMA(50K:50K) PMMA(146K).

INSTRUMENT USED:	DATE OF REPORT:	EXPERIMENT NO.:
Posy II	6/19/92	1450

TITLE:
Diffusion of Polymers in Crosslinked Polymer Networks

AUTHORS AND AFFILIATIONS:
Bryan Sauer, John VanAlsten, Dave Walsh duPont

DATES OF EXPERIMENT: 4/17 -4/20, 1992

☒ APPROVED BY PROGRAM COMMITTEE, OR

☐ PART OF INSTRUMENT SCIENTIST ALLOCATION

REPORT RECEIVED:

EXPERIMENTAL REPORT (or Abstract of Publication)

Adsorbed Polymer Profiles and Exchange Kinetics at the Polymer-Melt/Solid Interface Studied by Neutron Reflection(NR)

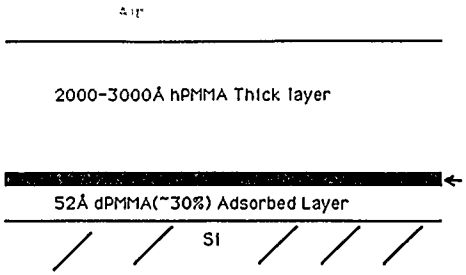
Because of the high depth resolution needed and difficulty in resolving surface adsorbed species from bulk species, little if any experimental information on polymer conformation at a solid surface in the melt state has been obtained. For the same reason, polymer exchange and diffusion at the solid/melt interface has not been experimentally addressed. For the length scales of interest, NR is the only technique applicable. To provide this necessary discrimination between adsorbed and bulk species, we pre-adsorb a single layer of deuterated poly(methyl methacrylate) (dPMMA) on a Si wafer out of dilute solution for 24 hrs.(Figure A) After extensively rinsing with solvent, a second thick layer of hydrogenated (hPMMA) is then applied on top by spin coating.

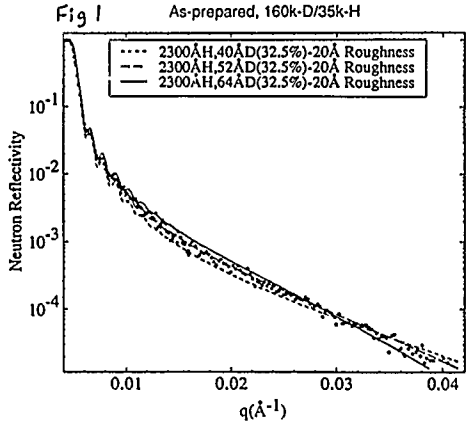
Figure 1 illustrates the sensitivity of the technique to the deuterated layer thickness in comparison to a representative experiment. The roughness indicated on the plot is introduced between the dPMMA and hPMMA layers and is effectively a diffuse interface between the layers.

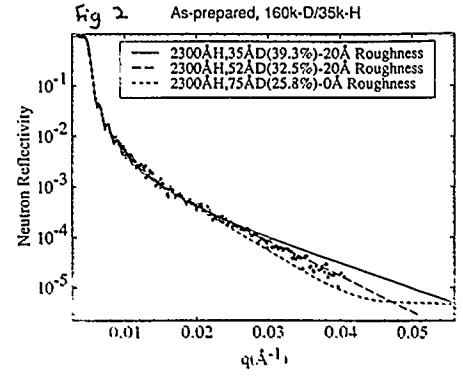
Because the layers are so thin, there are limitations in determining both the concentration and thickness of deuterated species at the solid surface. An example of just how much one can say about the profile of the deuterated species at the Si surface is shown in Figure 2. The best fit is shown in Figure 2 for a 52Å dPMMA layer(32.5%) and 20Å(error function) roughness. Attempting to find best fits by fixing the thicknesses at 35Å and 75Å and allowing the concentration and roughness to vary, gave the other two fits shown in Figure 2. They are not satisfactory. Thus, the thickness determined is 52Å±7Å. The precision is actually ~2Å if the concentration is fixed. This type of dimension is physically reasonable since the Rg of a 160k dPMMA molecule is ~100Å. The fact that the "deuterated" layer is only ~33% dPMMA indicates that the adsorbed molecules are highly swollen. The roughness needed to model the data indicates that the segmental density of the adsorbed species is higher near the surface as expected.

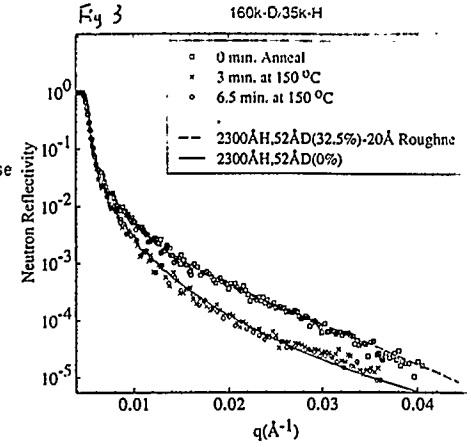
The bilayer samples of hPMMA/dPMMA/Si were annealed in a convection oven. After only 3 minutes at 150 °C the dPMMA concentration for one sample was reduced to 0%.(Figure 3) Further annealing for 6.5 minutes total lead to no discernable change in the spectra. This was the lowest M.W. hPMMA studied and exchange was rather rapid. For a bilayer with a higher hPMMA M.W., the exchange is slower as is indicated by the data in Figure 5.

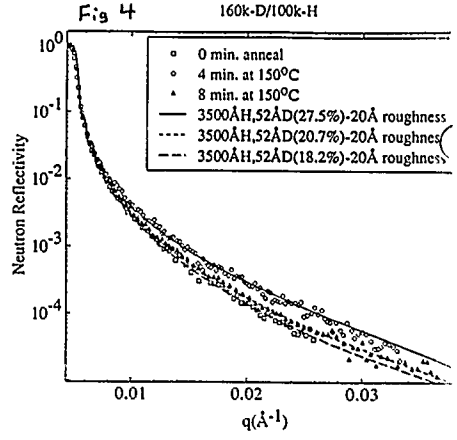
The kinetics data is summarized in Figure 5 in terms of the variation in hPMMA M.W. at constant dPMMA M.W. The thickness was fixed at 52Å(for reasons discussed above), and the concentration was varied to obtain the best fit. The precision is very good. There is a systematic trend with exchange occurring faster for lower hPMMA molecular weights. Variation of the dPMMA M.W. has not yet been performed.

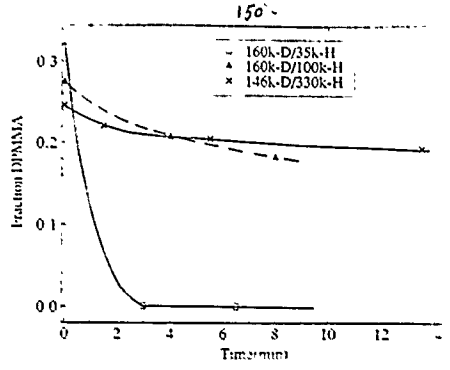












INSTRUMENT USED: POSY II

DATE OF REPORT: 7/31/92

EXPERIMENT NO: 1568

TITLE: Polyimide Interfaces: Imidization and Interdiffusion by Neutron Reflectrometry

AUTHORS AND AFFILIATIONS: N.C.Stoffel, E.J. Kramer (Cornell U); T.P. Russell, W.Volksen (IBM ARC).

DATES OF EXPERIMENT: 6/17/92-6/23/92

✓ APPROVED BY PROGRAM COMMITTEE, OR

— PART OF INSTRUMENT SCIENTIST ALLOCATION

REPORT RECEIVED:

EXPERIMENTAL REPORT (or Abstract of Publication)

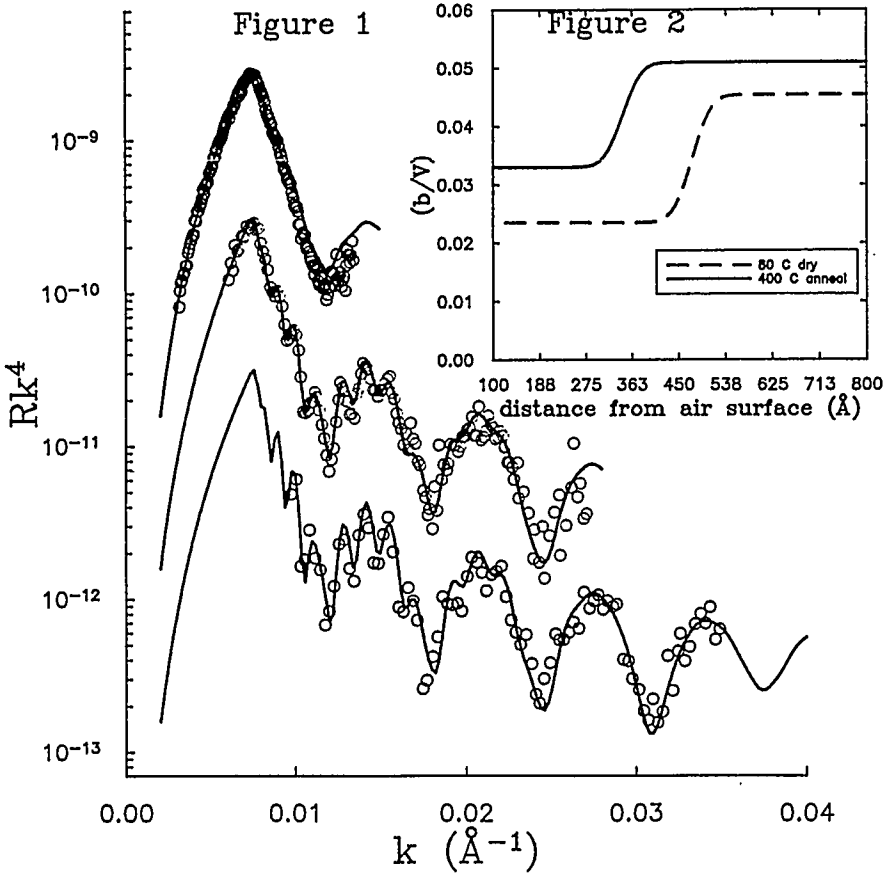
Forward recoil spectrometry (FRES) measurements show that the interdiffusion distance w decreases markedly as the imide fraction f of the polyimide is increased toward 1. These w's correlate with fracture toughness Gc of the interface, but further decreases in Gc are found as f approaches 1 where w is too small to be measured by FRES. Neutron reflectivity was used here to determine w under these conditions.

In order to make diffusion measurements possible the meta isomer of the polyamic ethyl ester (PAE) of PMDA-ODA was synthesized in both a hydrogenated version (PAE), and a deuterated version (d-PAE) where the hydrogens of the oxydianiline moeity (ODA) were replaced with deuterium. Prior to our interdiffusion studies, we measured the (b/V) profile of single layer polyimide films. When spuncast from DMSO, the (b/V) was constant. In contrast, films spun-cast from NMP displayed a region of lower scattering length density in a region ~70Å below the air surface. X-ray reflectivity confirmed these observations.

Neutron reflectivity measurements were made on a bilayer sample prepared by spin-casting a d-PAE base layer from DMSO onto silicon, baking at 300 °C to cause imidization (f=0.9), and then spin-casting a PAE layer on top, and finally drying at 80°C. A plot of Rk^4 vs. k (Where R is the reflectivity and k is the perpendicular component of the neutron wavevector) for this bilayer sample is shown in Figure 1. The fit is calculated from the scattering length density profile seen in the dashed line of Figure 2, and yields w=30 Å. This value may be compared to the interfacial width of the same sample after a 400 °C thermal treatment, where w has increased to 40Å, as shown in the solid line of Figure 2. We are continuing analysis of neutron reflectivity data for bilayers cast from NMP with base layer anneals at 300 °C and 400 °C (corresponding to f = 0.9 and 1 respectively), both before and after annealing. In order to complete this study, one additional sample, cast from DMSO, with a base layer anneal at 400 °C must be run both after drying, and after annealing.

References:

1.) "Diffusion and Self-Adhesion of the Polyimide, PMDA-ODA", H.R. Brown, A.C.-M. Yang, T.P. Russell, W. Volksen and E.J. Kramer, (MSC Report # 6311), Polymer, 29 , 1807-1811 (1988).



INSTRUMENT USED:	DATE OF REPORT:	EXPERIMENT NO.:
POSY II	7/25/94	7

TITLE: Interfacial Broadening of Segmented Poly Urethane Ureas)

AUTHORS AND AFFILIATIONS:

DATES OF EXPERIMENT: Nov 16-19, 1993

☒ APPROVED BY PROGRAM COMMITTEE, OR

☐ PART OF INSTRUMENT SCIENTIST ALLOCATION

REPORT RECEIVED:

INTERFACIAL BROADENING SEGMENTED POLY(URETHANE UREAS) STUDIED BY NEUTRON REFLECTION

John G. Van Alsten, Bryan B. Sauer, Craig R. Gochanour, Katherine L. Faron
Central Research and Development
E. I. DuPont de Nemours & Company, Wilmington, DE 19880-0356

William D. Dozier
Building 223, Argonne National Laboratory, Argonne, IL 60439

Summary: We have studied the development of the interface between bilayers of a segmented Poly(Urethane Urea) (PUU) elastomers using neutron reflection and mechanical measurements. Neutron contrast was obtained by using partially deuterated PUU in thin film bilayers with its hydrogenated analog. The interface widths broaden to ca. 7 nm after a few days of annealing at room temperature, with only small increases seen after further annealing at high temperatures. Interpenetration is likely limited by phase separated hard segment domains which act as physical cross-links between the soft segments. The final interface width is somewhat larger than the dimension of the low glass transition soft segment blocks in PUU which are believed responsible for the self-adhesion. The rate of peel strength is strongly temperature dependent, even though the temperature is well above the soft-segment melting point. It is speculated that diffusion of chain ends consisting mainly of soft segments is responsible for interdiffusion.

The PUU studied here is a micro-phase separated segmented block copolymer consisting of 85% by volume poly(tetramethylene oxide) (PTMeO) soft segments and 15% aromatic urethane-urea linked hard segments.[3] The overall M_w of PUU is about 60,000. The PUU samples are micro-phase separated, which is typical of this type of polyurethane-urea. For our studies, a deuterium-labeled material was prepared by substituting per-deuterated poly(tetramethylene oxide) (d-PTMeO) for PTMeO.

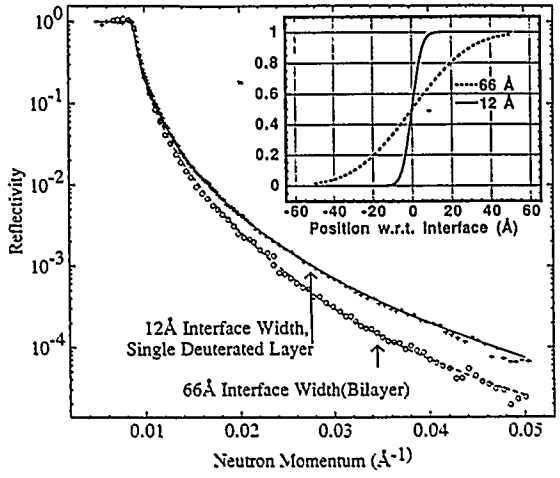
The following conditions were found to give films and bilayers of acceptable quality. Individual d-PUU films (0.7 μm thick by ellipsometry) were spun at 45 °C onto 2 inch diameter silicon wafers from a ca. 7% by weight solution in DMAC. h-PUU films (ca. 1 μm thick) were prepared by solution coating at T>45 °C onto poly(ethylene terephthalate) (PET, Mylar® film) and bilayers of the two were produced by pressing the h-PUU film onto the d-PUU film and running a wedge across the PET surface to remove air bubbles at T>40 °C, before removing the PET film.

The interface widths reported here are full widths defined in terms of a linear gradient profile. In Figure 1 the experimental and model results are compared for a single layer of d-PUU and a h-PUU/d-PUU bilayer, with schematics of the corresponding interfacial profiles shown in the inset. For the single d-PUU layer, the air/polymer interface has a characteristically sharp interface width of 1.2±0.5 nm typical of a single layer of amorphous polymer on a Si wafer. The interface of the bilayer prepared by "bonding" at 60 °C for 1 minute with a subsequent 3 day anneal at 23 °C, broadened to 6.6 ± 0.3 nm indicating that there is significant interpenetration of d- and h-chains across the interface (inset Figure 3). Other data are given in Table1.

Table 1
Interfacial Widths (in nm) as a Function of Thermal History

PUU-A(Single Layer of d-PUU)	
as prepared, 45 °C	1.2± 0.5
+15 min., 80 °C	1.2± 0.5
+10 min., 120 °C	1.2± 0.5
PUU-B(Bilayer "Bonded" at 60 °C for 1 minute)*	
+ 3 days at 23 °C	6.6 ± 0.3
+15 min., 80 °C	6.6 ± 0.3
+25 min., 120 °C	8.0 ± 0.5

Figure 1) Comparison of the reflectivity vs. momentum transfer from a single d-PUU layer and a d-PUU/h-PUU bilayer, both on Si wafer. The interfacial broadening of the bilayer is indicative of substantial chain interdiffusion caused by annealing at 60 °C for 1 minute plus 3 days at 23 °C (Table 1).
Inset. Schematic of compositional profiles normal to the interface for air/d-PUU and d-PUU/h-PUU.



INSTRUMENT USED:	DATE OF REPORT:	EXPERIMENT NO.:
POSY II	8/3/90	1359

TITLE: Neutron Reflection Studies of Polymer Interfaces

AUTHORS AND AFFILIATIONS: David J. Walsh and Bryan B. Sauer
E.I. Du Pont de Nemours & Co., Experimental Station, Wilmington, DE 19880-0356

DATES OF EXPERIMENT: 10/17/89-10/20-89

☒ APPROVED BY PROGRAM COMMITTEE, OR

☐ PART OF INSTRUMENT SCIENTIST ALLOCATION

REPORT RECEIVED:

EXPERIMENTAL REPORT (or Abstract of Publication)

Neutron Reflection Studies of Polymer Interfaces

Abstract: Neutron reflection(NR) was used to study the evolution of the buried interface between spin-coated thin films of the miscible pair, poly(vinyl methyl ether)(PVME) and polystyrene(PS)(Figure 3) as a function of time and temperature. At temperatures around the glass transition of PS(T_g =104°C), interdiffusion was too rapid to monitor due to the high mobility of PVME(T_g = -31°C). At 80°C the interdiffusion occurred slow enough so that the interface could be monitored as a function of annealing time.

The reflectivity profiles for two different as-spun PVME/PS/Glass bilayer samples are shown in Figure 1. The reproducibility of the experiment is extremely good from sample to sample as is indicated in the figure. NR is not sensitive to the PVME and PS layer thicknesses(both approximately 800 nm), but is sensitive to interfacial roughness, which is in most cases, indistinguishable from interfacial broadening due to interdiffusion. The data was modelled using an error function interfacial profile(Gaussian segmental density profile as distance is varied normal to the plane of the interface) or an linear gradient profile. The simulated spectra were essentially identical using these two interfacial profiles, except the error function $\langle z^2\rangle^{1/2}$ parameter is as effective as a linear gradient thickness twice as wide. Thus, in all the discussion that follows, we will present the interface dimension in terms of equivalent of the linear gradient profile; i.e., the error function parameter $\langle z^2\rangle^{1/2}$ times 2.

Only small increases in thickness occurred after annealing for 2 minutes and 12 minutes at 80°C as is indicated in Figure 2 and Table I. The value of b/V of the PVME phase also apparently increases about 20% to 2.6(±0.2) x 10^{-10} cm^{-2} due to dissolution of deuterated PS in the PVME layer. The contribution of b/V for the PVME phase generally influences the calculated spectra in the high q region so the effects can easily be uncorrelated from those due to variations in the interfacial thickness.

The model that we have extracted from these experiments, is that PVME penetrates the PS surface and imparts significant mobility to PS in the interfacial layer by reducing T_g. Thus, the PVME etches away the PS in a thin dynamic interfacial layer at 80°C even though the PS has no mobility in the bulk, at this temperature. The interface broadens from 11 nm to 14 nm after 12 minutes at 80°C and the neutron scattering length of the PVME phase increases 20% due to the PS which has dissolved and diffused away from the interface.

EXPERIMENTAL REPORT (CONTD.)

Figure 1. Reflected neutron intensity versus momentum transfer (q) for two different as-spun films of PVME/PS/Glass.

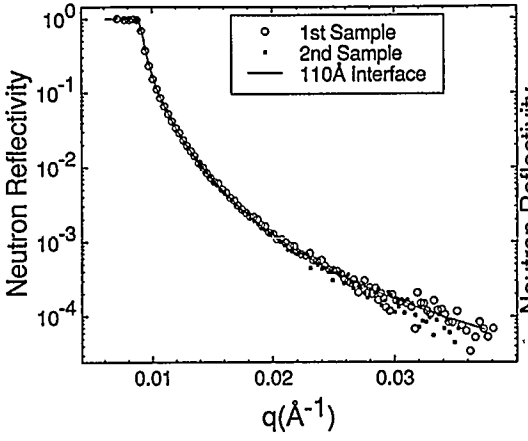
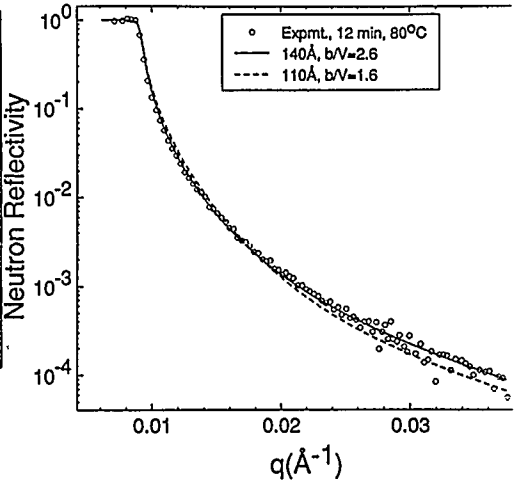


Figure 2. Reflectivity vs. q for PVME/PS/Glass annealed at 80°C. The simulated curve from Figure 1 is included to indicat the total change due to annealing.



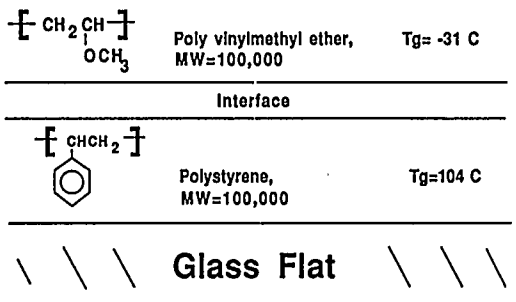


Table I Interfacial Thickness, PVME/PS/Glass

	Interfacial Thickness (nm)	$(b/V)_{PVME}$ ($\times 10^{-10}$ cm^{-2})
As Spun	11±0.3	1.6
2 min. @ 80°C	12±0.5	2.0
12 min. @ 80°C	14±0.5	2.3

INSTRUMENT USED:	DATE OF REPORT:	EXPERIMENT NO.:
POSY II	1/21/91	1359

TITLE:
Neutron Reflection Studies of Polymer Interfaces

AUTHORS AND AFFILIATIONS: David J. Walsh and Bryan B. Sauer
E.I. Du Pont de Nemours & Co., Experimental Station, Wilmington, DE 19880-0356

DATES OF EXPERIMENT: 9/11/90 - 9/13/90

☒ APPROVED BY PROGRAM COMMITTEE, OR

☐ PART OF INSTRUMENT SCIENTIST ALLOCATION

REPORT RECEIVED:

EXPERIMENTAL REPORT (or Abstract of Publication)

Neutron Reflection Studies of Polymer Interfaces

Abstract: Neutron reflection(NR) was used to study the evolution of the interface between spin-coated thin films of the miscible pair, poly(vinyl methyl ether)(PVME, MW=100K) and polystyrene(PS)(MW=10K, 100K, 1,000K). In a previous report it was found that PVME swells and etches away the PS at 80°C even though the PS has no mobility in the bulk at this temperature. The more recent experiments reported here indicate that marked non-Fickian diffusion is occurring ~20°C below the glass transition of PS(T_g ~100°C). This is partially because of the high mobility of PVME(T_g = -31°C). No interdiffusion was observed below 70°C. The goal of the experiments reported here is to understand the mechanism of interdiffusion and the polymer properties which govern the rate. It was found that NR was sensitive to some features of an asymmetric interface profile and these features also contribute to understanding of the mechanism involved.

The position of the penetration front of PVME into PS is plotted vs. time in Figure 1. The interdiffusion rate was extremely sensitive to temperature, and changed orders of magnitude as T was varied a few degrees around 80°C. Note also that non-Fickian diffusion is observed, as is indicated by the linear variation with time. To further understand why the rate was so sensitive to T in this narrow range well below T_g, experiments were performed as a function of molecular weight of PS(MW listed in Table I). This allows one to effectively change T_g without perturbing any of the chemical driving forces for miscibility. Because T_g is related to reciprocal MW($T_g = T_{g,\infty}$ - Const./MW), the asymptotic high MW limit of T_g is almost reached at MW=100K. Thus, the T_g 's for 100K and 1,000K PS are about the same while T_g for 10K PS is about 6°C lower(Table I). At 80°C the rate of interdiffusion is about the same for 100K and 1,000K while markedly higher for 10K(Figure 2). This proves that the mechanical relaxations in the solid(glassy) PS phase, which are governed by the proximity to T_g (see Table I), are dominant. Neither diffusion of PVME through the partially swollen network of different molecular weights of PS or reptation of PS away from the interfacial region are the rate determining steps.

Other features of NR which are consistent with a non-Fickian diffusion process, are the occurrence of an asymmetric profile with an extended tail of PVME penetrating into the glassy PS phase. An example of a sample annealed for 12 min. at 80°C is shown in Fig. 3. The upper part of the figure shows that the symmetric and asymmetric profile apparently give the same quality of fit(schematic of profiles given in Fig. 4). Only upon expanding the region near the critical angle(lower part of Fig. 3), is the improvement in fit using the asymmetric profile seen. The asymmetric profile shown is consistent with the ellipsometric data for the same systems although ellipsometry is not as sensitive. The profile is not an unique one for the NR data, but we feel that one must assume some sort of extended tail of PVME into PS to get a reasonable fit.

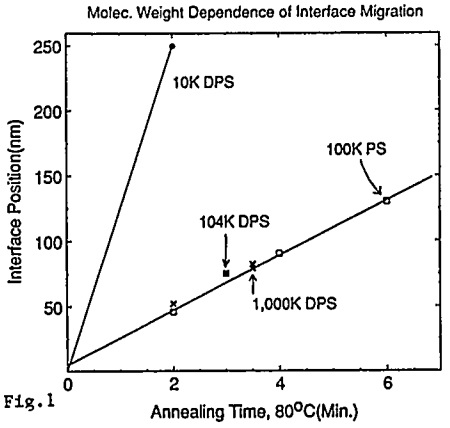


Fig.1

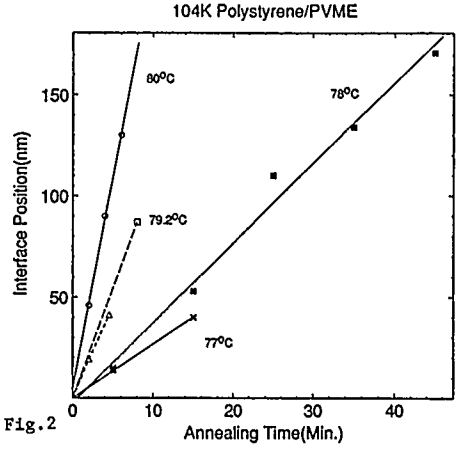
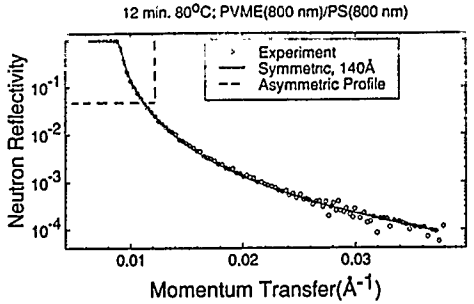


Fig.2

Table I. MW Dependence of T_g as is Related to Annealing Experiments at 80°C.

	T_g (°C)	T_g-T_{anneal} (°C)
10K PS	98	18
100K PS	104	24
1,000K PS	104.6	24.6



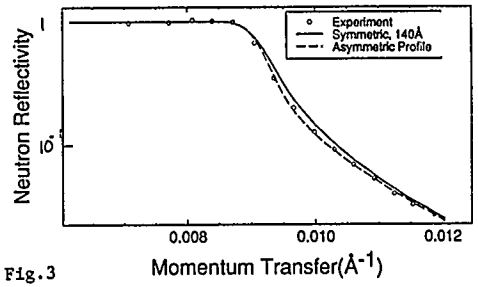


Fig.3

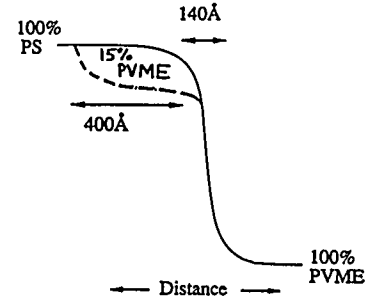


Fig.4

Fig. 1. Variation of penetration front of PVME into PS as a function of annealing temp.
Fig. 2. Variation of penetration front of PVME into different molecular weights of PS after annealing at 80°C.
Fig. 3. Top: Reflectivity vs. q for PVME(100K)/ PS(100K) bilayer annealed at 80°C.
Bottom: Expanded view of dashed box area showing improvement in fit.
Fig. 4. Asymmetric profile(dashed line) superimposed with symmetric profile used to fit NR data in Fig. 3.

INSTRUMENT USED:	DATE OF REPORT:	EXPERIMENT NO.:
Posy II	5/20/91	1359

TITLE: Neutron Reflection Studies of Polymer Interfaces

AUTHORS AND AFFILIATIONS: Dave Walsh and Bryan Sauer, John Van Alsten, duPont Co.

DATES OF EXPERIMENT: April 7-10, 1991

☒ APPROVED BY PROGRAM COMMITTEE, OR

☐ PART OF INSTRUMENT SCIENTIST ALLOCATION

REPORT RECEIVED:

Neutron Reflection Studies of Polymer Interfaces

Abstract: Neutron reflection(NR) was used to study the early stages of poly(vinyl methyl ether)(PVME) diffusing into deuterated polystyrene(dPS) at temperatures well below the glass transition of PS(T_g =104°C). We have also started preliminary experiments looking at the exchange kinetics of a thin(~2 nm) adsorbed layer of deuterated poly(methyl methacrylate) (dPMMA) with a thick reservoir(~200 nm) of hPMMA in the absence of solvent.

PS/PVME

Data is presented below for experiments performed well below the Tg of PS between 60oC and 70oC where interdiffusion is extremely slow. Earlier studies were performed at T>75oC showing relatively rapid interdiffusion and some hints of an asymmetric profile which was obscured to a certain extent by the large diffusion lengths. The temperatures chosen here are well above Tg of PVME(-31°C).

The reflectivity profile for a PVME(100k)/dPS(1000k)/Glass bilayer system annealed at 67oC for 3 minutes is shown in Figure 1. NR is not sensitive to the PVME layer thicknesses(approximately 317 nm by ellipsometry). Very slight modulations can be seen due to the dPS layer thickness of 287 nm. The linear gradient interfacial thickness for the as spun sample(data not shown) was 5±0.3 nm where the linear gradient profile is equivalent to the error function parameter $\langle z^2 \rangle^{1/2}$ times 2. After annealing(Figure 1), the interface broadens quite asymmetrically. The best fit shown in Figure 1 was generated using an asymmetric tail 15 nm wide of 13% PVME extending into the dPS layer superimposed onto a 10 nm linear gradient profile. The best fit using a 11 nm (110Å) symmetric profile is also shown. It is evident that the asymmetric profile fits the data much better.

Other experiments were performed at 60oC with lower MW dPS(83k, 218 nm thick) and the same PVME. Under these conditions the rate of PVME penetration is so slow that the dPS has time to relax and the interface stays symmetric.(Figure 2) This agrees with our modelling of this case II diffusion process. As is indicated in Figure 2, the interface broadens from 7.2 nm to 16.4 nm(164Å) after 3 min. at 60oC. After 13 minutes at 60oC the interface thickness stays at 16.4±0.2 nm but ~10 more nm of the dPS layer is dissolved away.(data not shown) The interface also remains symmetric as expected. As we have proposed earlier, the asymmetric profile in combination with the non-Fickian penetration rate of PVME into dPS indicates that this is an example of case II diffusion typically seen for solvent penetration into polymer well below Tg.

PMMA Exchange Kinetics

The samples were prepared by adsorbing dPMMA(1.8 nm) from solution onto a Si wafer and then spin-coating hPMMA(200 nm) on top. Unlike experiments of exchange

kinetics from solution, where the large number of contacts and the high binding strength lead to very long exchange times and questionable degrees of equilibration because of kinetic factors, exchange from the bulk at T>>Tg increases the thermal energy of the segments compared to the binding strength and it is possible to perform the experiments in a reasonable amount of time. Preliminary experiments indicate that no exchange occurs for dPMMA(100k)/ hPMMA(300k) at 140oC for 30 min. while at 160oC the exchange progresses quite rapidly in tens of minutes. With dPMMA as the thin layer NR is very sensitive to small changes in adsorbed amount. Only neutron reflection can provide the combination of spatial and compositional sensitivity required for these studies. Representative data is shown in Figure 3 for an as-prepared dPMMA/hPMMA bilayer(fit was made using 3.2 nm 50% dPMMA layer and a 200 nm hPMMA layer on top). After annealing for 23 min at 160oC the concentration of dPMMA at the Si surface was essentially zero as is indicated by the fit with a 200 nm hPMMA layer and no deuterated layer.(Figure 3) It is evident that the changes are easily observed in the dPMMA layer concentration and we have a few other points for shorter annealing times at 160oC indicating the gradual loss of dPMMA from the surface.

In order to get more information on the profile of the adsorbed layer of dPMMA we need to cover a wider range in q.

PVME/dPS(1000k)

Fig 1

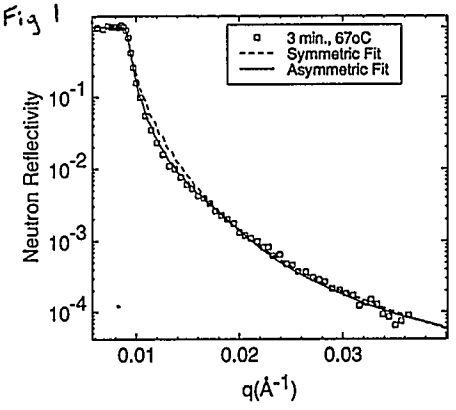


Fig 2

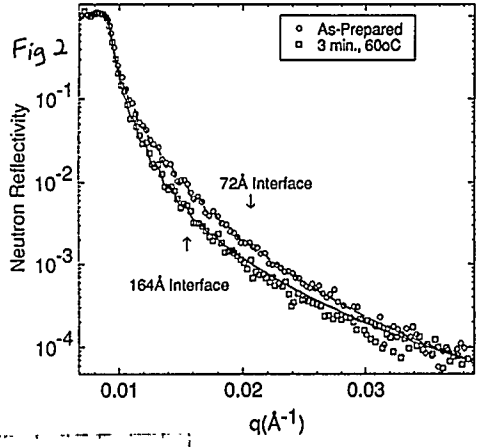
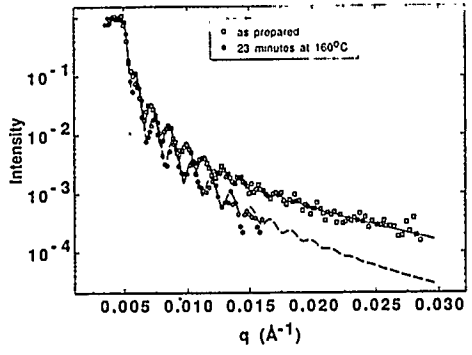


Fig 3



INSTRUMENT USED:	DATE OF REPORT:	EXPERIMENT NO.:
POSY 2	7-27-90	[1]

TITLE:

"Structure of Polymer Interfaces"

AUTHORS AND AFFILIATIONS:

R. P. Wool, K. L. Foster and H. Zhang / University of Illinois

DATES OF EXPERIMENT: Feb 26 - March 2, 1990

☐ APPROVED BY PROGRAM COMMITTEE, OR

☐ PART OF INSTRUMENT SCIENTIST ALLOCATION

REPORT RECEIVED:

EXPERIMENTAL REPORT (or Abstract of Publication)

REPORT ON MEASUREMENTS CARRIED OUT AT IPNS

Structure of Polymer-Polymer Interfaces

Concentration profiles of several amorphous polymer-polymer interfaces were examined with specular neutron refelctivity (SNR). With SNR, the contrast between a protonated and deuterated polymer film leads to a reflection of neutrons that is characteristic of the concentration profile. The theoretical concentration profile, C(z,t), where z is the distance from the interface and t is the diffusion time, was used to calculate the reflectivity as a function of neutron wave length and compared to an experimental reflectivities as specific diffusion times. Preliminary analysis has found that the experimental results for a symmetric case were in agreement with theoretical concentration profiles previously derived[1,2] by Zhang and Wool.

EXPERIMENTAL

Bilayer films of polymers were prepared on a silicon substrate by conventional solvent spinning techniques and heated for specific diffusion times at 125°C. Three different types of films were prepared. The first was a symmetric case of deuterated polystyrene (D-PS) - protonated polystyrene (H-PS) of 708,000 and 650,000 molecular weight (M_w) respectively. It will be described in more detail in the results section. The second was an asymmetric study with a D-PS film of 203,000 M_w on top of a 4 million M_w H-PS film. Diffusion times less than the reptation time of the low molecular weight species have been examined. These films were prepared to examine the validity of a molecular dynamics approach to determining the concentration profile of polymers in diffusion. A third study was prepared to examine the temperature and kinetic effects of the mixing of incompatible polymers PS and polymethylmethacrylate (PMMA) as well as the emulsifying effects of block copolymers have on the interfacial mixing of incompatible polymers. Samples were prepared consisting of H-PS on a deuterated (D-PMMA) film.

RESULTS

Symmetric Interfaces:

Theoretical and experimental data was compared for diffusion times of 0, 10, 42, 120, and 242 minutes at 125°C. Plans had been made to complete this run for diffusion times as high as the reptation time (1850 min.) but beam down time temporarily interrupted this study. There was a significant difference in the calculated

EXPERIMENTAL REPORT (CONTD.)

RESULTS CONT'D

reflectivities determined at 0.1 s and 1 s while there was little difference between 1 and 2 s calculated results. This indicates that the local non-equilibrium chain conformations relax very fast, less than 1 s, in agreement with Rouse dynamics theory. The agreement at 10 minutes is not as great as the control but comparisons at greater diffusion times improve. Further investigation of the assumptions involved in the theoretical expressions are being conducted and will be examined in the future. Several publications are pending[3,4]. The analysis of asymmetric interfaces is in progress.

SUMMARY AND FUTURE WORK

Theoretical concentration profiles have been compared to results obtained with SNR of a model symmetric polymer interface with good agreement. These results suggest the potential for significant polymer motion and relaxation to occur during very short diffusion times. An Asymmetric interface composed of a large and small molecular weight polymer films was examined experimentally but analysis with theoretical predictions has not yet been completed. Initial studies on incompatible polymer mixing were inconclusive probably due to choice of solvent used in the spinning procedure.

Future work includes completion of the reflectivity measurements and subsequent analysis for the symmetric system at diffusion times approaching the reptation time. Also a repeat of the incompatible study is planned. In addition, analysis of the asymmetric experimental results will be completed during this next quarter.

REFERENCES

1. Zhang, H. and Wool, R. P.; Macromolecules 22, 3019 (1989).
2. Zhang, H.; Ph.D. thesis, University of Illinois, (1989).
3. Zhang, H. and Wool, R. P., A.C.S. Polymer Preprints, Washington, D.C., Aug. (1990).
4. Zhang, H., Foster, K. L., Wool, R. P., Karim, A., and Felcher, G. P., in revision with authors, for Macromolecules (1990)

INSTRUMENT USED:	DATE OF REPORT:	EXPERIMENT NO.:
POSY-II	12/5-12/7, 1990	No. 1353

TITLE: Evaluation of Minor Chain Reptation Model Using Triblock Interfaces

AUTHORS AND AFFILIATIONS: H. Zhang, G. Agrawal, R.P. Wool-U. of IL at Urbana-Champaign; T.P. Russell-IBM Almaden Res. Cntr., San Jose, CA*

DATES OF EXPERIMENT: 12/5 - 12/7, 1990

☒ APPROVED BY PROGRAM COMMITTEE, OR

☐ PART OF INSTRUMENT SCIENTIST ALLOCATION

REPORT RECEIVED:

EXPERIMENTAL REPORT (or Abstract of Publication)

In order to evaluate the Minor chains reptation model (MC), the segment density distribution of triblock interfaces was investigated by use of neutron reflectivity using POSY-II at IPNS. Reflectivity measurements were performed on the interfaces made of center-deuterated triblock polystyrene (HDH) and homogeneous polystyrene, protonated (HPS) or fully deuterated (DPS). The characteristics of the interfaces are the following:

1. HPS(M=233,000)/HDH(M=190,000)/Si
2. HPS(M=475,000)/HDH(M=510,000)/Si
3. DPS(M=203,000)/HDH(M=190,000)/Si
4. HDH with degree of polymerization of 420, 958, and 420

   HDH with degree of polymerization of 888, 2497, and 888

Specimens were prepared by spin coating technique. Before reflectivity measurements, sample 1 and 3 were heated at 120° C for different periods of time, while sample 2 was heated at 125° C for different periods of

EXPERIMENTAL REPORT (CONTD.)

The reflectivity data are partially shown in the figures attached. These data are analyzing currently using the MC model.

* G.P. Feltcher, W.D. Dozier-Argonne Nat'l. Lab.

INSTRUMENT USED: QENS	DATE OF REPORT: 6/20/95	EXPERIMENT NO :

TITLE: Non-Fermi Liquid Scaling in UBe_{13}

AUTHORS AND AFFILIATIONS:
M.C. Aronson (Univ. of Michigan) F. Trouw (IPNS)

DATES OF EXPERIMENT:
6/6/95 - 6/22/95

CHECK ALL APPLICABLE BOXES:

- [X] APPROVED BY PROGRAM COMMITTEE
- [ ] INSTRUMENT SCIENTIST ALLOCATION
- [ ] DO NOT PUBLISH
- [ ] PROPRIETARY RESEARCH
- [ ] PRT ALLOCATION

EXPERIMENTAL REPORT (or Abstract of Publication)

In a recent QENS experiment, we have been studying the magnetic excitations of the heavy fermion superconductor UBe_{13}. An early spin polarized triple axis experiment[1] identified a broad, dispersionless, magnetic excitation, modelled as a quasielastic Lorenzian in energy transfer, with a half width of approximately 15 meV. Little can be discerned about the magnetic excitations for energy transfers of less than ~ 10 meV from this experiment. Accordingly, a second experiment [2] was performed on IN6 which identified almost featureless magnetic scattering over the energy transfer range from 0.25 meV-1.8 meV. These excitations were modelled as the low energy tail of a quasielastic Lorentzian, with a half width of 1-2 meV. In this experiment, we have qualitatively reproduced both these results in the course of explicating the magnetic response of UBe_{13} over the continuous energy transfer range of 0.5 meV - 100 meV, as depicted in Fig. 1. The magnetic scattering is limited primarily to the range 0.5 meV< ω < 20 meV, and is almost energy independent down to the lowest energies studied.

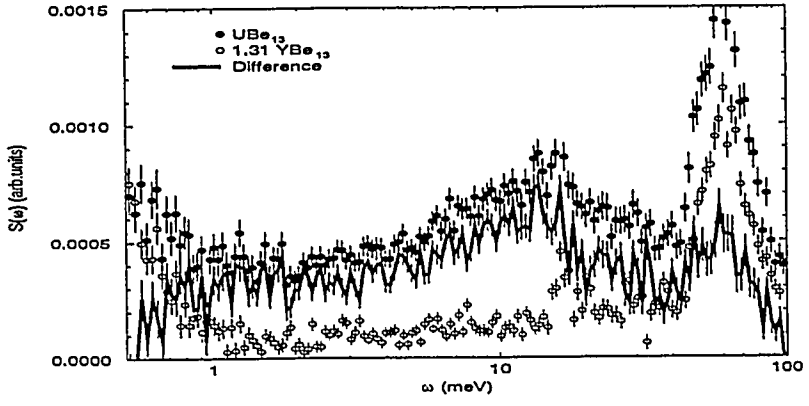


Fig. 1

Scattered neutron intensity for UBe13 and isostructural, nonmagnetic YBe13, collected at a fixed detector angle of 90 degrees. Each is normalized by the integrated elastic line. The experimental temperature is 1.5 K.

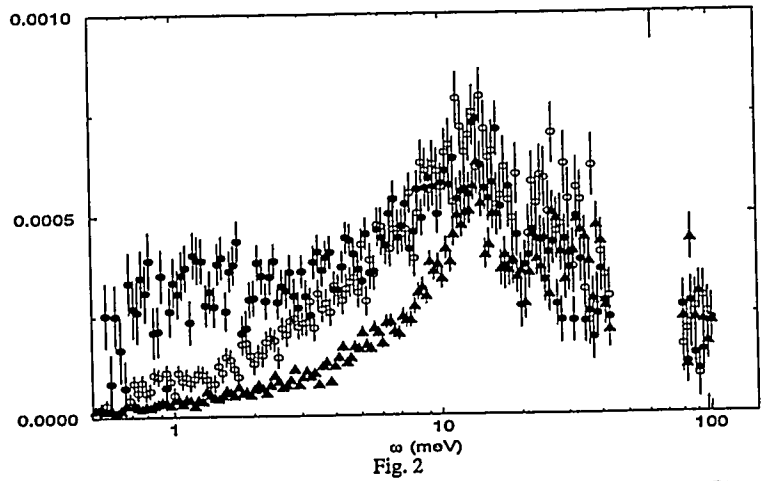


Fig. 2

Dynamic susceptibility $\chi''(\omega)$ of UBe_{13} for fixed temperatures of 1.5 K(●), 50 K(○), and 150 K(▲). Magnetic scattering has been isolated by direct subtraction of scattering from nonmagnetic YBe_{13}.

Recent nonlinear susceptibility measurements[3] suggest that the scaling properties of the magnetic excitations in UBe_{13} are anomalous, depending not on a fixed energy scale, but on temperature itself. In this respect, UBe_{13} is similar to $UCu_{5-x}Pd_x$ (x=1.5,1), a system which we have recently found to have this "non-Fermi liquid " scaling.[4] The basic attribute of systems obeying non-Fermi liquid scaling is that the spectrum of their electronic excitations is qualitatively different for energies which are either larger or smaller than the experimental temperature. Our recent results on UBe_{13}, reproduced in Fig. 2, suggest that its magnetic excitations have exactly this property. Note the crossover in $\chi''(\omega)$ in the 50 K data set for ω~T, to a temperature independent form displayed by the 1.5 K data set, which has T <ω always. A completely different form for $\chi''(\omega)$ is found for ω < T, a condition realized in the 150 K data set.

References

1. A. I. Goldman, S. M. Shapiro, G. Shirane, J. L. Smith, and Z. Fisk, Phys. Rev. B 33, 1627 (1986)

2. G. H. Lander, S. M. Shapiro, C. Vettier, and A. J. Dianoux, Phys. Rev. B46, 5387 (1992)

3. A. P. Ramirez, P. Coleman, P. Chandra, E. Bruck, A. A. Menovsky, Z. Fisk, and E. Bucher, Phys. Rev. Lett. 68, 2680(1992).

4. M. C. Aronson, R. Osborn, R. A. Robinson, J. W. Lynn, M. B. Maple, C. L. Seaman, and R. Chau, Phys. Rev. Lett.(to appear); M. C. Aronson, M. B. Maple, R. Osborn,. P. de Sa, and A. M. Tsvelik, Phys. Rev. Lett. (submitted).

INSTRUMENT USED: QENS	DATE OF REPORT: July 1992	EXPERIMENT NO.: 1581

TITLE: Effect of Plasticizer on polymer dynamics

AUTHORS AND AFFILIATIONS: V. Arrighi and J.S. Higgins - Imperial College - London (U.K.)

DATES OF EXPERIMENT: 2nd June 1992

CHECK ALL APPLICABLE BOXES:

- ☐ APPROVED BY PROGRAM COMMITTEE
- ☐ INSTRUMENT SCIENTIST ALLOCATION
- ☐ DO NOT PUBLISH
- ☐ PROPRIETARY RESEARCH
- ☐ PRT ALLOCATION

EXPERIMENTAL REPORT (or Abstract of Publication)

Many applications of polymeric materials involve the use of additives in order to tailor the physical properties to specific needs. The addition of low molecular weight molecules may give rise to the so called "plasticization effect" which consists in a reduction of the modulus and the glass transition temperature of the polymeric material. The macroscopic properties of the "plasticized " polymer depend on the mobility and concentration of the diluent as well as on the molecular interactions between the polymer matrix and the diluent[1].

We have recently performed Quasielastic Neutron Scattering (QENS) experiments to investigate the effect of plasticizers on the polymer dynamics close to the glass transition[2]. Our system consisted of solution chlorinated polyethylene (SCPE, T_g = 317K) plasticized with selectivily deuterated di-2-ethylhexylphthalate (DOP, T_g = 189K). QENS measurements were performed on the IRIS back-scattering spectrometer at the ISIS pulsed neutron source (Rutherford Appleton Laboratory, U.K.). Both the pure solvent (DOP) and a sample consisting of 75% SCPE and 25% DOP (T_g = 279K). QENS measurements were carried out in the Q range from 0.33 to 1.84 Å^{-1}, from 4 to 400 K. The energy resolution of the spectrometer was 11μeV (FWHH) and the energy range from -0.4 to 0.4 meV.

The QENS results relative to the neat solvent (DOP) indicated the existence of three processes: (1) a "fast" (τ~ 0.1 ps) Q-independent motion with weak temperature dependence (E_a = 1.54 kcal/mol), (2) a "slow" Q-dependent motion and (3) a flat background increasing with Q and T. The Q-dependence is illustrated in Figure 1 for DOP at 312 K.

The localized motion associated with the phenyl group has been assumed to be responsible for the "fast process" whereas the "slow" process was discussed in terms of the jump-diffusion model[2]. A very good agreement was found between theory and the Q-dependence of the experimental linewidth.

During the QENS experiment on IRIS we were able to extract useful information on the dynamics of DOP and the plasticized polymer. However, there remained some unresolved issues, namely the significant background increasing with both temperature and momentum transfer Q (Figure 1). Our speculation was that the background in the QENS spectra was due to the fast methyl group rotation of DOP. This process is expected to contribute to a quasielastic broadening of 0.32 and 0.42 meV (hwhh) at 265

and 300 K, respectively[3]. Quasielastic broadening of the order of 0.8 meV (FWHH) appears in fact as a flat background within the energy window of our experiment on IRIS.

The spectrometer QENS at IPNS provides a wider energy range with respect to IRIS and therefore enables us to test our hypothesis. QENS measurements were performed on the pure solvent DOP in the temperature range from 180 to 312 K. For T> 210K the measured spectra were fitted with a curve consisting of a delta function (elastic part), a Lorentzian (quasielastic component) and a flat background. A typical spectra is given in Figure 2. The measured linewidth (FWHH) increases from 0.5 meV at 230 K to 1.8 meV at 312 K and appears to be approximately Q-independent at a given temperature as expected for methyl group rotations. In addition the linewidth of the quasielastic broadening compares well with values obtained for PMMA.

The "slow" and "fast" processes observed with IRIS contribute in this case to the elastic peak as a consequence of the lower resolution of QENS (15μeV for IRIS and 70μeV for QENS) for T< 265 K. At higher temperature the best fit to the experimental data was obtained by including a second Lorentzian function with a linewidth from 0.08 meV at 265 K to 0.170 meV at 312 K. This finding is in very good agreement with the linewidth relative to the "fast" process measured on IRIS

REFERENCES

(1) see for example: G.Fytas, A.Rizos, G. Floudas, T.P. Lodge *J. Chem. Phys.* **93**, 5096 (1990); G.Floudas, G.Fytas, W.Brown *J. Chem. Phys.*, submitted.
(2) G.Floudas, J.S.Higgins and G.Fytas *J. Chem. Phys.*, submitted
(3) B.Gabrys, J.S.Higgins, K.T.Ma and J.E.Roots *Macromolecules*, **17**, 560 (1984)

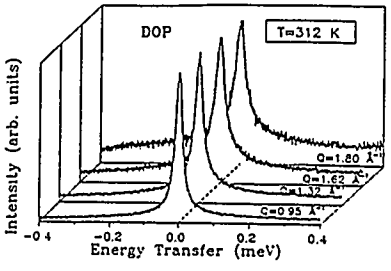


Figure 1.

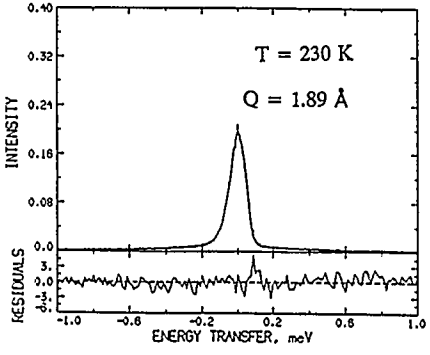


Figure 2.

INSTRUMENT USED: QENS	DATE OF REPORT: 3 APRIL 1995	EXPERIMENT NO.: 1958
TITLE: Dynamics of Small Molecules in Large Pore Zeolites		
AUTHORS AND AFFILIATIONS:	K. Edler, J. W. White (Research School of Chemistry, Australian National University), Frans Trouw (IPNS)	
DATES OF EXPERIMENT: 12/7/94 TO 12/17/94		

CHECK ALL APPLICABLE BOXES:

X APPROVED BY PROGRAM COMMITTEE
☐ INSTRUMENT SCIENTIST ALLOCATION
☐ DO NOT PUBLISH
☐ PROPRIETARY RESEARCH
☐ PRT ALLOCATION

EXPERIMENTAL REPORT (or Abstract of Publication)

Large pore zeolite materials, such as MCM-41, produced by using liquid crystalline templates, are attractive materials for studying the effect of pore size on molecular and solid state properties. The channel structure of the zeolite MCM-41 is highly regular and we are interested in the effect of these highly regular channels on molecular packing and dynamics. This has relevance to catalytic and microdot molecular properties. The range of pore sizes available now is from *ca.* 20Å - 100Å and the extreme uniformity of the pores is reflected in the adsorption isotherms. This makes the systems ideal for computer simulation studies of new phase transitions and size dependent effects. These studies have been conducted in collaboration with Professor Keith Gubbins at Cornell[1].

QENS measurements have allowed us to probe the melting behaviour (as reflected by the dynamics and diffraction) of methane confined in 36Å channels in MCM-41.This experiment complements the work on adsorption isotherms.

A sample of highly crystalline MCM-41 was prepared using the method of Beck et al[2], and characterised by means of nitrogen and methane adsorption isotherms and small angle x-ray scattering. After evacuation at 350°C overnight, the pore system was completely filled with methane at 140K in order to provide a good signal to noise ratio. The behaviour of the quasielastic scattering function $S(Q, \omega)$ of methane as a function of temperature was followed. A broad survey of the phase transitions for this molecular system in the material MCM-41 was attempted with a temperature range from 1.5K (to see rotational tunneling) to 180K, where all gas was essentially desorbed. Given that the walls are approximately 8Å thick, we should therefore be looking at pieces of molecular material which may be only 5-8 molecular diameters wide in one dimension although they are extended along the channels of the silicate. A series of runs on bulk methane over a smaller range of temperatures were also carried out for purposes of comparison. The data was fitted, in the case of methane confined in MCM-41, by a delta function (corresponding to the elastic scattering component of the system) and a single Lorentzian (for the quasielastic component). Fitting of the bulk data was more complicated and required three Lorentzian functions.

Analysis of the data was carried out using the pattern from empty MCM-41 at 15K as a resolution function for the system. The quasielastic scattering from MCM-41 itself showed an interesting variation with temperature which has not yet been fully investigated. We define Q as the momentum transfer, $Q = 4\pi/\lambda \sin\theta$. For temperatures below 60K the width as a function of Q^2 is a constant, behaviour typical of a system in which only rotational diffusion of the protons is occurring. For 60K and above the width as a function of Q^2 increases linearly with increasing Q^2, a signature of translational diffusion. The methane in the 36Å channels of the MCM-41 shows evidence of considerable translational diffusion at temperatures below the 92K melting point of bulk methane. The data thus show clear differences between the behaviour of bulk methane and that confined in the MCM-41 channel system. . Further analysis of the data obtained is being carried out in order to make a more detailed comparison of the differing diffusion constants between the nanophase methane and the bulk sample. The Q dependence of the Elastic Incoherent Scattering Function contains more useful dynamical data. In addition at low temperatures there is a suggestion, not properly resolved, of the onset of tunnelling behaviour.

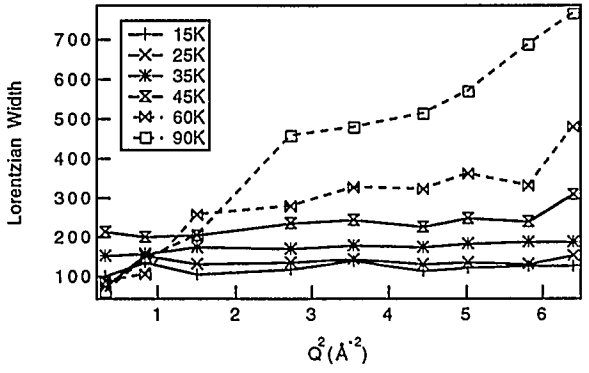


Figure 1: Lorentzian width against Q^2 for temperatures from 15K to 90K showing the change from rotational diffusion to translational diffusion for methane confined in 36 Å pores in MCM-41.

References

1 Gubbins, K. unpublished data, 1994.

2 Beck, J.S., Vartuli, J.C., Roth, W.J., Leonowicz, M.E., Kresge, C.T., Schmitt, K.D., Chu, C.T.-W., Olson, D.H., Sheppard, E.W., McCullen, S.B., Higgins, J.B. and Schlenker, J.L. *J. Am. Chem. Soc.*, 1992, 114, 10834.

INSTRUMENT USED:	DATE OF REPORT:	EXPERIMENT NO.:
QENS	9/25/91	1305

TITLE:

A QUASIELASTIC AND LOW-ENERGY INELASTIC STUDY OF ETHANOL ON A GRAPHITE SURFACE

AUTHORS AND AFFILIATIONS:

K. W. Herwig and F. R. Trouw, IPNS/ANL

DATES OF EXPERIMENT: 7/11/90 - 7/25/90 and 9/5/90 - 9/16/90

☒ APPROVED BY PROGRAM COMMITTEE, OR

☒ PART OF INSTRUMENT SCIENTIST ALLOCATION

REPORT RECEIVED:

EXPERIMENTAL REPORT (or Abstract of Publication)

The structure and dynamics of hydrocarbons physisorbed onto a graphite surface have been the subject of numerous investigations.[1] These efforts have concentrated on systems where the adsorbate-adsorbate interactions are relatively simple. As these interactions become more complex, one may expect to observe novel and intriguing behavior in these systems. We have focused our attention in this series of experiments on ethanol, C_2H_5OH, physisorbed on the basal planes of graphite. Hydrogen bonding is a major factor in determining the structure and dynamics of this two-dimensional system. Using QENS, we have measured the quasielastic spectra at two f temperatures over a range of momentum transfers, Q.

Figure 1 shows the width of the Lorentzian peak as a function of Q^2 for the data obtained for a sample temperature of 194 K. At this temperature the system is in a two-dimensional solid phase. The data at all Q's could be well fit with a constant Lorentzian width of 120 μeV. Figure 2 shows the intensity of the Lorentzian as a function of Q for this temperature. The behavior of the quasielastic scattering is strongly indicative of rotational diffusion. Details about this diffusion await further analysis and insight from a molecular dynamics simulation.

We also measured the scattering from the specimen at a sample temperature of 290 K. At this temperature, the system has melted and is a two-dimensional liquid. Figure 3 shows the width of the Lorentzian peak for this temperature, while Figure 4 shows the intensity. This scattering is of the form one expects to observe for Brownian translational diffusion. The data indicate a diffusion constant near 10 10^{-5} cm^2/sec. This agrees very well with the result obtained from our simulation, 12 10^{-5} cm^2/sec.

REFERENCES

[1] See for example, Neutron Scattering Studies of the Structure, Phase Transitions, and Dynamics of Commensurate Herringbone Monolayers Physisorbed on Graphite, H. Taub in The Time Domain in surface and Structural Dynamics, NATO ASI series, ed. G.J. Long and F. Gradjean, p. 467-498, 1988.

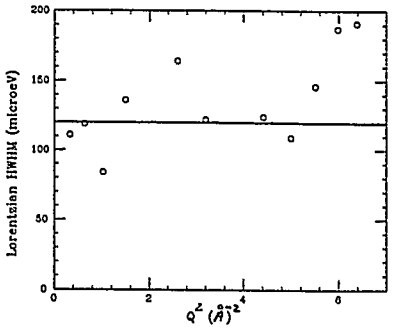


Fig. 1 Lorentzian width at 194 K.

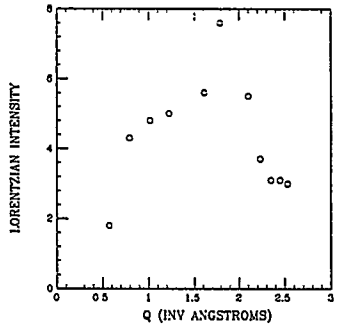


Fig. 2 Lorentzian intensity at 194 K.

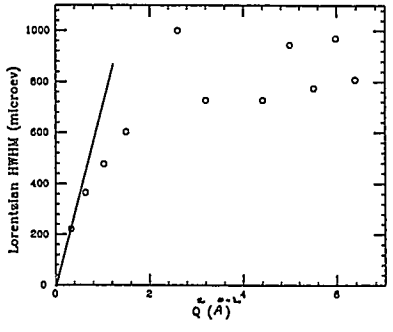


Fig. 3 Lorentzian intensity at 290 K.

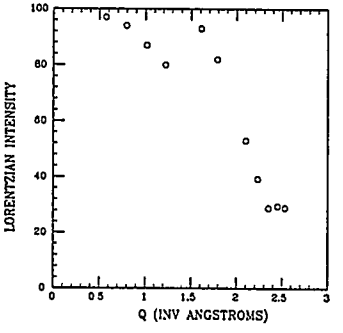


Fig. 4 Lorentzian intensity at 290 K.

INSTRUMENT USED:	DATE OF REPORT:	EXPERIMENT NO.:
QENS	7/25/91	1394

TITLE:

A LOW_ENERGY INELASTIC STUDY OF ETHANOL ON A GRAPHITE SURFACE

AUTHORS AND AFFILIATIONS:

K. W. Herwig and F. R. Trouw IPNS/ANL

DATES OF EXPERIMENT: 9/12/90 - 9/16/90

☒ APPROVED BY PROGRAM COMMITTEE, OR

☐ PART OF INSTRUMENT SCIENTIST ALLOCATION

REPORT RECEIVED:

EXPERIMENTAL REPORT (or Abstract of Publication)

The structure and dynamics of hydrocarbons physisorbed onto a graphite surface have been the subject of numerous investigations.[1] These efforts have concentrated on systems where the adsorbate-adsorbate interactions are relatively simple. As these interactions become more complex, one may expect to observe novel and intriguing behavior in these systems. We have focused our attention in this series of experiments on ethanol, C_2H_5OH, physisorbed on the basal planes of graphite. Hydrogen bonding is a major factor in determining the structure and dynamics of this two-dimensional system. Using QENS, we have measured the inelastic spectra from 0 to approximately 60 meV.

Figure 1 shows the inelastic spectra measured at low temperatures from crystalline bulk ethanol, C_2H_5OH. Peaks in the bulk spectra below 20 meV may be associated with lattice modes. The CH_3 torsional mode should appear near 30 meV. Three peaks are observed in this region. Upon deuteration of the methyl and methylene groups, the two lower energy peaks at approximately 30 and 34 meV, shift down in energy as expected for an isotope shift, however the peak at 36 meV is unaffected. As there are two unique molecules per unit cell in the bulk structure, it may be that the torsional mode is split due to two differing environments. The origin of the peak at 36 meV is not understood at present but is most likely associated with motion of the hydroxyl proton. Also present in the inelastic spectra are two peaks near 54 meV which may be associated with the CCO in-plane bend. The appearance of two peaks may again be due to differing environments in the bulk crystal.

Figure 2 shows the data obtained from C_2H_5OH physisorbed onto graphite powder. The peak near 32 meV occurs between the two peaks we associated with rotation of the methyl group in the bulk spectra. The presence of a single peak indicates that a single environment exists for the methyl group in the physisorbed system. The two peaks occuring at lower energy transfers may be associated with whole body motions of the molecule. Our molecular dynamics simulation predicts peaks in the inelastic spectra near these energy transfers. The peak near 8 meV is due to an in-plane reorientation of the long axis of the physisorbed molecule. The peak near 14 meV is due to reorientation of the short axis of the molecule out of the graphite basal plane.

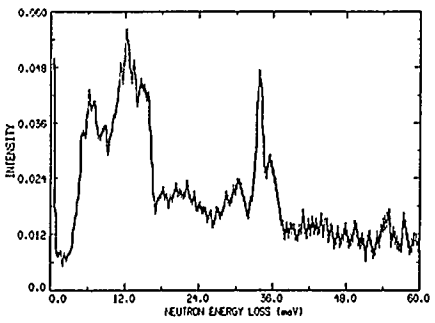


Fig. 1 The inelastic spectra of bulk ethanol.

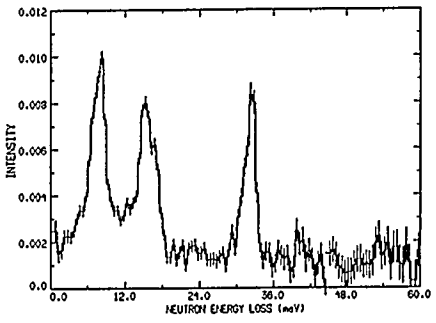


Fig. 2 The inelastic spectra of C_2H_5OH physisorbed on graphite.

REFERENCES

[1] See for example, Neutron Scattering Studies of the Structure, Phase Transitions, and Dynamics of Commensurate Herringbone Monolayers Physisorbed on Graphite, H. Taub in The Time Domain in surface and Structural Dynamics, NATO ASI series, ed. G.J. Long and F. Gradjean, p. 467-498, 1988.

INSTRUMENT USED:	DATE OF REPORT:	EXPERIMENT NO.:
QENS	11/21/95	1880

TITLE: A quasielastic neutron scattering study of the diffusive motion of water molecules in a water-oil microemulsion

AUTHORS AND AFFILIATIONS: K. W. Herwig, University of Missouri-Columbia; W. D. Dozier, Argonne National Laboratory; J. S. Huang, Exxon Research

DATES OF EXPERIMENT: May 10-16, 1994

☒ APPROVED BY PROGRAM COMMITTEE, OR

☐ PART OF INSTRUMENT SCIENTIST ALLOCATION

REPORT RECEIVED:

EXPERIMENTAL REPORT (or Abstract of Publication)

We have used quasielastic neutron scattering (QNS) to investigate the dynamics of water molecules in an oil-continuous microemulsion (water/deuterated decane/AOT). These emulsions have been extensively studied by SANS and their phase diagram is well known.[1-3] Our study is aimed at understanding how the translational and rotational dynamics of water molecules are modified (relative to bulk water) by the confining geometry provided by the relatively immobile surfactant layer. By studying the water dynamics in various sized droplets, we can determine to what distance such an interface exerts influence on the water molecules. This information is relevant to our understanding of interfacial water in a variety of other systems including water in biological gels.

We collected QNS spectra from two microemulsions having water core radii of 38 Å and 20 Å at a temperature of 297 K. The data were analyzed using a model previously employed to describe the dynamics of bulk water.[4,5] This model treats the water molecule's translational diffusion with random jumps and its rotational component as the diffusion of protons on the surface of a sphere. Figure 1 shows the HWHM of the translational component of the quasielastic scattering as it varies with Q for three samples: bulk water, 38 Å radius droplets, and 20 Å radius droplets. The solid curves are fits to the jump diffusion model. Both the jump distance and average residence time increase significantly with decreasing droplet size. In bulk water, this behavior was interpreted as due to changes in the hydrogen-bonded network with decreasing temperature. In our case, the interpretation is that the hydrogen-bonded network is strongly affected by the presence of the relatively immobile surfactant layer and the water molecules tightly pinned to it. As the droplet radius is decreased, the influence of the surface becomes stronger, resulting in a hydrogen-bonded

EXPERIMENTAL REPORT (CONTD.)

network which is far from ideal. Surprisingly, the translational diffusion is strongly modified (relative to bulk water) in even the largest droplet studied. In fact, the translational dynamics of the droplets strongly resembles that of bulk water cooled to 10.5 °C and -20 °C for the 38 Å and 20 Å droplets respectively.

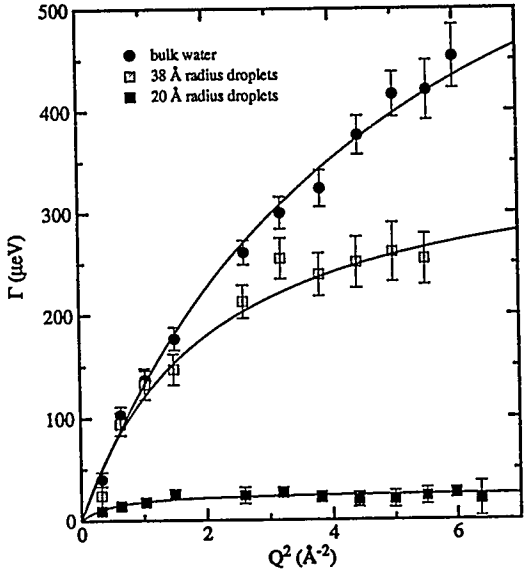


Figure 1. The HWHM of the translational component of the quasielastic spectra collected from room temperature samples. The solid curves are fits to the data using the jump diffusion model described in the text.

REFERENCES

[1] M. Kotlarchyk, et al., J. Phys. Chem 86,3273 (1982).
[2] M. Kotlarchyk, et al., Phys. Rev. A 29, 2054 (1984).
[3] M. Kotlarchyk, et al., J. Phys. Chem. 89, 4382 (1985).
[4] S-H Chen, et al., Phys. Rev. A 26, 3477 (1982).
[5] J. Teixeira, et al., Phys. Rev. A 31, 1913 (1985).

INSTRUMENT USED: QENS	DATE OF REPORT: 8/22/94	EXPERIMENT NO.: 1881

TITLE: Diffusion of Water in a Biological Gel Matrix

AUTHORS AND AFFILIATIONS:
K. W. Herwig, T. Wong, E. Blaine; University of Missouri-Columbia

DATES OF EXPERIMENT: March 19-25, 1994

CHECK ALL APPLICABLE BOXES:

- [X] APPROVED BY PROGRAM COMMITTEE
- [ ] INSTRUMENT SCIENTIST ALLOCATION
- [ ] DO NOT PUBLISH
- [ ] PROPRIETARY RESEARCH
- [ ] PRT ALLOCATION

EXPERIMENTAL REPORT (or Abstract of Publication)

We are conducting a multi-disciplinary research project aimed at understanding how fluid is sequestered and released from gel matrices.[1] In its initial stages, the study is focused on investigating the physicochemical properties of gel and viscoelastic solutions formed by hyaluronan (hyaluronic acid and its salts, hereafter abbreviated as HA) in water and mixtures of HA and collagen in water.[2,3] This particular system forms the basis of a biological gel which contains three-fourths of the extracellular fluid found in the body. This fluid is the principal defense of blood volume during times of depletion, such as hemorrhage or severe exercise. Thus, determining the diffusion coefficients and diffusion mechanism of water (and solute) in these gel matrices is an important step in understanding the physiological mechanism of water regulation in the human body. Our QENS experiments are designed to investigate the mobility of water in these systems.

Preliminary quasielastic neutron scattering (QNS) measurements have been made on three HA gel samples at concentrations of 3 mg/ml, 10 mg/ml, and a 10 mg/ml concentration treated with HAdase. Due to the limited amount of time available on QENS, only room temperature measurements were obtained and thus no activation energies for the various diffusive motions of the water could be obtained. The data were analyzed in terms of a model incorporating both jump and rotational diffusion which had been previously used in studies of both bulk and biological water.[4,5] The rotational diffusion constant was very similar to that observed for bulk water but the jump diffusion was dependent on the HA concentration. The QNS data were fit to two parameters, L and τ_0, where L is the mean jump distance and τ_0 is the mean time between jumps (the residence time). As the concentration of HA increased, so did both L and τ_0. The interpretation is that as the concentration of polymer increases, the distance a water proton must jump in order to make a new hydrogen bond increases and so does the time it remains hydrogen bonded. The translational diffusion coefficient may be calculated within this model as $L^2/6\tau_0$, and did not vary significantly at the two concentrations studied, but was approximately 4% lower than that of bulk water at the same temperature, consistent with QNS studies of agarose gels.[5] Interestingly, the sample treated with HAdase exhibited little difference when compared with the sample at identical HA concentration.

Future studies will focus on systems more closely approximating those found in the human body. For example, samples of aqueous gel of HA and collagen in proportions more closely mimicking gel matrices found in the human body are possible candidates. Finally, with an understanding gained from studies of these model systems, our goal is to compare measurements made on *in vivo* samples with those made on *in vitro* specimens. The findings of these QNS measurements will be compared with the results of other techniques such as NMR. It is anticipated that these results will provide a coherent picture of water and solute mobility and diffusion mechanisms in HA gels, and will form the physical basis for the interpretation of the physiological role the HA interstitial matrix plays in fluid regulation.

REFERENCES

REFERENCES

[1] K. Aukland and R. K. Reed, Physiological Reviews 73, 1 (1993).

[2] W. D. Comper and O. Zamparo, Biochem. J. 269, 561 (1990).

[3] V. Crescenzi, M. Dentini, and T. Coviello, Biophys. Chem. 41, 61 (1991).

[4] see for example, J. Teixeira, M. -C. Bellissent-Funel, S. H. Chen, and A. J. Dianoux, Phys. Rev. A 31, 1913 (1985).

[5] A. Deriu, F. Cavatorta, D. Cabrini, C. J. Carlile, and H. D. Middendorf, Europhys.Lett. 24, 351 (1993).

INSTRUMENT USED:	DATE OF REPORT:	EXPERIMENT NO.:
QENS	12/15/93	1692

TITLE:
A Quasielastic Neutron Scattering Study of the Diffusive Motion of Water Molecules in a Water-Oil Microemulsion

AUTHORS AND AFFILIATIONS:
K. W. Herwig (Univ. of Missouri), W. D. Dozier(ANL), J. S. Huang (Exxon Research)

DATES OF EXPERIMENT:
10/21/93-10/25/93

CHECK ALL APPLICABLE BOXES:

- [x] APPROVED BY PROGRAM COMMITTEE
- [ ] INSTRUMENT SCIENTIST ALLOCATION
- [ ] DO NOT PUBLISH
- [ ] PROPRIETARY RESEARCH
- [ ] PRT ALLOCATION

EXPERIMENTAL REPORT (or Abstract of Publication)

The structure and dynamics of molecules in restricted geometries is a topic of much current theoretical and experimental interest. These systems range from various species physisorbed onto surfaces, to molecules adsorbed into the relatively narrow "pores" of zeolites or glasses such as Vycor. Another fascinating system, with a somewhat different geometry is that of water-in-oil microemulsions. Microemulsions are mixtures of water and oil stabilized by a surfactant which is present at the interface between the two. Small droplets of water are surrounded by the surfactant and dispersed throughout the oil. We have finished a preliminary set of measurements using QENS to probe the diffusive behavior of water in such a microemulsion. The particular system we studied consisted of water, decane, and a single surfactant, AOT (sodium di-2-ethylhexyl-sulfosuccinate). This particular microemulsion has been extensively studied by small angle neutron scattering [1-3] and the phase diagram is well known.

Due to a limited amount of available beam time (4.5 days) , only two specimens could be studied, a pure AOT-decane sample as a reference and 14% by volume water in an H_2O-decane - AOT sample with water droplet radius of approximately 50 Å. Both samples were measured at a series of 3 temperatures, 230, 265, and 300 K, at a single table setting of QENS (arm 1 = 25 deg). At 300 K, data were collected from both samples over the full Q-range accessible to QENS. For analysis, the signal from the reference sample was subtracted from the water sample.

As a first stage in the analysis, the data were analyzed as a sum of Lorentzians convoluted with the instrumental resolution of QENS. As seen in previous studies of pure water, the data could be analyzed by a sum of narrow and broad components.[4,5] The narrow component has been associated with jump diffusion while the broad component is related to rotational motion. The translational component we observe at room temperature is only half as broad as that of the corresponding signal reported for bulk water.[4,5] Hence, the translational motion of water in these small droplets is greatly suppressed relative to that of bulk water. This component could be observed only at the two higher temperatures studied, 265 and 300 K. At the lower temperature no quasielastic scattering was observed.

We are currently implementing into the QENS analysis code the model for water diffusion used in the analysis of the data of reference [5]. Once this has been accomplished a more detailed comparison of the dynamics of water in these small droplets can be made with that of bulk water.

REFERENCES

[1] M. Kotlarchyk, et al., J. Phys. Chem 86,3273 (1982).
[2] M. Kotlarchyk, et al., Phys. Rev. A 29, 2054 (1984).
[3] M. Kotlarchyk, et al., J. Phys. Chem. 89, 4382 (1985).
[4] S-H Chen, et al., Phys. Rev. A 26, 3477 (1982).
[5] J. Teixeira, et al., Phys. Rev. A 31, 1913 (1985).

INSTRUMENT USED:	DATE OF REPORT:	EXPERIMENT NO.:
QENS	28-JUL-92	1392

TITLE:
Thermal Behavior of the Inelastic Response of UF4

AUTHORS AND AFFILIATIONS:
S. Kern (Colorado State U.), F. Trouw, C. K. Loong, G. H. Lander and B. Cort

DATES OF EXPERIMENT:
April 1991

CHECK ALL APPLICABLE BOXES:

- [X] APPROVED BY PROGRAM COMMITTEE
- [ ] INSTRUMENT SCIENTIST ALLOCATION
- [ ] DO NOT PUBLISH
- [ ] PROPRIETARY RESEARCH
- [ ] PRT ALLOCATION

EXPERIMENTAL REPORT (or Abstract of Publication)

Thermal Behavior of the Inelastic Response of UF_4

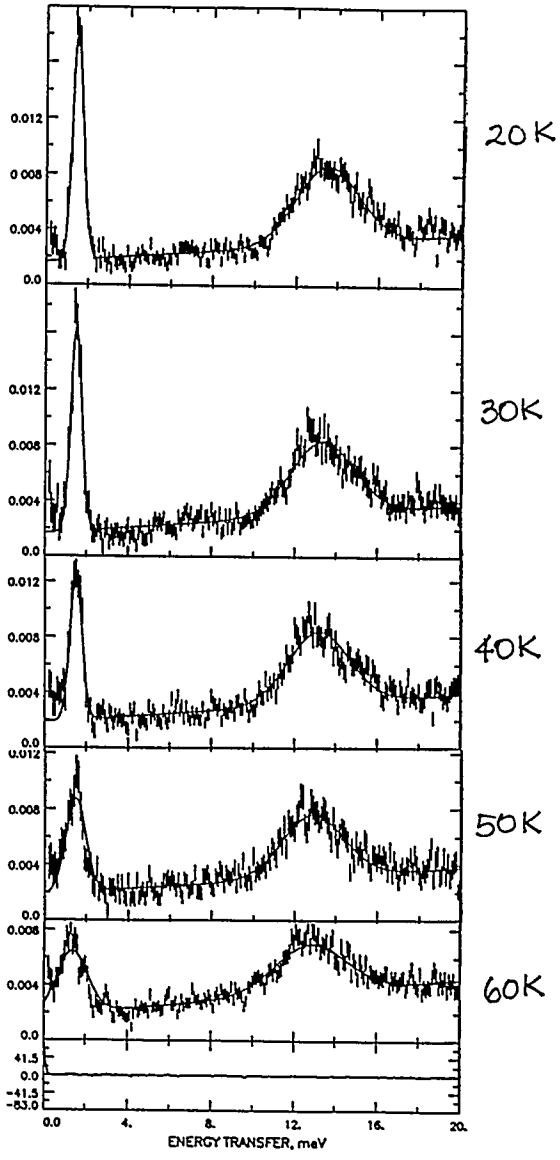
The inelastic spectrum of UF_4 was measured on QENS at 20,30,40,50,and 60K. Contrary to our initial expectations we were not able to resolve the 14meV peak ,that we had previously seen on HRMECS, into any further components. Unexpectedly, however, we did find an additional peak at low energy, 1.5meV.

This 1.5 meV peak acts to corroborate a conjecture made on the basis of magnetic susceptibilty measurements made 30 years ago that there should be an electronic level in UF_4 some 15K above the ground state. We have repeated the susceptibility measurements and find good agreement with the older results. The presence of this level also helps to explain the near disappearance of the crystal field levels seen on HRMECS when the temperature was raised from 15K to 150K as simply due to level population effects.

In the Figure is shown the temperature variation of the response of the 1.5 meV peak as well as that of the 14meV transition.The relative magnitude of the peaks closely follows calculations that take into account the thermal population of the levels as a function of temperature. Higher levels are not expected to contribute appreciably.

The detection of this 1.5meV level has important consequences for the interpretation of the crystal fields in UF_4. The bulk of our information comes from visible and infrared spectroscopy, but these are generally unable to firmly establish the nature of the ground state, which is the determiner of most thermodynamically important properties at room temperature and below. Often the predictions for the ground state, made on the basis of fittings optimized for higher levels, prove inadequate. UF_4 falls into this category, for we see levels that are not predicted from the spectroscopic models and do not see others that they predict to be strongly present. Furthermore, we seem at present to be unable to distinguish between the response caused by the two slightly different Uranium sites in UF_4. It is possible that their energy level scheme is very similar, or there are other factors in operation.

This experiment on QENS was a beauty.



INSTRUMENT USED: QENS	DATE OF REPORT: 6-29-92	EXPERIMENT NO.: 1654

TITLE: Molecular Motions in Ammonia-Ammonium Intercalated Titanium Disulfide

AUTHORS AND AFFILIATIONS: E.W. Ong and J. Eckert, LANL; L.A. Dotson, ASU; F. Trouw, ANL

DATES OF EXPERIMENT: June 11, 1992 thru June 23, 1992

CHECK ALL APPLICABLE BOXES:

- ☐ APPROVED BY PROGRAM COMMITTEE
- ☒ INSTRUMENT SCIENTIST ALLOCATION
- ☐ DO NOT PUBLISH
- ☐ PROPRIETARY RESEARCH
- ☐ PRT ALLOCATION

EXPERIMENTAL REPORT (or Abstract of Publication)

It has been known for some time that ammonia-intercalated titanium disulfide contained ammonia molecules (NH_3) and ammonium ions (NH_4^+), as distinguishable entities [1-5]. The results of numerous experiments, which include: thermogravimetric analysis, differential scanning calorimetry, x-ray photoelectron spectroscopy, neutron diffraction, and nuclear magnetic resonance (NMR) has yielded a consistent picture about the coexistence of the above chemical species within titanium disulfide (TiS_2). Recently, McMillan etal [6] proposed that ammonia-intercalated titanium disulfide contained non-molecular nitrogen and hydrogen species. They based their conclusions on observing the resonance frequency of protons in the compound, using magic-angle-spinning NMR. In this model, no rotational diffusive motions of the species are possible. To further study the motions of chemical species within the ammonia-intercalated titanium disulfide system, we have performed quasi-elastic neutron spectroscopy experiments during the last IPNS run cycle, utilizing the Quasi-Elastic Neutron Spectrometer (QENS).

Two samples were studied. Their stoichiometries were: $(NH_4^+)_{0.25}(NH_3)_{0.37}TiS_2^{0.25-}$ and $Rb^+_{0.27}(NH_3)_{0.37}TiS_2^{0.27-}$. The quasi-elastic spectra of these compounds were measured at momentum transfers (Q) ranging from 0.57 $Å^{-1}$ to 2.53 $Å^{-1}$. These experiments were performed at temperatures of 15 K, 100 K, 200 K and 300 K. The temperatures were chosen because previous NMR experiments have found linewidth changes at 130 K and 270 K, suggesting transitions in the dynamic behavior of the intercalated species [5]. A vanadium sample was also measured at 300 K to determine the resolution function for the instrument. The data obtained to date indicate that rotational motion is present for all temperatures studied. The observed spectra for both compounds consist of a delta function component, which strongly suggests spatially confined motions like those from rotations, and Lorentzian components. Purely translational diffusion, as suggested by McMillan's model, would give a negligible delta function component to the quasi-elastic spectra. The presence of rotationally diffusive motions is consistent with the findings of

previous experiments cited above, and is contrary to McMillan's conclusion. Previously, it was assumed that the interaction between NH_3 and NH_4^+ to be similar to those between NH_3 and Rb^+. The hydrogen-weighted vibrational density-of-state portion of the spectra indicates that this assumption is wrong. To ascertain how NH_3 molecules influence the dynamics of NH_4^+ ions in TiS_2, a sample of $(NH_4^+)_{0.25}TiS_2^{0.25-}$ must also be examined. We have submitted a proposal to study this compound using QENS during the next IPNS run cycle.

References:

1. R. Schollhorn and H.D. Zagefka, *Angew. Chem. Int. Ed. Engl.* **16**, 199 (1977).

2. M.J. McKelvy and W.S. Glaunsinger, *J. Solid State Chem.* **67**, 142 (1987).

3. E.W. Ong, M.J. McKelvy, L.A. Dotson and W.S. Glaunsinger, *Chem. Mater.* **3**, 17 (1991).

4. V.G. Young, Jr., M.J. McKelvy, W.S. Glaunsinger and R.B. Von Dreele, *Solid State Ionics* **26**, 47 (1988).

5. G.W. O'Bannon, W.S. Glaunsinger and R.F. Marzke, *Solid State Ionics* **26**, 15 (1988).

6. P.F. McMillan, V. Cajipe, P. Molinie, M.F. Quinton, V. Goulaouen and P. Colombet, *Chem. Mater.* **3**, (1992).

INSTRUMENT USED: QENS	DATE OF REPORT: 3 May 1993	EXPERIMENT NO.: 1638

TITLE: Quasielastic Scattering from YbBiPt

AUTHORS AND AFFILIATIONS: R. A. Robinson (LANSCE), F. Trouw (IPNS), P. C. Canfield (LANL)

DATES OF EXPERIMENT: 9 - 17 February 1993

CHECK ALL APPLICABLE BOXES:

- ☒ APPROVED BY PROGRAM COMMITTEE
- ☐ INSTRUMENT SCIENTIST ALLOCATION
- ☐ DO NOT PUBLISH
- ☐ PROPRIETARY RESEARCH
- ☐ PRT ALLOCATION

EXPERIMENTAL REPORT (or Abstract of Publication)

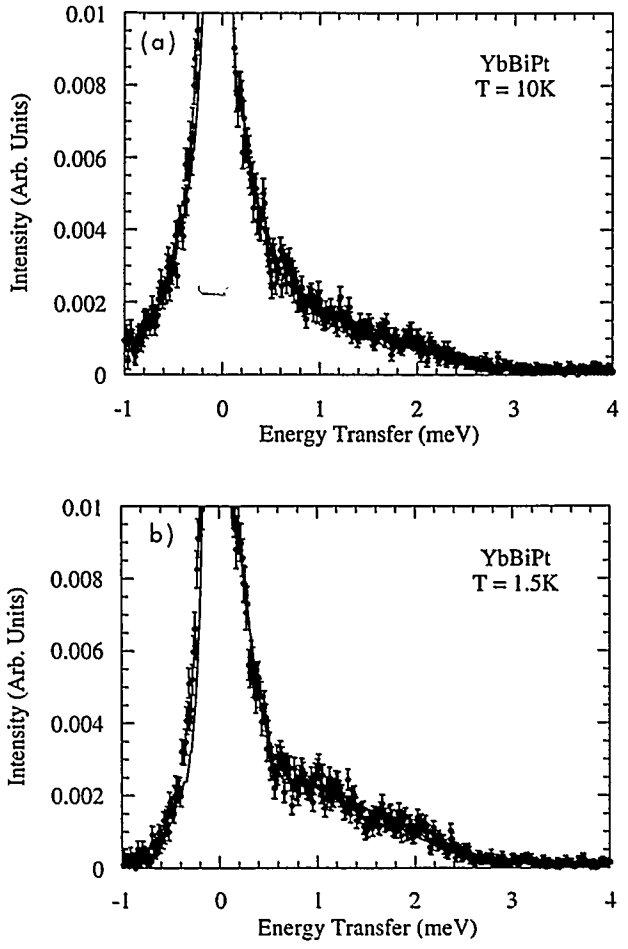
The super-heavy fermion compound YbBiPt has the largest known linear specific heat coefficient $\gamma = 8 J mol^{-1} K^{-2}$, and the source of this enormous "electronic" specific heat is of great current interest[1,2]. In a previous experiment[3] on the LAM-40 spectrometer at the Japanese spallation source KENS, we showed that there is a crystal-field level at approximately 6meV together with a rather complicated quasielastic response. This quasielastic response can be fit to a two-component gaussian lineshape and we assign these gaussians to the Γ_7 and Γ_8 crystal field levels, which are almost degenerate and which are hybridised with the d-electrons in different ways. LAM-40 has resolution of approximately 350 μeV, and the purpose of the present experiment was to study the quasielastic response with better resolution (70 μeV) using QENS. In addition we were able to go to lower temperature (1.5K) by pumping on the cryostat, something that was not possible at KENS. Our new results at 1.5K and 10K are shown in Figure 1, and they are qualitatively similar to the Japanese data. Again, a two-component response works quite well (the separation is more definitive in this experiment) and gaussians are definitely preferred over lorentzians, indicating that intersite correlations must be important. Note however that some structure is present in the broader quasielastic component at 1.5K. This may be associated with the closeness of a phase transition at 0.4K, and a field that is splitting the crystal-field degeneracy in some way. The Γ_8 quartet is known to be particularly sensitive to this sort of thing. Finally, within the assumption that our crystal-field assignment is correct (i.e. that the narrow response belongs to Γ_7, and the broad to Γ_8), and that the widths are as observed ($\sigma = 0.2$ meV for the narrow and $\sigma = 0.9$ meV for the broad), one can calculate the electronic specific heat by taking appropriate integrals over the density of possible excited states. When this is done, we obtain $\gamma = 10 J mol^{-1} K^{-2}$, which is within 20% of the observed electronic specific heat. The physical picture is that the ground state consists of two almost degenerate crystal field levels, each of which is hybridised weakly with the d-electrons but in different ways.

[1] P. C. Canfield, J. D. Thompson, W. P. Beyermann, A. Lacerda, M. F. Hundley, E. Peterson, Z. Fisk and H. R. Ott, J. Appl. Phys. 70, 5800 (1991).

[2] Z. Fisk, P. C. Canfield, W. P. Beyermann, J. D. Thompson, M. F. Hundley, H. R. Ott, E. Felder, M. B. Maple, M. A. Lopez de la Torre, P. Visani and C. Seaman, Phys. Rev. Lett. 67, 3310 (1991).

[3] R. A. Robinson, M. Kohgi, T. Osakabe, P. C. Canfield, T. Kamiyama, T. Nakane, Z. Fisk and J. D. Thompson, Physica B (in press) 1993.

Figure 1 Observed low-energy spectra for YbBiPt at (a) 10K and (b) 1.5K. The solid line is a fit to a convolution of the known spectrometer resolution function and a two-component gaussian quasielastic response.



INSTRUMENT USED: QENS	DATE OF REPORT: 2.2.95	EXPERIMENT NO.: 1954

TITLE: Crystalline electric-field and molecular-field behaviour in $Y_{1-x}Tb_xBa_2Cu_3O_y$

AUTHORS AND AFFILIATIONS: U. Staub, L. Soderholm, CHM Argonne

DATES OF EXPERIMENT:

CHECK ALL APPLICABLE BOXES:

- ☒ APPROVED BY PROGRAM COMMITTEE
- ☐ INSTRUMENT SCIENTIST ALLOCATION
- ☐ DO NOT PUBLISH
- ☐ PROPRIETARY RESEARCH
- ☐ PRT ALLOCATION

EXPERIMENTAL REPORT (or Abstract of Publication)

It is now well known that the spin dynamics in the CuO_2 planes in high temperature superconductors are important for understanding of the fundamental mechanism of high temperature superconductivity. Inelastic neutron scattering on the crystalline electric-field (CEF) excitations is a useful tool to investigate the spin dynamics. Such studies have been reported for BCS-type superconductors [1] as well as for the $Y_{1-y}R_yBa_2Cu_3O_x$ system [2]. The studies are focused on the temperature dependence of the line width of the CEF transitions which is proportional to the imaginary part of the susceptibility of the surrounding CuO_2 planes summed over the Brillouin zone.

One of the best candidates for such an investigation is R=Tb. Tb has a singlet ground-state followed by another singlet separated by only 10 μeV, which behaves like a doublet because of their very small energy separation. [3] The next CEF states are at energies above 20 meV so that excited-state transitions will not disturb this experiment and thermal depopulation will not significantly decrease the observed intensity of the ground-state transitions. In addition, the transition within the quasi ground-doublet is very strong, containing about 90 % of the scattering from the entire multiplet. QENS is therefore an ideal spectrometer to determine the intensity and half-width of the expected quasi-elastic scattering.

Fig. 1 show the energy spectra of $Y_{0.9}Tb_{0.1}Ba_2Cu_3O_7$ at T=160K. At this temperature we observe two magnetic components which are superimposed on the nuclear elastic background. There is a relatively strong quasi-elastic component which reflect the scattering from within the quasi-doublet ground state. The second contribution is a for this temperature smaller magnetic elastic contribution which indicate that the Tb ground-state wave function can not be described by the CEF Hamiltonian alone but needs an additional mean-field term. The intensity of the magnetic elastic component versus temperature is shown in Fig. 2. The accurate determination of the width of the quasi-elastic component, which inherently contain information about the Cu spin fluctuations is currently under way.

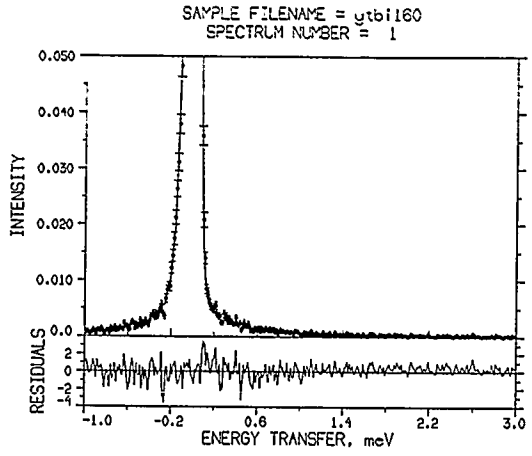


Fig. 1 Energy spectra of $Y_{0.9}Tb_{0.1}Ba_2Cu_3O_7$ at T=160K. The solid line correspond to a fit with a quasi-elastic component (broad Lorentzian) and a elastic (resolution limited Gaussian).

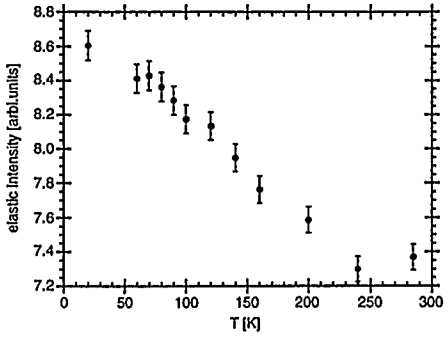


Fig. 2 Temperature dependence of the integrated magnetic elastic intensity.

1 R. Feile, M. Loewenhaupt, J. K. Kjems, and H. E. Hoenig, Phys. Rev. Lett. 47, 610 (1981).
2 R. Osborn and E. A. Goremychkin, Physica C 185, 1179 (1991).
3 U. Staub, M. R. Antonio, L. Soderholm, M. Guillaume, W. Henggeler, and A. Furrer, Phys. Rev. B 1 (1994).

INSTRUMENT USED:	DATE OF REPORT:	EXPERIMENT NO.:
QENS	January 19, 1991	1254

TITLE:
Quasielastic Neutron Scattering from Butane and Hexane Monolayers Adsorbed on Graphite

AUTHORS AND AFFILIATIONS: Haskell Taub and Pencheng Dai, University of Missouri-Columbia; F. Y. Hansen, The Technical University of Denmark; Torben Brun, LANSCE; Frans Trouw, IPNS

DATES OF EXPERIMENT: September 5-11, 1990

☒ APPROVED BY PROGRAM COMMITTEE, OR

☐ PART OF INSTRUMENT SCIENTIST ALLOCATION

REPORT RECEIVED:

EXPERIMENTAL REPORT (or Abstract of Publication)

The present run was the second in a series of experiments to study how the melting of physisorbed monolayers is influenced by the steric properties of the constituent molecules. Our interest in this subject has been motivated by the fact that the most convincing evidence of the continuous melting predicted in two dimensions (2D) by the well-known KTHNY theory [1] has been found for ethylene and ethane monolayers adsorbed on graphite [2] in which the molecules are distinctly nonspherical. By investigating the diffusion of rod-shaped molecules in monolayers near their melting point, we hope to learn what role molecular steric properties play in quasi 2D melting as opposed to the topological defects in the KTHNY theory.

Our experimental approach has been to investigate monolayer melting on graphite for a series of isostructural rod-shaped molecules, the *n*-alkanes (C_nH_{2n+2}), as a function of their length (n). In our first run, we observed the quasielastic scattering from a butane monolayer (n =4) adsorbed on an exfoliated graphite substrate (Papyex). We found no observable quasielastic broadening below the butane monolayer melting point of T_m = 116 K. However, broadening was easily observed above T_m with essentially no elastic scattering from the butane monolayer remaining above 150 K. This behavior is consistent with the results of molecular dynamics (MD) simulations [3] which show that both the rotational and translational order in the monolayer are lost abruptly at the melting point.

In the present run, we performed similar quasielastic measurements on a hexane monolayer (n = 6). As before, our sample consisted of a Papyex substrate in a cylindrical aluminum cell 5 in long and 1/2 in diameter. This diameter results in an instrumental energy resolution of ~100 μeV. The sample was mounted in a Displex cryostat which we brought from Missouri along with our own gas handling system. Prior to arriving at Argonne, the surface area of the substrate was determined to be 245 m^2 from a nitrogen vapor pressure isotherm measurement at 78 K.

It was necessary to perform a background measurement of the quasielastic scattering from the bare graphite substrate first, since the hexane cannot easily be pumped off the surface at room temperature. Then, from the known herringbone structure of the hexane monolayer on graphite (002) surface [4,5] and the measured surface area of the substrate, we were able to introduce a well-defined hexane coverage of 1.02 layers into the cell. Quasielastic spectra were obtained at temperatures of 13 K, 145 K, 155 K, 184 K, and 300 K.

EXPERIMENTAL REPORT (CONTD.)

During the entire run, data collection was hampered by malfunctioning of the detectors on arm #3 of QENS. This limited the Q range of our measurements to 0.58 $Å^{-1} < Q < 2.12$ $Å^{-1}$ and resulted in poor statistics in the vibrational spectra covering energy transfers up to 50 meV. Also, the heater on our cryostat burned out in the 5th day which thereafter limited our measurements to room temperature.

Despite these equipment problems, we were able to observe several internal vibrational modes of the hexane molecule at 13 K. At higher temperatures, the vibrational spectra were characterized by a long tail of inelastic scattering extending out to energy transfers of 10 meV. This may result from anharmonic effects in the monolayer. It will be interesting to see whether MD simulations now in progress can offer a more detailed explanation of this behavior.

Upon heating, the first quasielastic broadening was observed at 155 K which is below the monolayer melting point of 170 K inferred from neutron and x ray diffraction [4,5]. Since no broadening was observed for the butane monolayer below its melting point, this behavior may reflect the greater flexibility of the longer hexane molecule. However, one must be careful in relating the quasielastic data to the diffraction experiments since the latter were performed on deuterated samples which could have a different melting point. We have subsequently performed synchrotron x ray diffraction on a protonated hexane monolayer and are now analyzing the results.

Perhaps the most interesting result for the hexane monolayer is that elastic scattering is observed to persist even up to 300 K. This is consistent with neutron diffraction patterns [4,5] which show a much higher degree of translational order above the melting point for the hexane monolayer compared to butane. It is also consistent with the MD simulations which indicate a coexistence of two phases at high temperatures: a rectangular-centered monolayer solid (albeit with a short coherence length, 15-20 Å) and a disordered phase containing a significant number of *gauche* molecules. We are planning additional quasielastic experiments on both the butane and hexane monolayers in order to make a quantitative comparison with the translational and rotational diffusion rates calculated from the MD simulations.

1. J. M. Kosterlitz and D. J. Thouless, J. Phys. C **6**, 1181 (1973); B. I. Halperin and D. R. Nelson, Phys. Rev. Lett. **41**, 121 (1978); D. R. Nelson and B. I. Halperin, Phys. Rev. B **19**, 2457 (1979); and A. P. Young, Phys. Rev. B **19**, 1855 (1979).
2. H. K. Kim, Q. M. Zhang, and M. W. H. Chan, Phys. Rev. Lett. **56**, 1579 (1986); J. Z. Larese, *et al.*, Phys. Rev. Lett. **61**, 432 (1988); and S. Zhang and A. D Migone, Phys. Rev. B 38, 12039 (1988).
3. F. Y. Hansen and and H. Taub, in *Phase Transitions at Surfaces*, NATO Advanced Study Institute Series B, edited by H. Taub, G. Torzo, H. J. Lauter, and S. C. Fain, Jr., (Plenum, New York, 1991); and F. Y. Hansen, N. C. Newton, and H. Taub, to be published.
4. H. Taub, in *The Time Domain in Surface and Structural Dynamics*, NATO Advanced Study Institute Series, Vol. C228, edited by G. J. Long and F. Grandjean (Kluwer, Dordrecht, 1988), p. 467.
5. J. C. Newton, Ph.D. thesis, University of Missouri-Columbia, 1989 (unpublished).

Supported by NSF Grant Nos. DMR-8704938 and DMR-9011069, Pittsburg Supercomputing Center Grant No. DMR-880008P, and by Danish NSF Grant No. M 11-7015.

INSTRUMENT USED:	DATE OF REPORT:	EXPERIMENT NO.:
QENS	September 26, 1991	1253

TITLE:

Lattice Dynamics of Polymer Chains II: Polyamides

AUTHORS AND AFFILIATIONS:
A. Xenopoulos, B. Wunderlich, and A. H. Narten, Chemistry Department, The University of Tennessee, Knoxville, TN 37996 AND Chemistry Division, Oak Ridge National Laboratory, Oak Ridge, TN 37831

DATES OF EXPERIMENT: 3/5-20/91

☒ APPROVED BY PROGRAM COMMITTEE, OR

☐ PART OF INSTRUMENT SCIENTIST ALLOCATION

REPORT RECEIVED:

EXPERIMENTAL REPORT (or Abstract of Publication)

In continuation of our ongoing effort to understand the proton motions in aliphatic nylons by incoherent quasielastic neutron scattering, we performed two more sets of experiments to complement our initial work on solution-crystallized nylon 6.6 (#1051, September 1989). Data were collected for melt-crystallized nylon 6.6 at 300, 400, and 500 K; this sample was of lower crystallinity (29%) than the solution crystallized material (47%).

We also collected data on nylon 6 at 20, 200, 300, 350, 400, and 525 K. This material, having a structure similar to nylon 6.6, does not show the Brill transition seen in that material.

The results of our studies are summarized in the following abstract.

ABSTRACT of paper "PROTON MOTIONS IN ALIPHATIC NYLONS FROM NEUTRON SCATTERING," to be submitted to the Journal of Chemical Physics:

Quasielastic neutron scattering studies on samples of aliphatic nylons with different crystallinity show that at temperatures below the glass transition (310-330 K), the scattering is elastic, indicating that the protons, and hence the methylene groups to which they are bound, undergo only small-amplitude motions about their equilibrium positions. As the temperature increases, the elastic scattering decreases gradually, to be replaced by quasielastic components which can be fitted by single Lorentzians. The decrease in elastic intensity is largest for nylon 6.6, where at temperatures 40 K below melting the methylene groups undergo large amplitude motions. These observations are in agreement with the concept of conformational disorder in the crystal and with thermal analysis work on the same samples.

EXPERIMENTAL REPORT (CONTD.)

INSTRUMENT USED: QENS, HIPD	DATE OF REPORT: 12/12/93	EXPERIMENT NO.: 1768
TITLE: Tunnelling and Inelastic Scattering from Ternary Intercalates of C_{60}		
AUTHORS AND AFFILIATIONS:	J. W. White*, P. Reynolds*, R. Durand*, F. Trouw‡ * Research School of Chemistry, Australian National University ‡ IPNS, Argonne National Laboratory	
DATES OF EXPERIMENT: 10/11/93 to 17/11/93		

CHECK ALL APPLICABLE BOXES:

- ☐ APPROVED BY PROGRAM COMMITTEE
- ☐ INSTRUMENT SCIENTIST ALLOCATION
- ☐ DO NOT PUBLISH
- ☐ PROPRIETARY RESEARCH
- ☐ PRT ALLOCATION

EXPERIMENTAL REPORT (or Abstract of Publication)

We have found that alkali metal C_{60} intercalates, such as Rb_3C_{60} may be ternarily doped with ammonia at room temperature to produce phases which resemble those which we have previously studied in the graphite alkali metal intercalation compounds.[1,2] This doping also changes the superconducting behaviour of the C_{60} intercalate.

The mechanism of superconductivity in these compounds has been suggested to be explainable by the BCS theory of superconductivity [3] which is based on electron-phonon coupling. In particular the intramolecular modes of C_{60} having symmetry Hg have been implicated in this interaction [4]. Changes in the superconducting behaviour should therefore be apparent as changes in the strengths and widths of these modes.

To examine the NH_3 tunnelling and the effect of doping on the C_{60} Hg vibrational modes we examined two samples on QENS. The first was Rb_3C_{60} doped with ca. 4 moles of NH_3 per C_{60}. The second was Rb_3C_{60} doped with ca. 1 mole of ND_3 per C_{60}. The results indicate that doping with ammonia does strongly affect the vibrational modes of C_{60} and that doping at a stoichiometry of ca. 1:1 of ammonia:Rb_3C_{60} results in a mixture of two phases, pure Rb_3C_{60} and $Rb_3C_{60}(ND_3)_4$. The inelastic spectrum from QENS shows prominent NH_3 librational peaks for the NH_3 material.

HIPD Diffraction results (see Fig. 1)

The pattern of the ND_3 doped material exhibits a mixture of strong sharp, and weak broad peaks. The latter correspond with similar peaks in the NH_3 doped material. The ND_3 material is a mixture of ca. 80% pure Rb_3C_{60} and 20% $Rb_3C_{60}(ND_3)_{4\pm1}$. This is confirmed by Rietveld fitting of the profiles (see Fig. 2), from which we obtain the first Rb_3C_{60} structure. Examination of this structure shows voids around the Rb site at $^1/_2,^1/_2,^1/_2$ of a size capable of accommodating ammonia molecules. The NH_3 doped material has a similar cell size, indicating filling of voids by ammonia, but the cell indexes as primitive cubic, not Fm3m, as in Rb_3C_{60}. In addition peaks are broad, and somewhat shifted indicating poorer crystal quality.

QENS Inelastic results :

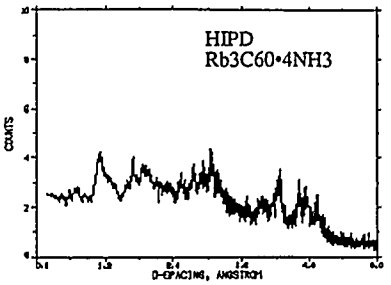
The inelastic spectra from QENS for the NH_3 and ND_3 materials (see Fig. 3) clearly show the prominent NH_3 librational peaks for the NH_3 material, at 3.7 and 8.4 meV. We also observe distinct differences at higher energies in which the relatively sharp Rb_3C_{60} peaks at 43.9, 49.6 and 60.4 meV are broadened in the $Rb_3C_{60}(NH_3)_4$. Thus ammonia doping markedly affects the "C_{60}" vibrational modes although we cannot yet definitively say if this broadening is due to electron phonon interaction or due to structural disorder.

1 .....Two Dimensional Caesium-ammonia Solid Solutions in $C_{28}Cs(NH_3)_x$
Carlile C.J., Jamie I. McL., Lockhart G., and White J.W., *Mol. Phys.*, 76, 173, (1992)

2 .....Temperature Dependence of the Lattice Dynamics of Rb_3C_{60}
White J.W., Lindsell G., Pang, L., Palmisano A., Sivia D.S., and Tompkinson J., *Chem. Phys. Lett.*, 191, 92-96, (1992)

3 .....Theory of Superconductivity
Bardeen J., Cooper L.N., Schrieffer J.R., *Phys. Rev.*, 108(5), 1175, (1957)

4 .....Schluter M.A., *preprint*



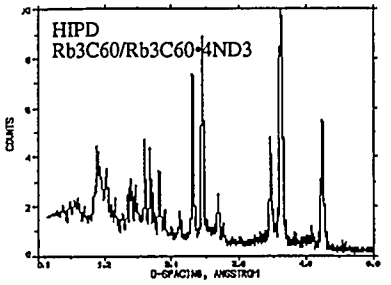


FIGURE 1

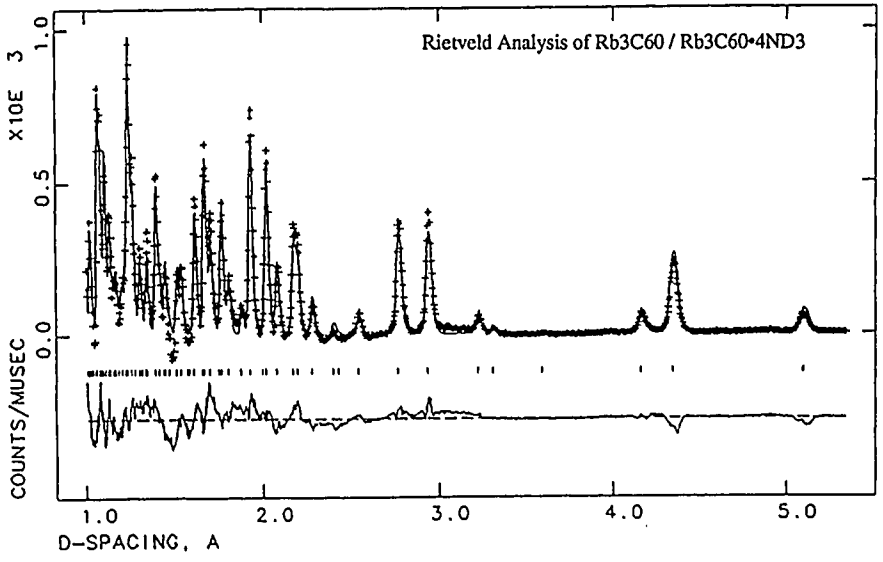
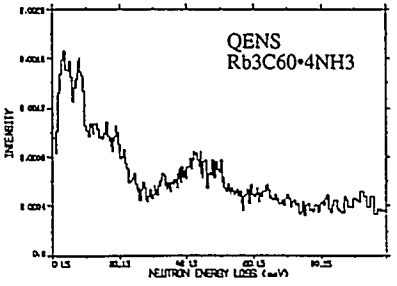


FIGURE 2



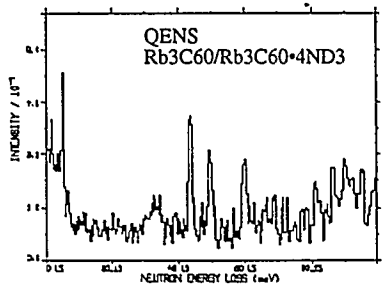


FIGURE 3

INSTRUMENT USED: QENS, HIPD	DATE OF REPORT: 8/2/94	EXPERIMENT NO.: 1878

TITLE: Inelastic Scattering from Ternary Intercalates of C_{60}

AUTHORS AND AFFILIATIONS: J. W. White, P. Reynolds, R. Durand
Research School of Chemistry, Australian National University

DATES OF EXPERIMENTS: 4/12/94 to 4/25/94

CHECK ALL APPLICABLE BOXES:

- [X] APPROVED BY PROGRAM COMMITTEE
- [ ] INSTRUMENT SCIENTIST ALLOCATION
- [ ] DO NOT PUBLISH
- [ ] PROPRIETARY RESEARCH
- [ ] PRT ALLOCATION

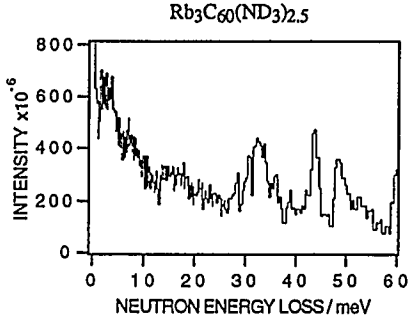
EXPERIMENTAL REPORT (or Abstract of Publication)

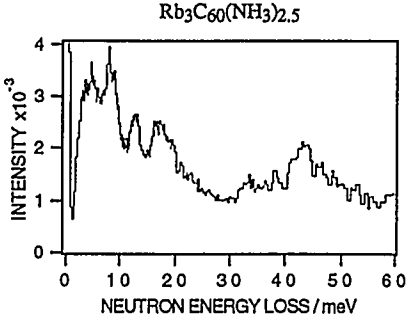
This is a continuation of Experiment No. 1768 in which two ammonia doped Rb_3C_{60} samples were examined by elastic (HIPD) and inelastic (QENS) neutron scattering. As outlined in the report on #1768, this is an experiment to elucidate the mechanism of high temperature superconductivity in these materials.

Two further samples, of improved crystallinity and different doping were examined on QENS and HIPD. We now have results from Rb_3C_{60}; $Rb_3C_{60}(NH_3)_{0.96}$; $Rb_3C_{60}(NH_3)_{2.5}$ and $Rb_3C_{60}(ND_3)_{2.5}$.

These new results confirm that the internal vibrational modes of C_{60} in Rb_3C_{60} are strongly affected by ammonia doping, the density of states reverting to something much closer to that in pure C_{60}. In addition there are now, by comparison of spectra, sufficient data to assign all the observed inelastic peaks both in the tunnelling (μeV) and vibrational (meV) regions. The NH_3 and ND_3 torsional and tunnelling peaks may be fitted by a model in which the -NH_3 rotor exists within a threefold potential with a mean barrier height of 12 meV.

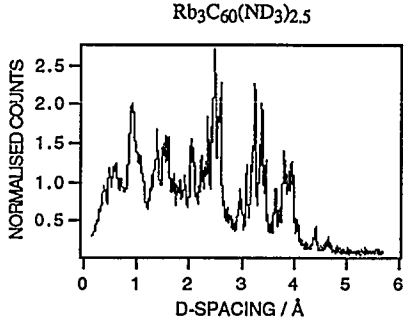
QENS Inelastic Results The new QENS inelastic spectrum for $Rb_3C_{60}(NH_3)_{2.5}$ shows more structure than the $Rb_3C_{60}(NH_3)_{0.96}$ spectrum of #1768. In addition to the lattice peak at 4 meV and the NH_3 torsional mode at 8.5, we can now resolve two further torsional peaks at 13.0 and 17.5 meV. In addition for ND_3 we observe torsions at 7.9 and 16.3 meV. All these energies may be fitted by a threefold rotational potential with barrier height 12 meV. δ bending modes of N-Rb-N may be assigned at 35 and 45 meV (NH_3) and 27 meV (ND_3) at their expected values. A comparison of Rb_3C_{60} and $Rb_3C_{60}(NH_3)_{2.5}$ shows similar C_{60} internal vibrational modes, many very narrow. But in $Rb_3C_{60}(NH_3)_{2.5}$, as in C_{60} itself, the $H_g(2)$ (54 meV) and T_{1u}(70-74 meV) modes are apparent which they are not in Rb_3C_{60}. This appears to be due to strong electron-phonon coupling.

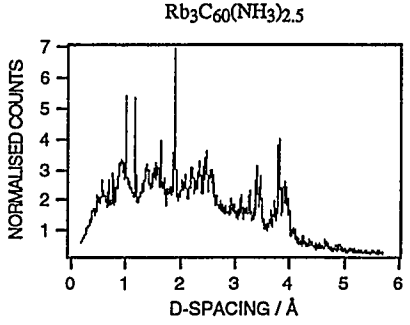




EXPERIMENTAL REPORT (CONTD.)

HIPD Diffraction Results The diffraction patterns here show many more resolved peaks than the previous samples, reflecting the improved crystallinity. The peaks indexed as primitive cubic are now much split. The material is not single phase, but is composed of a number of superlattices all derived from a basic cubic $Im\bar{3}m$ (a=12.10Å) cell, by modulation along the three principal axes. This is supported by both X-ray diffraction measurements, and measurements on the corresponding lithium compounds. The C_{60} - C_{60} distances remain constant while the modulation doubles and in aged samples the cell dimensions triple with substantial rearrangement of unit cell contents. These superlattices may be interpreted as low order approximants to an icosahedral quasicrystal. The peaks observed correspond to those strongest in such a quasicrystal. We can infer that the commensurate modulation is such as to produce, for much of the unit cell content, a more icosahedral local coordination around the C_{60} fragments.





INSTRUMENT USED:	DATE OF REPORT:	EXPERIMENT NO.:
SAD	August 1991	#1402 and #1458

TITLE:

Magnesium Hydroxide Gels Monitored by SANS Contrast-Variation Techniques

AUTHORS AND AFFILIATIONS:
K. A. Carrado (CHM) and P. Thiyagarajan (PNS), Argonne National Lab

DATES OF EXPERIMENT: February, 25-27 (#1402) and June, 13-15 (#1458) 1991

☒ APPROVED BY PROGRAM COMMITTEE, OR

☐ PART OF INSTRUMENT SCIENTIST ALLOCATION

REPORT RECEIVED:

EXPERIMENTAL REPORT (or Abstract of Publication)

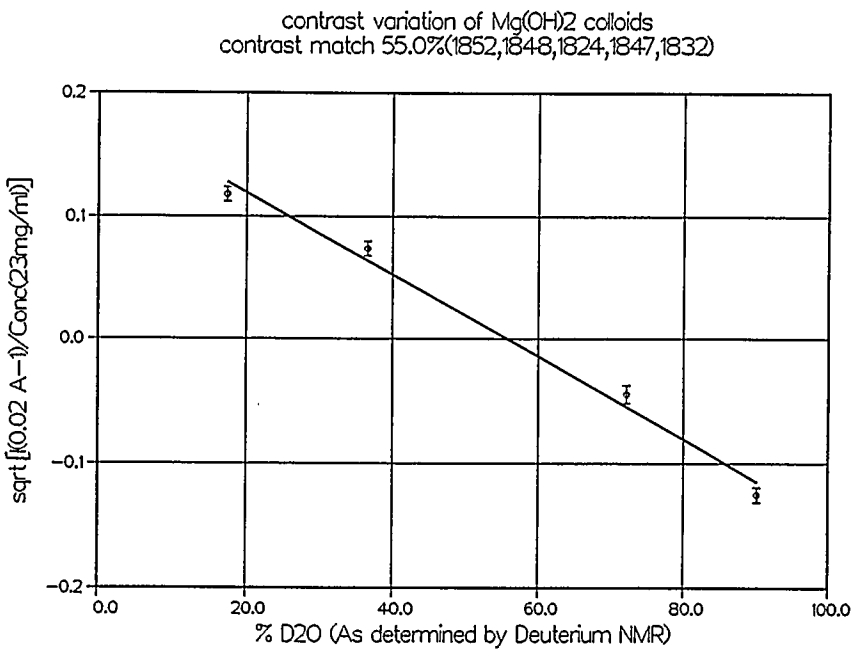
A better understanding of the gel chemistry involved in processes wherein synthetic clays incorporate a pillaring species *in situ* is needed in order to probe the details of gel structure and crystal nucleation phenomena. With such information, it is hoped that the gel chemistry and, ultimately, the structure of the final products can be better controlled. The clay gels consist of colloidal silica sol and magnesium hydroxide, lithium fluoride and organic template.

When it is present, the scattering from unreacted magnesium hydroxide dominates the scattering, so that finer details in the scattering profiles cannot be observed. This component therefore needs to be contrast-matched, or made "invisible" in the neutron scattering profile. This is done by adjusting mixtures of heavy and light water to precisely match the scattering power of a specific component. The component of interest here is freshly prepared magnesium hydroxide, which is colloidal in nature and whose density is unknown. The density of the natural mineral of magnesium hydroxide, brucite (2.36 g/cm^3), was used as the closest approximation in the calculation for determining the scattering length density of $Mg(OH)_2$, which is equivalent to 41.6% D_2O. In the first experiment (#1402), the magnesium hydroxide samples were prepared by direct precipitation of magnesium chloride in ammonium hydroxide diluted in the various D_2O/H_2O mixtures. However, due to H-D exchange the contrast match point could not be determined.

For experiment #1458, a solution of magnesium hydroxide colloids was prepared fresh in distilled water, divided into equal portions, and these were dialyzed in the various D_2O/H_2O mixtures. This dialysis technique proved to be very efficient, and a contrast match point of 55% D_2O was obtained, as seen in Figure 1. Precise D_2O/H_2O ratios of the dialysates were needed for the calculations; these values were determined by ^1H and ^2D NMR on a 300 MHz GE NMR Omega spectrometer.

The actual contrast match value of 55% D_2O is quite different from the calculated value of 42%. This may be due to a combination of factors, such as assumptions in the calculation regarding density and a limited degree of H-D exchange on the colloidal surfaces. Further experiments can now be performed using this contrast match value to mask scattering due to unreacted magnesium hydroxide. Interactions between this component and colloidal silica in the reactive clay gel should therefore become more dominant in the scattering profiles.

Figure 1



INSTRUMENT USED: SAD-1	DATE OF REPORT: 1/9/95	EXPERIMENT NO.: 1832

TITLE: Small angle neutron scattering in the dilute concentration limit of PVME in PSD

AUTHORS AND AFFILIATIONS: Robert M. Briber

DATES OF EXPERIMENT: From September 19, 1994 To September 23, 1994

CHECK ALL APPLICABLE BOXES:

- ☐ APPROVED BY PROGRAM COMMITTEE
- ☐ PROPRIETARY RESEARCH
- ☒ INSTRUMENT SCIENTIST ALLOCATION
- ☐ PRT ALLOCATION
- ☐ DO NOT PUBLISH

EXPERIMENTAL REPORT (or Abstract of Publication)

1. INTRODUCTION

Poly(vinylmethylether)(PVME)/deuterated polystyrene(PSD) blends were examined by SANS in the limit of dilute PVME concentration. Zimm analysis and the random phase approximation (RPA) were used to analyze the data. The object of this work is to study the interaction parameter and radius of gyration for PVME in PSD as a function of composition and temperature in the dilute PVME concentration regime.

2. EXPERIMENTAL

The PVME was cationically polymerized in toluene using boron trifluoride-ethyl ether complex as the catalyst. The molecular weight of the PVME was determined using gel permeation chromatography. The samples for neutron scattering were prepared by dissolving the PVME and PSD in toluene and then allowing the solution to evaporate in a Teflon petridish and form a thin film. The film was then dried in vacuum to remove the remaining toluene. The scattering experiment was carried out as a function of temperature at the Intense Pulsed Neutron Source Argonne National Laboratory using SAD-1.

3. DATA ANALYSIS

The raw data were obtained at 120 °C, 130 °C, 140 °C, 150 °C, 160 °C, and 170 °C for each concentration. The raw data were corrected for scattering from the empty cell, background matrix scattering, detector dark current and sensitivity, sample transmission and thickness, placed on an absolute scale using a calibrated secondary standard and circularly averaged to produce the I(q) versus q plots. The data at each temperature were extrapolated to the limit of zero concentration at every value of q.

The classical Zimm equation gives the scattering from a dilute mixture of a polymer in a solvent to be[1-4]

$$\frac{k_n\phi_a}{I(q)} = \frac{1}{\langle N_a\rangle_n v_a \langle P_a(q)\rangle_w} + 2A_2\phi_a \qquad (1)$$

where I(q) is the measured scattered intensity, $\langle P_a(q)\rangle_w$ is the *weight* average single particle form factor for species a, ϕ_a is the volume fraction of the dilute polymer, $\langle N_a\rangle_n$ is the number average degree of polymerization of polymer a, v_a is the specific volume of polymer a, A_2 is the second virial coefficient, and k_n is the contrast factor for neutrons. By taking the limit as $\phi_a \to 0$

$$\lim_{\phi\to 0}\left(\frac{I(q)}{\phi_a}\right) = k_n \langle N_a\rangle_w v_a \langle P_a(q)\rangle_w. \qquad (2)$$

$\langle P_a(q)\rangle_w$ is given by[5,6] $\langle P(q)\rangle_w = \frac{2}{\langle x\rangle_n^2}[\langle x\rangle_n - 1 + (\frac{h}{h+\langle x\rangle_n})^h]$ (3a)

where $h = \frac{1}{(\frac{\langle N\rangle_w}{\langle N\rangle_n} - 1)}$ and $\langle x\rangle_n = \langle N\rangle_n l^2 q^2/6 = \langle r_g^2\rangle_n q^2$. (3b,c)

$\langle N\rangle_w$ and $\langle N\rangle_n$ are the weight and number average degrees of polymerization, l is the statistical segment length, q is the scattering vector, and $\langle r_g^2\rangle_n$ is the number average square of the radius of gyration. The statistical step length and radius of gyration for PVME were obtained by fitting the data to equation (2). The values of the step length and radius of gyration at six different temperatures are shown in table 1.

Temperature	R_{gPVME}(Å)	l_{PVME}(Å)
120 °C	48	5.9
130 °C	46	5.6
140 °C	46	5.6
150 °C	47	5.8
160 °C	48	5.8
170 °C	48	5.8

Table 1. Step length of PVME in PSD from zero concentration extrapolated scattering data. Average value of l_{PVME} = 5.75 Å

By taking the limit as q→0 for the Zimm equation

$$\frac{k_n\phi_a}{I(0)} = \frac{1}{\langle N_a\rangle_w v_a} + 2A_2\phi_a. \qquad (4)$$

The weight average molecular weight and the second virial coefficient can be determined from a plot of $\phi_a/I(0)$ versus ϕ_a. The $\phi/I(0)$ data were obtained from linear least square fit of $1/I(q)$ versus q^2 plots. The $\phi/I(0)$ data obtained at q=0 were plotted as a function of concentration for different temperatures. The values of $\langle N_a\rangle_w$ were obtained from the intercept of the line with y-axis using equation (4). The average value of $\langle N_a\rangle_w$ was found to be 662, which is the same as the value determined from GPC.

de Gennes has developed an expression for the total coherent scattering from binary (miscible) mixture of polymers using the random phase approximation[7,8]. The total scattering is given by

$$\frac{k_n}{I(q)} = \frac{1}{\langle N_a\rangle_n v_a\phi_a\langle P_a(q)\rangle_w} + \frac{1}{\langle N_b\rangle_n v_b\phi_b\langle P_b(q)\rangle_w} - 2\frac{\chi}{v_0}. \qquad (5)$$

By fitting this equation to the data we obtained the value of the interaction parameter. By extrapolating the data to the point $\chi/v_0 = \chi_s/v_0$ on a plot of χ/v_0 versus 1/T the spinodal temperature, T_s, was obtained. For the blend with ϕ_{PVME}=0.09362 the extrapolated spinodal temperature was found to be T_s=312 °C.

4. CONCLUSION

The data obtained by SANS was extrapolated to zero concentration and were fit to obtain the value of the radius of gyration using a modified Debye function. The value of the statistical segment length found for PVME was 5.75 Å. The temperature dependence of χ/v_0 indicates that phase separation will occur in the range of 310 °C for ϕ_{PVME}≅9 %.

REFERENCES

1. S. Sakurai, H. Hasegawa, T. Hashimoto, and C. C. Han; *Polym. Comm.*, 31, 99(1990)
2. A. Maconnachie, R. P. Kambour, D. M. White, S. Rostami, and D. J. Walsh; *Macromolecules*, 17, 2645(1984)
3. B. H. Zimm; *J. Chem. Phys.*, 16, 1093(1948)
4. B. H. Zimm; *J. Chem. Phys.*, 16, 1099(1948)
5. G. V. Z. Schultz; *Phys. Chem. Abt.*, B43, 25(1939)
6. K. Mori, H. Tanaka, H. Hasegawa, and T. Hashimoto; *Polym.*, 30, 1389(1989)
7. P. G. de Gennes; *Scaling Concepts In Polymer Physics*, Cornell University, New York, 1979.
8. M. Shibayama, H. Yang, R. S. Stein, C. C. Han; *Macromolecules*, 18, 2179(1985)

INSTRUMENT USED:	DATE OF REPORT:	EXPERIMENT NO:
SAD	10 August 1994	1745

TITLE:
The Accessibility of Organic Liquids to the Pore Network of Activated Carbons

AUTHORS AND AFFILIATIONS:
J. M. Calo, Division of Engineering, Box D, Brown University, Providence, RI 02912, U.S.A.
P. J. Hall, Department of Pure and Applied Chemistry, University of Strathclyde, Glasgow, U.K.

DATES OF EXPERIMENT:
March 19, 20, 1994

CHECK ALL APPLICABLE BOXES:

- ☑ APPROVED BY PROGRAM COMMITTEE
- ☐ INSTRUMENT SCIENTIST ALLOCATION
- ☐ DO NOT PUBLISH
- ☐ PROPRIETARY RESEARCH
- ☐ PRT ALLOCATION

EXPERIMENTAL REPORT (or Abstract of Publication)

Data from SANS experiments conducted on the IPNS SAD instrument were used to investigate porosity development in a phenol-formaldehyde resin char and Pittsburgh #8 coal (Argonne Premium Coal Sample Bank) char samples. SANS was performed on freshly pyrolyzed, unactivated samples, as well as samples that were progressively activated by gasification in air at 400°C. Scattering from the dry, powdered samples results from both porosity that is accessible or "open" to the exterior of the particles, as well as inaccessible or "closed" porosity. These two different types of porosity were differentiated using a contrast matching technique. Essentially, SANS data were obtained for both "dry" char samples, and then for the same samples following saturation with deuterated toluene in an ultrasonic bath for four hours. This treatment causes the solvent to enter and fill the accessible porosity. The deuterated toluene closely contrast matches the carbon in these samples such that the resultant SANS data are almost entirely due to the inaccessible or closed porosity.

Figures 1 and 2 present some selected SANS results for the resin char and Pittsburgh #8 coal char samples, respectively. These data reveal some interesting features about the pore structures of these two chars. The level of scattering at high wave vector values suggests that both have relatively low levels of microporosity. This conclusion was confirmed by nitrogen gas adsorption isotherms that were obtained for sample characterization. The effect of contrast matching, however, is different for both chars. The contrast matched resin char still exhibits significant scattering in comparison to the corresponding "dry" sample. This indicates that this carbon has a significant, well-developed, but inaccessible pore structure. The SANS data for the progressively burned-off resin char samples demonstrate that gasification of this carbon proceeds primarily *via* "opening up" of the closed porosity.

As indicated in Figure 2, however, the data for the coal char samples are quite different. The contrast-matched Pittsburgh #8 sample exhibits considerably reduced scattering intensity in comparison to the corresponding "dry" sample. This indicates that this coal char exhibits very little "closed" porosity. Moreover, the SANS data for the progressively burned-off samples clearly show that porosity development in this coal char proceeds primarily *via* the production of new pores produced during the gasification process, rather than the opening up of pre-existing closed porosity. That is, essentially all the observed porosity is accessible to the deuterated toluene.

With this set of experiments on these two very different chars, we have successfully demonstrated that contrast matching using deuterated solvents is a potentially powerful technique for the investigation and quantification of porosity development in activated carbons. We are currently in the process of analyzing our SANS data using a bimodal, Fully Penetrable Polydisperse Spheres (FPPS) porosity model in order to quantitatively characterize porosity development in these carbons.

Publications:

P. J. Hall, M. M. Antxustegi, and J. M. Calo, *Proc. Int. Carbon Conf. Carbon '94*, Granada, Spain, 1994, p. 164.
Two papers in preparation.

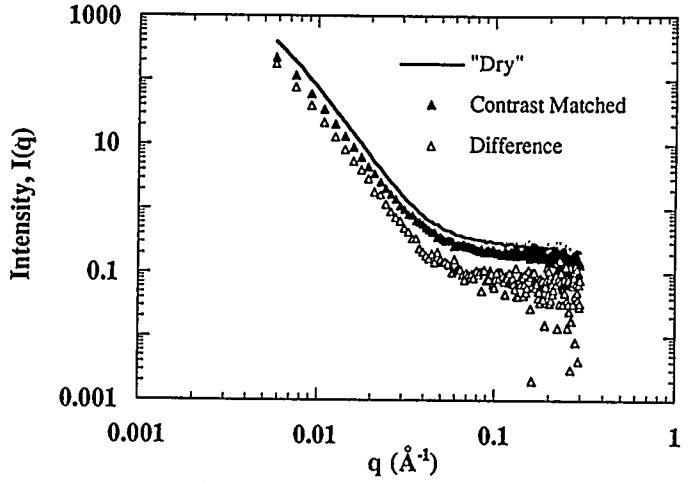


Figure 1. SANS data for unactivated resin char.

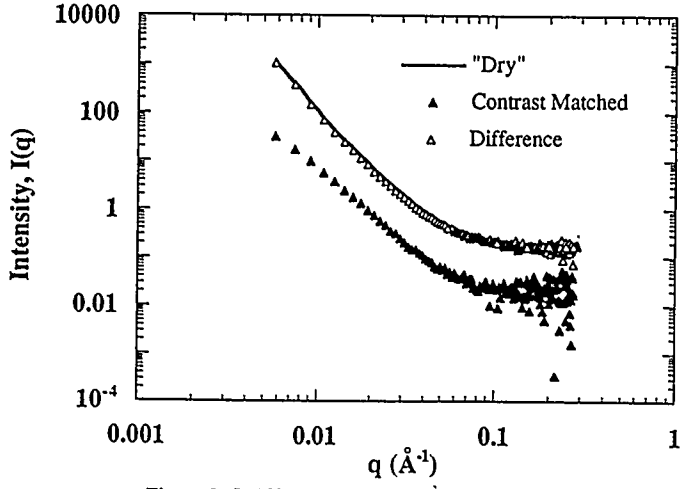


Figure 2. SANS data for unactivated Pittsburgh #8 coal char.

INSTRUMENT USED: SAD	DATE OF REPORT: 1 December 1995	EXPERIMENT NO.: 1968

TITLE:

Connectivity of Porosity in Coals

AUTHORS AND AFFILIATIONS: J.M. Calo, Division of Engineering, Brown University, Providence, RI
P.J. Hall, Dept. Pure & Appl. Chemistry, University of Strathclyde, Glasgow, UK.

DATES OF EXPERIMENT: March 10-12, 1995

CHECK ALL APPLICABLE BOXES:

- ☐ APPROVED BY PROGRAM COMMITTEE
- ☐ PROPRIETARY RESEARCH
- ☐ INSTRUMENT SCIENTIST ALLOCATION
- ☐ PRT LOCATION
- ☐ DO NOT PUBLISH

EXPERIMENTAL REPORT (or Abstract of Publication)

The following are abstracts of two papers based upon the data obtained at IPNS which have been submitted to the journal Energy & Fuels:

1. The Effect of Interparticle Scattering on the Interpretation of Small Angle Neutron Scattering and the Development of Porosity in Pittsburgh No. 8 Coal Char

Peter J. Hall, M. Mirari Antxustegi, J.M. Calo, and P. Thiyagarajan

Contrast matching small angle neutron scattering has been used to investigate the development of porosity in Pittsburgh #8 coal char following gasification in air at 673K. The ungasified char contains very little porosity, although the char exhibits considerable scattering in the small angle region. Contrast matching with deuterated toluene shows that the origin of this scattering is from interparticle voids. As porosity develops during gasification so does the scattering intensity. A method is presented whereby scattering from gasified chars can be corrected for interparticle scattering, such that the development of the actual porosity can be properly monitored.

2. The Use of Contrast Matching Small Angle Neutron Scattering to Monitor "Closed" Porosity in Carbons

Peter J. Hall, M. Mirari Antxustegi, J.M. Calo, and P. Thiyagarajan

Small angle neutron scattering has been performed on unactivated phenolic resin char (PRC) and PRC activated to 21% burn-off. Char samples were contrast-matched with deuterated toluene. It is shown that scattering from the contrast matched samples arises predominantly from closed porosity. The difference in scattering between the dry and contrast matched samples is shown to be from interparticle scattering and from the porosity filled with deuterated toluene. It is shown how interparticle scattering convolutes the interpretation of small angle scattering data and how the activation process develops porosity in the size range <240Å. It is concluded that considerable care must be taken concerning the proper interpretation of small angle scattering data in terms of porosity development in carbons and chars.

Other Publications:

P.J. Hall, M.M. Antxustegi, J.M. Calo, and P. Thiyagarajan, *Proc. Carbon '94*, p. 164, 1994, Granada, Spain.

P.J. Hall, M.M. Antxustegi, J.M. Calo, and P. Thiyagarajan, *Proc. Carbon '95*, p. 378, 1995, U.C. San Diego, CA.

INSTRUMENT USED: SAD	DATE OF REPORT: 1/18/95	EXPERIMENT NO.: 1889

TITLE: SANS Studies of the Mechanism of Incorporation of Water-Soluble Polymers in Clays During Hydrothermal Crystallization

AUTHORS AND AFFILIATIONS: K. A. Carrado, Chemistry Division, and P. Thiyagarajan, Pulsed Neutron Source Division, Argonne National Laboratory

DATES OF EXPERIMENT: May 14-16, 1994

☐ APPROVED BY PROGRAM COMMITTEE, OR

☐ PART OF INSTRUMENT SCIENTIST ALLOCATION

REPORT RECEIVED:

EXPERIMENTAL REPORT (or Abstract of Publication)

EXPERIMENTAL REPORT

We proposed to examine by small-angle neutron scattering methods the conformational changes that occur for water-soluble polymers during the crystallization of layered silicate clay minerals from a gel. The uncoiling behavior and structural changes in polyvinyl alcohol (PVA) as a function of temperature and the presence of a clay matrix are of interest for this experiment. These are fundamentally important phenomena that have not yet been directly observed, therefore any new data will be of immediate interest to materials science.

Our laboratory has developed a method for preparing synthetic clays with direct incorporation of a wide variety of organic and organometallic molecules (*1*), including water-soluble polymers such as polyvinyl alcohol (PVA) and those that are cellulosic (*2*). A series of PVA samples varying in molecular weight from 9,000 to 146,000 have been successfully employed. All are incorporated at approximately the 20% (w/w) level, and all separate the clay layers by approximately 10 Å in the final dried products. Polymer-clay complexes of PVA have been previously examined in detail (*3*). The adsorption of PVA by natural montmorillonite clays has been found to be influenced by the nature of the exchangeable cation and by ionic strength. The complex with Na-montmorillonite, for example, at maximum adsorption (ca. 80 wt%) has a gallery height of about 20 Å, corresponding to a flat, extended monolayer of PVA on each of the two opposing interlayer surfaces (*3*), with an average loop length of 10 Å each. Our samples incorporate PVA at about 1/4 of this level, with gallery heights corresponding to a single, flat extended monolayer of PVA.

We began with a PVA sample of molecular weight 50,000. PVA alone in an approximately 65% D_2O solution, which is the contrast match medium for our particular silica sol (*4*), was measured at both room temperature and after heating at 100°C. The solution was well-dispersed and no agglomeration upon heating was evident. Another factor of interest was ionic strength. SANS of PVA solutions was both in the absence of any salt and in 0.1M NaCl. The radius of gyration R(g) and the I(0) values were observed to decrease at high ionic strengths, implying shrinkage of the polymers. This factor was examined because ionic strength is clearly a factor in clay gel crystallization.

The cationic poly(dimethyl diallyl ammonium) chloride has also been observed to intercalate directly within the layers of a clay as they crystallize from a gel (*2*). SANS of PDDA with a molecular weight of 100,000 in D_2O was measured. Since the monomer of PDDA has a

positive chage it resembles a polyelectrolyte, and the SANS signal was strongly affected by the interparticle interactions. With the addition of a series of increasing NaCl concentrations, we observed the SANS signals in the low q-region to increase. This indicates a decrease in interparticle interactions, see Figure 1.

The layering process of smectite clay formation from a gel has been reported by our group (*4*) using SANS, and the results support the generally accepted mechanism whereby tetrahedral silica layers condense on preexisting brucitic sheets. Additional information regarding this mechanism may be obtained after determining the changes in phase and structural conformations relevant to the polymers of interest.

REFERENCES

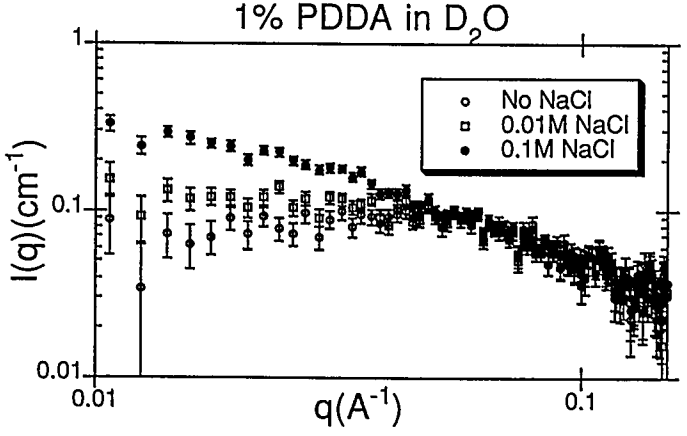
1. K. A. Carrado, *Industrial and Engineering Chemistry Research* **1993**, *31*, 1654.

2. K. A. Carrado and D. L. Elder, *Chemistry of Materials* 1995, submitted.

3. (a) D. J. Greenland, *J. Coll. Sci.* **1963**, *18*, 647; (b) B. K. G. Theng, *Clays Clay Miner.* **1982**, *30*, 1; (c) B. K. G. Theng, *Formation and Properties of Clay-Polymer Complexes* **1979**, Elsevier: Amsterdam.

4. K. A. Carrado, P. Thiyagarajan, R. E. Winans, R. E. Botto, *Inorganic Chemistry* **1991**, *30*, 794.

FIGURE 1.



INSTRUMENT USED:	DATE OF REPORT:	EXPERIMENT NO.:
SAD	August 9, 1990	1263

TITLE: Characterization of Template-Mediated Layer Silicate Crystallization Processes by Small-Angle Neutron Scattering

AUTHORS AND AFFILIATIONS:

K. A. Carrado, P. Thiyagarajan, R. E. Winans

DATES OF EXPERIMENT: May 14 - 16, 1990

☒ APPROVED BY PROGRAM COMMITTEE, OR

☒ PART OF INSTRUMENT SCIENTIST ALLOCATION

REPORT RECEIVED:

EXPERIMENTAL REPORT (or Abstract of Publication)

Clays are layered silicates that have been used extensively as solid acids in catalytic cracking reactions of large hydrocarbons[1]. Zeolite-based materials are the currently used commercial fluid-cracking catalysts, but a limited pore size range (2-8Å) restricts their utility for converting high molecular weight hydrocarbons like those found in heavy oils. Pillared clays, where the clay layers are propped open by columns of alumina, offer an expanded pore size range[2] with rectangular openings of about 8 x 15Å. To date, all pillared clays have been prepared by ion-exchange of clay minerals in solution. A new method is being developed wherein clays are synthesized to incorporate a pillaring species *in situ*. This process is similar to zeolite synthesis, where organic molecules present in a silicate gel are used to direct specific structure types, and are then burned out of the framework leaving cages and channels in a porous network. It is critical to establish a better understanding of the gel chemistry involved in such templating processes, because the details of gel structure and crystal nucleation phenomena are not well understood for even the much-studied zeolite systems[3].

We have previously used small-angle neutron scattering (SANS) to follow the layering process of synthetic clays from colloidal silica sols[4]. A typical preparation of a hectorite clay involves refluxing an aqueous gel of silica sol, magnesium hydroxide, lithium fluoride and an organic template. The organic templates examined thus far have been water-soluble porphyrins and metalloporphyrins. In order to obtain more chemical information, porphyrin was also added to each gel component individually and the scattering was analyzed[5]. This work is continued in the present report, in addition to further studies described below.

A 'template theory' has been developed to explain the structure-directing effect of organic molecules in zeolite synthesis. Charge distribution and size and shape of a templating molecule are believed to cause this behavior[6]. On the other hand, alteration of the gel chemistry by the additive may be equal or greater importance than the templating action[6]. Resolving this issue is a major key to the overall understanding of the action of templates, and is necessary to guide the design of more elaborate systems. Comparison of organic template molecules in our clay syntheses reveals that large, flat macrocycles like porphyrins induce crystallization at much faster rates than traditional organics, such as alkylammonium cations. The significant decrease in reaction time may be attributed to 'templating'. Although Si/Al ratios, concentrations, and crystallization temperatures were all held constant, the effect of other factors in the gel chemistry, such as pH, could not be dismissed without further investigation. It was decided to probe pH effects on silica sol alone using SANS, and probe interactions at the particulate level of the gel. Modifications in pH were accomplished by adding HCl, NaOH, NH_4OH or NaOH to span a pH range of 6.6 to 11.5. As can be seen in Figure 1, particle-particle interactions increase dramatically when the pH is outside the range of a normal clay synthesis gel preparation (pH 9.5-10). When this happens the larger effective size of the sol particles leads to a much lower surface area for reaction, and a more inefficient process results.

In addition, various combinations of the multi-component system were examined separately. While our previous study[5] looked only at porphyrin interactions (porphyrin-silica and porphyrin-$Mg(OH)_2$), we have now completed a much more comprehensive series. This includes a comparison of porphyrin (P) vs. tetramethyl ammonium (TMA) templates as well. Silica reacted with LiF and with $Mg(OH)_2$ separately were two of the systems. It was already known and demonstrated that reaction of silica, $Mg(OH)_2$ and LiF together results in crystallization of the purely inorganic clay synthetic Li-hectorite. TMA-silica systems were compared with P-silica, and then TMA- and P-$Mg(OH)_2$ systems were probed. The effect of refluxing all systems for one day was also measured. Figs. 2a and 2b show the effects of adding LiF and TMA to the silica sol. At pH conditions where the sol exhibits strong interparticle interactions, these additives seem to reduce those interactions, and probably promote the growth of chainlike particles involving silica and the additives.

EXPERIMENTAL REPORT (CONTD.)

Various combinations of three of the gel components were then examined: TMA- and P-LiF-silica, P-$Mg(OH)_2$-silica, and P-LiF-$Mg(OH)_2$. The presence of $Mg(OH)_2$ in any system was found to be so dominant that all subtle features of scattering due to interactions were masked. As a result, it is essential that contrast-matching experiments be performed next.

REFERENCES

1. Pinnavaia, T. J. *Science* 1983, *220*, 365.

2. Shabtai, J.; Rosell, M.; Tokarz, M. *Clays & Clay Mins.* 1984, *32*, 99.

3. Gabelica, Z.; Derouane, E. G.; Blom, N. *ACS Symp. Ser.* 1984, *248*, 219.

4. Carrado, K. A.; Thiyagarajan, P.; Winans, R. E. *Experimental Report* 1989, IPNS Expt. #0988.

5. Carrado, K. A.; Thiyagarajan, P.; Winans, R. E. *Experimental Report* 1990, IPNS Expt. 0988, continued. (b) Carrado, K. A.; Thiyagarajan, P.; Winans, R. E.; Botto, R. E. *Inorg. Chem.* 1990, submitted as "Hydrothermal crystallization of porphyrin-containing layer silicates".

6. Lok, B. M.; Cannan, T. R.; Messina, C. A. *Zeolites* 1983, *3*, 282.

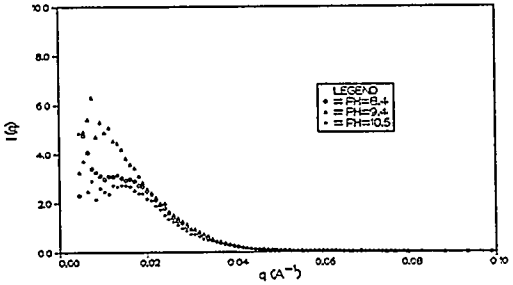


Figure 1. Effect of pH on scattering of silica sol.

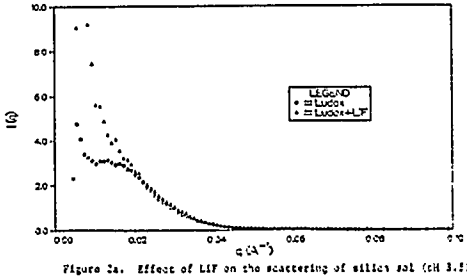


Figure 2a. Effect of LiF on the scattering of silica sol (pH 9.5).

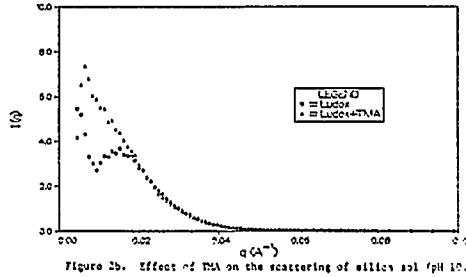


Figure 2b. Effect of TMA on the scattering of silica sol (pH 10.

INSTRUMENT USED:	DATE OF REPORT:	EXPERIMENT NO.:
SAD	January 30, 1990	1185

TITLE: Effect of Lattice Mismatch Strain on the Morphology Change in Ni-Al-Si Ternary Alloys

AUTHORS AND AFFILIATIONS:

Haydn Chen and G. Muralidharan, University of Illinois

DATES OF EXPERIMENT: 13 - 16 December, 1989 (3 days)

☒ APPROVED BY PROGRAM COMMITTEE, OR

☐ PART OF INSTRUMENT SCIENTIST ALLOCATION

REPORT RECEIVED:

EXPERIMENTAL REPORT (or Abstract of Publication)

OBJECTIVE:

To study the effects of lattice mismatch strain on the morphology change, the interparticle correlation, the dynamical scaling behavior, and the coarsening kinetics in a Ni-Al-Si ternary system. The strain field and the volume fraction of the γ' precipitates can be systematically adjusted by controlling the relative Al to Si content in the system.

EXPERIMENTAL:

A polycrystalline sample of Ni-4at.%Al-8at.%Si was prepared using arc melting technique. This composition is selected because the minimum lattice mismatch is expected. Solution treatment was conducted at 1100°C for 2 hours in an evacuated quartz capsule, followed by a gravity driven quench into iced water. Wide-angle x-ray diffraction measurements show that the as-quenched alloy is basically of single phase. Weak superlattice reflections are noticeable, suggesting the existence of either a short-range ordered state or embryos of γ' particles.

In Situ SANS measurements were carried out on the IPNS-SAD facility for three days using time-resolved counting mode. Due to time limitation, it was only possible to complete one series of measurements at 700°C. Multiple scattering was not found to be serious despite the use of a polycrystalline specimen. Data were corrected for parasitic scattering, and converted to absolute scales.

RESULTS:

As shown in Fig.1, the scattering in the as-quenched (or as-received) condition was very weak. No peak was discernible when only the channels with λ's above the Bragg cutoff are used. Upon aging a shoulder appeared in the spectrum and intensities increased. The Guinier radius increases very rapidly as shown in Table 1. The later runs show a nearly linear ln(I)-ln(Q) behavior. Slopes (Sp)were then obtained and tabulated. Clearly, this slope converges toward the value of -4 (Porod's constant) that one would expect from particles with sharp boundaries.

In summary, it would appear that the reaction went rather rapidly at 700°C. The equilibrium condition is reached after about 16 hours aging. For future measurements, a lower aging temperature is desirable in order to investigate the early stages of precipitation. In addition, the alloy composition will be changed to study the effect of lattice mismatch strain on various phenomena as described in the objectives.

Table 1

Aging Time (hrs)	Rg (Å)	Sp
as rec	-	-
0.5	207	-
1.0	209	-
2.5	211	-
5.5	266	-4.3
10.5	315	-3.99
16.5	326	-3.9
22.5	340	-3.87
28.5	339	-3.92
34.5	346	-3.97
40.5	349	-3.99
45.3	334	-4.02

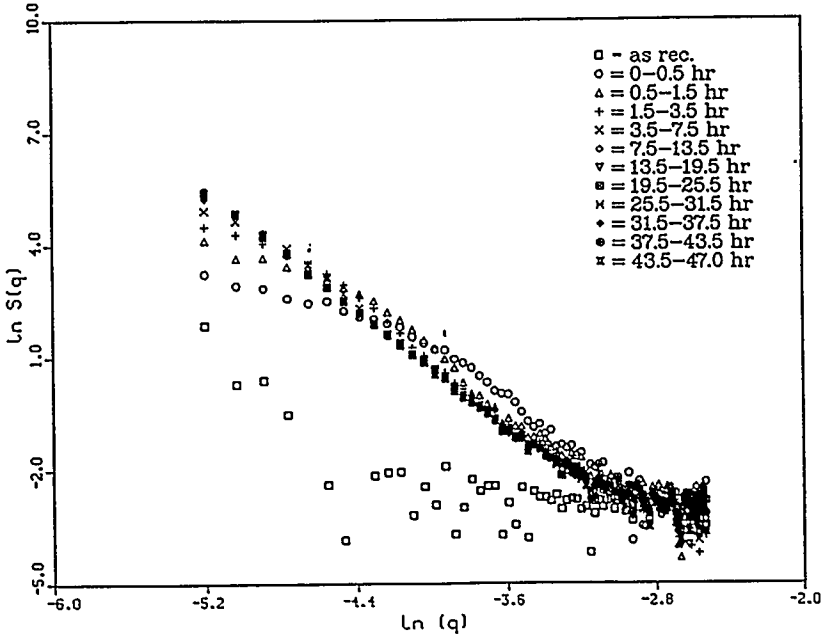


Figure 1 SANS spectra of a Ni-4at.%Al-8at.%Si alloy aged at 700°C

INSTRUMENT USED:	DATE OF REPORT:	EXPERIMENT NO:
SAD	December 13, 1993	1825

TITLE:

The Solution Structure of the Coal Macromolecule

AUTHORS AND AFFILIATIONS:

G.D.Cody(CHM,ANL),P.Thiyagarajan(IPNS,ANL),R.E.Botto(CHM,ANL),J.E.Hunt(CHM,ANL
R.E.Winans(CHM,ANL)

DATES OF EXPERIMENT:

October 22 - 26, 1993

CHECK ALL APPLICABLE BOXES:

- [x] APPROVED BY PROGRAM COMMITTEE
- [ ] INSTRUMENT SCIENTIST ALLOCATION
- [ ] DO NOT PUBLISH
- [ ] PROPRIETARY RESEARCH
- [ ] PRT ALLOCATION

EXPERIMENTAL REPORT (or Abstract of Publication)

From the early 1960's up until very recently the predominant model employed to describe the macromolecular structure of bituminous coals considered the occurrence of two fundamental phases; a solvent extractible macromolecular fraction and a non-extractible covalently cross-linked network fraction. Given such a model of coal structure, commercial conversion strategies have focused on depolymerization of the network, both thermally and catalytically. These are, as a rule, expensive technologies.

Very recently, however, there have been significant advances in our understanding of coal structure which challenge the model described above. Chemists in Japan have demonstrated that extractibilities well beyond those achievable in pyridine are possible given mixed solvents systems. In a different set of experiments, a research group at Penn State demonstrated that bituminous rank coals exhibit viscous compliance which is entirely incompatible with a covalently cross-linked coal structure. The potential for ambient temperature solubilization has profound implications for low cost conversion processes. By circumventing the mass transport limitations associated with attempting intra-network chemistry, one can begin to seriously explore promising solution chemistry.

In light of the recent evolution of our understanding of coal structure we set out to determine the solution state of the solvent extractible macromolecular fraction dispersed in solvent. In the present report we describe the results of these experiments. We chose pyridine as it is generally considered one of the best solvents for coal; moreover, recent statistical thermodynamic models of coal-pyridine interactions predict that pyridine is a "good" solvent capable of solvating all non-covalently bound organics within coal. Intermediate rank coals typically have extractibilities in the 25 to 30 % wt. range, thus the extracts constitute a significant proportion of the whole coal.

Small angle neutron scattering was applied to dilute coal extracts (1,3, and 5% wt.) in pyridine from three different coals, APCS #2, APCS # 3, APCS #8. In order to probe the role of strong interactions between acid functional groups in coal and the basic nitrogen of pyridine we investigated the scattering behavior of both O-methylated and pristine (untreated) extracts.

Figures 1 presents the scattering data for one of the extracts, APCS # 2 pristine, with the scattering intensities normalized to concentration, 1, 3, and 5 %, respectively. In this sample, as well as all of the samples, there was no evidence of interparticle interactions or other concentration dependent effects at these concentrations.

APCS # 3 pristine and alkylated are presented in Figure 2. The pristine extract exhibits an upper bound in the scattering behavior at low Q. Analysis of the Guinier region indicates a single, R_G on the order of 37.5 Å. With O-methylation, however, the scattering behavior changes dramatically. A power law dependence in the scattering intensity is evident at low Q indicating linear scaling of the log of the density-density correlation length, c(r), with log of the distance, r. The power law exponent, *d*, is on the order of 1.7 for all concentrations.

In the case of the other two coals, fractal scattering behavior is indicated for both the pristine and alkylated extracts. In the case of neat APCS # 2 (Figure 3) the scaling exponent is on the order of 1.80, however, with O-methylation *d* increases to around 2.5. The results of Neat APCS # 8 indicates *d* is on the order of 2.1; upon O-methylation this increases to 2.3.

Finally, Porod type behavior, i.e. Q^{-4} vs I(Q), is evident at high Q for all three coals (Figures 1, 2, 3, and 4) indicating a lower limit of the fractal behavior and the presence of fundamental particles. Laser Desorption Mass spectrometry of these extracts, however, reveals only low mass material indicating that even the fundamental particles are probably aggregates of lower molecular weight material.

The effect of O-methylation may be interpreted in terms of the role of hydrogen bonding interactions on coal-solvent solution thermodynamics. In the case of APCS # 3 (Figure 2) suppression of hydrogen bonding interactions results in a system of small clusters to aggregate into an extended ramified (open) structure. In the case of APCS # 2 and # 8; the shift in *d* corresponds to a densification of an open aggregated system with suppression of the strong solvent-solute interactions.

The results of these experiments reveal that although pyridine is capable of extracting large quantities of material from coals, the quality of the resulting solution is very low. This conclusion is contrary to conventional wisdom regarding the relationship between pyridine derived coal extracts and the "insoluble" residue. Furthermore, the presence of such solution structure demonstrates a significant departure from random mixing, a key assumption implicit in most thermodynamic treatments of coal-pyridine systems. Future work will address the thermodynamics of the aggregation in the presence and absence of hydrogen bonding interactions as a function of temperature and solvent activity.

The results of this work have been submitted for publication in Energy & Fuels.

Figure 1

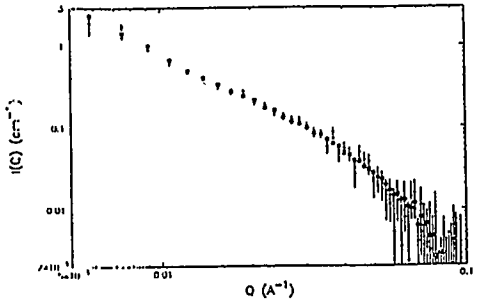


Figure 2

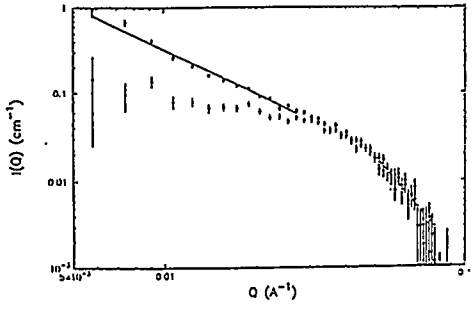


Figure 3

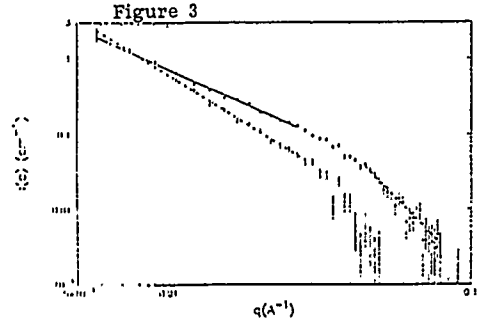
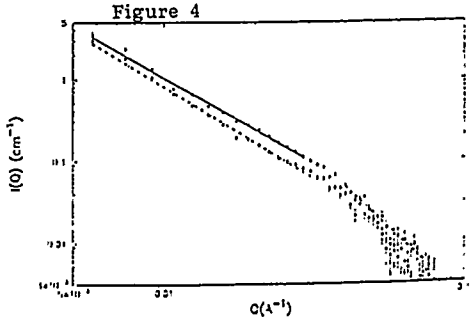


Figure 4



INSTRUMENT USED:	DATE OF REPORT:	EXPERIMENT NO.:
SAD	May 16, 1990	1069/1146

TITLE: Thermodynamics of Polyethylene-Copolymer Blends

AUTHORS AND AFFILIATIONS: B. Crist and J.W. Rhee, Northwestern University

DATES OF EXPERIMENT: October 16-18, 1989 and January 29-31, 1990

☒ APPROVED BY PROGRAM COMMITTEE, OR

☐ PART OF INSTRUMENT SCIENTIST ALLOCATION

REPORT RECEIVED:

EXPERIMENTAL REPORT (or Abstract of Publication)

Thermodynamic interaction parameters, χ, of short chain (ethyl) branched polyethylene (PE) blends were measured varying temperature and composition. Partially deuterated polybutadiene (DPB) and hydrogenated polybutadiene (HPB) were used.

Thermodynamic interaction of highly branched PE blends were much higher than we expected from low blanched PE blend [1]. A large isotope effect which results in unexpectedly large χ was observed for highly branched polymers. This effect can be qualitatively explained by the thermodynamic interaction between hydrogenated and deuterated monomer units.

Sample polymers were prepared by saturated reaction of nearly monodisperse (polydispersity index ≈ 1.1) PBs. Table 1 shows the properties of sample polymers. All SANS experiments were done in the melt to avoid any possible problems from crystallization, i.e., density fluctuation from semicrystallized polymers or phase separation resulting from the different crystallization temperatures of blended polymers. Table 2 shows the thermodynamic interaction parameters of DPB/HPB blends.

For a blend of two polymers of composition (A_xB_{1-x}) and (C_wD_{1-w}), the interaction parameter χ between the two copolymer can be expressed as [2],

$$\chi_{(A/B)(C/D)} = xw\chi_{AC} + (1-x)w\chi_{BC} + x(1-w)\chi_{AD} + (1-x)(1-w)\chi_{BD} - x(1-x)\chi_{AB} - w(1-w)\chi_{CD} \quad (1)$$

where x and w are volume fractions of one component in each copolymer.

For the case of a blend of two copolymers which differ in both chemical composition and isotopic content, A is the linear C_4H_8 unit of unlabeled copolymer, B the branched C_4H_8 (butene-1) unit of unlabeled copolymer, and C, D are the linear and branched $C_4H_{8(1-y)}D_{8y}$ units of labeled copolymer. With the use of random copolymer theory, χ can be separated into χ_{hd} ($= \chi_{ac} = \chi_{bd}$), χ_{lb} ($= \chi_{ab} = \chi_{cd}$), and χ_{hdlb} ($= \chi_{ad} = \chi_{bc}$). Then eq. 1 can be written as,

$$\chi = \chi_{hd} + (x-w)^2\chi_{lb} + (x+w-2xw)\chi_{div} \quad (2)$$

where $\chi_{div} = \chi_{hdlb} - \chi_{hd} - \chi_{lb}$.

When $\chi_{div} > 0$, eq. 2 qualitatively explains not only the branch concentration difference, x-w, dependence of χ but also the average branch concentration dependence of χ.

For matched system (x=w), eq. 2 can be simplified as

$$\chi = \chi_{hd} + 2x(1-x)\chi_{div} \quad (3)$$

With eq. 3, branch concentration dependence of χ of matched system can be explained.

So far the value of χ_{hdlb} and χ_{lb} is not clear and more researches will be followed.

Table 1. Saturated polybutadienes used for SANS experiments.

Sample	MW[a]	ρ_H (g/cm³)	ρ_D (g/cm³)	y
HPB17(DPB17)	102,200	0.90	0.98	0.53
HPB101(DPB101)	101,600	0.86	0.92	0.42
HPB115(DPH115)	40,960	0.86	0.92	0.45
HPB203(DPB203)	37,700	0.86	0.91	0.41

[a] HPB molecular weights were calculated from the molecular weights of polybutadienes assuming 100% saturation.

Table 2. Thermodynamic interaction parameters of saturated polybutadiene blends.

Sample	X_{br}	T(°C)	ϕ_H	$\chi(10^4)$
HPB17/DPB17	7	160	0.50	1.3
HPB101/DPB101	34	150	0.49	4.7
HPB115/DPB115	38	55	0.50	9.3
		190	0.50	8.8
HPB203/DPB203	58	190	0.50	13.1
HPB17/DPB115	7/38	160	0.75	17.8
HPB115/DPB203	38/58	55	0.50	>28.6[a]
		55	0.75	>29.2[a]
		120	0.50	>28.6[a]
		190	0.50	>28.6[a]
		190	0.75	33.8

[a] Minimum χ values ($\chi N=2$) for phase seperated blends.

REFERENCES

1] J. C. Nicholson, T. M. Finerman, and B. C. Crist, Jr., *Polymer*, in press.

2] D. R. Paul and J. W. Barlow, *Polymer*, 25, 487(1084).

3] F. S. Bates, S. B. Dierker, and W. C. Wignall, *Macromolecules*, 21, 1086(1988).

INSTRUMENT USED:	DATE OF REPORT:	EXPERIMENT NO.:
Small Angle Diffractometer	July, 11, 1991	1282 and 1347

TITLE: Thermodynamics of model polyethylene blends

AUTHORS AND AFFILIATIONS: Buckley Crist and Jangweon Rhee
Chemical Engineering Department, Northwestern University

DATES OF EXPERIMENT: Sept., 9 - Sept, 11, 1990 and Apr.,20 - Apr.,23, 1991

☒ APPROVED BY PROGRAM COMMITTEE, OR

☐ PART OF INSTRUMENT SCIENTIST ALLOCATION

REPORT RECEIVED:

EXPERIMENTAL REPORT (or Abstract of Publication)

ANOMALOUS COIL DIMENSIONS OF MODEL ETHYLENE COPOLYMERS BY SMALL-ANGLE NEUTRON SCATTERING

Buckley Crist* and Jangweon Rhee
Department of Chemical Engineering
Northwestern University
Evanston, IL 60208-3108

ABSTRACT

The relation between mean square radius of gyration and molecular weight, $R_g^2 = a^2M$, is examined for a series hydrogenated polybutadienes (HPB) which emulate random ethylene - butene copolymers. Analyses of SANS patterns in the low q and intermediate q regimes give consistent values of the coil dimension parameter a^2 which show an expected decrease of 40% as the fraction of branched C_4H_8 repeat units increases from 0.07 to 0.60. The unusual finding is that a^2 for these model copolymers is 55±10% larger than values derived from viscometry in low molecular weight θ solvents. This large coil expansion is tentatively associated with partial labeling of deuterated polybutadiene (DPB) used in the SANS experiments.

EXPERIMENTAL REPORT (CONTD.)

Effects of Isotope and Microstructure on Thermodynamic Interaction for Model Ethylene–Butene-1 Copolymer by Small-Angle Neutron Scattering

Jangweon Rhee and Buckley Crist**

Department of Chemical Engineering,
Northwestern University, Evanston, IL 60208

ABSTRACT

Combined isotope and microstructure effects on segment-segment thermodynamic interactions are examined for model ethylene–butene-1 copolymer blend. By "switching" experiment, it has been found that mismatched blends that more branched component has deuterium have 100±50% larger thermodynamic interaction χ than their pairs that less branched component has deuterium. New thermodynamic interaction analysis, using four interaction parameter terms, has been employed to explain "switching" effect. Four parameter analysis works well for low branched copolymer blends while medium branched copolymer blends have maximum 410% larger χ than calculated value. This average branch concentration dependence of thermodynamic interaction is tentatively related with the effect of sequence distribution.

** First paper has been summitted to *Macromolecules* on June, 1991.
Second paper is in preparation and to be summitted to *Journal of Physical Chemistry* on July, 1991.

INSTRUMENT USED:	DATE OF REPORT:	EXPERIMENT NO.:
SAD	11/20/92	1469

TITLE: Thermodynamics of Model Polyethylene Blends

AUTHORS AND AFFILIATIONS:
B. Crist and J. Rhee, Northwestern Univ.

DATES OF EXPERIMENT: 4/15/92 - 4/20/92

☑ APPROVED BY PROGRAM COMMITTEE, OR

☐ PART OF INSTRUMENT SCIENTIST ALLOCATION

REPORT RECEIVED:

EXPERIMENTAL REPORT (or Abstract of Publication)

ANOMALOUS COIL DIMENSIONS OF MODEL ETHYLENE COPOLYMERS BY SMALL-ANGLE NEUTRON SCATTERING

Buckley Crist and Jangweon Rhee
Department of Chemical Engineering
Northwestern University
Evanston, IL 60208-3120

ABSTRACT

The relation between mean square radius of gyration and molecular weight, $R_g^2 = a^2M$, is examined at 150°C for a series hydrogenated polybutadienes (HPB) which emulate random ethylene -butene copolymers. Analyses of SANS patterns in the low q and intermediate q regimes give self-consistent values of the coil dimension parameter a^2 which show the expected decrease as the fraction of branched C_4H_8 repeat units increases from 0.06 to 0.60. The unusual finding is that a^2 for these model copolymers is 50% larger than values derived from viscometry in low molecular weight θ solvents. This large coil expansion is tentatively associated with isotope labeling of deuterated polybutadiene (DPB) used in the SANS experiments.

Isotope and Microstructure Interactions in Blends of Random Copolymers

Jangweon Rhee and Buckley Crist
Department of Chemical Engineering
Northwestern University, Evanston, IL 60208

ABSTRACT

Combined isotope and microstructure effects on thermodynamic interactions are examined by small-angle neutron scattering from binary blends of random copolymers having one partially deuterated component. These copolymers are based on linear and ethyl branched C_4H_8 units and are models for poly(ethylene-*co*-butene-1). The Flory-Huggins interaction parameter χ is found to be ~100% larger for blends in which the more branched copolymer is labeled with deuterium. This "switching" effect, where the chemical microstructure of the labeled component affects χ, is confirmed by critical temperatures in blends having all possible isotope combinations. Parallel studies by Graessley, et al. show the same effects with copolymers having higher branch concentrations. Analysis in terms of copolymer/copolymer theory indicates that the repulsive interactions between monomers differing in both chemical microstructure and isotope depend on which repeat unit, linear or branched, is labeled with deuterium. A simple model based on molar volumes of linear and branched, hydrogenous and deuterous repeat units accounts for the observed effects in a semiquantitative manner. The contribution to χ from chemical microstructure does not obey simple copolymer theory; the strength of repulsive interactions depends on the average composition of the chains in addition to the composition difference between components.

Key words: ethylene copolymers, thermodynamics, neutron scattering, deuteration

Submitted to *Journal of Chemical Physics* October, 1992

INSTRUMENT USED: SAD	DATE OF REPORT: 22 JANUARY 1996	EXPERIMENT NO.: 2017
TITLE: Aging Process and Template Content in MCM-41		
AUTHORS AND AFFILIATIONS:	K. Edler, J. W. White, P.A. Reynolds(Research School of Chemistry, Australian National University)	
DATES OF EXPERIMENT: 16/6/95-18/6/95		

CHECK ALL APPLICABLE BOXES:

X APPROVED BY PROGRAM COMMITTEE
☐ INSTRUMENT SCIENTIST ALLOCATION
☐ DO NOT PUBLISH
☐ PROPRIETARY RESEARCH
☐ PRT ALLOCATION

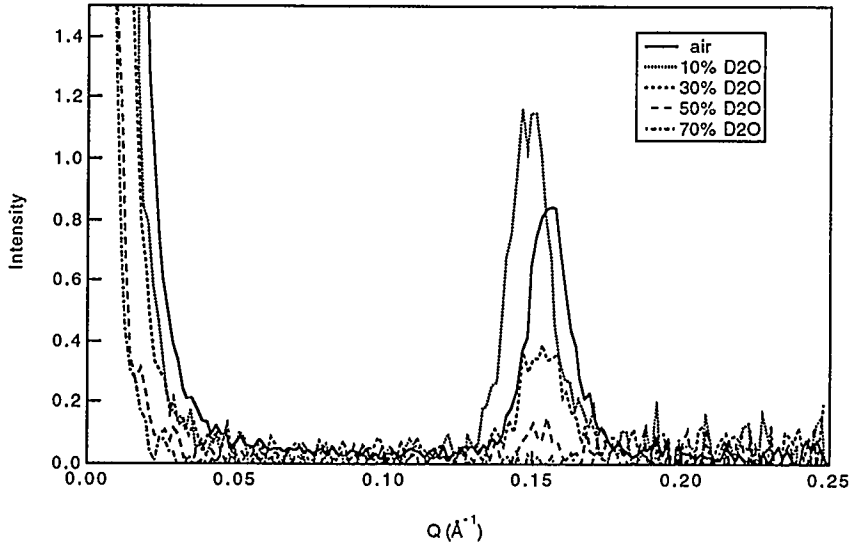
EXPERIMENTAL REPORT (or Abstract of Publication)

The mesoporous molecular sieve, MCM-41, is formed by use of a surfactant template which imparts a honeycomb-like hexagonal structure to amorphous silica.[1] The as-synthesised product when isolated from the reaction gel is made up of hollow surfactant-filled silicate tubes of around 40Å diameter which are packed together to form a network of parallel channels. During the synthesis process, the d-spacing observable in X-ray diffraction measurements decreases significantly from that in the synthesis gel as the sample is washed, dried and finally calcined. The hexagonal structure of this material is retained throughout this shrinkage of 6-7Å, indicating a remarkable flexibility in the silicate walls[2]. The wall structure of this material at various stages of the synthesis is therefore of considerable interest, especially since, from X-ray diffraction, it appears to be amorphous.

We therefore carried out a small angle neutron scattering experiment on samples synthesised from two different preparations at the stage where the material had been washed and dried, but the template still remained intact in the channels, and also after calcination where the template was totally removed. One set of samples was prepared using the optimised preparation derived from Beck et al[1] published previously[3] , and the other was prepared following the method of Ryoo and Kim[4] which involves titration with acetic acid during synthesis. The second method produces much more highly crystalline materials than the first and we were looking to find differences in wall density between the two preparations. Contrast series were run on each of these samples by immersing them in H_2O/D_2O mixtures and varying the composition of this solvent to find the contrast match point. The hydrogenous surfactant and the silicate walls should have very different scattering length densities and so different contrast match points and so be distinguishable in the scattering experiment.

In each sample both small angle scattering and a diffraction peak at *ca* 40Å were seen to vary in intensity with H_2O/D_2O contrast (Figure 1). Using I(0) values from the small angle scattering, contrast match points were found to be around 65% for the calcined, pure silica samples, and around 23% for the template filled, uncalcined sample. In the pure silica samples the diffraction peak contrasted out at much the same point as the small angle scattering, but in the template filled sample the intensity of the peak did not vary linearly with D_2O concentration. This behaviour is probably due to the interaction between scattering from the surfactant on the interior of the channels and the silicate walls which have very different scattering length densities and work is continuing into resolving these components from this data. The much lower contrast match point for the uncalcined sample indicates a considerably lower scattering length density than in the calcined samples, possibly due to very porous silicate walls containing some surfactant molecules.

Figure 1: Small angle neutron scattering from a highly crystalline, calcined MCM-41 sample from a preparation titrated with acetic acid during synthesis, showing the variation in the small angle scattering and the diffraction peak with H_2O/D_2O concentrations.



References:

1. Beck, J.S., *et al. J. Am. Chem. Soc.* 114, 10834-10843 (1992).
2. Edler, K.J. & White, J.W. *J. Chem. Soc., Chem. Commun.* 155-156 (1995).
3. Edler, K.J., *et al. Colloids and Surfaces A*, 102, 213-230, (1995).
4. Ryoo, R. & Kim, J.M. *J. Chem. Soc., Chem. Commun.* 711-712 (1995).

INSTRUMENT USED:	DATE OF REPORT:	EXPERIMENT NO.:
SAD	29 July 1990	/255

TITLE:

Time Resolved Neutron Small Angle Scattering

AUTHORS AND AFFILIATIONS: E.P. Epperson , J.W. White , D. Dorset and R. Snyder *

DATES OF EXPERIMENT: 20 May 1990 to 23 May 1990

☑ APPROVED BY PROGRAM COMMITTEE, OR

☐ PART OF INSTRUMENT SCIENTIST ALLOCATION

REPORT RECEIVED:

EXPERIMENTAL REPORT (or Abstract of Publication)

We show that neutron small angle scattering can sensitively detect microphase separation in solid solutions of $C_{30}H_{62}$:$C_{36}D_{74}$ mixed paraffins. By scanning the sample temperature at ca. 2·5°C per minute complementary information to that from differential heat capacity measurement is obtained from the total small angle count rate and its first temperature derivative.

Figure 1 shows the effect of annealling the $C_{30}H_{62}$:$C_{36}D_{74}$; 1:4 sample (after long-time ageing) at 40°C, 47°C, 56°C and 65°C. Clearly signal is first lost from the mid Q range (near ln Q = -2·5, Q = 0·08Å^{-1}, d = 77Å) then (at 56°C) near ln Q = 3·7, Q = 0·025, d = 250Å, but before the sample melts there remains signal at the lowest Q values. The experiments have assigned these different contributions to the scattering and, using a temperature scan rate about the same as that used in the scanning calorimetry - so as to have comparable nonequilibrium effects, permit a more precise determination of the onset temperatures for the changes seen in Figure 1. Figure 2(a) shows the total counts in the detector, $\bar{c}^*$, arising from small angle scattering by the 1:4 $C_{30}H_{62}$:$C_{36}D_{74}$ sample as a function of sample temperature. By calculating the invariants [10] for the individual five minute runs in this series and comparing them with those for the slowly annealed cases (Figure 1) it can be seen that the major contribution to the intensity change between 36°C and 53°C is due to the loss of the scattering near Q = 0·08. The data were fitted with a cubic spline and the differential with respect to temperature taken to produce the curve of Figure 2(b) for comparison with heat capacity data like that of Figure 1. It can be seen that a major change in detector counts occurs, $\bar{c}^*$ occurs at a temperature of 46°C. There is a subsidiary change in, $\bar{c}^*$, at about 65°C where the low angle part of the scattering begins to alternate. This low angle part is completely quenched at the melting point.

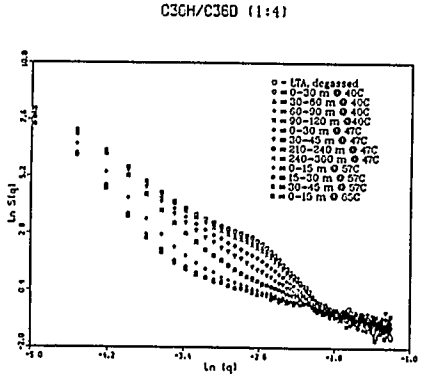


FIGURE 1

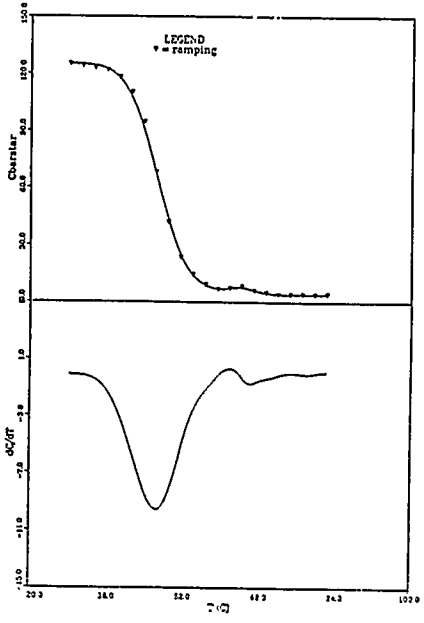


FIGURE 2(a)

FIGURE 2(b)

* Argonne National Laboratory USA, Australian National University Canberra Australia, Medical Foundation Buffalo NY USA,Chemistry Dept. Berkeley California.

INSTRUMENT USED:	DATE OF REPORT:	EXPERIMENT NO.:
SAD	July 23, 1991	1538

TITLE:

Determination of the Miscibility Gap in the Fe-Cr System

AUTHORS AND AFFILIATIONS:

J. E. Epperson, K. A. Hawick (Edinburgh Univ.), S. K. Chan and D. G. Wozniak

DATES OF EXPERIMENT: May 12-13, 1991

☐ APPROVED BY PROGRAM COMMITTEE, OR

☒ PART OF INSTRUMENT SCIENTIST ALLOCATION

REPORT RECEIVED:

EXPERIMENTAL REPORT (or Abstract of Publication)

As part of our studies on phase separation in the Fe-Cr alloy system, we are mapping out the miscibility gap. The Fe-Cr alloys are, of course, the basis for our steels, and phase separation governed by the miscibility gap is thought to be responsible for the loss of ductility in many commercially important materials.

The classical version of the miscibility gap from Williams (1958) is shown in Fig. 1 and is characterized by a broad, flat top. Subsequently, theoretical work by Nishizawa, Hasebe and Ko (1979) predicted a rather different form, as shown in Fig. 2. In particular, they predicted a "horn" on the miscibility gap where it is intersected by the curve of Curie temperature vs composition. We have annealed at 5°C intervals a series of polycrystalline Fe-Cr samples with compositions ranging from 20 to 62 at.% Cr. The presence of an interference peak in the SANS profile was taken as evidence that the anneal had occurred within the miscibility gap. We have also determined the Curie temperature for pure Fe and for three Fe-Cr alloys. As shown in Fig. 3, a bulge on the miscibility gap does occur, and the curve of Curie temperature vs composition intersects the gap at this bulge, in essential agreement with the theoretical predictions. This result is sufficient to indicate that the magnetic energy makes a significant contribution to the free energy for this alloy system. There are, however, obvious differences with regards to the shape of the miscibility gap at high Cr contents. Additional work is needed to map out the flanks of the gap. This data will then allow the magnetic and chemical energies to be determined.

References:

1. R. O. Williams, Trans AIME 212, 497-502 (1958).
2. T. Nishizawa, M. Hasebe, and M. Ko, Acta Met. 27, 817-828 (1979).

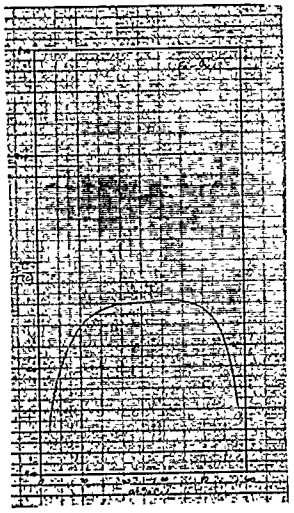


Fig. 1. Miscibility gap in the Fe-Cr System as reported by Williams (1958).

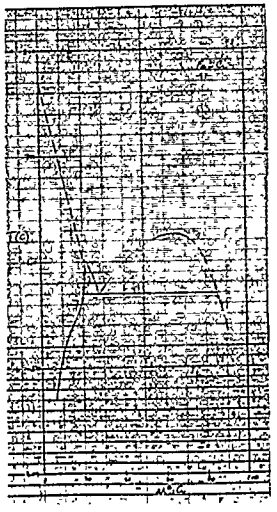


Fig. 2 Theoretical miscibility gap in Fe–Cr system, after Nishizawa, Hasebe and Ko (1979).

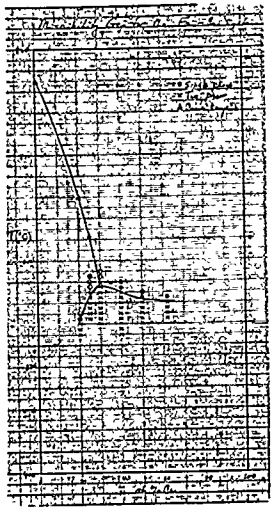


Fig. 3. Top portion of the miscibility gap for the Fe-Cr system and the Curie temperatures from this work.

INSTRUMENT USED: Small angle diffractometer	DATE OF REPORT: July 7, 1993	EXPERIMENT NO.: 1615

TITLE: Clouding phenomenon in non-ionic micellar solutions: Applicability of Baxter's sticky hard sphere model

AUTHORS AND AFFILIATIONS: P.S.Goyal, S.V.G.Menon, B.A.Dasannacharya, BARC, India; P.Thiyagarajan, ANL, Argonne

DATES OF EXPERIMENT: March 11-March 14, 1993

CHECK ALL APPLICABLE BOXES:

- ☑ APPROVED BY PROGRAM COMMITTEE
- ☐ PROPRIETARY RESEARCH
- ☐ INSTRUMENT SCIENTIST ALLOCATION
- ☐ PRT ALLOCATION
- ☐ DO NOT PUBLISH

EXPERIMENTAL REPORT (or Abstract of Publication)

Micellar solutions of non-ionic surfactant Triton x-100 become cloudy at a well defined temperature T_{cp} ($\sim$ 338 K) called the cloud point. At T_{cp}, the solution separates into two phases - one rich and the other dilute in micellar concentration. T_{cp} varies with surfactant concentration ϕ in the solution. The co-existence curve between high and low temperature phases shows a minimum at $\phi_c \sim 0.06$ and $T_c \sim$ 334 K and is asymmetric about ϕ_c.

The clouding in above solutions is connected with the fact that interaction potential between micelles changes with temperature; it becomes more attractive as one approaches T_{cp}. Baxtor's sticky hard sphere model /1/ which assumes a narrow square well potential for the attractive part, has been used to explain the phase diagram and a limited amount of SANS data from non-ionic micellar solutions /2, 3/. To test the validity of above model over a large range of the phase diagram and to determine the shape/size of micelles, we have carried out SANS experiments on micellar solutions of Triton X-100. Measurements have been made for ϕ = .01, .02, .04, .08, .12, .15 and data were taken at 5-6 temperatures between 295 K and the clouding temperature, for each sample. Fig.1 shows the effect of variation in concentration on the SANS distribution at 295 K. [illegible] The effect of temperature on SANS distribution for ϕ = 0.08 is shown in Fig.2 for T = 295, 313, 323, 328, 331, 333 and 334 K. The observed changes in the distributions are arising because of changes in S(Q) with temperature.

At low concentrations and at low temperatures inter-micellar interference effects are negligible ($S(Q) \sim 1$) and thus the data corresponding to ϕ = 0.01 at 295 K have been used to obtain form factor $P(Q)$ of the micelle. This analysis showed that micelles are oblate in shape (a = b = 95 Å, c = 45 Å) and that there are about 90 molecules of water per surfactant molecule in the hydrophilic region of the micelle. At higher surfactant concentrations, $S(Q) \neq 1$ even at 295 K, the interaction at low temperature (= 295 K) is dominated by repulsive forces due to the hydration of the micelle. The high concentration data were analysed by modelling this repulsive force by an effective hard sphere. The solid lines in Fig.1 are the calculated curves and this gave a hydration layer of $\sim$ 5 Å.

The temperature dependence of above data was analysed using Baxter model for S(Q). The particle diameter obtained from 295 K data was kept fixed throughout. The solid lines in Fig.2 are the results

of this analysis. The fits are good for $Q > 0.01$ Å^{-1}. The results of this analysis will be communicated for publication. It should be noted that there are significant deviations at lower Q values suggesting that Baxter model needs modification. In particular, it seems that the long range part of the attractive potential /4/ should be incorporated in the calculation of S(Q). Such an analysis is in progress.

/1/. R.J. Baxter, J. Chem. Phys. 49, 2770 (1968).

/2/. S.V.G.Menon et al., Phys.Rev. A43, 1130 (1991).

/3/. K.S.Rao et al. Physica 174, 170 (1991).

/4/. L.Reatto et al. in Surfactants in Solutions, Vol.7 (1989).

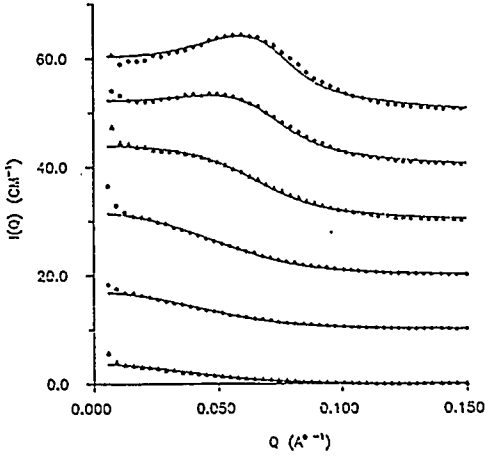


Fig.1

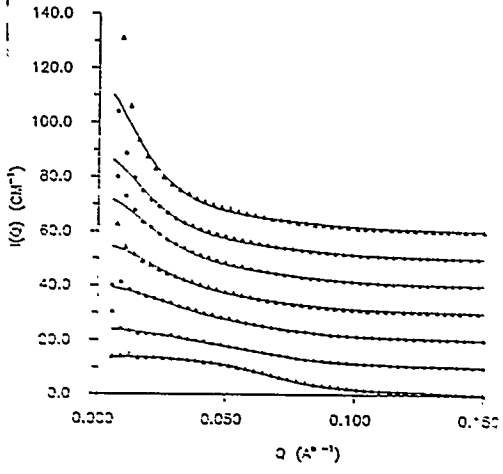


Fig. 2

INSTRUMENT USED:	DATE OF REPORT:	EXPERIMENT NO.:
SAD	August 5	1259

TITLE:

The Structure of Protein/SDS Complex in Low Ionic Strength Solution

AUTHORS AND AFFILIATIONS:

X.H. GUO, S.H. Chen (MIT), P. Thyagq (IPNS)

DATES OF EXPERIMENT: July 22 --- July 25 (3 days)

☒ APPROVED BY PROGRAM COMMITTEE, OR

☐ PART OF INSTRUMENT SCIENTIST ALLOCATION

REPORT RECEIVED:

EXPERIMENTAL REPORT (or Abstract of Publication)

We have performed a small-angle neutron scattering experiment on the protein/SDS complexes in low ionic strength solution. Two types of phosphate buffer (pH7.2, I=0.1M) were used: (1) 40%D_2O and 60%H_2O, (2) 100%D_2O. The scattering length density of buffer(1) is $2.2*10^{-6}$ $Å^{-2}$ which matches those of the proteins (bovine serum albumin, ovalbumin) under study. Specifically, we look into the structure of polypeptide chain when buffer(1) is used, or surfactant aggregates when buffer(2) is used. The experimental result showed that the scattering intensity distribution I(Q) from BSA/SDS and OVA/SDS complexes are similar regardless of the difference of their amino acid sequences. Therefore, we only report our preliminary analysis for the BSA/SDS case.

(A) Buffer(1)

A plot, LogI(Q) vs LogQ, was presented in Fig.1(a). We can see that there is cross-over behavior for I(Q) at $Q_c \simeq 0.025 Å^{-1}$, namely the unfolded polypeptide chain behaves like a flexible chain in large distance ($L > 1/Q_c = 40 Å$), but has a stiff segment in short distance. Furthermore, a plot, Log[Q*I(Q)] vs Q^2 in Fig.1(b), showed that the slope is very small, close to zero. This analysis indicated that the cross-sectional radius of the unfolded polypeptide chain is very small, about a few Å. This result provided new evidence that the protein had lost its tertiary structure due to the binding of SDS molecules, and unfolded into a chain object. The stiff segment reflects those amino acide residues along the polypeptide chain interacting tightly with the SDS micelle.

(B) Buffer(2)

We used a new formula of the differential scattering cross section, derived by using the concept of blob model in polymer literature. We can obtain the following parameters by fitting the SANS data: fractal dimension D, mean distance between two neighbouring micelles, numbers of micelle in a unfolded chain N, the micelle size (a,b). The fitting result was shown in Fig. 2. The D=1.0 indicates that the excluded volume effect due to the electrostatic and steric repulsion between two micelle-like clusters in a chain is very significant.

We also formulate the diferential scattering cross section for a cylindrical micelle. The calculated result, using the structral parameters given in "the flexible helix" model, was also presented in Fig.2. We found that the latter model failed to describe quantitatively the SANS data.

We hope to perform further SANS studies on this system. Especially, we hope to achieve a better data statistics in high Q range by using high concentration sample. We hope to vary the ionic strength of the solution between 0.1M and 0.3M, and to study how the excluded volume effect characterized by D would alter. This experiment would provide information to verify critically the polymer model.

INSTRUMENT USED: SAD	DATE OF REPORT: 11/10/95	EXPERIMENT NO.: 2009

TITLE: SANS Investigation of Deuterium Precipitation in Nb: Effect of Deformation

AUTHORS AND AFFILIATIONS:
BJ Heuser, Univ. Illinois & JS King, Univ. Michigan

DATES OF EXPERIMENT: October 17-23, 1995

CHECK ALL APPLICABLE BOXES:

- ☒ APPROVED BY PROGRAM COMMITTEE
- ☐ INSTRUMENT SCIENTIST ALLOCATION
- ☐ DO NOT PUBLISH
- ☐ PROPRIETARY RESEARCH
- ☐ PRT ALLOCATION

EXPERIMENTAL REPORT (or Abstract of Publication)

SANS measurements of 4 single crystal Nb samples, two loaded with approximately 25000 appm deuterium and two loaded with approximately 7000 appm deuterium, were successfully completed on October 17-23, 1995. One sample at each bulk D concentration was deformed to 50% thickness reduction. The purpose of the experiments was to observe the effect that deformation had on deuteride phase formation as the sample temperature was reduced below the solvus line. This set of experiments greatly expanded on the original IPNS-SAD experiments in May, 1995.

In order to better characterize phase precipitation of deuterium in Nb, the SANS response was monitored as the sample temperature was gradually (but incrementally) lowered into the two phase region. Figure 1 shows the SANS response as a function of inverse temperature for the 7000 appm, undeformed sample. The SANS response is actually represented as the total detector counts in time bins 48 to 67 (all time bins above the Bragg cutoff), corrected for sample transmission, empty beam, and dark current. The open and solid boxes in Fig. 1 represent the observed response as the temperature was decreased and increased, respectively. The most interesting observation is the large hysteresis present; the large increase/decrease in SANS response due to the formation/dis-solution of deuteride particles are separated by 100 K. The high concentration, undeformed sample exhibited a similar hysteresis and is not showed. On the other hand, temperature cycling of the deformed, high concentration sample did not produce as strong an effect; although a hysteresis was present, the splitting was approximately 40 K. Furthermore, the hysteresis effect was shifted to temperatures above the solvus line for the deformed, high concentration sample. In fact, a five-fold increase in SANS response occurred immediately as the solvus line was crossed. This is significantly different than the behavior of the undeformed, high concentration sample and that of NbSC7. We believe the dislocations created by deformation assist deuteride precipitation, thereby altering the hysteresis accordingly.

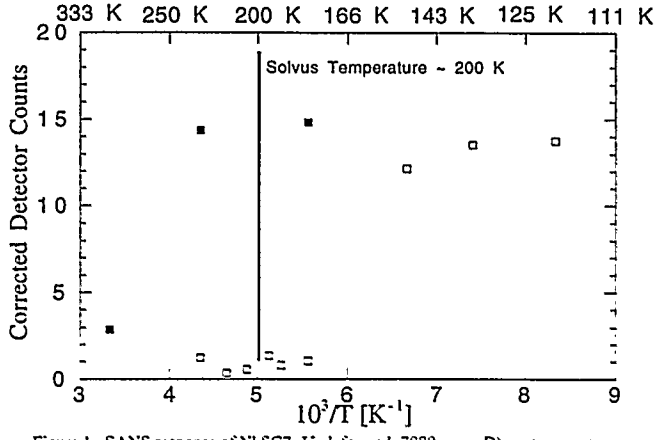


Figure 1. SANS response of NbSC7 (Undeformed, 7000 appm D) vs. temperature.

Additional proof of this hypothesis is given in Fig. 2 which shows the response of both high concentration samples at 120 K. Radially-averaged, absolute, macroscopic, differential cross sections versus wave-vector transfer are plotted in ln-ln format in Fig. 2. Notice that while the scattering at low Q is equal for both samples, the response above approximately 0.015 1/Å (lnQ~-4.2) is not. This high Q scattering follows a $1/Q^2$ power law indicative of a plate-like particle morphology. The scattering response at low Q follows a $1/Q^4$ Porod law.

A tentative explanation of this response is that the dislocation defects, which are know to be distributed in a highly heterogeneous cell-like structure, initially trap deuterium and, as the temperature is lower, act as a framework for deuteride precipitation. In other words, deuteride precipitation follows the cellular or plate-like dislocation substructure. Deuterium trapping and subsequent precipitation in regions of high dislocation density may also explain the absence of a significant hysteresis; hysteresis are thought to be the result of a dislocation-creation barrier being overcome at the onset of precipitation. This barrier may be eliminated by the large lattice distortions present in the deformed sample.

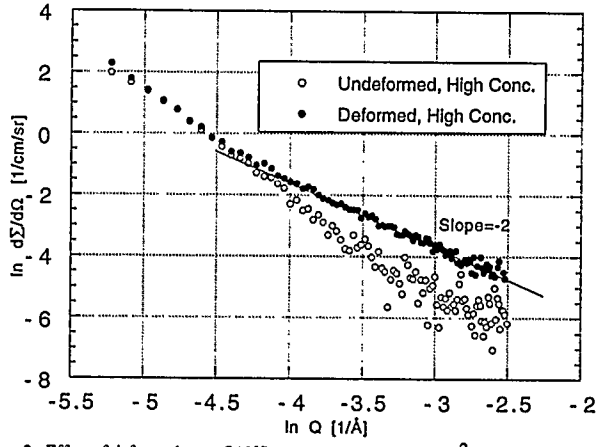


Figure 2. Effect of deformation on SANS response. Note strong $1/Q^2$ scattering at higher Q.

The discussion presented above is not the entire story. The deformed samples exhibit strongly anisotropic scattering responses with two-fold symmetry. This anisotropy is characterized by an anisotropy ratio, the scattering in strongest direction divided by the scattering 90° from the strongest direction (again, for two-fold symmetry). These ratios exceed 10 at lowest Q and are approximately two at high Q. As expected, the $1/Q^2$ response is anisotropic as well. The direction of most intense scattering was found to coincide with the deformation rolling direction. Efforts are now underway to relate this anisotropy to the know bcc dislocation slip systems and ultimately the dislocation cell wall planar directions.

INSTRUMENT USED: SAD | DATE OF REPORT: 5/31/95 | EXPERIMENT NO.: 2009

TITLE: SANS Investigation of Deuterium Trapping at Dislocations in Nb at Low Temp.

AUTHORS AND AFFILIATIONS: B.J. HEUSER, Univ. of Illinois, Urbana, IL & J.S. KING, Univ. Mich., Ann Arbor

DATES OF EXPERIMENT: May 13-16, 1995

CHECK ALL APPLICABLE BOXES:

- [x] APPROVED BY PROGRAM COMMITTEE
- [ ] INSTRUMENT SCIENTIST ALLOCATION
- [ ] DO NOT PUBLISH
- [ ] PROPRIETARY RESEARCH
- [ ] PRT ALLOCATION

EXPERIMENTAL REPORT (or Abstract of Publication)

SANS measurements of 3 single crystal Nb samples, two loaded with approximately 8000 appm deuterium and one of these deformed to 49% thickness reduction, were successfully completed on May 13-16, 1995. The original purpose of the experiments was to observe enhanced trapping of deuterium at dislocations in deformed Nb at reduced temperature. The characteristic 1/Q signal expected from deuterium trapped at dislocations [1] was adequately observed in a deformed, deuterium-loaded sample, but only at temperatures below 230 K. We attribute this to the very low 1/Q scattering cross section near room temperature--runs at RT and 230 K were recorded, but a 1/Q signal could not be separated from the background scattering. Still, the measurements as a function of temperature provided interesting results, as described below.

One anticipated effect was a separate SANS signal from the precipitation of the deuteride phase as the two-phase solvus line was crossed at low temperature. This signal did appear quite strongly, but in general did not interfere with our ability to characterize deuterium-dislocation trapping in the low temperature regime. A comparison at 120 K of two single crystal Nb samples, one deformed to 49% thickness reduction (Nb2), the other undeformed (Nb1), are shown in Fig. 1. Both samples were loaded with approximately 8000 at. ppm deuterium. Notice that the $1/Q^4$ Porod scattering, which we attribute to the formation of deuteride phase particles as solvus line is crossed (at approximately 220 K for 8000 appm deuterium in Nb), is a factor of four larger in Nb1. Also notice that a significant deuterium-dislocation 1/Q component is present in the deformed Nb2 sample, but not in the undeformed Nb1 sample.

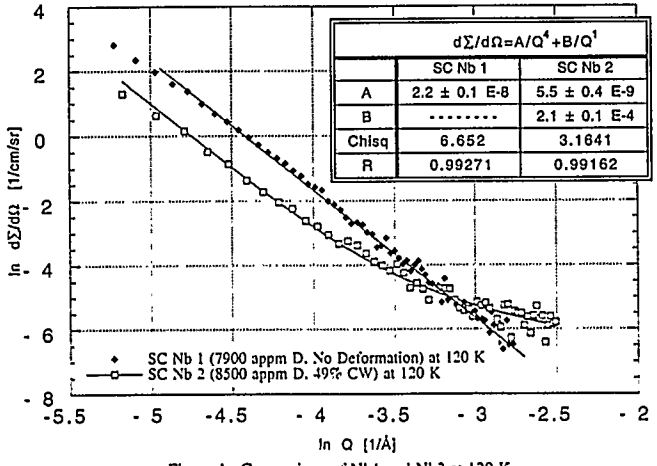


Figure 1. Comparison of Nb1 and Nb2 at 120 K.

EXPERIMENTAL REPORT (CONTD.)

Because both samples had nearly identical deuterium concentrations, we might expect nearly identical amounts of the low-temperature deuteride phase to form, giving rise to equal Porod intensities. However, as observed, a significant fraction of the deuterium in the deformed Nb2 sample is trapped at dislocations at 120 K. We believe these measurements provide proof that this trapped deuterium is not available to form the deuteride phase. This may be in contradiction to the long held hypothesis that dislocations serve as nucleation sites for the precipitation of low temperature deuteride phases in Nb [2].

Although the Porod law fits the strong scattering over a partial Q range in Fig. 1, it is not the entire solution. Notice at lowest Q the data from both samples falls away from the best-fit line, which includes only the Porod law. We suspect this is a precipitate size effect, so that the Porod law requirement, $\ell Q \gg 1$, is not valid at lowest Q.

The deformed Nb2 sample was measured five different temperatures; RT, 230, 175, 120, and 70 K. As shown in Fig. 2, the RT and 230 K responses were identical within the statistical precision of the measurements. The most significant change in Fig. 2 occurs between 230 to 175 K, as the solvus line is crossed, creating the deuteride ε phase. Differences in the SANS response between the 175, 120, and 70 K runs are significant as well and are currently being analyzed.

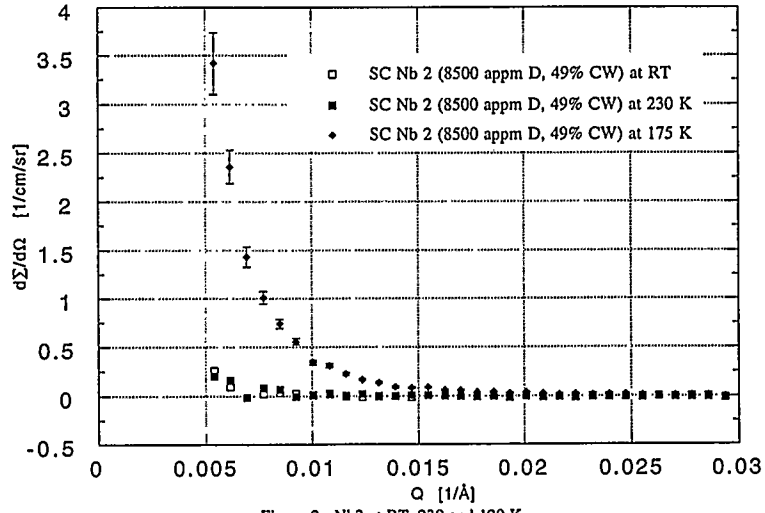


Figure 2. Nb2 at RT, 230 and 120 K.

In addition to these measurements, a deformed single crystal Nb sample without deuterium loading (Nb5, not shown) was measured at RT and at 175 K. As expected, the scattering response of this sample did not change with respect to temperature, verifying that the observed effect in Nb1 and Nb2 was not an experimental artifact.

References

1. B.J. Heuser, J.S. King, G.C. Summerfield, F. Boue, and J.E. Epperson, "SANS Measurement of Deuterium Trapping at Dislocations and Grain Boundaries in Palladium." Acta metall. mater., 39 2815 (1991).

2. T. Schober, "The Niobium-Hydrogen System-An Electron Microscope Study II. Low-Temperature Structures." Phys. Stat. Sol. A, 37 107 (1975).

INSTRUMENT USED:	DATE OF REPORT:	EXPERIMENT NO.:
SAD	7/31/90	1237

TITLE:
Dislocation-Deuterium Interaction in Pd

AUTHORS AND AFFILIATIONS:
B. J. Heuser, G. C. Summerfield, J. S. King (U.M.); J. E. Epperson (ANL)

DATES OF EXPERIMENT: July 10-12, 1990

☒ APPROVED BY PROGRAM COMMITTEE, OR

☐ PART OF INSTRUMENT SCIENTIST ALLOCATION

REPORT RECEIVED:

EXPERIMENTAL REPORT (or Abstract of Publication)

Two experiments were attempted, which were ancillary to previous results. First, we sought to confirm at low Q (.006 to .02$\AA^{-1}$) that grain boundary scattering, seen in polycrystal, annealed Pd at Saclay, would be observable on SAD. Our results, on one sample only, were inconclusive due to statistical limits. Second, we undertook to confirm, by a series of increasingly cold-worked (0%, 10%, 20%, 30%, 42%, 54%, 65%) polycrystal Cu samples that dislocation scattering, without deuterium gas would show a systematic and true Q^{-3} Atkinson-type scattering. Although electronic difficulties at SAD prevented measurements on the complete series we did obtain good data on the 0%, 10%, 20%, and 65% cases. We found that the net scattering (when 0% cw counts are subtracted) from (65%-0%) was negative, but positive for (20%-0%), and strongly positive for (10%-0%). This most interesting result (which we believe is due to mosaic extinction) needs a model, and definitely should be examined for Pd.

EXPERIMENTAL REPORT (CONTD.)

INSTRUMENT USED:	DATE OF REPORT:	EXPERIMENT NO:
SAD	17 December 1993	1820

TITLE: Particle Morphology in Mixed Aqueous Colloids of Monoglycerides and Biles Salts

AUTHORS AND AFFILIATIONS: Rex P. Hjelm (LANL), Alan Hofmann & Claudio Schteingart (UC San Diego), P. Thiyagarajan (ANL)

DATES OF EXPERIMENT: 10-13 December 1993

CHECK ALL APPLICABLE BOXES:

- [X] APPROVED BY PROGRAM COMMITTEE
- [ ] INSTRUMENT SCIENTIST ALLOCATION
- [ ] DO NOT PUBLISH
- [ ] PROPRIETARY RESEARCH
- [ ] PRT ALLOCATION

EXPERIMENTAL REPORT (or Abstract of Publication)

Background: Mixtures of bile salts (Figs. 1a & b) and appropriate lipids (Figs. 2a-c) serve as models for the structure and action of bile—basically an emulsifying and solubilizing agent in the billary tract and intestine for the transport of lipids, and work on these systems serves to further our understanding of the physiological processes of cholesterol solubilization in bile, as well as lipid digestion and absorption in the small intestine. These systems are also important in understanding the efficacy of some oral drug delivery formulations, as solubilization is often rate limiting in drug adsorption in some cases, and an understanding of bile-drug interactions could lead to improvements in uptake. Because the formation of some types of gall stones involves precipitation of bile, an understanding of the physico-chemistry of model systems can lead to effective drug therapies for this painful and debilitating condition. The concepts that must be developed are in the physico-chemistry and colloid physics of these mixed colloid systems, and this is what we are studying.

The self assembly of mixed colloids containing detergents, the (conjugated bile acids) and appropriate lipids is proving to be highly tractable to study by SANS. Our work in this area has changed the picture of this system [1-4]. We have showed that mixed micelles in mixtures of phosphatidylcholines (Fig 2c) with bile salts these systems are rodlike, and that the hydrocarbon chains of the lipids are arranged radially in the rod. The bile salt (or bile acid) lies parallel to the rod axis, near the surface of the micelle, and acts as a wedge between the charged heads of the lipids to induce curvature between the lipids. There is a concentration-induced transition from rodlike micelles to single bilayer vesicles with dilution, which can be reversed by the addition of bile salts.

We have been exploring the self assembly of particles in these mixtures. Our approach has been to consider fats having different character with the aim of understanding what factors are important to particle self assembly. In our first such studies we used the glycerol-1-monoester shown in Fig. 2b. In this case there is only one fatty acid, and the head group contains only the glyceryl moiety, the zwitterionic phosphatidylcholine moiety not being present (Fig. 2a, b). The surprising observation was that mixtures of monoolein with either cholylglycine or chenodeoxycholylglycine (Figs 1a,b) formed particles that where identical to those formed with these same bile salts with phosphatidylcholine. The implications were that neither the zwitterionic nor the two tailed nature of the phosphatidylcholine where important in the self assembly of these systems. Further, these results indicate that the curvature needed to induce mixed micelle and vesicle shape is due solely to the bile salt component.

Objective: We wanted to take this approach one step further by looking at the behavior of the mixtures containing the bile salts with oleic acid-sodium oleate (Fig 2c), a singly charged fatty acid. We measured the scattering from particles formed as a function of total amphiphile concentration, as done previously.

Results: The results for the cholylglycine mixtures are shown in Figs 3 and 4. Even without detailed analysis they show that the particles formed in the bile salt-oleate-oleic acid mixtures are the same as with the monoolein mixtures. The curve shapes imply rodlike mixed micelles with a concentration induced transition to vesicles, just like the other mixtures studied. The same conclusion is drawn for the mixtures with chenodeoxycholylglycine. Thus we can reduce the determinant of the self assembly of these systems to the bile salt and the fatty acid chains. We a doing more detailed analysis to further refine this picture.

Physiological Implications: The implications of this work on the determinants of self assembly in these systems is important to an understanding of bile physiology. In the intestine the phosphatidylcholine is hydrolyzed to lysophosphatidylcholine (LPC) and fatty acid. The LPC is replaced by monoolein and

EXPERIMENTAL REPORT (CONTD.)

fatty acid and fatty acid anion molecules. This work implies that the bile particles are conserved during this process and that this may be important in the function of bile in facilitating digestive enzyme action and in the adsorption of the lipid components into the intestinal wall.

REFERENCES:

1 Hjelm, R.P., Thiyagarajan, P., and Alkan, H. (1988), *J. Appl. Cryst.*, 21, 858-863.
2. Hjelm, R.P., Thiyagarajan, P., and Alkan, H. (1990), *Mol. Cryst. Liq. Cryst.*, 180A, 155-164
3. Hjelm, R.P., Thiyagarajan, P, Sivia, D., Lindner. P., Alkan, H., and Schwahn, D. (1990), *Prog. Coll Polymer Sci.*, 81, 225-231.
4. Hjelm, R.P., Thiyagarajan, P., and Alkan, H, *J. Phys. Chem.*, 96, 8653-8661 (1992).

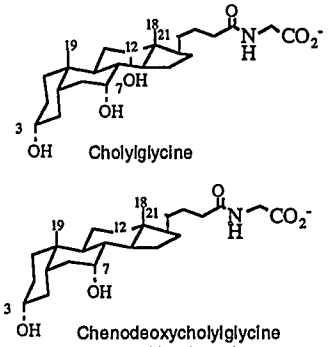


Fig 1: *Bile Salts used in this Study.*

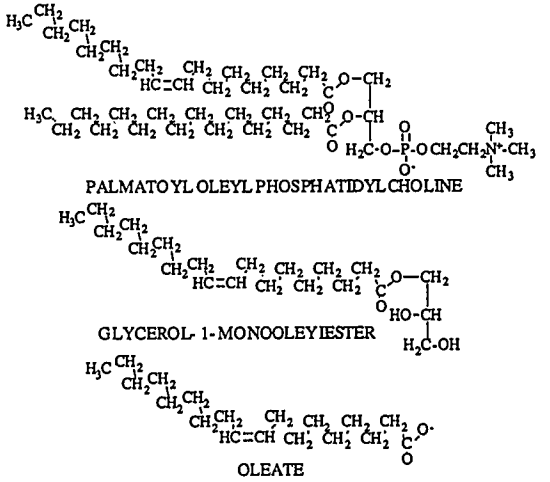


Fig. 2: *Lipids Referred to in the Text.*

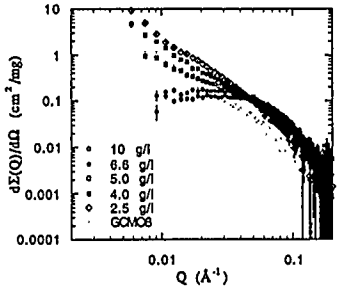


Fig. 3: *SANS of Cholylglycine-Monoolein Mixtures*

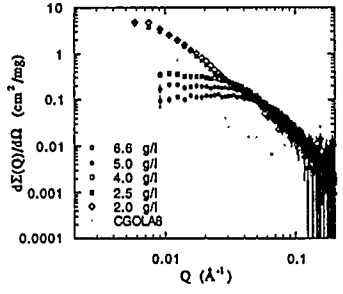


Fig. 4: *SANS of Cholylglycine-Oleic Acid-Sodium Oleate Mixtures*

INSTRUMENT USED:	DATE OF REPORT:	EXPERIMENT NO.:
~~ADD~~SAD	06 SEPT 1990	1227 & 1291

TITLE:

SANS OF MIXED BILE SALT-LECITHIN COLLOIDS

AUTHORS AND AFFILIATIONS:

R.P. Hjelm (LANL), P. THIYAGARAJAN IPNS), A. ALKAN (U of Illinois)

DATES OF EXPERIMENT: 24,26 JAN 1990 & JULY 15 1990

☒ APPROVED BY PROGRAM COMMITTEE, OR

☒ PART OF INSTRUMENT SCIENTIST ALLOCATION

REPORT RECEIVED:

EXPERIMENTAL REPORT (or Abstract of Publication)

Introduction: Mixed aqueous colloids of bile salts and lecithin serve as models for bile in physiology and pharmacology. Thus SANS studies of these systems have proved to be important in understanding the physiology of bile and in drug therapy of certain disorders, such as gall stones. These systems also are of interest in pharmaceutical applications, where they are being studies as novel drug delivery systems. They are also important in understanding mixed aqueous colloid systems, in general.

Our work on mixtures of glycocholate (GC) and lecithin has given important new information on the microstructure of these colloids in the isotropic phases [1-3]. There are, however, several bile salts excreted by the liver, the most common of which are the glycine and taurine conjugates of cholic acid, GC and taurocholate (TC), and chenodeoxycholic acid, glycochenodeoxycholate (GCDC) and taurochenodeoxycholate (TCDC). In these studies we look at the microstructure in the isotropic phases of TC-lecithin and GCDC-lecithin mixed colloids. The studies are intended to give a better understanding of the role of different conjugates and the C12-hydroxy group (see Fig 1) in particle formation. Measurements were done in each case on dilution series for lecithin to bile salt molar ratios, Γ, of 0.5 and 0.8.

Results: *Taurocholate:* TC-lecithin samples at $\Gamma = 0.5$ and 0.8 show the same general progression of growth and shape transformation as seen in the GC-lecithin mixed colloids when the stock solutions (50 gl^{-1}) are diluted. Taking the $\Gamma = 0.5$ series as an example (Fig 2): At 16.7 gl^{-1} globular particles with R_g = 23Å are seen. Dilution to 4.7 gl^{-1} results in rods with R_c = 20Å. Particles at formed concentrations between these extremes show increasing elongation with decreasing concentration. The dimension for globular and rod-like particles are the same in TC- and GC-lecithin systems [1-3]. Vesicular forms are seen at 3.3 gl^{-1}. The vesicles decrease size as the concentration is reduced further, which is the same result obtained with the GC system. Though the trends for the dependence of particle microstructure on Γ and total lipid concentration for TC-lecithin and GC-lecithin are the same, the two systems differ in detail. For example TC-lecithin $\Gamma = 0.5$ dilution series shows features seen in GC-lecithin, $\Gamma = 0.3$. Likewise, the TC-lecithin, $\Gamma = 0.8$ shows transformations characteristic of smaller Γ in the GC series.

Glycochenodeoxycholate: Again, the general characteristics seen in TC- and GC-lecithin systems are observed in GCDC-lecithin. However there are substantial differences. At higher concentrations there is significant intensity at very low-Q, indicative of large aggregates. These may be simple bile salt micelles. At $\Gamma = 0.5$ (Fig 3) no transition to vesicles is observed, even at the lowest total lipid concentration measured, 0.5 gl^{-1}. The scattering is characteristic of coiled and/or loosely-aggregated linear micelles. At $\Gamma = 0.8$, however, some indication of vesicles is evident at 0.6 gl^{-1}. In samples where standard analysis can be applied, we find the same dimensions for particles seen in TC- and GC-lecithin samples.

Conclusions: Bile salts differing in the conjugated moiety (glycine or taurine) or in the presence of a hydroxy group at C12 (Fig 1) show the same general characteristics of Γ- and concentration-dependent particle formation. In each case the globular and rod-like forms appear to be of the same size. This indicates that common principles govern the microstructure of these systems, regardless of the bile salt. On the other hand, there are differences which undoubtedly are related to physical chemical attributes of the bile salts—solubility, for example. The balance of bile salt in bile may be important in maintaining the structure of the colloid particle under physiological conditions. Further analysis and comparisons of these data may help in understanding the role of different bile salts in bile function.

References:

1 Hjelm, R.P., Thiyagarajan, P., and Alkan, H. (1988), *J. Appl. Cryst.*, 21, 858-863.
2. Hjelm, R.P., Thiyagarajan, P., and Alkan, H. (1990), *Mol. Cryst. Liq. Cryst.*, 180A, 155-164
3. Hjelm, R.P., Thiyagarajan, P, Sivia, D., Lindner. P., Alkan, H., and Schwahn, D. (1990), *Prog. Coll. Polymer Sci.*, 81 (in press)

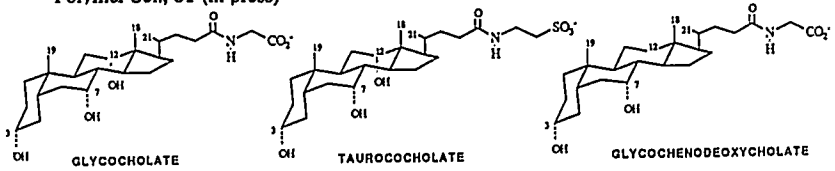


Figure 1: *Structures of Bile Salts Used in These Studies*

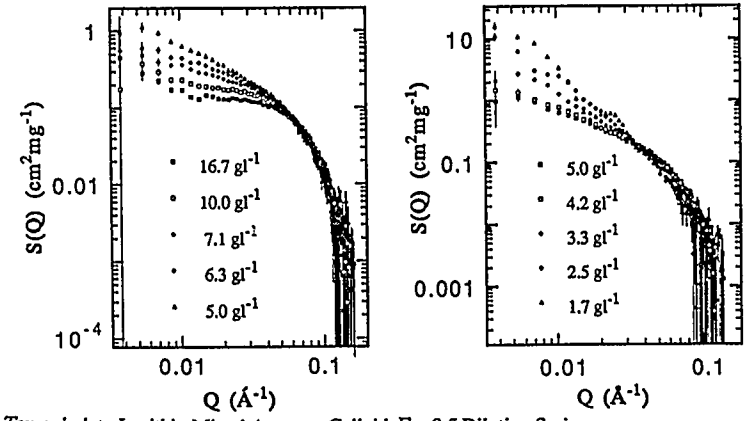


Figure 2: *Taurocholate-Lecithin Mixed Aqueous Colloid, $\Gamma = 0.5$ Dilution Series*

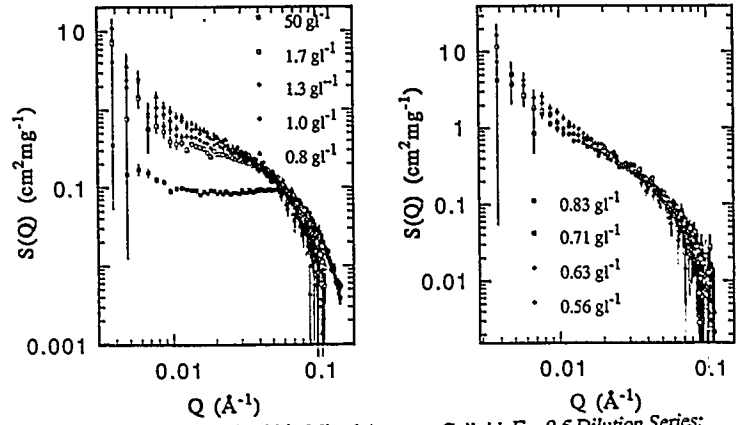


Figure 3: *Glycochenodeoxycholate-Lecithin Mixed Aqueous Colloid, $\Gamma = 0.5$ Dilution Series:*

INSTRUMENT USED:	DATE OF REPORT:	EXPERIMENT NO.:
SAD	11 SEPT 1990	1291

TITLE:

SANS OF MIXED BILE SALT-LECITHIN COLLOIDS

AUTHORS AND AFFILIATIONS:

R.P. HJELM (LANL), P. THIYAGARAJAN (IPNS) & H. ALKAN (U OF ILLINOIS)

DATES OF EXPERIMENT: JULY 14, 16, 1990

☐ APPROVED BY PROGRAM COMMITTEE, OR

☒ PART OF INSTRUMENT SCIENTIST ALLOCATION

REPORT RECEIVED:

EXPERIMENTAL REPORT (or Abstract of Publication)

Introduction: One long range objective of our work on the microstructures of the isotropic phases of mixed aqueous colloids of lecithin and bile salts is to understand the thermodynamics of particle formation in these systems. thus temperature and pressure dependence of the microstructure is being studied. In our preliminary work on the pressure dependence, we found that in glycocholate-lecithin mixtures in an isotropic phase containing rod-like mixed micelles the application of 370 atm (37MPa) pressure resulted in complete collapse into a lamellar phase. The characteristic repeat expected for stacked bilayers of lecithin is 50 Å, consistent with the observations. We proposed that the transformation is the result of bile salt being squeezed out of the particles, and is indicative of a finite, negative ΔV associated with the process bile salt bound to lecithin → bile salt free in solution. The pressures at which this process is driven to completion are well below pressures where the lecithin bilayer undergoes phase changes. We wanted to get more information on this by looking at intermediate pressures, different isotropic phases and different bile salts.

Experimental: Two sample were prepared for these measurements: a) A glycocholate-lecithin (GC) sample in a vesicular isotropic phase. b) A taurocholate-lecithin (TC) sample also in an isotropic phase, but consisting of linear mixed micelles. Application of the different pressures was done sequentially with 30 minutes equilibration before the subsequent measurement. During the course of the measurement, the absolute data rates are checked to determine if counting rates are varying, a sign that the transformation is not yet complete. In each case the instantaneous rates are constant.

Results: *TC-Lecithin:* Figure 1 shows the data for this series. Samples at NTP in the pressure cell show the same scattering as that measured using a standard quartz cell. The features are characteristic of scattering from quasi-one-dimensional particles. The application of 35 atm (3.5MPa) pressure does not change the scattering. The application of 69 atm (6.8MPa) and higher pressures leads to progressive changes which include: smaller differential cross section, S(Q); $S(Q) \sim Q^{-2}$ at low Q; The appearance of a correlation peak at 0.12Å^{-1}. All of this is consistent with a transformation from an isotropic phase of quasi-one-dimensional objects to a lamellar phase having a repeat of ~ 50Å. This repeat is expected for a single lecithin bilayer. The transformation is not readily reversible as incubation of the sample at NTP after the application of 69 MPa does not cause the scattering curve to revert to its original form. Visually, the sample became quite turbid at a result of the pressure treatment.

GC-Lecithin: The results of the progressive application of pressure to the GC-lecithin sample are shown in figure 2. The scattering from sample in standard quartz cell and from the sample at NTP (0.1MPa) in the pressure cell is the same, and is indicative of single bilayer vesicles. The application of 35 atm (3.5MPa) results in considerable changes in the scattering: S(Q) decreases, but the overall vesicular form of the particles is still apparent. Pressurization to 69 atm (6.8 MPa) results in complete disappearance of the vesicle scattering. Much of the curve can be described as $S(Q) \sim Q^{-3}$. These changes, and subsequent ones are concomitant with the appearance of a correlation peak at 0.12Å^{-1}. The application of 173 atm and higher pressures results in changes of the scattering such that $S(Q) \sim Q^{-2}$. The curve as 518 atm (51.8MPa) (Fig 2) is indistinguishable from that for the TC-lecithin mixture at the same pressure (Fig 1).

EXPERIMENTAL REPORT (CONTD.)

Conclusions: A lamellar state results from the applications of the highest pressures\ in both TC- and GC-lecithin systems. The characteristic repeat of 50Å is consistent with the presence of lecithin bilayers. The mixtures do not readily revert from the high pressure forms back to the forms observed at NTP. The response of the GC-lecithin mixture initially in a vesicular phase to low pressures is different from that of the TC-lecithin mixture containing rod-like mixed micelles. There is some intermediate (perhaps metastable) state at moderate pressures in the GC- mixture not observed in the TC- system. The GC- system in the vesicular phase is more susceptible to moderate pressure than the TC- system containing rod-like particles.

Figure 1: *Taurocholate-lecithin, $\Gamma = 0.5, 3.3$ gl^{-1}*

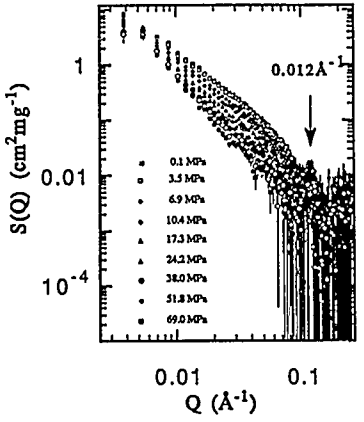
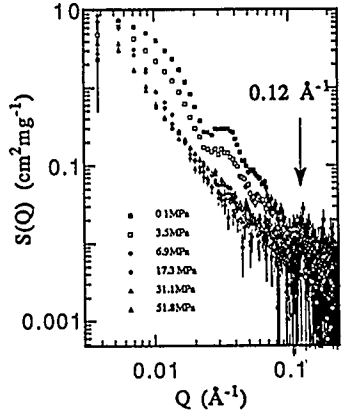


Figure 2: *Glycocholate-lecithin, $\Gamma = 0.8, 2.0$ gl^{-1}*



INSTRUMENT USED:	DATE OF REPORT:	EXPERIMENT NO.:
SAD	8/12/91	1507

TITLE:
Arrangement and Assembly of Lecithin and Bilesalts in mIxed Micelles

AUTHORS AND AFFILIATIONS: R. P. Hjelm Jr. (LANL), P. Thiyagarajan (ANL), H. Alkan (U of I,Chicago)

DATES OF EXPERIMENT: 4/18/91 to 4/20/91

☒ APPROVED BY PROGRAM COMMITTEE, OR

☐ PART OF INSTRUMENT SCIENTIST ALLOCATION

REPORT RECEIVED:

EXPERIMENTAL REPORT (or Abstract of Publication)

SIGNIFICANCE: Aqueous mixed colloids of bile salts and the phosphatidylcholine, lecithin, are important as models of the structure and function of bile. Bile is essential in the transport of lipophilic waste products from the liver into the upper intestine where the bile is required for the solubilization or transport of dietary lipids in the aqueous environment of the digestive tract. In these functions the solubilizing detergent action of the bile salt form particles with the lecithin which are the lipid carriers. Further, the bile salt-lecithin system may be of pharmaceutical interest in the production of liposomes for drug delivery systems in that vesicles are known to form spontaneously on dilution [1,2]. This work on particle morphology and the thermodynamics of their formation impacts on issues associated with the function of bile and on the potential applications of the lecithin-bile salt system. The question of particle formation in mixed micelles is also of interest, and this work impacts on this also.

Our earlier work [1-3] had shown the existence of rod-like structures in areas of the phase map where mixed micelles are present. The organization of lecithin an bile salt in the micellar rods is not known. There are two ways to insert the rod-like lecithin into the micelle, radially or axially. Both models have been proposed. We had proposed an axial arrangement of lecithin in stacked bilayers [3] with the detergent bile salt covering the surface of the rod, giving it the necessary hydrophilic surface for the structure. This was similar to an earlier proposal by Shankland [4]. A radial arrangement has been proposed by Nichols and Ozarowski [5]. A similar model previously proposed for rod-like structures in the hexagonal phase of this system [6]. The question we addressed with these measurements was which of these models is correct.

EXPERIMENTAL: The lecithin chosen for these studies was dipalmtoylphosphatidylcholine (DPPC) mixed with the bile salt taurocholate. We had shown hat this system behaves similarly to the egg lecithin glycocholate mixtures studied previously [1-3]. Mixtures were made with DPPC and DPPC deuterated at the cholate methyl groups (DPPC-d_9. The approach was to measure the scattering from the two mixtures at different concentrations where mixed micelles are present in D_2O and H_2O. The analysis would focus on the cross sectional radius of gyration, Rc, derived from the modified Guinier expression for a long, rod-like particle, $I(Q) = Q^{-1} \Delta m_0 \exp(-Q^2 Rc^2)$. Here Q is momentum transfer, I is the scattering intensity, and Δm_0 is the excess scattering mass per unit length in the rod. The expectation for radially arrayed lecithin is that Rc would be smaller for the deuterated mixtures than the protonated mixtures in D_2O, and *vise versa* in H_2O. If the lecithin is axially inserted, no change is expectred, and the periodic changes in scattering length density along the rod afforded by the deuterated component may show a characteristic signature in the scattering curve.

RESULTS: Samples where initially measured in both H_2O and D_2O, but there was insufficient signal in H_2O; thus the study was continued using only D_2O. Figure 1 shows the result of the Guinier analysis at different total lipid concentrations. In each case the most concentrated sample shows a rod-like morphology apparent from the straight line. The scattering from the sample at 6.25 g/dl can be interpreted as being from a short rod-like particle ~~particle~~. Further there is no significant scattering because of a regular repeat in the rod. These results are consistent with our earlier work on egg lecithin-glycocholate mixtures. Table I lists the values of Rc and Δm_0 for both the protonated and non-deuterated samples. In each and every case the deuterated samples show consistently significantly smaller values of Rc. This is consistent with a radial distribution of lecitrum in micelles. Further analysis is underway using the entirety of the scattering curves to assure the validity of this conclusion.

REFERENCES
1. Thiyagarajan, P., and Alkan, H. (1990) *J. Phys. Chem.* [illegible]
2. Hjelm, R.P., Thiyagarajan, P., and Alkan, H. (1988) *Prog. Colloid Polymer Sci.* 78, 254-259.
3. Hjelm, R.P., Thiyagarajan, P., Lindner, P., Alkan, H. [illegible] *in Colloid and Polymer Science* 31, 225-231.
4. Shankland, W. (1970), *Chem. Phys. Lipids*, 4, 109-130.
5. Nichols, J.W., and Ozarowski, J., (1990) *Biochemistry*, 29, 4600-4606.
6. Ulmius, J., Lindblom, G., Wennerstrom H, Johansson, L. B.-A., Fontell, K., Söderman, O., Arvidson, G. (1982), *Biochemistry*, 21, 1553-1560.
7. Hjelm, R.P. (1985), *J. Appl. Cryst.*, 18, 452-460.

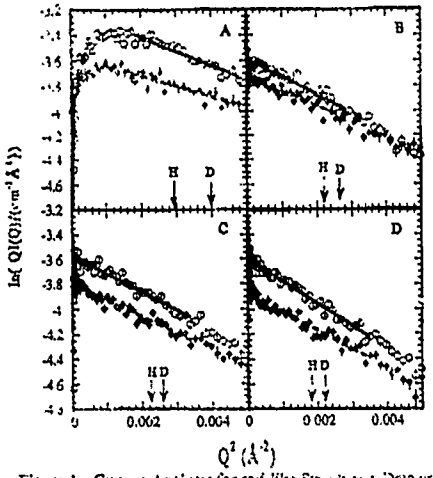


Figure 1. *Guinier Analysis for rod-like Structure*. Data are for ○, DPPC-taurocholate and ◆, DPPC-d_9-Taurocholate mixtures in D_2O. Lines are fits of the data using the Guinier equation for rod-like particles. A, 5.25 g/dl; B, 4.00 g/l; C, 3.33 g/l; D, 2.50 g/l total lipid concentration

Table I
Mass per Unit Length and Cross sectional Radius of Gyration
Derived from Modified Guinier Analysis[a]

[lipid][b]	Δm_0 (10^3 cm^2 mg^{-1} Å^{-1})		R_c (Å)	
(g/l)	DPPC-TC[c]	DPPC-d_9-TC[d]	DPPC-TC[c]	DPPC-d_9-TC[d]
6.25	6.34 (0.16)	4.56 (0.11)	15.0 (0.7)	12.6 (0.9)
5.00	5.66 (0.28)	6.30 (0.37)	17.1 (0.6)	15.3 [illegible]
3.33	[illegible]	5.75 (0.37)	[illegible]	[illegible]
[illegible]	[illegible]	7.24 (0.07)	[illegible]	[illegible]
2.50		3.05 (0.02)		

a From the regress on analysis given in Figure 1
b Numbers in parentheses are the rms values from the regression
b Total lipid concentration in g/l
c DPPC taurocholate mixtures.
d DPPC-d_9-taurocholate mixture.

INSTRUMENT USED:	DATE OF REPORT:	EXPERIMENT NO.:
SAD	17 June 1993	1710

TITLE: SANS AS A PROBE OF THE STRUCTURE OF LIQUID CRYSTAL POLYMER-REINFORCED COMPOSITES

AUTHORS AND AFFILIATIONS:
Rex P. Hjelm (LANSCE, LANL), Brian Benicewicz & Elliot Douglas (MST-7, LANL), & P. Thiyagarajan

DATES OF EXPERIMENT: 4-8 March 1993

CHECK ALL APPLICABLE BOXES:

- [X] APPROVED BY PROGRAM COMMITTEE
- [ ] INSTRUMENT SCIENTIST ALLOCATION
- [ ] DO NOT PUBLISH
- [ ] PROPRIETARY RESEARCH
- [ ] PRT ALLOCATION

EXPERIMENTAL REPORT (or Abstract of Publication)

Introduction: There is a great deal of interest in the concept of molecular composites due to the large increases in mechanical properties which may be realized from this type of composite material. [1,2] Fiber composite theory predicts that reinforcement of a matrix is controlled by the aspect ratio of the reinforcing element. Increasing the aspect ratio of the fiber is reported to increase tensile modulus by up to two orders of magnitude. Thus, the expected property improvements in molecular composites result from the reinforcement of a matrix at the molecular level by individually dispersed rigid rod polymer molecules. In addition, the formation of a molecular composite may alleviate the problem in conventional composites of failure at discrete phase separated fiber-matrix interfaces. In general, the major obstacle to overcome in the formation of a true molecular dispersion is the immiscibility of the rigid reinforcement and flexible matrix polymers.

We have been exploring a new approach to molecular composites [3], which uses a mixture of a liquid crystalline polymer (LCP) reinforcement in a liquid crystalline thermoset (LCT) matrix. Composites made from LCPs and LCTs are expected to show enhanced miscibility as a consequence of both components' ability to form nematic liquid crystalline phases. Subsequent crosslinking of the thermoset should result in a homogeneous dispersion of rigid-rod polymer in a continuous three dimensional crosslinked network. In this report, we describe our preliminary results on a mixture of a LCP and a LCT, shown in Fig. 1.

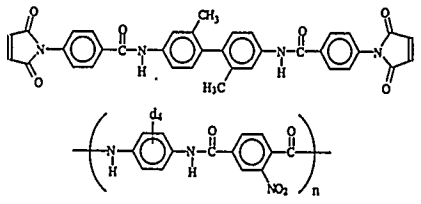


Fig. 1. Chemical structures of the LCT and deuterated LCP used.

Table I
Parameters from the Debye-Bueche Analysis

$f_{d\text{-}LCP}$ [a]	$d\Sigma(0)/d\Omega$ (cm^{-1}) [b]	ξ (Å) [b]
0.0	23 (1)	74 (2)
0.50	70 (5)	80 (2)
0.75	69 (3)	74 (1)
1.0	173 (14)	88 (2)

a Weight fraction of total LCP that is deuterated.
b Number in parentheses are root mean squared deviations from the regression.

Experimental: The liquid crystalline thermoset, shown in Fig. 1, was synthesized as described previously. [4] Solutions of the mixtures were made by dissolving the LCP and LCT in NMP at a total concentration of approximately 5 %. The films considered here where made from 60/40 (w%/w%) LCP/LCT solutions in NMP and cast from the isotropic solution in NMP at 60°C onto glass plates and allowed to air dry for 24 hours, followed by oven drying at 60° C. The films were then dried in vacuum at 150° C overnight. Four such films were considered, each differing by the amount of d_4-LCP (Fig. 1). In this case there were 0, 0.50, 0.75 and 1.0 weight fraction of deuterated verses non-deuterated material.

Results: We interpret the scattering data using the model of Debye and Bueche,[6] which was originally used to describe inhomogeneities in acrylic resins. This model is characterized as a pair of randomly interpenetrating phases having different scattering length densities. The scattering expected for this model is given by, $d\Sigma(Q)/d\Omega = d\Sigma(0)/d\Omega/(1 + Q^2\zeta^2)^2$. Here, ζ is the characteristic correlation distance. The SANS data plotted using the Debye-Bueche analysis is shown in Fig. 2, from which we see that a straight line is a good approximation to the data. At this stage we have not exhausted all other possible models in fitting the data. Thus the analysis must be considered preliminary as to the details of phase morphology. Regardless, the general conclusions drawn here are independent the details of the model.

Table I summarizes the $d\Sigma(0)/d\Omega$ and ζ parameters derived from the Debye-Bueche analysis of Fig. 1. $d\Sigma(0)/d\Omega$ varies with the fraction of d_4- LCP, $f_{d\text{-}LCP}$. The characteristic correlation distance, ζ, is in the range of 70-80 Å.

Debye and collaborators [7] showed that for random interpenetrating phases, $\langle\Delta\rho^2\rangle = \Delta\rho_{a,b}^2\,\Phi(1\text{-}\Phi)$, where Φ is the volume fraction of one of the two phases; $\langle\Delta\rho^2\rangle$ is the averaged squared scattering length density fluctuation; $\Delta\rho_{ab}$ is the difference in scattering length density between the two phases and is given as [3] $\Delta\rho_{a,b}^2 = (\phi_a\text{-}\phi_b)^2\,(f_{d\text{-}LCP}^2\,\Delta\rho_{dh}^2 + 2f_{d\text{-}LCP}^2\,\Delta\rho_{dh}\Delta\rho_{PT} + \Delta\rho_{PT}^2)$. Here ϕ_a and ϕ_b are the volume fractions of LCP in, respectively, phase a (the LCP-rich phase) and b (the LCT-rich phase); $\Delta\rho_{dh}$ is the difference between the scattering length densities of the deuterated and protonated LCP's; and $\Delta\rho_{PT}$ is the difference in between the scattering length densities of the protonated LCP and LCT.

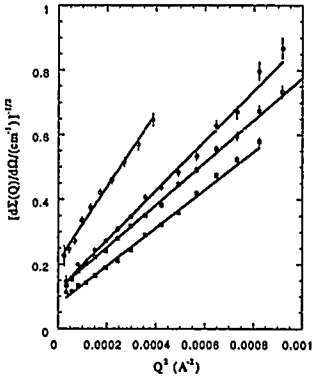


Fig.2. Debye-B euche Analysis of Small-angle Neutron Scattering Data: ○, $f_{d\text{-}LCP}$ = 0; ●, $f_{d\text{-}LCP}$ = 0.5; □, $f_{d\text{-}LCP}$ = 0.75; ■, $f_{d\text{-}LCP}$ = 1.0.

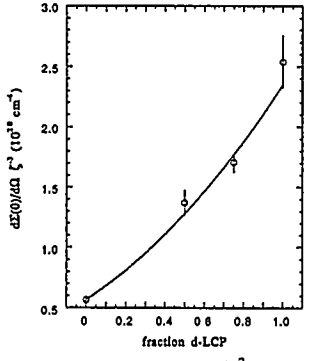


Fig. 3. Dependence of $d\Sigma(0)/d\Omega\ \zeta^{-3}$ on the fraction of Deuterated LCP: ○, Values computed from the data given in Table I: ——, least-squares regression of the data as discussed in the text.

It is easy to show that $d\Sigma(0)/d\Omega = 8\pi\zeta^3\,\Delta\rho_{a,b}^2\,\Phi(1\text{-}\Phi)$, from which and the expression for $\Delta\rho_{a,b}^2$ we see that a plot of $d\Sigma(Q)/d\Omega\,\zeta^{-3}$ verses $f_{d\text{-}LCP}$ will give a parabola, assuming that the volume fraction of each phase, Φ, does not change with $f_{d\text{-}LCP}$. A plot for this data is given in Fig. 3 and the regression parameters are given in Table II. The values for $\Phi(1\text{-}\Phi)(\phi_a\text{-}\phi_b)^2$ are calculated by equating the regression parameters with the coefficients for like powers in $f_{d\text{-}LCP}$. We observe no significant differences in these values, with 0.035 being the most likely. In the completely phase separated case $\Phi = 0.59$, $\phi_a = 1$ and $\phi_b = 0$, in which case $\Phi(1\text{-}\Phi)(\phi_a\text{-}\phi_b)^2 = 0.24$, nearly an order of magnitude higher than the experimental values. This result strongly suggests that there is partial mixing of LCP and LCT in the two phases, with each phase being rich in one component but having substantial amounts of the minor component also present.

Conclusions: The two important conclusions derived from this study are that there is phase separation in this system on the scale of 70-80 Å, and that each phase is not composed of the pure components, but rather is a mixture of LCP and LCT. This work also shows that current theoretical models [8] do not adequately describe these systems.

References:

1. Hwang, W.-F., D.R. Wiff, C.L. Benner and T.E. Helminiak (1983), *J. Macromol. Sci. - Phys.*, B22(2), 231-257.
2. Pawlikowski, G.T., D. Dutta and R.A. Weiss (1991), *Annu. Rev. Mater. Sci.*, 21, 159-84.
3. Benicewicz, B.C., E.P. Douglas, and R.P. Hjelm (1993), *Proceedings of the International Workshop on Liquid Crystalline Polymers* Plenum Press, in press.
4. Hoyt, A.E. and B.C. Benicewicz (1990), *J. Polym. Sci.: Part A: Polym. Chem.*, 28, 3403-3415.
5. Higashi, F., S. Ogata and Y. Aoki (1982), *J. Polym. Sci.: Polym. Chem. Ed.*, 20, 2081-2087.
6. Debye, P. and A.M. Bueche (1949), *J. Appl. Phys.*, 20, 518-525.
7. Debye, P., R. Anderson and H. Brumberger (1957), *J. Appl. Phys.*, 28, 679-683.
8. Abe, A. and P.J. Flory (1978), *Macromolecules*, 11, 1122-1126

Table II
Parameters of Fitting the Dependence of $d\Sigma(0)/d\Omega\,\zeta^{-3}$ on $f_{d\text{-}LCP}$

Term	Regression Parameter (10^{-4} cm^{-4})	$\Phi(1\text{-}\Phi)(\phi_a\text{-}\phi_b)^2$
$8\pi\Phi(1\text{-}\Phi)(\phi_a\text{-}\phi_b)^2\Delta\rho_{PT}^2$	0.57 (0.04)	0.035 (0.002)
$16\pi\Phi(1\text{-}\Phi)(\phi_a\text{-}\phi_b)^2\Delta\rho_{dh}\Delta\rho_{PT}$	1.1 (0.7)	0.02 (0.01)
$8\pi\Phi(1\text{-}\Phi)(\phi_a\text{-}\phi_b)^2\Delta\rho_{dh}^2$	0.7 (0.8)	0.02 (0.02)

INSTRUMENT USED:	DATE OF REPORT:	EXPERIMENT NO
SAD	24 Sept 1992	

TITLE:

SANS AS A PROBE OF LIQUID CRYSTAL EPOXY-LIQUID CRYSTAL POLYMER COMPOSITES

AUTHORS AND AFFILIATIONS:
Rex P. Hjelm (LANSCE), Brian Benicewicz (MST-7, LANL) and P. Thiyagarajan (IPNS)

DATES OF EXPERIMENT:
6-10 June 1992

CHECK ALL APPLICABLE BOXES:

- ☐ APPROVED BY PROGRAM COMMITTEE
- ☒ INSTRUMENT SCIENTIST ALLOCATION
- ☐ DO NOT PUBLISH
- ☐ PROPRIETARY RESEARCH
- ☐ PRT ALLOCATION

EXPERIMENTAL REPORT (or Abstract of Publication)

Background and Significance: Composite materials form the bases of highly important technologies. These range from reinforcement of elastomers by carbon black used in automobile tires to advanced molecular composite materials used in advanced military aircraft applications. The strategy of composite design is to produce a material with enhancements of beneficial characteristics of the constituents. Most important among these is mechanical properties such as toughness and strength. This report describes our first attempts to obtain nanoscale and molecular level information on the mechanism of improved mechanical properties in composites, specifically those containing a matrix of liquid crystal thermoset epoxy (LCT), reinforced by rigid-rod, liquid crystal polymers (LCP),. This information will be used in further work on the development of new, more effective composites.

Objectives: A successful strategy in the production of molecularly reinforced LCP-matrix composites must deal with difficulties in dispersing the LCP in the matrix material. The difficulty is due to unfavorable free energy of mixing between the components. Rather complex schemes have been devised to process melts of the polymers into a "homogeneous phase" followed by a deep quench below the glass transition. However, the mixtures almost always show some phase separation, at least on the microscale level, limiting the theoretically achievable strength. Further, the mixtures are thermodynamically unstable, and phase separation inevitably results with time.

There are unexplored strategies to deal with these problems. One of these is to use a matrix which will better disperse the LCP phase. This strategy is the bases of our novel approach in which an LCT is mixed with LCP. The mixture is melted, homogenized, then the temperature of the melt is raised above the thermoset point of the epoxy. It is anticipated that this process will give LCP well dispersed in the matrix material. We believe that these materials will offer a new class of composite materials with significant improvements in stiffness, toughness and strength. However, there is no data on the characteristics of these mixtures, and this study provides the first information on this. Our initial interest is to determine the behavior of the system under a variety of conditions in order to determine the "rules" that govern the interaction between rodlike polymers and molecules. This will serve as the bases for the design of definitive experiments to understand the nature of the interaction further. This problem has interest in its own right as there is presently little understanding on the interactions of rodlike molecules and polymers.

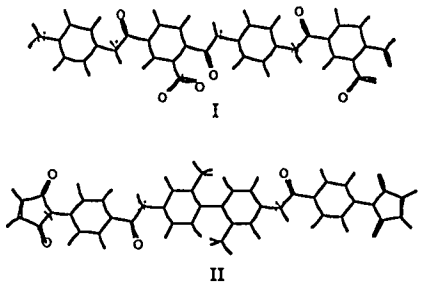


Figure 1. Liquid Crystal Polymer and Liquid Crystal Thermoset Epoxy Used in this Study. I: Nitro-substituted Liquid Crystal Polymer Segment of Two monomers. II: Liquid Crystal Thermoset Epoxy

Experimental: Films were cast from solution of nitro-substituted kevlar-like LCP, a segment of which is shown in II of Figure 1, and mixtures of this with an LCT, shown as I in Figure 1, in the isotropic phase. The mixtures were made in different ratios of LCP/LCT as 80/20 (%/%) and 60/40. Samples were prepared with different proportions of LCP deuterated at the four positions of the unsubstituted benzene ring (Fig. 1 II). The proportions of LCP-d4 were 0, 25, 50, 75 and 100%. Samples were measured freshly prepared and annealed for 5 hours at 200°C.

Results: The SANS from LCP-LCT films show microphase separation of LCP and LCT on length scales accessible on SAD ($2\pi Q^{-1} \leq$ 1200Å) that is dependent on the composition. The 80/20 LCT/LCP films show scattering characteristic of rodlike morphology with a cross sectional radius of gyration, $R_c \approx 80$ Å (Fig. 2). The particles appear to be distinct phases of LCP and LCT- rich domains, as the scattering shows a Porod law, and the intensity scales with LCP-d_4 content. The 60/40 films scatter scattering as a two phase, randomly interpenetrating. The characteristic length calculated for the Debye-Bueche model is, $\xi \approx 80$Å (Fig. 3). The higher Q data does not follow a Porod law. Annealing does not have a strong effect on the scattering from the mixtures. These conclusion are provisional on further analysis must be and further experimental measurements.

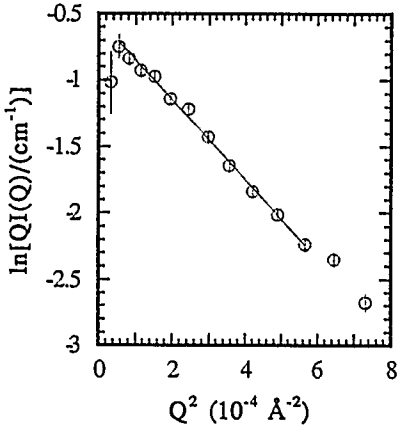


Figure 2. Guinier Analysis for Rodlike Particles for Data from an LCP-LCT Film. Data from a sample of LCP-LCP mixed in the ratio 80/20 (%/%). The analysis assumes that the scattering has the form $I(Q) = \Delta m_0 \exp(-Q^2 R_c/2)$.

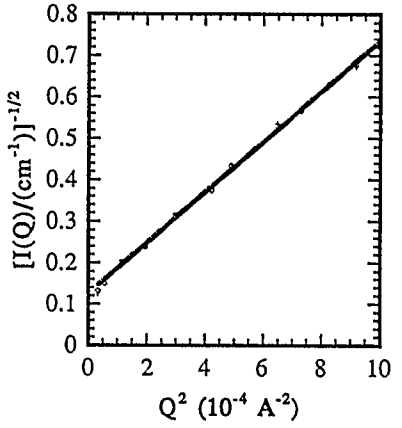


Figure 3. Debye-Bueche Analysis of Data from a LCP-LCT film. Data from a sample of LCP-LCT mixed at a ratio of 60/40. Analysis assumes that the scattering is $I(Q) = I(0)/(1 + \xi^2 Q^2)^2$.

INSTRUMENT USED:	DATE OF REPORT:	EXPERIMENT NO:
SAD	17 November 1995	2072

TITLE: **Mixed Colloid-Drug Interactions in Drug Delivery Systems**

AUTHORS AND AFFILIATIONS:
Rex P. Hjelm, LANSCE, Los Alamos National Laboratory
Sharon Ayd and Hayat Alkan-Onyuksel, Department of Pharmaceutics, Univeristy of Illinois, Chicago
P. Thiyagarajan, IPNS, Argonne National Laobroratory

DATES OF EXPERIMENT:
12-13 June 1995

CHECK ALL APPLICABLE BOXES:

- [x] APPROVED BY PROGRAM COMMITTEE
- [ ] INSTRUMENT SCIENTIST ALLOCATION
- [ ] DO NOT PUBLISH
- [ ] PROPRIETARY RESEARCH
- [ ] PRT ALLOCATION

EXPERIMENTAL REPORT (or Abstract of Publication)

A significant number of drug compounds exhibit inadequate aqueous solubility which creates a serious formulation problem. Several approaches including pH adjustment, and the use of co-solvent, pro-drug, emulsions, cyclodextrins and liposomes have been used in an attempt to address this issue. Each of these techniques has its own disadvantage. Another technique is to use mixed micelles composed of a soluble (bile salt-BS) and insoluble (lecithin-L) amphiphile to solubilize hydrophobic drug compounds. The rationale of incorporating L into the micellar vehicle is based on the assumption that lecithin will increase the hydrophobic core of the bile salt simple micelles and increase the solubilization capacity. Removal of bile salt monomers from the mixed micelles occurs spontaneously upon aqueous dilution and is the result of attempts by the system to sustain the intermicellar concentration in the bulk solution. When enough bile salt monomers have been removed the remaining L molecules spontaneously form bilayer vesicles which is known as the micelle-to-vesicle transition and the result is that hydrophobic drug molecules can be kept solubilized in the L vesicles after the transition has occurred. (1) This is a major advantage of this technique. (2) The composition of the mixed micelle depends on that of the starting mixture as well as the ability of each component to self associate as given by the critical micelle concentration (CMC). It is believed that disc-shaped bimolecular leaflets of lecithin molecules form the core of the mixed micelle with the hydrocarbon sides of the bile salts associating with their counterparts on the lecithin disc. The addition of lecithin to a bile salt may considerably increase the solubilization of a hydrophobic drug molecule as a result of the formation of mixed micelles.

Thus, overall success in this approach would increase the availability of insoluble drugs and, in some cases would improve drug efficacy by increasing bioavailability. For oral formulations, bioavailability might be affected by drug/bile interactions through changes in bile particle morphology, and this is a hypothesis that needs to be tested. With these applications in mind we have been investigating the structure of particles formed in mixed aqueous colloids of bile salt and lecithin. In our previous work we demonstrated a linear relationship between total amphiphile concentration and L/BS ratio. This relationship was based on the boundary between single phase-clear isotropic mixed micelle and two phase-elongated mixed micelle/vesicle systems. The significance of the linear relationship is that it represents optimized L/BS/H_2O systems in which the aggregates exist only as spherical mixed micelles. The effect of model drug entities on the shapes of micelles and the formation of vesicles will give important information on the self assembly of mixed micellar systems. Current notions point to the importance of the molecular shape of included drug molecules in determining the geometries of the structures and the elastic behavior (3) of the structures. This proposal will provide validation of these ideas.

SANS provides information on the structure over length scales most relevant to mixed micelle particle morphology in the isotropic phase (4-8). The high contrast afforded by SANS of the L/BS particle in D_2O allows the system to be studied over a broad range of concentrations, an essential condition for the study of self assembly of colloid particles.

EXPERIMENTAL REPORT (CONTD.)

OBJECTIVE: To investigate the solubilization potential of optimized mixed micellar vehicles for two drugs (hydrocortisone & deoxycorticosterone) of differing polarity. We want to analyze some key formulations to further our understanding about structural changes that may occur in the mixed micelles as they incorporate drug: 1) is there a change in mixed micelle size, structure, or dimensions that occurs when drug is solubilized, 2) is this change, if any, in mixed micelle shape/size dependent on the molecular weight or polarity or shape of the solubilized drug, or the polarity of the soluble amphiphile in the mixed micelle.

Experimental: Mixed micelle solutions of L and the bile salts, cholyltaurine (CT) or deoxycholyltaurine (DT) were made up in D_2O by the method of co-precipitation. Hydrocortisone (HC) and deoxycorticosterone (DC) containing solutions were made up in a similar manner at drug concentrations slightly less than saturation. Solutions without drug were measured as empty "controls". Samples included: 1) constant total amphiphile content but with different soluble amphiphile and no insoluble amphiphile (simple micelles), 2) constant number of micelles but with different soluble amphiphile and again no insoluble amphiphile, 3) constant L/CT ratio but with different soluble amphiphile and L as insoluble amphiphile (mixed micelles), and 4) constant total amphiphile content but with different soluble amphiphile and again L as insoluble amphiphile. In all cases, samples will contain either DC, DC, or no drug.

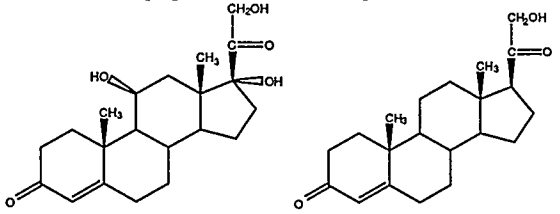


Figure 1: Hydrocortisone (left) and deoxycorticosterone (right)

Results: We note first of all that both HC and CD contain a cholesterol-like core, and thus have analogous structures to the bile salts. They differ, however in their polarity. In shape these molecules are wedge-like. L/TC was chosen so that mixed micelles were present of the same size and shape. but at different concentrations. Guinier analysis of these solutions with 300 µg/ml of added hydrocortisone show that the globular particle seen in the L/CT solutions have become long rods of approximately the same radius. On the the hand the addition of 100 µg/ml of deoxycorticosterone, completely disrupts the micelle structure. Similar measurements on solutions containing the less polar bile salt, DT, showed that neither the addition of hydrocortisone at 100 µg/ml nor the addition of deoxycorticosterone had any affect on the micelle structure what so ever. Curiously, however, 80 µg/ml hydrocortisone had the effect of causing rod elongation. We plan further experiments to evaluate these results and there implications on mixed micelle self assembly.

References:

1. R. P. Hjelm, P. Thiyagarajan, and H. Alkan-Onyuksel, Organization of Phosphatidylcholine and Bile Salt In Rodlike Mixed Micelles, J. Physical Chemistry, 96, 1992
2. H. Alkan-Onyuksel, S. Ramakrishnan, H. Chai, and J. Pezzuto, A Mixed Micellar Formulation Suitable for the Parenteral Administration of Taxol, Pharm. Res., Vol. 11, No. 2, 1994.
3. S. A. Safran, P. Pincus, D. Andelman, and F. C. MacKintosh, Phys. Rev. A. 43, 1071, 1991.
4. R. P. Hjelm, P. Thiyagarajan, and H. Alkan, J. Appl. Cryst., 21, 858, 1988,
5. R. P. Hjelm, P. Thiyagarajan, and H. Alkan, Mol. Cryst. Liq. Cryst. 180A, 55, 1990,
6. R. P. Hjelm, P. Thiyagarajan, D. Sivia, P. Lindner, H. Alkan, and D. Schwahn, Prog. Coll. Polymer Sci.. 225, 1990,
7. R. P. Hjelm, P. Thiyagarajan, and H. Alkan-Onyuksel, J. Phys. Chem., 96, 8653, 1992,
8. R. P. Hjelm, P. Thiyagarajan, C. Schteingart, A. F. Hofman, and H. Alkan-Onyuksel, Falk Symposium Bile Acids in Gastroenterology: Basic and Clinical Advances, Kluwer pp 41-58 (1995)

((Typed version will be submitted later))

INSTRUMENT USED: SAD	DATE OF REPORT: Feb-9,	EXPERIMENT NO.: 1939

TITLE: In-plane Scattering of Peptides in Membranes

AUTHORS AND AFFILIATIONS: Huey W. Huang, Rice University

DATES OF EXPERIMENT: Feb 8-11, 1995

CHECK ALL APPLICABLE BOXES:

- [x] APPROVED BY PROGRAM COMMITTEE
- [ ] INSTRUMENT SCIENTIST ALLOCATION
- [ ] DO NOT PUBLISH
- [ ] PROPRIETARY RESEARCH
- [ ] PRT ALLOCATION

EXPERIMENTAL REPORT (or Abstract of Publication)

Membrane-active peptides have been discovered from the host-defense systems of animals. They are potentially important new kinds of antibiotics which exert their activity directly on the lipid bilayer of the cell membrane, rather than on some protein targets. In our previous publications we have shown that these peptides show an interesting transition when interacting with membranes. At low concentrations, they absorb on the membrane surface. Above a critical concentration, they insert into the membrane. This insertion transition is the ~~molecular~~ mechanism of the peptides' antibiotic activity.

In order to understand this peptide insertion transition we performed neutron in-plane scattering of membranes with peptides inserted. We used undeuterated peptide and lipid but hydrated with D_2O. The attached figure show preliminary data obtained on Feb-9. The solid line is membrane without peptide. The peak is the The lamellar Bragg peak due to inevitable smectic

EXPERIMENTAL REPORT (CONTD.)

defects of the multilayer sample. The dots are for membranes with peptides. Clearly there is signals in addition to a Bragg peak. (The reason the solid line peak is so much stronger is that there were more defects in the sample without peptide.) The signal is due to D_2O penetrating the membrane because of the inserted peptide. If we subtract the Bragg peak, we will see 2 bumps due to D_2O penetrating the membranes. ~~Tentatively we~~ This ~~conclude~~ ~~infer~~ implies that the peptide formed ion channels in the membrane ~~with~~ and the water is in the core of the ion channel.

INSTRUMENT USED: SAD	DATE OF REPORT: May 12, 1995	EXPERIMENT NO.: 2079

TITLE: In-plane Scattering of Peptides in Membranes

AUTHORS AND AFFILIATIONS: Huey W. Huang, Rice Univ.

DATES OF EXPERIMENT: May 9-12, 1995

CHECK ALL APPLICABLE BOXES:

- [x] APPROVED BY PROGRAM COMMITTEE
- [ ] INSTRUMENT SCIENTIST ALLOCATION
- [ ] DO NOT PUBLISH
- [ ] PROPRIETARY RESEARCH
- [ ] PRT ALLOCATION

EXPERIMENTAL REPORT (or Abstract of Publication)

The attached data represent in-plane scattering of alamethicin (20 amino acid helical peptide) embedded in membranes. The neutron scattering length contrast between peptide and lipid (membrane) is very small. The signal indicates that D_2O (which was used to hydrate the membranes) penetrates the lipid bilayer along with peptides. The same sample without peptide does not show such scattering ~~sing~~ signals.

The scattering curves resemble a liquid scattering, in this case a 2-D liquid of channels: We modeled a channel as a cylinder lined by ~~pe~~ helical peptides in the barrel-stack fashion. The cylindrical hole in the center is filled with water (in this case D_2O). The ~~theor~~ scattering curve agrees with a simulation of cylinders in 2D very well (to be published). The data indicates that in DLPC the channel is composed of about 8 monomers. However in DPhPC the channels are larger, ~~#~~ about 9 ~~or~~ to 10 monomers.

It is well known that the peptide-lipid interaction is strongly lipid dependent. Which aspect of the lipids determine ~~#~~ the channel size is an interesting question.

Another puzzle is the peptide concentration dependence. Consistently we have observed that the channel size decreases with peptide concentration.

EXPERIMENTAL REPORT (CONTD.)

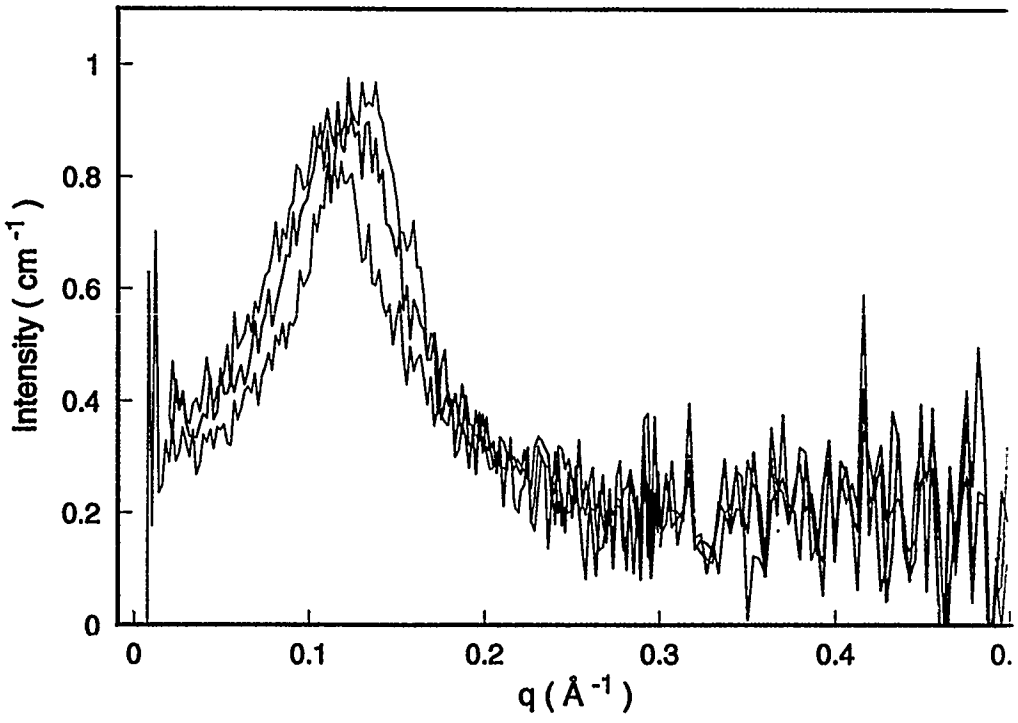


Fig. caption: In-plane scattering of alamethicin channels in DLPC bilayer membranes. The peptide to lipid molar ratios are 1/10 (red), 1/15 (blue), and 1/20 (green). The scattering curves agree with ~~sim~~ computer simulations of cylindrical channels freely diffusion in ~~#~~ a 2D plane. Each channel is composed of about 8 peptide monomers, slightly larger for lower concentrations.

INSTRUMENT USED: SAD	DATE OF REPORT: Nov 10, 95	EXPERIMENT NO.: 2094

TITLE: In-plane Scattering of Peptides in Membranes

AUTHORS AND AFFILIATIONS: Huey W Huang, Rice University

DATES OF EXPERIMENT: Oct 9-13, 1995

CHECK ALL APPLICABLE BOXES:

- ☒ APPROVED BY PROGRAM COMMITTEE
- ☐ INSTRUMENT SCIENTIST ALLOCATION
- ☐ DO NOT PUBLISH
- ☐ PROPRIETARY RESEARCH
- ☐ PRT ALLOCATION

EXPERIMENTAL REPORT (or Abstract of Publication)

Abstract of K. He, S J Ludtke, H.W. Huang, D L. Worcester "Antimicrobial Peptide Pores in Membranes Detected by Neutron In-plane Scattering" to be published in Biochemistry (Accelerated Publication, Dec 1995):

~~Antimicrobial peptides isolated from the host defense systems of animals have been~~

ABSTRACT

A technique of neutron in-plane scattering for studying the structures of peptide pores in membranes is described. Alamethicin in the inserted state was prepared in undeuterated and deuterated dilauroyl phosphatidylcholine (DLPC) hydrated with D_2O or H_2O. Neutron in-plane scattering showed a strong dependence on deuteration, clearly indicating that water is a part of the high order structure of inserted alamethicin. The data is consisttent with the simple barrel-stave model originally proposed by Baumann and Mueller. The theoretical curves computed on this model at four different deuteration conditions agree with the data in all cases. Both the diameter of the water pore and the effective outside diameter of the channel are determined accurately. Alamethicin forms pores in a narrow range of size. In a given sample condition, >70% of the peptide forms pores of n and $n \pm 1$ monomers. The pore size varies with hydration and with lipid. In DLPC, the pores are made of $n = 8 - 9$, with a water pore $\sim$ 18 Å in diameter and with an effective outside diameter $\sim$ 40 Å. In diphytanoyl phosphatidylcholine, the pores are made of $n \sim 11$ monomers, with a water pore $\sim$ 26 Å in diameter and with an effective outside diameter $\sim$ 50 Å.

INSTRUMENT USED:	DATE OF REPORT:	EXPERIMENT NO.:
Small angle diffractometer	5 August, 1991	1370

TITLE: ZSM-5 CRYSTALLISATION BY LIQUID PHASE ION TRANSPORT

AUTHORS AND AFFILIATIONS:
Dr. L.E. ITON (Argonne National Laboratory); Professor J.W. WHITE (Australian National University)

DATES OF EXPERIMENT: 31 July 1991 to 3 August 1991

☑ APPROVED BY PROGRAM COMMITTEE, OR

☐ PART OF INSTRUMENT SCIENTIST ALLOCATION

REPORT RECEIVED:

EXPERIMENTAL REPORT (or Abstract of Publication)

In an earlier experiment we have shown that in the crystallisation of high silica - ZSM-5 zeolites from aluminosilicate gels[1] the behaviour of the neutron small angle scattering before hydrothermal treatment is critically dependent upon the nature of the gel. In particular, gels made up with soluble silicate suffer an immediate transformation through the addition of "template" molecules such as the tetrapropylammonium ion, whilst those based upon colloidal silica (ludox) have essentially unchanged neutron scattering patterns for hours or days after mixing. The latter experiments appear to be good models for the liquid phase ion transport (LPIT) mechanism of zeolite crystallisation but detailed interpretation of the scattering at intervals up to a few days of mixing, and during heating requires careful contrast matching of the remaining silica.

In the experiment reported here the first system in which there is no particulate phase present in the start solutions has been studied. This is a preparation designed by von Balmoos[2] which gives a very pure ZSM-5 product when heated at temperatures above 120° C in the hydrothermal process. From a neutron scattering point of view it is very interesting because no solid separates in the early part of the hydrothermal process and there is, in principle, a low background of scattering against which incipient zeolite nucleation could be detected.

The experiment tested the assumption of a low background and at one contrast, looked for the first appearance of nucleation in heated samples. As can be seen from Figure 1 the results are very promising in that, for the start solutions there is essentially no scattering background over the whole Q range of the SAD instrument and that with heating for 4, 12 and 24 hours there is a progressive growth of the low angle scattering associated with the crystallisation process. It thus looks as if this system might well prove to be a good paradigm for the LPIT mechanism and is worth following up in detail with a variety of contrast and heating experiments.

In Figure 2 we show the time development of the small angle scattering intensity extrapolated to zero momentum transfer (I(0)) and of the radius of gyration of the scattering particles. This may be the first time that nucleation from a homogeneous zeolite fluid has been detected. In further experiments we plan to identify the scattering intensity of the particles produced and, if possible, extend the measurements to lower momentum transfers.

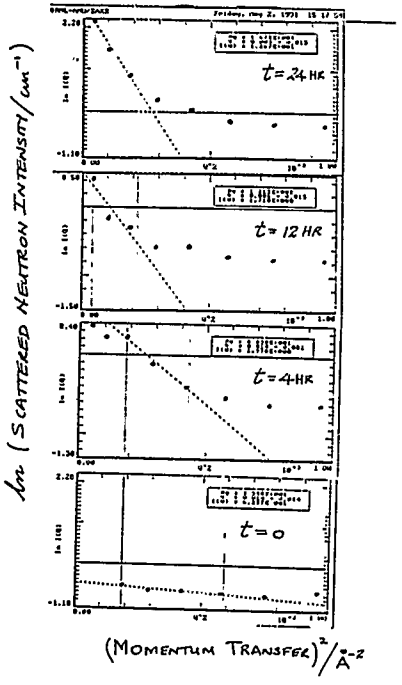


FIGURE 1

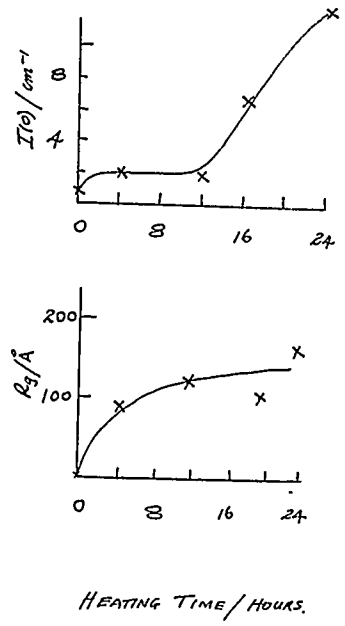


FIGURE 2.

References:

1. L.E. Iton, F. Trouw, T.O. Brun, J.E. Epperson, J.W. White and S.J. Henderson, Langmuir, 1991, in press.
2. van Balmoos, private communication.

INSTRUMENT USED: SAD	DATE OF REPORT: 31-7-92	EXPERIMENT NO.: 1575, 1152, 1245, 1411

TITLE: ZSM-5 CRYSTALLISATION BY LIQUID PHASE ION TRANSPORT

AUTHORS AND AFFILIATIONS: Dr. L.E. ITON (Argonne National Laboratory); J. DOUGHERTY, ANU
Professor J.W. WHITE (Australian National University)

DATES OF EXPERIMENT: 13 JULY 1992 to 17 July 1992 (Detector then failed)

CHECK ALL APPLICABLE BOXES:

- ☑ APPROVED BY PROGRAM COMMITTEE
- ☐ INSTRUMENT SCIENTIST ALLOCATION
- ☐ DO NOT PUBLISH
- ☐ PROPRIETARY RESEARCH
- ☐ PRT ALLOCATION

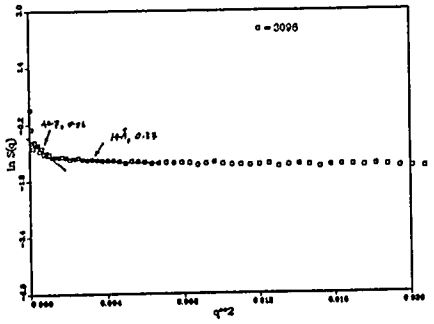
EXPERIMENTAL REPORT (or Abstract of Publication)

This experiment was an attempt to repeat those in July 1991on the evolution of the scattering with hydrothermal treatment, which failed due to the target problems. Despite the fact that again the work was curtailed due to a detector problem an interesting and tantalising result was found for the start solutions on which we had already done small angle X-ray work. In earlier experiments we have shown that in the crystallisation of high silica - ZSM-5 zeolites from aluminosilicate gels[1] the behaviour of the neutron small angle scattering before hydrothermal treatment is critically dependent upon the nature of the gel.

It will be recalled that the present system, originated by von Balmoos[2], when heated to ca 150C crystallises ZSM-5 from start solutions which have no visible solid matter in suspension. It is thus possible to attempt absolute measurements of the scattering intensity in the start solution aging and the high temperature hydrothermal treatment processes to follow the evolution of zeolite nucleation and growth. In the small angle X-ray experiments an aging process has been detected in the start solutions with particles present whose radii of gyration increase with time at room temperature from ca 15Å to 50-70Å. The X-ray scattering from these systems is quite strong.

In the two successful runs of the present experiment long runs were done (to take account of the reduced flux at present) on solutions of the same composition and aging as were used for the X-ray experiments but made up in both H_2O and D_2O as extrema for an intended contrast matching series to detect the scattering length density of the scattering objects. Careful backgrounds were run for each solution and a weak but clear scattering signal detected. Figure 1 shows the data for the system made up in D_2O. There is a distinct break in the scattering function at Q~ 0.02Å^{-1}with Guinier radii /Å^{-1}, I(0) /cm^{-1} below and above it of (43,0.6) and (14,.4) respectively. For the H_2O system the incoherent background was much larger but again careful subtraction gave a very similar scattering function. The parameters for the higher Q part were Rg = 26Å, I(0) = 0.2 cm^{-1}.

SNET3098.DAT



References:

1. T.O. Brun, J.E. Epperson, S.J. Henderson, L.E. Iton, F. Trouw and J.W. White *Langmuir*, 8, 1045-1048, 1992
2. van Balmoos, private communication.

INSTRUMENT USED:	DATE OF REPORT:	EXPERIMENT NO.:
SAD	29-02-'92	IPNS 1499

TITLE: Characterization of the Pore Structure in Activated Carbons

AUTHORS AND AFFILIATIONS: John Kieffer, Depar. of Matl's Sci & Eng., Univ. of Illinois

DATES OF EXPERIMENT: Nov. '91

☒ APPROVED BY PROGRAM COMMITTEE, OR

☐ PART OF INSTRUMENT SCIENTIST ALLOCATION

REPORT RECEIVED:

EXPERIMENTAL REPORT (or Abstract of Publication)

In this experiment we used small-angle neutron scattering for the characterization of small internal pores in activated carbon fibers, information that is difficult to access with other techniques. The principal conclusion of this work is that the chemical activation process of carbons involves the erosion of larger size domains without changing the structure of the adsorption sites on the surface itself. The higher adsorption capacity results from the opening of passageways that grant better access to internal pores.

These conclusions were based on an analysis of the scattering intensities for which we developed a new method. Our method is designed to eliminate truncation effects upon Fourier transforming the structure factor, by first fitting a linear combination of functionals to the raw data. The functionals are theoretical curves expected for certain extreme cases of sample geometries.

EXPERIMENTAL REPORT (CONTD.)

The publication resulting from this experiment:

J. Kieffer, "Investigation of the transitional pore structure of activated carbon fibers by small angle neutron scattering", *J. Appl. Phys.* 72, 5649-56 (1992)

Abstract

The small angle neutron scattering technique was used to determine the geometry of transitional pores in activated carbon fibers, as a function of the degree of activation. A refined numerical method for the data reduction is introduced. This procedure allows one to determine the characteristic size of structural features from density-density correlation functions. Based on this analysis, the activation of the fibers can be described as an erosion process, producing a microporous granular structure. The largest structural features have a radius of gyration of approximately 260 Å. These define the pore structure. The size of these granules is reduced as the activation treatment progresses and the specific surface area increases. A smaller feature, with a radius of gyration of close to 80 Å, was also observed. The size of this structural element is not affected by the activation process. The description of the pore structure within the bulk of the fibers, as deduced from the scattering data, is consistent with scanning electron microscope pictures of the surface of the fibers.

INSTRUMENT USED: SAD	DATE OF REPORT: 8/11/92	EXPERIMENT NO.: 1560

TITLE: SANS from D_2OSwollen Reverse Osmosis and Ultrafiltration Membranes

AUTHORS AND AFFILIATIONS: S. Kulkarni and S. Krause, Rensselaer Polytechnic Inst.
P. Thiyagarajan, ANL

DATES OF EXPERIMENT: June 4-6, 1992

CHECK ALL APPLICABLE BOXES:

- [X] APPROVED BY PROGRAM COMMITTEE
- [ ] INSTRUMENT SCIENTIST ALLOCATION
- [ ] DO NOT PUBLISH
- [ ] PROPRIETARY RESEARCH
- [ ] PRT ALLOCATION

EXPERIMENTAL REPORT (or Abstract of Publication)

INTRODUCTION

These experiments were aimed at elucidating the pore structure of synthetic Reverse Osmosis (RO) and Ultrafiltration (UF) membranes. Another objective of this study was to investigate whether or not pores exist in the surface ("skin") layer of asymmetric RO membranes.

EXPERIMENTAL

A multilayered sample of ultrathin (~ 1000 Å thick) cellulose acetate (CA) films, referred to as active layers, was studied because these film mimic the properties of the skin layer in RO membranes. Samples of an asymmetric CA UF membrane, a CA RO membrane, a Polysulfone UF membrane and a polyamide composite RO membrane were also studied. In all cases small-angle neutron scattering (SANS) was carried out first on dry membranes and then on D_2O swollen membranes. A constant incoherent background of 0.12 cm^{-1} was subtracted in the case of all CA membranes. While this is not quite accurate (especially at low Q), we were unable to run a suitable incoherent scatterer (such as a piece of non porous CA film). Such a sample will be run some time in the future.

RESULTS

The dry active layer sample exhibited mainly incoherent scattering although there was a small coherent scattering component at low Q. Figure 1 shows a log-log scattering plot for the D_2O swollen CA active layers. The absence of Porod's law dependence at high Q indicates the possibility that very small scattering structures (pores) may be present, although deviation from the fourth power relationship may also arise due to a roughness of the pore surfaces (resulting in a fractal dimension larger than 2.0). In any case the strong forward scattering confirms the existence of (D_2O swollen) porous regions in the membrane. A Debye-Bueche two phase approximation as described by Moritani[1] was used in the analysis of the data. An estimate for the short range correlation length of ~ 10 Å was obtained from the high Q region, which most likely corresponds to the size of interstitial pores formed due to close packing of polymer "nodules" or primary particles[2]. The low Q region shows the presence of multiple long range correlation lengths, which probably correspond to the sizes of the "nodules", roughly 150 - 300 Å in diameter.

Figure 2 shows the scattering curves for the dry and D_2O swollen samples of asymmetric CA RO membranes. As in the case of the active layers there is no region of Porod's law dependence. The two-phase model gave a value of 9 Å for the short range correlation length and presence of multiple long range correlations (~ 200 - 300 Å) was observed.

Figure 3 shows the scattering curve for dry and D_2O swollen CA UF membranes. Both curves follow Porod's law quite well at high Q. This indicates that the pore surface is smooth and very well defined with a fractal dimension of 2.0. The two phase approximation gave a single value of correlation length (for the entire Q region) of ~180 Å for the D_2O swollen membrane and ~ 150 Å for the dry membrane.

Data obtained for polysulfone UF membrane and the composite RO membrane showed trends similar to the CA UF membrane and CA RO membrane respectively, but this data has not been included here due to limitations of space.

REFERENCES

1. M. Moritani, T. Inoue, M. Motegi, and H. Kawai, Macromolecules, 3, 433 (1970).

2. R. D. Schultz and S. K. Asunmaa, Recent Prog. Surf. Sci., 3, 291 (1970)

Figure 1. I vs Q plot for D_2O swollen CA active layers

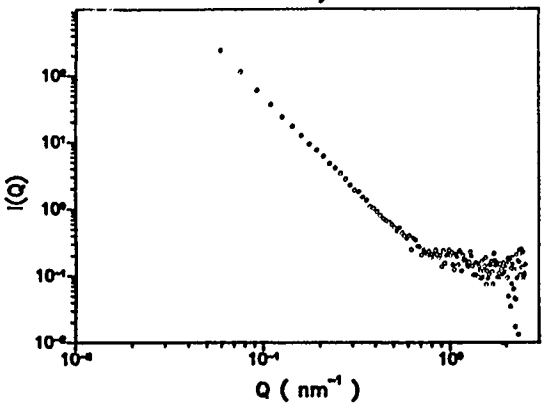


Figure 2. I vs Q plot for dry and D_2O swollen CA RO membrane

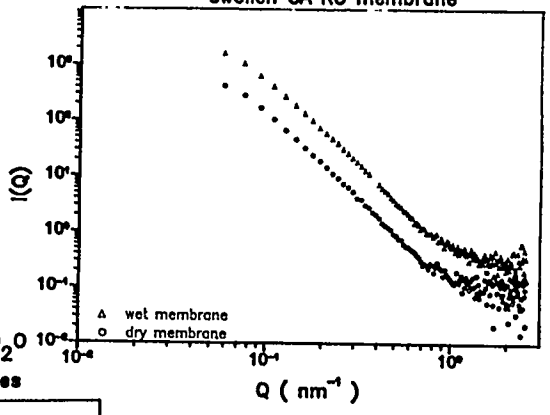
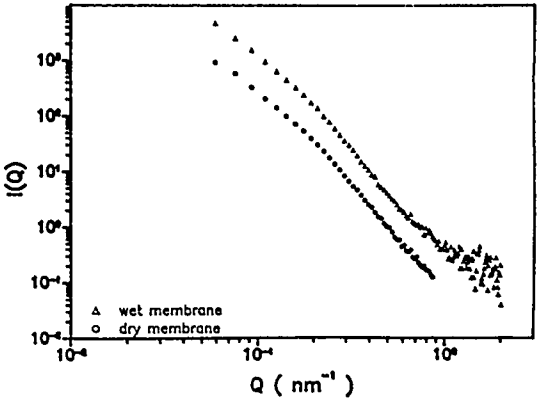


Figure 3. I vs Q plot for dry and D_2O swollen CA UF membranes



INSTRUMENT USED: SAD	DATE OF REPORT: June 25, 1992	EXPERIMENT NO.:

TITLE: Block Copolymers

AUTHORS AND AFFILIATIONS: C.W. Lantman - Miles, Inc.; P. Thiyagarajan - IPNS

DATES OF EXPERIMENT: 6/4 - 6/5/91

CHECK ALL APPLICABLE BOXES:

- ☐ APPROVED BY PROGRAM COMMITTEE
- ☐ PROPRIETARY RESEARCH
- ☑ INSTRUMENT SCIENTIST ALLOCATION
- ☐ PRT ALLOCATION
- ☐ DO NOT PUBLISH

EXPERIMENTAL REPORT (or Abstract of Publication)

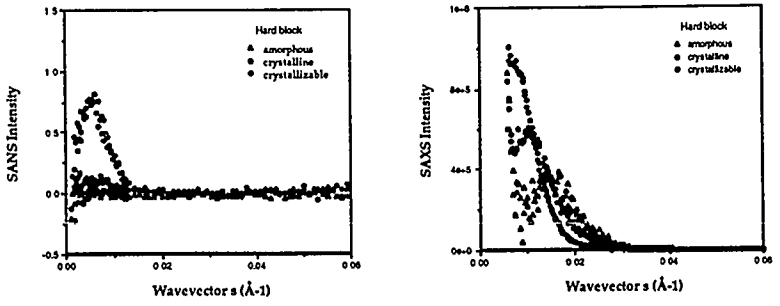
This work examines the influence of relative miscibility and crystallizability in determining the morphology of block copolymers. This phenomenon is of large practical importance in such technological applications as thermoplastic elastomers and reaction-injection molding processes. It is also of fundamental scientific interest to determine what factors control the state of microphase separation in block copolymer systems.

In the current study, we examine polyurethane block copolymers. These materials are known to microphase separate into hard and soft domains.(1) Here we consider copolymers of matched block ratios but with differing hard segments. The hard segment is chosen to be either amorphous or crystalline at room temperature and to have known solubility in the soft phase. Specifically, we examine copolymers of poly(butylene adipate) polyol and either 4,4'-dicyclohexylmethane diisocyanate or 4,4'-diphenylmethane diisocyanate. Additionally, the hard segments are synthesized using 2,2,3,3,-d4-1,4-butanediol as the chain extender. This effectively labels the hard blocks and enables the use of small-angle neutron scattering (SANS).

It is of interest to compare the scattering results obtained from SANS with those obtained independently by X-ray scattering (SAXS). A representative comparison is shown in the following two figures. The SAXS patterns were collected with a slit geometry (Kratky camera) and hence have been corrected for smearing effects.

Previous SANS investigations of polyurethane copolymers have focused on the single chain radius of gyration.(2, 3) In this study, we concentrate on the long period as calculated from the peak position. This spacing is characteristic of the average separation between hard segment domains.(4) In each case, the spacing determined by SAXS is 80-85% smaller than when measured by SANS. The cause of this difference is not yet known.

EXPERIMENTAL REPORT (CONTD.)



The results reveal the dimension and degree of perfection of microphase separation present in these systems. The copolymer containing amorphous hard blocks do not assemble into well-defined morphologies. This is confirmed by the absence of a strong peak in the SANS curve. Those systems containing crystallizable hard blocks, on the other hand, form strongly microphase separated domains. The size and degree of perfection in these domains appears to be controlled by a balance between the crystallization energy and the miscibility with the soft phase.

It is noteworthy that these findings correlate well with the observed physical properties of the materials. Those copolymers containing crystallizable hard blocks form more cleanly microphase separated morphologies which in turn yield stronger physical crosslinks and superior mechanical properties.

References

1. Leung, L.; Koberstein, J.T.; Macromolecules 1986, 19, 706.
2. Cooper, S.L.; Miller, J.A.; Rubber Chem. Tech. 1986, 58, 899.
3. Cooper, S.L.; Miller, J.A.; Han, C.C.; Pruckmayr, G.; Macromolecules 1984, 17, 1063.
4. Baltá-Calleja, F.J.; Vonk, C.G.; *"X-Ray Scattering of Synthetic Polymers"*, Elsevier, Amsterdam 1989.

INSTRUMENT USED:	DATE OF REPORT:	EXPERIMENT NO.:
SAD	July 26, 1991	1439

TITLE:

Effect of Sequence Distribution on Copolymer Adsorption

AUTHORS AND AFFILIATIONS:

C. W. Lantman - Mobay M. Galvin - AT + T A. C. Balazs - Pitt

DATES OF EXPERIMENT: June 5 - 7, 1991

☑ APPROVED BY PROGRAM COMMITTEE, OR

☐ PART OF INSTRUMENT SCIENTIST ALLOCATION

REPORT RECEIVED:

EXPERIMENTAL REPORT (or Abstract of Publication)

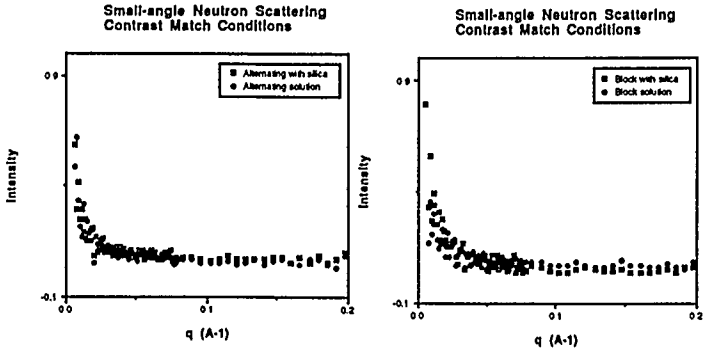
This work examines the role of sequence distribution in copolymer adsorption. The selective adsorption of copolymers at solid-fluid interfaces is technologically very important. Notable practical examples are the steric stabilization of particulate dispersions and the fabrication of thin films. Since copolymer adsorption is driven by competing solvation effects, the composition and distribution of lyophobic segments within the polymer chain is important. These measurements are important for comparison with ongoing theoretical work [1].

The adsorption system consisted of copolymers of polystyrene (PS) and polymethylmethacrylate (PMMA), silica particles, and partially deuterated 1,2,3,4-tetrahydronapthalene (Tetralin) whose composition was calculated to be at contrast match with the silica. Since the scattering length densities of the solvent and particle were equal under these contrast match conditions, the observed scattering arises only from the adsorbed polymer layer.

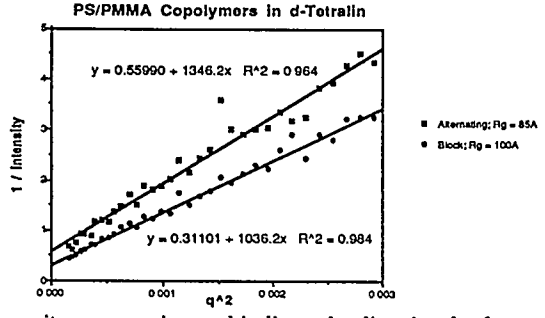
This is a relatively good solvent for PS (χ = .1-.2) and only a moderate solvent for PMMA (χ = .9-1.0) and hence has a large difference in interaction energy between the two comonomers. In this way, we were able to study polymer adsorption driven purely by competing solvation effects.

Due to time limitations, it was not possible to complete our studies however we nonetheless determined several interesting phenomena. First, we demonstrate that it is possible to perform measurements at contrast-match conditions in this system.

Second, we found that the difference in interaction energy between Tetralin-PS and Tetralin-PMMA is not sufficient to drive adsorption of the alternating copolymer. This can be seen below where the scattering profiles for solutions with and without silica particles are compared. An analogous result was found when block copolymers were used. This result is more surprizing since the associative comonomers are grouped into blocks and hence there is a stronger local driving force for adsorption. Nonetheless we do not observe adsorption. This is an interesting result because it indicates that an unfavorable solvent environment as well as a large difference in interaction energy is required for adsorption to occur.



Since these copolymers remain freely dissolved in solution under these conditions, it is possible to determine the Rg of the copolymer from the scattering profile. As shown below, the alternating copolymer, which has a Mw of 259,000, has a Rg of ~85Å and the block copolymer, whose Mw = 282,000, has a Rg of ~100Å. These values are consistent with the solvent conditions. The chain dimensions represent a balance between the unfavorable PMMA-Tetralin interactions and the less costly PS-Tetralin interactions. Hence the overall copolymer chain dimensions are significantly collapsed relative to a pure PS chain of the same mass.



These results are quite encouraging and indicate the direction for future study. In order for adsoprtion to occur, it is necessary to have both a large difference in interaction energy and an attraction to the surface. For this reason, we will next study adsorption in a different solvent, one which is poor for one block and marginal for the second. In this way, we should be able to drive adsorption.

1. Balazs, A.C.; Gempe, M.; Lantman, C.W.; Macromolecules 1991, 24, 168.
2. Stober, W.; Fink, A.; Bohn, E.; J. Colloid Interface Sci. 1968, 26, 62.
3. Cosgrove, T.; Finch, N.A.; Webster, R.P.; Macromolecules 1990, 23, 3353.
4. Cosgrove, T.; Heath, T.G.; Ryan, K.; Macromolecules 1987, 20, 2879.

INSTRUMENT USED: SAD	DATE OF REPORT: June 25, 1992	EXPERIMENT NO.: 1545

TITLE: Copolymer Adsorption

AUTHORS AND AFFILIATIONS: C.W. Lantman - Miles, Inc.; P.Thiyagarajan - IPNS
A.C. Balazs - UPitt; M. Galvin - AT&T Bell Labs

DATES OF EXPERIMENT:
4/4 - 4/6/92

CHECK ALL APPLICABLE BOXES:

- ☑ APPROVED BY PROGRAM COMMITTEE
- ☐ INSTRUMENT SCIENTIST ALLOCATION
- ☐ DO NOT PUBLISH
- ☐ PROPRIETARY RESEARCH
- ☐ PRT ALLOCATION

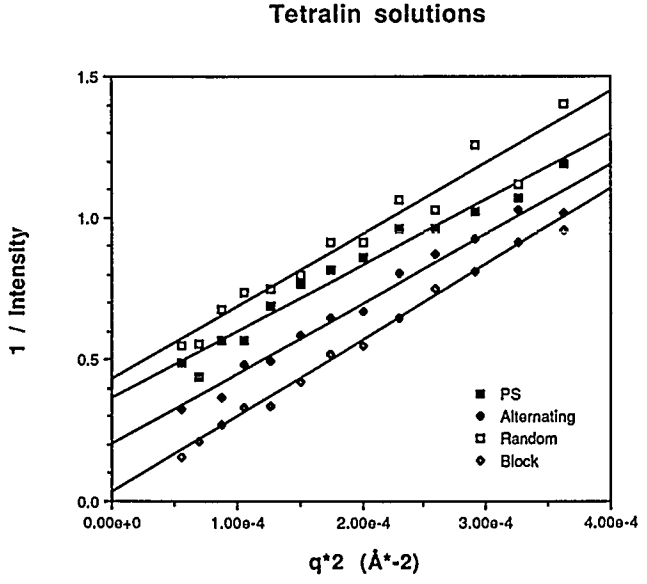
EXPERIMENTAL REPORT (or Abstract of Publication)

This study explores the solution behavior of copolymers and determines the relative roles of sequence distribution and solvent-polymer interaction strength. Understanding and controlling the solution conformation of copolymer chains is of technological importance as well as fundamental scientific interest. Similar copolymer systems find practical utility as viscosity modifiers and interfacial agents.

The solution properties of these copolymer systems are presumably dictated by chain conformation. Since the final conformation assumed by the copolymer chain will be governed by competing solvent-monomer interactions, the location and distribution of lyophobic segments within the copolymer chain should be important. The relative strength of the interaction between the solvent and each comonomer should also play a critical role. In order to determine the influences of these factors on chain conformation, we studied a series of copolymers of polystyrene (PS) and polymethylmethacrylate (PMMA) with specific sequence distributions. The solvents of choice were perdeuterated 1,2,3,4-tetrahydronapthalene (Tetralin-d12) and perdeuterated tetrahydrofuran (THF-d8). In each case, comparisons were made to homopolystyrene in the same solvent. We focus our attention on polymer solutions well below the overlap concentration, c*.

In the case of Teralin-d12, the PS segments of the copolymer are in a relatively good solvent environment ($\chi_{PS\text{-}Tetralin}$ = .1-.2) while the PMMA segments are in a poor solvent ($\chi_{PMMA\text{-}THF}$ > 1.0). Hence there is a large difference in the solvent interaction energies between the two comonomers.

Through use of the Debye formalism (1) with appropriate corrections for limited angular range (2) it was possible to determine the radius of gyration Rg as a function of sequence distribution. Through calibration with homopolystyrene of known molecular weight, it was possible to obtain absolute molecular weight values as well. Representative modified Zimm plots are shown in the following figure.



In the case of THF-d8, both PS and PMMA segments are in a relatively good solvent environment and hence the selective solvent effect should be largely mitigated. To verify this, we repeated analogous experiments in THF-d8 to those described above.

The results of this study show that copolymer chain conformation in solution is dependent upon sequence length n_s and solvent-polymer interaction strength χ. Our findings suggest that a critical relationship exists for the product $n_s\chi$ in governing chain conformation and hence solution properties.

References

1. Debye. P.; J. Phys. Colloid Chem. 1947, 51, 18.
2. Ullman, R.; J. Polym. Sci., Polym. Phys. 1985, 23, 1477.

INSTRUMENT USED: SAD	DATE OF REPORT: 21 July 1994	EXPERIMENT NO.:

TITLE: Small Angle Neutron Scattering in $Ni_{1-x}Al_x$ Alloys

AUTHORS AND AFFILIATIONS: A. C. Lawson and J. D. Cotton, LANL; R. D. Noebe, NASA Lewis Research Center; P. Thiyagarajan and D. Wozniak, ANL

DATES OF EXPERIMENT: 17 May 1994

CHECK ALL APPLICABLE BOXES:

- ☐ APPROVED BY PROGRAM COMMITTEE
- ☐ INSTRUMENT SCIENTIST ALLOCATION
- ☐ DO NOT PUBLISH
- ☐ PROPRIETARY RESEARCH
- ☐ PRT ALLOCATION

EXPERIMENTAL REPORT (or Abstract of Publication)

NiAl is a CsCl-structured intermetallic which is of commercial interest as a turbine engine material due to its high melting point and good oxidation resistance. Although highly ordered, this compound displays a large solubility range. Deviations from stoichiometry are accommodated by the presence of either antisite (Ni_{Al}) or vacancy (V_{Ni}) constitutional point defects. The same deviations are accompanied by large increases in the ambient flow stress. Based on various indirect measurements, it has been surmised that these point defects cluster to form barriers to dislocation motion. In fact, to produce the large strengthening effects observed, slip obstacles (defect clusters) on the order of at least 10 Å should be present. Electron microscopy has not revealed such clusters, although anomalous diffraction phenomena in off-stoichiometric alloys have been variously interpreted as: strain due to local ordering, premartensitic effects or local "omega" defects produced by phonon trapping. At present there are insufficient data to determine whether these phenomena are related to clustering. Such a relationship would explain the sensitivity of the mechanical properties to stoichiometry and provide guidance for the development of this compound for practical applications.

We purchased one day of beam-time on SAD to examine the small-angle scattering from NiAl alloys. We examined the scattering from 4 $Ni_{1-x}Al_x$ alloys and an additional Cr bearing specimen which is not discussed in this report. Log-log plots from the scattering data are shown in Fig. 1. The results were scaled to the incoherent scattering of Ni, which was subtracted from the data. Guinier plots are shown in Fig. 2, and the derived Guinier constants are given in Table 1. For further data

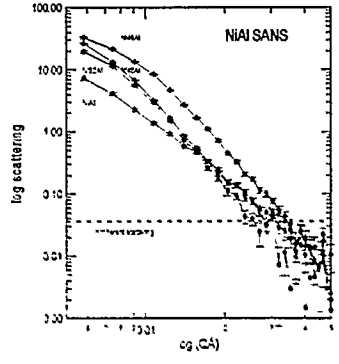


Fig. 1. Small angle scattering for NiAl alloys.

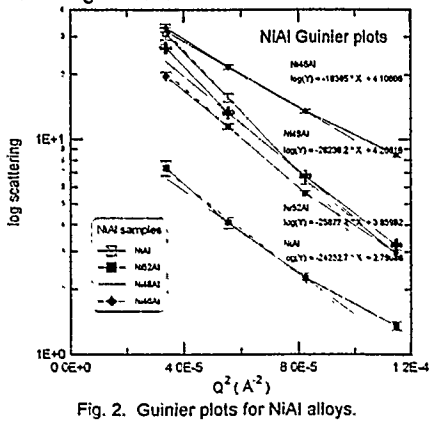


Fig. 2. Guinier plots for NiAl alloys.

Table 1. Guinier constants for NiAl alloys.

Sample	R_g (Å)	V_s (10^{-17} cm^3)	C_g (cm^{-1})	$C_g/(V_s^2.(\Delta c)^2)(10^{12}$ $cm^{-3})$
NiAl	270	8.24	93,7	1.52
Ni52Al	279	9.10	273.1	1.01
Ni48Al	291	10.30	387.6	1.12
Ni46Al	235	5.44	350.7	3.62

analysis, we *assumed* that the scattering is caused by voids; these have previously been observed in NiAl single crystals [1]. Under this hypothesis, we can plot the volume fraction of voids versus composition, as in Fig. 3. It is intriguing to note that the concentration dependence of the void volume fraction is very similar to that reported for the yield strength. But there are potential problems

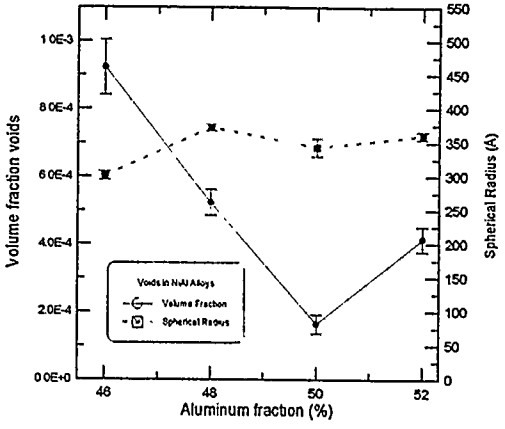


Fig. 3. Spherical radius and volume fraction for postulated voids in NiAl alloys.

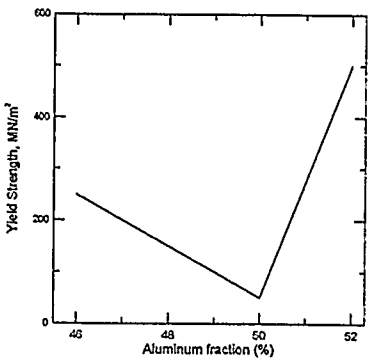


Fig. 4. Schematic yield strength vs. composition.

with this interpretation, as it is difficult to see how voids can provide the observed strengthening [2].

A electron microscopic search for voids is underway. Meanwhile, the trend of Fig. 3 ineeds to be better established: we are planning to repeat these experiments on more NiAl samples with different compositions and quenching conditions

References

[1] J. E. Epperson, K. W. Kerstenberg, D. Berner, G. Kostorz and C. Ortiz, Phil. Mag. A 38 529 (1978)

[2] R. D. Noebe, R. R. Bowman and M. V. Nathal, Int. Mat. Rev. 38 193 (1993).

INSTRUMENT USED:	DATE OF REPORT:	EXPERIMENT NO.:
SAD	August 2, 1990	1321

TITLE:

Critical phase transition of binary fluids in random media

AUTHORS AND AFFILIATIONS:

M.Y.Lin, NIST/S.K.Sinha, BNL/J.M.Drake, Exxon/X.L.Wu, U.of Pittsburgh

DATES OF EXPERIMENT: May 8-10, 1990

☒ APPROVED BY PROGRAM COMMITTEE, OR

☐ PART OF INSTRUMENT SCIENTIST ALLOCATION

REPORT RECEIVED:

EXPERIMENTAL REPORT (or Abstract of Publication)

We study the phase separation process of a binary fluid in a porous medium, Vycor glass. The fluid trapped in the porous glass is a mixture of H_2O, D_2O and 2,6 lutidine near its critical composition. Due to the difference in the affinity of glass surface to water and lutidine, the porous structure of the glass may be considered to exert a type of chemical random field on the trapped binary fluid.

The experiment was performed at ANL/IPNS using the small angle diffractometer (SAD). We found that the phase separation process was broadened considerably in temperature, with the critical fluctuation dominated scattering continuing to increase from 20° C to 80° C. The large Q behavior of the scattering intensity can be expressed as $I(Q) \sim Q^{-n}$, with $n \approx 2$ at room temperature (before phase separation) to $n \approx 4$ at the highest temperature. This suggests that a Lorentzian-squared term in the scattering grows as the phase separation progresses, in addition to the Lorentzian term present at the low temperature. Similar behavior has been found for the same binary fluid system trapped in a cross-linked gel medium, and is predicted by the random field Ising model and a theory of deGennes.

A derivatized Vycor sample was also used in the experiment, in a hope that derivatized surfaces in the porous glass may change the preferential wetting of the binary fluid. No qualitative change, however, was seen in the scattering compared with that of the regular Vycor samples.

The H_2O/D_2O/lutidine was chosen so that in the homogeneous phase almost complete contrast matching should have occurred with the Vycor. In fact, the Vycor scattering was decreased by a factor of ~ 100, but the existence of preferential wetting of lutidine prevented the complete extinction of bulk Vycor scattering. The results are currently being analyzed in terms of static wetting layers plus critical fluctuations as giving arise to the scattering.

We consider this a successful but unfinished experiment. We were given 2 days time in asking for an estimated 5 day duration. Therefore, consideration to grant more time in using the SAD to continue the experiment is greatly appreciated.

EXPERIMENTAL REPORT (CONTD.)

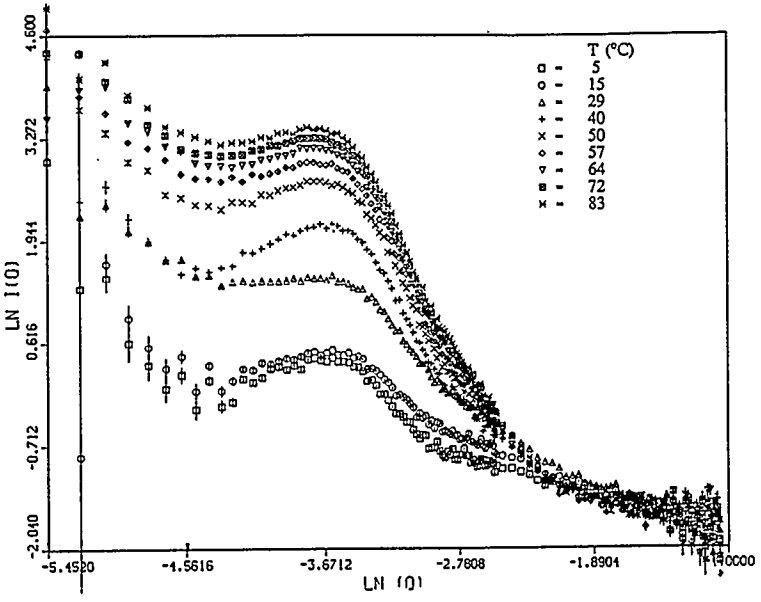


FIG. 1 Neutron scattering intensity I(Q) as a function of Q of binary fluid trapped inside a Vycor glass sample, for a temperature range of 5° C to 85° C. The peak at $Q \approx 0.02$ /Å is due to the structure of Vycor. However, the overall increase in the intensity is due to the phase separation process.

INSTRUMENT USED	DATE OF REPORT	EXPERIMENT NO.:
SAD	August 3, 1989	1148

TITLE: SANS Studies on the Formation of Sol-Clay Complexes and Its Dependance on pH and Particle size

AUTHORS AND AFFILIATIONS: A. Moini, C. A. Polansky, J. Amarasekera, and T.J. Pinnavaia, Michigan State University, East Lansing, Michigan 48824; and P. Thiyagarajan, Argonne National Laboratory, Argonne, Il 60439.

DATES OF EXPERIMENT: March 29-30 1990

[x] APPROVED BY PROGRAM COMMITTEE, OR

[ ] PART OF INSTRUMENT SCIENTIST ALLOCATION

REPORT RECEIVED:

EXPERIMENTAL REPORT (or Abstract of Publication)

Formation of new sol-clay composite products has been established by our previous SANS studies[1-4]. All these results were obtained on solid silica-montmorillonite composites prepared under acidic conditions. We now report the preliminary results from our systematic study where we have evaluated the effect of pH and the type of clay on silica sol. The results are summarized below.

I. Silica-montmorillonite complexes. These studies centered on silica-montmorillonite complexes in aqueous solutions. The complexes were prepared both at the silica sol's isoelectric point and at pHs below the isoelectric point to study how negatively charged silica and positively charged silica interact with clay platelets.The results revealed that silica sol aggregate both in acidic and alkaline aqueous solutions. The scattering data for the silica aggregates in alkaline solutions conform to an ellipsoidal model, with a cross sectional diameter of about 45 Å and a length of 750 Å or more. In the presence of Na^+-montmorillonite clay these long aggregates break down to form clay-sol composites, through the delamination of clay layers. Addition of acid to these sol-clay mixtures results in aggregation of these particles. Treatment of the silica sol with acid prior to the reaction with clay, prevented the aggregation, and resulted in higher binding interactions between the sol and clay. It is clear that the reduction in pH is an essential step in synthesis of sol-clay complexes.

The SANS data on solid products isolated from these slurries also confirmed the above observations. The data for the pure silica product showed a high degree of scattering in the low-Q region. The log-log plot showed a slope of -3.21(2) at low Q values indicating the formation of a large extended network of the smaller particles. The scattering curves for the silica-montmorillonite products formed under basic conditions showed the presence of highly aggregated silica, with some contribution to the scattering from clay platelets. The power-law regime due to clay scattering for 10:1 complex had a slope of -2.26(4). In comparison, the 10:1 silica-clay product prepared by reacting the clay with acidified silica had a log-log slope of -1.55(6). These results clearly indicate that in basic conditions the clay layers are not delaminated as efficiently as in acidic conditions.

II. Silica-Fluorohectorite and Silica-Laponite® Complexes. The charge densities of these clays are quite different from Na^+-montmorillonite. Fluorohectorite has a higher charge density [Cation Exchange Capacity (CEC): 120 meq/100 g] than montmorillonite (CEC: 80 meq/100 g) whereas Laponite® has a lower charge density (CEC: 48 meq/100 g). The difference in charge densities should result in different interactions with silica sol; therefore, we have studied the composites formed from the reaction of these clays with silica using SANS.

The power law regime due to clay scattering extends over a wide range in Q with slopes of -2.82(1) and -2.66(5) for 10:1 and 15:1, respectively for fluorohectorite-silica complexes. These values are much lower than those obtained for the montmorillonite products [-1.79(3) for a 4:1 silica-montmorillonite[4]]. The range of these slopes is indicative of the presence of stacked layers of fluorohectorite. It is possible that, the layers have a higher tendency of forming oriented structures even in the presence of sol particles due to their large clay particle size.

The shape of the scattering curves from Laponite®-silica composites suggest that the scattering from hydrolyzed silica, which had previously[4] given a peak at $Q = 0.0856$ Å^{-1}, had now moved to a lower Q regions. This is an indication of the formation of larger particles by the silica sol in the presence of Laponite®. Attempts to subtract the Laponite® scattering from the silica-Laponite® data made little change in the overall shape of the scattering curve. These preliminary results suggest that in the presence of Laponite® the interaction between silica and clay is not favorable, therefore the aggregation of the silica sol is promoted.

In order to further understand the interactions between silica sol and fluorohectorite and Laponite® we plan to study these complexes in aqueous suspensions. The results of these studies will be compared to results obtained for montmorillonite-silica composite, giving a broader picture of interactions between clays and silica sol.

References

1. IPNS Report, July 12, 1987, IPNS Progress Report, 1988.
2. IPNS Report for Experiment 973.
3. IPNS Report for Experiment 876, IPNS Progress Report, 1988.
4. Moini, A.; Pinnavaia, T. J.; Thiyagarajan, P.; White, J. W. *J. Appl. Crystallogr.* 1988, *21*, 840.

INSTRUMENT USED:	DATE OF REPORT:	EXPERIMENT NO.:
Small Angle Diffractometer	August 2, 1991	1246

TITLE:

Effect of Lattice Mismatch Strain on Phase Separation in Ni-Al-Si Alloys.

AUTHORS AND AFFILIATIONS:

G. Muralidharan, H. Chen, University of Illinois and J.E. Epperson, Argonne National Lab

DATES OF EXPERIMENT:

☒ APPROVED BY PROGRAM COMMITTEE, OR

☐ PART OF INSTRUMENT SCIENTIST ALLOCATION

REPORT RECEIVED:

EXPERIMENTAL REPORT (or Abstract of Publication)

Objective: The aim of the current series of experiments is to study the effect of lattice mismatch on the coarsening kinetics of γ' precipitates in Ni-Al-Si alloys. The lattice mismatch between γ and γ' can be altered by varying the Si to Al ratio.

Experimental: Three different compositions of the ternary Ni-Al-Si alloys were selected. The compositions and the calculated lattice mismatch values ($\delta = (a_{\gamma'} - a_{\gamma})/a_{\gamma}$) are shown below:

1. Ni-8.1 at.% Si- 3.9 at.% Al (-0.02%)
2. Ni-9.5 at.% Si- 2.5 at.% Al (-0.15%)
3. Ni- 11.0 at.% Si- 1.0 at.% Al (-0.28%)

Polycrystalline samples of the above nominal compositions were prepared by arc melting, were homogenized, solutioned at 1020° C for 6 hours in an evacuated quartz capsule and quenched rapidly to avoid formation of γ'.

In-situ SANS measurements were carried out on IPNS-SAD facility using time resolved counting mode. In the first cycle of experiments, three sets of measurements were carried out on alloy 2, one at each of the following temperatures: 481° C, 531°C and 582°C. In the second round of experiments, similar measurements were done at the same temperatures, but this time on alloy 3. Further, one set of measurements was carrried out on alloy 1 at 531°C. All data collected were corrected for parasitic scattering.

Results: Ostwald ripening theories predict the following temporal evolution for the average particle size:

$$R^3 - R_0^3 = K(t - t_0)$$

where R is the average radius at time t
R_0 is the average radius at time t_0
K is the rate constant

For spherical precipitates, the rate constant is given by the expression

$$K = 8\gamma C_e D V_m^2 / 9RT$$

where γ is the interfacial energy of the particle-matrix interface
C_e is the equilibrium concentration of the matrix
V_m is the molar volume.

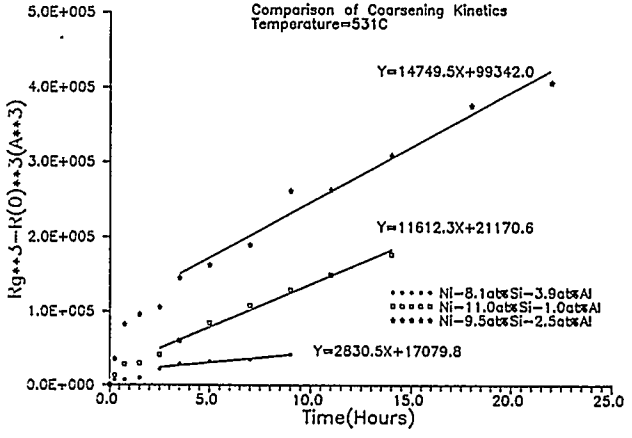
EXPERIMENTAL REPORT (CONTD.)

Fig.1 shows the variation of $R^3 - R_0^3$ with time at 531° C observed in this study, for all three alloys. Note that R here is the Guinier radius obtained from the SANS profile. It is clear that in all three cases there is a pronounced linear portion in the curve, the slope of which gives the rate constant K. By assuming that γ and C_e are not strongly dependent on the temperature, the activation enegy for coarsening in alloy 2 was found to be 39.7 kcal/mole. It is interesting to note that this value is much lower than those observed in the Ni-Si system(66.5 kcal/mole) and Ni-Al system(62.3 kcal/mole) in previous experiments done in our laboratory. It is possible that this discrepancy is due to enhanced diffusion at low temperatures from a non-equilibrium concentration of vacancies.

Another interesting feature in this study is the variation of the coarsening rate constant with composition. As the Si to Al ratio increases, the coarsening rate is first observed to increase and then decrease. Current work is focussed on understanding this behavior. Wide angle diffraction is being carried out on the samples used in the study to determine the actual value of the misfit. TEM studies are underway to look at the morphology and coherency of the precipitates. An important fact to be considered is the size of the precipitates at the beginning of the in-situ SANS study. In case of alloy 2, the samples showed significant scattering in the as-quenched condition(Guinier radius of the order of 35-45 A) whereas the alloy samples 1 and 3 aged at 531°C did not show any significant scattering in the as-quenched condition. It is possible that the precipitates in the different alloys were in different stages of coherency. It is hoped that the TEM studies will answer this question.

Future work: All the samples used in this series of experiments have been designed to have a negative misfit. The next series of experiments will be aimed at studying the effect of change in the sign of misfit on the coarsening kinetics. Other interesting questions still to be addressed include, the effect of volume fraction on the coarsening rate, morphology changes during coarsening and the effect of misfit on the scaling behavior, which will be the subject of study in future experiments.

Fig. 1



INSTRUMENT USED:	DATE OF REPORT:	EXPERIMENT NO.:
SAD	August 3, 1992	1562

TITLE:
Effect of Lattice Mismatch Strains on Phase Separation in Ni-Al-Si Alloys

AUTHORS AND AFFILIATIONS:
G. Muralidharan, H. Chen, University of Illinois and J. E. Epperson, Argonne National Labs

DATES OF EXPERIMENT:

CHECK ALL APPLICABLE BOXES:

- [x] APPROVED BY PROGRAM COMMITTEE
- [ ] INSTRUMENT SCIENTIST ALLOCATION
- [ ] DO NOT PUBLISH
- [ ] PROPRIETARY RESEARCH
- [ ] PRT ALLOCATION

EXPERIMENTAL REPORT (or Abstract of Publication)

Objective: The focus of the current series of experiments is to study the relationship between the misfit parameter (hence coherency strains) and the kinetics of coarsening of the second phase (γ') in the ternary Ni-Al-Si system.

Experimental: Four different compositions of the ternary Ni-Al-Si alloys were used. The compositions and the calculated lattice mismatch values ($\delta = (a\gamma' - a\gamma)/a\gamma$) are shown in Table I. Polycrystalline samples with the nominal compositions were prepared by arc melting, were homogenized, solutioned at 1020° C for 1 hour in flowing helium and quenched rapidly into iced brine to avoid the formation of γ'. In-situ SANS measurements were carried out on IPNS-SAD facility using time resolved counting mode. All data collected were corrected for parasitic scattering. Table I shows the alloys studied and the temperatures used in the study.

Table I. Composition, misfit parameters and coarsening temperatures for the different alloys used for the study

Alloy #	Composition	δ	Temperatures (°C)
1.	Ni- 8.1 at.% Si- 3.9 at.% Al	-0.02%	531, 600
2.	Ni- 9.5 at.% Si- 2.5 at.% Al	-0.15%	481, 531, 550, 582, 600
3.	Ni-11.0 at.% Si- 1.0 at.% Al	-0.28%	481, 531, 550, 582, 600
4.	Ni- 4.0 at.%Si- 8.0 at.% Al	+0.35%	550, 600

Results: Ostwald ripening theories predict the following temporal evolution for the average particle size:

$$R^3 - R_0^3 = K(t - t_0) \quad (1)$$

where R is the average radius at time t
R_0 is the average radius at time t_0
K is the rate constant

For spherical precipitates, the rate constant is given by the expression

$$K = 8\gamma C_e D V_m^2 / 9RT \quad (2)$$

where γ is the interfacial energy of the particle-matrix interface
C_e is the equilibrium concentration of the matrix
V_m is the molar volume.

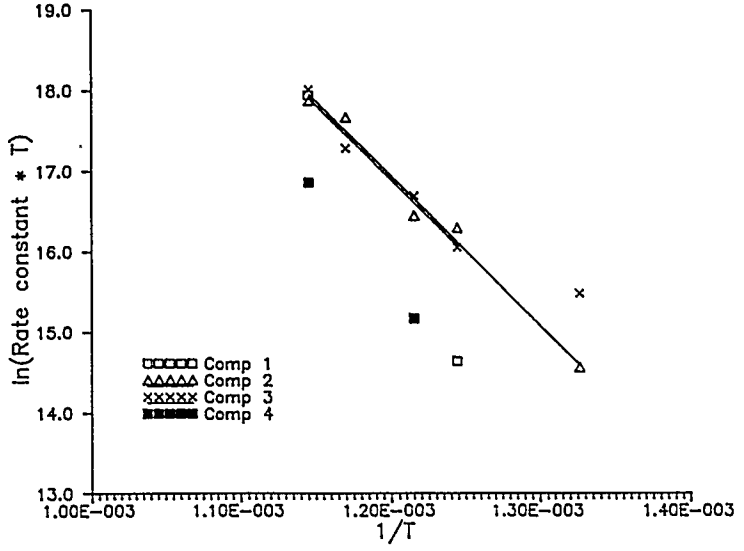
Table II shows a summary of results obtained at three different tempertures. It is interesting to note that the coarsening rate increases when the Si content increases from 4.0 at.% to 11.0 at.% although not necessarily in a monotonic manner. Note that at 531°C, Comp 2 shows a comparatively large coarsening rate and at 600°C, Comp 1 shows similar behavior. It is not clear whether this behavior is composition related or sample history dependent. Further work is necessary to clarify this point.

Table II Relationship between composition and coarsening rates.

Alloy	Si content	Coarsening rate (A^3/hour) at 531°C	550°C	600°C
Comp 4	4.0 at. %	------	4726.7	24021.4
Comp 1	8.1 at. %	2830.5	------	70674.4
Comp 2	9.5 at. %	14749.5	16766.3	65944.8
Comp 3	11.0 at. %	11612.3	21560.0	76296.3 72918.2

Fig 1 shows a plot of ln(KT) as a funtion of 1/T for all the alloys studied. Note that the activation energies for alloys of Comp 2 and 3 (given by the slope of the line) are almost identical (37.2 kcal/mole). Further information is needed to obtain a value for the activation energy for alloys 1 and 4. Rate constants obtained at additional temperatures would help confirm the value of activation energy obtained from the data available at this time.

Fig. 1 Variation of ln(KT) as a function of 1/T



INSTRUMENT USED: SAD	DATE OF REPORT: 6/28/93	EXPERIMENT NO: 1649

TITLE:
Effect of Coherency Strains on the Kinetics of Coarsening in Ni-Al-Si Alloys

AUTHORS AND AFFILIATIONS:
G. Muralidharan (University of Illinois/ANL), J. E. Epperson (MSD/ANL) and Haydn Chen (University of Illinois)

DATES OF EXPERIMENT:
10-23-92 to 10-27-92, 11-3-92 to 11-6-92

CHECK ALL APPLICABLE BOXES:

- [x] APPROVED BY PROGRAM COMMITTEE
- [ ] INSTRUMENT SCIENTIST ALLOCATION
- [ ] DO NOT PUBLISH
- [ ] PROPRIETARY RESEARCH
- [ ] PRT ALLOCATION

EXPERIMENTAL REPORT (or Abstract of Publication)

Objective: The focus of the current series of experiments is to study the relationship between the misfit parameter (hence coherency strains) and the kinetics of coarsening of the second phase (γ') in the ternary Ni-Al-Si system.

Experimental: Five different compositions in the ternary Ni-Al-Si system were used. The compositions and the calculated lattice mismatch values ($\delta = (a_{\gamma'} - a_{\gamma})/a_{\gamma}$) are shown in Table I. Polycrystalline samples with the nominal compositions were prepared by arc melting, were homogenized, solutioned at 1020° C for 1 hour in flowing helium (except for the binary Ni-Si alloys which were solutioned for 5 hours) and quenched rapidly into iced brine to avoid the formation of γ'. Single crystals of alloys with compositions 1 and 3 were grown using the vertical Bridgmann growth technique. Small disks cut from the ampoules were initially homogenized at 1100°C, then solutioned at 1020°C for 1 hour in flowing helium and were subsequently quenched in iced-brine. In-situ SANS measurements were carried out on IPNS-SAD facility using time resolved counting mode. All data collected were corrected for parasitic scattering. Table I shows the alloys studied and the temperatures used in the study.

Table I. Composition, misfit parameters and coarsening temperatures for the different alloys used for the study

Alloy #	Composition	δ	Temperatures (°C)
1.	Ni- 8.1 at.% Si- 3.9 at.% Al	-0.02%	531, 600
2.	Ni- 9.5 at.% Si- 2.5 at.% Al	-0.15%	481, 531, 550, 582, 600
3.	Ni-11.0 at.% Si- 1.0 at.% Al -	-0.28%	481, 531, 550*, 582, 600
4.	Ni- 4.0 at.%Si- 8.0 at.% Al	+0.35%	550, 600*
5.	Ni-12.5 at.% Si	-0.35%	481, 550, 600

* indicates that single crystals were also studied at the temperature

Results: Ostwald ripening theories predict the following temporal evolution for the average particle size:

EXPERIMENTAL REPORT (CONTD.)

$$R^3 - R_0^3 = K(t - t_0) \quad (1)$$

where R is the average radius at time t
R_0 is the average radius at time t_0
K is the rate constant

For spherical precipitates, the rate constant is given by the expression

$$K = 8\gamma C_e D V_m^2 / 9RT \quad (2)$$

where γ is the interfacial energy of the particle-matrix interface
C_e is the equilibrium concentration of the matrix
V_m is the molar volume.

Table II shows a summary of results obtained at three different tempertures. It is interesting to note that the coarsening rate increases when the Si content increases from 4.0 at.% to 12.5 at.% although not necessarily in a monotonic manner, except at 600°C. Note that at 531°C, Comp 2 shows a coarsening rate that is larger than that of both comp 1 and comp 3 and at 550°C, Comp 1 seems to show a similar behaviour. It is possible that this effect could be due to deviation from the overall composition of the alloy due to segregation during solidification. The composition of these alloys is being studied by x-ray analysis on the Scanning Electron Microscope (SEM). However, at this time, in the samples that have been studied, there is no evidence of significant deviation from the nominal composition of the alloys.

Table II Relationship between composition and coarsening rates.

Alloy	Si content	Coarsening rate (A^3/hour) at 481°C	531°C	550°C	582°C	600°C
Comp 4	4.0 at. %		4704.0	4726.7		24,021.4
Single Xtal						27,730.4
Comp 1	8.1 at. %		2830.5	25,320.0		95,210.0
Comp 2	9.5 at. %	2805.7	14,749.5	16,766.3	73,420.0	100,300.0
Comp 3	11.0 at. %	7021.4	11,612.3	21,560.0	99,900.0	131,700.0
Single Xtal				23,360.0		131,100.0
Ni-Si	12.5 at. %	6337.0	----------	71,290.0		494,800.0

One probable explanation for this behaviour is that it is related to the relative values of the thermal expansion coefficients of both γ and γ'. Based upon the evidence available in other systems, there is reason to believe that the γ' would have a lower thermal expansion coefficient compared to the matrix (We propose to study this in another experiment on the GPPD). Hence the alloys in which the lattice paramater of γ' is larger than that of the matrix, the misfit will tend to decrease (become more negative) with an increase in temperature thus influencing the coarsening rates. Since the experimental values of the misfit parameter are unknown at this stage, it is not possible to analyze this in further detail. The following experimental coarsening data will be required to get a better understanding of the variation of coarsening rates with composition and temperature:

1. Coarsening data at 500°C for all alloys and at 582°C for Comp 1 and Comp 4.
2. Introduce another alloy with a Si content of about 6.0 at.% and study the coarsening rate for this alloy at all relevant temperatures.

It is believed that this data together with the data from the GPPD experiments will give a more complete understanding of the effect of coherency strains on coarsening.

INSTRUMENT USED:	DATE OF REPORT:	EXPERIMENT NO:
SAD	12/15/93	1813

TITLE:
Effect of Coherency Strains on the Kinetics of Coarsening in Ni-Al-Si Alloys

AUTHORS AND AFFILIATIONS:
G. Muralidharan (University of Illinois/ANL), J. E. Epperson (MSD/ANL) and Haydn Chen (University of Illinois)

DATES OF EXPERIMENT:
10-23-92 to 10-27-92, 11-3-92 to 11-6-92, 10-12-93 to 10-15-93

CHECK ALL APPLICABLE BOXES:

- [x] APPROVED BY PROGRAM COMMITTEE
- [ ] INSTRUMENT SCIENTIST ALLOCATION
- [ ] DO NOT PUBLISH
- [ ] PROPRIETARY RESEARCH
- [ ] PRT ALLOCATION

EXPERIMENTAL REPORT (or Abstract of Publication)

Objective: The focus of the current series of experiments is to study the relationship between the misfit parameter (hence coherency strains) and the kinetics of coarsening of the second phase (γ') in the ternary Ni-Al-Si system.

Experimental: Seven different compositions in the ternary Ni-Al-Si system were used. The compositions and the calculated lattice mismatch values ($\delta = (a_{\gamma'}-a_{\gamma})/a_{\gamma}$) are shown in Table I. Polycrystalline samples with the nominal compositions were prepared by arc melting, were homogenized, solutioned at 1020° C for 1-5 hours in flowing helium and quenched rapidly into iced brine to avoid the formation of γ'. Single crystals of alloys of compositions 1 and 3 were grown using the vertical Bridgmann growth technique. Small disks cut from the ampoules were initially homogenized at 1100°C, then solutioned at 1020°C for 1 hour in flowing helium and were subsequently quenched in iced-brine. In-situ SANS measurements were carried out on IPNS-SAD facility using time resolved counting mode. All data collected were corrected for parasitic scattering. Table I shows the alloys studied and the temperatures used in the study.

Table I. Composition, misfit parameters and coarsening temperatures for the different alloys used for the study

Alloy #	Composition	δ	Temperatures (°C)
1.	Ni- 8.1 at.% Si- 3.9 at.% Al	-0.02%	531, 600
2.	Ni- 9.5 at.% Si- 2.5 at.% Al	-0.15%	481, 531, 550, 582, 600
3.	Ni-11.0 at.% Si- 1.0 at.% Al -	-0.28%	481, 531, 550*, 582, 600
4.	Ni- 4.0 at.%Si- 8.0 at.% Al	+0.35%	550, 600*
5.	Ni- 6.0 at.%Si-6.0 at.% Al	+0.17%	550, 600
6.	Ni-10.25at.% Si-1.25 at.% Al	-0.26	550, 582, 600
7.	Ni-12.5 at.% Si	-0.35%	481, 550, 600

* indicates that single crystals were also studied at the temperature

Results: Ostwald ripening theories predict the following temporal evolution for the average particle size:

$$R^3-R_0^3=K(t-t_0) \quad (1)$$

where R is the average radius at time t
R_0 is the average radius at time t_0
K is the rate constant

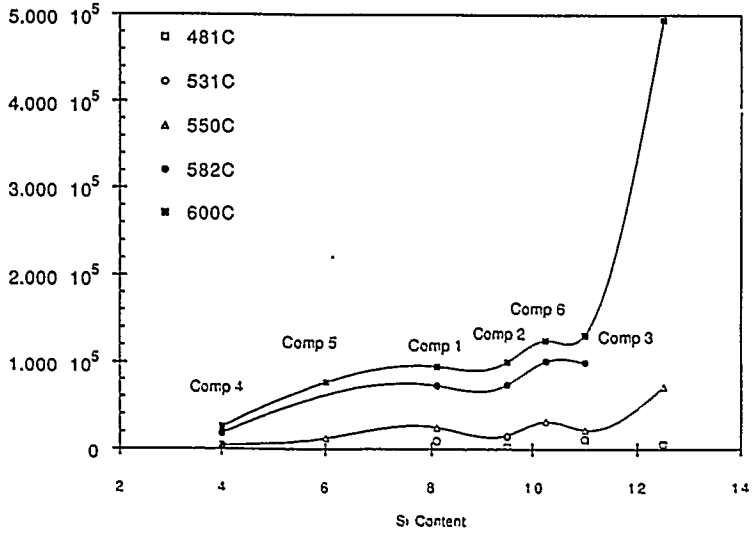
For spherical precipitates, the rate constant is given by the expression

$$K= 8\gamma C_e D V_m^2/9RT \quad (2)$$

where γ is the interfacial energy of the particle-matrix interface
C_e is the equilibrium concentration of the matrix
V_m is the molar volume.

Fig. 1 shows the variation of coarsening rates as a function of the Si content at the different temperatures. The data points are connected by a simple spline fit. Note that the overall trend is for the coarsening rate to increase with an increase in the Si content. This trend is significantly altered at around a composition of 8-10 at. % Si. There seems to be a small lowering of the coarsening rate around 9.0 at. % Si. A calculation of the misfit parameters (see Table I) shows that the misfit tends to zero at around 8.0 at. % Si. However, since these values have been calculated based on the assumption that the tie-lines pass through the Ni- corner of the phase diagram and hence are only approximate, experiments are currently being carried out to measure the lattice parameters of γ and γ' in these alloys, to see if this decrease in coarsening rate corresponds to a zero misfit parameter value. To competely account for the temperature dependence of the variation of coarsening rates with composition, one also has to measure the misfit as a function of temperature accounting for the difference in thermal expansion coefficients of γ and γ'. A series of experiments have been proposed to measure both the thermal expansion coefficients and the actual lattice parameters of the two phases in these alloys. Diffusion coefficients in the ternary system are being measured to account for the variation in coarsening rates with changes in the diffusion coefficients with composition. Thus, a complete analysis of the contribution from the misfit strains should be possible once the results from these experiments become available.

Fig. 1 Coarsening Rates vs. Composition



INSTRUMENT USED:	DATE OF REPORT:	EXPERIMENT NO:
SAD	8/01/94	1813

TITLE:
Effect of Coherency Strains on the Kinetics of Coarsening in Ni-Al-Si Alloys

AUTHORS AND AFFILIATIONS:
G. Muralidharan (University of Illinois/ANL), J. E. Epperson (MSD/ANL) and Haydn Chen (University of Illinois)

DATES OF EXPERIMENT:
10-23-92 to 10-27-92, 11-3-92 to 11-6-92, 10-12-93 to 10-15-93

CHECK ALL APPLICABLE BOXES:

- [x] APPROVED BY PROGRAM COMMITTEE
- [ ] INSTRUMENT SCIENTIST ALLOCATION
- [ ] DO NOT PUBLISH
- [ ] PROPRIETARY RESEARCH
- [ ] PRT ALLOCATION

EXPERIMENTAL REPORT (or Abstract of Publication)

Objective: The focus of the current series of experiments is to study the relationship between the misfit parameter (hence coherency strains) and the kinetics of coarsening of the second phase (γ') in the ternary Ni-Al-Si system.

Experimental: Nine different compositions in the ternary Ni-Al-Si system were used. The compositions and the calculated lattice mismatch values ($\delta = (a_{\gamma'}-a_{\gamma})/a_{\gamma}$) are shown in Table I. Polycrystalline samples with the nominal compositions were prepared by arc melting, were homogenized, solutioned at 1020° C for 1-5 hours in flowing helium and quenched rapidly into iced brine to avoid the formation of γ'. Single crystals of alloys of compositions 1 and 3 were grown using the vertical Bridgmann growth technique. Small disks cut from the ampoules were initially homogenized at 1100°C, then solutioned at 1020°C for 1 hour in flowing helium and were subsequently quenched in iced-brine. In-situ SANS measurements were carried out on IPNS-SAD facility using time resolved counting mode. All data collected were corrected for parasitic scattering. Table I shows the alloys studied and the temperatures used in the study.

Table I. Composition, misfit parameters and coarsening temperatures for the different alloys used for the study

Alloy #	Composition	δ	Temperatures (°C)
4.	Ni- 4.0 at.%Si- 8.0 at.% Al	+0.35%	550, 600*
9.	Ni- 7.0 at.%Si-5.0at. % Al	+0.08%	600
1.	Ni- 8.1 at.% Si- 3.9 at.% Al	-0.02%	531, 600
8.	Ni-8.75 at. %Si-3.25 at.%Al	-0.08%	600
2.	Ni- 9.5 at.% Si- 2.5 at.% Al	-0.15%	481, 531, 550, 582, 600
3.	Ni-11.0 at.% Si- 1.0 at.% Al	-0.28%	481, 531, 550*, 582, 600
6.	Ni-10.25at.% Si-1.25 at.% Al	-0.26%	550, 582, 600
7.	Ni- 9.75at. %Si-2.25 at. % Al	-0.17%	550, 600
10	Ni-12.5 at.% Si	-0.35%	481, 550, 600

* indicates that single crystals were also studied at the temperature

EXPERIMENTAL REPORT (CONTD.)

Results: Ostwald ripening theories predict the following temporal evolution for the average particle size:

$$R^3-R_0^3=K(t-t_0) \quad (1)$$

where R is the average radius at time t
R_0 is the average radius at time t_0
K is the rate constant

For spherical precipitates, the rate constant is given by the expression

$$K= 8\gamma C_e D V_m^2/9RT \quad (2)$$

where γ is the interfacial energy of the particle-matrix interface
C_e is the equilibrium concentration of the matrix
V_m is the molar volume.

Fig. 1 shows the variation of coarsening rates as a function of the Si content at the different temperatures. The data points are connected by a simple spline fit. Note that the overall trend is for the coarsening rate to increase with an increase in the Si content. This trend is significantly altered at around a composition of 8-10 at. % Si. There seems to be a small lowering of the coarsening rate around 9.0 at. % Si. A calculation of the misfit parameters (see Table I) shows that the misfit tends to zero at around 8.0 at. % Si. However, since these values have been calculated based on the assumption that the tie-lines pass through the Ni- corner of the phase diagram and hence are only approximate, experiments are currently being carried out to measure the lattice parameters of γ and γ' in these alloys, to see if this decrease in coarsening rate corresponds to a zero misfit parameter value.

Fig.1 Coarsening rates vs. Si content

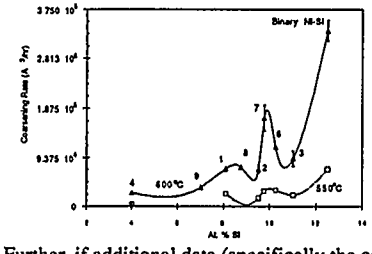
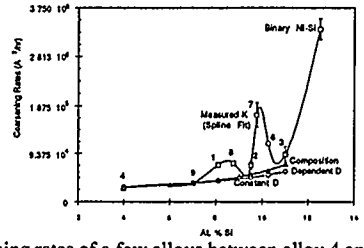


Fig. 2. Comparison of measured and calculated rates



Further, if additional data (specifically the coarsening rates of a few alloys between alloy 4 and alloy 9 and between alloy 9 and alloy 8) are obtained at both 550°C and 600°C, it should be possible to obtain a quantitative estimate of the effect of coherency strains for the first time. The details of this procedure are briefly illustrated in the second figure above. The figure shows the coarsening rates measured at 600°C and the calculated variation in the coarsening rates due to the composition of the alloy arising solely from the effects of composition and the diffusion coefficients. We believe that the two small peaks are related to the coherency strain effect: we need additional data at both these temperatures to support our claim.

INSTRUMENT USED:	DATE OF REPORT:	EXPERIMENT NO:
SAD	2/13/95	1813

TITLE:
Effect of Coherency Strains on the Kinetics of Coarsening in Ni-Al-Si Alloys

AUTHORS AND AFFILIATIONS:
G. Muralidharan (University of Illinois/ANL), J. E. Epperson (MSD/ANL)
P. Thiyagarajan (IPNS/ANL) and Haydn Chen (University of Illinois)

DATES OF EXPERIMENT:
10-23-92 to 10-27-92, 11-3-92 to 11-6-92, 10-12-93 to 10-15-93, 12/94

CHECK ALL APPLICABLE BOXES:

- [x] APPROVED BY PROGRAM COMMITTEE
- [ ] INSTRUMENT SCIENTIST ALLOCATION
- [ ] DO NOT PUBLISH
- [ ] PROPRIETARY RESEARCH
- [ ] PRT ALLOCATION

EXPERIMENTAL REPORT (or Abstract of Publication)

Objective: The focus of the current series of experiments is to study the relationship between the misfit parameter (hence coherency strains) and the kinetics of coarsening of the second phase (γ') in the ternary Ni-Al-Si system.

Experimental: Fourteen different compositions in the ternary Ni-Al-Si system have been used. Polycrystalline samples with the nominal compositions were prepared by arc melting, were homogenized, solutioned at 1020° C for 1-5 hours in flowing helium and quenched rapidly into iced brine to avoid the formation of γ. Single crystals of alloys of compositions 1 and 3 were grown using the vertical Bridgmann growth technique. Small disks cut from the ampoules were initially homogenized at 1100°C, then solutioned at 1020°C for 1 hour in flowing helium and were subsequently quenched in iced-brine. *In-situ* SANS measurements were carried out at the IPNS-SAD facility. Since the previous run cycle, additional alloys have been cast in order to clarify some crucial points that were not quite clear at the conclusion of experiments in the previous run cycle:
1. Two peaks over the background were identified earlier (see Fig. 1). However, the breadth of these peaks were not very clear and had to be established, particularly on the low Si side. Further, the maximum value at the peak could not be established with the available data.
2. The behavior at lower temperatures was not clear. The behavior at 550°C had to be studied.

Results: Ostwald ripening theories predict the following temporal evolution for the average particle size:

$$R^3-R_0^3=K(t-t_0) \qquad (1)$$

where R is the average radius at time t
R_0 is the average radius at time t_0
K is the rate constant

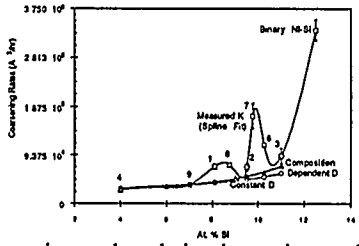
For spherical precipitates, the rate constant is given by the expression

$$K= 8\gamma C_e D V_m^2/9RT \qquad (2)$$

where γ is the interfacial energy of the particle-matrix interface
C_e is the equilibrium concentration of the matrix
V_m is the molar volume.

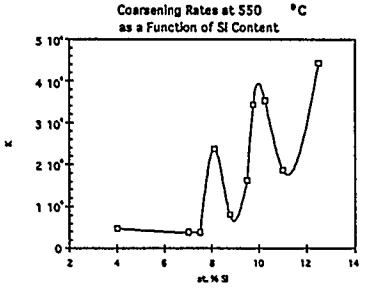
EXPERIMENTAL REPORT (CONTD.)

Fig. 1. Comparison of measured coarsening rates at 600°C and calculated rates



Since then, additional experiments done during the previous cycle have shown clearly that this peak on the lower Si side extends from roughly from 7.75 at. % Si to 9.5 at. % Si and the coarsening rate at the maximum of the peak is not much higher than indicated above. Further, the coarsening rates at 550°C for additional alloys have been measured and the trend looks very similar to the 600°C data shown above (see Fig. 2 below). Thus we have succeeded in establishing the role of coherency strains on coarsening kinetics. What is left to be done is to map out the interaction between volume fraction and coherency strains. In some previous work we have measured coarsening rates at 550°C in 4 different alloys with a higher volume fraction of precipitates. We request an additional 5 days in this cycle to complete this work and conclude our experiments on Ni-Al-Si alloys.

Figure 2



INSTRUMENT USED:	DATE OF REPORT:	EXPERIMENT NO:
SAD	8/1/1994	1875

TITLE: Effect of the Interaction of Coherency Strains and Volume Fraction on the Coarsening of γ' in Ni-Al-Si alloys

AUTHORS AND AFFILIATIONS: G. Muralidharan (IPNS/MSD/Univ of Illinois), J. E. Epperson (MSD), Haydn Chen (Univ of Illinois, Urbana)

DATES OF EXPERIMENT:

CHECK ALL APPLICABLE BOXES:

- [X] APPROVED BY PROGRAM COMMITTEE
- [ ] INSTRUMENT SCIENTIST ALLOCATION
- [ ] DO NOT PUBLISH
- [ ] PROPRIETARY RESEARCH
- [ ] PRT ALLOCATION

EXPERIMENTAL REPORT (or Abstract of Publication)

Objective: The focus of the current series of experiments is to study the effect of the misfit parameter (hence coherency strains) and the volume fraction on the kinetics of coarsening of the second phase (γ) in the ternary Ni-Al-Si system.

Experimental: Four different compositions in the ternary Ni-Al-Si system were used. In contrast to the previous series of experiments (Please see other attached report), the Ni content in these alloys was reduced to 86.0 at. % from 88.0 at. %, thus increasing the volume fraction of the second phase precipitates. However, the ratio of Si/Al was maintained similar to the previous alloys and hence the misfit parameters are similar to the low volume fraction alloys. The compositions and the calculated lattice mismatch values ($\delta = (a_\gamma - a_\gamma)/a_\gamma$) are shown in Table I. Polycrystalline samples with the nominal compositions were prepared by arc melting, were homogenized, solutioned at 1020° C for 1-8 hours in flowing helium and quenched rapidly into iced brine to avoid the formation of γ. In-situ SANS measurements were carried out on IPNS-SAD facility using time resolved counting mode. All data collected were corrected for parasitic scattering. Table I shows the alloys studied and the temperatures used in the study.

Table 1 Composition and Calculated Misfit Parameters for Alloys with a Higher Volume Fraction of γ

Alloy #	Composition	δ	Temperature (°C)
1A	Ni-4.5at. % Al-9.5 at.%Si	-0.02%	550
2A	Ni-2.9at. % Al-11.1at.%Si	-0.15%	550
3A	Ni-1.2at. %Al-12.8at.%Si	-0.28%	550
4A	Ni-7.0at.%Al-7.0at.%Si	+0.17%	550

Results: Ostwald ripening theories predict the following temporal evolution for the average particle size:

$$R^3 - R_0^3 = K(t - t_0) \qquad (1)$$

EXPERIMENTAL REPORT (CONTD.)

where R is the average radius at time t
R_0 is the average radius at time t_0
K is the rate constant

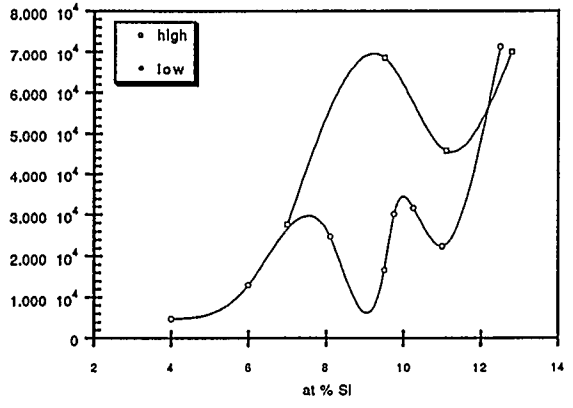
For spherical precipitates, the rate constant is given by the expression

$$K = 8\gamma C_e D V_m^2 / 9RT \qquad (2)$$

where γ is the interfacial energy of the particle-matrix interface
C_e is the equilibrium concentration of the matrix
V_m is the molar volume.

Fig. 1 shows a comparison of the variation of coarsening rates in both the series of alloys at 550°C. One obvious feature of these curves is that, the alloys with the higher volume fraction of the second phase precipitates, shows a faster kinetics. Also note that both series show similar trends in coarsening rates with at. % Si: both series of alloys do not show a monotically increasing coarsening rates with Si content. Coarsening rates must be measured in more alloys to determine the correlation between coarsening rates, misfit parameters and volume fraction.

Fig. 1 Comparison of Coarsening Rates in the Two Series of Alloys (High and Low Volume Fraction)



INSTRUMENT USED:	DATE OF REPORT:	EXPERIMENT NO.:
SAD	1/9/95	1847

TITLE: Distribution of Labeled Species in Polymers and Copolymers

AUTHORS AND AFFILIATIONS: N. S. Murthy, AlliedSignal Inc.

DATES OF EXPERIMENT: 10/11/94 to 10/13/94

CHECK ALL APPLICABLE BOXES:

- [X] APPROVED BY PROGRAM COMMITTEE
- [X] INSTRUMENT SCIENTIST ALLOCATION
- [ ] DO NOT PUBLISH
- [ ] PROPRIETARY RESEARCH
- [ ] PRT ALLOCATION

EXPERIMENTAL REPORT (or Abstract of Publication)

Hydration in Nylon Fibers

The objective of these measurements was to understand the diffusion behavior of water in these commercial fibers, and relate it to the practical problems of dye diffusion. These data will also be useful in understanding the structure of the amorphous phase, since molecules such as water are known to diffuse almost exclusively into the amorphous regions.

One set of data were collected from undrawn (1x) and drawn (4.5x) nylon 6 fibers at various levels of water (D_2O) content. Specifically, data were collected from 1x fiber at 100% RH, during initial stages of drying, after drying at 60°C for 8 min., after complete drying, and at 80% RH. Data from 4.5x fiber were obtained at 100% RH, during initial stages of drying, and from a fully dried fiber. Data were collected between Q ranges of 0.005 to 0.25 $Å^{-1}$. Preliminary interpretation of the data are based on sector-averaged intensities along and perpendicular to the fiber-axis, i.e., along the meridional and equatorial directions. The variations in the equatorial and the meridional intensities show that the amount of water diffuses at different rates into the interfibrillar and interlamellar regions. Further analysis of the data is required to come to any firm conclusions. Furthermore, a comparison of the intensities from dry and 100% RH (H_2O) fiber shows that H_2O gives rise to both meridional and equatorial intensities suggesting that the negative cross section of excess hydrogen is sufficient to give rise to a measurable intensity.

A second set of data were collected to understand the effect of heat setting in NA and NB fibers. These measurements were designed so that we can compare the diffusion characteristics of NA and NB fibers before and after annealing (heat setting). Both these fibers were heatset by Superba and Suessen processes. The present set of measurements were carried out at 80% RH. The degree of water diffusion, as determined by the intensity of the SANS peak (shown in parenthesis) varies as follows: NHS NA (1.0) <Suessen NA (1.5) < Superba NA (2.0) < NHS NB (2.5)<Suessen NB (3.0) < Superba NB (5.0). Thus, among the heat-set fibers, Superba NB is most porous and Suessen NA is least porous. Further analysis of the data is in progress.

Copolymers of VF_2 and CTFE

The objective of these measurements was to determine the changes in the distribution of the VF_2 comonomer during crystallization. Data were collected for PCTFE films with and with out VF_2 , and before and after crystallization. The lamellar intensity increased by an order of magnitude upon annealing. However, this increase in intensity could be due both redistribution of VF_2 and to the changes in the crystalline and amorphous densities. SAXS measurements on these same samples will be performed to determine contributions to the observed increase in the intensity from the density differences and the redistribution VF_2.

Acknowledgment

I would like to thank P. Thiyagarajan and D. Wozniak who went out of their way in making this a fruitful visit.

INSTRUMENT USED:	DATE OF REPORT:	EXPERIMENT NO.:
SAD	11/8/95	2044

TITLE:
Study of Amorphous Domains in Febers, Blends and Networks

AUTHORS AND AFFILIATIONS:
N. S. Murthy, AlliedSignal Inc.

DATES OF EXPERIMENT:
9/23/95 to 9/26/95

CHECK ALL APPLICABLE BOXES:

- [x] APPROVED BY PROGRAM COMMITTEE
- [ ] INSTRUMENT SCIENTIST ALLOCATION
- [ ] DO NOT PUBLISH
- [ ] PROPRIETARY RESEARCH
- [ ] PRT ALLOCATION

EXPERIMENTAL REPORT (or Abstract of Publication)

SANS data were collected to study the diffusion behavior of water and ethylene glycol in various nylons. During this visit, experiments were carried out on two nylons (nylon 6 and nylon 66) exposed to five ratios of water/ethylene glycol mixtures (100/0, 75/25, 50/50, 25/75 and 0/100) at two temperatures (121 and 140°C). Measurements were also carried out at with nylon 6 at various temperatures in D_2O.

Data in Figure 1 show the feasibility of carrying out variable temperature measurements using our sample cell on samples immersed in various types of liquids. Such experiments are required for studying the diffusion of liquids and dissolution of the polymer. These measurements will be continued during future visits.

The effect ethylene glycol on the lamellar structure appears to be more dramatic than we had expected. For instance, at 140 °C, the lamellar spacing of nylon 6 increase to 140 Å in water, and to 190 Å in ethylene glycol. This indicates that ethylene glycol is a more efficient swelling agent than water. Surprisingly, contrary to our expectations, the coherence length of the lamellar stacks does not decreases significantly at these elevated temperatures even in the presence of ethylene glycol. The data also show that ethylene glycol may begin to diffuse into the interlamellar space in both nylon 6 and nylon 66 only when it is present in excess of 25/75 at 121°C and 50/50 at 140°C.

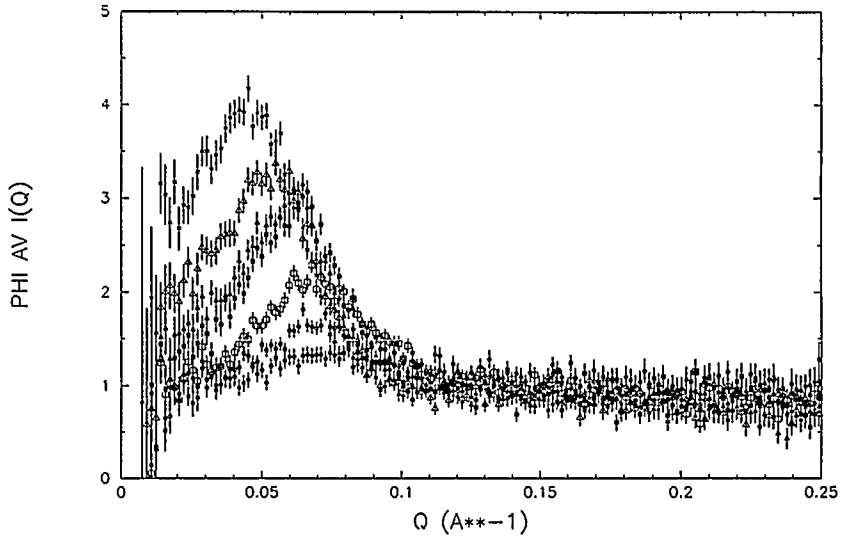


Figure 1. SANS scans of a nylon 6 specimen immersed in D_2O at tempertaures of 22, 60, 80, 120,130, 140 and 150 °C.

The lamellar peak is weak at 140 °C in water (100/0), disappears at 75/25, and is replaced by an intense diffuse scattering at 50/50. The lamellar peak reappears at 75/25 and grows in intensity at 0/100. These interesting series of observations could be due to the inversion of contrast. We have observed similar phenomenon before (Preprints, ACS-PMSE, Fall 1994, pp.293-294), and will be explored further in future visits. H_2O alone gives rise to a weak lamellar reflection at these temperatures, possibly due to the density difference between the crystalline and the amorphous domains. The differences between the behavior of various nylons is being investigated.

INSTRUMENT USED:	DATE OF REPORT:	EXPERIMENT NO.:
SAD	August 2, 1991	1275

TITLE:
SANS Studies of the Microstructure of Alumina Sol-Gels

AUTHORS AND AFFILIATIONS:
L.F. Nazar, D.C. Napier and D. Lapham, University of Waterloo, Department of Chemistry and J.E. Epperson, Material Science Division, Argonne National Labs

DATES OF EXPERIMENT: May 17-20 + continuation due to flux problems July 29-31

☒ APPROVED BY PROGRAM COMMITTEE, OR

☐ PART OF INSTRUMENT SCIENTIST ALLOCATION

REPORT RECEIVED:

EXPERIMENTAL REPORT (or Abstract of Publication)

Information on the microstructure of alumina sol-gels was obtained using small-angle neutron scattering (SANS) and static light scattering. The sol-gels were prepared by the hydrolysis and subsequent peptization of aluminum tri-sec-butoxide in solutions of varying HNO_3 concentration. Temperatures of 20°C ("low-temperature") and 90°C ("high-temperature") for hydrolysis and HNO_3 to aluminum ratios of 0.07 to 0.6 for peptization were employed. The alumina sol-gels have been studied previously by ^{27}Al-NMR, and rheology. Differences were found in the microstructure of the sol-gels prepared under various processing conditions.

Power law dependances were observed for neutron scattering in the Porod regime for these sol-gels which suggest mass fractal dimensions of 1.4 to 1.8. For the high temperature sol-gels, the apparent fractal dimensions increased with increased ratio of acid to aluminum content. The higher-acid, high-temperature sol-gels show fractal dimensions of 1.8 which is close to that expected (1.75-1.80) for mass fractals formed by rapid diffusion limited cluster-cluster agregation in three dimensions. It is suggested that the lower fractal dimension (1.4-1.5) for the lower-acid high-temperature sol-gels could be explained by invoking cluster polarisability effects. The SANS data supports a proposed model that is consistent with results from static light-scattering, ^{27}Al-NMR, and rheological studies of these systems.

"Small-Angle Neutron Scattering and ^{27}Al NMR Studies on the Microstructure and Composition of Alumina Sol-Gels", L.F. Nazar, D.G. Napier, D. Lapham and J.E. Epperson, Better Ceramics Through Chemistry IV, Mat. Res. Soc., 180, 117 (1990); "Small-Angle Neutron Scattering Study of Aluminum Tri-sec-Butoxide Derived Sol-Gels", L.F. Nazar, D.G. Napier, D. Lapham, and J.E. Epperson, submitted J. Phys. Chem., 1991.

INSTRUMENT USED:	DATE OF REPORT:	EXPERIMENT NO:
SAD	Feb. 20, 1996	2057

TITLE:
Study of porous texture and adsorption process in rare-earth modified zirconia gels

AUTHORS AND AFFILIATIONS:
M. Ozawa and S. Suzuki (Nagoya Institute of Technology)
C.-K. Loong and P. Thiyagarajan (IPNS-ANL)

DATES OF EXPERIMENT:
Sept 17-20, 1995

CHECK ALL APPLICABLE BOXES:

- [X] APPROVED BY PROGRAM COMMITTEE
- [ ] INSTRUMENT SCIENTIST ALLOCATION
- [ ] DO NOT PUBLISH
- [ ] PROPRIETARY RESEARCH
- [ ] PRT ALLOCATION

EXPERIMENTAL REPORT (or Abstract of Publication)

Fine powders of ZrO_2-R_2O_3 oxides (R = rare earths), prepared by a low-temperature coprecipitation method, are useful support and promoter components for catalytic functions in chemical syntheses and pollution controlling reactions. High surface area and stable structure at elevated temperatures are the key desirable properties for these catalysts. Neutron small-angle scattering was used to study the microstructural change and crystal growth in Ce- and Nd-doped ZrO_2 as well as in pure ZrO_2 powders. Different porosity and particle-size distribution were observed for these powders at various heat-treatment temperatures and this may be due to the different oxidation states of Ce and Nd ions. Doping rare-earths into zirconia to form a solid solution of R-Zr oxide system is an effective approach to improve stability and maintain large surface area over a wide temperature range.

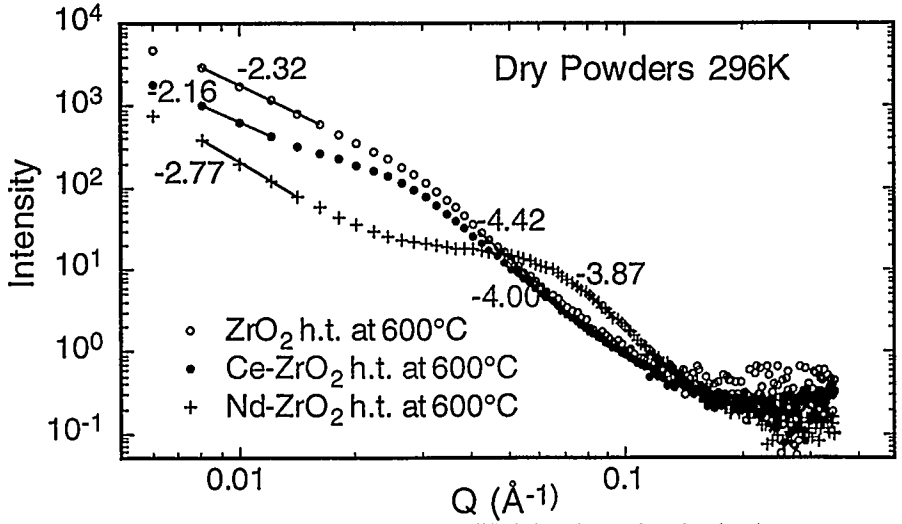


Fig. 1. Small-angle-scattering spectra of rare-earth modified zirconia powders showing the effect of rare-earth dopants on the texture of the materials.

EXPERIMENTAL REPORT (CONTD.)

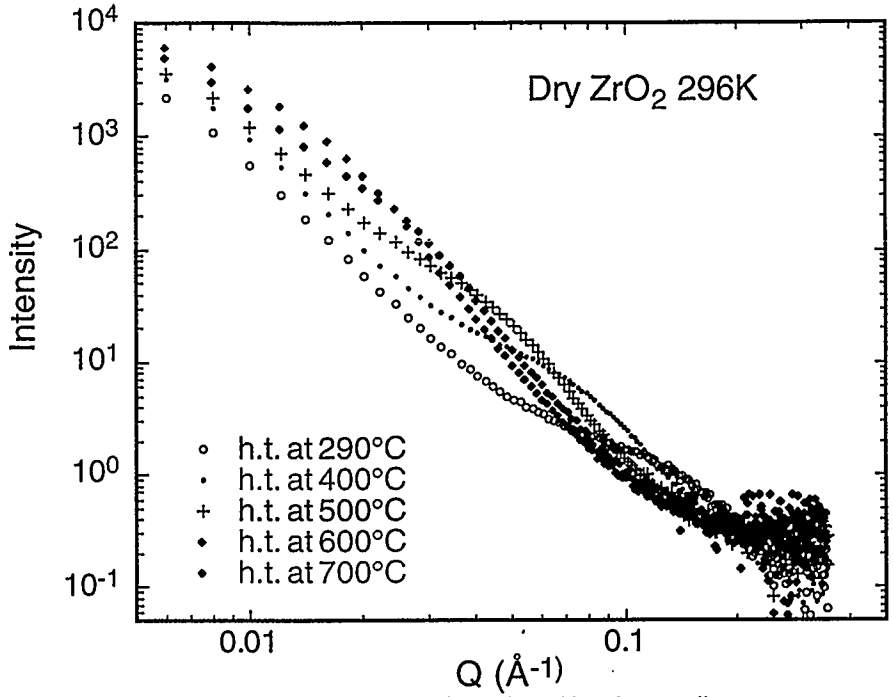


Fig. 2. Small-angle-scattering spectra of pure zirconia powders subjected to annealing at different temperatures, showing the effect of sintering on the texture of the materials.

INSTRUMENT USED:	DATE OF REPORT:	EXPERIMENT NO.:
IPNS	6/6/95	2043

TITLE:
Small Angle Neutron Scattering Study of Phase Separation in Bulk Metallic Glasses

AUTHORS AND AFFILIATIONS:
S. Schneider, U. Geyer, P. Thiyagarajan and W. L. Johnson

DATES OF EXPERIMENT:
May 17-20, 1995

CHECK ALL APPLICABLE BOXES:

- ☐ APPROVED BY PROGRAM COMMITTEE
- ☐ INSTRUMENT SCIENTIST ALLOCATION
- ☐ DO NOT PUBLISH
- ☐ PROPRIETARY RESEARCH
- ☐ PRT ALLOCATION

EXPERIMENTAL REPORT (or Abstract of Publication)

The aim of our SANS investigation was to study the long and short-range compositional variations in the amorphous phase of two different alloys $Zr_{41.2}Ti_{13.8}Cu_{12.5}Ni_{10}Be_{22.5}$ and $Zr_{46.8}Ti_{8.2}$ $Cu_{7.5}$ Ni_{10} $Be_{27.5}$ during annealing.

The samples were prepared and homogenized from a mixture of the pure elements by induction melting on a water-cooled silver boat under Ti gettered argon atmosphere. The ZrTiCuNiBe ingots were remelted in silica tubes with an inner diameter of 10mm and then water quenched. For changing the cooling rate from 40K/s to about 10K/s the amorphous $Zr_{41.2}Ti_{13.8}Cu_{12.5}Ni_{10}Be_{22.5}$ alloy was also prepared in a 14mm silica tube. For the SANS measurements disks with a thickness of 2.7mm were cut from the rods. These disks were annealed below and above the glass transition temperature (T_g) between 320C and 410C for different times. After each heat treatment the samples were analyzed by x-ray diffraction to confirm their amorphous structure.

$Zr_{46.8}Ti_{8.2}$ $Cu_{7.5}$ Ni_{10} $Be_{27.5}$ alloy

SANS was measured for selected isothermal annealing times. The results are shown in Fig.1 as log s(q) versus log (q) plots. The intensity exhibits a power law within a region $0.005Å^{-1}<q<0.025Å^{-1}$. This corresponds to characteristic lengths between 1250Å and 250Å. All Porod-slopes m are noninteger with values between -3.6 and -3.5. However, no significant difference is observed in the scattering intensity from annealed and as quenched samples.
The increase of scattering intensity can be either due to density and/or composition. fluctuations in the amorphous phase. The substantial change in scattering intensity at low q suggests a phase separation in two amorphous phases with different composition Most likely, the scattering is caused by relatively rough interfaces between decomposed regions.
Thus the phase separation already occurs by passing the miscibility gap in the undercooled liquid region during the quenching process. Then the amorphous alloy $Zr_{46.8}Ti_{8.2}Cu_{7.5}Ni_{10}$ $Be_{27.5}$ approaches a metastable equilibrium of at least two phases in the glassy state.

$Zr_{41.2}Ti_{13.8}Cu_{12.5}Ni_{10}Be_{22.5}$ alloy

In Fig.2 the SANS intensity s(q) versus scattering vector q are depicted for the $Zr_{41.2}Ti_{13.8}Cu_{12.5}Ni_{10}Be_{22.5}$ alloy annealed at 350C for three different time durations. The profiles show a interference peak which grows for longer annealing durations. The Guinier approximation has been applied to estimate the size of the scattering particles.

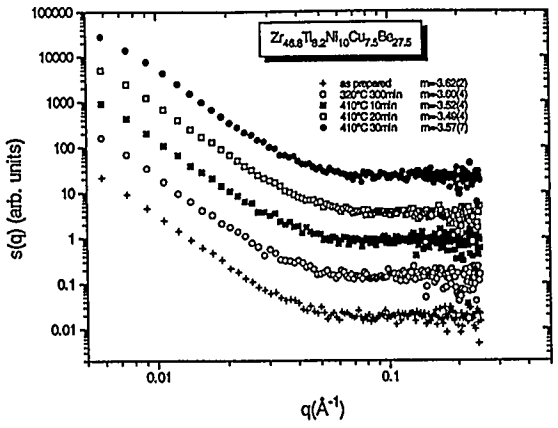


Fig.1 Porod plot

The data can be fitted to the Guinier law as illustrated in Fig.3. The calculated Guinier radii of the particles are 11Å to 14Å. It is not quite clear yet if this peak indicates a phase separation in the amorphous phase or the beginning of primary crystallization into a nano phase[1]. The x-ray pattern of the samples show no evidence of crystallization. Further investigations have to be carried out by TEM to provide additional microstructural informations. The as prepared sample does not show any contrast, even though significant composition fluctuations with respect to the Zr and Be concentration are found in the as prepared $Zr_{41.2}Ti_{13.8}Cu_{12.5}Ni_{10}Be_{22.5}$ alloy by atom probe field ion microscopy[2]. An explanation might be the small difference in the scattering length of Be and Zr.
Samples prepared from the 10mm rod and anealed at 320C for 240min, 250min and 280min reveal an increase of scattering intensity for $q < 0.05Å^{-1}$ The first one can be fitted to the Guinier law (R_g=18.5nm) the latter to the Porod law (m=-3.6). Within an annealing duration of 40min below the glass transition temperature a substantial change in the medium-range order of the amorphous alloy has ocurred. The samples cut from the 14mm rod show only background scattering for $0.005Å^{-1}<q<0.25A^{-1}$. (data will be presented in a new proposal)

[1] S. Schneider: unpublished research (1995)
[2] R. Busch, S. Schneider, A.Peker and W.L. Johnson, Appl.Phys.Lett. (1995)

INSTRUMENT USED:	DATE OF REPORT:	EXPERIMENT NO.:
SAD	8/10/92	1496

TITLE: Reacted Asphaltenes in Polar Solvents

AUTHORS AND AFFILIATIONS:
Eric Y. Sheu and Maureen De Tar; Texaco R & D

DATES OF EXPERIMENT: Apr. 23 1992

☑ APPROVED BY PROGRAM COMMITTEE, OR

☐ PART OF INSTRUMENT SCIENTIST ALLOCATION

REPORT RECEIVED:

EXPERIMENTAL REPORT (or Abstract of Publication)

REACTED ASPHALTENES IN POLAR SOLVENTS

Eric Y. Sheu and Maureen M. De Tar, Texaco R&D, P.O. Box 509
Beacon, New York 12508

Asphaltenes, derived from Ratawi (Neutral Zone) crude oil, form micelles in toluene with high association energy. Dispersing these micelles or lowering the association energy is crucial for refiining efficiency. In ordrer to lower the association energy we treated the asphaltene with base or reacted with methyl iodide to break C-S bonds, or combine these two processes. SANS was then used to examine the effects of base treatment and the reaction.

Fig. 1 shows that the non-pretreated and non-reacxted (NPNR) asphaltene micelles are about 33 Å on average. For the base treated but not reacted sample (PNR), the particle size distribution is much wider, with the average particle size similar to NPNR case. This may indicate that the monomers have smaller molecular weight, but form similar size micelles of larger polydispersity. The gel permeation chromatography (GPC) data shows similar conclusion. This is because the entropic energy increases, due to increaing number density of the monomers, equivalent to increasing monomer concentration. From the Gibb's equilibrium condition point of view, a wider size distribution is a natural result of increasing concentration. The reaction (NPR) and the combine cases (PR) show similar effect. If this picture is correct, both base treatment and methyl iodide reaction lower the association energy.

The future study of this problem is to perform SANS as a function of temperature for NPNR, PNR, NPR, and PR cases, to quantitatively determined the effect of base treatment and C-S bonds cleavage on lowering of the association energy.

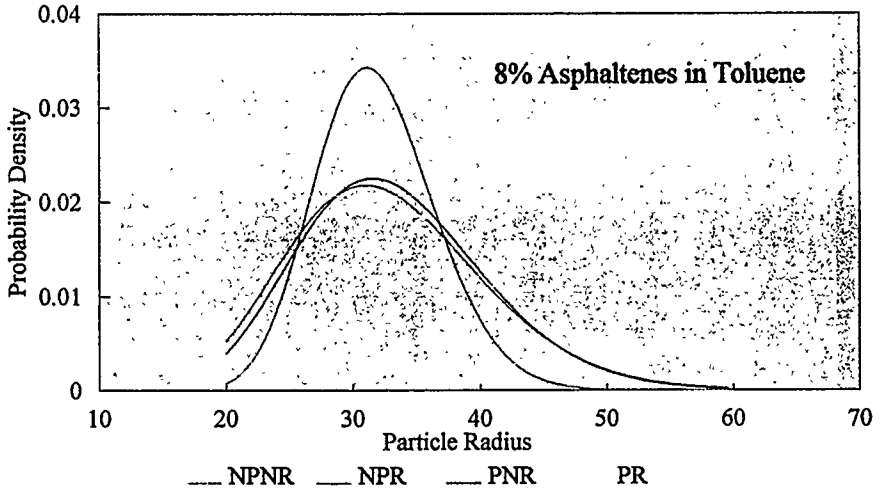


Fig. 1 The size distributions for 8% NPNR, PNR, NPR, PR asphaltenes in toluene.

INSTRUMENT USED:	DATE OF REPORT:	EXPERIMENT NO.:
SAD	July 17, 1990	1238

TITLE:
Asphaltenes in Polar Solvents

AUTHORS AND AFFILIATIONS:
Eric Y. Sheu, Maureen M. DeTar, and Dave A. Storm,
Texaco Research Center, Beacon, NY 12508

DATES OF EXPERIMENT: May 11, 1990 to May 13, 1990

☒ APPROVED BY PROGRAM COMMITTEE, OR

☐ PART OF INSTRUMENT SCIENTIST ALLOCATION

REPORT RECEIVED:

EXPERIMENTAL REPORT (or Abstract of Publication)

Asphaltene is a component extracted from vacuum residue following the refining of petroleum products. This material has a complex molecular structure consisting of aromatics with aliphatic side chains and a considerable amount of heteroatoms such as sulphur, nitrogen, nickel, and vanadium. Although this material is structurally similar to the discotic molecules which form columnnar liquid crystals in the thermotropic phase, via London forces between molecules [1], the association energy of asphaltene molecules is much higher [2]. It is thus interesting to investigate the free energies involved in asphaltene self-association.

We study the association energy by looking at the structure and the size distribution of the aggregates, as well as their response to physical parameters such as concentration and solvent dielectricity [3-5]. Among the available techniques for structural study of a colloidal system of size between 15-50 Å, small angle neutron scattering (SANS) appears to be the most appropriate technique [6]. In this experiment, we systematically varied asphaltene concentration and solvent dielectricity (by mixing toluene and pyridine) to study the response of the particle structure and polydispersity.

For data treatment we fitted the scattering intensity distribution using various structural and polydispersity models. We the selected the most appropriate model according to the method recently proposed by Sheu [7]. Based on our analysis we found that the asphaltene colloids, to the first order of approximation, are spherical in shape and the size distribution follows the Schultz distribution function. Figure 1 shows a typical scattering intensity distribution. The solid line is the fit based on the above structural and polydispersity model.

As for the response of structure and polydispersity to concentration and/or solvent dielectricity, no significant change was obsevered. From a thermodynamics point of view, this result reflects a low association energy [3]. And, it apparently contradicts the reported temperature study [2], which concludes a strong association energy between asphaltene molecules. To explain this dilemma based on thermodynamics, there must exist an additional free energy which restricts the growth of the particles in spite of the strong association energy. We attribute this energy to be the packing constraint based on the fact that the molecular structure of asphaltenes is complicated and non-uniform. To confirm our argument, further studies are necessary in the following steps. First of all one needs to identify the type of free energy leading to asphaltene association. Charge transformation energy originating from the heteroatoms has been suspected to be the main free energy responsible for this association [8]. Should this be true, the association energy would be strong as suggested in the temperature study [2]. Secondly, if the association is mainly caused by the charge transformation eneryg and the packing constraint is indeed the free energy term that restricts the particle growth, then the aggregates must be formed in such a way that no charge transfer sites are available on the surface. To verify this point, a future study is necessary. This can be achieved by studying the structure of asphaltene colloids in solvents that provide charge transformation sites. Finally, if the charge transfer sites come from the heteroatoms, then one can quantify this energy by systematically varying the heteroatom content and look at the structural evolution by SANS.

(1) E. Y. Sheu, K. S. Liang, and L. Y. Chiang, J. Phys. France 50 1279 (1989).
(2) E. Y. Sheu, K. S. Liang, S. K. Sinha, and R. Overfield, "Polydispersity of Asphaltene Aggregates in Toluene." unpublished.
(3) P. Missel, N. A. Mazer, G. B. Benedek, C. Y. Young, and M. C. Carey, J. Phys. Chem., 84 1044 (1980).
(4) E. Y. Sheu and S. H. Chen, J. Phys. Chem., 92 4466 (1988).
(5) J. Sung, E. Y. Sheu, and J. S. Huang, "The significance of Solvent Dielectric Constant on Micellization of didodecyldimethyammonium Bromide", submitted to J. Coll. Int. Sci.
(6) C. G. Winsor, J. Appl. Cryst. 21 582 (1988).
(7) E. Y. Sheu, "Particle Size Distribution of a Noninteracting Dispersed System Studied by Small Angle Scattering", submitted to J. Coll. Int. Sci.
(8) B. Siffert, J. Kuczinskl, and E. Papirer, J. Coll. Int. Sci., 135 107 (1990).

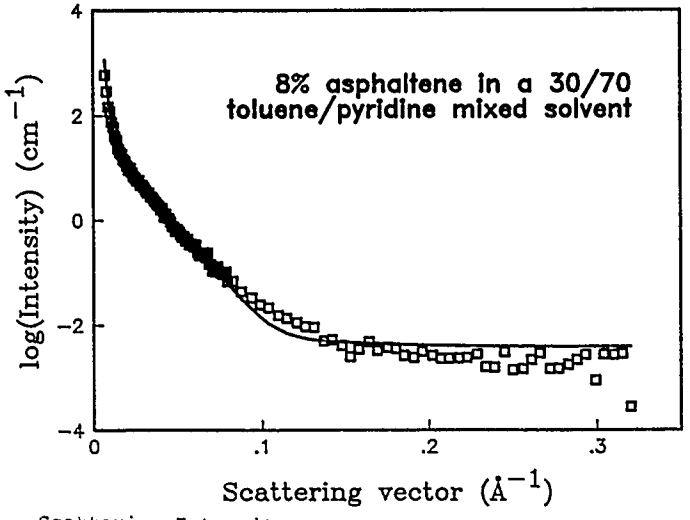


Fig. 1. Scattering Intensity vs Q. The solid line is a fit (see text).

INSTRUMENT USED: SAD	DATE OF REPORT: JULY 1, 1991	EXPERIMENTAL NO.: 1346

TITLE:
THE STUDY OF ASPHALTENE FORMATION ENERGY IN POLAR SOLVENTS

AUTHORS AND AFFILIATIONS:
E. Y. Sheu, M.M. De Tar and D.A. Storm
Texaco Research Center Beacon, New York.12508

DATES OF EXPERIMENT: APRIL 2-6, 1991.

□ APPROVED BY PROGRAM COMMITTEE, OR

□ PART OF INSTRUMENT SCIENTIST ALLOCATION

REPORT RECEIVED:

EXPERIMENTAL REPORT (OR ABSTRACT OF PUBLICATION)

Two experiments were performed in this study. The first experiment was designed to measure the dependence of asphaltene colloidal structure in toluene, when equilibrated with caustic solutions of increasing sodium hydroxide concentration. A paralell experiment has been performed at Texaco Research Center using a Krüss Surface Tensiometer (Model K10ST). The results indicated that the adsorption isotherm is enhanced when the NaOH concentration increased, but became saturated for [NaOH] > 1 N. Fig. 1 shows the SANS results for this study. Clearly, the asphaltene particles become smaller when equilibrated with a caustic solution. However, no significant changes were found for [NaOH] > 0.01 N, this differs from the interfacial tension measurement (IFT). A series of IFT measurements for a similar system are currently underway at Texaco Research Center, in order to resolve the quantitative discrepancy between the SANS results and the IFT measurements. A more systematic investigation will be proposed for the upcoming IPNS cycle.

The second experiment was designed to investigate the structural transition of poly(vinyl)pyridine (PVP) in pyridine/H_2O mixtures. Pyridine is a good solvent for PVP, while PVP is not soluble in H_2O. We thus expected either a structural transition, or a phase separation to occur along the pyridine/H_2O mixture axis. A previous dynamic light scattering experiment had indicated that there exists an "agglomeration-like" structural transition near pyridine/H_2O = 70/30, at room temperature. However, the SANS results suggests a gradual growth of the dispersed particle size along the solvent axis, rather than a rapid structural transition (see Fig. 2). This indicates that the structural transition or phase separation should occur at pyridine volume ratio less than 50 %. Again, there is a quantitative discrepancy between the dynamic light scattering and the SANS results. Our recent dielectric relaxation study (not yet completed) seems to support the SANS results. However, the whole picture of the transition physics will not be exposed until the dielectric study is completed and more SANS data is collected.

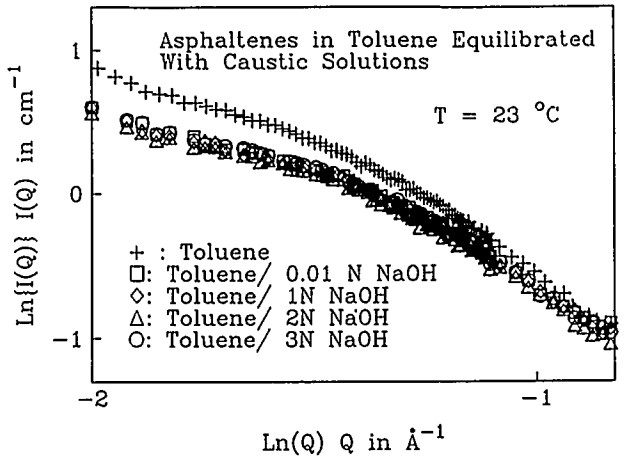


Fig 1

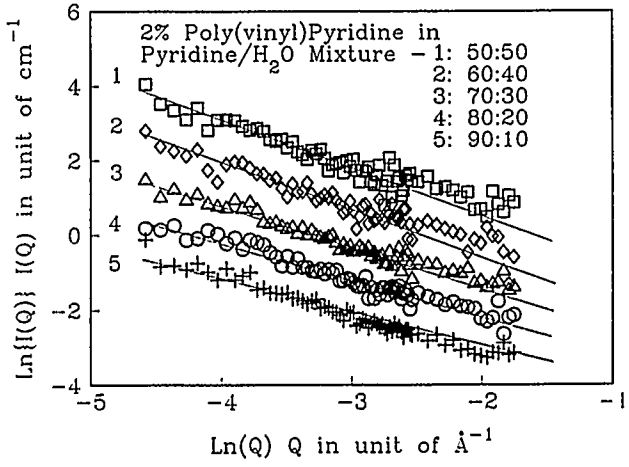


Fig 2

INSTRUMENT USED:	DATE OF REPORT:	EXPERIMENT NO.:
SAD	Feb 15 1993	1651

TITLE: Structure of Bioremediation Surfactants in Soil/Water/ Surfactant complexes.

AUTHORS AND AFFILIATIONS: ERIC Y. SHEU, Texaco R & D, P.O. Box 509, Beacon NY 12508

DATES OF EXPERIMENT: Dec 18 to Dec 21

☐ APPROVED BY PROGRAM COMMITTEE, OR

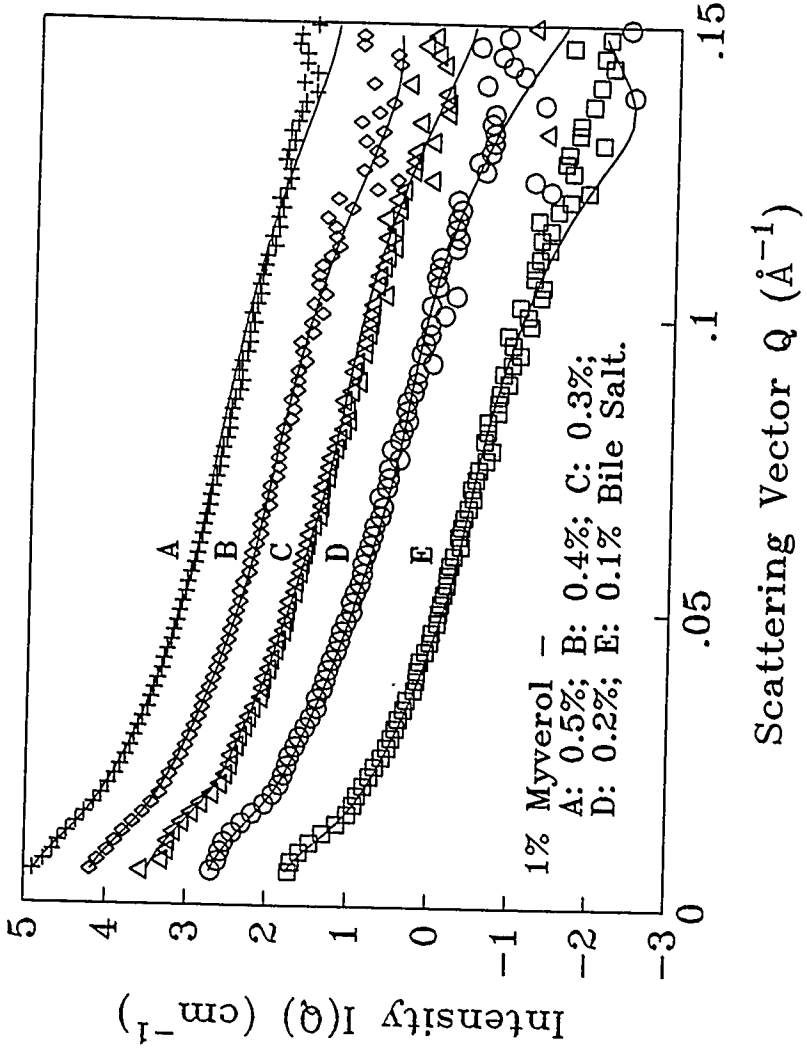
☑ PART OF INSTRUMENT SCIENTIST ALLOCATION

REPORT RECEIVED:

EXPERIMENTAL REPORT (or Abstract of Publication)

Two systems were studied in this experiment. The first system involved the CGS bio-surfactant used for bioremediation of hydrocarbon containing soil. This surfactants form micelles at 0.1% (by weight) in water, but do not form micelles until 1.0% when 4:10 (gm:cc) contaminated soils is introduced to the water solution (the soil contains ~ 1.5 hydrocarbon). The surface tension measurement results was confirmed by SANS. In addition, SANS gives the micellar shape and size information for this nitrogen containing surfactant.

The second system was a drug delivery system called Myverol. It contains 75% of Monoolein and 25% of salts. It forms cubic structure, when swelled by water. However, it solubility in water is relatively low (< 0.5 WT %). In order to make use of the cubic phase for delivering drug, one needs to disperse the cubic phase to form a dilute solution, while maintaining the cubic structure. One way of achieving it is to add the bile salt containing 50% of sodium cholate and 50% sodium deoxycholate. The wide angle X-ray performed here in Taxeco laboratory suggested that at 0.6% of bile salt and 1% myverol, the solution is well dispersed, and the myverol structure remain cubic. The SANS data showed that the cubic structure extends to a length scale of ~ 500 Å. Surprisingly, this cubic region has a structure of thin plate on which the cubic structure was formed. The SANS data was first analyzed by simply plotting $Ln[Q^2I(Q)]$ vs Q^2, from which the thickness of the plate was found to be about 37 Å. Later, the data was analyzed via assuming the structure to be thin plate of thickness T and cross section radius R, with a Guassian distributed polydispersity of R. The calculated I(Q) agreed with the data well, except at the low bile salt concentration (0.1% bile salt). Fig. 1 shows the fitting. The extracted T was 39±0.5 Å, close to the 37 Å obtained from the crude analysis. The SANS clearly showed that for bile salt > 0.8%, the cubic no longer exist, since the bile salt starts to form ionic-like micelle with a pronounced scattering peak.



INSTRUMENT USED: SAD	DATE OF REPORT: Dec 16,1993	EXPERIMENT NO: 1669

TITLE:

In situ Sintering of Nanophase Pd

DATES OF EXPERIMENT: July 9-14,1993

CHECK ALL APPLICABLE BOXES:

- [X] APPROVED BY PROGRAM COMMITTEE
- [X] INSTRUMENT SCIENTIST ALLOCATION
- [ ] DO NOT PUBLISH
- [ ] PROPRIETARY RESEARCH
- [ ] PRT ALLOCATION

EXPERIMENTAL REPORT (or Abstract of Publication)

We have made *in situ* SANS measurements at 100°C, 200°C, 250°C, 275°C and 300°C on uncompacted, nanophase Pd. Survey ln S(q) vs ln q plots of the scattering at the respective sintering temperatures are shown in Fig.1. At the lower temperatures, there was very little, if any, change in the scattering profile. However, 300°C sintering resulted in rapid changes; in fact, most of the change took place within the first 30 minutes of the anneal., making it impossible to map out the microstructural changes given the relatively low neutron flux available at IPNS.

Earlier SAXS work [1] on compacted and uncompacted nanophase Pd has shown that the small angle scattering seen above the break in slope shown in Fig. 1 can be understood in terms of scattering from individual nanophase particles. The scattering below the break is largely due to pore fractal behavior, that is void space associated with the boundary regions.

If this model is correct, there must be additional information [2], in the immediate vicinity of the break in slope, about the non-fractal, local ordering among the nanophase particles. Such information about how such particles are packed together during sintering would offer a useful, detailed look at an important materials consolidation process; however, before the proper analysis can be carried out SANS data throughout the sintering process must be available. Given the low flux at IPNS, it would appear that the best approach would be to carry out the anneals ex situ and transfer the sintered sample to the SAD instrument for the measurements.

1). J. E. Epperson, R. W. Siegel, Jongtae Lee and J. S. Lin, manuscript in preparation (1993)

2). P. Dimon, S. K. Sinha, D. A. Weitz, C. R. Safina, W. A. Varady and H. M. Lindsay, Phys Rev. Letters 57, 595 (1986).

EXPERIMENTAL REPORT (CONTD.)

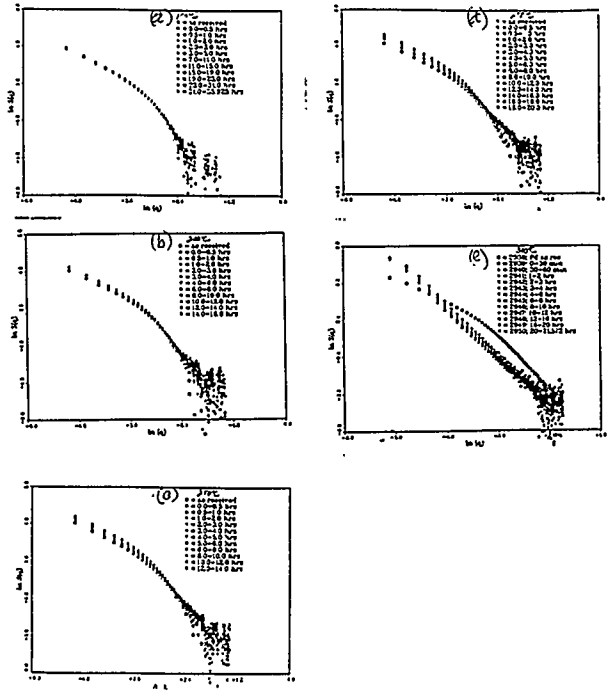


Fig. 1. ln S(q) vs ln q plots summarizing the SANS profiles measured during isothermal, in situ sintering of nanophase Pd at (a). 100C, (b). 200C, (c). 250C, (d). 275C and (e). 300C.

INSTRUMENT USED.	DATE OF REPORT:	EXPERIMENT NO
SAD	12/21/93	1824

TITLE:Physico-Chemical Properties of Detergents used for Membrane Protein Crystallization in Presence of Salt, Small Amphiphiles and Polyethylene Glycol.

AUTHORS AND AFFILIATIONS:
P. Thiyagarajan (IPNS, ANL), David M. Tiede (Chemistry,ANL)

DATES OF EXPERIMENT: September 24-28, 1993

CHECK ALL APPLICABLE BOXES:

- [X] APPROVED BY PROGRAM COMMITTEE
- [X] INSTRUMENT SCIENTIST ALLOCATION
- [ ] DO NOT PUBLISH
- [ ] PROPRIETARY RESEARCH
- [ ] PRT ALLOCATION

EXPERIMENTAL REPORT (or Abstract of Publication)

A large part of the surface of the tertiary structures of the membrane proteins is hydrophobic in nature and they are soluble only in detergent solutions. These proteins play key roles in the important biological processes such as respiration, vision, nerve conduction and photosynthesis. An understanding of the membrane proteins in terms of their structure and self assembly will provide useful insights into these biological processes. Since X-ray crystallography is the most useful tool for obtaining structural details at atomic resolution, these proteins need to be crystallized. To date about 400 water soluble proteins have been solved by X-ray crystallography, but structures of only two membrane proteins are understood. This is mainly due to the difficulties in growing good protein crystals and lack of rational schemes for that.

For the crystallization of the membrane proteins, a number of components such a detergent, salt, polyethylene glycol and small amphiphilic molecules are added. The physical chemistry of interaction between the added ingredients and the proteins is not well understood. This is essential for the development of rational schemes for crystallization of membrane proteins. SANS is useful for studying multicomponent systems where a particular component can be contrast matched and its effect on the rest of the system can be studied by adjusting the deuteration levels of either that component and/or the solvent.

We have carried out systematic SANS studies on the structure of the particles formed in two widely used detergent solutions, namely, Dodecyl dimethylamine-N-oxide (LDAO) and β-Octyl glucoside (BOG) as a function of their concentration, salt type and its concentration, and the concentration of small amphiphilic molecule, heptane 1,2,3 triol (HT). We also studied the aggregation properties of the photosynthetic reaction center (RC) protein in these detergent solutions as a function of ionic strength. Our studies reveal that these detergents form spherical micelles above their cmc. Further particle growth occurs depending on the type of detergent and ionic strength. Thus BOG solutions contain large aggregates at high NaCl concentration while LDAO solutions do not at that ionic strength. However both form large aggregates in 1M $(NH_4)_2SO_4$ solutions. The addition of HT to the pure detergent solution leads to mixed micelle formation whereas in the case of detergent solutions containing $(NH_4)_2SO_4$ the larger aggregates are broken into smaller mixed micelles. We also found that the RC protein is in equilibrium between monomeric and chainlike aggregates and the direction of equilibrium towards monomer is shifted by the type of detergent and ionic strength of the solution.

The aggregation properties of the detergents under conditions used for the crystallization of membrtane proteins have not been addressed so far while setting up crystallization experiments. While creating super saturation conditions for the crystallization of membrane proteins it so happens that those conditions super saturate the detergents as well. This results in large aggregation of the detergent micelles, thus depleting the amount of micelles necessary for the solubilization of the membrane proteins. As a consequence the proteins can aggregate irreversibly and thus hinder the crystallization process. We propose to generate all the necessary data on the physical chemistry of the systems used for membrane protein crystallization both in the presence and absence of membrane proteins which may pave a way for the development of rational schemes for their crystallization.

EXPERIMENTAL REPORT (CONTD.)

INSTRUMENT USED:	DATE OF REPORT:	EXPERIMENT NO:
SAD	6/12/95	1948

TITLE: The Solution Structure of Untreated and O-methylated Coal Extracts in Pyridine: A Contrast Variation SANS Analysis.

AUTHORS AND AFFILIATIONS:
P. Thiyagarajan, G.D. Cody and R.E. Winans.

DATES OF EXPERIMENT:
Feb 1995.

CHECK ALL APPLICABLE BOXES:

- [X] APPROVED BY PROGRAM COMMITTEE
- [ ] INSTRUMENT SCIENTIST ALLOCATION
- [ ] DO NOT PUBLISH
- [ ] PROPRIETARY RESEARCH
- [ ] PRT ALLOCATION

EXPERIMENTAL REPORT (or Abstract of Publication)

Small angle neutron scattering (SANS) has been used to investigate the solution structure of pyridine extracts obtained from three Argonne Premium coals; APCS # 3, 2, and 8. In order to investigate the role of specific solvent-solute interactions, both untreated and O-methylated extracts were investigated. SANS analysis reveals that the solution structure of lower rank coal extracts exist as small particles, with a radius around 80 A, which further aggregate into topologically complex structures. The power-law behavior of the scattering intensity as a function of the wave-vector indicates a mass fractal topology, and the dimensionality of the aggregate depends on the rank of the coal. O-methylation increases the densification of the extended solution structure. Temperature dependent scattering studies indicate that the size of the aggregates from the pyridine extracts of APCS #3 dispersed in deuterated pyridine does not decrease significantly with increasing temeperature upto 90C. Contrast variation studies of the above reveals a solution density of 1.18 for the coal extract in pyridine which is larger than expected based on comparison with the solvent swollen coal.

INSTRUMENT USED:	DATE OF REPORT:	EXPERIMENT NO:
SAD	12/21/93	1823

TITLE.STRUCTURE OF LIGHT HARVESTING COMPLEXES IN DETERGENT SOLUTIONS

AUTHORS AND AFFILIATIONS:
D. M. Tiede (Chemistry, ANL) and P. Thiyagarajan (IPNS, ANL)

DATES OF EXPERIMENT:
September 15-18, Dec 13-15, 1993

CHECK ALL APPLICABLE BOXES:

- [X] APPROVED BY PROGRAM COMMITTEE
- [ ] INSTRUMENT SCIENTIST ALLOCATION
- [ ] DO NOT PUBLISH
- [ ] PROPRIETARY RESEARCH
- [ ] PRT ALLOCATION

EXPERIMENTAL REPORT (or Abstract of Publication)

INTRODUCTION

The goal of these experiments was to determine the size and shape of light-harvesting chlorophyll-protein complexes, LH, isolated from the photosynthetic bacterium Rb. sphaeroides in detergent micelles. There are two spectroscopically distinguishable forms of the LH complex, called LH I and LH II, each consisting of short peptides, a, b (48 to 58 amino acid residues) that are associated with one chlorophyll molecule. In the natural membrane, the a/b peptides form an array that allows rapid, efficient energy transfer among up to 200 chlorophyll molecules. Numerous spectroscopic studies have examined the LH II complex in micelles of the detergent lauryldimethylamine-N-oxide, LDAO, and the detergent n-octyl-B-D-glucopyranoside, OG. OG has also proven to be a detergent from which it is possible to crystallize the LH I and LH II complexes, although these crystals have not been amenable for high-resolution structural analysis. Much of the literature on LH complexes suggest that a a6b6 complex with six-fold symmetry is the smallest functional unit, but recent equilibrium sedimentation studies suggest that LH II may be an a8b8 complex in detergent micelles.

We have used the Small Angle Diffractometer, SAD, to characterize the size and aggregation states of the isolated LH complexes in LDAO and OG detergent micelles. Small angle neutron scattering, SANS, profiles were measured for perdeuterated LH complexes, under conditions in which the scattering from the detergent was minimized by contrast matching to the H2O/D2O ratio of the solvent.

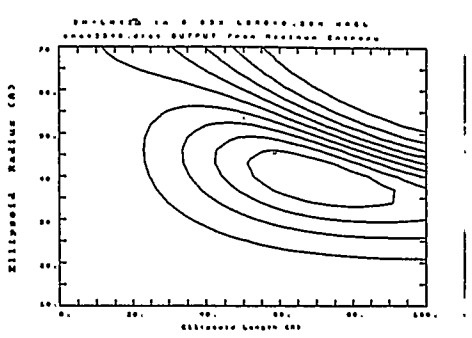
RESULTS AND DISCUSSION

Our SANS measurements found striking differences in the aggregation state of the LH II in LDAO and OG detergents. Maximum entropy analysis found that the SANS profiles for the LH II could be fit by a cylindrical form factor in both detergents, figures 1 and 2. However, polydispersity and the presence of large aggregates of proteins were found to be considerably higher in LDAO than in OG. The LH II complex in OG could be fit as cylindrical particle with a length of approx. 62 A and radius of 35 A. These dimensions are not consistent with the a6b6 model for LH II, but they are compatible with a a8b8 complex.

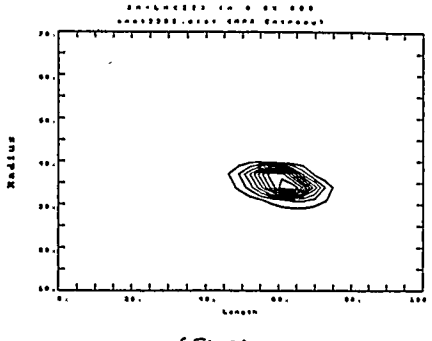
EXPERIMENTAL REPORT (CONTD.)

The detergent dependence on the aggregation state and polydispersity of the LH II complex parallels our findings for the reaction center protein in these detergents, and suggests that these may be general features of the interaction of these detergents with proteins.

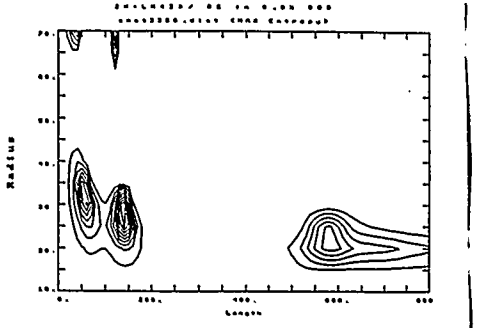
The LH I complex is not stable in LDAO, but spectroscopic analysis and crystallization have been achieved in OG. The SANS profiles measured for LH I were found to be more complex that those for LH II. Preliminary maximum entropy analysis, figure 3, found that the profiles could only be fit with multiple components with relatively small polydispersity. Further analysis will test other structural details.



(Fig. 1)



(Fig. 2)



(Fig. 3)

INSTRUMENT USED:	DATE OF REPORT:	EXPERIMENT NO.:
SAD	4-29-91	1341

TITLE:
Ionomer Chain Dimensions in the Vicinity of the Ionic Aggregates

AUTHORS AND AFFILIATIONS:
Susan A. Visser, Stuart L. Cooper (Univ. of Wisconsin) and Gefried Pruckmayr (DuPont)

DATES OF EXPERIMENT: Dec. 7-10, 1990

☒ APPROVED BY PROGRAM COMMITTEE, OR

☐ PART OF INSTRUMENT SCIENTIST ALLOCATION

REPORT RECEIVED:

EXPERIMENTAL REPORT (or Abstract of Publication)

The influence of ionic aggregation on polymer chain dimensions remains a subject of controversy. Theoretical predictions by Forsman et al. and Dreyfus et al. suggest that ionic aggregation will cause measurable chain expansion, while the theory of Squires et al. predicts that chains will retain their unperturbed dimensions. Experimental tests have been inconclusive; aggregation of labled chains in SANS studies, failure to use morpologically matched samples for a subtraction technique, or other experimental difficulties have marred previous work. In this work, these experimental difficulties were overcome. Sodium sulfonated model polyurethane ionomers were labeled with various concentrations of deuterated PTMO segments, and the PTMO polymer subchain dimensions were measured using small-angle neutron scattering. Morphological matching of ionomers which differ only in labeling level, as well as the presence of ionic aggregation, was verified by small-angle x-ray scattering. SANS results for sodium sulfonated ionomers based on 1000 and 2000 m.w. PTMO subchains confirmed that no chain expansion occurs upon ionic aggregation, in agreement with the theoretical predictions of Squires et al. Data were analyzed with a wormlike chain model which accounts for the polydispersity of the PTMO subchains. A number of other models for analyzing SANS data were also evaluated, and results from all models confirmed the no-expansion result.

(Full manuscript submitted to Macromolecules)

EXPERIMENTAL REPORT (CONTD.)

INSTRUMENT USED: SAD	DATE OF REPORT: 5TH DECEMBER, 1995.	EXPERIMENT NO: 1959
TITLE: SURFACE MODIFICATION OF PHASE SEPARATION IN *n*-PARAFFIN SOLUTIONS		
AUTHORS AND AFFILIATIONS:	J.W. White, E.P. Gilbert and P.A. Reynolds Research School of Chemistry, Australian National University	
DATES OF EXPERIMENT: 1ST - 6TH MARCH, 1995.		

CHECK ALL APPLICABLE BOXES:

X APPROVED BY PROGRAM COMMITTEE

☐ INSTRUMENT SCIENTIST ALLOCATION

☐ DO NOT PUBLISH

☐ PROPRIETARY RESEARCH

☐ PRT ALLOCATION

EXPERIMENTAL REPORT (or Abstract of Publication)

Introduction

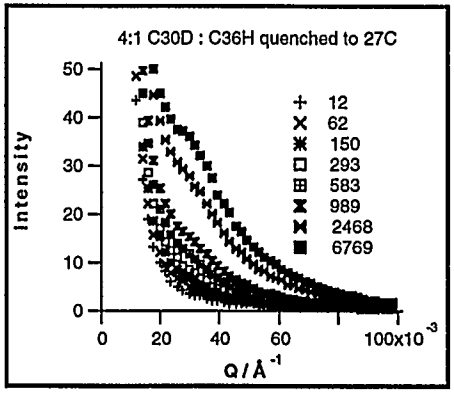
Equimolar binary mixtures of $C_{30}H_{62}$:$C_{36}D_{74}$ and $C_{30}D_{62}$:$C_{36}H_{74}$, when quenched from the melt to some 40 to 50 degrees below the melting point, undergo solid state phase separation in a period of about 12 hours. Using small angle neutron scattering, it is possible to follow this demixing behaviour which is characterised by the growth of a microphase peak around 0.07 $Å^{-1}$. For systems unbalanced in concentration, e.g. with 1:4 and 4:1 molar composition, demixing still occurs but with the peak appearing at significantly lower Q values. We have made extensive investigations of this process and have found scaling laws from the late stages of this bulk property (1).

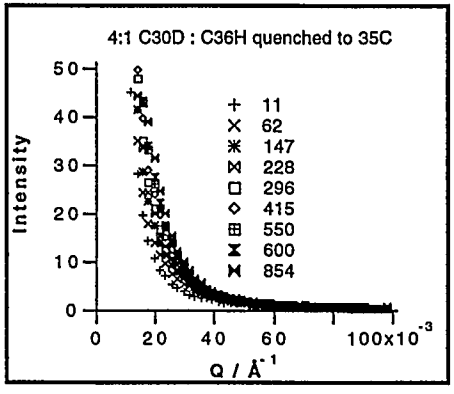
Graphite has a high affinity for normal alkanes, with the latter being physisorbed at the basal plane of the substrate. STM experiments carried out in our own laboratory (2) have indicated that long-chain alkanes are preferentially adsorbed to those of lower carbon number. In experiments performed on the LOQ instrument at the Rutherford Appleton Laboratory (3), we found that when equimolar mixtures were doped inside the cavities present in porous graphite, microphase separation still occurred but the demixing was greatly modified by the adsorption process. Demixing was found to occur more rapidly and, for the $C_{30}D_{62}$:$C_{36}H_{74}$ system, a significantly more ordered microphase structure was found.

In this series of experiments performed on SAD, we extended our studies on both the equimolar and non-equimolar mixtures adsorbed on graphite, to provide a set of data fully comparable to those for the bulk material. The preparation and procedure used were identical to those of earlier LOQ experiments. The samples are strong scatterers and, consequently, it was possible to obtain data with very good statistics in a period of about 15 minutes. During the five day experiment, we were able to study all the binary systems at quench temperatures ranging from 20 to 43C.

Results

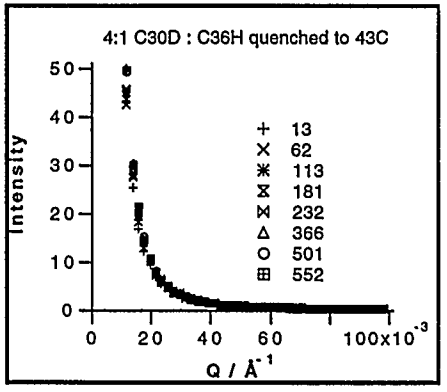
We discuss here only a fraction of the data available. The figures show the time-resolved SANS from 4:1 $C_{30}D_{62}$:$C_{36}H_{74}$ doped into the porous graphite substrate and quenched from 140C to 27C, 35C and 43C respectively. The number of minutes elapsed after the quench is also indicated in the figures.





At the lowest temperature, intensity is found to develop most quickly for Q < 0.05 $Å^{-1}$. As expected, this is at a lower Q value than that observed for the equimolar alkane-graphite systems. On increasing the quench temperature, the development in scattering is significantly reduced. This is most apparent at 43C, where no significant microphase growth was found to occur. These observations can be correlated with recent Raman spectroscopy measurements on the bulk systems, which indicate that the chains undergo an abrupt increase in conformational disorder some 15C above room temperature (4). This disorder can be seen here to cause the chains to mix and therefore destroy the microphase.

Further analysis of the data is underway to understand the influence of the graphite substrate on the demixing of these binary alkanes and to obtain scaling laws for the microphase separation process.



1. P.W. Zhu, PhD thesis, A.N.U. (1993).
2. E.P. Gilbert, T.J. Senden, J.W. White, unpublished data.
3. E.P. Gilbert, P.A. Reynolds, J.W. White, ISIS report on RB no. 6431 (1995).
4. R.G. Snyder, G. Conti, H.L. Strauss, D.L. Dorset, J. Phys. Chem 97 (1993) 7342.

INSTRUMENT USED:	DATE OF REPORT:	EXPERIMENT NO:
SAD	August 17, 1994	1896

TITLE:
SANS of Petroleum Resid and Their Interaction with Dispersed Catalysts

AUTHORS AND AFFILIATIONS:
R. E. Winans, J. E. Hunt, P. Thiyagarajan **ANL**
K. B. Anderson **Amoco Oil Co.**

DATES OF EXPERIMENT:
May 11-15, 1994

CHECK ALL APPLICABLE BOXES:
- [√] APPROVED BY PROGRAM COMMITTEE
- [√] INSTRUMENT SCIENTIST ALLOCATION
- [ ] DO NOT PUBLISH
- [ ] PROPRIETARY RESEARCH
- [ ] PRT ALLOCATION

EXPERIMENTAL REPORT (or Abstract of Publication)

Paper in preparation for Energy and Fuels. The title, authors and abstract follow.

SANS Study of Temperature-Dependent Structrural Changes ofAsphaltene Micelles in 2-methylnaphthalene

P. Thiyagarajan, Jerry E. Hunt†, Randall E. Winans†, Ken Anderson* and Jeffrey Miller*

Intense Pulsed Neutron Source Division

†Chemistry Division,
Argonne National Laboratory
Argonne, Il 60439

*AMOCO Research Corporation
Naperville, Il

*This work was performed under the auspices of the U. S. Department of Energy, CRADA No. 9300901 between Amoco Oil Co. and Argonne National Laboratory, under contract number W-31-109-ENG-38.

Abstract

Small angle neutron scattering (SANS) has been used to investigate the temperature-dependent structural changes of a 5% asphaltene in perdeuterated 2-methylnaphthalene solution in a temperature range of 20 - 400°C. A special stainless steel cell was constructed and used for the measurements. The

EXPERIMENTAL REPORT (CONTD.)

SANS data measured at temperatures of 20C, 50C, 100C, 150C, 200C, 250C, 300C, 320C, 340C and 400C continuosly vary and the decrease in the signal intensity as a function of increasing temperature suggests that the disaggreagation and eventual demicellization of asphaltenes. Guinier analysis of the data in the low temperature region suggested polydispersity in the sizes and was not useful in obtaining reasonable information on the size. Attempts to fit the SANS data using the expression for the form factor of ellipsoid were not satisfactory either. Hence we have carried out maximum entropy analysis on the paticle size distributions by using the form factor for a cylinder. This permitted extraction of particle size distributions in two dimensions, namely, radius and length and the fits were extremely good. The asphaltenes self associate in 2-methylnaphtahlene and at room temperature, forming long rod shaped particles whose radii fall in the range of 10-20Å and lengths larger than 500Å (see fig. 1). As the temperature is increased to 50°C the disaggregation takes place. In the temperature range of 100 - 320°C particle sizes become smaller and their polydispersity also varies. Between 340 to 400°C, the particles are small having a spherical shape with a radius of 12Å and monomeric. Cooling the sample back to 20°C did not show any measurable signal at all and thus the particles have completely disintegrated the sample forming a crud on the walls of the cell.

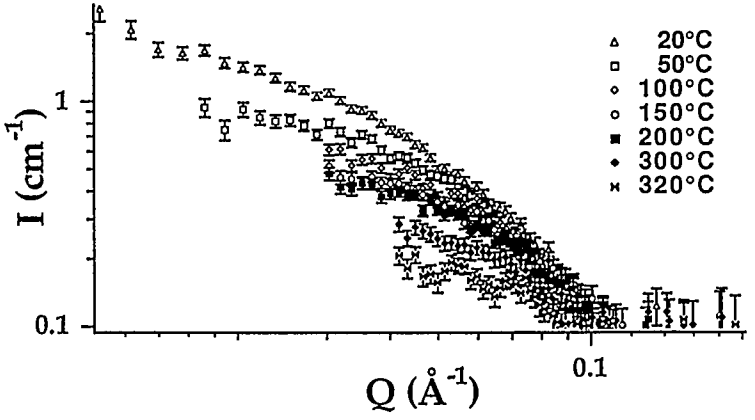


Figure 1. SANS of 5% Asphaltene in d10-methyl naphthalene

INSTRUMENT USED:	DATE OF REPORT:	EXPERIMENT NO:
SAD	February 8, 1995	1896

TITLE:
SANS of Petroleum Resid and Their Interaction with Dispersed Catalysts

AUTHORS AND AFFILIATIONS:
R. E. Winans, J. E. Hunt, P. Thiyagarajan — ANL
K. B. Anderson, J. T. Miller — Amoco Corp.

DATES OF EXPERIMENT:
December 7-9, 1994

CHECK ALL APPLICABLE BOXES:

- [√] APPROVED BY PROGRAM COMMITTEE
- [√] INSTRUMENT SCIENTIST ALLOCATION
- [ ] DO NOT PUBLISH
- [ ] PROPRIETARY RESEARCH
- [ ] PRT ALLOCATION

EXPERIMENTAL REPORT (or Abstract of Publication)

Small angle neutron scattering (SANS) was used to investigate the structural changes of a 5 wt.% asphaltene solution in perdeuterated 1-methylnaphthalene (d-1MN) as a function of temperature. A special stainless steel cell was constructed and used for the measurements. The SANS data measured at various temperatures from 20°C to 400°C show that the scattering intensity continuosly decrease with increasing temperature.A nonlinear curve in the Guinier plot for asphaltene solutions at 20°C suggested polydispersity in the sizes. Maximum entropy analysis using the form factor for a cylinder allowed extraction of particle size distributions in the radius and length space. At 20°C the asphaltenes self-associate in d-1MN forming long rod-shaped particles whose radius was around 18Å, but vary in length over 500Å. At 50°C these aggregates break down, as evidenced by the decrease in signal intensity. In the temperature range of 100 - 320°C the maximum length of the particles decreases and the polydispersity varies in both radius and length dimensions. Between 340 and 400°C, the particles become smaller having a spherical shape with a radius around 12Å. Upon returning the sample to 20°C, the SANS signal was too weak to derive any structural information, implying irreversible thermochemistry. Interestingly, the structural properties of asphaltenes in d-1MN at temperatures below irreversibility are remarkably reproducible, irrespective of the temperature sequence steps. We also carried out similar studies on the deasphalted oil (DAO) in d-1MN at 20°C, 100°C and 200°C, but the SANS signals were very weak and no changes in the scattering behavior were seen as a function of temperature. We are currently analyzing data on the temperature reversibilty of asphaltene aggregation, taking a close look at the hysteresis in their formation and disaggregation, before the onset of irreversible thermochemistry. Figure 1 shows that maximum entropy analysis is very effective in obtaining the morphology and polydispersity information of the asphaltenes. Figure 2 shows the length distribution for particles of a given radius at 4 different temperatures.

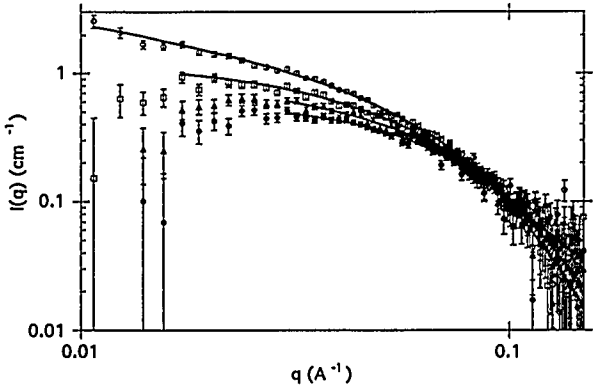


Figure 1:MaxEnt fits of the SANS data for 5 wt.% asphaltenes in d-1MN at 20°C (o), 50°C (square), 150°C (triangle) and 400°C (filled o).

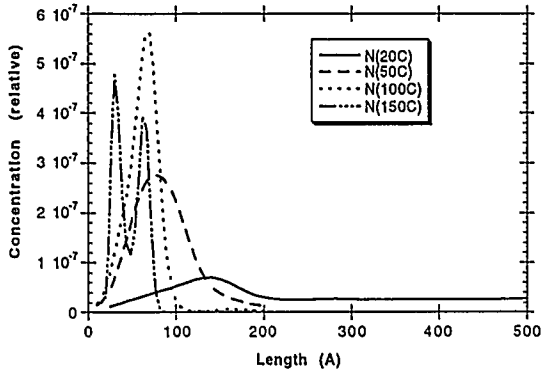


Figure 2: The length distributions for the asphaltene solutions in d-1MN: 20°C (solid line), 50°C(dashed line), 100°C (dotted line), 150°C (dashed-dotted line). See text for the radius of the particles at those temperatures.

INSTRUMENT USED:	DATE OF REPORT:	EXPERIMENT NO:
SAD	June 5, 1995	1896

TITLE:
SANS of Petroleum Resid and Their Interaction with Dispersed Catalysts

AUTHORS AND AFFILIATIONS:
R. E. Winans, J. E. Hunt, P. Thiyagarajan — ANL
K. B. Anderson, J. T. Miller — Amoco Corp.

DATES OF EXPERIMENT:
June 6-9, 1995

CHECK ALL APPLICABLE BOXES:

- [√] APPROVED BY PROGRAM COMMITTEE
- [√] INSTRUMENT SCIENTIST ALLOCATION
- [ ] DO NOT PUBLISH
- [ ] PROPRIETARY RESEARCH
- [ ] PRT ALLOCATION

EXPERIMENTAL REPORT (or Abstract of Publication)

Asphaltenes, the heptane insoluble fraction of petroleum resids, are known to interfere in the upgrading and refining processes of petroleum by forming colloidal objects. The characterization of petroleum resid is a primary component of our CRADA agreement with Amoco Oil Company. Asphaltene is an important component in petroleum, and has long been considered as the most refractory one. Petroleum resid are hydrogen deficient, high boiling (540°C+), heavy petroleum fractions that are difficult to upgrade to gasoline range products. Major problems associated with their upgrading are coke formation and difficulty in removing heteroatoms and metals. It is believed that most of the problems can be attributed to multinuclear aromatic clusters, which contain major portions of the metals and heteroatoms. In the previous experiments we used SANS to obtain details on the aromatic structure, molecular size, and shape distributions of asphaltenes at reaction temperatures and pressures and to define the temperature limits for reversibility in the transformation of asphaltene size and shape. We also found that the oils and resins from which the asphlatenes were precipitated shows no aggregation behavior. A manuscript has been accepted by *Energy and Fuels* and is attached.

Recently, our CRADA partner, Jeff Miller at Amoco, has been successful in further separating the asphaltenes into two subfractions. The heavier of the subfractions behaves much as the unseparated fraction. However, the lighter fraction shows characteristics in between that of the whole asphlatene and the deasphalted oil. In the most recent SANS results from early June 1995, we have determined that the lighter fraction aggregates strongly at room temperture, but falls apart to smaller sizes with even a slight increase in temperature. The heavier fraction also aggregates at RT, but maintains large particle sizes up to a temperature of 300°C. SANS has produced the first experimental evidence of a real difference in these two samples which is not only of scientific interest in terms of aggregation, but also impacts on the process conditions used in industry.

SAD	5 March, 1990	1100

TITLE:
Hydrostatic Pressure Analysis of Teleost Myelin Stability

AUTHORS AND AFFILIATIONS: D.L. Worcester, UMC, Columbia, Missouri.
A.E. Blaurock, Kraft Technology Center, Glenview

DATES OF EXPERIMENT: 14 October, 1989

☑ APPROVED BY PROGRAM COMMITTEE, OR

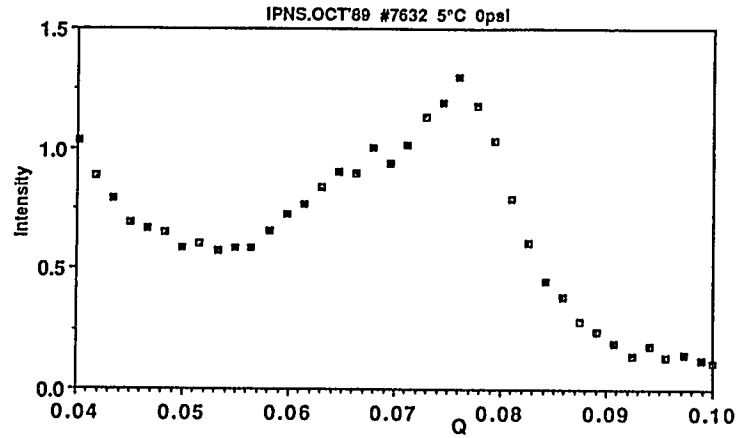
☐ PART OF INSTRUMENT SCIENTIST ALLOCATION

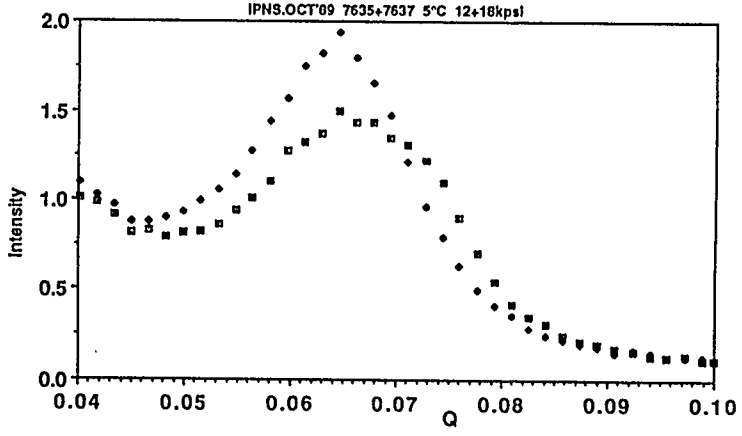
REPORT RECEIVED:

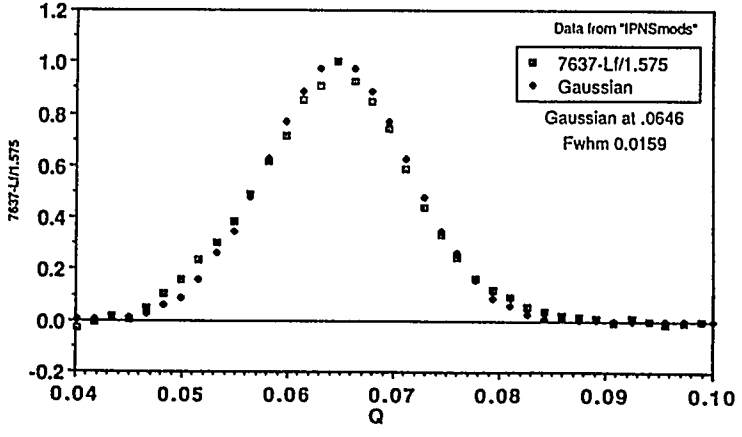
EXPERIMENTAL REPORT (or Abstract of Publication)

First measurements of teleost myelin membrane spacings at different hydrostatic pressures has provided data sets at 5, 22 and 37°C and pressures up to 18kpsi. All measurements were made on a single sample within 20 hours of dissection. The strong second order diffraction peak was used to determine membrane spacing changes. The position of this peak gives the single membrane spacing for the centrosymmetric unit cell containing two membranes. Other diffraction orders could not be measured in the time available, so it could not be determined whether the changes were cytoplasmic or extracellular. Apart from this limitation, teleost myelin was found to be qualitatively similar to mammalian and amphibian myelins, for which membrane spacings increase with pressure. However, the teleost CNS myelin changed in a quantitatively different way than other CNS myelins. This probably reflects differences between the proteins which form membrane contacts and adhesion in these different myelins.

Further analysis is needed, and measurements at higher pressures would be of value. A small discrepancy with X-ray spacings at zero pressure is being examined. One difficulty encountered in this first work was the sensitivity of teleost myelin to Ca++, which resulted in an extra diffraction spacing in some spectra. Better Ca++ control in future will alleviate this. Data are shown on the right for 5°C in the region of the second order diffraction peak. The extra peak due to Ca++ is present in the data at the top at low Q values. At higher pressures (center), all of the myelin has changed to about this spacing. The changes with pressure are fully reversible (not shown). Analysis of the 18kpsi data is shown at the bottom, for which diffuse scattering background on both sides of the peak has been fitted and subtracted. The remaining peak is shown, together with a gaussian curve to give the peak position and width.







INSTRUMENT USED:	DATE OF REPORT:	EXPERIMENT NO.:
SAD	Sept. 9, '95	2060

TITLE: Density of Liquid Cyclohexane Inside Small Pores in Porous Glass

AUTHORS AND AFFILIATIONS: T.W. Zerda, Y. Shao, Texas Christian University
R. Hjelm, Los Alamos National Lab

DATES OF EXPERIMENT: June 9-12, 1995

CHECK ALL APPLICABLE BOXES:

- [x] APPROVED BY PROGRAM COMMITTEE
- [ ] INSTRUMENT SCIENTIST ALLOCATION
- [x] DO NOT PUBLISH
- [ ] PROPRIETARY RESEARCH
- [ ] PRT ALLOCATION

EXPERIMENTAL REPORT (or Abstract of Publication)

We planned to measure the density of liquid cyclohexane inside small pores in a series of two independent experiments. The first set of measurements was conducted at IPNS. Although we obtained good spectra at ambient conditions, we failed at low temperatures and at high pressures. Now we know how to improve the experiment and its second part will be conducted at LANSCE by the end of October.

EXPERIMENTAL REPORT (CONTD.)

INSTRUMENT USED: SCD	DATE OF REPORT: Feb. 28, 1995	EXPERIMENT NO.: 1884

TITLE: Single-Crystal Structure of Saccharinatotetraamminecopper(II) Saccharinate Hydrate

AUTHORS AND AFFILIATIONS: L. R. Falvello and I. Pascual; University of Zaragoza

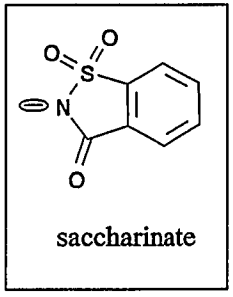
DATES OF EXPERIMENT: November 15-22, 1994

CHECK ALL APPLICABLE BOXES:

- ☒ APPROVED BY PROGRAM COMMITTEE
- ☒ INSTRUMENT SCIENTIST ALLOCATION
- ☐ DO NOT PUBLISH
- ☐ PROPRIETARY RESEARCH
- ☐ PRT ALLOCATION

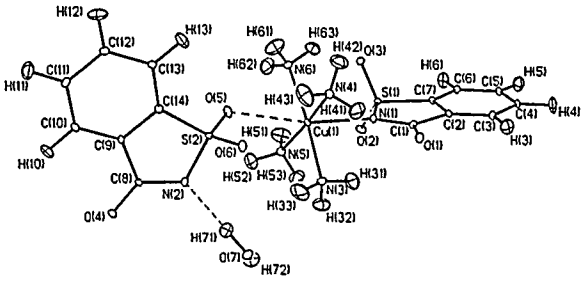
EXPERIMENTAL REPORT (or Abstract of Publication)

Compounds of first-row transition elements with polyfunctional ligands have been found to yield molecular crystalline materials exhibiting structural topologies in which the intermolecular interactions have determinative importance equal to or greater than that of the usually more prominent intra-molecular forces associated with covalent bonding. Among the ligands which have given such results are cyanurate-N, 5,5-diethylbarbiturate, and saccharinate (sac), $C_7H_4NO_3S$, which is the subject of the present study.



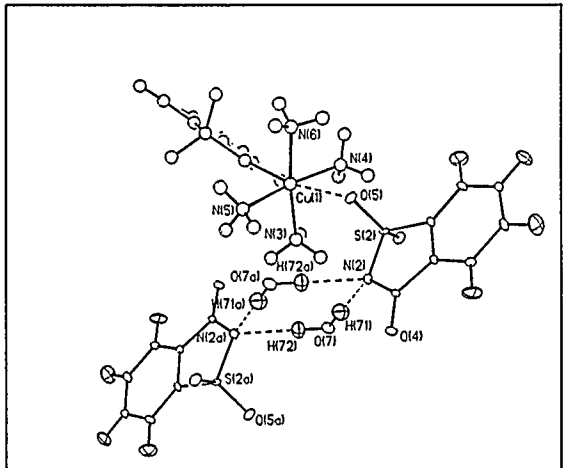
saccharinate

In this experiment the structure of $[Cu(sac)(NH_3)_4](sac)\cdot H_2O$ was determined on the Single Crystal Diffractometer at IPNS. This compound was studied because the normal six-coordinate structure about the copper center is disrupted by the formation of a supramolecular aggregate between free saccharinate and water moieties. The copper atom is left with effective five-coordination, with one saccharinate and four ammine ligands ligated in the usual way. In the sixth coordination position, there is a distant (~2.7 Å) contact to a sulfonyl oxygen atom of a saccharinate moiety that forms part of the supramolecular aggregate.



The contents of one asymmetric unit of a crystal of $[Cu(sac)(NH_3)_4](sac)\cdot H_2O$, from the neutron structure.

This compound forms rapidly in the reaction of hexaaquocopper(II) chloride with saccharinate in the presence of ammonia and water. The corresponding bis-(saccharinato)tetraamminecopper(II) complex can only be formed through non-aqueous chemistry, and converts rapidly into the present compound in the presence of even atmospheric water. The formation of the supramolecular aggregate is the driving force behind these chemical transformations. Its characterization was not complete until the structure was determined by neutron diffraction, since x-ray diffraction -- although it yielded an apparently accurate structure determination -- still did not unambiguously prove the identities of the H_2O and NH_3 moieties. The neutron analysis has resolved all outstanding questions.



The supramolecular aggregate formed by two saccharinate ions and two water molecules in $[Cu(sac)(NH_3)_4](sac)\cdot H_2O$, from the neutron structure.

Table I. Summary Data for the Neutron Single-crystal Structure of $[Cu(sac)(NH_3)_4](sac)\cdot H_2O$.

Space group	triclinic, P(-1)	V, Å^3	998.2 (3)
a, Å	6.998 (1)	No. obsd. data	7258
b, Å	10.528 (2)	No. parameters	504
c, Å	13.881 (2)	$R(F_o)$	0.098
α, °	97.55 (2)	$Rw(F_o)$	0.049
β, °	92.46 (2)	Instrument	SCD (IPNS)
γ, °	99.35 (2)	Refinement	GSAS

INSTRUMENT USED:	DATE OF REPORT:	EXPERIMENT NO.:
SCD	2/3/90	1249

TITLE: Hydrogen bonding and stress in molecular solid solutions exhibiting the cooperative Jahn-Teller effect

AUTHORS AND AFFILIATIONS: L.R. Falvello, F.A. Cotton (Texas A&M Univ.), C.A. Murillo (Univ. of Costa Rica)

DATES OF EXPERIMENT: May 14 - 25, 1990

☑ APPROVED BY PROGRAM COMMITTEE, OR

☐ PART OF INSTRUMENT SCIENTIST ALLOCATION

REPORT RECEIVED:

EXPERIMENTAL REPORT (or Abstract of Publication)

Four crystals of $Cu(sacch)_2(H_2O)_4 \cdot 2H_2O$, where sacch is saccharinate, $C_7H_4NO_3S^-$, were examined on the SCD and two were selected for data collection. One set of data was obtained at 15 K under vacuum (LTV) and a second data set was obtained at 15 K under an applied pressure of 1.3 kbar (LTP). In both cases, a quadrant of data were measured, and Bragg peaks were integrated and reduced to structure factor amplitudes. For the LTV structure there are 5796 reflections with $I > 3s(I)$, whereas for the LTP structure the number is 3594 since a smaller crystal had to be used for the high pressure sample holder. Both structures are currently being refined and have R-factors of about 10%. Upon completion of the refinements, the structures will be examined in detail to see if there are any changes in the copper coordination geometry due to the application of pressure.

EXPERIMENTAL REPORT (CONTD.)

INSTRUMENT USED:	DATE OF REPORT:	EXPERIMENT NO.:
SCD	May 25, 1993	1648

TITLE:

Hydrogen Bonding in the Crystal Structure of Vanadium Sulfate Hydrate

AUTHORS AND AFFILIATIONS: Larry R. Falvello (University of Zaragoza), Carlos A. Murillo (University of Costa Rica & TAMU) and F. Albert Cotton (Texas A&M University)

DATES OF EXPERIMENT: February 9 - 22, 1993

☒ APPROVED BY PROGRAM COMMITTEE, OR

☐ PART OF INSTRUMENT SCIENTIST ALLOCATION

REPORT RECEIVED:

EXPERIMENTAL REPORT (or Abstract of Publication)

As a result of the measurements made in February, we are submitting two manuscripts to Inorganic Chemistry. The abstracts of these two papers follow:

The Neutron and X-ray Structural Characterization of the Hexaaquavanadium(II) Compound $VSO_4 \cdot 7H_2O$.

F. Albert Cotton, Larry R. Falvello, Carlos A. Murillo, Isabel Pascual, Arthur J. Schultz and Milagros Tomás

The title compound, for which crystals are more reactive towards oxygen than the chemically similar compound $VSO_4 \cdot 6H_2O$, has been prepared as large single crystals and characterized by both x-ray diffraction at room temperature and neutron diffraction at 11 - 16 K. $VSO_4 \cdot 7H_2O$ crystallizes in the monoclinic space group $P2_1/c$, Z = 4, with the following cell dimensions, where in each case the x-ray value is given first followed by the neutron value: a = 14.130(3) Å, 14.013(2) Å; b = 6.501(1) Å, 6.481(1) Å; c = 11.017 Å, 10.981(2) Å; β = 105.64(2)°, 105.39(1)°; V = 974.5(3) Å^3, 961.5 Å^3. The structure was refined to residuals of R = 0.0289, 0.0766, and quality of fit = 1.047, 1.427, for x-ray and neutron data, respectively. It consists of two independent centrosymmetric $V(H_2O)_6^{2+}$ ions connected to a sulfate ion and an interstitial water molecule by an extensive network of hydrogen bonds. The room temperature and low-temperature structures are qualitatively identical. Each hydrogen atom is involved in a hydrogen bond. The network of hydrogen bonds is implicated in the stability of $VSO_4 \cdot 7H_2O$ in the solid state in dry surroundings.

EXPERIMENTAL REPORT (CONTD.)

Solid Solutions of a Jahn-Teller Compound in an Undistorted Host. 4. Neutron and X-ray Single-crystal Structures of a Cr/Zn Tutton Salt Solid Solution, and Their Implications for the Determination of Homogeneity.

F. Albert Cotton, Lee M. Daniels, Larry R. Falvello, Carlos A. Murillo and Arthur J. Schultz

Fragments of a solid solution cleaved from a large single crystal of the ammonium Tutton salt, $(NH_4)_2[Cr_{0.10}Zn_{0.90}(H_2O)_6](SO_2)_2$ have been studied by single x-ray diffraction at room temperature and neutron diffraction at 11 - 16 K, as well as atomic absorption, AA, analysis. It crystallizes in the monoclinic space group $P2_1/c$, Z = 4, with the following cell dimensions, where in each case the x-ray value is given first followed by the neutron value: a = 6.249(2) Å, 6,286(1) Å; b = 12.508(3) Å, 12.367(2) Å; c = 9.237(2) Å, 9.147(2) Å; β = 106.82(2)°, 106.87(1)°; V = 691.1(3) Å^3, 680.4(2) Å^3. The structure was refined to residuals of R = 0.0226, 0.0670, and quality of fit = 1.099, 1.165, for x-ray and neutron data, respectively. The anisotropic displacement parameters of the oxygen and hydrogen atoms from the neutron diffraction study are examined for their implications as to the presence or absence of disorder in the ligands about the composite Cr/Zn metal center. The results indicate that there is no disorder in the crystallographic sites in question, and thus that the solid solution is indeed geometrically homogeneous. A comparison of the x-ray and neutron results is used to infer the reliability of x-ray analysis in determining the homogeneity of such systems.

INSTRUMENT USED: SCD	DATE OF REPORT: April 20, 1994	EXPERIMENT NO.: 1731

TITLE: Hydrogen Bonding and Strain in Molecular Solid Solutions Exhibiting the Cooperative Jahn-Teller Effect

AUTHORS AND AFFILIATIONS: Larry R. Falvello (University of Zaragoza) and Carlos A. Murillo and F. A. Cotton (Texas AM University)

DATES OF EXPERIMENT: December 7 - 15, 1993

CHECK ALL APPLICABLE BOXES:

- ☑ APPROVED BY PROGRAM COMMITTEE
- ☐ INSTRUMENT SCIENTIST ALLOCATION
- ☐ DO NOT PUBLISH
- ☐ PROPRIETARY RESEARCH
- ☐ PRT ALLOCATION

EXPERIMENTAL REPORT (or Abstract of Publication)

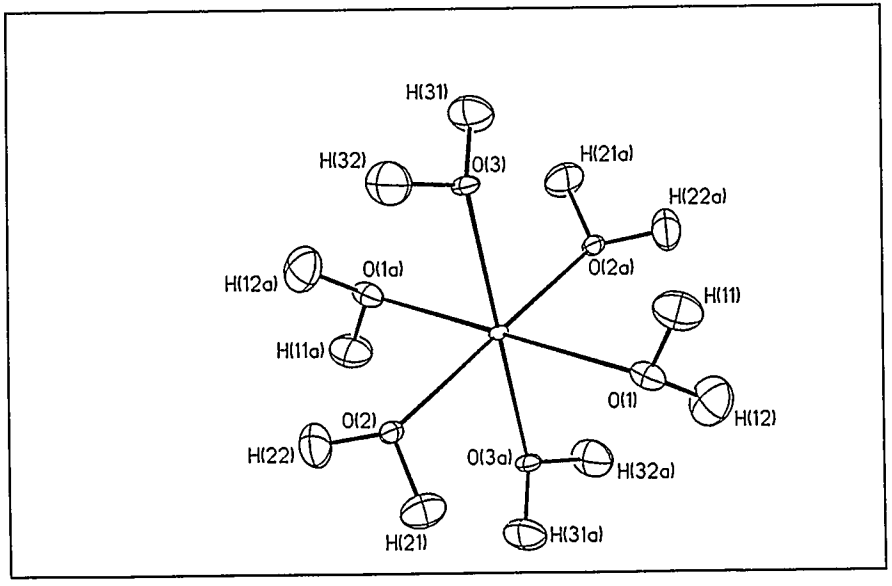
Solid Solutions of a Jahn-Teller Compound in an Undistorted Host. 4. Neutron and X-ray Single-crystal Structures of Two Cr/Zn Tutton Salt Solid Solutions, and the Observation of Disorder by Low-temperature Neutron Diffraction

F. Albert Cotton, Lee M. Daniels, Larry R. Falvello,* Carlos A. Murillo,* and Arthur J. Schultz*

Abstract

Solid solutions of the ammonium Cr/Zn Tutton salt with two different compositions, $(NH_4)_2[Cr_{0.10}Zn_{0.90}(H_2O)_6](SO_4)_2$, **1**, and $(NH_4)_2[Cr_{0.22}Zn_{0.78}(H_2O)_6](SO_4)_2$, **2**, have been studied by single crystal x-ray diffraction at room temperature and by neutron diffraction at 11 - 16 K for **1** and at 11 - 17 K for **2**. Composition **1** was also characterized by atomic absorption, AA, analysis. The solid solutions, which are isotypic at a given temperature, crystallize in the monoclinic space group $P2_1/c$, Z = 2, with the following cell dimensions, where in each case the room temperature x-ray value is given first followed by the low-temperature neutron value: For **1**, a = 6.249(2), 6.286(1) Å; b = 12.508(3), 12.367(2) Å; c = 9.237(2), 9.147(2) Å; β = 106.82(2), 106.87(1)°; V = 691.1(3), 680.4(2) Å^3. For **2**, a = 6.252(1), 6.260(1) Å; b = 12.503(1), 12.242(2) Å; c = 9.247(1), 9.093(1) Å; β = 106.77(1), 106.89(2)°; V = 692.1(1) Å^3, 666.8(2)(2) Å^3. The structure of **1** was refined to residuals of R = 0.0226, 0.0670, and quality of fit = 1.099, 1.165, for x-ray and neutron data, respectively; the corresponding residuals for the x-ray and neutron structures of **2** are R = 0.0215, 0.0682, and quality-of-fit = 1.057, 0.994. The anisotropic displacement parameters of the oxygen and hydrogen atoms from the neutron diffraction studies are examined for their implications as to the presence or absence of disorder in the ligands about the composite Cr/Zn metal center. The results for composition **2**, x(Cr) = 0.22, clearly indicate the presence of disorder for the aqua ligand affected by Jahn-Teller distortion in the pure chromium complex. For composition **1**, x(Cr) = 0.10, the observation of disorder is not clear. The structures of **1** and **2** are isotypic at a given temperature, but the room-temperature and low-temperature structures differ subtly in the hydrogen bonding pattern.

The manuscript that accompanies this abstract contains a description of the first clear and undoubtable observation we have made of disorder in molecular solid solutions. The oxygen atom affected by Jahn-Teller distortion on the pure chromium sample, O(1) in the figure below, has displacement parameters that show elongation roughly parallel to the M-O bond. The use of low-temperature SCD data has thus made possible the resolution of an important question in the mechanism of molecular solid solution formation -- that is, whether there is disorder or not in the Tutton salt system.



INSTRUMENT USED:	DATE OF REPORT:	EXPERIMENT NO.:
SINGLE-CRYSTAL DIFFRACTOMETER	6/10/91	1209

TITLE: ANALYZING CARBOXYLIC ACID AND AMINO-NITRO HYDROGEN-BOND GEOMETRY IN THE COCRYSTAL OF 4-AMINOBENZOIC ACID AND 3,5-DINITROBENZOIC ACID BY USE OF 298K X-RAY and 15K NEUTRON DIFFRACTION

AUTHORS AND AFFILIATIONS: GAYLE M. FRANKENBACH, ARTHUR J. SCHULTZ, JACK M. WILLIAMS (ARGONNE) MARGARET C. ETTER (U. OF MINNESOTA)

DATES OF EXPERIMENT: November 15-22, 1989

☒ APPROVED BY PROGRAM COMMITTEE, OR

☐ PART OF INSTRUMENT SCIENTIST ALLOCATION

REPORT RECEIVED:

EXPERIMENTAL REPORT (or Abstract of Publication)

The structure of the cocrystal (**1**) of 4-aminobenzoic acid (**2**) and 3,5-dinitrobenzoic acid (**3**), $C_7H_7NO_2 \cdot C_7H_4N_2O_6$, $M_r = 349.26$, has been determined at 298 K by use of X-ray diffraction and at 15 K by use of neutron diffraction techniques. X-ray diffraction structure: Fdd2, $a = 21.49$ (3), $b = 7.041$ (7), $c = 20.65$ (2) Å, V= 3120 (1) Å^3, Z = 8, $D_x = 1.48$ Mg·m^{-3}, λ(Mo Kα) = 0.71073 Å, $\mu = 1.17$ cm^{-1}, F(000) = 1440, $R(F_o) = 0.032$, $R_w(F_o) = 0.029$. Neutron diffraction structure: $a = 21.135$ (3), $b = 6.8567$ (7), $c = 20.602$ (2) Å, V= 2985.6 (6) Å^3, Z = 8, $D_x = 1.5541$ Mg·m^{-3}, time of flight neutron diffraction, λ = 0.7-4.2 Å, $\mu = 0.968$-2.896 cm^{-1}, $R(F_o) = 0.061$, $R_w(F_o^2) = 0.118$. In **1**, hydrogen-bond formation between the acid groups of **2** and **3** results in a cyclic heterodimer. Neutron diffraction data were collected to accurately locate the acid protons and to determine the geometry of the hydrogen bonds. The two acid hydrogen bonds are related by a two-fold crystallographic rotation axis and the protons are disordered over two sites. The heterodimers are organized into two-dimensional polar sheets as a consequence of hydrogen bonding between an amine group and nitro groups on neighboring heterodimers. Determining the structure of **1** at two different temperatures revealed significant changes in the amino-nitro hydrogen-bond geometry, but virtually no change in the acid-acid hydrogen-bond geometry.

EXPERIMENTAL REPORT (CONTD.)

PAPER SUBMITTED TO: ACTA CRYSTALLOGRAPHICA C
JUNE 1991

INSTRUMENT USED:	DATE OF REPORT:	EXPERIMENT NO.:
Single crystal diffractometer	3 June, 1994	1430

TITLE:
Neutron diffraction study of the effect of pressure on the structure of $(NH_4)_2[Cr(H_2O)_6](SO_4)_2$

AUTHORS AND AFFILIATIONS:
M.A. Hitchman, H. Stratemeier, C.J. Simmons, A.J. Schultz, B.N. Figgis

DATES OF EXPERIMENT:
15 March - 25 March, 1994

CHECK ALL APPLICABLE BOXES:

- ☐ APPROVED BY PROGRAM COMMITTEE
- ☐ INSTRUMENT SCIENTIST ALLOCATION
- ☐ DO NOT PUBLISH
- ☐ PROPRIETARY RESEARCH
- ☐ PRT ALLOCATION

EXPERIMENTAL REPORT (or Abstract of Publication)

Background

As part of a general investigation of static and dynamic Jahn-Teller distortions in transition metal complexes, we have studied the Tutton salts, $X_2[M(H_2O)_6](SO_4)_2$, where X is a monovalent cation and M a divalent metal ion. When M = Cu^{2+} and Cr^{2+} the Jahn-Teller effect causes the $M(H_2O)_6^{2+}$ ions to adopt tetragonally elongated octahedral coordination geometries and the salts with X=NH_4 are particularly interesting, because here the direction of the long M-(H_2O) bonds in the lattice varies with temperature. Moreover, for the Cu^{2+} compound, this direction differs for the hydrogenous and deuterated compound. In a previous study at Argonne using the single crystal scanning neutron diffractometer at 15K, the geometry of the deuterated salt was observed to change to that of the hydrogenous salt at a pressure of 1.5kbar, the only known example of a Jahn-Teller 'switch' of this kind (*J. Am. Chem. Soc.* **1993**, *115*, 11304). The difference in structure, and the reason for the pressure switch, both appear to be related to the delicate balance in this lattice between hydrogen bonding interactions and the Jahn-Teller distortion of the $Cu(H_2O)_6^{2+}$ complex.

The hydrogenous and deuterated ammonium salts of Cr^{2+} both adopt the low-pressure structure of the deuterated Cu^{2+} compound, though work by another group has shown that 'doping' with a small percentage of Zn^{2+} ions causes the structure to change to that of the hydrogenous Cu^{2+} compound. This suggests that the Cr^{2+} compounds may undergo a change in structure at high pressure analogous to that shown by the deuterated Cu^{2+} compound. To investigate this point, and study in detail the dependence of the hydrogen bonding lattice interactions on the nature of the metal, it was decided to look at the effect of pressure on the structure of $(NH_4)_2[Cr(H_2O)_6](SO_4)_2$.

Results

Initially, several crystals of $(NH_4)_2[Cr(H_2O)_6](SO_4)_2$ were mounted on the single crystal diffractometer and subjected to a pressure of ~1.5kbar, both at room temperature and 15K, but on each occasion the crystal shattered. On close examination under a microscope, it was observed that the crystals contained small bubbles, and this probably led to their inability to withstand high pressure. It was therefore decided to collect a data set at room temperature and ambient pressure.

EXPERIMENTAL REPORT (CONTD.)

Data collection and refinement of the structure proceeded smoothly, leading to a final R(F_0) value of 0.069. The parameters of the monoclinic unit cell, a = 9.368(2), b = 12.621(4), c = 6.177(1)Å, β = 106.64°, space group $P2_1/a$, and atomic positions agree well with those from the previous X-ray study. The accurate hydrogen positions obtained in the present neutron study allow a detailed analysis of the hydrogen bonding interactions, and this is currently under way. Comparison with the data already available from the neutron studies of the hydrogenous and deuterated Cu^{2+} compounds at high and low pressure should provide a detailed picture of the inter-relationships between the orientation of the Jahn-Teller distortion of the two metal ions and the hydrogen bonding network in the lattices.

In addition, the neutron diffraction data collected earlier for $K_2[Cu(H_2O)_6](SO_4)_2$ at 15K and 1.4kbar were analysed. The refinement converged to an R(F_0) value of 0.049, yielding cell parameters a = 9.030(2), b = 12.022(3), c = 6.121(2)Å, β = 104.29(3)°. At ambient pressure, the orientation of the Jahn-Teller distorted $Cu(H_2O)_6^{2+}$ ions in this lattice was known from a previous X-ray study to be similar to that in deuterated $(NH_4)_2[Cu(H_2O)_6](SO_4)_2$. In contrast to the latter compound, it was found that no switch in the direction of the long bonds of the $Cu(H_2O)_6^{2+}$ group occurs at high pressure for the potassium salt. Comparison of the high and low pressure structures of $K_2[Cu(H_2O)_6](SO_4)_2$ therefore provides a useful guide to the effect of pressure on the Cu-O bond distances and hydrogen bonding interactions in the absence of a change in the packing of the $Cu(H_2O)_6^{2+}$ groups. A detailed comparison of the structure of the potassium salt with those of the high and low pressure forms of the deuterated ammonium compound is currently under way to establish the role of the monovalent cations in the hydrogen bonding network, and the influence this has on the orientation of the Jahn-Teller axis of distortion.

INSTRUMENT USED:	DATE OF REPORT:	EXPERIMENT NO.:
5CD	7/16/91	1114

TITLE: Accurate determination of changes in structural parameters in NiF_2 due to magnetic ordering

AUTHORS AND AFFILIATIONS: W. Jauch, Hahn-Meitner Inst. Berlin
A. Schultz, ANL

DATES OF EXPERIMENT: July 11-25 1989

☒ APPROVED BY PROGRAM COMMITTEE, OR

☐ PART OF INSTRUMENT SCIENTIST ALLOCATION

REPORT RECEIVED:

EXPERIMENTAL REPORT (or Abstract of Publication)

Introduction:

Neutron data have been collected at 3 temperatures from the same sample used for an extended γ-ray investigation. The primary goal of the neutron work consisted in determining reliable values of the mean thermal positions of the fluorine nuclei. The present study is essential to probing the influence of magnetic order on the charge density.

Refinement conditions:

- refinements based on F^2, no data threshold;
- weighting scheme: $w^{-1} = \sigma_{cs}^2 + (0.04\ F^2)^2 + \text{const.}$;
- extinction correction: Becker-Coppens Lorentzian;
- T = 15 K: reflections with h+k+l = odd and $\sin\Theta/\lambda < 0.6$ Å^{-1} are excluded since they may contain magnetic contributions.

Comments:

- refined mosaic width is strongly temperature dependent;
- T = 295 K: excellent agreement with positional parameter as obtained from γ-ray diffraction: x(γ-ray) = 0.30365(9);
- T = 15 K: results probably affected by the magnetic domain structure (90° domains, orthorhombic symmetry due to weak ferromagnetic component).

EXPERIMENTAL REPORT (CONTD.)

Structural results for NiF_2 (T_N = 73 K):

		295 K	80 K	15 K
g'		1.69(4)	0.94(2)	0.60(1)
Ni:	U_{11}(Å^2)	0.00494(4)	0.00208(4)	0.00210(4)
	U_{33}	0.00373(5)	0.00170(5)	0.00158(5)
	U_{12}	-0.00037(3)	-0.00012(2)	-0.00009(2)
F:	x	0.30365(4)	0.30352(4)	0.30335(3)
	U_{11}(Å^2)	0.00931(7)	0.00445(5)	0.00429(4)
	U_{33}	0.00603(7)	0.00340(6)	0.00333(5)
	U_{12}	-0.00426(5)	-0.00146(4)	-0.00130(3)
n		1751	1758	1693
R(F)		0.0384	0.0385	0.0323
$R(F^2)$		0.0532	0.0643	0.0471
$wR(F^2)$		0.0712	0.0801	0.0693

INSTRUMENT USED:	DATE OF REPORT:	EXPERIMENT NO.:
SCD	3/6/91	1483

TITLE: Texture analysis of $YBa_2Cu_3O_x$ specimens

AUTHORS AND AFFILIATIONS: J.S. Kalland - IIT
A.C. Biondo, A.J. Schultz, K.C. Goretta - ANL

DATES OF EXPERIMENT: Sept. 14-18, 1990

☒ APPROVED BY PROGRAM COMMITTEE, OR

☐ PART OF INSTRUMENT SCIENTIST ALLOCATION

REPORT RECEIVED:

EXPERIMENTAL REPORT (or Abstract of Publication)

TEXTURE ANALYSIS OF BULK $YBa_2Cu_3O_x$ BY NEUTRON DIFFRACTION

J. S. Kallend
Illinois Institute of Technology, Chicago, Illinois 60616
A. C. Biondo, A. J. Schultz, and K. C. Goretta
Argonne National Laboratory, Argonne, Illinois 60439

ABSTRACT

Neutron diffraction has been used to generate Orientation Distribution Functions for two sinter-forged $YBa_2Cu_3O_x$ specimens. Sinter forging imparted a strong texture, with *c* axes of crystals preferentially aligned parallel to the forging direction. The distribution of *a* and *b* axes was not uniform, which may have implications to critical current density.

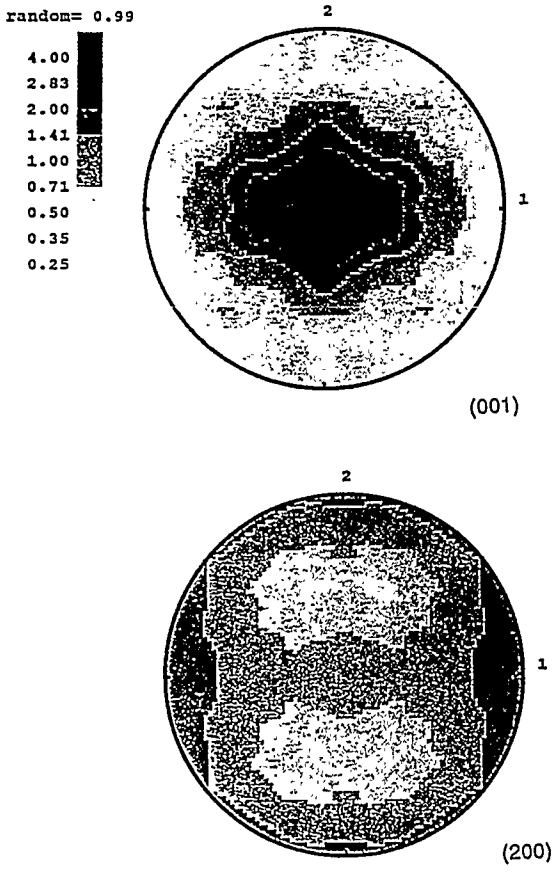


Figure 4. Representatine pole figures for first sinter forging.

CONCLUSION

Neutron diffraction was used to generate Orientation Distribution Functions of sinter-forged $YBa_2Cu_3O_x$. The sinter forgings had strong textures, with *c* axes being preferentially aligned with the forging direction. Grain growth during forging appeared to enhance texture slightly. The ODFs reveal that the *a* and *b* axes of the sinter forgings are distributed nonrandomly.

INSTRUMENT USED:	DATE OF REPORT:	EXPERIMENT NO.:
SCD		1145

TITLE:
Crystal Chemistry and Crystal Physics of Neptunite

AUTHORS AND AFFILIATIONS:
M. Kunz, Th. Armbruster, G.A. Lager, Art Schultz, R.J. Goyette

DATES OF EXPERIMENT: March 20 - April 1, 1996

☒ APPROVED BY PROGRAM COMMITTEE, OR

☐ PART OF INSTRUMENT SCIENTIST ALLOCATION

REPORT RECEIVED:

EXPERIMENTAL REPORT (or Abstract of Publication)

Fe/Ti-ordering in neptunite ($KNa_2LiTi_2Fe_2Si_8O_{24}$).

Martin Kunz, Thomas Armbruster, University of Berne (Switzerland);
G.A. Lager, University of Louisville;
Art Schultz, R.J. Goyette, Argonne National Laboratory.

The crystal structure of neptunite was first described by Canillo et al. (1966) in space group C2/c. The structure basically consists of Fe/Ti-octahedral chains running along [110] and [$\bar{1}$ 10]. These octahedra are interlaced with SiO_4-tetrahedral chains. The alkali cations Na, Li, and K are situated in large cavities within this framework. A subsequently observed piezoelectric effect was in contradiction to the centric space group. Therefore, the authors proposed a refinement in space group Cc (Canillo et al. 1966). The acentric refinement was recently performed with X-ray experiments preceding the present neutron single crystal study. However, the metal distribution on the octahedral sites, which was believed to be the cause of the acentricity, could not be resolved with the X-ray experiments.
Thus, the primary goal of this neutron single crystal study was to refine the Fe/Ti ordering on the octahedral metal sites. An additional experiment was performed with a self-constructed pressure cell to obtain insight into the structural dependence of the piezoelectric effect.

The following results were obtained:

a) Data collection at 15 K and 293 K enabled refinements of the positional parameters and the displacement parameters as well as the metal scattering lengths. Despite some correlation problems between pseudo-centro-symmetric equivalent positions, the refinements converged to R(F) and wR(F^2)-values of 5.25% and 9.75%, respectively.

The refinement of the metal scattering lengths yielded a coarse ordering into two Ti sites and two Fe sites. The exact distribution of the metal atoms within these four sites, however, was not so easy to resolve due to minor amounts of Mn and Mg that also occupy the metal sites.
Coupling the neutron observation with the X-ray results, we assumed that Mn and Mg concentrate on the two Fe-sites. With this constraint, we were able to derive the following Fe/Ti ordering scheme from the neutron data:

Ti1: 100% Ti
Ti2: 90% Ti, 10% Fe
Fe1 + Fe2: 70% Fe, 10% Ti, 10% Mn, 10% Mg.

Thus, Ti and Fe are highly ordered and therefore induce the observed acentricity. Whether this ordering is caused by differences in polyhedral distortion or whether these distortions are generated as a result of ordering is a topic of further investigations.

b) The aim of a third run was to relate structural changes at pressure to the piezoelectric effect observed for neptunite. For this purpose, a mechanical pressure cell was constructed. The experiment was performed with a pressure of about 80 bars directed parallel to the crystallographic a-axis and applied to the same crystal used for the first two runs.
Unfortunately, the Al-housing of the pressure apparatus may have been too thick. Absorption as well as Al-powder peaks affected the data strongly. As a consequence, we were not able to carry out a satisfactory refinement. Fixing all displacement parameters at the values obtained from the 293 K refinement, the R(F) value converged to 8.1%. However, the standard deviations are large and the results of the pressure experiment are difficult to interpret.

Refernce: Canillo. E., Mazzi, F., Rossi, G. (1966): The Crystal Structure of Neptunite. Acta Crystallographica, 21, 200 - 208.

INSTRUMENT USED:	DATE OF REPORT:	EXPERIMENT NO.:
SCD	December 4th, 1990	NSF-15

TITLE: Structure and Processing Relationships in Single Crystal $Y_{1-x}Pr_xBa_2Cu_3O_{7-d}$

AUTHORS AND AFFILIATIONS: J.R. LaGraff, P.D. Han, and D.A.Payne: UIUC
A. Schultz and R. Goyette: ANL

DATES OF EXPERIMENT: 9/5-9/10/90

☒ APPROVED BY PROGRAM COMMITTEE, OR

☐ PART OF INSTRUMENT SCIENTIST ALLOCATION

REPORT RECEIVED:

EXPERIMENTAL REPORT (or Abstract of Publication)

Relatively few $YBa_2Cu_3O_{7-\delta}$ single crystals of sufficient size (>1mm^3) have been available for neutron diffraction studies. The authors have found that crystals grown with high levels of praseodymium (Pr) are generally an order of magnitude larger in the c-direction than pure $YBa_2Cu_3O_{7-\delta}$. The reason for this is not yet known. Preliminary measurements were made on a Pr-doped single crystal of dimensions ~3x3x0.8mm^3 in order to determine site occupancies for Y, Pr, and chain oxygen. The self-flux from which the crystal was grown had a nominal Pr concentration of x=0.4; however, preliminary analysis gives a site occupancy of 0.48 which indicates that Pr has a higher affinity for the Y-site than yttrium. The calculated chain oxygen site occupancy of 0.9 (δ~0.1) suggests almost complete oxygenation of the crystal. Assuming ideal {110} twinning when fitting the data does not yield satisfactory results. This indicates a mosaic structure due to either mismatch of the twin boundary orientations throughout the bulk of the crystal or to the mismatch of successive layers during the growth of the crystal. The latter could have important implications on the optimal growth conditions for single crystals of these materials. Efforts are underway to detwin large crystals in order to look for the 60K superstructure (orthorhombic II phase) which has been observed by electron diffraction, but not yet by neutron diffraction.

INSTRUMENT USED: SCD	DATE OF REPORT: June 14, 1995	EXPERIMENT NO.: 2056

TITLE:
Impurity-Induced Electronic Conductivity and Ferroelectricity in Ca-doped $KTa_{1-x}Nb_xO_3$

AUTHORS AND AFFILIATIONS: Chun Loong, Argonne National Laboratory
Hans-Martin Christen and Lynn A. Boatner, Oak Ridge National Lab.

DATES OF EXPERIMENT: May 9 - 15, 1995

CHECK ALL APPLICABLE BOXES:

- [X] APPROVED BY PROGRAM COMMITTEE
- [ ] INSTRUMENT SCIENTIST ALLOCATION
- [ ] DO NOT PUBLISH
- [ ] PROPRIETARY RESEARCH
- [ ] PRT ALLOCATION

EXPERIMENTAL REPORT (or Abstract of Publication)

Introduction

It has recently become possible to grow high-quality ferroelectric $K(Ta_xNb_{1-x})O_3$ single crystals with the addition of small amounts (approx. 0.05 % molar) of Ba, Ca, or Sr. The resulting material is a semiconductor with a high room-temperature electrical conductivity.

The transition temperature of insulating $K(Ta_xNb_{1-x})O_3$ varies with the Nb-concentration, and the character of the transition changes from first order to second order to quantum ferroelectric with increasing x.

At this time it is not clear how the presence of electrical carriers affects this structural transition. The present study was undertaken as a first step to shed light on this issue.

Neutron diffraction was chosen as a method due to the difficulties involved in alternative experiments. For example, dielectric measurements will only probe the behavior of the depleted portion of the sample (which is expected to behave very similarly to the undoped crystals). Due to the limited penetration depth of x-rays in electrically conducting materials, x-ray diffraction suffers the same difficulty.

Semiconductive perovskites with a high dielectric polarisability are known to exhibit a large depletion layer at a bare surface (H.-M. Christen *et al.*, *Phys. Rev. B* 49 12095 (1994)), and thus fine-grained powders may once more reflect the behavior of the insulating material only. It is therefore natural to study these materials using a single crystal diffractometer.

The aim of this study is to determine if semiconducting $K(Ta_xNb_{1-x})O_3$ undergoes a structural phase transition similar to the insulating material, and how the transition temperature of the semiconducting material compares to that of the insulating crystal.

Experiment

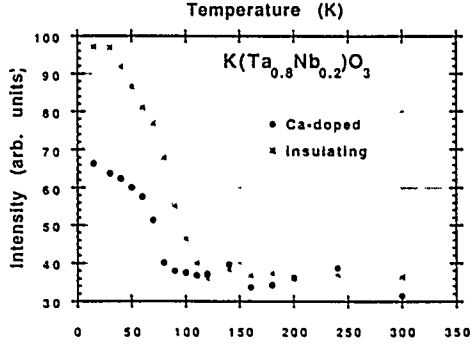
Single crystals of insulating and semiconducting $K(Ta_xNb_{1-x})O_3$ with x=0.2 and x=0.52 have been cut into pieces of approximately 10 - 20 mm^3. Several Bragg reflections of the room temperature cubic structure have been followed across the known transition temperature of the insulating material. Since the crystal is known to break up into domains much smaller than the sample size, no average distortion from the cubic phase is expected, however it was carefully checked whether a splitting of one of the peaks could be observed. In particular, it is known that the splitting of the (024) reflection can easily be detected by x-rays (P. M. Gehring *et al.*, *Ferroelectrics* 150 47 (1993)).

The resolution of the present neutron scattering set-up unfortunately proved to be insufficient to detect any peak splitting. As an alternative means to detect a phase transition, the integrated intensity of a single Bragg reflection was studied as a function of temperature. A relief of extinction resulting in an increased peak intensity has previously been observed to parallel the cubic-to-ferroelectric phase transition in $K(Ta_xNb_{1-x})O_3$ (P. M. Gehring *et al.*, *op. cit*).

Results

The figure shows the temperature dependence of the peak intensity of the (200) Bragg reflection upon cooling. As evident from the data (and as also observed on the x=0.52 sample) the sharp increase of the intensity occurs at a different temperature for each sample. In fact, the present measurement shows that the phase transition temperature is reduced by as much as 25% as a consequence of the 0.05% Ca doping.

To our knowledge, this is the first observation of this type of an effect. Additional experiments will be required to fully understand the mechanism that couples the electrical carriers to this structural phase transition.



INSTRUMENT USED:	DATE OF REPORT:	EXPERIMENT NO.:
SCD	June 30, 1995	2073

TITLE: Structural Studies on a Nanoporous Coordinational Network

AUTHORS AND AFFILIATIONS: J. S. Moore and D. Venkataraman, Dept. of Chemistry, University of Illinois at Urbana-Champaign

DATES OF EXPERIMENT: June 15-19, 1995

CHECK ALL APPLICABLE BOXES:

- [X] APPROVED BY PROGRAM COMMITTEE
- [ ] PROPRIETARY RESEARCH
- [ ] INSTRUMENT SCIENTIST ALLOCATION
- [ ] PRT LOCATION
- [ ] DO NOT PUBLISH

EXPERIMENTAL REPORT (or Abstract of Publication)

Data collection was initiated on a large crystal of a framework material composed of a trigonal aromatic nitrile. The cavities have diameters of about 10 Å and in this particular study, contain both deuterated and protiated benzene.

A large crystal was selected from a solution of the mother liquor. Intiially, the data were very good and we were very optimistic of obtaining sufficient data for a combined x-ray/neutron structure analysis as we had successfully done with a related compound. Since the x-ray data were collected at room temperature, and since the x-ray crystal had remained stable over a 2 week period in the air in the x-ray beam, it was decided to collect the neutron data at room temperature and ambient pressure. However, over a period of several days the diffraction from the sample decreased and finally disappeared. There was not sufficient time available to try a second crystal.

For a future experiment, we will first try to obtain low temperature x-ray data. This will allow us to cool the crystal in the neutron data collection, which should reduce the possible of thermal decomposition and improve the data. In addition, we will coat the crystal with a fluorinated grease or epoxy to reduce the probably of loosing guest molecules.

EXPERIMENTAL REPORT (CONTD.)

INSTRUMENT USED:	DATE OF REPORT:	EXPERIMENT NO:
SCD	Nov. 20, 95	1928

TITLE:

Magnetic Structure of UCu_3Al_2

AUTHORS AND AFFILIATIONS:

H. Nakotte,and R.A. Robinson
LANSCE, Los Alamos National Laboratory, Los Alamos NM 87545, USA
E. Brück, K. Prokeš and F.R. de Boer
University of Amsterdam, 1018 XE Amsterdam, The Netherlands

DATES OF EXPERIMENT:

Feb. 2-9, 1995

CHECK ALL APPLICABLE BOXES:

- [x] APPROVED BY PROGRAM COMMITTEE
- [ ] INSTRUMENT SCIENTIST ALLOCATION
- [ ] DO NOT PUBLISH
- [ ] PROPRIETARY RESEARCH
- [ ] PRT ALLOCATION

EXPERIMENTAL REPORT (or Abstract of Publication)

We performed neutron-diffraction experiments on a single crystal of UCu_3Al_2 in order to clarify the origin of an anomaly, which is appears around 10 K, in the temperature dependencies of the magnetic susceptibility, the electrical resistivity and the specific heat. For this purpose, we have collected diffraction patterns on SCD at 300 K (3 histograms), 20 K (5 histograms) and 6 K (11 histograms). The sample was cooled by means of a Heli-Tran, which had been reconfigured for this experiment, and it was found to work perfectly.

Above 10 K, almost all of the observed reflections could be indexed in the appropriate crystal structure previously reported for UCu_3Al_2 [1]. However, extremely broad peak indicate extremely poor quality of the present crystal due to large mosaicity. Closer inspection indicated an angular spread up to about 15° within the hexagonal basal plane, while the c-axis orientation seems to be well-defined.

EXPERIMENTAL REPORT (CONTD.)

At 6 K, our neutron-diffraction results did not reveal additional peaks, which would be of magnetic origin. Also triangular configuration of the moments which gives rise to magnetic contributions on nuclear reflections only (see e.g. [2]) is not supported by our data. Assuming different magnetic configurations, our data indicate that any ordered moment must be less than 0.02 μ_B. At present, we do not know whether the observed anomalies in bulk investigations indicate long-range order of even smaller magnetic moments or should be attributed to other correlation effects (e.g. spin-glass behavior).

[1] H. Nakotte, E. Brück, J.H.V.J. Brabers, K. Prokeš, F.R. de Boer, V. Sechovsky, K.H.J. Buschow, A.V. Andreev, R.A. Robinson, A. Purwanto and J.W. Lynn; IEEE Transactions on magnetics **30** (1994) 1217-9.

[2] A. Purwanto, R.A. Robinson, K. Prokeš, H. Nakotte, F.R. de Boer, L. Havela, V. Sechovsky, N.C. Tuan, Y. Kergadallan, J.C. Spirlet and J. Rebizant; J. Appl. Phys. **76** (1994) 7040-2.

INSTRUMENT USED: SCD	DATE OF REPORT: 2-13-96	EXPERIMENT NO.: 1546

TITLE: Structural parameters in NiF_2 at 15 K from a single domain crystal in a magnetic field

AUTHORS AND AFFILIATIONS: A. Palmer, W. Jauch (Hahn-Meitner Institute, Berlin), A. J. Schultz (ANL)

DATES OF EXPERIMENT: June 2-8, 1992

CHECK ALL APPLICABLE BOXES:

- [X] APPROVED BY PROGRAM COMMITTEE
- [ ] PROPRIETARY RESEARCH
- [ ] INSTRUMENT SCIENTIST ALLOCATION
- [ ] PRT LOCATION
- [ ] DO NOT PUBLISH

EXPERIMENTAL REPORT (or Abstract of Publication)

It has been predicted that the magnetic ordering in transition-metal difluorides is accompanied by small internal magnetostrictive shifts of the anions. In MnF_2, such a shift has been established by exteded γ-ray and neutron diffraction studies. In this experiment we examine NiF_2.

Data were collected at 295, 80, and 15 K. In order to exclued any distrubing influence of twinning on the results, the 15 K data were collected from a single domain crystal. Here, the sample was mounted between two CoSm permanent magnets generating a field of about 200 Oe along the *a* direction.

A predicted internal displacement is validated in NiF_2. The positional parameters are in excellent agreement with those obtained from γ-ray diffraction data. In view of this excellent agreement there is no evidence for any polarization effects in the antiferromagnetic phase.

EXPERIMENTAL REPORT (CONTD.)

INSTRUMENT USED: SCD	DATE OF REPORT: 2/14/96	EXPERIMENT NO.: Disc.

TITLE: Oxygen defect structure in Nd_2CuO_y

AUTHORS AND AFFILIATIONS: P. G. Radaelli, J. D. Jorgensen, A. J. Schultz (ANL); J. L. Peng, R. L. Greene (Univ. of Maryland)

DATES OF EXPERIMENT: March 9-19, 1993

CHECK ALL APPLICABLE BOXES:

- ☐ APPROVED BY PROGRAM COMMITTEE
- ☐ PROPRIETARY RESEARCH
- ☒ INSTRUMENT SCIENTIST ALLOCATION
- ☐ PRT LOCATION
- ☐ DO NOT PUBLISH

EXPERIMENTAL REPORT (or Abstract of Publication)

The defect structure of oxygenated and reduced Nd_2CuO_y ($y \approx 4$) was investigated by single-crystal neutron diffraction. Structural refinements indicate the presence of interstitial oxygen atoms in the "apical" O(3) position, directly above or below the copper atoms. The occupancy of the apical oxygen site is ~0.10 (per formula unit) for the oxygenated sample and ~0.04 for the reduced one. Both the in-plane O(1) and the out-of-plane O(2) oxygen sites were found to be deficient, but their occupancy did not vary, within the error bars, between the two crystals. The difference in oxygen content between the two crystals, as calculated from the structural refinements, is consistent, within the error bars, with the thermogravimetric analysis values reported in the literature.

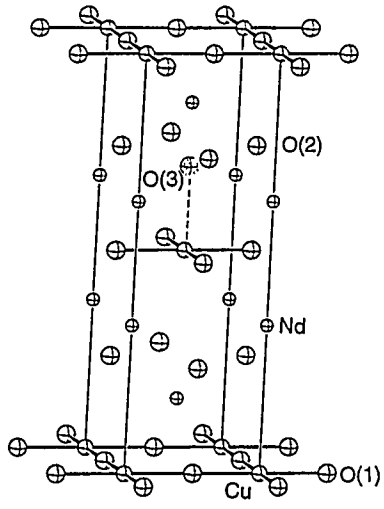


FIG. 1. Crystal structure of Nd_2CuO_y. O(3) is a defect site in the "apical" position, which we determined to have variable concentration (see text). Since the defect site occupancy is small and the defect may not obey the symmetry of the host lattice, its symmetry equivalent sites are not shown.

INSTRUMENT USED: SCD	DATE OF REPORT: 2/14/96	EXPERIMENT NO.: NSF

TITLE: Structure of superconducting $La_2CuO_{4+\delta}$ phases ($\delta \approx 0.08, 0.12$) prepared by electrochemical oxidation

AUTHORS AND AFFILIATIONS: P. G. Radaelli, J. D. Jorgensen, A. J. Schultz, B. A. Hunter, J. L. Wagner (ANL); F. C. Chou, D. C. Johnston (Iowa State Univ.)

DATES OF EXPERIMENT: Sept. 17 – Oct. 19, 1992

CHECK ALL APPLICABLE BOXES:

- [X] APPROVED BY PROGRAM COMMITTEE
- [ ] PROPRIETARY RESEARCH
- [ ] INSTRUMENT SCIENTIST ALLOCATION
- [ ] PRT LOCATION
- [ ] DO NOT PUBLISH

EXPERIMENTAL REPORT (or Abstract of Publication)

Two powder samples of electrochemically oxidized $La_2CuO_{4+\delta}$ (nominally $\delta \approx 0.08$ and 0.12) and one single crystal ($\delta \approx 0.1$), with superconducting critical temperatures of 32, 42, and 40 K, respectively, were studied using neutron diffraction. All samples appear to be single phase, both at room temperature and at low temperature (10–18 K), as evidenced by sharp Bragg peaks, indicating that these samples have compositions beyond the phase-separated region of the phase diagram. A detailed analysis of the Bragg reflections demonstrated that the basic crystallographic structure of all samples has *Fmmm* symmetry, with the excess oxygen located between adjacent LaO layers. However, a number of low-intensity peaks in the powder data suggested the existence of a very large superstructure. The satellites could be clearly identified in the single-crystal data, allowing the propagation vectors of the modulation to be determined. Rietveld refinements of the average structure, based on the main Bragg peaks, are presented here for samples prepared with this technique.

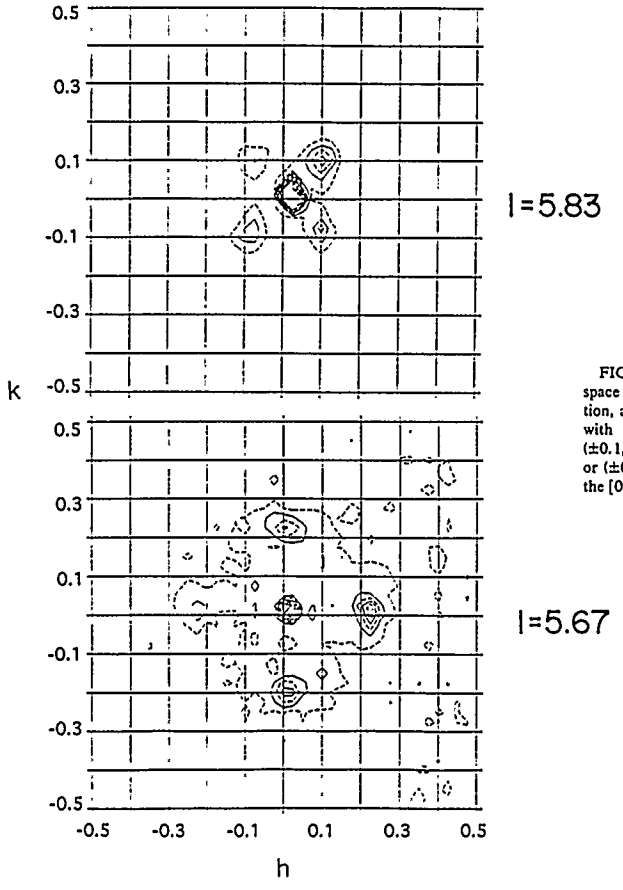


FIG. 5. Intensity contour plots of reciprocal space sections perpendicular to the c^* direction, at (a) $l \approx 5.83$ and (b) $l \approx 5.67$. Satellites with propagation vectors (a) $(\pm 0.1, \pm 0.1, -0.167)$ and (b) $(0, \pm 0.2, -0.333)$ or $(\pm 0.2, 0, -0.333)$ appear around the tail of the [0,0,6] Bragg reflection.

INSTRUMENT USED:	DATE OF REPORT:	EXPERIMENT NO.:
SCD	7/15/94	1725

TITLE: Differential ordering in minerals: The role of surface structure during growth

AUTHORS AND AFFILIATIONS: John Rakovan, Richard Reeder (SUNY Stony Brook) Art Schultz (IPNS)

DATES OF EXPERIMENT: Nov. 17-23, 1993

CHECK ALL APPLICABLE BOXES:

- ☐ APPROVED BY PROGRAM COMMITTEE
- ☐ INSTRUMENT SCIENTIST ALLOCATION
- ☐ DO NOT PUBLISH
- ☐ PROPRIETARY RESEARCH
- ☐ PRT ALLOCATION

EXPERIMENTAL REPORT (or Abstract of Publication)

Single Crystal Neutron Diffraction Study of Apatite Exhibiting Growth Related Sectoral and Intrasectoral Dissymmetrization.

John Rakovan and Richard J. Reeder. Department of Earth and Space Sciences, State University of New York at Stony Brook, Stony Brook, New York.
Arthur J. Schultz Argonne National Laboratory.

Surfaces play an important role in the partitioning of trace elements into crystals as well as in the ordering of trace and major elements during growth. Samples of natural hydroxy-fluorapatite have been found that show regions of dissymmetrization, from hexagonal to monoclinic or triclinic symmetry, that correlate directly to different growth sectors and subsectors within single crystals (see figure). Sectors formed under the {00.1} faces are uniaxial negative and exhibit a continuous extinction when viewed in optic axis sections under crossed polars. Sectors that have grown under the {10.1}, {11.1} and {10.0} faces, however, are not uniaxial. These regions are biaxial and show differential extinction orientation, in sections cut perpendicular to the c axial direction, between and within different sectors. Within time equivalent portions of a given sector, subsectors of different extinction orientation are polygonized and may show differences in optic angle (2V) as large as 13 degrees.

Rakovan and Reeder (1994) studied a number of apatites from different locations, including those in this study, that display sectoral and intrasectoral zoning of a large number of trace elements. In all of these samples, compositional heterogeneities correspond directly to different faces and symmetrically nonequivalent growth steps on a given face. Hence, it is postulated that this differential distribution of trace elements occurred during growth and was controlled by the structure of the crystal surface. The optical observations suggest that differences in surface structure are also affecting the ordering of atoms as they are incorporated into the crystals. Thus far, sectoral and intrasectoral dissymmetrization are only seen in the hydroxy-fluorapatites investigated here. These samples are the only ones from Rakovan and reeder (1994) with a detectable OH component. The lack of anomalous optical behavior in the OH-free

apatites suggests that the most probable cause of the reduction of symmetry in the biaxial sectors is positional ordering of OH and or OH/F ordering.

Quantitative characterization of the differential ordering is essential for the interpretation of possible surface structural influences. Single, optically homogeneous, subsectors were cut for neutron diffraction. Intensity data from one full hemisphere of reciprocal space were obtained. Structural refinement is not yet complete, however, the data collected are not consistent with $P2_1/b$ symmetry, which is the symmetry of almost all other non-$P6_3/m$ hexagonal apatites. Rather, the optical data combined with such observed reflections as 00l, l=3n, indicate a nonhexagonal space group not yet observed in apatite.

Rakovan and Reeder (1994) Dissymmetrization and differential incorporation of trace elements in apatite: The role of surface structure during growth. American Mineralogist. in press.

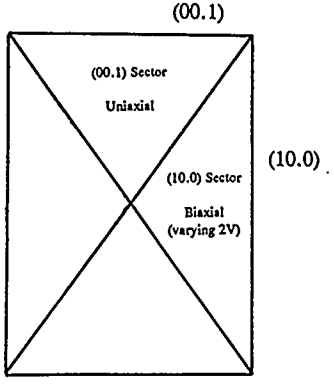


Fig. 1 Idealized crossection of an apatite single crystal showing optical variation between {00.1} and {10.0} sectors.

INSTRUMENT USED: SCD	DATE OF REPORT: 8/2/94	EXPERIMENT NO.: 1835

TITLE: The Crystal Structure of $Ru(ND_3)_6(SCN)_3$

AUTHORS AND AFFILIATIONS: P. Reynolds, R. Durand, B.N. Figgis (Univ. Western Australia)
Research School of Chemistry, Australian National University

DATES OF EXPERIMENTS: 5/5/94 to 5/10/94

CHECK ALL APPLICABLE BOXES:

- X APPROVED BY PROGRAM COMMITTEE
- ☐ INSTRUMENT SCIENTIST ALLOCATION
- ☐ DO NOT PUBLISH
- ☐ PROPRIETARY RESEARCH
- ☐ PRT ALLOCATION

EXPERIMENTAL REPORT (or Abstract of Publication)

A 40 mg single crystal of $Ru(ND_3)_6(SCN)_3$ was mounted on the time-of-flight single crystal diffractometer SCD, and cooled to 20K. A unique set of Bragg reflections was obtained from 25 crystal orientational settings. A single crystal orientation was sampled at ten temperatures from 100 to 290K.

The 20K data index on a $P2_1/n$ cell of very similar dimensions to that of the C2/c polymorph which we previously observed [1,2]. The $P2_1/n$ structure is clearly related to the C2/c by breaking symmetry in the latter. The $P2_1/n$ structure was solved by a bootstrap procedure, starting at the C2/c parameters. The h+k even data in $P2_1/n$ were refined.with isotropic thermal parameters after splitting the C2/c atom sites into two. The resulting sites were assembled into a $P2_1/n$ cell by forming molecules with reasonable bond lengths and angles from the split atom sites. The final model with anisotropic thermal parameters and extinction gave $R(F^2)= .13$ and a goodness-of-fit of 0.84 for 15507 unique reflections. Restricting the data to those with $I>6\sigma(I)$ gives R(F)=.042, but the parameter errors are much increased. The time-of-flight method extends to higher momentum transfer than is normal with conventional neutron diffraction. While this data is weak and degrades the R-factor, it markedly improves the standard deviations of the model parameters. In addition the R-factor is higher in this case because the "C-centred" data is systematically weak.

The $P2_1/n$ structure contains a unique $Ru(ND_3)_6$ fragment and two independent SCN fragments in the unit cell. The bond lengths, bond angles, and thermal parameters are as expected. The only unusual feature is that there is disorder remaining, even at 20K, in two of the six independent NH_3 rotors.

The data between 100 and 290K were fitted at each temperature to a highly constrained structural model, since we have only ca 5% of the 20K data. A phase transition to the C2/c structure is observed at 282(2)K. The transition is quite reversible, our single crystal showing no change in mosaic spread or visible damage after passing through the transition four times.

The C2/c structure is derived from the $P2_1/n$ by allowing one of the unique SCN fragments to disorder end-over end. This produces an extra centre of inversion, giving C-centring. At the same time The Ru atom moves onto a site of inversion symmetry. The SCN order parameter, and the Ru translation exhibit a temperature dependence typical of second order phase transitions.

The motive for study of this crystal structure is that this is a rare example of a paramagnetic heavy transition metal simple inorganic complex which can be easily grown as large single crystals. It is thus suitable for both polarised neutron diffraction study of its magnetisation density and x-ray diffraction study of its electron density. These experiments give a great deal of information about chemical bonding in heavy metal (and other) complexes. In particular relativistic effects on such bonding can be studied.

Although the 20K $P2_1/n$ structure is more complicated than the C2/c, this SCD experiment has defined it with sufficient accuracy that we can proceed to the further diffraction experiments.

EXPERIMENTAL REPORT (CONTD.)

It is a great virtue of the SCD experiment that this unexpected extra complexity required no change in the experiment, the extra peaks are automatically collected, and refinement gives a structure as accurate as that expected for the expected C2/c structure. This contrasts with the traditional experiment where a doubling of counting time would be necessary.

1 A.B.Blake, C.D.Delfs, L.M.Engelhardt, B.N.Figgis, P.A.Reynolds, B.Moubaraki, and K.S.Murray, *J.Chem.Soc.Dalton Trans.*, 1993, 1417.

2 B.N.Figgis, P.A.Reynolds, and A.N.Sobolev, *J.Chem.Soc.Dalton Trans.*, 1994, 1429.

INSTRUMENT USED:	DATE OF REPORT:	EXPERIMENT NO.:
SCD	8-13-90	121C

TITLE: Low temperature structure of $(NH_4)_2(TiOPO_4)_2$

AUTHORS AND AFFILIATIONS: A. J. Schultz (ANL), W. T. A. Harrison and G. D. Stucky (U.C., Santa Barbara)

DATES OF EXPERIMENT: December 5-12, 1989

☑ APPROVED BY PROGRAM COMMITTEE, OR

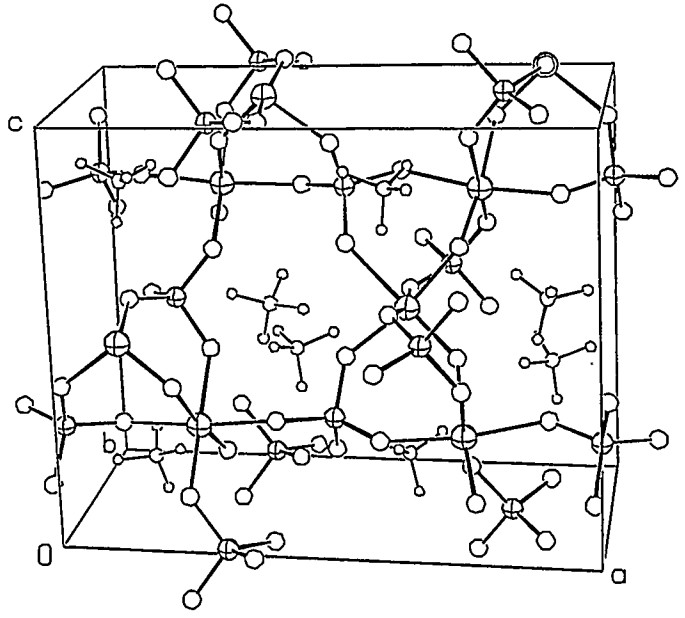
☐ PART OF INSTRUMENT SCIENTIST ALLOCATION

REPORT RECEIVED:

EXPERIMENTAL REPORT (or Abstract of Publication)

The second harmonic generation (SHG) of ammonium derivatives of $KTiOPO_4$ (KTP) and $KTiOAsO_4$ (KTA) can be controlled by proton-framework interactions. The nature of this interaction has been probed by elastic and quasielastic neutron scattering. The crystal structure of ammonium titanyl phosphate, NH_4TiOPO_4 (NTP), has been determined at 15 K using single crystal time-of-flight neutron diffraction. NTP is isostructural with KTP and crystallizes in the acentric space group $Pna2_1$ with **a** = 12.823(4) Å, **b** = 6.485(3) Å, **c** = 10.570(2) Å, V = 879 Å^3 and Z = 8. The titanium-oxygen octahedra show a similar degree of distortion to that found in the KTP structure, and the characteristic short-long Ti–O bonding geometry in the helical TiO_6 chains. The hydrogen-bonding scheme in NTP has been established: each ammonium makes 2 close contacts to the framework, and has two "floating" protons. The SHG responses for KTP and NTP are substantially similar, although the bonding scheemes for the potassium and ammonium cations appear to be different when hydrogen-bonding is taken into account.

EXPERIMENTAL REPORT (CONTD.)



INSTRUMENT USED: SCD	DATE OF REPORT: 2/14/96	EXPERIMENT NO.: NSF.

TITLE: Structures of reduced and oxygenated $Nd_{2-x}Ce_xCuO_y$

AUTHORS AND AFFILIATIONS: A. J. Schultz, J. D. Jorgensen (ANL); J. L. Peng, R. L. Greene (Univ. of Maryland)

DATES OF EXPERIMENT: Dec. 16–22, 1993; Feb. 22–March 1, 1994

CHECK ALL APPLICABLE BOXES:

- ☐ APPROVED BY PROGRAM COMMITTEE
- ☐ PROPRIETARY RESEARCH
- ☐ INSTRUMENT SCIENTIST ALLOCATION
- ☐ PRT LOCATION
- ☐ DO NOT PUBLISH

EXPERIMENTAL REPORT (or Abstract of Publication)

Single crystals of $Nd_{1.85}Ce_{0.15}CuO_y$ were grown by a flux method. Two nearly identical platelike crystals of dimensions 5 x 2.5 x ~0.05 mm^3 were selected for the experiment. The oxygenated (nonsuperconducting) crystal was annealed in pure oxygen at 950°C for 24 h, and then slowly cooled for 48 h to room temperature. The reduced (superconducting) crystal was annealed in pure nitrogen at 900°C for 24 h, followed by cooling to room temperature over a period of 5 h. A measurement of the Meissner effect shows a T_c onset of 24 K.

Single-crystal neutron diffraction data were obtained using the time-of-flight single crystal diffractometer (SCD) at IPNS with the sample at 15 K. The SCD is equipped with a large area (30 x 30 cm^2) position-sensitive detector, a Huber crystal orienter, and a closed-cycle helium refrigerator. With a stationary crystal and detector, a three-dimensional histogram of a portion of reciprocal space is obtained. For this study, 14 histograms with the crystal in different orientations were collected so that more than one octant of reciprocal space was covered.

The structures of single crystals of oxygenated and reduced (T_c = 24 K) $Nd_{1.85}Ce_{0.15}CuO_y$ ($y \approx 4$) were examined by neutron diffraction. Although refinements of various models including interstitial oxygen atoms was inconclusive, Fourier maps of the oxygenated crystal exhibit peaks at the apical O(3) oxygen site. This peak is almost entirely absent in the superconducting reduced crystal. These results are consistent with results from a previous study of oxygenated and reduced Nd_2CuO_y.

EXPERIMENTAL REPORT (CONTD.)

INSTRUMENT USED: SCD	DATE OF REPORT: 2-13-96	EXPERIMENT NO.: 1625

TITLE: The low temperature, high pressure crystal structure of $K_2[FeCl_5(H_2O)]$

AUTHORS AND AFFILIATIONS: A. J. Schultz (ANL), R. L. Carlin (University of Illinois–Chicago)

DATES OF EXPERIMENT: December 8-22, 1992

CHECK ALL APPLICABLE BOXES:

- [X] APPROVED BY PROGRAM COMMITTEE
- [ ] PROPRIETARY RESEARCH
- [ ] INSTRUMENT SCIENTIST ALLOCATION
- [ ] PRT LOCATION
- [ ] DO NOT PUBLISH

EXPERIMENTAL REPORT (or Abstract of Publication)

The crystal structure of $K_2[FeCl_5(H_2O)]$ was examined at 15 K and ambient pressure (1 bar = 0.1 MPa) and at 15 K and 0.14 GPa (1.4 kbar) by single-crystal time-of-flight neutron diffraction in order to search for structural changes coincident with the discontinuity in the slope of the spin flop transition field (H_{SF}) vs. pressure at 60 MPa. It is found that intramolecular and hydrogen bond distances and angles are statistically equivalent at the two pressures. However, there are significant changes of as much as 0.049(3) Å in the intramolecular Cl···Cl distances which may effect the Fe–Cl···Cl–Fe superexchange pathways and the discontinuity in H_{SF}. Dipotassium aquapentachloroferrate(III), $M_r = 329.3$, $F(000) = 636$, orthorhombic, *Pnma*, $Z = 4$. At 15 K and ambient pressure (0.1 MPa), $a = 13.452(5)$, $b = 9.631(2)$, $c = 7.003(2)$ Å, $V = 907.3(5)$ Å^3, $D_x = 2.41$ g cm^{-3}. At 15 K and 0.14 GPa, $a = 13.391(4)$, $b = 9.648(2)$, $c = 6.942(2)$ Å, $V = 896.9(4)$ Å^3, $D_x = 2.44$ g cm^{-3}. The a and c axes decrease slightly, whereas the b axis increases slightly, under applied pressure.

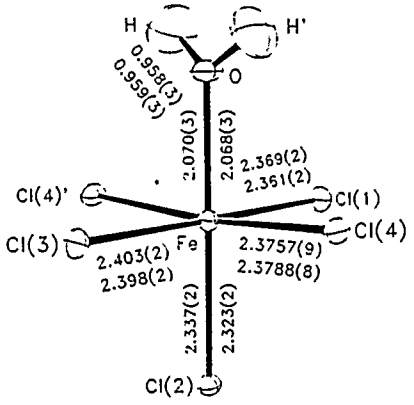


Fig. 1. Perspective drawing of the $[FeCl_5(H_2O)]^{2-}$ anion at 15 K and ambient pressure (0.1 MPa). Atoms are drawn at the 75% probability level. For each bond length (Å), the top number is for 15 K, 0.1 MPa and the lower number is for 15 K, 0.14 GPa.

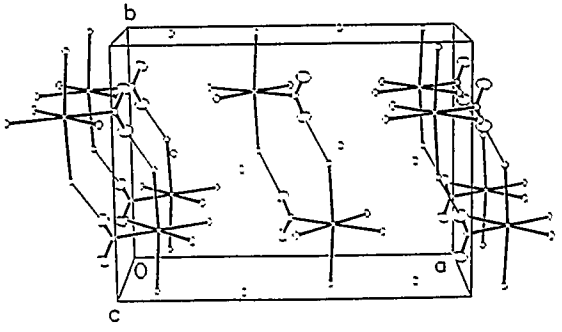


Fig. 2. Perspective view of the unit cell of $K_2[FeCl_5(H_2O)]$ at 15 K and ambient pressure (0.1 MPa). Atoms are drawn at the 50% probability level. H···Cl(4) hydrogen bonds are shown as thin lines.

INSTRUMENT USED:	DATE OF REPORT:	EXPERIMENT NO.:
SCD	July 18, 1991	1430

TITLE:

Single Crystal Neutron Diffraction Study of $(NH_4)Cu(H_2O)_6(SO_4)_2$...

AUTHORS AND AFFILIATIONS:

Charles Simmons (BYU-Hawaii Campus), Michael Hitchman (University of Tasmania), Brian Hathaway (University College, Cork)

DATES OF EXPERIMENT: April 2-9, 1991

☒ APPROVED BY PROGRAM COMMITTEE, OR

☐ PART OF INSTRUMENT SCIENTIST ALLOCATION

REPORT RECEIVED:

EXPERIMENTAL REPORT (or Abstract of Publication)

The family of Tutton salts have the general formula $X_2M(YO_4)\cdot 6H_2O$, where X represents a monovalent cation and Y is either S or Se. These complexes contain discrete $M(H_2O)_6^{2+}$ units. All crystallize in the space group $P2_1/a$, Z = 2 and the chromophores have a center of inversion.

Because a $Cu(H_2O)_6^{2+}$ complex has a ^2E_g electronic ground state, it is susceptible to a Jahn-Teller distortion. Previous X-ray and neutron studies have shown that two 90° misaligned elongated rhombic chromophores result from this distortion. The energy difference between the two chromophores, δE, is lowest for the NH_4^+ and ND_4^+ salts, as revealed by the greater temperature variation of their Cu-O bond lengths.

The NH_4^+ and ND_4^+ Tutton salts are the most interesting to study because in all of the alkali isomorphs (including ND_4^+), the Cu-O(8) bond is elongated and the Cu-O(7) bond compressed, while in the NH_4^+ salt, the distortion pattern is reversed. Tentative explanations given for this effect include differences in the librational motion between NH_4^+ and ND_4^+ and slight differences in hydrogen-bonding interactions.

In order to better understand the structural differences between the NH_4^+ and ND_4^+ Tutton salts, an experiment (#1430) was conducted at IPNS using SCD between April 2-6, 1991. Data were collected at 15K ambient pressure and at 15 K 1.5 kbar on the same deuterated ammonium salt crystal.

EXPERIMENTAL REPORT (CONTD.)

The results indicate that the unit cell a and b axes decreased about 0.3 and 0.5 Å, while the c axis increased nearly 0.4 Å upon the application of 1.5 kbar of pressure, suggesting a possible structural rearrangement of the copper chromophore. The space group remained the same, however.

Both structures were solved using direct methods and were refined using full-matrix least-squares procedures. The final R values are 5%. It is found that the Cu-O(7), Cu-O(8), and Cu-O(9) bond lengths are 2.022, 2.311, and 1.969 Å at 15 K ambient pressure. However, at 15 K and 1.5 kbar, the Cu-O(7), Cu-O(8), and Cu-O(9) bond lengths are 2.290, 2.014, and 1.988 Å, indicating a change in the distortion pattern of the $Cu(H_2O)_6^{2+}$ chromophore.

It has been demonstrated that the application of 1.5 kbar of pressure to a ND_4^+ Tutton salt crystal "flips" or reverses the bond lengths in a $Cu(H_2O)_6^{2+}$ chromophore. The distortion pattern of the deuterated ammonium salt at high pressure is the same as that of the hydrogenous compound at ambient pressure. ORTEP packing diagrams reveal a shift in the positions of the ND_4^{+2} and SO_4^{-2} ions. These slight shifts, apparently, greatly influence the distortional behavior of the copper chromophore.

This is the first diffraction experiment on a Jahn-Teller crystal under high pressure. Interestingly, the application of pressure not only affects the direction of distorion, but also the amount of distortion. This is revealed by the Jahn-Teller radius, $R_{JT} = \sum(d_i - \bar{d})^2$, where d_i are the individual Cu-O bond lengths and $\bar{d}$ is the mean Cu-O bond length. R_{JT} is 0.37 Å at ambient pressure, but is reduced about 10% to 0.33 Å at 1.5 kbars of pressure. Further experiments with the hydrogenous compound at low temperatures and high pressures would be most interesting.

INSTRUMENT USED:	DATE OF REPORT:	EXPERIMENT NO.:
SCD	8/10/92	1529

TITLE: Single Crystal Neutron Diffraction Study of $(NH_4)_2Cu(H_2O)_2(SO_4)_2$ at 15 K ambient and 1.5 kbar pressure

AUTHORS AND AFFILIATIONS: C. J. Simmons – BYU-Hawaii Campus; A. J. Schultz – ANL; M. A. Hitchmann – Univ. of Tasmania

DATES OF EXPERIMENT: April 14 – 24, 1992

☒ APPROVED BY PROGRAM COMMITTEE, OR

☐ PART OF INSTRUMENT SCIENTIST ALLOCATION

REPORT RECEIVED:

EXPERIMENTAL REPORT (or Abstract of Publication)

To be submitted to JACS:

High Pressure, Low Temperature, Single Crystal Neutron Diffraction Study of Deuterated and Protonated Ammonium Hexaaquacopper(II) Sulphate (Tutton's Salt): A Switchable Jahn-Teller Distortion

Charles J. Simmons

Math, Science and Technology Division
Brigham Young University–Hawaii Campus
Laie, Hawaii 96762

Arthur J. Schultz

Chemistry and Materials Science Divisions
Argonne National Laboratory
Argonne, Illinois 60439

and

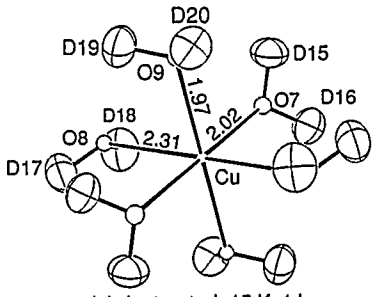
Michael A. Hitchman

Department of Chemistry
University of Tasmania
Tasmania, Australia

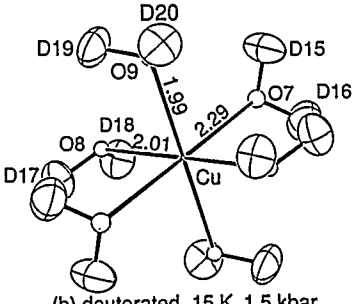
Abstract

Single crystal time-of-flight neutron diffraction at low temperature and at low temperature and high pressure was used to study the Jahn-Teller distortion in deuterated and protonated $(NH_4)_2[Cu(H_2O)_6](SO_4)_2$. At ambient pressure, there is a structural isotope effect which produces a switch of the Jahn-Teller distorion between the protonated and dueterated crystals as previously shown by Hathaway and Hewat.[1] Application of pressure to the deuterated crystal switches the distortion by 90° so that it is isostructural with the protonated crystal. The Cu-O(7) bond length increases from 2.022(2) to 2.290(2) Å, and the Cu-O(8) bond length decreases from 2.310(2) to 2.014(2) Å. Hydrogen bonding interactions are shown to be important in the switching. Space group is monoclinic $P2_1/a$ with unit cell parameters: for $(ND_4)_2[Cu(D_2O)_6](SO_4)_2$ at 15 K and 1 bar, a = 9.451(2), b = 12.736(3), c = 6.096(1) Å, β = 107.13(2)°, V = 701.2(3) Å^3; for $(ND_4)_2[Cu(D_2O)_6](SO_4)_2$ at 15 K and 1.5 kbar, a = 9.136(1), b = 12.285(2), c = 6.371(1) Å, β = 106.28(2)°, V = 686.4(2) Å^3; for $(NH_4)_2[Cu(H_2O)_6](SO_4)_2$ at 14 K and 1.4 kbar, a = 9.068(2), b = 12.232(2), c = 6.340(1) Å, β = 106.44(2)°, V = 674.5(2) Å^3.

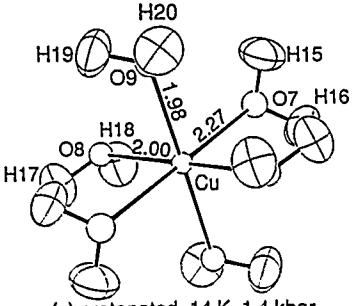
EXPERIMENTAL REPORT (CONTD.)



(a) deuterated, 15 K, 1 bar



(b) deuterated, 15 K, 1.5 kbar



(c) protonated, 14 K, 1.4 kbar

INSTRUMENT USED:	DATE OF REPORT:	EXPERIMENT NO.:
SEPD	8/12/91	Pilot Center

TITLE: Thermal Expansion Measurements Using Neutron Diffraction of $(Bi,Pb)_2Ca_2Sr_2Cu_3O_x$

AUTHORS AND AFFILIATIONS: Ronald H. Arendt, Mary F. Garbauskas, & Charles A. Meyer, GE Corporate Research & Development, Schenectady, NY 12301--Frank J. Rotella, James D. Jorgensen, & Richard Hitterman, Argonne National Laboratory, Argonne, IL 60439

DATES OF EXPERIMENT: 3/11/91-3/12/91 and 5/10/91-5/13/91

☐ APPROVED BY PROGRAM COMMITTEE, OR

☐ PART OF INSTRUMENT SCIENTIST ALLOCATION

REPORT RECEIVED:

EXPERIMENTAL REPORT (or Abstract of Publication)

The high temperature superconductor, $(Bi,Pb)_2Ca_2Sr_2Cu_3O_x$, Bi-(2223), will likely be used in the form of metal sheathed tapes of the oxide, in which the crystals of the material are aligned relative to the surface of the tape. In order to properly engineer these composite structures, a detailed knowledge of the physical properties of the components is required, one parameter being the anisotropic thermal expansion of the superconducting oxide. Dilatometry measurements do not lend themselves to a convenient and reliable determination of this parameter, particularly when free-standing bodies are as structurally weak as are those of the superconductor. X-ray measurements, which can measure the anisotropic nature of the thermal expansion, give data representative of only the surface of this x-ray opaque material. Also, this technique has limited applicability in the present case due to the potential for surface decomposition of the material due to evaporative loss of Bi_2O_3 at high temperatures. Only neutron powder diffraction provides a means for reliably studying the bulk anisotropic thermal expansion of this material over the entire range of temperatures of interest. Results will be presented on the thermal expansion of Bi-(2223) under various oxygen partial pressures. Comparisons with companion x-ray data on the same material, and with published data, will be made.

EXPERIMENTAL REPORT (CONTD.)

INSTRUMENT USED:	DATE OF REPORT:	EXPERIMENT NO.:
SEPD	8/12/91	Pilot Center

TITLE:

Thermal Expansion Measurements Using Neutron Diffraction of $Bi_2CaSr_2Cu_2O_x$

AUTHORS AND AFFILIATIONS: Ronald H. Arendt, Mary F. Garbauskas, & Charles A. Meyer, GE Corporate Research & Development, Schenectady, NY 12301--Frank J. Rotella, James J. Rotella, James D. Jorgensen, & Richard L. Hitterman, Argonne National Laboratory, Argonne, IL 60439

DATES OF EXPERIMENT: 9/10/90-9/14/90

☐ APPROVED BY PROGRAM COMMITTEE, OR

☐ PART OF INSTRUMENT SCIENTIST ALLOCATION

REPORT RECEIVED:

EXPERIMENTAL REPORT (or Abstract of Publication)

The differential thermal expansion of $Bi_2CaSr_2Cu_2O_x$, Bi-(2122), has been measured using high-temperature neutron powder diffraction in air, 0.980% oxygen in nitrogen, and pure argon. Thermal expansion in the c-axis direction is greater by a factor of about 1.4 than that in either the a- or b-axis direction for all sample environments. The neutron results for Bi-(2122) in air are compared with results from similar x-ray powder diffraction measurements.

Presented at American Crystallographic Association meeting July, 1991.
Submitted for publication Physica C, 1991.

EXPERIMENTAL REPORT (CONTD.)

INSTRUMENT USED:	DATE OF REPORT:	EXPERIMENT NO.:
SEPD	8/9/92	1457

TITLE: Comparison of the local atomic structure of reduced and unreduced samples of $Nd_{1.83}Ce_{0.17}CuO_{4-y}$.

AUTHORS AND AFFILIATIONS: S.J.L. Billinge and T. Egami, Dept. of Materials Science and Engineering, University of Pennsylvania.

DATES OF EXPERIMENT: 3/11/92----3/15/92

☒ APPROVED BY PROGRAM COMMITTEE, OR

☐ PART OF INSTRUMENT SCIENTIST ALLOCATION

REPORT RECEIVED:

EXPERIMENTAL REPORT (or Abstract of Publication)

$Nd_{2-x}Ce_xCuO_{4-y}$ is one of the class of n-doped high temperature superconductors. One of the most intriguing outstanding questions about this material relates to the reducing anneal that samples are subjected to during fabrication. No superconductivity has been observed in any sample, with any cerium content, without this reducing anneal. However, iodometric titration[1] and neutron diffraction[2] indicate that the change in oxygen concentration in the samples as a result of the anneal is no more than $\delta y < 0.01$. This corresponds to a very small change in nominal carrier concentration, and cannot explain the profound change in the properties of the material. Apparently, the sample must be undergoing some further change which is not understood. Neutron diffraction experiments indicated no significant change in the long range atomic structure as a result of the reducing step.[2]

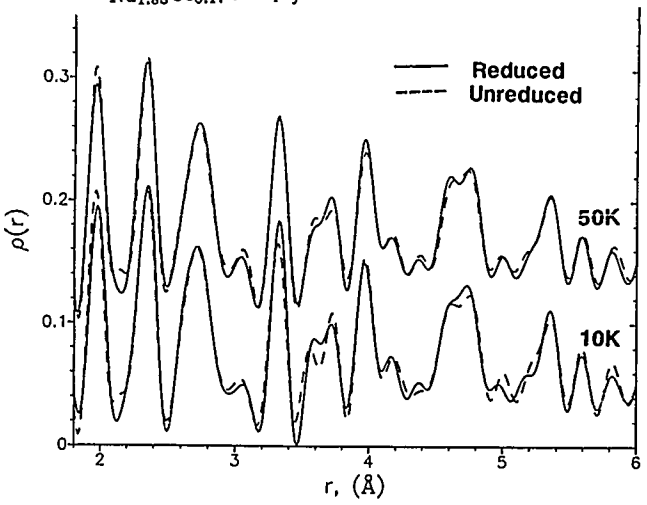
Various techniques which are sensitive to atomic structure on a local scale have indicated anomalous behaviour which could be associated with the appearance of superconductivity. EXAFS[3], Ion-channeling[4] and the pair distribution function[5] (PDF) all exhibited anomalies at T_c in various superconductors. It thus appears that structure on a mesoscopic scale may determine the superconducting properties of a cuprate material. The PDF analysis of pulsed neutron powder diffraction data has shown itself to be very sensitive to structure on these length scales.

The experiment that was carried out on the SEPD diffractometer at the IPNS was to compare the PDF from samples of $Nd_{1.83}Ce_{0.17}CuO_{4-y}$ which had, and had not, been given the reducing anneal. The PDF is a real space representation of the structure which is obtained by fourier transforming diffraction data. In this way the important *local* structure could be examined for changes produced by the reduction step.

The preliminary results are shown in Fig. 1. This shows the PDF's of the superconducting (reduced) and non-superconducting (unreduced) samples compared at two temperatures. Data from the reduced samples are shown as solid curves, and those from the

EXPERIMENTAL REPORT (CONTD.)

Figure 1. Comparison of PDF's from Reduced and Unreduced Samples of $Nd_{1.83}Ce_{0.17}CuO_{4-y}$



unreduced samples by dashed lines. Data are shown at two temperatures, 10K and 50K which are below and above T_c respectively. The expected errors due to the counting fluctuations in the data are approximately $\Delta\rho = 0.01\text{Å}^{-3}$ at $r \approx 4$Å, and decrease as $1/r$. It appears that above T_c the differences between the two samples are rather small and barely significant. However, below T_c a number of significant differences are apparent, in particular to the features close to 3.7Å and close to 5.1Å. These features involve Cu-O1, Cu-O2 and O1-O2 correlations. A more detailed analysis of the data is currently in progress. However, it does appear that at low temperature, the oxygen sublattice of the material is sensitive to the processing history of the sample. This is in agreement with our earlier PDF studies of the similar material, with x=0.165, which indicated a change in the oxygen sublattice which accompanied the appearance of superconductivity. This was explained as a change in the local ordering arrangement of the small oxygen displacements[6] which appear to be intrinsic to these materials.

[1] Y. Tokura *et. al.*, Nature **337**, 345 (1989).
[2] G.H. Kwei *et. al.*, Phys. Rev. **40**, 9370 (1989).
[3] S.D. Conradson and I.D. Raistrick, Science **243**, 1340 (1989).
[4] R.P. Sharma *et. al.*, Phys. Rev. Lett. **62**, 2869 (1989).
[5] B.H. Toby *et. al.*, Phys. Rev. Lett. **64**, 2414 (1990).
[6] S.J.L. Billinge *et. al.*, Physica C**179**, 279 (1991).

INSTRUMENT USED:	DATE OF REPORT:	EXPERIMENT NO.:
SEPD	Dec. 15, 1993	1757

TITLE:

Local Structure of Superconducting $YBa_2Cu_4O_8$

AUTHORS AND AFFILIATIONS:

W. Dmowski, T. R. Sendyka and T. Egami University of Pennsylvania

DATES OF EXPERIMENT: Sept. 22 26, Nov. 11 - 16, 1993

☒ APPROVED BY PROGRAM COMMITTEE, OR

☐ PART OF INSTRUMENT SCIENTIST ALLOCATION

REPORT RECEIVED:

EXPERIMENTAL REPORT (or Abstract of Publication)

Local structure of $YBa_2Cu_4O_8$ and its temperature dependence was studied by the atomic pair-distribution function (PDF) analysis. The PDF is obtained by Fourier-transforming the normalized powder diffraction intensity, S(Q), determined by SEPD up to high momentum transfer (35 $Å^{-1}$). As shown in Fig. 1, the experimentally determined PDF differs significantly from the PDF calculated for the crystallographic structure. By the real-space modeling of the PDF, i.e. by constructing a model of which PDF agrees with the experimental PDF, we found that the Cu-O chains in this compound are shifted along its length direction by about 0.1 Å. Two adjacent chains are shifted in opposing directions. The shift, however, remains local, and does not affect the long range order.

We also found that the height of certain PDF peaks changes anomalously with temperature. As shown in Fig. 2, the height of the peak at 3.43 Å decreases rapidly with temperature, while over the same temperature range the height of other peaks decreases by about 40 % due to increased thermal motion. This rapid decrease in the height of the 3.43 Å peak is due to the increased local buckling motion in the CuO_2 plane, according to the real-space modeling. It is interesting to note that the temperature range over which this peak precipitously decreases agrees with the temperature range over which the NMR spin-lattice relaxation time T_1 shows anomalous behavior. The behavior of T_1 is explained by the opening of the spin-gap due to increased spin correlation. However, the present observation suggest that the origin of the spin-gap may partly be structural, such as the formation of bi-polarons. The results have significant implications to the mechanism of high temperature superconductivity.

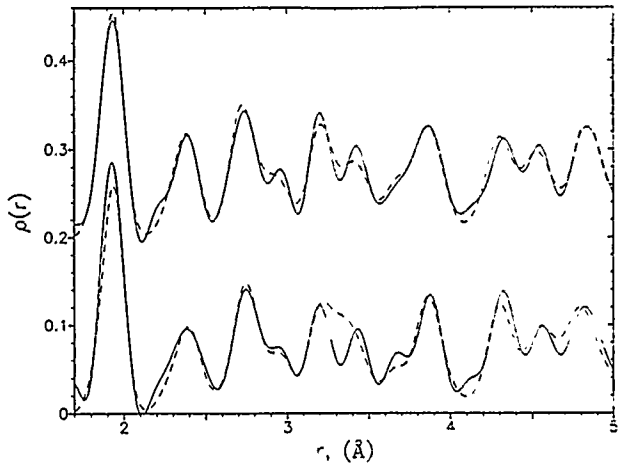


Fig. 1. The PDF of $YBa_2Cu_3O_7$ (above, solid line) and that of $YBa_2Cu_4O_8$ at T = 10 K (below, solid line), compared to the PDF's calculated for the crystallographic structure (dashed lines).

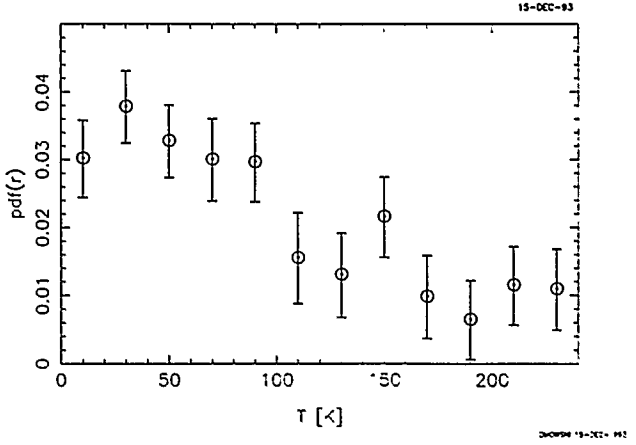


Fig. 2. Temperature dependence of PDF(3.43 Å) - PDF(3.33 Å). The PDF has a peak at 3.43 Å and a valley at 3.33 Å.

INSTRUMENT USED:	DATE OF REPORT:	EXPERIMENT NO.:
SEPD	1/25/91	1381

TITLE:
Local Structure of Superconducting Oxides

AUTHORS AND AFFILIATIONS:
T. Egami, S. Billinge and B.H. Toby, University of Pennsylvania

DATES OF EXPERIMENT: Nov. 13 - 15, 1990

☒ APPROVED BY PROGRAM COMMITTEE, OR

☐ PART OF INSTRUMENT SCIENTIST ALLOCATION

REPORT RECEIVED:

EXPERIMENTAL REPORT (or Abstract of Publication)

Powder diffraction data were collected at various temperatures using the SEPD, for $Nd_{1.835}Ce_{.165}CuO_4$ [NdCe214] which is an electron (n-type) superconductor, and for $YBa_2Cu_4O_8$ [YBaCul24]. The temperature points taken were T = 10, 20, 25, 30, 40 and 50 K for NdCe214, and 10, 45, 60, 75, 90 and 105 K for YBaCul24. In order to achieve high statistical accuracy the measurement was made for 4 hrs. at each temperature. The data were Fourier-transformed to obtain the atomic pair distribution function (PDF), using the modified GLASS package. The purpose of obtaining the PDF is to detect non-periodic or non-crystallographic deviations from the perfect crystal structure.

The PDF's of $Nd_{1.835}Ce_{.165}CuO_4$ at four temperatures (T = 10, 25, 30, 50 K) are shown in Fig. 1. In this sample T_c is 28 K, but the Meissner transition is broad, ranging down to 10 K. Fig. 1 shows that below T_c a shoulder develops at 2.6 Å on the right hand side of the PDF peak at 2.4 Å. This indicates that the distance between the oxygen atom in the Cu-O plane and the oxygen in the (Nd,Ce)-O plane above becomes bifurcated below T_c. Such an anomalous change in the local structure below T_c was observed earlier for other oxide superconductors, namely $Tl_2Ba_2CaCu_2O_8$ [1], $La_{2-x}(Sr,Ba)_xCuO_4$ [2], $YBa_2Cu_3O_7$ and $(Ba_{.6}K_{.4})BiO_3$. The results altogether strongly suggest that the local structural change at T_c is the common feature of the high-T_c oxides, and implies an important role the lattice plays in producing superconductivity. The data on YBaCul24 are presently being analyzed.

EXPERIMENTAL REPORT (CONTD.)

[1] B.H. Toby, T. Egami, J.D. Jorgensen, and M.A. Subramanian, Phys. Rev. Lett., 64, 2414 (1990).
[2] T. Egami, W. Dmowski, J. D. Jorgensen, D. G. Hinks, D. W. Capone, II, C. U. Segre and K. Zhang, Rev. Solid St. Sci., 1, 247 (1987).

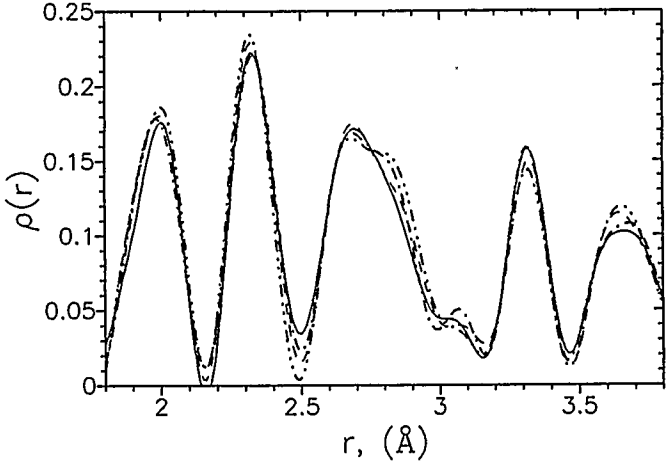


Fig. 1. Pair distribution function of $Nd_{1.835}Ce_{.165}CuO_4$ at T = 10 (-•••-•••-), 25 (-•-•-•-), 30 (-----), and 50 (———) K.

INSTRUMENT USED:	DATE OF REPORT:	EXPERIMENT NO.:
SEPD	Aug. 8, 1991	1381

TITLE:

Local Structure of Superconducting La-Nd-Sr-Cu-O and $YBa_2Cu_4O_8$

AUTHORS AND AFFILIATIONS:

T. Egami, B.H. Toby, H.D. Rosenfeld, U. of Pennsylvania, M.K. Crawford, du Pont

DATES OF EXPERIMENT: ~~Feb. 20 - 26, 1991~~

☒ APPROVED BY PROGRAM COMMITTEE, OR

☐ PART OF INSTRUMENT SCIENTIST ALLOCATION

REPORT RECEIVED:

EXPERIMENTAL REPORT (or Abstract of Publication)

The local atomic structure and its temperature dependence of superconducting $La_{1.85-x}Nd_xSr_{.12}CuO_4$ (x = .2, .6) and $YBa_2Cu_4O_8$ was studied by the atomic pair-distribution function (PDF) analysis. The PDF is obtained by the Fourier transformation of the normalized neutron structure factor, and describes the orientationally averaged distribution of interatomic distances. It is well known that the low temperature structural transition from the orthorhombic (LTO) phase to the tetragonal (LTT) phase in $La_{1.875}Ba_{.125}CuO_4$ suppresses superconductivity [1]. In La-Sr-Cu-O system this transition is not observed, but replacing a part of La by Nd induces this transition and concomitant depression of T_c. In order to understand the reason why the transition to the LTT phase results in the depression of T_c, we studied the local structure of this system. Understanding why a certain local structure kills superconductivity may lead to the understanding of why the superconductivity occurs in the first place.

The PDF of $La_{1.68}Nd_{.2}Sr_{.12}CuO_4$ is shown in Fig. 1. The temperature dependence of the height of the shoulder at r = 2.98 Å is shown in Fig. 2. This shoulder is absent in the ideal (crystallographic) structure, but it has been always observed in all of the 214 compounds [2]. The height of this shoulder is a very sensitive parameter of the local distortion in the CuO_6 octahedron, since the ideal distance between the apical oxygen (O2) and the in-plane oxygen (O1) is 3.2 Å. We conjectured earlier that the local distortion described by this peak may be crucial in producing superconductivity [2]. However, Fig. 2 show that the distortion of the CuO_6 octahedron is largest during the transition from LTO to LTT structure at T = 40 K, and the distortion does not completely disappear even at low temperatures. Thus unfortunately the result shows that the depression of T_c does not coincide with the disappearance of the local distortion, apparently negating the simplest ansatz. Nevertheless a more detailed modelling work has to be done before deriving the conclusion, and such an effort is in progress. The PDF of $YBa_2Cu_4O_8$ shows interesting temperature anomalies similar to the one observed for $YBa_2Cu_3O_7$. However, we need more statistics before confirming the presence of anomaly.

[1] J. D. Axe et al., Phys. Rev. Lett., 62, 2751 (1989).
[2] T. Egami et al., Rev. Solid St. Sci., 1, 247 (1987).

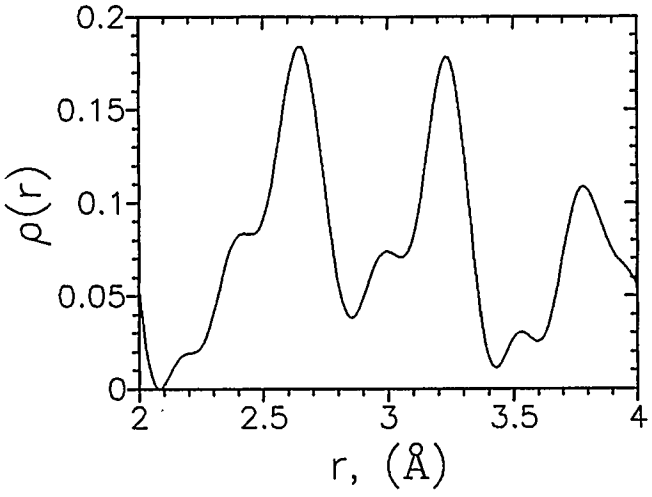


Fig. 1. Atomic pair-distribution function of $La_{1.68}Nd_{.2}Sr_{.12}CuO_4$ at T = 10 K

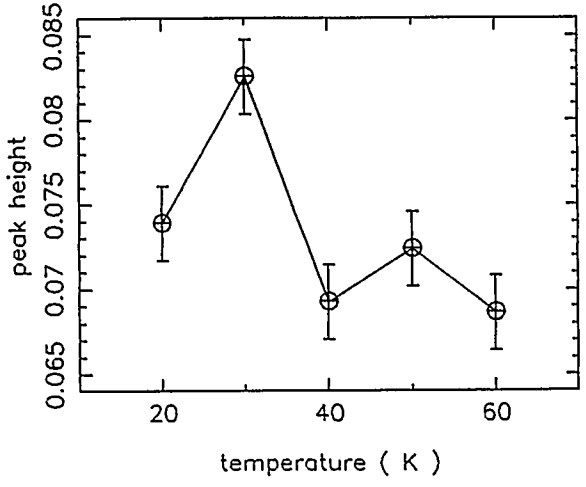


Fig. 2. Temperature dependence of the height of the shoulder at r = 2.98 Å of the PDF of $La_{1.68}Nd_{.2}Sr_{.12}CuO_4$.

INSTRUMENT USED:	DATE OF REPORT:	EXPERIMENT NO.:
SEPD	Aug 23 '91	1491

TITLE: Structural Ordering in Liquid Potassium-Tellurium Alloys

AUTHORS AND AFFILIATIONS: J. Fortner, M.-L. Saboungi, & J. E. Enderby*; ANL * Bristol, U.K.

DATES OF EXPERIMENT: June 11-14 1991

CHECK ALL APPLICABLE BOXES:

- ☒ APPROVED BY PROGRAM COMMITTEE
- ☐ INSTRUMENT SCIENTIST ALLOCATION
- ☐ DO NOT PUBLISH
- ☐ PROPRIETARY RESEARCH
- ☐ PRT ALLOCATION

EXPERIMENTAL REPORT (or Abstract of Publication)

Neutron diffraction from molten K_xTe_{1-x} is reported for x=.12 and x=.50 semiconducting alloys. The measured radial distribution functions (rdf) demonstrate the persistence of 2-fold coordinated covalent tellurium chains in the liquid. The rdf of the liquid $K_{0.12}Te_{0.88}$, which is dominated by the Te-Te contribution, is remarkably similar to that of pure liquid tellurium, the notable exception being that the nearest neighbor peak is largely resolved and found to have a coordination number slightly less than 2. The $K_{0.50}Te_{0.50}$ rdf clearly indicates Te-Te pairing in the melt, an unexpected departure from the presumed similar $Cu_{0.50}Te_{0.50}$. These paired tellurium are most likely of the form $(Te_2)^{2-}$ Zintl ions.

Recent thermodynamic investigations of the potassium-tellurium system[1] have shown that for several compositions there is considerable "excess stability," indicative of chemical ordering. Of particular interest is the nature of this ordering at the approximate compositions $K_{0.12}Te_{0.88}$ and $K_{0.50}Te_{0.50}$ corresponding to local maxima in the excess stability function.[1] Near the equiatomic composition, one expects an "ionic alloy" type of ordering due to the large electronegativity difference between K and Te.[1-3] For compositions much less than 50% K, the tendency for Te to form covalently bonded chains, which are known to survive into the melt, will be significant.[2,4] Neutron diffraction was then used to measure the total structure factors for these two compositions and the radial distribution functions were thereby obtained.

EXPERIMENTAL REPORT (CONTD.)

The reduced rdf, T(r), for the molten $K_{0.12}Te_{0.88}$ alloy shows clear separation of the first peak in the rdf from the rest of the neighbors. This first peak, at a distance of 2.8 Å and with an area of 1.6 atoms, indicates Te chains (about 5 atoms long) persisting into the melt. It is interesting to note, additionally, that otherwise the rdf is quite similar to that of pure liquid Te, suggesting 2-fold, rather than 3-fold bonding in the pure system. An additional peak at 3.6Å, matching the sum of the K^+ and Te^{2-} ionic radii, is attributed to the K-Te first coordination sphere.

The T(r) for liquid $K_{0.50}Te_{0.50}$ shows that there is again a first Te-Te coordination peak at 2.8 , having in this case a coordination of 0.96. This virtually complete pairing of tellurium atoms to form $(Te_2)^{2-}$ Zintl ions[1,3] is in sharp contrast to the heterocoordination of liquid CuTe and the partial pairing of Se in liquid CuSe.[2]

REFERENCES

1. A. Petric, A. D. Pelton, and M.-L. Saboungi, J. Chem. Phys. 89 (8) 5070 (1988).
2. J. E. Enderby and A. C. Barnes, Rep. Prog. Phys. 53, 85 (1990).
3. M.-L. Saboungi, W. Geertsma, and D. L. Price, Annu. Rev. Phys. Chem. 41, 207 (1990).
4. A. Menelle, R. Bellissent, and A. M. Flank, Europhys. Lett. 4 (6) 705 (1987).

INSTRUMENT USED:	DATE OF REPORT:	EXPERIMENT NO.:
SEPD	August 16th, 1990	#1033

TITLE:

Structure Determination in BCC Solid ^3He-^4He

AUTHORS AND AFFILIATIONS:

M. A. Fradkin (UIUC), R. C. Blasdell (ANL-IPNS), R. O. Simmons (UIUC)

DATES OF EXPERIMENT: 5/9 - 5/11/90

☒ APPROVED BY PROGRAM COMMITTEE, OR

☐ PART OF INSTRUMENT SCIENTIST ALLOCATION

REPORT RECEIVED:

EXPERIMENTAL REPORT (or Abstract of Publication)

In this experiment we sought from the sample any superlattice peaks which would arise if isotopic short-range ordering were occurring at temperatures just below melting. Due to a superfluid leak on our cryostat pot assembly we were unable to reach temperatures below 2.2 K. This limitation prevented us from taking data on a $^3He_{0.5}$ - $^4He_{0.5}$ bcc mixture, whose melting temperature is at about 1.2 K, as we had originally intended. We instead took data on: a) an hcp mixture, $^3He_{0.25}$ -$^4He_{0.75}$, which melts at a higher temperature, at a variety of sample orientations using our cryostat's rotating vacuum seal; b) a reference liquid of the same isotopic composition. Preliminary analysis of the data has failed to reveal any diffraction peaks due to the sample. We note that due to the presence of ^3He, a strong neutron absorber, and unfavorable Debye-Waller factors we expect any He diffraction peaks which are present will be quite weak. A more detailed analysis of the data is in progress.

INSTRUMENT USED:	DATE OF REPORT:	EXPERIMENT NO.:
SEPD	8/12/91	Pilot Center

TITLE:
High-Temperature Neutron Diffraction Study of the Melting Behavior of $Bi_2CaSr_2Cu_2O_x$

AUTHORS AND AFFILIATIONS:
• Mary F. Garbauskas and Ronald H. Arendt, General Electric Corporate Research & Development, Schenectady, NY 12301 • James D. Jorgensen and Richard L. Hitterman, Materials Science Division, Argonne National Laboratory, Argonne, IL 60439

DATES OF EXPERIMENT: 10/11/89-10/13/89

☐ APPROVED BY PROGRAM COMMITTEE, OR

☐ PART OF INSTRUMENT SCIENTIST ALLOCATION

REPORT RECEIVED:

EXPERIMENTAL REPORT (or Abstract of Publication)

High temperature neutron powder diffraction has been used to study the melting, and subsequent re-formation, behavior of $Bi_2CaSr_2Cu_2O_x$, (2122), the 80K transition temperature oxide superconductor. It was found that the (2122) substantially re-forms upon return to a temperature just below the peritectic melting point of the material. This finding implies that difficulties encountered in melt processing this material may be due largely to gross segregation of the constituents while the material is partially molten, as opposed to slow formation kinetics for this species.

Appl. Phys. Lett. 58, 2987 (1991).

EXPERIMENTAL REPORT (CONTD.)

INSTRUMENT USED: SEPD	DATE OF REPORT: 30/06/94	EXPERIMENT NO.: 1858

TITLE: STRUCTURAL STUDY OF $Na_2Bi_2O_5$ AND $Pb_2Bi_6O_{11}$

AUTHORS AND AFFILIATIONS: J.T.S. IRVINE, S.M. FRAY, UNIVERSITY OF ABERDEEN

DATES OF EXPERIMENT: 17/03/94

CHECK ALL APPLICABLE BOXES:

- [xxx] APPROVED BY PROGRAM COMMITTEE
- [ ] INSTRUMENT SCIENTIST ALLOCATION
- [xxx] DO NOT PUBLISH
- [ ] PROPRIETARY RESEARCH
- [ ] PRT ALLOCATION

EXPERIMENTAL REPORT (or Abstract of Publication)

This report details progress to date: structural analysis is ongoing and a more complete report will follow.

Two samples were investigated; "$Na_2Bi_2O_5$"(3.7 g) and $Pb_2Bi_6O_{11}$(6.0g), a smaller, higher purity batch of "$Na_2Bi_2O_5$" proved to be too small to diffract sufficiently. Good data were obtained; however, the $Na_2Bi_2O_5$ sample was clearly biphasic, containing both $Na_2Bi_2O_5$ and a new cubic rocksalt polymorph of Na_3BiO_4. $Na_2Bi_2O_5$ appears to be structurally very closely related to $Pb_2Bi_6O_{11}$. As $Pb_2Bi_6O_{11}$ gave a better diffraction pattern and was single phase, initial attention focused on this phase.

X-ray powder data from $Pb_2Bi_6O_{11}$ indexed well on a monoclinic cell:

$a = 5.992$ Å
$b = 5.553$ Å
$c = 4.808$ Å
$\beta = 92.9°$

The geometry of this cell corresponded quite well with that of $Ca_2Mn_2O_5$, which might be expected to be analogous to $Na_2Bi_2O_5$. Data obtained from low angle banks show reflections with d-spacings of about 9.0 and 11.6Å, inconsistent with the above model. Electron diffraction has further confirmed the larger unit cell, indicating a triclinic cell which may described with the following alternative settings:

	pseudo-monoclinic A centred	triclinic
a	11.969	10.360
b	5.628	5.624
c	19.940	11.960
α	90.22	90.71
β	105.33	104.98
γ	89.11	74.07

Good indexing has been achieved of both X-ray and neutron data for both settings, although the pseudo-monoclinic cell seems slightly better. It should also be noted that incommensurate superstructure reflections corresponding to a repeat of 48Å were also observed in electron diffraction.

The next stage in the refinement, is to utilise Patterson methods to locate the heavy atom positions from X-ray data, both triclinic settings will be tested. After this GSAS will be utilised to refine the complete structure, including oxygens from neutron data.

For the $Na_2Bi_2O_5$, we intend to use the final structure of $Pb_2Bi_6O_{11}$ as our structural model for Rietveld refinement; however, the structure of Na_3BiO_4 has been refined without optimisation of the $Na_2Bi_2O_5$ phase. The structure refines well to a disordered rocksalt with a cell edge of 4.740Å. The refinement of this structure, including site occupancies will be completed in conjunction with the refinement of the $Na_2Bi_2O_5$ structure.

INSTRUMENT USED:	DATE OF REPORT:	EXPERIMENT NO.:
SEPD	June 17, 1991	1398

TITLE:
Crystal Structures of $Tl_2Ba_2CuO_{6+z}$ under High Pressure

AUTHORS AND AFFILIATIONS:
F. Izumi, Y. Kubo*, Y. Shimakawa*, T. Manako* *NEC, Fundamental Res. Lab. Natl. Inst. Res. Inorg. Mater.

DATES OF EXPERIMENT: March 14–17, 1991

☑ APPROVED BY PROGRAM COMMITTEE, OR

☐ PART OF INSTRUMENT SCIENTIST ALLOCATION

REPORT RECEIVED:

EXPERIMENTAL REPORT (or Abstract of Publication)

$Tl_2Ba_2CuO_{6+z}$ is known to be doped with excessive hole carriers. Figure 1 illustrates the crystal structure of this superconducting oxide. Its superconducting transition temperature, T_c, is lowered by increasing content of excess oxygen, which occupy an interstitial site sandwiched between two TlO sheets.[1] Môri *et al.*[2] showed that $Tl_2Ba_2CuO_{6+z}$ has large negative pressure coefficients, dT_c/dp, and that these coefficients vary with changing z value. These experimental results suggest that the pressure-induced lowering of T_c may be caused by increases in hole concentration on two-dimensional CuO_2 sheets. We investigated structural changes of $Tl_2Ba_2CuO_{6+z}$ under high pressure to confirm this idea.

Three samples of $Tl_2Ba_2CuO_{6+z}$ with T_c = 0, 46, and 79 K were prepared by solid-state reactions. TOF neutron-powder-diffraction data (six points) were taken on the SEPD diffractometer over the pressure range from 0 GPa to 0.622 GPa using a He gas pressure cell,[3] with which pressure can be precisely controlled and measured under perfect hydrostatic conditions.

The unit-cell dimensions a and c, and therefore, the unit-cell volume, V, decreased linearly with increasing pressure. Table 1 summarizes linear and volume compressibilities, and bulk moduli, K, of the three samples. Some bulk moduli of other superconductors[3–5] are also given below this Table. The values of K for $Tl_2Ba_2CuO_{6+z}$ are evidently smaller than those of the other superconductors. It is interesting to note that the linear compressibilities for a are very high; that is, the Cu–O(1) bond parallel to the a axis is compressed very easily under high pressure. This finding presents unambiguous evidence for the pressure-induced increase in hole concentration on the CuO_2 sheet.

The compressibilities for the bond between Cu and apical O(2) atoms, $-(1/l_0)(dl/dp)$, were 0.0071(9), 0.0102(12), and 0.0081(5), respectively. Thus, $-(1/l_0)(dl/dp)$ for the Cu–O(2) bond is 2–3 times as large as $-(1/c_0)(dc/dp)$. Such marked approach of the O(2) atom toward Cu under high pressure must contribute considerably to the increase in hole concentration on the CuO_2 sheet, lowering the T_c of this superconductor.

References

1) Y. Shimakawa, Y. Kubo, T. Manako, H. Igarashi, F. Izumi, and H. Asano, *Phys. Rev. B*, **42**, 10165 (1990).
2) N. Môri, H. Takahashi, Y. Shimakawa, T. Manako, and Y. Kubo, *J. Phys. Soc. Jpn.*, **59**, 3839 (1990).
3) J.D. Jorgensen, Shiyou Pei, P. Lightfoot, D.G. Hinks, B.W. Veal, B. Dabrowski, A.P. Paulikas, and R. Kleb, *Physica C*, **171**, 93 (1990).
4) Y. Yamada, J.D. Jorgensen, Shiyou Pei, P. Lightfoot, Y. Kodama, T. Matsumoto, and F. Izumi, *Physica C*, **173**, 185 (1991).
5) Shiyou Pei, J.D. Jorgensen, D.G. Hinks, B.D. Dabrowski, P. Lightfoot, and D.R. Richards, *Physica C*, **169**, 179 (1990).

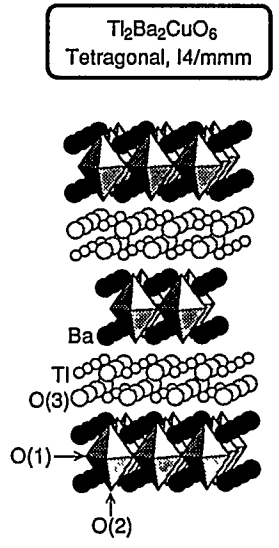


Fig. 1 Crystal structure of $Tl_2Ba_2CuO_6$

Table 1. Linear and volume compressibilities and bulk moduli at zero pressure

T_c/K	0	46	79
$-(1/a_0)(da/dp)$/GPa^{-1}	0.00404(4)	0.00427(5)	0.00428(6)
$-(1/c_0)(dc/dp)$/GPa^{-1}	0.00337(5)	0.00356(6)	0.00363(5)
$-(1/V_0)(dV/dp)$/GPa^{-1}	0.01141(13)	0.01208(15)	0.01217(17)
K/GPa^{-1}	87.6(10)	82.8(10)	82.2(11)

$Ba_2YCu_3O_{6.93}$: K = 123 GPa^{-1}; $Ba_2YCu_4O_8$: K = 118 GPa^{-1}
$(Nd_{1-x}Sr_x)(Nd_{1-y}Ce_y)CuO_{4-z}$: K = 143 GPa^{-1}
$La_{1.85}Sr_{0.15}CuO_4$: K = 147 GPa^{-1}

INSTRUMENT USED:	DATE OF REPORT.	EXPERIMENT NO.:
SEPD	10th February 1995	#1886

TITLE: Determination of the Differential Pair Distribution Functions for $YBa_2Cu_3O_{6+x}$...

AUTHORS AND AFFILIATIONS:
George H. Kwei, LLNL, and Simon J. L. Billinge, Michigan State University.

DATES OF EXPERIMENT: October 1994

CHECK ALL APPLICABLE BOXES:

- ☑ APPROVED BY PROGRAM COMMITTEE
- ☐ INSTRUMENT SCIENTIST ALLOCATION
- ☑ DO NOT PUBLISH
- ☐ PROPRIETARY RESEARCH
- ☐ PRT ALLOCATION

EXPERIMENTAL REPORT (or Abstract of Publication)

Determination of the differential pair distribution functions for $YBa_2Cu_3O_{6+x}$ near T_c using ^{63}Cu and ^{65}Cu labeled samples

Structural frustrations are widespread in the high-T_c superconducting materials leading to structural phase transitions, incommensurate structures and lattice instabilities [1]. It is of great interest to know whether, and how, structural instabilities couple to the electronic system and affect the material properties. For example, there is some experimental evidence that structural instabilities couple to the superconducting transition [1]. One such result, which remains controversial to this day, is the observation of a "double-well" for the axial oxygen in $YBa_2Cu_3O_{6+x}$. This was first reported from x-ray absorption measurements (XAS) [2]. More recent XAS data have confirmed the observation [3] (though not reproduced any temperature dependence of the double well parameters); however, there appears to be no evidence from other techniques such as x-ray and neutron scattering [4,5] to support the presence of the double well. In this experiment on SEPD we have attempted to address this question using the pair distribution function (PDF) analysis of neutron powder diffraction data.

The PDF yields the local structure directly by Fourier transforming the corrected, normalized, scattering data from reciprocal space in to direct space. Data from SEPD are ideal because of the large flux available of high-energy neutrons which furnish the important high-Q information which gives us the resolution in real-space to resolve such a feature as the double well in $YBa_2Cu_3O_{6+x}$. One problem with $YBa_2Cu_3O_{6+x}$ is the complexity of the structure. The axial oxygen feature appears in the same place in the PDF as two correlations from Y to in-plane oxygen ions. These overlapping features are larger than the Cu2-O4 feature (because of its low multiplicity) and so swamp it in the *total* PDF.

Using SEPD, we have obtained the chemically resolved differential PDF (DPDF) for $YBa_2Cu_3O_{6+x}$. This gives only correlations involving Cu and so the Y-O correlations which overlap the Cu2-O4 peak are eliminated, allowing us to study the interesting Cu2-O4 peak alone. This is done experimentally by taking data using the isotopically labeled samples and taking the difference between these data-sets before Fourier transforming. We measured two 10g samples, one made with 100% ^{63}Cu and the other with 100% ^{65}Cu. Data were collected around Tc (107K, 92K and 77K) and Cu DPDFs obtained at these temperatures. These qualitatively reproduce the expected Cu DPDF based on the crystal structure, except the Cu2-O4 bond appears split into two peaks centered about the 2.41Å position where a single peak is expected. Thus, the preliminary result from the DPDF study is consistent with the earlier XAS observations and supports the idea that, locally, the Cu2-O4 bond is either short or long as compared to the average Cu2-O4 bond length. Unfortunately, there is significant noise in this region of the DPDFs as a consequence of some uncorrected background contribution to the data. We intend to repeat the measurement to eliminate this problem. A definitive statement about the real nature of the Cu2-O4 bond cannot be made until this result is reproduced in the absence of noise.

[1] See for example, *Lattice Effects in High-T_c Superconductors*, ed. by Y. Bar-Yam, T. Egami, J. Mustre-de Leon and A.R. Bishop, (World Scientific, Singapore, 1992).
[2] J. Mustre-de Leon, S.D. Conradson, I. Batistic and A.R. Bishop, Phys. Rev. B44, 2422 (1991) and references cited therein.
[3] E.A. Stern, M. Qian, Y. Yacobi, S.M. Heald and H. Maeda, in reference 1, p. 51; A. Bianconi, S. Della Longa, M. Missori, I. Pettiti and M. Pompa, in reference 1, p. 65.
[4] J.D. Sullivan, P. Bordet, M. Marezio, K. Takemaka and S. Uchida, Phys. Rev. B48, 10638 (1993).
[5] G.H. Kwei, A.C. Larson, W.L. Hults and J.L. Smith, Physica C169, 217 (1990).

INSTRUMENT USED:	DATE OF REPORT:	EXPERIMENT NO.:
SEPD	July 31, 1990	1211 & 1289

TITLE:
STRUCTURE OF AMORPHOUS CARBON

AUTHORS AND AFFILIATIONS:
FANG LI AND J. S. LANNIN, PENN STATE PHYSICS DEPT.

DATES OF EXPERIMENT: Dec. 15-18, 1989; May 11-14, 1990

☒ APPROVED BY PROGRAM COMMITTEE, OR

☐ PART OF INSTRUMENT SCIENTIST ALLOCATION

REPORT RECEIVED:

EXPERIMENTAL REPORT (or Abstract of Publication)

Radial Distribution Function of Amorphous Carbon

Fang Li and Jeffrey S. Lannin

Department of Physics

Penn State University

University Park, PA 16802

The radial distribution function obtained by pulsed neutron diffraction measurments on thick amorphous carbon films is compared to recent theoretical models. The first neighbor peak is found to be quite broad for an amorphous semiconductor, in qualitative agreement with the predictions of molecular dynamics. However, the detailed shape of the first two peaks, including additional contributions in the minimum region between the peaks, differs from all current models. Although the areas of the first two peaks indicate predominant three fold bonding, no evidence for a distinct peak associated with graphite-like, intra-hexagon third neighbors is observed. This distinguishes amorphous carbon from local two dimensionally ordered graphitic-like materials.

EXPERIMENTAL REPORT (CONTD.)

INSTRUMENT USED:	DATE OF REPORT:	EXPERIMENT NO:
SEPD	June 16, 1995	1971

TITLE: CRYSTAL STRUCTURE AND LATTICE DYNAMICS OF SLIP-CAST β-SIALONS

AUTHORS AND AFFILIATIONS:
C.-K. Loong and J. W. Richardson, Jr., Argonne National Laboratory, Argonne, IL 60439, U. S. A.; and S. Suzuki and M. Ozawa, Nagoya Institute of Technology, Tajimi, Gifu, 507, Japan.

DATES OF EXPERIMENT: Sept. 1994

CHECK ALL APPLICABLE BOXES:

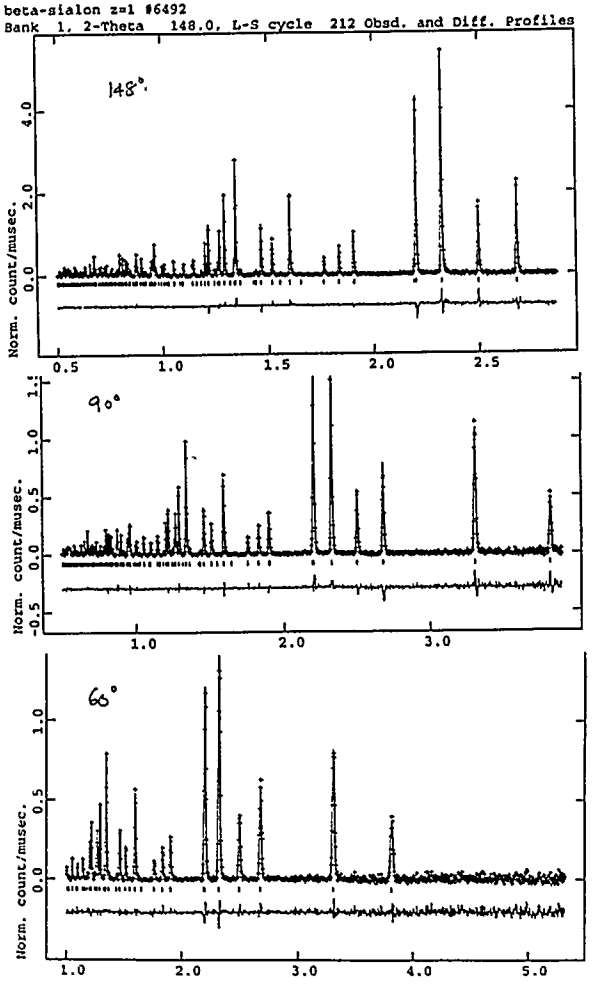
- [ ] APPROVED BY PROGRAM COMMITTEE
- [X] INSTRUMENT SCIENTIST ALLOCATION
- [ ] DO NOT PUBLISH
- [ ] PROPRIETARY RESEARCH
- [ ] PRT ALLOCATION

EXPERIMENTAL REPORT (or Abstract of Publication)

Abstract

The crystal structures and phonon densities of states (DOS) of β-Sialon ceramics, $Si_{6-z}Al_zO_zN_{8-z}$ ($0 \le z \le 6$), prepared by a novel slip-cast method were studied by neutron scattering techniques. A Rietveld analysis of the diffraction patterns shows that samples of $z < 4$ form a single-phase solid solution of Si-Al-O-N isostructural to β-Si_3N_4 (space group $P6_3/m$). Within this structure there is a consistent preferred occupation of O on the 2c sites and N on the 6h sites. For $z > 4$ the materials exhibit multiple-phase structure. The observed phonon DOS of the $0 \le z \le 4$ ceramics displays phonon bands at about 50, 80, and 120 meV. These features are considerably broader than the corresponding ones in β-Si_3N_4 powder. As z increases, effects due to atomic disorder lead to an overlap of the three phonon bands and a complete fill up of the phonon gap at ~100 meV observed in Si_3N_4. Work performed at Argonne National Laboratory is supported by the U. S. DOE-BES under the contract No. W-31-109-ENG-38.

EXPERIMENTAL REPORT (CONTD.)



INSTRUMENT USED:	DATE OF REPORT:	EXPERIMENT NO.:
SEPD	May 25, 1995	1931

TITLE: Structural Investigation of Lithiated Oxides for Rechargeable Lithium Batteries

AUTHORS AND AFFILIATIONS:
M. F. Mansuetto (CMT), M. M. Thackeray (CMT), D. N. Argyriou (MSD) and J. J. Jorgenson (MSD)

DATES OF EXPERIMENT:

CHECK ALL APPLICABLE BOXES:

- [X] APPROVED BY PROGRAM COMMITTEE
- [ ] INSTRUMENT SCIENTIST ALLOCATION
- [X] DO NOT PUBLISH
- [X] PROPRIETARY RESEARCH
- [ ] PRT ALLOCATION

EXPERIMENTAL REPORT (or Abstract of Publication)

Data Collection and Structural Refinement of $Li_{1.2}V_3O_8$

Data Collection. Several samples of $Li_{1.2}V_3O_8$ prepared at various processing temperatures were submitted to IPNS-SEPD for data collection. The presence of Li and V in these samples made them good candidates for a combined X-ray/Neutron refinement. X-ray data were collected on a Philips X-Ray Diffractometer in CMT. Fig. 1 shows the X-ray diffraction pattern of $Li_{1.2}V_3O_8$ prepared at 400°C. Fig. 2 shows the diffraction pattern of $Li_{1.2}V_3O_8$ prepared at 600°C. Changes in the intensity of the 001 reflection as a function of processing temperature was observed in these patterns. This change appears to result from a preferred orientation effect. Additional grinding of the samples eliminated some but not all of the preferred orientation. The neutron diffraction patterns of $Li_{1.2}V_3O_8$ prepared at 400°C and 600°C are shown in Fig. 3 and Fig. 4 respectively. The large size and random orientation of the sample in the sample holder eliminates any preferred orientation in the neutron diffraction patterns, and in fact the patterns are nearly identical.

Refinement. Combined Rietveld refinement of the X-Ray and neutron data of $Li_{1.2}V_3O_8$ prepared at 400°C was carried out with the program GSAS (General Structure Analysis System) operated on a PC. The lattice parameters were calculated from the X-ray data and then fixed for the refinement of the neutron data. Refined parameters for both the X-ray and neutron patterns included: scale factors, background coefficients, and profile coefficients. An absorption coefficient was refined for the neutron data only, while a preferred orientation parameter was refined for the X-ray data. Atomic positions and anisotropic temperature factors were refined for all the V and O atoms. Atomic positions and an isotropic temperature factor were refined for Li(1), while the position, occupancy, and temperature factor for Li(2) were fixed. The final refined positions of the atoms are in good agreement with the positions of the atoms determined in a single crystal X-Ray structure determination of $Li_{1.2}V_3O_8$[1]. A view of the structure of $Li_{1.2}V_3O_8$ is shown in Fig. 5.

1. L. A. de Picciotto, K. T. Adendorff, D. C. Liles and M. M. Thackeray, *Solid State Ionics*, 62 (1993) 297.

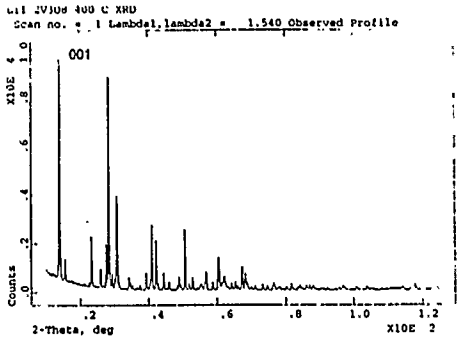


Fig. 1. The X-ray diffraction pattern of $Li_{1.2}V_3O_8$ (400°C)

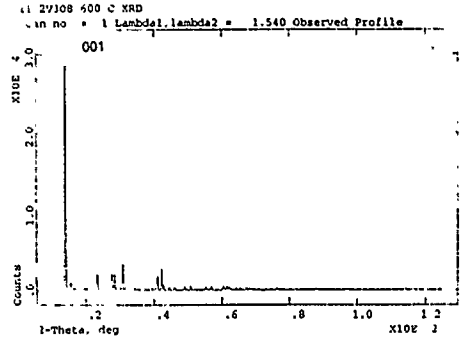


Fig. 2. The X-ray diffraction pattern of $Li_{1.2}V_3O_8$ (600°C)

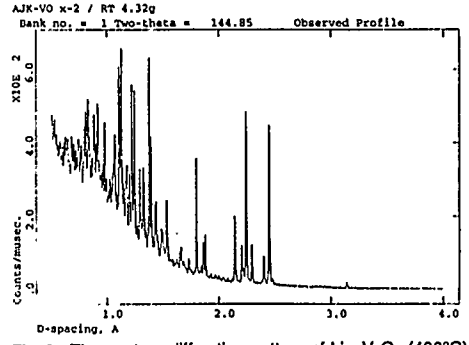


Fig. 3. The neutron diffraction pattern of $Li_{1.2}V_3O_8$ (400°C)

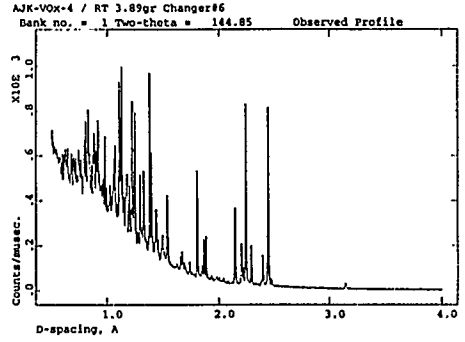


Fig. 4. The neutron diffraction pattern of $Li_{1.2}V_3O_8$ (600°C

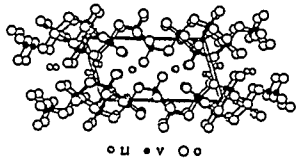


Fig. 5. The crystal structure of $Li_{1.2}V_3O_8$ as determined by combined X-ray and neutron diffraction.

INSTRUMENT USED:	DATE OF REPORT:	EXPERIMENT NO.:
SEPD	July 31, 1990	1268

TITLE:

Local Structure of Superconducting La-Sr-Cu-O

AUTHORS AND AFFILIATIONS:

H. D. Rosenfeld, B. H. Toby and T. Egami, Univ. of Pennsylvania

DATES OF EXPERIMENT: May 20 - 24, 1990

☑ APPROVED BY PROGRAM COMMITTEE, OR

☐ PART OF INSTRUMENT SCIENTIST ALLOCATION

REPORT RECEIVED:

EXPERIMENTAL REPORT (or Abstract of Publication)

Powder diffraction data were collected at the SEPD for superconducting $La_{2-x}Sr_xCuO_4$ (x = 0.12, 0.15) at various temperatures ranging from 10 K to 65 K. In order to achieve high statistical accuracy the measurement was made for 4 hrs. at each temperature. The data were Fourier-transformed to obtain the atomic pair distribution function (PDF), using the GLASS package modified so that the data from different detector banks are overlapped rather than joinedand the statistical error of the PDF can be estimated. The purpose of obtaining the PDF is to detect both dynamic and static non-periodic or non-crystallographic deviations from the perfect crystal structure.

An example of the PDF (for x = .12 at T = 10 K) is shown in Fig. 1. The PDF is in good agreement with the previous results, including the small peak at 2.9 Å which indicates non-crystallographic oxygen deviations [1]. It was found that several peaks show anomalous behavior at the superconducting transition temperature. For example, as shown in Fig. 2 the height of the Cu-O peak of the x = .12 sample (T_c = 32 K) at 1.92 Å appreciably decreases below T_c, indicating the softening of the Cu-O bond. On the other hand x = .15 sample (T_c = 38 K) shows a slight hardening below T_c. It is interesting to note that the x = .12 sample showed a large oxygen isotope effect, while x = .15 sample did not [2].

Similar softening behavior was found also in $(Ba_{.6}K_{.4})BiO_3$ and in $YBa_2Cu_3O_7$. A possible explanation is that the phonon self-energy becomes reduced due to the resonance with the superconducting gap [3]. In conventional superconductors such a softening is very small. For instance in Nb a softening by only 0.2 % is seen. In $YBa_2Cu_3O_7$ a softening of an optical phonon by 2.4 % was observed [4]. On the other hand 10 % change in the peak height observed in Fig. 2 corresponds to a change in the phonon frequency by as much as 20 %, which is by an order of magnitude larger than reasonably expected from the strong coupling theory [3]. Thus the present result provides a powerful evidence that the electron-lattice interaction in these oxides is anomalously strong, and a fundamental re-thinking of this interaction is required.

[1] T. Egami, W. Dmowski, J. D. Jorgensen, D. G. Hinks, D. W. Capone, II, C. U. Segre and K. Zhang, Rev. Solid St. Sci., 1, 247 (1987).
[2] M. K. Crawford, M. Kunchur, W. E. Farneth, E. M. McCarron and S. J. Poon, Physica, C, 162-164, 755 (1989).
[3] R. Zeyher and G. Zwicknagl, Solid St. Commun., 66, 617 (1988).
[4] R. M. Macfarlane, H. Rosen and H. Seki, Solid St. Commun., 63, 831 (1987).

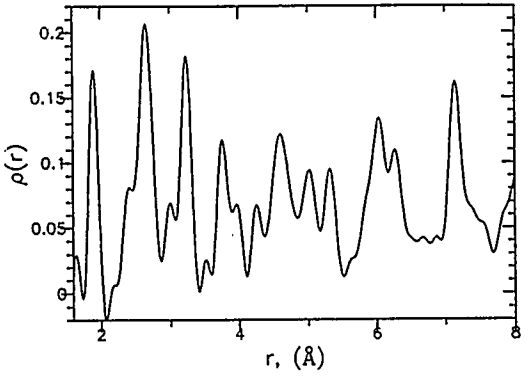


Fig. 1. Pair distribution function of $La_{1.88}Sr_{.12}CuO_4$ at T = 10 K.

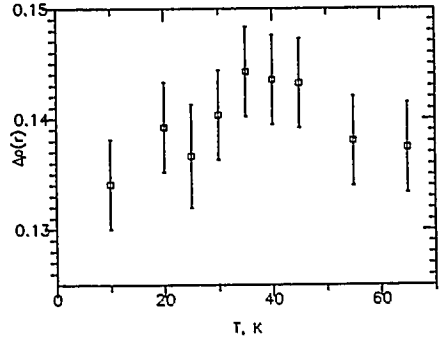


Fig. 2. Temperature dependence of the PDF peak height at 1.93 Å for $La_{1.88}Sr_{.12}CuO_4$.

INSTRUMENT USED:	DATE OF REPORT:	EXPERIMENT NO.:
SEPD	10/17/90	1323

TITLE:

Crystal Chemistry of Si/Al in Bi-processed Aluminosilicates

AUTHORS AND AFFILIATIONS: K.B. Schwartz, R.W. Dupon, and M.S. Thompson

Raychem Corporation, 300 Constitution Drive, Menlo Park, CA 94025

DATES OF EXPERIMENT: 7/20-21/90

☒ APPROVED BY PROGRAM COMMITTEE, OR

☐ PART OF INSTRUMENT SCIENTIST ALLOCATION

REPORT RECEIVED:

EXPERIMENTAL REPORT (or Abstract of Publication)

Cordierite, $Mg_2Al_4Si_5O_{18}$, is a refractory aluminosilicate whose low dielectric constant and favorable thermal expansion properties are valued in applications of ceramic technology.[1] Naturally occurring cordierites have been used as geothermometers in the study of metamorphic rocks.[2] Recently, a new process has been reported for the preparation of cordierite below 1000°C using a bismuth oxide flux.[3] This process produces dense cordierite bodies containing residual amounts of bismuth oxide flux at grain boundaries and triple points. The dielectric constant of the bodies appears unperturbed by the presence of the bismuth oxide.

Neutron powder diffraction data for three synthetic cordierite samples were collected on the SEPD. The samples were prepared with the addition of 2 at%, 5 at%, and 10 at% bismuth ion, respectively, to a stoichiometric mix of SiO_2 and $MgAl_2O_4$ spinel. The data were used to refine the structure and examine the crystal chemistry of the three samples in conjunction with x-ray powder diffraction data collected on a Siemens D-500 diffractometer with a single-crystal quartz monochromator and position sensitive detector. Combining data from the SEPD with XRD data is useful in this case as it allows for an unambiguous identification of channel constituents in the cordierite structure. The use of XRD data is particularly effective at detecting small amounts of Bi suspected of occupying the channel sites. Simultaneously, ND data can constrain the thermal parameters and probe the nature of Si/Al distribution in these samples. The joint refinements were performed using GSAS.[4]

The structures of the 5 at% Bi and 10 at% Bi samples were refined in the orthorhombic space group, Cccm. Orthorhombic, or low, cordierite is the ordered form of the structure and contains five distinct tetrahedral sites. Aluminum and silicon are ordered amongst the sites, with two sites ($T_1$1 and $T_2$6) containing Al and three sites ($T_1$6, $T_2$1 and $T_2$3) fully occupied by Si.[5] Ordering of Si/Al in synthetic cordierite is unusual, as most synthetic samples are actually the disordered hexagonal polymorph, indialite.[6] Both the 5 at% Bi and and 10 at% Bi samples contain significant amounts of Bi in the two channel sites, C1 and C2 (see Table 1). χ^2 for the final cycle of refinement are 3.52 and 3.07, respectively. Metal-oxygen bond distances are given for the samples and other cordierites for comparison in Table 2.

Refinement of the structure of the 2 at% Bi sample has been problematic, but the most satisfactory model has the indialite structure, space group P6/mcc. Though χ^2=5.81, refinements in the lower symmetry orthorhombic structure do not significantly improve the agreement factors. Indialite, with two distinct tetrahedral sites, is disordered "high cordierite," and Al/Si distribution is fixed at complete disorder. Comparison of bond distances with naturally occurring, partially ordered indialites (Table 2) indicate partial ordering may also occur in this sample. Site occupancy refinements for Al and Si between T_1 and T_2 show no significant improvement in χ^2. Bi occupancy of the channel sites is comparable with the other samples, but with a more even distribution of Bi between C1 and C2 (see Table 1).

Implications of the change in symmetry between low-Bi and high-Bi-processed cordierites are currently under investigation.

[1] U. Chowdry and A.W. Sleight, Ann. Rev. Mat. Sci. 17, 323-40 (1987).
[2] K.L. Currie, Contrib. Mineral. Petrol. 33, 215-26 (1971).
[3] R.W. Dupon, R.L. McConville, D.J. Musolf, A.C. Tanous, and M.S. Thompson, J. Am. Cer. Soc. 73, 335-39 (1990).
[4] A.C. Larsen and R.B. von Dreele, LAUR 86-748, Los Alamos National Laboratory (1986).
[5] E.P. Meagher and G.V. Gibbs, Canad. Mineral. 15, 43-9 (1977).
[6] M.F. Hochella,Jr. and G.E. Brown,Jr., J. Am. Cer. Soc. 69, 13-18 (1986).
[7] G.V. Gibbs, Amer. Mineral. 51, 1068-87 (1966).
[8] J.P. Cohen, F.K. Ross, and G.V. Gibbs, Am. Mineral. 62, 67-78 (1977).
[9] Cordierite glass synthesized by Bill Jackson of Stanford University.
[10] Y.H. Kim, D. Mercurio, J.P. Mercurio, and B. Frit, Mat. Res. Bull. 19, 209-17 (1984).

Table 1: Bismuth Occupancy in Channel Sites of Cordierite Structure

	C1 (0,0,.25)	C2 (0,0,0)
2 at% Bi	0.062(3)	0.056(3)
5 at% Bi	0.089(4)	0.038(4)
10 at% Bi	0.092(5)	0.055(5)

Table 2: Metal-Oxygen Bond Distances in Cordierite and Indialite

Cordierite

	Mg-O	$T_1$1-O	$T_1$6-O	$T_2$1-O	$T_2$3-O	$T_2$6-O
5 at% Bi	2.100(3)	1.750(4)	1.643(2)	1.635(4)	1.620(4)	1.720(4)
10 at% Bi	2.100(3)	1.752(4)	1.636(2)	1.634(3)	1.620(3)	1.724(4)
Guilford[7]	2.119(3)	1.753(4)	1.621(5)	1.611(4)	1.612(4)	1.744(4)
White Wells[8]	2.108(1)	1.758(1)	1.626(2)	1.614(1)	1.617(1)	1.742(1)

Indialite

	Mg-O	T_1	T_2
2 at% Bi	2.104(1)	1.719(1)	1.652(2)
xlized glass[9]	2.083(3)	1.743(3)	1.652(5)
Bokaro[5]	2.108(5)	1.719(5)	1.653(7)
K-substituted[10]	2.114(3)	1.725(4)	1.653(6)

INSTRUMENT USED:	DATE OF REPORT:	EXPERIMENT NO.:
SEPD	AUG. 3, 1992	1457

TITLE:
Local Structure of Superconducting Oxides

AUTHORS AND AFFILIATIONS:
T. Sendyka and T. Egami, University of Pennsylvania

DATES OF EXPERIMENT: July 14 - 18, 1992

☒ APPROVED BY PROGRAM COMMITTEE, OR

☐ PART OF INSTRUMENT SCIENTIST ALLOCATION

REPORT RECEIVED:

EXPERIMENTAL REPORT (or Abstract of Publication)

The local atomic structure and its changes with temperature of superconducting 2-1-4 materials $La_{2-x}Sr_xCuO_4$, (x = .125, 0.15) and $La_{2-x}Ba_xCuO_4$ (x = 0.125) were studied by the Pair Distribution Function (PDF) Analysis. The PDF is the Fourier transformation of the normalized neutron structure factor, and describes the orientationally averaged distribution of interatomic distances. It is well known that the low temperature structural transition from the orthorombic (LTO) phase, to tetragonal (LTT) phase in $La_{1.875}Ba_{1.25}CuO_4$ coincides with the suppression of the superconductivity. Though in $La_{2-x}Sr_xCuO_4$ system this transition is not observed a small amount of suppression of Tc around x=.125 has been confirmed. While the origin of supression of Tc appears to be electronic, by comparing the two systems one can see how the supression of superconductivity would affect the local structure. Such a knowledge would be important in an attempt to understand the mechanism of superconductivity.

The PDF of $La_{1.875}Ba_{1.25}CuO_4$ is shown in Fig. 1. The observed PDF differs from the one of ideal crystallographic structure. The most visible differences are the presence of small peaks at r = 3.0 Å, and r = 3.5 Å. These peaks - absent in the ideal structure - has always been observed in all the 214 compounds. Initial structural modelling suggests that these peaks are due to the distance between the apical (O2) and in-plane (O1) oxygens in the CuO_6 octahedron. Since O1-O2 distance is 3.2 Å in the ideal crystallographic structure, the PDF clearly shows that the CuO_6 octahedra are distorted, and this may be crucial in producing superconductivity. Extensive modeling of local structure of all three compounds is under way.

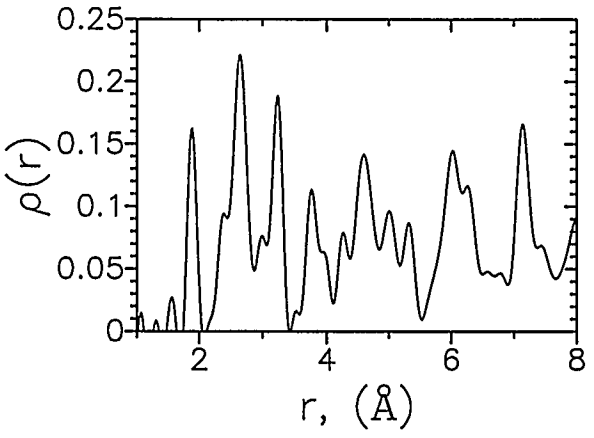


Fig. 1. Atomic pair distribution function of $La_{1.875}Ba_{1.25}CuO_4$ at T = 30 K, determined with SEPD.

INSTRUMENT USED:	DATE OF REPORT:	EXPERIMENT NO.:
SEPD	Dec. 15, 1993	1755

TITLE:

Local Structure of Relaxor Ferroelectric PLZT

AUTHORS AND AFFILIATIONS:

S. Teslic and T. Egami, Univ. of Pennsylvania

DATES OF EXPERIMENT: Nov. 11 - 13, 1993

☒ APPROVED BY PROGRAM COMMITTEE, OR

☐ PART OF INSTRUMENT SCIENTIST ALLOCATION

REPORT RECEIVED:

EXPERIMENTAL REPORT (or Abstract of Publication)

$(Pb_{1-x}La_x)(Zr_{1-y}Ti_y)O_3$ (PLZT) system is a family of transparent ferroelectric ceramic materials suitable for a variety of electrooptic as well as piezoelectric applications [1,2]. Materials of particular interest have compositions in the range $5<x<15$, and $y = 0.35$. The structures of these materials are based on cubic perovskite, and the distortion of the crystal lattice at the ferroelectric transition can be observed by standard diffraction experiments [3]. However, presumption of long range order in the conventional crystallographic analysis obscures subtle effects which lead to various features of ferroelectric behavior, in particular the relaxor ferroelectric behavior. In relaxor ferroelectric solids ferroelectric transition takes place gradually as the temperature is changed, just as the spin-glass transition. The use of the atomic pair distribution function (PDF) analysis provides more direct information regarding the local atomic structure without the assumption of long range periodicity [4,5]. The PDF is obtained by Fourier-transforming the normalized powder neutron scattering intensity, S(Q), and describes the distribution of the interatomic distances, weighted by the scattering amplitude of each atom and averaged over space and time. The neutron PDF of PLZT ($x = 0.12$, $y = 0.35$, solid curve) obtained by Fourier transforming S(Q) up to Q=30 Å is shown in Figure 1 of the report, compared with the PDF calculated for an average perovskite structure (dotted curve). In calculating the model PDF the neutron scattering length of each atom, the vibrational amplitude of 0.05 Å, and a lattice constant of 4.09 Å were assumed. The profound difference between two PDF's indicates that the real atomic structure in this solid is very far from periodic, and departs significantly from the crystallographic lattice structure. We have studied earlier another relaxor ferroelectric material $Pb(Mg_{1/3}Nb_{2/3})O_3$ (PMN), which is described crystallographically as a cubic perovskite. We observed also very significant deviation from the crystallographic structure. A structural model developed by the means of the dual space refinement technique (our new method to build a model by achieving agreement both in the reciprocal and real spaces) shows that the displacements of cations and anions are not correlated over long (crystallographic) distances, and that the correct crystallographic description is a cubic disorder model [6]. The neutron PDF of PMN is very similar to that of PLZT implying similarities of atomic displacements between PMN and PLZT and, in turn, similarities in chemical bonding requirements in these materials.

EXPERIMENTAL REPORT (CONTD.)

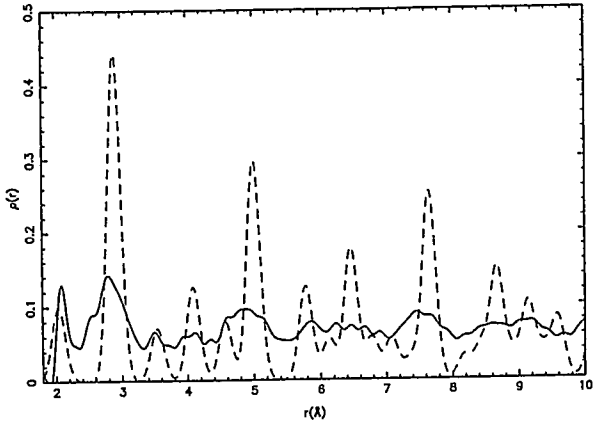


Fig. 1. The PDF of $(Pb_{.88}La_{.12})(Zr_{.65}Ti_{.35})O_3$ (PLZT, solid curve) compared with the PDF of the average perovskite structure.

INSTRUMENT USED:	DATE OF REPORT:	EXPERIMENT NO.:
SEPD	July 31, 1990	1268

TITLE:

Local Structure of Superconducting (Ba,K)BiO_3

AUTHORS AND AFFILIATIONS:

B. H. Toby and T. Egami, Univ. Penna., K. Volin and J. D. Jorgensen, IPNS

DATES OF EXPERIMENT: Mar. 14 - 16, 1990

☐ APPROVED BY PROGRAM COMMITTEE, OR

☑ PART OF INSTRUMENT SCIENTIST ALLOCATION

REPORT RECEIVED:

EXPERIMENTAL REPORT (or Abstract of Publication)

Powder diffraction data were collected at the SEPD for superconducting $(Ba_{.6}K_{.4})BiO_3$ at various temperatures ranging from 10 K to 100 K. In order to achieve high statistical accuracy the measurement was made for 4 hrs. at each temperature. The data were Fourier-transformed to obtain the atomic pair distribution function (PDF), using the GLASS package modified so that the data from different detector banks are overlapped rather than joinedand the statistical error of the PDF can be estimated. The PDF describes dynamic as well as static distribution of the interatomic distances. The purpose of obtaining the PDF is to detect both dynamic and static non-periodic or non-crystallographic deviations from the perfect crystal structure.

An example of the PDF (at T = 10 K) is shown in Fig. 1. While the first peak (Bi-O correlation), third (Bi-Ba,K) and forth (a-axis translation) peaks are reasonably sharp, the second peak which describes the Ba,K-O correlation is rather broad, indicating the presence of local tilting of BiO_6 octahedra, although for this composition there is no macroscopic tilting. Collective tilting of BiO_6 occurs at lower concentrations of K, leading to a lowering of the crystal symmetry [1]. At lower concentrations also a Bi-O breathing mode instability develops, leading to the charge disproportionation of Bi. Although at this moment we do not see an obvious sign of local breathing modes, while more detailed modelling is required on this point, it is of a great interest to note that a tendency of softening of the Bi-O correlation was observed below T_c. In other words, the height of the Bi-O peak at 2.15 Å decreased by about 3 % below T_c, corresponding to the decrease in the vibrational frequency by 6 %. Similar, but even larger softening was observed for the Cu-O peak of $La_{1.88}Sr_{.12}CuO_4$ (Report for Experiment 1268). The amount of softening observed here is larger than the one observed by Raman scattering for $YBa_2Cu_3O_7$ (2.4 %) [2], and is much larger than in conventional superconductors (in Nb a softening by only 0.2 % is seen). A possible explanation of this softening is that the phonon self-energy becomes reduced due to the resonance with the superconducting gap [3].

However, the magnitude of softening is larger than reasonably expected from the strong coupling theory [3]. Thus the present result provides another evidence that the electron-lattice interaction in these oxides is anomalously strong, and the nature of the interaction may be quite different from the ordinary one.

[1] S. Pei, J. D. Jorgensen, B. Dabrowski, D. G. Hinks, D. R. Richards, A. W. Mitchell, J. M. Newsam, S. K. Sinha, D. Vaknin and A. J. Jacobson, Phys. Rev., B41, 4126 (1990).

[2] R. M. Macfarlane, H. Rosen and H. Seki, Solid St. Commun., 63, 831 (1987).

[3] R. Zeyher and G. Zwicknagl, Solid St. Commun., 66, 617 (1988).

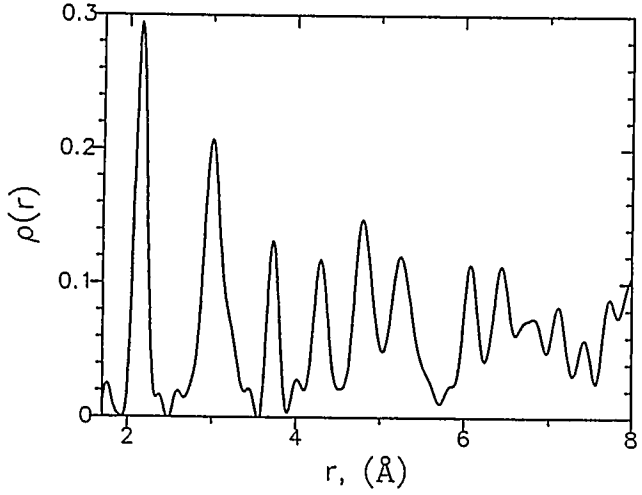


Fig. 1. Pair distribution function of $(Ba_{.6}K_{.4})BiO_3$ at T = 10 K.

INSTRUMENT USED:	DATE OF REPORT:	EXPERIMENT NO.:
SEPD	3 AUG 1992	1329

TITLE: Structure of an Ambient-Temperature Molten Salt $ImHCl_2$

AUTHORS AND AFFILIATIONS: P. C. Trulove (The Frank J. Seiler Research Laboratory, USAF Academy, CO); D. L. Price (ANL); R. A. Osteryoung (Dept. of Chemistry, North Carolina State Univ., Raliegh, NC).

DATES OF EXPERIMENT: April 12-14, 1991

☐ APPROVED BY PROGRAM COMMITTEE, OR

☐ PART OF INSTRUMENT SCIENTIST ALLOCATION

REPORT RECEIVED:

EXPERIMENTAL REPORT (or Abstract of Publication)

The structure of 1-ethyl-3-methylimidazolium hydrogen dichloride ($ImHCl_2$) was investigated using neutron diffraction. Experiments were performed on four samples of $ImHCl_2$ with differing combinations of H-D substitution on the imidazolium ring and HCl_2^-. The incomplete deuteration of the imidazolium cation (i.e. the ethyl and methyl groups were not deuterated) resulted in a large incoherent scattering background. This, in turn, greatly complicated data analysis. However, through the analysis of diffraction differences from H-D substitution using the program for H-D substitution by H. A. Soper, it was still possible to extract some interesting information about the $ImHCl_2$ melt structure.

Analysis of first order differences due to deuteration of HCl_2^- gave three (or possibly only two) intrastructural peaks. These results indicate that the HCl_2^- exists as an unsymmetrical ion in the $ImHCl_2$ molten salt. This is quite remarkable considering that the HCl_2^- ion in $AlCl_3$:ImCl molten salts is linearly with the hydrogen symmetrically placed between the two chlorides.[1] Furthermore, to our knowledge, unsymmetrical HCl_2^- ions have only been observed in the solid-state.[2] An unsymmetrical HCl_2^- implies some type of interaction with an additional species. The samples of $ImHCl_2$ used for these experiments had a small molar excess of ImCl and, therefore, contained some free Cl^-. As shown in Figure 1, this free Cl^- could weakly H-bond to the hydrogen in HCl_2^- resulting in an unsymmetrical ion. Alternatively, an unsymmetrical ion could be formed if one chloride from the HCl_2^- ion H-bonds to a hydrogen on the imidazolium ring (Figure 2). The chlorides in the HCl_2^- ion are capable of acting as H-bond acceptors as demonstrated by the presence of anions of the type $Cl(HCl)_n^-$ in the $ImHCl_2$ melts containing excess HCl.[3] In addition, the imidazolium ring hydrogens have been shown to strongly H-bond to Cl^- in $AlCl_3$:ImCl molten salts.[4]

EXPERIMENTAL REPORT (CONTD.)

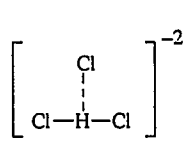


Figure 1

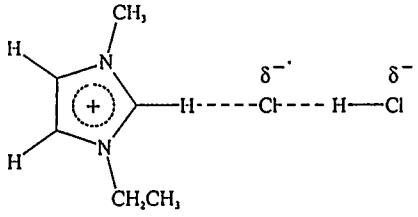


Figure 2

Analysis of second order differences due to correlations between hydrogens on the imidazolium cation ring and HCl_2^- gave a pronounced peak near r = 4 Å. The area for this peak corresponded to 2-3 hydrogens about a hydrogen at the origin, suggesting a quite ordered arrangement in the $ImHCl_2$ melt. The manner of this ordering and the nature of the HCl_2^- ion structure are a matter for future experiments.

References

1. Trulove, P. C.; Osteryoung, R. A. *Inorg. Chem.* in press.

2. Evans, J. C.; Lo, G. Y-S. *J. Phys. Chem.* **1966**, *70*, 11-19.

3. Campbell, J. L. E.; Johnson, K. E. In *Proceedings of the Eighth International Symposium on Molten Salts*; The Electrochemical Society: Pennington, NJ, 1992: in press.

4. Dieter, K. M.; Dymeck, C. J.; Heimer, N. E.; Rovang, J. W.; Wilkes, J. S. *J. Am. Chem. Soc.* **1988**, *110*, 2722-2726.

INSTRUMENT USED:	DATE OF REPORT:	EXPERIMENT NO.:
SEPD	16th October 1990	1240

TITLE:

Structural Study of the Liquid Alloy $Mg_{.50}Ba_{.50}$

AUTHORS AND AFFILIATIONS: J.B. Van Zytveld,
Physics Department, Calvin College, Grand Rapids, Michigan 49546

DATES OF EXPERIMENT: 18 - 20 July 1990

☒ APPROVED BY PROGRAM COMMITTEE, OR

☐ PART OF INSTRUMENT SCIENTIST ALLOCATION

REPORT RECEIVED:

EXPERIMENTAL REPORT (or Abstract of Publication)

The structure of the liquid alloy $Mg_{.50}Ba_{.50}$ has been measured at two temperatures, 600°C and 800°C, by means of neutron diffraction. These temperatures are respectively 75°C and 275°C above the alloy melting temperature. The experiments were carried out on the Special Environment Powder Diffractometer (SEPD) at the Intense Pulsed Neutron source (IPNS) at Argonne National Laboratory. The sample was held in a cylindrical vanadium tube and heated in a vanadium furnace; separate diffraction measurements on an empty sample tube and on the empty furnace permitted subtraction of the scattering due to these sources. Standard analysis resulted in the reduction of the experimental data to the total structure factor, S(Q), and the total distribution function, T(r). (T(r)=n(r)/r, where n(r) is the radial distribution function.) · Curve-fitting analysis of T(r) for the 600°C experiment indicates a first major coordination shell, of coordination number (C.N.) approximately 9, centered at r=3.89A, and a second smaller shell, C.N.=4, centered at r=5.00A. A very small shell of C.N.=0.5 may exist at about r=2.7A as well. No significant change in these parameters is seen for the higher temperature measurement, indicating a relatively temperature- independent liquid structure. This observation is significant, since an earlier measurement of the electrical resistivity of this sample showed a large and unusual temperature dependence; this observed dependence is therefore to be attributed to electronic changes, and not to temperature-dependent structure effects.

If a liquid structure characterized by a random packing of hard spheres is assumed, one would expect to see evidence of primary ionic separations of approximately 2.7A (Mg-Mg), 3.9A (Ba-Ba) and 3.3A (Mg-Ba). Very little evidence for the 2.7A separation is found, and the 3.3A separation is totally missing. Spectroscopic studies of the solid alloy, however, show a stable hexagonal structure formed by the stacking of polyhedra with Mg_2Ba stoichiometry. If such a local packing involving individual (non-stacked) polyhedra were also preferred in the liquid alloy, one would expect to see coordinations characteristic of the individual polyhedra as well as of excess Ba. If we assume a Friauf polyhedron, the primary coordination is that of (Mg-Ba), with a separation of r=3.8A. This would be indistinguishable in this experiement from the pure Ba separation of 3.9A. Thus these measurements are consistent with a liquid alloy composed of locally-ordered Friauf polyhedra which incorporate nearly all of the Mg ions, and which are awash in excess Ba. The existance of such polyhedra in the liquid, however, do not require electronic bonding.

The essential and substantial assistance of K. Volin and D. Price with the experiment and with the data reduction, respectively, is warmly acknowledged. This work also benefited substantially from the assistance of students W. Schotanus, E. Van Timmeren, and H. Schnyders.

EXPERIMENTAL REPORT (CONTD.)

Disclaimer

This report was prepared as an account of work sponsored by an agency of the United States Government. Neither the United States Government nor any agency thereof, nor any of their employees, makes any warranty, express or implied, or assumes any legal liability or responsibility for the accuracy, completeness, or usefulness of any information, apparatus, product, or process disclosed, or represents that its use would not infringe privately owned rights. Reference herein to any specific commercial product, process, or service by trade name, trademark, manufacturer, or otherwise, does not necessarily constitute or imply its endorsement, recommendation, or favoring by the United States Government or any agency thereof. The views and opinions of authors expressed herein do not necessarily state or reflect those of the United States Government or any agency thereof.



Argonne National Laboratory
Operated by the University of Chicago
for the U.S. Department of Energy



Printed on recycled paper